INTERNATIONAL COUNCIL FOR RESEARCH AND INNOVATION
IN BUILDING AND CONSTRUCTION

WORKING COMMISSION W18 - TIMBER STRUCTURES

CIB - W18

MEETING THIRTY-EIGHT

KARLSRUHE

GERMANY

AUGUST 2005

CONTENTS

CIB-W18 Papers 38-2-1 up to 38-102-3

0 List of Participants

INTERNATIONAL COUNCIL FOR RESEARCH AND INNOVATION IN BUILDING AND CONSTRUCTION
WORKING COMMISSION W18 - TIMBER STRUCTURES

MEETING THIRTY-EIGHT
Karlsruhe, Germany, 29 - 31 August 2005

LIST OF PARTICIPANTS

AUSTRALIA
B Leicester   CSIRO, Melbourne

AUSTRIA
G Schickhofer   TU Graz

CANADA
A Asiz   University of New Brunswick, Fredericton
F Lam   University of British Columbia, Vancouver
Chun Ni   Forintek, Vancouver
E Karacabeyli   Forintek, Vancouver
M Popovski   Forintek, Vancouver
P Quenneville   Royal Military College of Canada, Kingston

CZECH REPUBLIC
P Kuklik   TU Prague

CROATIA
V Rajcic   Faculty of Civil Engineering, Zagreb

DENMARK
H J Larsen   Copenhagen

FINLAND
A Kevarinmäki   VTT Technical Research Centre of Finland, Espoo
J Leskelä   Finnish Forest Industries, Helsinki
A Ranta-Maunus   VTT Technical Research Centre of Finland, Espoo

GERMANY
I Bejtka   Universität Karlsruhe
H J Blaß   Universität Karlsruhe
H Brüninghoff   Universität Wuppertal
J Denzler   Technical University of Munich
J Ehlbeck   Freiburg
P Fellmoser   Universität Karlsruhe
M Frese   Universität Karlsruhe
P Glos   Technical University of Munich
R Görlacher   Universität Karlsruhe
P Haller   TU Dresden
R Hartnack   Kulmbach
V Krämer   Universität Karlsruhe
K Rautenstrauch   Bauhaus University, Weimar
W Rug   Wittenberge
M Schmid   Universität Karlsruhe

T Uibel   Universität Karlsruhe
H Werner   University of Cooperative Education, Mosbach

ITALY
M Ballerini   University of Trento
M Follesa   Timber Engineering, Florence
M P Lauriola   Timber Engineering, Florence
M Moschi   IVALSA-CNR, Florence
M Rizzi   University of Trento
A Ceccotti   IVALSA-CNR, Florence

JAPAN
M Yasumura   Shizuoka University

LATVIA
L Ozola   Latvia University of Agriculture

NEW ZEALAND
A Buchanan   University of Canterbury

SLOVENIA
B Dujic   Faculty of Civil and Geodetic Engineering, Ljubljana

SWEDEN
J Jönsson   Lund University
B Källsner   Trätek, Stockholm
J König   Trätek, Stockholm
S Thelandersson   Lund University

SWITZERLAND
M Arnold   EMPA Wood Laboratory, Dübendorf
C Erchinger   ETH Zürich
A Frangi   ETH Zürich
J Köhler   ETH Zürich
V Schleifer   ETH Zürich
R Steiger   EMPA Wood Laboratory, Dübendorf

THE NETHERLANDS
A Jorissen   TU Eindhoven
J W van der Kuilen   TU Delft
A Leijten   TU Delft

UK
B Griffiths   BRE, Watford
A Kermani   Napier University, Edinburgh
A Lawrence   Arup, London
T Reichert   Napier University, Edinburgh

USA
B Yeh   American Plywood Association, Tacoma

1. Chairman's Introduction

2. General Topics

3. Timber Columns

4. Stress Grading

5. Stresses for Solid Timber

6. Timber Joints and Fasteners

7. Environmental Conditions

8. Structural Stability

9. Fire

10. Statistics and Data Analysis

11. Glued Joints

12. Loading Codes

13. Any Other Business

14. Venue and Program for Next Meeting

15. Close

INTERNATIONAL COUNCIL FOR RESEARCH AND INNOVATION IN BUILDING AND CONSTRUCTION

WORKING COMMISSION W18 - TIMBER STRUCTURES

MEETING THIRTY EIGHT

KARLSRUHE, GERMANY 28 TO 31 AUGUST 2005

M I N U T E S
(F Lam)

1 CHAIRMAN'S INTRODUCTION

Chairman Hans Blass opened the 38th CIB-W18 meeting and welcomed the delegates to Karlsruhe, Germany. This is the fourth meeting hosted by Germany. Previous to this meeting the 5th CIB-W18 meeting in 1975 was held in Karlsruhe, the 15th CIB-W18 meeting was held in Karlsruhe in 1982, and the 21st CIB-W18 meeting was held in Berlin (formerly East Germany) in 1989.

The chair informed the participants the Dr. B.S. Choo has sadly passed away in June 2005 and asked for a minute of silence in commemoration of Dr. Choo.

Papers brought directly to the meeting will not be accepted and papers without the presence of any of the authors will not be allowed to be presented by non-authors. Papers should fit to the overall goals towards translation of research results into rules in codes or development and harmonization of existing and new standards. Presenters are reminded that they should conclude the presentation with statements concerning impact of research to code applications.

2 GENERAL TOPICS

S. Thelandersson made an announcement of the second Timber Engineering Advance Course in Lund University in Oct and Nov 2005. The course is free and all are welcome. The participants have to pay for their own travel costs to and from Lund.

3 TIMBER COLUMNS

38 - 2 - 1   Long-term Load Bearing of Wooden Columns Influenced by Climate – View on Code - **R Hartnack, K Rautenstrauch**

Presented by R Hartnack

B Leicester commented that since the work was intended for code application, statistics such as mean and COV are important and asked whether data was available. Hartnack answered that this is a virtual exercise adapted to values in literature of small data set of full size specimens. H Larsen asked whether the method is aimed at design practice engineers and do they have any input to the method. The answer was yes. J Köhler asked how was model uncertainty handled? Hartnack answered there are more uncertainties in other part of the work compared with the uncertainties in the model. J Köhler asked how

1

to correspond the safety level cited in the paper to beta values. Hartnack answered the safety level cited was defined per the code equations. R Steiger commented how come the work neglected snow load. Hartnack answered that a 4 month snow load duration was tested and the influence was found to be small because after one year no influence on creep was observed. Data from Germany and Swedish Data was used.

E Karacabeyli commented that R Foschi's work clearly indicated snow load has a strong impact on bending performance. Hartnack answered that there is an impact on strength but not creep. J König commented that Figure 4 shows a big gap in safety and asked if this is supported by real life experience. Hartnack answered that real life experience did not indicate a problem. J König commented that no action is needed in code. Hartnack disagreed and stated that there is additional safety in real life but the code should be changed.

4   STRESS GRADING

38 - 5 - 1   Are Wind-Induced Compression Failures Grading Relevant - **M Arnold, R Steiger**

Presented by M Arnold

H Blass asked and received confirmation that the characteristic strength values reported were depth adjusted already. H Larsen commented this work shows the Swiss visual rules are too conservative and therefore the compression failure impact can still be tolerated. H Larsen said that compression failure should be excluded but question how this can be done as MSR is not effective. M Arnold mentioned that visual grading can detect this although this is not easy. In practice, problems are not seen with wood that has compression failures. F Lam mentioned in N. America graders detect "falling breaks" in grading which are compression failures induced during logging. B Leicester commented in Australia similar type of problem was observed where detection of defects was difficult. A proof test method was introduced. Proof test machine was built and standard was written. M Arnold responded that the proof load level has to be set fairly high for this to be effective. A Ranta-Maunus asked about the weakest values in the different compression failures classes. M Arnold answered that he cannot see differences in strength amongst different compression failure classes. A Buchanan received clarification that the compression failure was tested always on the tension side during bending. He also asked if the tree was damaged earlier would it mask the detection of compression failures. M Arnold answered that a portion of the tested pieces had previous damage from past wind and they could be detected. S Thelandersson commented that may be the MSR method could be calibrated against material which has a portion of compression wood. He also commented that with the conclusion that we have to be careful with storm damaged trees, can we still use the wood? M Arnold answered that it is a question of how to define storm damage and yes we need to be careful.

5   STRESSES FOR SOLID TIMBER

38 - 6 - 1   Design Specifications for Notched Beams in AS:1720 - **R H Leicester**

Presented by R H Leicester

A Buchanan questioned whether the theoretical notch is a practical notch with saw cut. B Leicester answered that the Fracture Mechanics (FM) approach assumes the existence of a slit and notch root has an effect. Designer does know whether there is a crack. H Larsen

commented European has strong interests but reference to their work is missing. Leicester mentioned that a companion paper has more comprehensive reference list. H Larsen questioned the general size effect concept in FM. He commented that there is no general size effect but a depth effect exists in a square relationship. The paper shows a factor 0.48 which agrees with the European results. He questions where is the general size effect as claimed? B Leicester answered that European has confirmed that general size effect findings also. Leicester also responded that in the case of two geometrically similar beams loaded the same way the general size effect can be seen. Also for metals this is true. A Jorissen received clarification that in the figure beam depth is the size in that case. If the beam is shallower than a certain depth we do not see an effect. A Buchanan related that this may be the case of finger jointed material as the lamination is relatively thin and also the case of LVL.

38 - 6 - 2   *Characteristic Bending Strength of Beech Glulam* -   **H J Blaß, M Frese**

Presented by M Frese

H Larsen received confirmation the Karlsruhe model was used and the failure established when outer lamination was cracked. H Larsen commented that the Karlsruhe model weakness is the redistribution of stress after 1st failure. M Frese mentioned that failure in the interior plies can happen first and stress redistribution is allowed until outer ply failure. S Thelandersson asked whether Beech is expensive compared to softwood. H Blass answered yes but red heart material that is not suitable for furniture is used here.

38 - 6 - 3   *Shear Strength of Glued Laminated Timber* -   **H Klapp, H Brüninghoff**

Presented by H Brüninghoff

P Kuklik commented on the detail of the connector at the support and commented that the changes in moisture in the connection may have caused tension perpendicular to grain stresses. Brüninghoff responded that the beam is free at the upper 2/3 portion and cracks outside the bolt area were also found. Density difference between adjacent ply may be an issue. A Ranta-Maunus asked about the weather information during failure. Brüninghoff responded that during winter the beam surface may have a 9% mc and 10% 5 cm deep from the surface. The climatic condition in the facility is quite stable.

G Schickhofer commented decrease in shear strength was found with increase in tension strength in previous work and micro and macro defects influence shear strength. Annular ring influence was found by Glos and Denzler. There is also knot effect. The work used data from small clear specimens which is not realistic for glulam. Brüninghoff agreed that more test on glulam may be appropriate. P Glos commented that EN 408 is not a good test and does not fit to solid timber. However in this case the failure indicate failure in wood along the glue line and does not have dowel effect; therefore, the data are good. P Glos also commented this is good work. S Thelandersson agreed with P Glos's comments in general. He mentioned also that one needs to define shear strength at the end of the beam where drying stresses may occur. This is an important point when evaluating this aspect in the lab.

R Steiger commented that this should be included in Eurocode 5 and ask what should be done from other country point of view. H Blass responded that Germany will take action. F Lam mentioned size effect for shear is in the Canadian code. A Ranta-Maunus commented that this has not been an issue in Nordic countries but will consider this information. A Buchanan suggested that may be a step function type approach can be used. F Lam commented this is the mention in Canada where beam larger than a certain size will have

3

shear strength reduced according to size. H Blass said that the alternative can also be considered where beams smaller than a certain size will be allowed a larger shear strength.

6 TIMBER JOINTS AND FASTENERS

38 - 7 - 1   A Numerical Investigation on the Splitting Strength of Beams Loaded Perpendicular-to-grain by Multiple-dowel Connections – **M Ballerini, M Rizzi**

Presented by M Ballerini

A. Jorissen asked and received explanation from M Ballerini about the form of Figure 8 in the paper. M Yasumura said similar work in pure tension was done previously and it will be interesting to compare results. He also questioned that since there is no shear between the two dowels, how can one explain the results. H Blass agreed that the shear force in that area is zero, however the Eurocode is derived from the single dowel case. M Ballerini mentioned that data is not available for his case and should look into whether it is conservative. H Blass mentioned that Eurocode is not meant to address the two dowels case. M Yasumura mentioned that if the spacing between the dowels is big enough cracks will propagate in each dowel. One has to be careful when applying Eurocode 5.

38 - 7 - 2   A Probabilistic Framework for the Reliability Assessment of Connections with Dowel Type Fasteners - **J Köhler**

Presented by J Köhler

F Lam commented that the embedment strength was modelled deterministically with a given randomly generated density and dowel diameter. It would be more realistic if the embedment strength is treated as a random variable for a given density and diameter. The overestimation of beta will probably be reduced. J Kohler answered the more accurate embedment strength was used last year and lower beta was found. However, there was concern if the assumed embedment model differs significantly from code.

38 - 7 - 3   Load Carrying Capacity of Curved Glulam Beams Reinforced with self-tapping Screws - **J Jönsson, S Thelandersson**

Presented by F J Jönsson

H Blass asked if decrease of splitting was observed when reinforcement was present. J Jönsson answered only without reinforcement cases were tested. A Buchanan received clarification that the double pitched fasteners were considered and questioned whether regular screws would work. A Ceccotti commented that well design beam with regular reinforcement should also work. A. Jorissen asked whether both FEM and design code based calculations were made. J Jönsson answered only FEM calculations were made.

38 - 7 - 4   Self-tapping Screws as Reinforcements in Connections with Dowel-Type Fasteners- **I Bejtka, H J Blaß**

Presented by I Bejtka

P Quenneville received clarification on the 3D diagram axis in the parametric study. V Rajcic received clarification that reducing the spacing will not result in timber failure.

38 - 7 - 5   The Yield Capacity of Dowel Type Fasteners - **A Jorissen, A Leijten**

Presented by A Jorissen

H Larsen pointed out that the bending case should not be an issue as this can be explained by the strain hardening of the fastener. A Jorissen responded that strain hardening is not an issue in small diameter bolts. H Larsen disagrees and further pointed out that the 3 point bending testing is no good. A Leijten mentioned that in the tension test no yielding was seen. They are aware of the material outside is different from the core material; however, no one would consider it as a non homogeneous material. H Blass pointed out that the statement of no shear force in the bending test is wrong. J W van de Kuilen mentioned the difference between model and experiment is the straining. C Ni received clarification that shear strength varies with diameter.

*38 - 7 - 6   Nails in Spruce - Splitting Sensitivity, End Grain Joints and Withdrawal
          Strength* - **A Kevarinmäki**

Presented by A Kevarinmäki

H Blass asked about the splitting sensitivity study where the nails were driven at 19% mc and wondered if 12% mc be a less favourable condition. A Kevarinmäki responded that they believe drying after nailing is more critical. H Blass questioned the low density of the timber used and commented that the proposal is independent of the strength class. A Kevarinmäki responded that high density pieces also show similar results. B Leicester commented that the end grain test apparatus may create friction from induced side pressure that could bias the results. M Schmidt questioned about hammer versus nail gun. A Kevarinmäki responded that hammer were used while ensure nail head is flushed with timber surface. A Leijten asked why withdrawal strength goes down with decrease in mc. A Kevarinmäki responded that as mc increase wood swells and increase the gripping on the nail. H Larsen commented about the relationship between the test standard and Eurocode 5. Standard should test at RH of 65%. If the standard is changed, it would invalidate past results. Correction to Eurocode 5 is the way to go. S Thelandersson commented that cyclic of climatic conditions should be considered. A Kevarinmäki responded that this information will be available in long term loading.

*38 - 7 - 7   Design of Timber Connections with Slotted-in Steel Plates and Small Diameter
          Steel Tube Fasteners* - **B Murty, I Smith, A Asiz**

Presented by A Asiz

H Blass commented that the oval cross section of the fastener under load would change the yield moment. A Asiz stated more test will come to confirm this. M Popovski asked about cyclic testing and behaviour in heavy timber. A Asiz said it would be interesting to consider cyclic testing and heavy timber is more appropriate. F Lam asked whether heavy timber would be tested. A Asiz agreed. F Lam also commented the lack of restraint in the tube compared to Delft's expansion tube. The tube can slide out of the connection and the behaviour between this and the original system is different. A Jorissen questioned and received clarification on figures in table for modification factor in relationship with numbers in the Table. A Leijten commented that the commercial application of the tube type connection is interesting and Delft's experience would be important.

7   ENVIRONMENTAL CONDITIONS

38 - 11 - 1   Design Specifications for the Durability of Timber – R H Leicester, C-H Wang, M Nguyen, G C Foliente

Presented by R H Leicester

S. Thelandersson asked how to generalize the findings on the building envelope study. B Leicester responded that in total 44 houses in two or three groups were considered. It was tried to use climatic information outside to predict the mc in the wall cavity. Wall cavity details are important. Knowledge on building physics needs to be used.

38 - 11 - 2   Consideration of Moisture Exposure of Timber Structures as an Action - M Häglund, S Thelandersson

Presented by S Thelandersson

A Ranta-Maunus commented that the model to moisture load on structure in future is important. For example dry period followed by wet period will be important to consider moisture load. J W van de Kuilen commented that their data agree with the Swedish findings and this is a good start. S Thelandersson responded that building physicists think that this is too simple as microclimatic condition rather than the macroclimatic conditions is important. The building physicists' approach is too complicated. A Ceccotti stated that this work is very important. The 5% mc change is a compromise to calculate the consequence. If 20% is used then every timber member may crack. Creep and mechano-sorptive effects are good things in this case as it can relax the stress built up in timber. J Köhler and S Thelandersson initiated a discussion on how to integrate the moisture load model in design with respect to load duration. V Rajcic asked how to introduce the concept in code? S Thelandersson responded that it would be nice to treat this from the external load perspective. Curved beams and notched beams cases are particularly influenced by mc. Reduced strength is also an option. A Ranta-Maunus stated that it is more important to consider moisture as a load otherwise the strength may be zero. A Jorissen commented that the effect of this may be more on the serviceability rather than strength issue.

8   STRUCTURAL STABILITY

38 - 15 - 1   Background Information on ISO STANDARD 16670 for Cyclic Testing of Connections - E Karacabeyli, M Yasumura, G C Foliente, A Ceccotti

Presented by E Karacabeyli

A Ceccotti stated that the EN12512 was written by a very small group. One can use ISO results to transfer to CEN standard which is used to support Eurocode 8 (yielding and ductility factors). M Yasumura stated that in Japan this is also used for shear walls. Japan has her own protocol which is similar but different. The question is how to adapt international standard to national standards. E Karacabeyli suggested testing according to both protocols.

A Leijten asked about equivalent damping ratio in the CEN standard is for the linear range only. No information on equivalent damping ratio for the non linear range. Is there any info in the ISO standard that can consider this. Chun Ni commented that connections and shear walls are tested using this standard and no nail fatigue breaking was observed. F. Lam asked whether it is true that nail fatigue was not observed. E Karacabeyli responded

that some nail fatigue failures are seen. This is also seen in walls subjected to multiple shake table tests.

A Leijten commented on the basis of loading cycle determination of the nail slip. In ASTM the determination of yielding slip is different. ISO does not define yield displacement. You can use EN standards to get yield displacement later. A Ceccotti stated that ductility definition is important. One must take into account calculation design code which is a national issue. The choice of not defining yield displacement is a good one.

P Quenneville stated provisions to test asymmetric loading is needed. E Karacabeyli stated that this is provided in the standard.

38 - 15 - 2   Testing & Product Standards – a Comparison of EN to ASTM, AS/NZ and ISO Standards – A Ranta-Maunus, V Enjily

Presented by A Ranta-Maunus

B Leicester commented that in the ISO and AS/NZ standard there is an attempt to draft equivalence and harmonisation for different standards. In general the idea is to try to test against the load capacity of the material in service. Shear testing is an example. Similar issue is for tension. In AS/NZ in service length was developed. Studies indicate that although the N. American standard requires the position of worst defect within the test span, it is possible to obtain lower results with the AS/NZ standard because it is difficult to accurately identify the "worst defect". A Ranta-Maunus said that the Europeans should be more involved in ISO process.

H Larsen stated the paper partly on testing and partly on code values for timber. These values may not be linked. Bending test is important and may be an issue. He is not too happy with the choices European had to set up their test standard as there was pressure fitting to a large existing data base of BRE. Difference in test method is a big problem for example for compression perpendicular to grain tests. Big problem when tested according to testing standard and values in the code is much too high which led to changes in the values in the code. Pre-stress bridge deck and concentrated load from column to sill are two examples of different applications for this issue.

F Lam stated the harmonisation work in ISO addresses MOR, MOE and tension. This paper points out more work need to be done in the area of harmonisation in area of shear and other properties. E Karacabeyli brought up the issue of poles and simply supported structures. S Thelandersson sees this as the same problem with concrete when one wants to characterize certain properties. In timber this is bending. One must consider how to use these values such as shear and perpendicular to grain properties. May be factors are needed. For example compression perpendicular o grain strength can be based on density. H Larsen restated that there is a need to have the same test method. Values in the code may not be 100% based on testing. BJ Yeh stated European tension test have shorter gauge length than the N. American, why are the strength lower in Europe compared to N. America. A Ranta-Maunus said that this is H Larsen's point.

J Ehlbeck said that if the standards are not used why not get rid of them. We need to do something. P Kuklic stated designers have trouble with some of the values. H Blass concluded that competitive aspect is one of the key issues of the paper.

38 - 15 - 3   Framework for Lateral Load Design Provisions for Engineered Wood Structures in Canada - M Popovski, E Karacabeyli

Presented by M Popovski

A Ceccotti stated that the structural behaviour depends on joint behaviour and Eurocode 8

has three statements about this. A Buchanan stated that there is useful information in this paper from loading to response. A concern that specification of how to design a timber building is not well set. If all the information is to be considered, the chapter in the Canadian code will be huge. May be better to have principles rather than details in the code and give designers the freedom to provide the ductility etc. M Popovski said connection work will go into another chapter. Guidelines can be provided.

F Lam stated that the next code cycle in Canada just started. To make it into the code will probably require information in 3.5 years. He asked how much manpower and resources are needed to complete the work. M Popovski agrees the timing is tight and will start be looking at existing information. He will look for input from within Canada and other outside Canada.

B Dujic questioned about R factors and which joint will fail to dissipate energy. M Popovski stated that the factors come from committee input some have data some based on educated guesses. R factors depend on system.

R Steiger commented that forces of acceleration increase from 475 to 2500 years return. One should have concerns with existing building and may be reliability method is needed to help justify. E Karacabeyli stated that other part of the equation was also changed so that the final demand is not changed too much.

S Thelandersson stated from a non seismic country point of view capacity design concept is interesting to design robust building to promote ductility. The question becomes how to guarantee that the dowels are not too strong.

E Karacabeyli stated that in Canada small building in Part 9 and engineered building in Part 4 of the code where all material are to be treated at the same level. A Ceccotti stated that Eurocode 8 considered all these issues.

38 - 15 - 4 Design of Shear Walls without Hold-Downs - **Chun Ni, E Karacabeyli**

Presented by Chun Ni

B Dujic commented that the vertical acceleration from earthquake may counteract the downward force that you are counting on. C Ni responded that this was considered in another paper as wind uplift load. B Griffith agrees with the findings in general and questioned that the testing deals with long panels without openings and how to treat such cases in design. C Ni answered that the sections with opening are ignored. B Griffith questioned how the 0.6 to 2.4 m length to determine vertical load is applied to the shorter panels. C Ni responded that the effective length is set no longer than wall height.

38 - 15 - 5 Plastic design of partially anchored wood-framed wall diaphragms with and
without openings - **B Källsner, U A Girhammar**

Presented by B Källsner

J Leskelä asked how to control deflection with the use of plastic method. B Källsner said that deflection calculation methods are needed. B Dujic received clarification about the source of the contact force being that of the panels. F Lam received confirmation that drift limits are not in Eurocode and confirmed that this is desirable. F Lam stated that deflection method is then needed.

A Buchanan stated that the last two papers deal with two similar topics but with different approach. The Canadian method deals with commonly built structures and looks into understanding the details about the forces. Europe seems to go the other way with a complicated design method. NZ uses the capacity design principle by identifying and

designing the fuses accordingly.

B Griffith commented that in practice timber designers need something simple, safe and workable. Maximize analysis tool to allow competitiveness of timber frame. A Buchanan stated that the difference may be between large displacement of earthquake load and serviceability concerns. E Karacabeyli stated that in Ni's study the openings in wall issues were verified against test data.

38 - 15 - 6 Racking of Wooden Walls Exposed to Different Boundary Conditions - B Dujič, S Aicher, R Žarnić

Presented by B Dujic

B Griffith received confirmation that the boundary condition as vertical load was applied to the frame. E Karacabeyli asked whether buckling was observed when heavy vertical load was applied. B Dujic responded that buckling was not observed.

H Blass asked whether much of the capacity of the nail was used up to carry the heavy vertical load. B Dujic responded that special hardware was provided to ensure the vertical load went directly to the studs. C Ni questioned whether the stiff upper boundary is reality for the case where the wall only has floor not another wall on top. B Dujic said that stiff floor is very common in Europe.

BJ Yeh commented in their work a 5% to 10% difference can be observed when a stiff loading beam was used in 2x4 wall tests. M Yasumura stated that in Japan hold downs at 4 corners are used to get the shear capacity. Other tests are used to develop information for the joints to develop calculation information for design.

E Karacabeyli stated that in terms of loading bar more effects were noted when walls have openings. V Rajcic commented in European system very stiff floor can result from concrete floors.

38 - 15 -7 A Portal Frame Design for Raised Wood Floor Applications - T G Williamson, Z A Martin, B Yeh

Presented by B Yeh

F Lam received clarification that the load deflection curves are obtained from sequential loading test. F Lam commented that although cost saving is an issue, the application of through bolts to connect inter storey and the use of the existing anchor bolts for hold down should not be too costly. BJ Yeh responded that the builders may build thousands of homes per year and they want the lowest cost option. Anchor bolts can be hidden which may be an issue for inspection.

E Karacabeyli commented that this help address the soft storey issues. He asked whether reference tests with full hold-down or through rods were performed. BJ Yeh responded that this was not directly done but the high end restraint information on reference wall has the hold downs installed.

38 - 15 - 8 Linear Elastic Design Method for Timber Framed Ceiling, Floor and Wall Diaphragms - J Leskelä

Presented by J Leskelä

M Yasumura asked whether deflection or capacity is of interest and how to define capacity. J Leskelä responded that they are both considered. The capacity is based on the code equations based on exceeding the strength of the fasteners. H Larsen liked the conclusion

that more research is needed and commented that since the work is based on design method, verification of such methods is needed. H Larsen further pointed out that design methods always have safety factors and asked if the level of deformation is known? J Leskelä responded that the level of deformation is not done in this exercise and commented that there is a need to do more tests. B Källsner stated that he has test results from the 80's and the method seems to be quite good. Nailing along the edge of sheathing with small spacing may lead to problems. H Larsen further questioned why one cannot use the plastic model if the elastic model can be used.

38 - 15 - 9   A Unified Design Method for the Racking Resistance of Timber Framed Walls for Inclusion in EUROCODE 5 - **R Griffiths, B Källsner, H J Blass, V Enjily**

Presented by R Griffiths

BJ Yeh stated in US the concept of relying on vertical load for uplift restraint is questioned as the load may not be there with wind uplift as an example. R Griffiths responded that in the case of 1 to 2 story building this is not an important issue. For 4 to 5 storey buildings the dead load is significant and should be considered.

E Karacabeyli asked whether ductility is considered in terms of comparisons. R Griffiths responded that for the large scale building test in the UK. Very high stiffness ~ 7 to 10 times design level was observed. In testing work he found this if brittle failure can be avoided then the timber frame is ductile. F Lam commented that stiffness and ductility should not be mixed as ductility is the ability of the system to carry load under large deformation. R Griffiths agreed.

9   **FIRE**

38 - 16 - 1   Fire Behaviour of Multiple Shear Steel-to-Timber Connections with Dowels - **C Erchinger, A Frangi, A Mischler**

Presented by C Erchinger

J König commented that he is happy about the work as the data is very good input to Eurocode 5; however, the idea of doubling is for end distance and not for member thickness and this would explain the findings. Also the one parameter exponential function is intended to yield conservative results. A two parameter function may be tried and may be more realistic. He asked whether additional models will be considered. C Erchinger responded that only 2 parameter model will be considered for now.

H Blass commented that 2 parameter model should not be fitted through one data point. J König said additional points are available and agreed that these points should not be too closely grouped.

A Buchanan received confirmation that longer BSB (plain) dowels were used in the extra thick specimens and commented that shorter dowel can also be considered so that there is no heat flux through the dowel. He further asked whether Johansen yield model were tried for both cold and hot dowel and whether bending of dowel in the fire case was observed. C Erchinger confirmed that some dowels were bent. A Frangi stated the yield theory was tried but did not give good match. The key is the change to wood failure mode in high temperature.

V Rajcic asked whether different configurations will be tried. C Erchinger confirmed that tests are finished and want to work on FEM. J König added that each configuration gives a different K and a lot of work is needed. A Buchanan stated data using LVL is available

and will offer results.

38 - 16 - 2 Fire Tests on Light Timber Frame Wall Assemblies - **V Schleifer, A Frangi**

Presented by V Schleifer

A Buchanan suggested a large volume of shear wall fire test data is available from NRC in Canada. He received confirmation that the tests were horizontally arranged and commented that the plaster boards may fall off and give non-realistic results for wall applications. He recommended using non-standard fire because the work can either have an objective to demonstrate product meet code or develop understanding of wall behaviour in fire to get how much time people have to leave a burning building. In the second case the use of standard fire has been shown to be not realistic because the temperature is too low.

BJ Yeh received confirmation that the wall was not loaded and commented that ISO standard may require loading. V Schleifer commented that large scale tests will be needed in such case. BJ Yeh received confirmation that failure was defined when the plaster board fell off.

10   STATISTIC AND DATA ANALYSIS

38 - 17 - 1 Analysis of Censored Data - Examples in Timber Engineering Research -
    R Steiger, J Köhler

Presented by R Steiger

S Thelandersson commented that one must be careful with consideration of the correlation factor especially in cases when within member correlation of properties may influence and bias the estimation of correlation factor. R Steiger agreed however finding the real correlation factor is difficult.

F Lam commented in the example of proof loading if point estimate is used to estimate a percentile property this technique will not help. If parametric approach is used than this technique is very useful. Work in the US with shear strength data is an example of the use of this technique. R Steiger agreed and stated the excel spreadsheet can be distributed for others to try. BJ Yeh confirmed his work on shear used this technique and the work is reported in previous CIB proceedings. H Larsen also suggested that Denzler's work can be re-analyzed with this technique for improvement.

11   GLUED JOINTS

38 - 18 - 1 Adhesive Performance at Elevated Temperatures for Engineered Wood
    Products - **B Yeh, B Herzog, T G Williamson**

Presented by B Yeh

A Buchanan stated that in NZ the fire-fighters will not go up onto the roof of a burning building. Shear failures or other failure modes beside glue failure can occur.

J König made a presentation of his views of this subject. The requirement may be too conservative as the temperature is too high. He presented data of Mischler and Frangi (2001), Fornather et al. (2004). Preheated specimens and short term tests as well as fire test information were presented. Real fire test is lower than preheat specimens and short term test. The reason is that the moisture content below the char level is increased as the

moisture front is created during the fire. Influence of the loading rate is also an issue.

The results agree with EN 1995-1-2. The N.A. Curve will punish a lot of adhesive manufacturers. Temperature gradient exists and may be a cause for decrease in strength of the member. Three recommendations were provided by J König: 1) do not ban adhesive that only passed moderate temperature test (200C); 2) specimens with low strength at high temperature should derive an alternative $k_{mod,f}$; 3) conduct comparative fire tests. BJ Yeh pointed out that some adhesives do have concerns.

A Frangi further explained that the US approach lacks consideration of the critical temperature for the glue. Wood failure between wood and glue is the real reason for failure. Additional failure of the glue from other tests can be considered and combined with EN 1995-1-2. A Frangi results published in Wood Science and Technology is available and will be sent.

BJ Yeh reiterated that the standard does not want to put adhesive manufacturers out of business. They can meet the standard with changes in their formulations. S Thelandersson stated that red curve and the test data may not be entirely comparable. A Frangi stated that some adhesive should not be used. Epoxy for example. All producers have some information.

12 LOADING CODES

38 - 102 - 1A New Generation of Timber Design Practices and Code Provisions Linking System and Connection Design - **A Asiz, I Smith**

Presented by A Asiz

S. Thelandersson pointed out the term "real" reliability level is meaning less and misleading as it is impossible to get and just a notion.

38 - 102-2 Uncertainties Involved in Structural Timber Design by Different Code Formats - **L Ozola, T Keskküla**

Presented by L Ozola

P Kuklic stated it is not proper to compare the Eurocode to the Latvian (Russian) National code as test method is different, safety factors are different, and test methods are different. It is not possible to compare.

Ozola responded that characteristics strengths are different. The work is based on testing of real structural elements not from small clear tests. In terms of connection Ozola agrees that the Eurocode accounts for plastic hinges. Her question is which one is predicted for service life.

J Ehlbeck asked whether the Eurocode is used in Latvia. Ozola said that the code is used by some designers and she taught her students about it. J Ehlbeck stated that one has to wait for national application document.

38 - 102-3 Comparison of the Eurocode 5 and Actual Croatian Codes for Wood Classification and Design With the Proposal for More Objective Way of Classification - **V Rajcic A Bjelanovic**

Presented by V Rajcic

JW van de Kuilen received confirmation that the specimens were small clear specimens. H

Blass commented that the characteristic strength should be based on full size tests. Rajcic responded that data was not available as the tests follow the previous DIN. JW van de Kuilen received confirmation that medium term was used for snow load. A Ceccotti stated that in Italian national annex snow load is always taken as short term except when C2 is nonzero then medium term is used.

13   ANY OTHER BUSINESS

None.

14   VENUE AND PROGRAMME FOR NEXT MEETING

The next meeting will be held in Firenze Italy August 28 to 31 2006 hosted by A Ceccotti. Details will be posted on CIB-W 18 Web site later.

The 2007 meeting will be held in Ljubljana, Slovenia invited by B Dujic and R Žarnic

The 2008 meeting will be held in New Brunswick, Canada invited by I Smith

A tentative invitation from Switzerland has been received for 2009

Master copy of the paper with any corrections should be sent to R Görlacher end of September 2005. A list of participants for 38th CIB-W18 and their contact information will be available from the password protected area of the CIB-W18 website.

B Dujic thanked the chair for the chance to host the 40th CIB-W18 meeting.

15   CLOSE

The chair thanked the speakers for their presentations and the delegates for their participation. Also thanks are extended to R Görlacher and P Eisentraud for their efforts to organise the meeting.

16. List of CIB-W18 Papers,
Karlsruhe, Germany 2005

List of CIB-W18 Papers, Karlsruhe, Germany 2005

2

17. Current List of CIB-W18(A) Papers

CURRENT LIST OF CIB-W18(A) PAPERS

Technical papers presented to CIB-W18(A) are identified by a code CIB-W18(A)/a-b-c, where:

a denotes the meeting at which the paper was presented. Meetings are classified in chronological order:

1 Princes Risborough, England; March 1973

2 Copenhagen, Denmark; October 1973

3 Delft, Netherlands; June 1974

4 Paris, France; February 1975

5 Karlsruhe, Federal Republic of Germany; October 1975

6 Aalborg, Denmark; June 1976

7 Stockholm, Sweden; February/March 1977

8 Brussels, Belgium; October 1977

9 Perth, Scotland; June 1978

10 Vancouver, Canada; August 1978

11 Vienna, Austria; March 1979

12 Bordeaux, France; October 1979

13 Otaniemi, Finland; June 1980

14 Warsaw, Poland; May 1981

15 Karlsruhe, Federal Republic of Germany; June 1982

16 Lillehammer, Norway; May/June 1983

17 Rapperswil, Switzerland; May 1984

18 Beit Oren, Israel; June 1985

19 Florence, Italy; September 1986

20 Dublin, Ireland; September 1987

21 Parksville, Canada; September 1988

22 Berlin, German Democratic Republic; September 1989

23 Lisbon, Portugal; September 1990

24 Oxford, United Kingdom; September 1991

25 Åhus, Sweden; August 1992

26 Athens, USA; August 1993

27 Sydney, Australia; July 1994

28 Copenhagen, Denmark; April 1995

29 Bordeaux, France; August 1996

30 Vancouver, Canada; August 1997

31 Savonlinna, Finland; August 1998

32 Graz, Austria, August 1999

33 Delft, The Netherlands; August 2000

34 Venice, Italy; August 2001

35 Kyoto, Japan; September 2002

36 Colorado, USA; August 2003

37 Edinburgh, Scotland, August 2004

38 Karlsruhe, Germany, August 2005

b   denotes the subject:

1   Limit State Design
2   Timber Columns
3   Symbols
4   Plywood
5   Stress Grading
6   Stresses for Solid Timber
7   Timber Joints and Fasteners
8   Load Sharing
9   Duration of Load
10   Timber Beams
11   Environmental Conditions
12   Laminated Members
13   Particle and Fibre Building Boards
14   Trussed Rafters
15   Structural Stability
16   Fire
17   Statistics and Data Analysis
18   Glued Joints
19   Fracture Mechanics
20   Serviceability
21   Test Methods
100 CIB Timber Code
101 Loading Codes
102 Structural Design Codes
103 International Standards Organisation
104 Joint Committee on Structural Safety
105 CIB Programme, Policy and Meetings
106 International Union of Forestry Research Organisations

c   is simply a number given to the papers in the order in which they appear:

Example: CIB-W18/4-102-5 refers to paper 5 on subject 102 presented at the fourth meeting of W18.

Listed below, by subjects, are all papers that have to date been presented to W18. When appropriate some papers are listed under more than one subject heading.

2

LIMIT STATE DESIGN

TIMBER COLUMNS

21-4-1	Modelling for Prediction of Strength of Veneer Having Knots - Y Hirashima
22-4-1	Scientific Research into Plywood and Plywood Building Constructions the Results and Findings of which are Incorporated into Construction Standard Specifications of the USSR - I M Guskov
22-4-2	Evaluation of Characteristic values for Wood-Based Sheet Materials - E G Elias
24-4-1	APA Structural-Use Design Values: An Update to Panel Design Capacities - A L Kuchar, E G Elias, B Yeh and M R O'Halloran

STRESS GRADING

1-5-1	Quality Specifications for Sawn Timber and Precision Timber - Norwegian Standard NS 3080
1-5-2	Specification for Timber Grades for Structural Use - British Standard BS 4978
4-5-1	Draft Proposal for an International Standard for Stress Grading Coniferous Sawn Softwood - ECE Timber Committee
16-5-1	Grading Errors in Practice - B Thunell
16-5-2	On the Effect of Measurement Errors when Grading Structural Timber - L Nordberg and B Thunell
19-5-1	Stress-Grading by ECE Standards of Italian-Grown Douglas-Fir Dimension Lumber from Young Thinnings - L Uzielli
19-5-2	Structural Softwood from Afforestation Regions in Western Norway - R Lackner
21-5-1	Non-Destructive Test by Frequency of Full Size Timber for Grading - T Nakai
22-5-1	Fundamental Vibration Frequency as a Parameter for Grading Sawn Timber - T Nakai, T Tanaka and H Nagao
24-5-1	Influence of Stress Grading System on Length Effect Factors for Lumber Loaded in Compression - A Campos and I Smith
26-5-1	Structural Properties of French Grown Timber According to Various Grading Methods - F Rouger, C De Lafond and A El Quadrani
28-5-1	Grading Methods for Structural Timber - Principles for Approval - S Ohlsson
28-5-2	Relationship of Moduli of Elasticity in Tension and in Bending of Solid Timber - N Burger and P Glos
29-5-1	The Effect of Edge Knots on the Strength of SPF MSR Lumber - T Courchene, F Lam and J D Barrett
29-5-2	Determination of Moment Configuration Factors using Grading Machine Readings - T D G Canisius and T Isaksson
31-5-1	Influence of Varying Growth Characteristics on Stiffness Grading of Structural Timber - S Ormarsson, H Petersson, O Dahlblom and K Persson
31-5-2	A Comparison of In-Grade Test Procedures - R H Leicester, H Breitinger and H Fordham
32-5-1	Actual Possibilities of the Machine Grading of Timber - K Frühwald and A Bernasconi
32-5-2	Detection of Severe Timber Defects by Machine Grading - A Bernasconi, L Boström and B Schacht
34-5-1	Influence of Proof Loading on the Reliability of Members – F Lam, S Abayakoon, S Svensson, C Gyamfi
36-5-1	Settings for Strength Grading Machines – Evaluation of the Procedure according to prEN 14081, part 2 - C Bengtsson, M Fonselius
36-5-2	A Probabilistic Approach to Cost Optimal Timber Grading - J Köhler, M H Faber

STRESSES FOR SOLID TIMBER

TIMBER JOINTS AND FASTENERS

LOAD SHARING

DURATION OF LOAD

TIMBER BEAMS

ENVIRONMENTAL CONDITIONS

LAMINATED MEMBERS

34-12-6	Determination of Shear Strength Values for GLT Using Visual and Machine Graded Spruce Laminations – G Schickhofer
34-12-7	Mechanically Jointed Beams: Possibilities of Analysis and some special Problems – H Kreuzinger
35-12-1	Glulam Beams with Round Holes – a Comparison of Different Design Approaches vs. Test Data - S Aicher L Höfflin
36-12-1	Problems with Shear and Bearing Strength of LVL in Highly Loaded Structures - H Bier
36-12-2	Weibull Based Design of Round Holes in Glulam - L Höfflin, S Aicher
37-12-1	Development of Structural LVL from Tropical Wood and Evaluation of Their Performance for the Structural Components of Wooden Houses. Part-1. Application of Tropical LVL to a Roof Truss - K Komatsu, Y Idris, S Yuwasdiki, B Subiyakto, A Firmanti
37-12-2	Reinforcement of LVL Beams With Bonded-in Plates and Rods - Effect of Placement of Steel and FRP Reinforcements on Beam Strength and Stiffness - P Alam, M P Ansell, D Smedley

PARTICLE AND FIBRE BUILDING BOARDS

7-13-1	Fibre Building Boards for CIB Timber Code (First Draft)- O Brynildsen
9-13-1	Determination of the Bearing Strength and the Load-Deformation Characteristics of Particleboard - K Möhler, T Budianto and J Ehlbeck
9-13-2	The Structural Use of Tempered Hardboard - W W L Chan
11-13-1	Tests on Laminated Beams from Hardboard under Short- and Longterm Load - W Nozynski
11-13-2	Determination of Deformation of Special Densified Hardboard under Long-term Load and Varying Temperature and Humidity Conditions - W Halfar
11-13-3	Determination of Deformation of Hardboard under Long-term Load in Changing Climate - W Halfar
14-4-1	An Introduction to Performance Standards for Wood-Base Panel Products - D H Brown
14-4-2	Proposal for Presenting Data on the Properties of Structural Panels - T Schmidt
16-13-1	Effect of Test Piece Size on Panel Bending Properties - P W Post
20-4-1	Considerations of Reliability - Based Design for Structural Composite Products - M R O'Halloran, J A Johnson, E G Elias and T P Cunningham
20-13-1	Classification Systems for Structural Wood-Based Sheet Materials - V C Kearley and A R Abbott
21-13-1	Design Values for Nailed Chipboard - Timber Joints - A R Abbott
25-13-1	Bending Strength and Stiffness of Izopanel Plates - Z Mielczarek
28-13-1	Background Information for "Design Rated Oriented Strand Board (OSB)" in CSA Standards - Summary of Short-term Test Results - E Karacabeyli, P Lau, C R Henderson, F V Meakes and W Deacon
28-13-2	Torsional Stiffness of Wood-Hardboard Composed I-Beam - P Olejniczak

TRUSSED RAFTERS

4-9-1	Long-term Loading of Trussed Rafters with Different Connection Systems - T Feldborg and M Johansen
6-9-3	Deflection of Trussed Rafters under Alternating Loading During a Year - T Feldborg and M Johansen

STRUCTURAL STABILITY

35-15-7	Design of timber structures in seismic zones according to EC8- 2002 version - A Ceccotti, T Toratti, B Dujič
35-15-8	Design Methods to Prevent Premature Failure of Joints at Shear Wall Corners - N Kawai, H Okiura
36-15-1	Monitoring Light-Frame Timber Buildings: Environmental Loads and Load Paths – I Smith et al.
36-15-2	Applicability of Design Methods to Prevent Premature Failure of Joints at Shear Wall Corners in Case of Post and Beam Construction - N Kawai, H Isoda
36-15-3	Effects of Screw Spacing and Edge Boards on the Cyclic Performance of Timber Frame and Structural Insulated Panel Roof Systems - D M Carradine, J D Dolan, F E Woeste
36-15-4	Pseudo-Dynamic Tests on Conventional Timber Structures with Shear Walls - M Yasumura
36-15-5	Experimental Investigation of Laminated Timber Frames with Fiber-reinforced Connections under Earthquake Loads - B Kasal, P Haller, S Pospisil, I Jirovsky, A Heiduschke, M Drdacky
36-15-6	Effect of Test Configurations and Protocols on the Performance of Shear Walls - F Lam, D Jossen, J Gu, N Yamaguchi, H G L Prion
36-15-7	Comparison of Monotonic and Cyclic Performance of Light-Frame Shear Walls - J D Dolan, A J Toothman
37-15-1	Estimating 3D Behavior of Conventional Timber Structures with Shear Walls by Pseudodynamic Tests - M Yasumura, M Uesugi, L Davenne
37-15-2	Testing of Racking Behavior of Massive Wooden Wall Panels - B Dujič, J Pucelj, R Žarnić
37-15-3	Influence of Framing Joints on Plastic Capacity of Partially Anchored Wood-Framed Shear Walls - B Källsner, U A Girhammar
37-15-4	Bracing of Timber Members in Compression - J Munch-Andersen
37-15-5	Acceptance Criteria for the Use of Structural Insulated Panels in High Risk Seismic Areas - B Yeh, T D Skaggs, T G Williamson Z A Martin
37-15-6	Predicting Load Paths in Shearwalls - Hongyong Mi, Ying-Hei Chui, I Smith, M Mohammad
38-15-1	Background Information on ISO STANDARD 16670 for Cyclic Testing of Connections - E Karacabeyli, M Yasumura, G C Foliente, A Ceccotti
38-15-2	Testing & Product Standards – a Comparison of EN to ASTM, AS/NZ and ISO Standards – A Ranta-Maunus, V Enjily
38-15-3	Framework for Lateral Load Design Provisions for Engineered Wood Structures in Canada - M Popovski, E Karacabeyli
38-15-4	Design of Shear Walls without Hold-Downs - Chun Ni, E Karacabeyli
38-15-5	Plastic design of partially anchored wood-framed wall diaphragms with and without openings - B Källsner, U A Girhammar
38-15-6	Racking of Wooden Walls Exposed to Different Boundary Conditions - B Dujič, S Aicher, R Žarnić
38-15-7	A Portal Frame Design for Raised Wood Floor Applications - T G Williamson, Z A Martin, B Yeh
38-15-8	Linear Elastic Design Method for Timber Framed Ceiling, Floor and Wall Diaphragms - Jarmo Leskelä
38-15-9	A Unified Design Method for the Racking Resistance of Timber Framed Walls for Inclusion in EUROCODE 5 - R Griffiths, B Källsner, H J Blass, V Enjily

FIRE

GLUED JOINTS

FRACTURE MECHANICS

SERVICEABILITY

TEST METHODS

CIB TIMBER CODE

2-100-1	A Framework for the Production of an International Code of Practice for the Structural Use of Timber - W T Curry
5-100-1	Design of Solid Timber Columns (First Draft) - H J Larsen
5-100-2	A Draft Outline of a Code for Timber Structures - L G Booth
6-100-1	Comments on Document 5-100-1; Design of Solid Timber Columns - H J Larsen and E Theilgaard
6-100-2	CIB Timber Code: CIB Timber Standards - H J Larsen and E Theilgaard
7-100-1	CIB Timber Code Chapter 5.3 Mechanical Fasteners; CIB Timber Standard 06 and 07 - H J Larsen
8-100-1	CIB Timber Code - List of Contents (Second Draft) - H J Larsen
9-100-1	The CIB Timber Code (Second Draft)
11-100-1	CIB Structural Timber Design Code (Third Draft)
11-100-2	Comments Received on the CIB Code U Saarelainen; Y M Ivanov, R H Leicester, W Nozynski, W R A Meyer, P Beckmann; R Marsh
11-100-3	CIB Structural Timber Design Code; Chapter 3 - H J Larsen
12-100-1	Comment on the CIB Code - Sous-Commission Glulam
12-100-2	Comment on the CIB Code - R H Leicester
12-100-3	CIB Structural Timber Design Code (Fourth Draft)
13-100-1	Agreed Changes to CIB Structural Timber Design Code
13-100-2	CIB Structural Timber Design Code. Chapter 9: Performance in Fire
13-100-3a	Comments on CIB Structural Timber Design Code
13-100-3b	Comments on CIB Structural Timber Design Code - W R A Meyer
13-100-3c	Comments on CIB Structural Timber Design Code - British Standards Institution
13-100-4	CIB Structural Timber Design Code. Proposal for Section 6.1.5 Nail Plates - N I Bovim
14-103-2	Comments on the CIB Structural Timber Design Code - R H Leicester
15-103-1	Resolutions of TC 165-meeting in Athens 1981-10-12/13
21-100-1	CIB Structural Timber Design Code. Proposed Changes of Sections on Lateral Instability, Columns and Nails - H J Larsen
22-100-1	Proposal for Including an Updated Design Method for Bearing Stresses in CIB W18 - Structural Timber Design Code - B Madsen
22-100-2	Proposal for Including Size Effects in CIB W18A Timber Design Code - B Madsen
22-100-3	CIB Structural Timber Design Code - Proposed Changes of Section on Thin-Flanged Beams - J König
22-100-4	Modification Factor for "Aggressive Media" - a Proposal for a Supplement to the CIB Model Code - K Erler and W Rug
22-100-5	Timber Design Code in Czechoslovakia and Comparison with CIB Model Code - P Dutko and B Kozelouh

LOADING CODES

4-101-1	Loading Regulations - Nordic Committee for Building Regulations
4-101-2	Comments on the Loading Regulations - Nordic Committee for Building Regulations

37-101-1	Action Combination Processing for the Eurocodes Basis of Software to Assist the Engineer - Y Robert, A V Page, R Thépaut, C J Mettem

STRUCTURAL DESIGN CODES

1-102-1	Survey of Status of Building Codes, Specifications etc., in USA - E G Stern
1-102-2	Australian Codes for Use of Timber in Structures - R H Leicester
1-102-3	Contemporary Concepts for Structural Timber Codes - R H Leicester
1-102-4	Revision of CP 112 - First Draft, July 1972 - British Standards Institution
4-102-1	Comparsion of Codes and Safety Requirements for Timber Structures in EEC Countries - Timber Research and Development Association
4-102-2	Nordic Proposals for Safety Code for Structures and Loading Code for Design of Structures - O A Brynildsen
4-102-3	Proposal for Safety Codes for Load-Carrying Structures - Nordic Committee for Building Regulations
4-102-4	Comments to Proposal for Safety Codes for Load-Carrying Structures - Nordic Committee for Building Regulations
4-102-5	Extract from Norwegian Standard NS 3470 "Timber Structures"
4-102-6	Draft for Revision of CP 112 "The Structural Use of Timber" - W T Curry
8-102-1	Polish Standard PN-73/B-03150: Timber Structures; Statistical Calculations and Designing
8-102-2	The Russian Timber Code: Summary of Contents
9-102-1	Svensk Byggnorm 1975 (2nd Edition); Chapter 27: Timber Construction
11-102-1	Eurocodes - H J Larsen
13-102-1	Program of Standardisation Work Involving Timber Structures and Wood-Based Products in Poland
17-102-1	Safety Principles - H J Larsen and H Riberholt
17-102-2	Partial Coefficients Limit States Design Codes for Structural Timberwork - I Smith
18-102-1	Antiseismic Rules for Timber Structures: an Italian Proposal - G Augusti and A Ceccotti
18-1-2	Eurocode 5, Timber Structures - H J Larsen
19-102-1	Eurocode 5 - Requirements to Timber - Drafting Panel Eurocode 5
19-102-2	Eurocode 5 and CIB Structural Timber Design Code - H J Larsen
19-102-3	Comments on the Format of Eurocode 5 - A R Fewell
19-102-4	New Developments of Limit States Design for the New GDR Timber Design Code - W Rug and M Badstube
19-7-3	Effectiveness of Multiple Fastener Joints According to National Codes and Eurocode 5 (Draft) - G Steck
19-7-6	The Derivation of Design Clauses for Nailed and Bolted Joints in Eurocode5 - L R J Whale and I Smith
19-14-1	Annex on Simplified Design of W-Trusses - H J Larsen
20-102-1	Development of a GDR Limit States Design Code for Timber Structures - W Rug and M Badstube
21-102-1	Research Activities Towards a New GDR Timber Design Code Based on Limit States Design - W Rug and M Badstube

INTERNATIONAL STANDARDS ORGANISATION

12-103-1	ISO/TC 165 Ottawa, September 1979
13-103-1	Report from ISO/TC 165 - A Sorensen
14-103-1	Comments on ISO/TC 165 N52 "Timber Structures; Solid Timber in Structural Sizes; Determination of Some Physical and Mechanical Properties"
14-103-2	Comments on the CIB Structural Timber Design Code - R H Leicester
21-103-1	Concept of a Complete Set of Standards - R H Leicester

JOINT COMMITTEE ON STRUCTURAL SAFETY

3-104-1	International System on Unified Standard Codes of Practice for Structures - Comité Européen du Béton (CEB)
7-104-1	Volume 1: Common Unified Rules for Different Types of Construction and Material – CEB
37-104-1	Proposal for a Probabilistic Model Code for Design of Timber Structures - J Köhler, H Faber

CIB PROGRAMME, POLICY AND MEETINGS

1-105-1	A Note on International Organisations Active in the Field of Utilisation of Timber - P Sonnemans
5-105-1	The Work and Objectives of CIB-W18-Timber Structures - J G Sunley
10-105-1	The Work of CIB-W18 Timber Structures - J G Sunley
15-105-1	Terms of Reference for Timber - Framed Housing Sub-Group of CIB-W18
19-105-1	Tropical and Hardwood Timbers Structures - R H Leicester
21-105-1	First Conference of CIB-W18B, Tropical and Hardwood Timber Structures Singapore, 26 - 28 October 1987 - R H Leicester

INTERNATIONAL UNION OF FORESTRY RESEARCH ORGANISATIONS

| 7-106-1 | Time and Moisture Effects - CIB W18/IUFRO 55.02-03 Working Party |

INTERNATIONAL COUNCIL FOR RESEARCH AND INNOVATION
IN BUILDING AND CONSTRUCTION

WORKING COMMISSION W18 - TIMBER STRUCTURES

LONG-TERM LOAD BEARING OF WOODEN COLUMNS
INFLUENCED BY CLIMATE –VIEW ON CODE–

R Hartnack

K Rautenstrauch

Bauhaus-University Weimar

GERMANY

Presented by R Hartnack

B Leicester commented that since the work was intended for code application, statistics such as mean and COV are important and asked whether data was available. Hartnack answered that this is a virtual exercise adapted to values in literature of small data set of full size specimens. H Larsen asked whether the method is aimed at design practice engineers and do they have any input to the method. The answer was yes. J Köhler asked how was model uncertainty handled? Hartnack answered there are more uncertainties in other part of the work compared with the uncertainties in the model. J Köhler asked how to correspond the safety level cited in the paper to beta values. Hartnack answered the safety level cited was defined per the code equations. R Steiger commented how come the work neglected snow load. Hartnack answered that a 4 month snow load duration was tested and the influence was found to be small because after one year no influence on creep was observed. Data from Germany and Swedish Data was used.

E Karacabeyli commented that R Foschi's work clearly indicated snow load has a strong impact on bending performance. Hartnack answered that there is an impact on strength but not creep. J König commented that Figure 4 shows a big gap in safety and asked if this is supported by real life experience. Hartnack answered that real life experience did not indicate a problem. J König commented that no action is needed in code. Hartnack disagreed and stated that there is additional safety in real life but the code should be changed.

Long-term load bearing of wooden columns influenced by climate –view on code–

R Hartnack, K Rautenstrauch

Bauhaus-University Weimar, Germany

1 Introduction

As already mentioned in our publications 35-2-1 [4] and 36-2-1 [6] of CIB, the reliability of timber columns depends on an large number of influences and their interaction. First of all the field of hygrothermal long-time effects and the principles of the simulation model was described in detail in [4]. Furthermore, in [6] the influence of the actions and the material parameters which spread on basis of stochastical principles, on the reliability of timber columns were explained.

The wide spread of the material parameters of the construction material wood especially leads to a broad spectrum of investigations. Both the expectable high costs, the great effort of time and great amount of specimens speak against a pure experimental procedure. Therefore virtual experiments were used. The objective of these investigations was to create a design criterion under different boundary conditions to enable an easy use. In the following the development and the use will be explained in principle. Details can be gathered from Hartnack [3].

2 Modelling

A detailed description of these models will not be given in this paper. I would like to draw attention, instead, to former publications ([4], [6]) and to [3]. Only for the facts that are relevant for the modelling an overview will be given. A special computer programme ISOBEAM (see [5], [3]) was developed to carry out virtual experiments.

2.1 Actions

Load, geometric imperfections and the changing moisture of wood resulting from the surrounding climate are actions on compressed members of wood. The load is defined in a deterministic way and is set on the wooden columns in different degrees of load. This means that the portion of permanent acting load of the total load is varied. A percentage of 43% of non-permanent acting load is considered as permanent acting (see [3]). The geometrical imperfections are based on real measured values which were approximated by a stochastic relation (see [3]). The unsteady moisture of wood is determined during the simulation based on the law of mass transport depending on the wooden moisture at the

edge of the cross-section which shows the equilibrium moisture content belonging to existing surrounding climate. The description of the surrounding climate was approximated to real measured climatic values and was modelled according to the service classes by DIN 1052 [1] and Eurocode 5 [2] (see [3]).

2.2 Resistances

The modulus of elasticity E and the strength f were modelled as resticances. These are derived from the stochastically described factors of influence, knot-density and bulk density. The correlations between the material parameters and the factors of influence can be taken from [3] or [6]. The relationship between strain and strength for compression is described elastic-plastically, while the material performance for tension was assumed as ideal elastical (see [3], [6]).

3 Investigations of variation

Before carrying out the investigations of variation, the model was verified. Using already published experiments with small and smallest specimen as well as with specimen with practical dimensions the verification was performed. Both experiments with short durations of execution and experiments with durations of more than seven years were considered. The comparison with virtual experiments produced reliable results (see [3]).

First of all, stochastical distributed material parameters and geometric imperfections were taken into account to generate 999 columns. Without considering the hygrothermal long-time effects the load-bearing capacity was calculated by virtual experiments in a first analysis. The simulated load-bearing capacities could be arranged in a ranking list. Taking hygrothermal long-time effects into consideration elements in the near of the 5-%-fractile were only used for further investigations.

These virtual experiments can initially be divided into three fields of investigation. First of all, the influence of cross-section dimension was investigated. Both the width and the height of the cross-section varied between 8 cm and 16 cm. It was assumed that the buckling of the compressed wooden member can only be possible in the direction of the cross-section height. The influence of the service classes by DIN 1052 [1] was examined in a further investigation. As already mentioned, the surrounding climate according to the service classes was adjusted to the measured data of climate (see [3], [4]). A further decisive influence derives from the quantity of the initial wooden moisture content which varies between 6 % and 30 % in these investigations.

The load degree (i. e. the portion of permanent acting load to total load) generally varied. Then the load degrees 0 %, 25 %, 50 %, 75 % and 100 % were investigated.

Because of the stochastic distributed material parameters and influences the results are also spreading. Owing to the already mentioned reduction resulting from the large scale the results already exist in the range of design (ultimate limit state).

2

4   Results

To analyse the results the simulated load-bearing capacities of the 5-%-fractile were understood to be resistances R_k and the maximum load-bearing capacities by Code were interpreted to be actions S_k. Using the semiprobabilistic safety concept of the new Code generation the following request can be given:

$$\frac{R_k}{S_k} \geq \frac{\gamma_F \cdot \gamma_M}{k_{mod}} \tag{1}$$

This procedure allows to compare the ratio between the simulated load-bearing capacity R_k and the maximum load-bearing capacity by Code S_k with the wanted safety level. If the equation (1) is true, the design by Code will be safe. If the equation (1) is not true, the design by Code will be unsafe. Next to the evaluation of existing design rules, this fact gives us the possibility to create alternative design proposals and verify them appropriately.

4.1   Load-bearing capacity after short term loading

First of all, the load-bearing capacities are analysed by equation (1) without taking the hygrothermal long-time effects into account. Figure (1) shows the analysis of equation (1) and confirms the Code values with the exception of compact columns between the slenderness ratios 0 and 60.
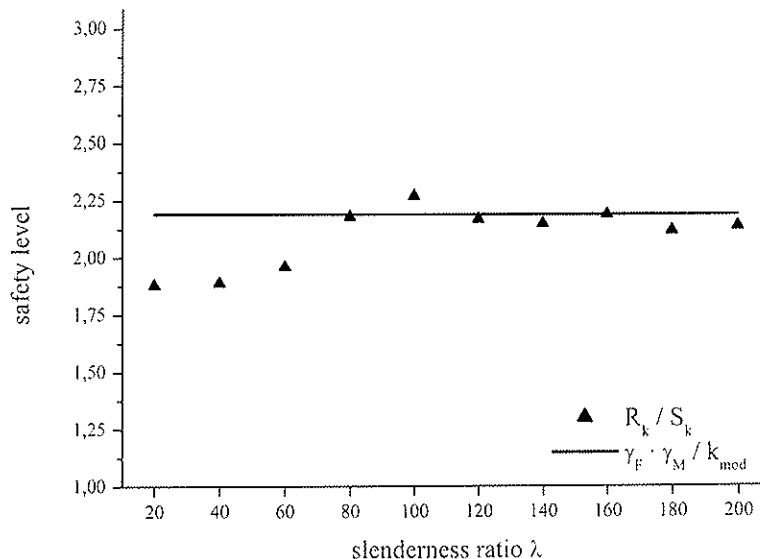
Fig. 1:   Comparison between the safety levels (equation (1)) from the results of virtual experiments with reference to DIN 1052 [1] –second order theory- with $k_{mod} = 0,8$ (load degree 1,0) (see [3])

The initial wooden moisture content also influences the so-called short-term load-bearing capacity. Figure (2) shows the relationship of the load-bearing capacity with defined initial wooden moisture content in reference to the initial wooden moisture content u = 12 %. As expected, the influence on compact columns is greater than the influence on slender columns. The result is that the influence of the wooden moisture on the compression strength (2,25 % per % in changing wooden moisture) was chosen bigger than the influence on the elastic modulus (1,5 % per % in changing wooden moisture). In Figure (2) you can also see that the sole failure criterion for compact columns (up to a slenderness

3

ratio of about 60) is the strength, while the sole failure criterion for slender columns (from a slenderness ratio of about 140) is their flexural stiffness. Between this two boarders both influences interact.
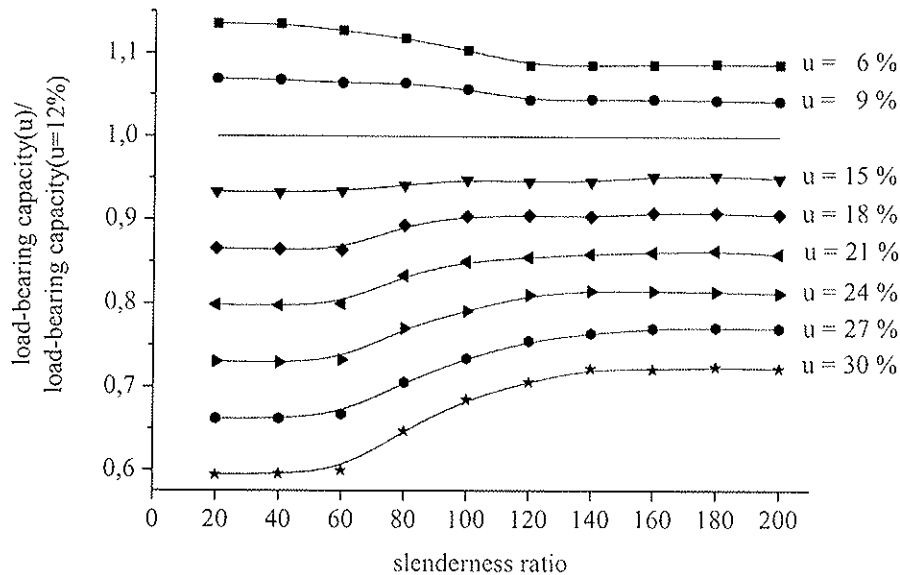
Fig. 2: The relation of the ratio of load-bearing capacity in its dependence of slenderness ratio with short-term loading for cross-section b/h = 16/16 cm at different initial moisture contents (5-%-fractiles) (see [3])

4.2 Load-bearing capacity after long term loading

Taking hygrothermal long-time effects into account, the influence of the service class and the influence of the initial wooden moisture content was examined. The influence of the cross-section will not explicitly be discussed in this work. For further details see [3].

As already mentioned, the service classes were modelled by an approximation to measured climate data. The climate data from the Deutscher Wetter Dienst (DWD) were identified as accompanying to service class 3. With respect to principles of building physics the data of service class 1 were derived and were applied on service class 2 by corresponding interpolation. The climate scenarios used for simulation can be taken from [3] or [4]. As a result for service class 3 it can be mentioned that the influence can only be seen at high load degrees (> 75 %). The losses of load-bearing capacity had a maximum of about 15 % and came across in the range of middle slenderness ratios. A decisive higher influence can be observed in service class 2, especially with the investigated load degrees 75 % and 100 %. Here the losses of load-bearing capacity are about 35 % (see also Figure (3) for the example of cross-section b/h = 8/8 cm). Generally it can be stated that the influences of the service class is a little smaller for the investigated cross-sections b/h = 12/12 cm and b/h = 16/16 cm. In service class 3 the influence is more significant than in the more convenient service classes. That means that the losses of load-bearing capacity are more decisive and the columns partly fail at the load degree 100 %. For cross-section b/h = 8/8 cm this affects columns with a slenderness ratio of 100 and more, for cross-section b/h = 12/12 cm this affects columns with a slenderness ratio of 120 and more and for cross-section b/h = 16/16 cm this affects columns with a slenderness ratio of 160 and more. Now the losses of load-bearing capacity are about 55 % in the range of middle slenderness ratios.

4
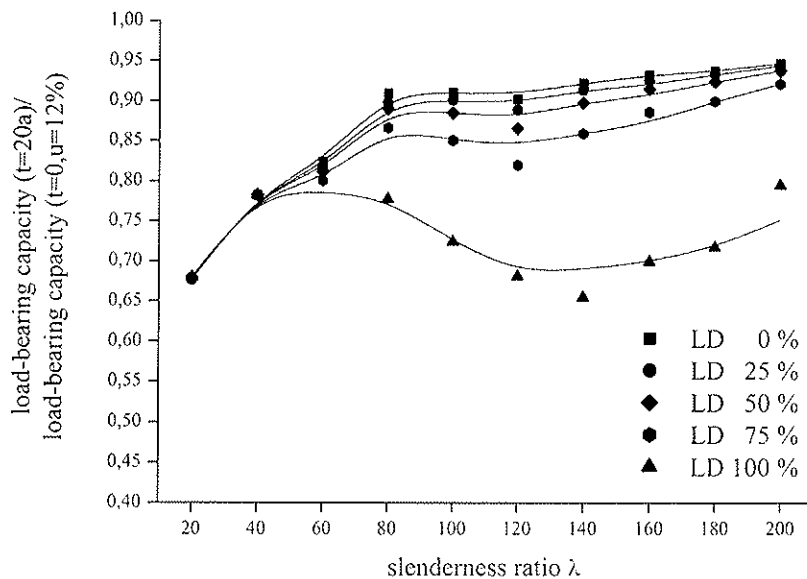
Fig. 3:   Ratio of load-bearing capacities in dependence of slenderness ratio and load
degree for cross-section b/h = 8/8 cm at service class 2 (5%-fractiles) (see [3])

Taking the hygrothermal long-time effects into account, the equation (1) can newly be
analysed using the calculated load-bearing capacities. The safety level (calculated from
simulation) can be compared to the safety level by Code. Figure (4) shows that the safety
level demanded by Code was decisively undercut in service class 1 and 2 (for example
cross-section b/h = 12/12 cm).
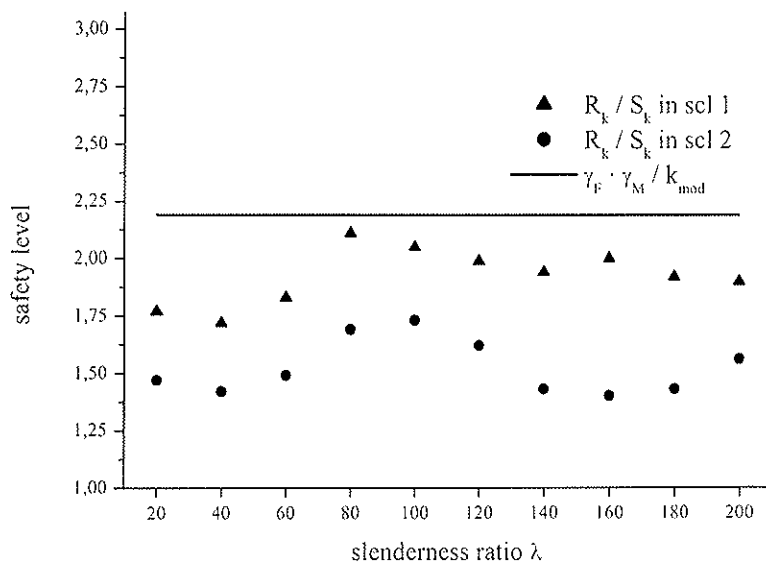
Fig. 4:   Comparison between the safety levels (equation (1)) from the results of virtual
experiments taking hygrothermal long-time effects into account with reference
to DIN 1052 [1] -second order theory- with $k_{mod} = 0,8$ (load degree 1,0) in
service classes 1 and 2 (see [3])

The results verify (and Figure (4) emphasizes this fact) that the ratio of simulated load-
bearing capacity under hygrothermal long-time effects and maximum load-bearing
capacity by Code undercuts the demanded safeties. This means that the mentioned effects
must be regarded for design and must influence the corresponding proofs of the Code.

5

5   Design by DIN 1052 at final state

Contrary to Eurocode 5 [2] the German Code DIN 1052 [1] (edition August 2004) regards and include the aforementioned hygrothermal long-time effects. The influence of creep should be taken into account for the design of compressed wooden members in service class 2 and 3. This is done by the reduction of stiffness with the factor $1/(1+k_{def})$. The modifying factor k_{def} is a deformation coefficient and can be understood as a creep factor. It depends on the service class and the structural material. The maximum load-bearing capacity is correspondingly reduced by reducing of stiffness. This leads to the fact that the distance to the simulated load-bearing capacity increases. Figure (5) proofs that the procedure of DIN 1052 [1] is safe for service class 2. It has to be mentioned here that the permanent load by DIN 1052 [1] was calculated without taking the aforementioned reduction of stiffness into account. This means that the permanent load used was overestimated. This fact leads to a further increase in safety. Furthermore, the Code uses design values of load to determine the load degree while in this work the load degree was calculated on the basis of the characteristic load. The small difference especially for high load degrees can be categorised as insignificant.
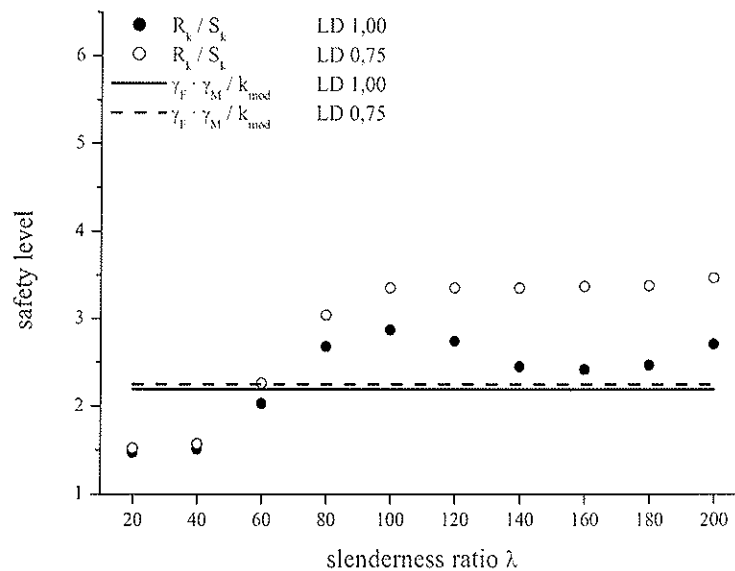
Fig. 5:   Comparison between the safety levels (equation (1)) from the results of virtual experiments taking hygrothermal long-time effects into account with reference to DIN 1052 [1] -second order theory (modified modulus of elasticity)- with b/h = 12/12 cm in service class 2 (see [3])

Now the existing safety level decisively lies above the demanded safety level. The matter is nearly the same in service class 3. But the existing safety level is about 5 or more for service class 3 and load degree 75 %. This led to the creation of alternative design proposals and to complete use of the results of virtual experiments.

6   Alternative design proposals

Besides the procedure of Code the consideration of hygrothermal long-time effects to design wooden columns can be done in different ways. First we must differentiate between the design procedures of DIN 1052 [1]. On the one hand it is possible to design wooden columns, using the so-called model column method, on the other hand the second order

theory can be used. Appropriately, it seemed to be practical to examine the alternative design proposals separately for both design procedures.

Using the second order theory, it is possible, first of all to complete additionally the prebend resulting from geometric imperfections with a prebend in order to take the hygrothermal long-time effects into account. A further possibility is to adapt the modifying factor k_{mod} to the results of virtual experiments. In the context of research this was done by the introduction of a further factor of k_{mod} which was defined as k_{creep}. A similar procedure is also possible for the model column method. Due to the different attempts by Code it is another value which was denominated k^*_{creep}. In principle it is also possible to adapt the coefficient β_c of the model column method in analogy to second order theory.

In the context of this paper we only deal with the additional prebend e_k for design with second order theory and the additional modifying factor k^*_{creep} for design with model column method. Further alternative design proposals can be taken from Hartnack [3].

6.1   Proposal with additional prebend e_k

The design with second order theory must first fulfil of all the proof of bending under normal force, whereas the bending moment comes into being as a result of the unwanted prebend by the effects of second order theory.

$$\left(\frac{\dfrac{\gamma_F \cdot N_k}{A}}{\dfrac{k_{mod} \cdot f_{c,0,k}}{\gamma_M}} \right)^2 + \frac{\dfrac{M^{II}}{W}}{\dfrac{k_{mod} \cdot f_{m,k}}{\gamma_M}} = 1 \tag{2}$$

with N_k characteristic load as normal force

$$M^{II} = (e + e_k) \cdot \gamma_F \cdot N_k \cdot \frac{N_{ki}}{N_{ki} - \gamma_F \cdot N_k} \tag{3}$$

The bending moment by second order theory is found out by taking the prebend into account, which results from an addition of the geometric imperfection and the additional prebend e_k. If you insert equation (3) into equation (2) and, furthermore, replace the characteristic load with the result of the virtual experiment and solve the equation to e_k, you will get the following destination equation (4):

$$e_k = \left\{ \left[1 - \frac{\left(R_{k,simulation} \right)^2}{\left(\dfrac{f_{c,0,k} \cdot A}{\gamma_{global}} \right)^2} \right] \cdot \frac{f_{m,k} \cdot W}{\gamma_{global}} \cdot \frac{N_{ki} - \gamma_F \cdot R_{k,simulation}}{N_{ki} \cdot R_{k,simulation}} \right\} - e \tag{4}$$

To simplify, another factor was additionally introduced:

$$\gamma_{global} = \frac{\gamma_F \cdot \gamma_M}{k_{mod}} \tag{5}$$

In dependence of service class, load degree and the height of the cross-section, the additional prebend can be derived from the destination equation (4). The results showed

7

that the prebend e_k can be described in proportion to the length of the column in good agreement:

$$e_k = \frac{L}{c} \tag{6}$$

The denominator c can be derived from the regression of the results of virtual experiments:

$$c = \left[\frac{g_k}{g_k + q_k} \cdot \left(c_1 \cdot \frac{g_k}{g_k + q_k} + 30 \right) \right] + c_0 \tag{7}$$

with c_1 factor to take service class into account

          service class 2: $c_1 = -325$

          service class 3: $c_1 = -100$

    c_0 factor to take service class and the height of cross-section into account (h is height of cross-section which is relevant for buckling)

          service class 2: $c_0 = \left[\dfrac{h}{32} \cdot (30 \cdot h - 400) \right] + 390$

          service class 3: $c_0 = \left[\dfrac{h}{32} \cdot (15 \cdot h - 220) \right] + 135$

With the aid of the equations (6) and (7) it is now possible to determine the additional prebend e_k and -as a result of this- to calculate the design bending moment, using second order theory. For practical use it is generally possible to provide the factor c as a table. Such a table can be taken from [3].
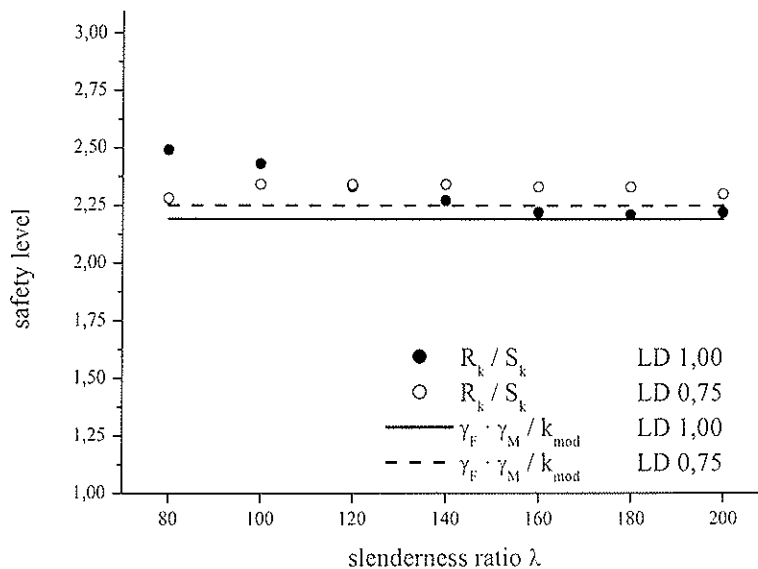
Fig. 6:   Comparison between the safety levels (equation (1)) from the results of virtual experiments taking hygrothermal long-time effects into account with reference to DIN 1052 [1] -second order theory (additional prebend e_k)- with b/h = 16/16 cm in service class 2 (see [3])

The verification of the design proposal can be done now in the same manner as it was already done with the procedure by DIN 1052 [1] by analysing the corresponding equation (1). In the context of this work it will be done for the example of cross-section b/h = 16/16 cm in service class 2. Figure (6) shows the good suitability of the procedure for the examined slenderness ratios of 80 and more. Now the calculated safety value lies

above the demanded safety values. But the differences between these values are not as great as those of the Code procedure.

6.2 Proposal with modifying factor k^*_{creep}

The second alternative design proposal refers to the model column method by DIN 1052 [1]. As already mentioned, the modifying factor k^*_{creep} should be an additional factor for k_{mod}. Using the model column method and taking the hygrothermal long-time effects into account, the proof for the border line case of 100 % capacity can be equated:

$$\frac{\dfrac{\gamma_F \cdot N_k}{A}}{k_c \cdot \dfrac{k^*_{creep} \cdot k_{mod} \cdot f_{c,0,k}}{\gamma_M}} = 1 \tag{8}$$

If you insert now in analogy to the equation (1)

$$\frac{k_{mod} \cdot R_{k,Simulation}}{\gamma_F \cdot \gamma_M} = N_k \tag{9}$$

in equation (8), you will get the following destination equation for k^*_{creep}:

$$k^*_{creep} = \frac{R_{k,Simulation}}{k_c \cdot f_{c,0,k} \cdot A} \tag{10}$$

Depending on the height of cross-section, the service class and the load degree the additional factor k^*_{creep} can be now calculated. In service class 2 cases like these must only be examined if the load degree is 75 % or more. Correspondingly, in service class 3 only load degrees of 50 % and more are relevant. Because k^*_{creep} is a reduction factor, a limitation to a maximum of 1.0 must be introduced.
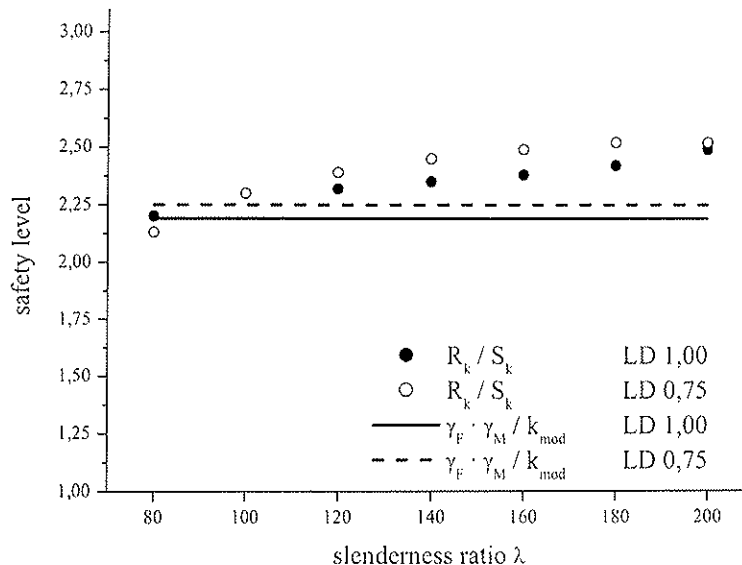
Fig. 7:   Comparison between the safety levels (equation (1)) from the results of virtual experiments taking hygrothermal long-time effects into account with reference to DIN 1052 [1] –model column method (modifying factor k^*_{creep})- with b/h = 16/16 cm in service class 2 (see [3])

In service class 2 the following relationship can be derived from the destination equation (10):

9

$$k^*_{creep} = \min\left\{\left[-0,48\cdot\left(\frac{g_k}{g_k+q_k}\right)^2 + \left(0,00219\cdot h^2 - 0,03625\cdot h + 0,32\right)\cdot\left(\frac{g_k}{g_k+q_k}\right) + 1,07\right]; 1,00\right\} \quad (11)$$

In service class 3 you get:

$$k^*_{creep} = \min\left\{\left[-0,96\cdot\left(\frac{g_k}{g_k+q_k}\right)^2 + \left(0,00156\cdot h^2 - 0,01875\cdot h + 0,50\right)\cdot\left(\frac{g_k}{g_k+q_k}\right) + 1,00\right]; 1,00\right\} \quad (12)$$

If you newly analyse the equation (1), the figure (7) will show that the required safety level is fulfilled for the slenderness ratios of 80 and more. The verification of the proposed design rules on the basis of virtual experiments is therefore made.

7   Summary

Virtual experiments represent an excellent alternative to real experiments if the used material model is sufficiently verified and a great amount of specimen is necessary because of stochastic aspects. Using the presented computer programme ISOBEAM, variation investigations like these were done with the objective to compare the safety level demanded by Code with the safety level reached by virtual experiments. As a result of the virtual experiments it can generally be stated that the additional condition of DIN 1052 [1] seems to be appropriate in order to take hygrothermal long-time effects for high load degrees into account. Furthermore, design proposals are discussed which can describe the mentioned long-term effects for designing with a minimum equal suitability alternative to the procedure of Code.

8   References

[1]   DIN 1052-2004:08 – Entwurf, Berechnung und Bemessung von Holzbauwerken, Allgemeine Bemessungsregeln für den Hochbau, 2004

[2]   DIN V ENV 1995-1-1 – Eurocode 5: Entwurf, Berechnung und Bemessung von Holzbauwerken, Teil 1-1: Bemessungsregeln für den Hochbau, 1994

[3]   Hartnack, R., Langzeittragverhalten von druckbeanspruchten Bauteilen aus Holz, PhD-Thesis, Bauhaus-University Weimar, Weimar, 2005

[4]   Hartnack, R., Schober, K.-U., Rautenstrauch, K., Computer simulations on the reliability of timber columns regarding hygrothermal effects, CIB-W18 meeting 35, paper 35-2-1, Kyoto, 2002

[5]   Rautenstrauch, K., Untersuchungen zur Beurteilung des Kriechverhaltens von Holzbiegeträgern, PhD-Thesis, University of Hannover, Hannover, 1989

[6]   Rautenstrauch, K., Hartnack, R., The reliability of timber columns based on stochastical principles, CIB-W18 meeting 36, paper 36-2-1, Colorado, 2003

INTERNATIONAL COUNCIL FOR RESEARCH AND INNOVATION
IN BUILDING AND CONSTRUCTION

WORKING COMMISSION W18 - TIMBER STRUCTURES

ARE WIND-INDUCED COMPRESSION FAILURES
GRADING RELEVANT?

M Arnold

R Steiger

Swiss Federal Laboratories for Materials Testing and Research (EMPA)

SWITZERLAND

Presented by M Arnold

H Blass asked and received confirmation that the characteristic strength values reported were depth adjusted already. H Larsen commented this work shows the Swiss visual rules are too conservative and therefore the compression failure impact can still be tolerated. H Larsen said that compression failure should be excluded but question how this can be done as MSR is not effective. M Arnold mentioned that visual grading can detect this although this is not easy. In practice, problems are not seen with wood that has compression failures. F Lam mentioned in N. America graders detect "falling breaks" in grading which are compression failures induced during logging. B Leicester commented in Australia similar type of problem was observed where detection of defects was difficult. A proof test method was introduced. Proof test machine was built and standard was written. M Arnold responded that the proof load level has to be set fairly high for this to be effective. A Ranta-Maunus asked about the weakest values in the different compression failures classes. M Arnold answered that he cannot see differences in strength amongst different compression failure classes. A Buchanan received clarification that the compression failure was tested always on the tension side during bending. He also asked if the tree was damaged earlier would it mask the detection of compression failures. M Arnold answered that a portion of the tested pieces had previous damage from past wind and they could be detected. S Thelandersson commented that may be the MSR method could be calibrated against material which has a portion of compression wood. He also commented that with the conclusion that we have to be careful with storm damaged trees, can we still use the wood? M Arnold answered that it is a question of how to define storm damage and yes we need to be careful.

Are wind-induced compression failures grading relevant?

M. Arnold, R. Steiger

Swiss Federal Laboratories for Materials Testing and Research (EMPA), Switzerland

1   Introduction

Compression failures (CF) are defects in the wood structure in the form of buckled cell walls of the wood fibres. They may be wind-induced in the standing trees, if the stems are bent so much by frequent or strong winds that the proportionality limit of the wood in axial compression is locally exceeded on the inward (leeward) side of the bow. The distorted fibres of CF remain as weak points in the wood and can lead to brittle fractures in processed timber already at a relatively low stress in bending or tension (Fig. 1). Therefore CF are regarded as unwanted structural defects.
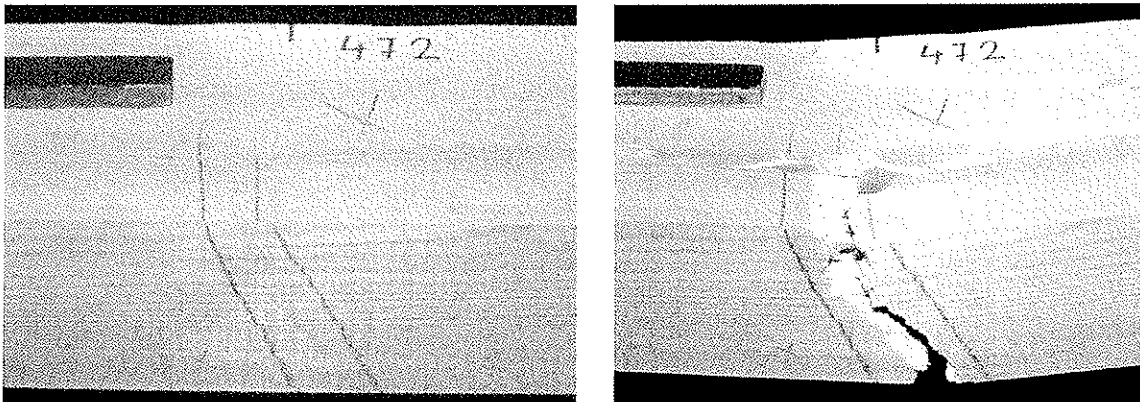
Fig. 1. A wind-induced compression failure in a squared timber beam before (left) and after (right) a destructive bending test. Initally the CF is barely visible on the planed surface, but the fracture was initiated directly in the previously marked CF and is extremely brittle and short-fibred.

CF are a well-known 'natural' phenomenon and are observed quite frequently in some of our lower density native softwoods such as spruce (Picea abies) [1-5]. Particularly after heavy storm damages in the forests, questions regarding their influence on the utilisation of timber from the salvaged trees arise anew.

CF are complex three-dimensional geometric structures with more or less fuzzy boundaries and appear in a broad range of intensities. Their size can range from minute deformations in the cell wall to wide bands of several millimetres in width, which can affect more than half of the stem's cross-section. Because of their diverse appearance various terms are in

use [6-7]. Regarding processing and grading it is important to note that CF are usually difficult to detect, particularly in rough sawn timber.

The consequences of CF on the utilisation of affected timber and particularly on its mechanical properties are still debated. While a reduction of the mechanical properties (mainly in bending and tension) at the fibre level [8] and in small clear wood specimens is generally acknowledged [5, 9], the effect is less clear with structural timber, where the effect of CF may be confounded by the presence of other defects such as knots or grain deviations [10-11]. Particularly regarding the effect of CF in structural timber only few comprehensive studies have been published so far.

However, because of their potential safety risk, many grading standards explicitly [12] or implicitly ('mechanical damages') exclude CF from timber elements in load bearing structures. CF therefore can impose serious restrictions on the utilization of wind-damaged timber and require additional efforts regarding grading and quality control. Historical example: CF used to be particularly feared of in the production of wooden ladder rails or wooden parts for airplanes (e.g. wings).

The presented work is part of an extensive research project in Switzerland started after the hurricane 'Lothar' in December 1999, aiming to collect more information regarding the extent and location, the causes, the detection, and the consequences of wind-induced CF [13].

The objective of this paper is to present new extensive data concerning the effect of wind-induced CF on the mechanical properties of structural timber stressed in bending and to draw conclusions regarding the consideration of CF in grading rules and procedures.

2   Material and methods

2.1   Sample material

The investigations were set up in the form of a case study. 30 spruce (Picea abies) trees were harvested in July 2000 from a mature, even-aged, heavily storm-damaged forest stand near Zurich, Switzerland. The selected trees were fully-grown and about 120 years old at the time of the hurricane. The diameter at breast height ranged from 39 cm to 72 cm, the tree height was between 35 m and 43 m.

3 to 5 logs of 5 m length were cut from each tree, graded and visually inspected for CF after partial debarking. 133 logs with a total volume of about 90 m^3 were processed. All logs were sawn into boards of 100 mm or 55 mm thickness, according to a systematic sawing pattern adjusted to the previously marked main wind direction of the storm (Fig. 2). This direction was corresponding mostly to the largest stem eccentricity, which again matches the usually westerly wind direction in this stand.
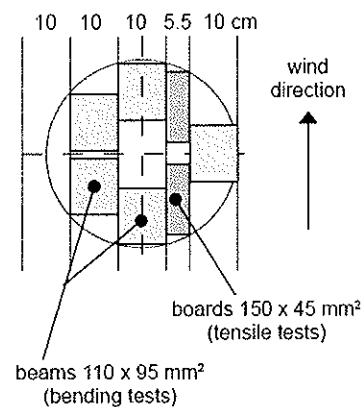
Fig. 2. Sawing pattern and arrangement of test pieces.

2

The sawn boards were subsequently cut into various test pieces (full-size structural timber as well as small clear specimens) for the assessment of various mechanical wood properties in bending, tension and compression. However, this paper is focusing only on the bending tests of structural timber. Results of the tests with small clear specimens from the same sample material have been published already earlier [9].

Each test piece was identified by its origin regarding tree, log and position in the stem cross-section. Depending on the diameter of the log, the sawing process resulted in a different number of timber pieces (1 to 11 pieces per log) with varying growth ring orientations. Since all harvested logs of the trees were converted into test pieces, a wide range of wood quality was included in the sample. All sawn pieces were kiln-dried to a wood moisture content of 15% and planed to their final dimension. A sample of 563 squared timber beams (2200·110·95 mm³) was finally available for testing.

2.2 Grading and detection of CF

Each beam was visually graded into 4 strength classes (I, II, III, ungraded) according to the supplementary specifications of the Swiss standard for the design of timber structures SIA 265/1 [12]. These visual grades are linked to the strength classes C24 (I+II) and C20 (III) according to the European standard EN 338 [14]. Due to practical reasons, visual grade I is currently assigned to C24 instead of the theoretically possible strength class C27. Deviating from the grading rules, beams with detected CF were not considered in the classification and therefore not excluded. Additionally, the wood density and the axial ultrasonic speed were measured. However, these additional parameters were not used to derive the strength classes, but recorded together with the main visual quality characteristics of each beam to be used later in the data analysis (Table 1).

Code	Parameter	Unit	Details
DENS	wood density	[kg/m³]	calculated from mass and volume of whole beam at 15% MC
USMIN	axial ultrasonic speed	[m/s]	minimum value of 2 measurements (device 'Sylvatest')
KMAX	diameter of largest knot	[mm]	between loading heads (inner third of span)
KCLU	size of largest knot cluster	[mm]	maximum sum of knot diameters (2 or more knots) within 150 mm length
CW	compression wood	[%]	affected cross-section (0, 5, 10, 20, 30, ..., 100%)
FUNG	discouloring fungal attack in sapwood	[%]	affected cross-section by blue stain or red stripe (0, 5, 10, 20, 30, ..., 100%)
SCSIA	strength class		I, II, III, ungraded (i.e. unfit for structural timber); by visual grading according to SIA 265/1 [12]

Table 1. Wood quality and grading parameters recorded during grading procedures.

Prior to testing all beams were carefully inspected for CF and the detected CF were marked (Fig. 1). A reliable detection of CF is difficult and depends on the light conditions, the angle of observation, the surface structure, and the experience of the observer. All macroscopically visible CF on the longitudinal faces of the beams were assessed. Because the inspection was done on planed surfaces, even rather fine CF could be detected. For each beam the 'intensity' of CF was recorded as the total number of identified CF and the 'size' of the largest CF (Table 2). The 'size' was assessed by a system simplifying the complex geometric structure of the CF to a one level defect plane, defined by its maximum axial 'width' (CFMAX, Table 3) and the visible length on the circumference of the beam (CFLEN, Table 2). This procedure resulted in 2 sub-samples of beams without and with CF (CFIND, Table 2).

Code	Parameter	Unit	Details
CFIND	binary indicator variable for presence of CF		0 = without CF, 1 = with CF
NCF	number of (single) detected CF		
CFMAX	axial 'width' of largest CF	[mm]	see Table 3
CFLEN	circumferential length of largest CF	[mm]	visible length on tension edge and side faces

Table 2. Assessment parameters of CF.

Max. (axial) width of CF	Definition	Remarks
0.1 mm	very fine CF; just visible with normal corrected vision	can be missed under insufficient illumination
0.5 mm	fine, but perceptible CF; clearly visible with normal corrected vision	will normally be detected by careful visual inspection of planed surfaces
1.0 mm	distinct CF; clearly visible	
>1 mm (1.5, 2.0, ...)	large and significant CF	classified in intervals of 0.5 mm

Table 3. Definition of discrete rating scale for visual assessment of axial 'width' of CF (CFMAX).

2.3 Bending tests

4-point static bending tests were conducted according to EN 408 [15] with the test configuration as shown in Fig. 3. The speed of the loading head was set to 0.2 mm/s, resulting in an average time to failure of 210 s. Time to failure was shorter than 180 s with 238 beams due to particular brittle fracture behaviour with a small deformation at maximum load (see 3.4). Deformation was measured on both side faces at the neutral axis over the total span as well as within the central gauge length and averaged over the two faces. The beams were cut such that the critical section with the expected failure location (e.g. knots, CF) was positioned between the inner loading points. To reproduce the original loading situation in the tree, the beams were loaded towards the nearer peripheral stem side (i.e. beams from the leeward side of the stem were loaded in the wind-direction and vice-versa). With this procedure, present CF were positioned in the majority on the tension edge and thus the beams were loaded in their most critical orientation. Resulting parameters were modulus of rupture (MOR), modulus of elasticity (MOE) and total deformation at maximum load (DMAX, Table 4).
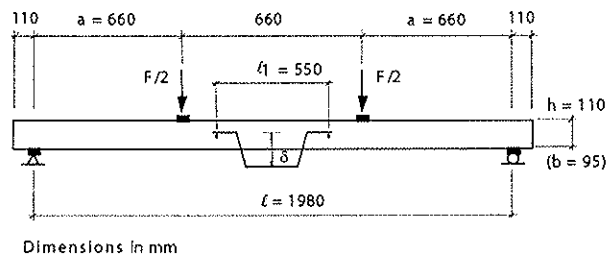
Fig. 3. Configuration of 4-point bending test according to EN 408.

Code	Parameter	Unit	Details
MOR	modulus of rupture	[N/mm^2]	calculated for nominal cross section of
MOE	modulus of elasticity	[N/mm^2]	110·95 mm (h·b)
DMAX	total deformation at maximum load	[mm]	measured at neutral axis over 1980 mm span

Table 4. Result parameters of bending test.

2.4 Data analysis

The test results were analysed with two different approaches focusing on the statistical significance and the practical relevance of the effect of CF on the mechanical properties. Further topics include the characterisation of the sample material, the effect of the 'size' of the CF and the fracture behaviour.

The statistical significance of the effect of CF on the mechanical properties was assessed with a multiple regression approach. A direct comparison of sub-sample means of beams without and with CF may be confounded due to differences in other quality parameters (e.g. density, knots, compression wood). The multiple regression methodology allows a simultaneous exploration of the effects of several 'independent' quality parameters on the 'dependent' mechanical properties, thus leading to 'adjusted' estimates of the single influencing factors.

The same main factor model without interaction terms was used for both dependent variables MOR and MOE as defined in formulas 1 and 2, thus allowing a comparison of the respective influence of the same factors in both models:

$$MOR = a_0 + a_1 \cdot DENS + a_2 \cdot USMIN + a_3 \cdot KMAX + a_4 \cdot KCLU +$$
$$a_5 \cdot CW + a_6 \cdot FUNG + a_7 \cdot CFIND + \varepsilon_1 \tag{1}$$

$$MOE = b_0 + b_1 \cdot DENS + b_2 \cdot USMIN + b_3 \cdot KMAX + b_4 \cdot KCLU +$$
$$b_5 \cdot CW + b_6 \cdot FUNG + b_7 \cdot CFIND + \varepsilon_2 \tag{2}$$

where a_0-a_7 and b_0-b_7 are regression coefficients and ε_1 and ε_2 are error terms in the models 1 and 2 respectively. The abbreviation codes for the regression variables are listed in Tables 1-4 and will be used throughout the presentation of the results.

The effect of CF was included as a binary variable, indicating only the absence (0) or presence (1) of CF within a beam (CFIND, Table 2). The estimated effect for CFIND is the nominal contribution of the CF on the tested dependent mechanical property. Interaction terms were not included in the models because they were not significant at the 5% level in most cases. All 563 tested beams have been included in this analysis.

The practical relevance of CF regarding the mechanical properties was assessed by comparing the characteristic values of the visually strength graded beams (including both beams without and with CF) as determined according to prEN 384 [16] with the limits of the given strength classes according to SIA 265 [17] and EN 338 [14]. 'Ungraded' beams were not included in this analysis.

3 Results and discussion

3.1 Properties of sample material

CF were found in 29 of the 30 investigated trees, which points to a rather high incidence of CF in the sample material [13]. In fact 200 (36%) of the 563 tested beams contained CF in various 'intensities' (Table 5). The proportion of beams containing CF increased in the lower strength classes. Only very few beams (24) were visually graded as strength class I, 145 and 197 beams were graded as strength class II and III respectively and a rather high number of beams (197) were graded unfit for structural timber ('ungraded'). Big knots and severe compression wood (CW > 20% in 127 of the beams) were the most frequent reasons for downgrading.

Frequency (Percent)	Strength class SCSIA				
CFIND	I C24 [1)]	II C24	III C20	un-graded	Total
0	23 (4.1%)	114 (20.3%)	120 (21.3%)	106 (18.8%)	363 (64.5%)
1	1 (0.2%)	31 (5.5%)	77 (13.7%)	91 (16.2%)	200 (35.5%)
Total	24 (4.3%)	145 (25.8%)	197 (35.0%)	197 (35.0%)	563 (100%)

Note: [1)] According to SIA 265/1 [12] visual grade I is assigned to C24 (see 2.2)

Table 5. Number of tested beams grouped by presence of CF (CFIND) and strength class (SCSIA).

Sample statistics for some selected wood quality and grading parameters are presented in Table 6. The wood density is typical for native spruce timber in Switzerland [18], but somewhat higher than in other recent studies on the effect of CF [10, 11]. The sample material covers a wide quality range from beams free of knots to beams from the upper logs with some rather large knots (diameter up to 55 mm). Except for wood density and the amount of compression wood, the wood quality parameters were very similar in both sub-samples of beams without and with CF.

	CFIND	n	Mean	Std	Min	Max
DENS	0	363	472	34	367	570
[kg/m³]	1	200	506	38	424	602
USMIN	0	363	5907	240	4834	6295
[m/s]	1	200	5850	243	5123	6284
KMAX	0	363	22.4	11.3	0	55
[mm]	1	200	23.5	10.6	0	50
KCLU	0	363	20.7	22.9	0	90
[mm]	1	200	17.5	21.3	0	90
CW	0	363	9.9	15.0	0	70
[%]	1	200	21.6	14.1	0	80
FUNG	0	363	8.7	8.9	0	40
[%]	1	200	9.6	9.0	0	40

Table 6. Sample statistics for selected wood quality parameters grouped by presence of CF (CFIND).

Beams with CF contained between 1 and 12 individual CF (NCF, Table 7). The average axial 'width' of the largest CF (CFMAX) was 0.7 mm, starting with a minimum of 0.1 mm as given in the rating scale in Table 3 to a maximum of 3 mm. 75 (38%) of the beams with CF contained rather large CF (CFMAX ≥ 1), while on the remaining 125 beams the largest CF was only detectable upon a careful visual inspection of the planed surfaces. The circumferential length on the tension edge and on the side faces of the largest CF (CFLEN) was on average 128 mm, with a range from 0 (CF on compression face only) to the maximum possible length of 315 mm (CF over full length of circumference).

For the interpretation of the results it must be noted that the sample material consisted of timber from a heavily storm-damaged forest stand. As a consequence of the prevailing westerly wind exposure of the whole stand, compression wood was concentrated on the lee sides of the stems, where also the vast majority of CF were located. Compared to earlier studies with structural timber [10, 11], we have tested a notably larger number of specimens with CF and with a higher 'intensity' of CF.

	CFIND	n	Mean	Std	Min	Max
NCF [pieces]	1	200	3.8	2.5	1	12
CFMAX [mm]	1	200	0.7	0.5	0.1	3.0
CFLEN [mm]	1	200	128	77	0	315

Table 7. Sample statistics for CF 'intensities' in beams with CF (CFIND=1).

3.2 Effect of CF on mechanical properties

Selected sample statistics for modulus of rupture (MOR), modulus of elasticity (MOE) and total deformation at maximum load (DMAX) are given in Table 8. Like with the wood density, MOR and MOE are in the usual range observed for spruce timber in Switzerland [18], but somewhat higher than in other recent studies [10, 11]. Variability (standard deviation) within the sub-samples without and with CF is very similar. The mean values of MOR and DMAX are distinctly lower in beams with CF, MOE differs only slightly. The effect of CF on MOR and MOE is further illustrated in Fig. 4, confirming a clear reducing effect on MOR, but only a small effect on MOE.

	CFIND	n	Mean	Std	Min	Max
MOR [N/mm^2]	0	363	53.0	9.9	23.1	76.3
	1	200	45.8	11.4	12.2	71.6
MOE [N/mm^2]	0	363	12451	2149	4550	16877
	1	200	12200	1971	6863	18041
DMAX [mm]	0	363	55.7	17.6	19.9	106.4
	1	200	39.3	14.7	12.4	81.5

Table 8. Sample statistics for bending test results grouped by presence of CF (CFIND).
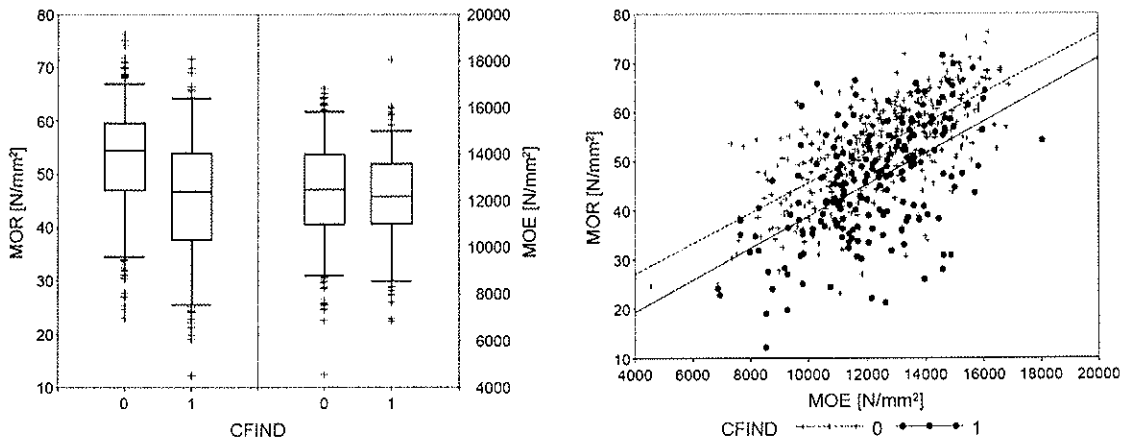
Fig. 4 Effect of the presence of CF (CFIND) on modulus of rupture (MOR) and modulus of elasticity (MOE). Box plots for sub-samples without and with CF (left, boxes show the median together with 25th and 75th percentiles, whiskers extend to 5th and 95th percentiles) and relationship between MOR and MOE (right, the dotted and the solid lines indicate the linear regression lines for the two groups of beams without and with CF respectively).

7

The results of the multiple regression analysis corresponding to model formulas 1 and 2 are listed in Table 9. Both models show a high overall statistical significance with a coefficient of determination (R-Square) of 0.45 for MOR and 0.69 for MOE. This agrees well with the usually observed better correlation between wood quality parameters and MOE than with MOR. Except for compression wood (CW) in the MOR model, all included factors are significant at the 5% error level. The diameter of the largest knot (KMAX) and the presence of CF (CFIND) are the most important factors in the MOR model, while wood density (DENS) and axial ultrasonic speed (USMIN) are particularly dominant in the MOE model.

```
                              Dependent Variable: MOR

                              Analysis of Variance

                                     Sum of        Mean
         Source             DF       Squares       Square    F Value    Pr > F

         Model               7        30903      4414.74762    65.35    <.0001
         Error             555        37495        67.55924
         Corrected Total   562        68399

                    Root MSE            8.21944    R-Square    0.4518
                    Dependent Mean     50.46490    Adj R-Sq    0.4449
                    Coeff Var          16.28744


                              Parameter Estimates

                     Parameter    Standard
    Variable   DF    Estimate      Error     t Value   Pr > |t|     95% Confidence Limits

    Intercept   1    -30.14410    10.83707    -2.78     0.0056    -51.43078     -8.85741
    DENS        1      0.07233     0.01107     6.53     <.0001      0.05057      0.09408
    USMIN       1      0.01025     0.00188     5.45     <.0001      0.00656      0.01394
    KMAX        1     -0.38636     0.03563   -10.84     <.0001     -0.45635     -0.31638
    KCLU        1     -0.06284     0.01793    -3.51     0.0005     -0.09806     -0.02763
    CW          1     -0.05921     0.03350    -1.77     0.0777     -0.12502      0.00660
    FUNG        1     -0.11295     0.03942    -2.86     0.0043     -0.19039     -0.03551
    CFIND       1     -8.07162     0.82103    -9.83     <.0001     -9.68432     -6.45892
```

```
                              Dependent Variable: MOE

                              Analysis of Variance

                                     Sum of          Mean
         Source             DF       Squares         Square      F Value    Pr > F

         Model               7     1696245177      242320740      177.80    <.0001
         Error             555      756402611        1362888
         Corrected Total   562     2452647788

                    Root MSE         1167.42777    R-Square    0.6916
                    Dependent Mean       12362    Adj R-Sq    0.6877
                    Coeff Var          9.44349


                              Parameter Estimates

                     Parameter     Standard
    Variable   DF    Estimate       Error      t Value   Pr > |t|     95% Confidence Limits

    Intercept   1      -24825    1539.21564    -16.13     <.0001     -27848       -21801
    DENS        1    26.34673      15.72989     16.75     <.0001    23.25699     29.43647
    USMIN       1     4.47382       0.26700     16.76     <.0001     3.94936      4.99828
    KMAX        1   -48.24031       5.06052     -9.53     <.0001   -58.18042    -38.30021
    KCLU        1    -7.40907       2.54625     -2.91     0.0038   -12.41054     -2.40760
    CW          1   -26.61012       4.75876     -5.59     <.0001   -35.95750    -17.26274
    FUNG        1   -11.22058       5.59959     -2.00     0.0456   -22.21956     -0.22159
    CFIND       1  -525.60071     116.61251     -4.51     <.0001  -754.65654   -296.54489
```

Table 9. Results of the multiple regression analysis for modulus of rupture (MOR, top) and modulus of elasticity (MOE, bottom) corresponding to model formulas 1 and 2 respectively.

The highly significant regression coefficient of the indicator variable for the presence of CF (CFIND) in both models indicates a statistically supported negative effect of the CF on both MOR and MOE. Because of the binary scale of the indicator variable CFIND, the parameter estimates give directly the nominal average effect of the presence of CF. For MOR this means that the presence of CF reduces the bending strength 'on average' by 8.1 N/mm^2 (with 95%-confidence limits between 9.7 and 6.5 N/mm^2). This estimate closely matches the difference of the mean values in Table 8 and the distance of the regression lines in Fig. 4. Related to the mean value of the beams without CF this corresponds to an average reduction of MOR by 15%. The estimate for the effect on MOE is -526 N/mm^2, which is a somewhat higher reduction than the nominal difference of the mean values (Table 8), but is still only a 4% reduction related to the mean value of the beams without CF. However, even this small reduction is statistically significant.

The identified more dominant effect of CF on MOR compared to MOE agrees well with earlier studies [9, 11] and is related to the higher sensitivity of MOR to single structural defects. As expected, the reduction of the mechanical properties of structural timber is slightly lower than with small clear specimens [9].

The above presented results are based on the whole sample of 563 beams, covering a wide range of wood quality and strength grades. Regression analysis stratified by strength classes and stem sections leads to very similar results regarding the effect of CF. This is interpreted as a confirmation of the validity of the used overall model.

In an alternative regression approach, a multiple regression model (model formula 1 without the indicator variable CFIND), was built on the sub-sample of beams without CF. The resulting regression coefficients were then used to calculate predicted MOR values for the beams with CF (without explicitly taking the visually detected CF into account), thus simulating a specifically calibrated machine stress grading system. An analysis of the deviations of the predicted and the observed MOR values is shown in Fig. 5. This approach disregarding the visually detected CF clearly predicts too high MOR values for many beams containing CF. Moreover the effect of CF is increasing slightly with higher strength values, which is most likely due to the decreasing amount of other structural defects.
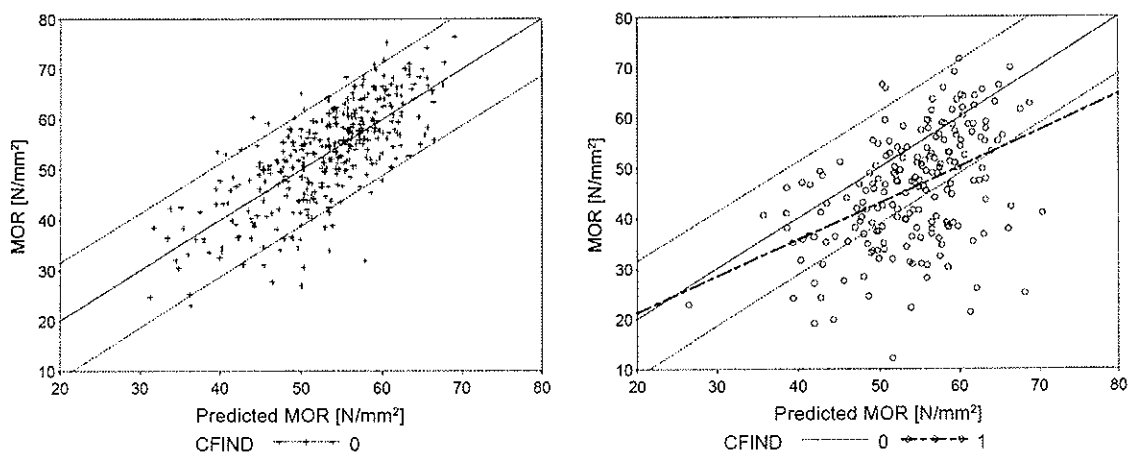
Fig. 5 Relationship between predicted and observed modulus of rupture (MOR) for the beams without (left) and with CF (right). The thin solid and dotted lines are the linear regression line and the 90% confidence bands for individual predicted values respectively of the regression model built on the sub-sample of the beams without CF. The thick dotted line is the linear regression line for the beams with CF.

A practical conclusion of this result is, that CF will not reliably be detected by machine stress grading methods relying on the dynamic or (low stress level) static assessment of the modulus of elasticity, as reported already in earlier studies [9, 19, 20]. Machine stress grading of timber containing CF without an additional visual inspection may therefore lead to an overestimation of expected MOR and wrong strength grades.

The verification of the characteristic values for MOR, MOE and DENS is documented in Table 10. In this approach the sub-samples of beams without and with CF were combined, but stratified by strength classes. The calculated characteristic values all exceed the limits in the given strength classes C20 and C24. This result means that in spite of the general and statistically significant reduction of the mechanical properties, visually graded structural timber even with CF meets the requirements with an adequate safety margin. Moreover, during the usual visual grading process in a sawmill, some of the beams with CF would have been detected and probably discarded.

Strength class [1]	Test results [2]					Adjustments to reference conditions [3]			Characteristic values [4]		
	n	Mean	Std	Min	5%-P	k_{MC} (factor)	k_h (divisor)	adjusted values	k_s (factor)	char. value	limit
MOR [N/mm^2]											
I+II / C24	169	56.6	9.0	22.2	**39.1**	-	1.064	36.8	0.89	**32.7**	24
III / C20	197	48.7	10.6	12.2	**30.1**			28.2	0.90	**25.5**	20
MOE [N/mm^2]											
I+II / C24	169	**13464**	1683	8608	10397	1.060	-	14272	-	**14272**	11000
III / C20	197	**12432**	1839	7362	9279			13178		**13178**	9500
Density [kg/m^3]											
I+II / C24	169	**475**	33	367	422	0.985	-	468 / 33	-	**414**	350
III / C20	197	**480**	35	395	427			473 / 34		**416**	330

Notes:
1) Strength class based on visual grading (without considering the presence of CF) according to the Swiss standard SIA 265/1 [12]
2) Abbreviations of sample statistics: n = sample size, **Mean** = arithmetic mean, **Std** = standard deviation, **Min** = minimum value, **5%-P** = empirical 5th percentile. The input values for the calculation of the characteristic values are printed in bold.
3) Conversion to reference conditions according to prEN 384: k_{mc}: Correction factor wood moisture content 15 → 12%, k_h: Correction factor timber size / height of beam $(150/110)^{0.2}$, **adjusted values**: property values at reference conditions. No adjustments to a pure bending MOE were made, which leads to a more conservative estimation of the characteristic values of MOE. Also no adjustments were made for the density as determined from mass and volume of the whole beams.
4) Verification of characteristic values: k_S: correction factor for sample size, **char. value**: characteristic value calculated from tested sample, **limit**: expected characteristic value according to EN 338 [14] for the given strength classes

Table 10. Verification of characteristic values of strength classes according to prEN 384 [16].

3.3 Effect of the 'size' of CF

Multiple regression analysis similar to the models presented under 3.2 failed to show evidence for an improvement of the model fit by the inclusion of the recorded CF 'intensity' variables NCF, CFMAX and CFLEN instead of the binary indicator variable for the presence of CF (CFIND). This is interpreted as a general difficulty to describe the 'damaging' dimensions of CF. Although on average there is an increasing negative effect on MOR with an increasing number and 'size' of CF, a strength prediction for single beams based on the macroscopic appearance of the CF would be unreliable due to the very high variability and hence wide confidence bands (Fig. 6). The lowest observed MOR values do not necessarily correspond to particularly 'large' CF. The correlation between the 'size' variables of CF and MOE is even lower.

Based on these findings, the use of allowable 'size' limits for CF in grading procedures seems neither safe nor practical. This result is in contrast to some earlier reports, where such limits have been proposed [10, 11].

10
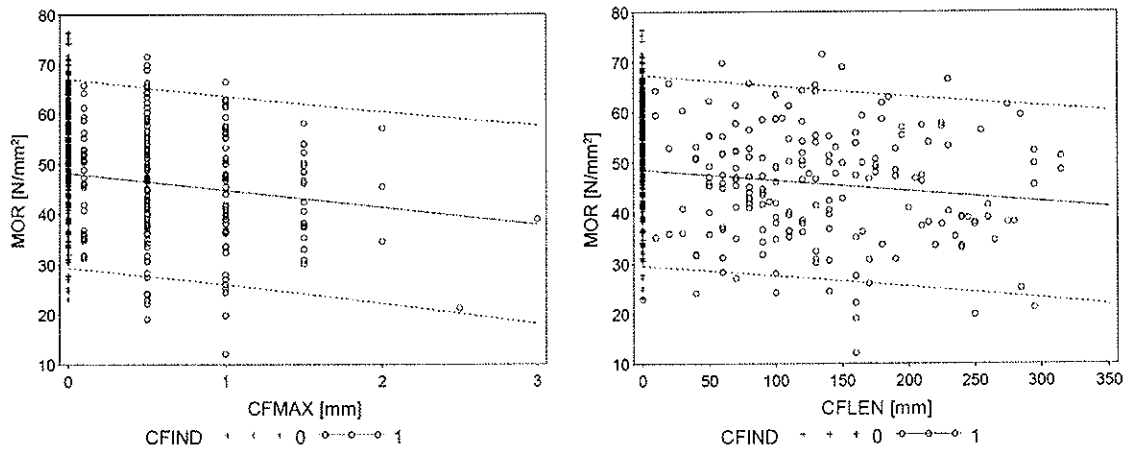
Fig. 6. Effect of the axial 'width' (CFMAX, left) and the circumferential length (CFLEN, right) of the largest CF on the modulus of rupture (MOR). The solid line indicates the linear regression line, the dotted lines enclose the 90% confidence band for individual predicted values for the beams with CF.

3.4 Fracture behaviour

If CF were involved in the mode of failure, frequently abnormally brittle and short-fibred fractures have been observed (Fig. 1). Fracture occurred often suddenly and without any prior indications. In some cases the beams were broken completely over the whole cross-section. The low-strain failure mode is also apparent in the total deflection at maximum load (DMAX, Fig. 7). Average total deflection at maximum load was only 39 mm in beams with CF compared to 56 mm in beams without CF, which corresponds to a reduction of 30% (Table 8). The beams with the lowest MOR all contained CF and exhibited very low deformations (Fig. 7).

This brittle fracture behaviour has been observed already in earlier studies [1, 5, 11]. Moreover, CF have been reported to be particularly sensitive to impact loads (e.g. impact bending tests), which showed a high strength reduction by CF [5, 9].
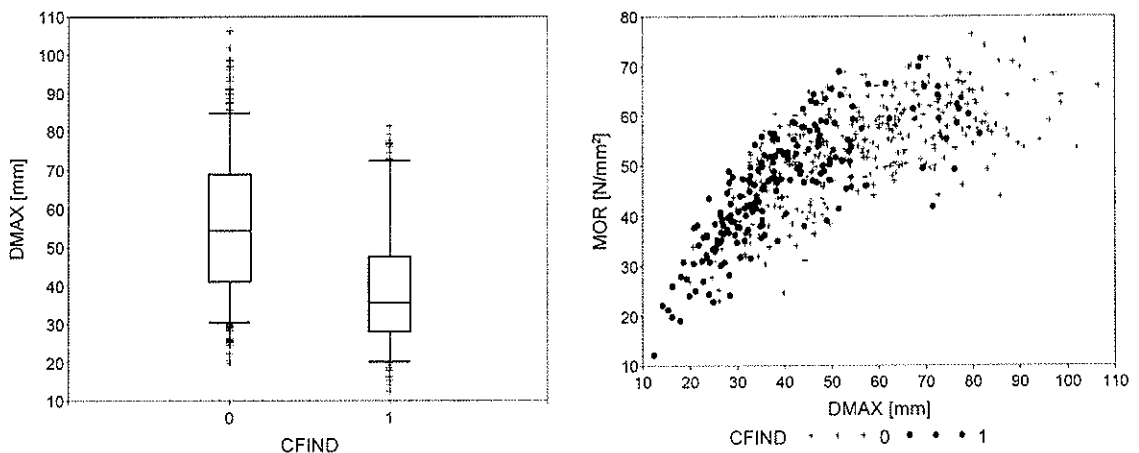
Fig. 7. Effect of the presence of CF (CFIND) on the total deformation at maximum load (DMAX) shown as box plots for sub-samples without and with CF (left, boxes show the median together with 25th and 75th percentiles, whiskers extend to 5th and 95th percentiles) and in relationship to the modulus of rupture (MOR, right).

11

4 Summary and conclusions

Based on this case study the following conclusions are drawn regarding the influence of wind-induced CF on the mechanical properties of spruce structural timber:

1. There is a statistically significant reduction of MOR and MOE in bending of squared timber beams containing CF compared to beams without visible CF. The effect is more pronounced regarding MOR than regarding MOE.

2. Despite the general reduction of strength and elasticity, the limits for the characteristic values of the strength classes C20 and C24 of visually graded structural timber (according to the Swiss standard SIA 265/1 [12]) are still exceeded. Considering the decreasing influence of other structural defects, this may however not be the case in the higher strength grades.

3. Because the modulus of elasticity is only slightly affected by the presence of CF, machine stress grading methods relying on the dynamic or (low stress level) static assessment of the modulus of elasticity are not able to reliably detect CF. Machine stress grading of timber containing CF without an additional visual inspection may therefore lead to an overestimation of expected MOR and wrong strength grades.

4. The macroscopically visible appearance ('size') of the CF is only a weak indicator for the potential reduction of MOR and MOE. This makes it impossible to distinguish between 'benign' and 'malignant' CF and to define allowable 'size' limits for CF for visual grading procedures. Thus only a strict exclusion of CF seems practical.

5. The failure behaviour of timber containing CF is frequently abnormally brittle and exhibits low-strain, short-fibred fractures.

6. Because of the potential safety risk and the difficult prediction of their strength reduction, detected CF should be excluded from load bearing structural elements stressed in tension or bending and explicitly addressed in the relevant grading standards (as in SIA 265/1 [12]). Timber containing CF should only be used in compression loaded or not load-critical applications.

Acknowledgements

References

[1] Trendelenburg R., 1940. Über Faserstauchungen in Holz und ihre Überwallung durch den Baum, Holz als Roh- und Werkstoff 3(7/8):209-221.

[2] Mergen F. and Winer H.I., 1952. Compression failures in the boles of living conifers, Journal of Forestry 50:677-679.

[3] Delorme A., 1974. Über das Auftreten von Faserstauchungen in Fichtensturmholz, Forstarchiv 45(7):121-128.

[4] Timell T.E., 1986. Compression Wood in Gymnosperms, Volume 3, Chapter 15.2.1.5, Springer, Berlin.

[5] Koch G., 1999. Sekundäre Veränderungen im Holz dynamisch beanspruchter Fichten (Picea abies [L.] Karst.) aus immissionsbelasteten und windexponierten Hochlagenbeständen, Mitteilungen der Bundesforschungsanstalt für Forst- und Holzwirtschaft, Hamburg, Nr. 192.

[6] Kucera L.J. and Bariska M., 1982. On the fracture morphology in wood. Part 1: A SEM-study of deformations in wood of spruce and aspen upon ultimate axial compression load, Wood Sci. Technol. 16:241-259.

[7] Wilkins A.P., 1986. The nomenclature of cell wall deformations, Wood Sci. Technol. 20:97-109.

[8] Terziev N., Geoffrey D. and Marklund A., 2005, Dislocations in Norway spruce fibres and their effect on properties of pulp and paper, Holzforschung 59:163-169.

[9] Sonderegger W. and Niemz P., 2004. The influence of compression failure on the bending, impact bending and tensile strength of spruce wood and the evaluation of non-destructive methods for early detection, Holz als Roh- und Werkstoff 62(5):335-342.

[10] Glos P. and Denzler J.K., 2004. Einfluss von Faserstauchungen auf die Festigkeit von Fichtenbauholz, Schweiz. Z. Forstwes. 155(12):528-532.

[11] Hoffmeyer P., 2003. Mechanical properties of timber from wind damaged Norway spruce, in Proceedings of the 'Second International Conference of the European Society for Wood Mechanics', Stockholm, Sweden, 25.-28. May 2003 (ESWM, Ed. L. Salmén, 2003).

[12] SIA 265/1, 2003. Holzbau – Ergänzende Festlegungen, Schweizerischer Ingenieur- und Architektenverein, Zürich.

[13] Arnold M., 2003. Compression Failures in wind-damaged Spruce Trees, in Proceedings International Conference 'Wind Effects on Trees', 16. – 18. September 2003, University of Karlsruhe, Germany, (Ed. B. Ruck et al., Karlsruhe), 253-260.

[14] EN 338, 2003. Structural timber – Strength classes.

[15] EN 408, 1995. Timber structures – Structural timber and glued laminated timber – Determination of some physical and mechanical properties.

[16] prEN 384, 2000. Structural timber – Determination of characteristic values of mechanical properties.

[17] SIA 265, 2003. Holzbau, Schweizerischer Ingenieur- und Architektenverein, Zürich.

[18] Steiger R., 1995. Biege-, Zug- und Druckversuche an Schweizer Fichtenholz, Forschungsbericht ETH/IBK Nr. 207, Birkhäuser, Basel.

[19] Steiger R., 1996. Mechanische Eigenschaften von Schweizer Fichten-Bauholz bei Biege-, Zug-, Druck- und kombinierter M/N-Beanspruchung; Sortierung von Rund- und Schnittholz mittels Ultraschall, Forschungsbericht ETH/IBK Nr. 221, Birkhäuser, Basel.

[20] Bernasconi A., Boström L. and Schacht B., 1999. Detection of severe timber defects by machine grading. Proceedings CIB-W18, 32. meeting, Graz, Austria, Paper 32-5-2.

INTERNATIONAL COUNCIL FOR RESEARCH AND INNOVATION
IN BUILDING AND CONSTRUCTION

WORKING COMMISSION W18 - TIMBER STRUCTURES

DESIGN SPECIFICATIONS FOR NOTCHED BEAMS IN AS 1720

R H Leicester

CSIRO

AUSTRALIA

Presented by R H Leicester

A Buchanan questioned whether the theoretical notch is a practical notch with saw cut. B Leicester answered that the Fracture Mechanics (FM) approach assumes the existence of a slit and notch root has an effect. Designer does know whether there is a crack. H Larsen commented European has strong interests but reference to their work is missing. Leicester mentioned that a companion paper has more comprehensive reference list. H Larsen questioned the general size effect concept in FM. He commented that there is no general size effect but a depth effect exists in a square relationship. The paper shows a factor 0.48 which agrees with the European results. He questions where is the general size effect as claimed? B Leicester answered that European has confirmed that general size effect findings also. Leicester also responded that in the case of two geometrically similar beams loaded the same way the general size effect can be seen. Also for metals this is true. A Jorissen received clarification that in the figure beam depth is the size in that case. If the beam is shallower than a certain depth we do not see an effect. A Buchanan related that this may be the case of finger jointed material as the lamination is relatively thin and also the case of LVL.

Design Specifications For Notched Beams in AS 1720

R.H. Leicester
CSIRO, Australia

Abstract

The design strength of notched beams has been in the Australian Standard AS 1720.1 for more than 30 years. In this paper these design rules are examined through the use of elastic fracture mechanics. Both stress intensity factors and critical stress intensity factors are evaluated for three notch angles in a beam element.

1. Introduction

As part of a proposed revision of the Australian Timber Engineering Design Code AS 1720 [8], it has been decided to reassess the design rules for the strength of notched beam elements. Although the basic concepts of elastic failure mechanics have been known since the 1970's, there has been little work on notched elements apart from some work on elements containing right angle notches [7,9,10,11]. The intent is to examine the design rules for notched beams in AS 1720.1.

The particular beam element chosen for investigation is illustrated in Figure 1. The notch angle will be defined by the notch slope ratio g/a. The dimensions of the element are defined by $d = D/2$, $a = D/2$, $L_1 = 2L_2$. For the case of $g/a = 0$ and 2, $L_2 = 2D$; and for the case of $g/a = 4$, $L_2 = 4D$.

The loads applied to the beam will be defined in terms of f_m and f_v, the nominal bending and shear stresses respectively on the cross-section at the notch root. These nominal stresses are defined by

$$f_m = (M + VL_2)(6/bd^2) \tag{1}$$

$$f_v = V(1.5/bd) \tag{2}$$

where M and V are the applied bending moment and shear force as shown in Figure 1, and b is the thickness of the timber beam.

The plane stress analysis of the beam was undertaken by means of a finite difference method. A regular rectangular mesh was used, with side lengths $\Delta x = L_2/24$ and $\Delta y = d/24$. No special elements were used.

Near the root of the notch an exact solution would predict that the stresses are expected to tend to infinity. However, provided the distortion zone is small compared to the eigenfields around the notch root, then the distortion does not effect the rest of the stress field of the

beam element. Thus the deformations of the distortion zone can be used as a measure of the eigenfield intensity. Such an approach, using finite element techniques, has been applied by Walsh [7,10,11].
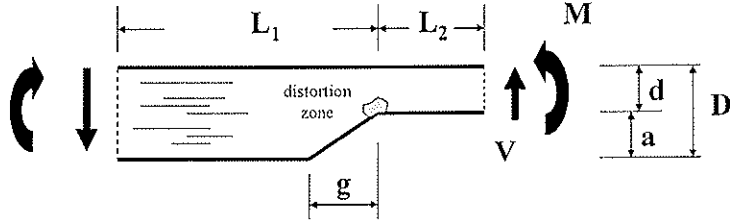
Figure 1. Notation for a beam-element.

2. Evaluation of K_A

2.1 Eigenfields Around A Notch Root

The stresses $\{\sigma_r, \sigma_\theta, \sigma_{r\theta}\}$ in the vicinity of a notch root such as that shown in Figure 2 can be written in terms of the polar coordinates (r, θ) in the following form [3,4]

$$\{\sigma_r, \sigma_\theta, \sigma_{r\theta}\} = \frac{K_A}{(2\pi r)^s} \{f_1(\theta), f_2(\theta), f_3(\theta)\} \tag{3}$$

and
$$\{\sigma_r, \sigma_\theta, \sigma_{r\theta}\} = \frac{K_B}{(2\pi r)^q} \{f_4(\theta), f_5(\theta), f_6(\theta)\} \tag{4}$$

where $f_1(\theta), f_2(\theta), \ldots$ are functions of θ only, s and q are constants that will be termed "size factors" and K_A and K_B are stress intensity factors defined by

$$\sigma_\theta\big|_{\theta=\pi} = K_A /(2\pi r)^s \tag{5}$$

$$\sigma_{r\theta}\big|_{\theta=\pi} = K_B /(2\pi r)^q \tag{6}$$

where $q \le s$.

The notation shown in Figure 2 will be used throughout this paper. It is assumed that the grain of the wood lies along the line $\theta = 0°$. and that the notch has free edges along the lines $\theta = 0$ and $\theta = 2\pi - \beta$, where β denotes the notch angle. Equations for other orientations of the notch have also been derived by Leicester [4].

Equations (5) and (6) describe stress singularities at $r = 0$. It was found that the singularity described by equation (5) exists for all notch angles $0 \le \beta < \pi$ and that the singularity of equation (6) exists for a notch angle $0 \le \beta < \alpha$, where α is roughly about 0.5 π.

2
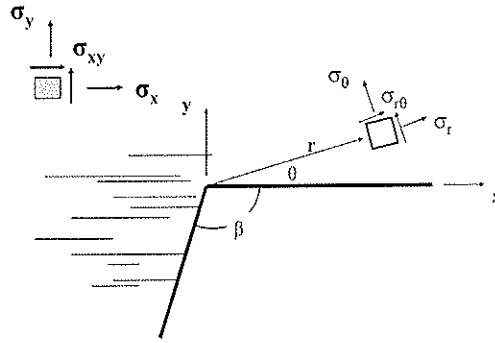
Figure 2. Notation used at a notch root.

2.2 Failure Criteria

For the condition $q < s$, the stress singularity described by equation (3) will always give rise to larger stresses near the notch root than those of equation (4) and hence the fracture criterion can be written

$$K_A = K_{AC} \tag{7}$$

where K_{AC} is termed the critical stress intensity factor.

2.3 Size Factor

An important aspect of the eigen equations (3) and (7) is that they imply a significant size factor in strength predictions. Using dimensional analysis, it can be shown that the value of K_A can be written in the form

$$K_A = AL^s \, \sigma_{nom} \tag{8}$$

where L is a characteristic dimension of the member, σ_{nom} is the nominal applied stress and A is a constant that depends on the shape of the structural element and the applied loading configuration.

Using the failure criterion of equation (7), the nominal stress at fracture for two members of different sizes (but having the same geometrical shapes and loading configuration) are related by

$$(\sigma_{ult,1}) / (\sigma_{ult,2}) = (L_2/L_1)^s \tag{9}$$

where the subscripts 1 and 2 refer to the two geometrically similar members, $\sigma_{ult,1}$ and $\sigma_{ult,2}$ denote the values of σ_{nom} at failure and L_1 and L_2 are the characteristic dimensions.

3

2.4   Equations of Plane Stress

Useful equations for solving a plane stress condition in an orthotropic material have been presented in previous papers [3,4,7]. These are conveniently stated in terms of a stress function ϕ defined by

$$\partial^2\phi/\partial x^2 = \sigma_y \ ; \ \ \partial^2\phi/\partial y^2 = \sigma_x \ ; \ \ -\partial^2\phi/\partial x\partial y = \sigma_{xy} \ . \tag{10}$$

The equation of compatibility then leads to

$$(\partial^4\phi/\partial x^4) + (2k/\in^2)(\partial^4\phi/\partial x^2\partial y^2) + (1/\in^4)(\partial 4^3\phi/\partial y^4) = 0 \ , \tag{11}$$

where

$$\in^4 = (E_x/E_y) \ , $$

$$k = 1/2(E_x/E_y)^{1/2} \ [(1/G_{xy}) - (\mu_{xy}/E_x) - (\mu_{yx}/E_y)] \ . \tag{12}$$

E, G and μ denote the modulus of elasticity, modulus of rigidity and Poisson's ratio, and the subscripts x and y denote properties relative to the x and y directions respectively.

Equation (11) is the field equation of the Airy stress function. It may also be written

$$\left[\left(\partial^2/\partial x^2\right)+\alpha_I^2\left(\partial^2/\partial y^2\right)\right]\left[\left(\partial^2/\partial x^2\right)+\alpha_{II}^2\left(\partial^2/\partial y^2\right)\right]\phi = 0 \tag{11}$$

where

$$\alpha_I^2 = \left(1/\in^2\right)\left[k+\left(k^2-1\right)^{1/2}\right],$$

$$\alpha_{II}^2 = \left(1/\in^2\right)\left[k-\left(k^2-1\right)^{1/2}\right].$$

Boundary conditions for the beam elements may be obtained by integrating the following functions around the boundary in an anti-clockwise direction [1].

$$\frac{\partial\phi}{\partial x} = \int\sigma_y dx - \sigma_{xy}dy \tag{14}$$

$$\frac{\partial\phi}{\partial y} = \int\sigma_x d_y - \sigma_{xy}dx \tag{15}$$

$$\phi = \int\left(\frac{\partial\phi}{\partial x}\right)dx + \left(\frac{\partial\phi}{\partial y}\right)dy \tag{16}$$

Elastic parameters $\in$ and k, computed from data reported by Hearmon [2] are shown in Figure 3 both for a single species and a group of species. The considerable scatter, even within a single species, is to be noted. For the analyses reported in this paper, the values used were $\in = k = 2$.

(a) data for all species   (b) data for spruce only
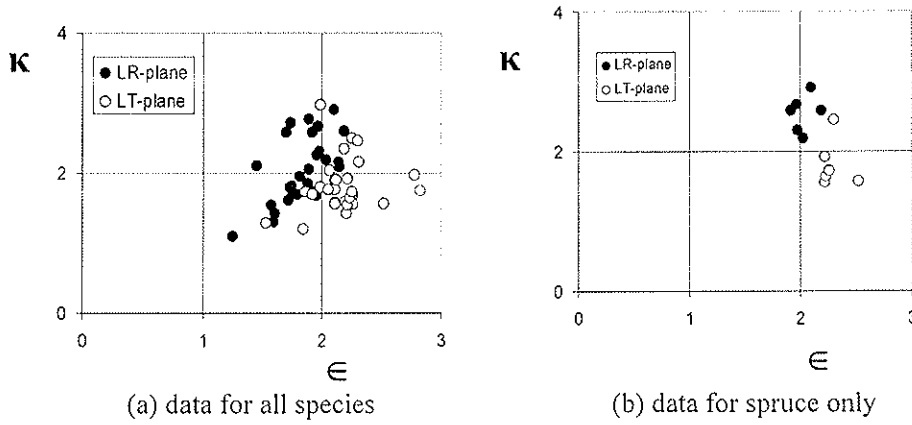
Figure 3. Elasticity parameters for wood.

2.5 Eigenfields

The solution of the field equation will be written in terms of transformed coordinates systems denoted by the subscripts I and II. These coordinates are defined by the equations

$$x = x_I = x_{II} \tag{17}$$

$$y = \alpha_I y_I = \alpha_{II} y_{II}. \tag{18}$$

The field equation (13) written in terms of the transformed coordinates is

$$\left[\left(\partial^2 / \partial x_I^2 \right) + \left(\partial^2 / \partial y_I^2 \right) \right]\left[\left(\partial^2 / \partial x_{II}^2 \right) + \left(\partial^2 / \partial y_{II}^2 \right) \right]\phi = 0 \tag{19}$$

A stress function which is which is suitable for the immediate vicinity of a notch root is

$$\phi = A_1 r_I^\lambda \cos\left(\lambda\theta_I\right) + A_2 r_I^\lambda \sin\left(\lambda\theta_I\right) + A_3 r_{II}^\lambda \cos\left(\lambda\theta_{II}\right) + A_4 r_{II}^\lambda \sin\left(\lambda\theta_{II}\right), \tag{20}$$

where A_1, ..., A_4 and λ are arbitrary real constants and the origin of the polar coordinates is taken at the notch root as shown in Figure 2. For the eigenfields, the condition $\sigma_\theta = \sigma r_\theta = 0$ must exist along edges of notch roots. Values of K_A for unit primary eigenfields for the three notch fields of interest are given in Table 1. Eignefields for other types of notch configurations have been discussed previously [4]. The size factors s and q are given by $s = \lambda_s - 2$ and $q = \lambda_q - 2$, where λ_s and λ_q are the power parameter λ for the primary and secondary eigenfields respectively.

Table 1. Parameters for the unit primary eigenfield

Notch slope	Notch angle β (deg.)	λ	s	A_1	A_2	A_3	A_4
$g/a = 0$	90.0	1.563	0.437	0.059	-0.559	-0.059	0.040
$g/a = 2$	153.4	1.637	0.363	0.155	-0.583	-0.155	0.042
$g/a = 4$	166.0	1.673	0.327	0.255	-0.613	-0.255	0.044

5

2.6   Numerical Analysis

A numerical analysis was undertaken using a relaxation technique. For the mesh used, about 3,0000,000 cycles of iteration were required and the time taken to do this using a Dell Latitude D400 computer was about one hour per solution.

As an example, Figure 4 shows the results of an analysis undertaken for the beam element subjected to boundary stresses corresponding to a unit eigenfield. The plot of computed stresses along the line $y = 0$, indicates that the distortion zone of the finite difference solution probably extends to about 5 nodes out from the notch root.
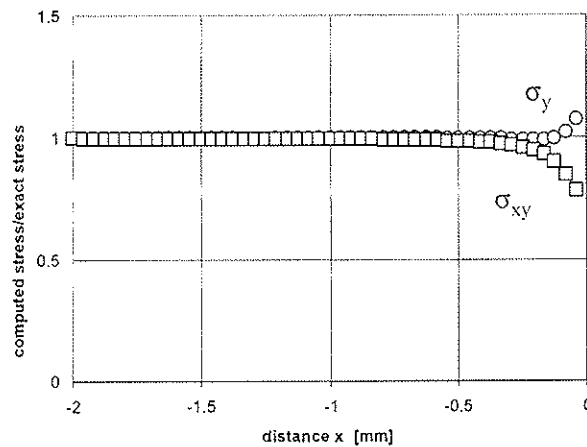
Figure 4. A comparison between the computed and exact stresses along $y = 0$ in an eigenfield for a beam with slope parameter $g/a = 4$.

To obtain the stress intensity factor for the beam loaded as shown in Figure 1, values at nodes near the notch root are compared with values obtained at the same nodes in a unit eignefield. The nodes used for this purpose are shown in Figure 5.
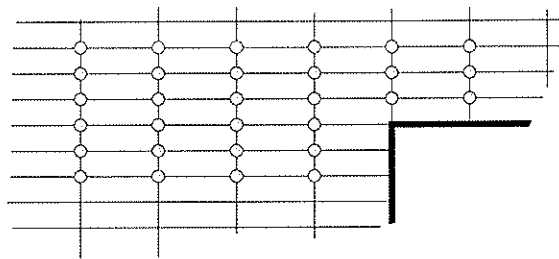
Figure 5. Nodes used for evaluating the magnitude of the eigenfield at a notch.

As an example, Figure 6 shows nodal comparisons for the case $M = 1$, $V = 0$, $D = 0.5$ and a notch with a slope ratio $g/a = 4$. From the plot of ϕ values, a value of $K_A = 0.86$ is derived and from the plot of σ_y values, a value of $K_A = 0.75$ is derived. By making a comparison of several such plots, an estimate of $K_A = 0.81$ was obtained which should be within 10% of the true value.

For the beam element loaded as shown in Figure 1, the primary stress intensity factor K_A obtained was

6

$$K_A = [f_m \, A_m + f_v \, A_v] D^s \qquad\qquad (21)$$

where the constants A_m and A_v are given in columns 2 and 3 of Table 2.

(a) ϕ values

(b) σ_y values
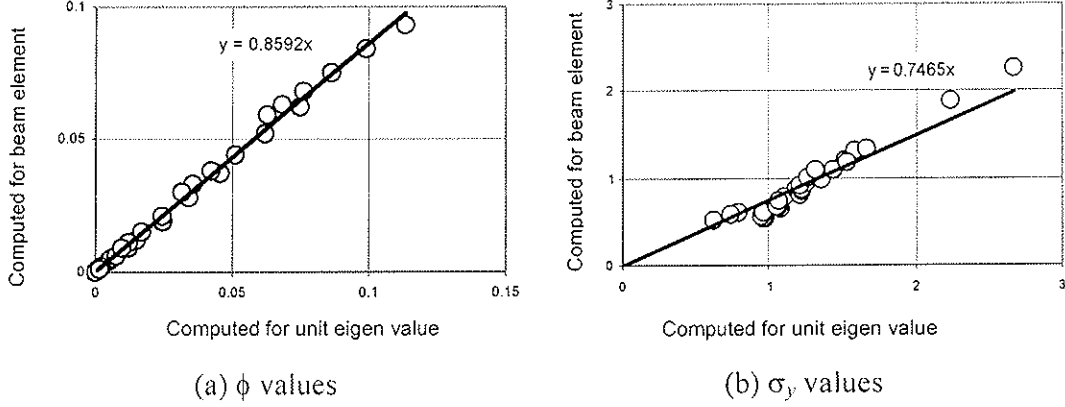
Figure 6. Comparison of node values for $g/a = 4$, $D = 0.5$, $M = 1$, $V = 0$.

Table 2. Strength and stress intensity parameters [N–mm units]
(Note. The density ρ is expressed in kg/m^3 units)

Notch slope	Stress intensity parameters		Strength parameters		Critical stress intensity factors	
	A_m	A_v	H_m	H_v	$K_{AC,m}/\rho$	$K_{AC,v}/\rho$
$g/a = 0$	0.0410	0.420	0.037	0.006	0.014	0.024
$g/a = 2$	0.0210	0.167	0.069	0.014	0.009	0.015
$g/a = 4$	0.0106	0.113	0.089	0.019	0.005	0.012

3. Measured Size Effect

The computed size parameters s and q for the notch shown in Figure 2 is given in Figure 7. Also shown plotted are the measured size effect parameters reported in an earlier paper [5] based on data from beam tests as shown in Figure 8.

Notch angle β [deg]

log₁₀ beam depth D (mm)
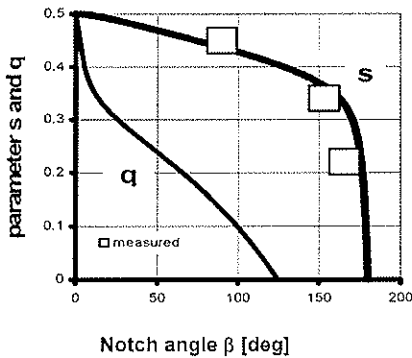
Figure 7. Size factors for the notch shown in Figure 2. (The measured values of *s* are from Figure 8).
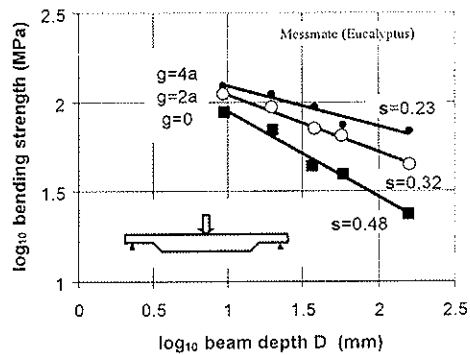
Figure 8. Measured nominal bending strengths for notched beams of various sizes [5].

4. Evaluation of K_{AC}

The measured bending and shear strength of notched beams with depth D = 150 mm has been described in an earlier paper [6]. This data is shown in Figures 9 and 10 for the case of notch slope parameters g/a = 0 and g/a = 4.
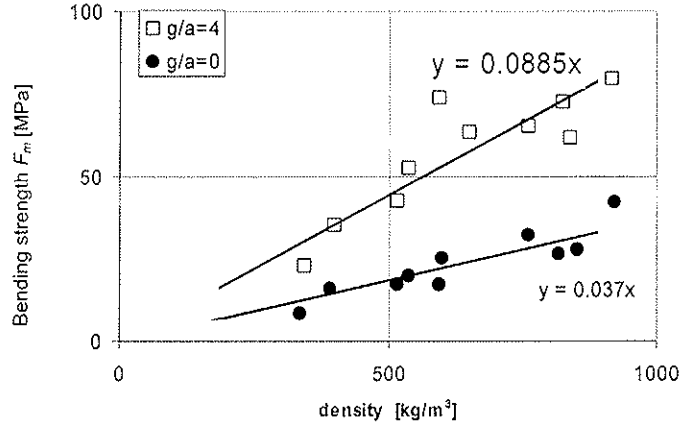
Figure 9. Measured bending strength of notched beams [6].
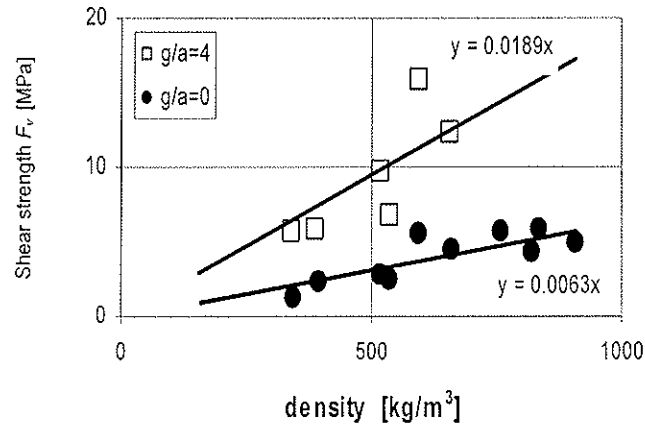
Figure 10. Measured shear strength of notched beams [6].

The fracture values of f_m and f_v will be denoted F_m and F_v and were found to be [6]

$$F_m = \rho H_m \tag{22a}$$

$$F_v = \rho H_v \tag{22b}$$

where ρ is the air dry density stated in kg/m^3 units and measured values of H_m and H_v are given in columns 4 and 5 of Table 2. The values of H_m and H_v for the cases of g/a = 0 and g/a = 4 are taken from Figures 9 and 10. The value for g/a = 2 has been interpolated by noting the values obtained for radiata pine beams [6].

Hence from (7), (21) and (22) the values of K_{AC} in N–mm units are

$$K_{AC} = K_{AC,m} + K_{AC,v}$$

$$= \rho\, H_m A_m\, (150)^s + \rho\, H_v A_v\, (150)^s \tag{23}$$

8

Values of K_{AC} computed according to equation (23) are shown in columns 6 and 7 of Table 2. Here the notations $K_{AC,m}$ and $K_{AC,v}$ are used to denote values of K_{AC} evaluated from pure bending and pure shear tests respectively. The effects of notch slope on the values of K_{AC} are shown plotted in Figure 11.
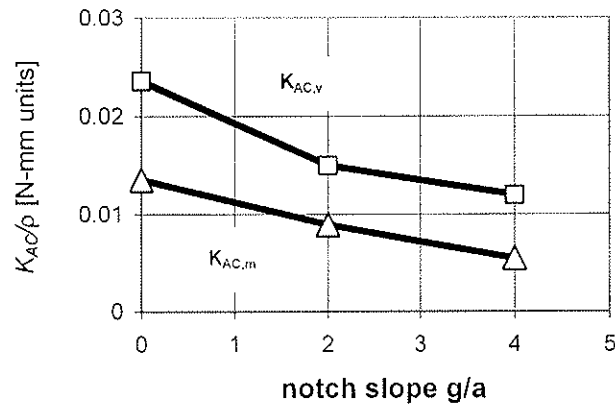
Figure 11. Effect of notch slope on the critical stress intensity factor.

Figure 12 shows the measured interaction between the bending and shear strength of notched radiata pine beams, reported in a previous paper [6]. Included also are the design rules of AS 1720 and the linear interaction expected for failure according to fracture mechanics concepts.
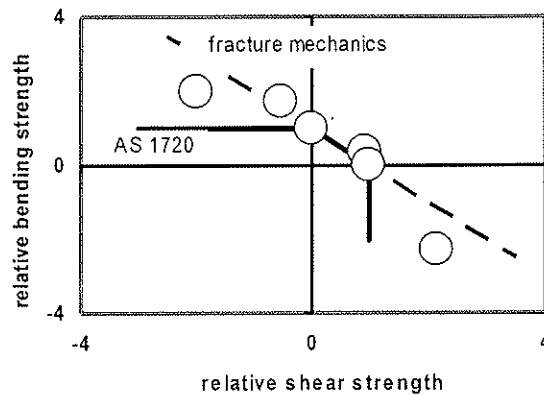
Figure 12. The interaction between bending and shear strength of a notched radiata pine beam [6].

5.   Discussion

The information reported in this paper is of uncertain accuracy because there is limited published data available for calibration and comparison purposes. The size effect for $g/a = 4$ is less than expected and may be due either to the use of incorrect elastic parameters for the computations or to the fact that the sizes of the beams tested may not be large enough to contain the critical eigenfield.

The critical stress intensity factors do not follow the expected relationship $K_{AC,m} = K_{AC,v}$ or the linear interaction equation shown in Figure 12. It would be useful to use fundamental wood properties to derive an expected effect of the notch slope parameter g/a on the critical stress intensity factor K_{AC}.

6. References

[1]   Allen, D.N. de G. (1954). Relaxation methods, McGraw Hill Book Co. Inc, New York, 257 pages.

[2]   Hearmon, R.F.S. (1948). The elasticity of wood and plywood, Spec. Rep. Forest Products Research. DSIR, No. 7, 5–9.

[3]   Leicester R.H. (1969). The size effect of notches, Division of Forest Products Reprint No. 817, CSIRO, Australia.

[4]   Leicester R.H. (1971). On some aspects of stress fields at sharp notches in orthotropic materials, Division of Forest Products Technological Paper No. 57 (Second series), CSIRO, Australia.

[5]   Leicester R.H. (1973). Effect of size on strength of structures, Division of Building Research Technological Paper No. 71, CSIRO, Australia.

[6]   Leicester R.H. and Poynter W.G. (1980). On the design strength of notched beams, *Proc. IUFRO Wood Engineering Conf.*, Oxford, UK, April, Topic 2/13.

[7]   Leicester R.H. and Walsh P.F. (1982). Numerical analysis for notches of arbitrary notch angle, *Proc. 5th Int. Conf. on Fracture Mechanics Technology Applied to Material Evaluation and Structure Design*, Melbourne, Australia, August.

[8]   Standards Association of Australia (1975). AS 1720: SAA Timber Engineering Code: Use of timber in structures, SAA, Sydney, Australia.

[9]   Walsh P.F., Leicester R.H. and Ryan A. (1973). The strength of glued lap joints in timber, *Forest Products J.*, **23**(5), May, 30–33.

[10]   Walsh P.F. (1974). Linear fracture mechanics in orthotropic materials, Division of Building Research Technological Paper No. 2 (Second series), CSIRO, Australia.

[11]   Walsh, P.F. (1975). Cracks, notches and finite elements, *Proc. National Congress on Pressure Vessels and Piping*, San Francisco. American Society of Mechanical Engineers, 49–61.

INTERNATIONAL COUNCIL FOR RESEARCH AND INNOVATION
IN BUILDING AND CONSTRUCTION

WORKING COMMISSION W18 - TIMBER STRUCTURES

BEECH GLULAM STRENGTH CLASSES

M Frese

H J Blaß

Universität Karlsruhe

GERMANY

Beech Glulam Strength Classes

M. Frese, H.J. Blaß
Lehrstuhl für Ingenieurholzbau und Baukonstruktionen
Universität Karlsruhe, Germany

1 Abstract

The following paper contains essential background information to provide an insight into the intended determination of characteristic values of the bending strength of beech glulam and of strength classes for beech glulam, respectively. The basis of this investigation is a research project performed at the Universität Karlsruhe [1].
Mechanical grading according to the dynamic MOE of 1888 beech boards for the production of 47 combined test beams is described. The results of bending tests of glulam beams according to EN 408 are presented. They confirm that mechanical grading using the dynamic MOE is an effective step towards high strength glulam beam production. These test results were used to verify a newly developed calculation model. It is suitable to determine both the characteristic tensile strength of boards and the characteristic bending strength of combined glulam beams. Using the calculation model, five different grading methods were numerically derived. They are based on visual and/or mechanical grading. Combined test beams are simulated taking into account the different grading methods and the beam load-carrying capacity was numerically determined depending on variable characteristic finger joint bending strength. The results of 235 bending tests on finger joints are presented. The specimens were produced from both, visually and mechanically graded boards. The results clarify the evident influence of the grading method on the characteristic strength values. They render possible strength classes up to GL48.

2 Background

2.1 Testing material and bending tests on beech glulam beams

Three sawmills located in Germany (Nordhessen, Schönbuch and Spessart) each delivered one third of the 1888 boards which were used to produce the test beams. The boards were graded using the dynamic MOE (= E_{dyn}) according to the scheme shown in Table 1. [2] gives the basis of the applicability of machine strength grading based on dynamic MOE from longitudinal vibration. The division based on MOE allowed a combined lay-up with lamellae of high stiffness in the outer zones of the test beams. Fig. 1 depicts the yield in the different grades. Table 2 and Table 3 give details of the beam lay-up. The total amount of 1888 boards was used to produce the beams. This confirms the economical aspect of the proposed grading scheme. Three strength classes and two beam heights were realised.

Fig. 2 shows the relation between the experimental data and the fitted normal density function of the beam bending strength. To provide a wider base to the statistical values the strength classes "very high" and "high" were merged for each beam height. Grading boards having a dynamic MOE over 15000 N/mm² ensures a characteristic bending strength of about 46,1 N/mm² (43,6 N/mm²) at a beam height of 340 mm (600 mm).

Table 1   Grading scheme according to dynamic MOE

grade	range of dynamic MOE (N/mm²)
1	$E_{dyn} \leq 13000$
2	$13000 < E_{dyn} \leq 14000$
3	$14000 < E_{dyn} \leq 15000$
4	$15000 < E_{dyn} \leq 16000$
5	$16000 < E_{dyn}$
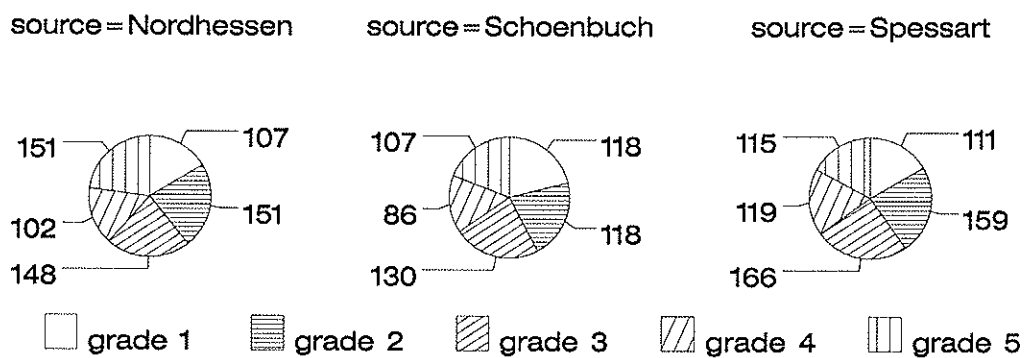
Fig. 1   Absolute yield in the 5 grades

Table 2   Acronym of strength class/sample size of the series and beam span

height h (mm)	340	600
strength class		
very high	VH-34 / 12	VH-60 / 10
high	H-34 / 12	H-60 / 8
low	L-34 / 5	-
span ℓ(m)	5,10	9,00

Table 3   Strength class and combined beam lay-up

strength class	grade of lamellae according Table 1	
	outer zone 1 (h/6)	inner zone 2 (4h/6)
very high	5	3
high	4	2
low	1	1

2
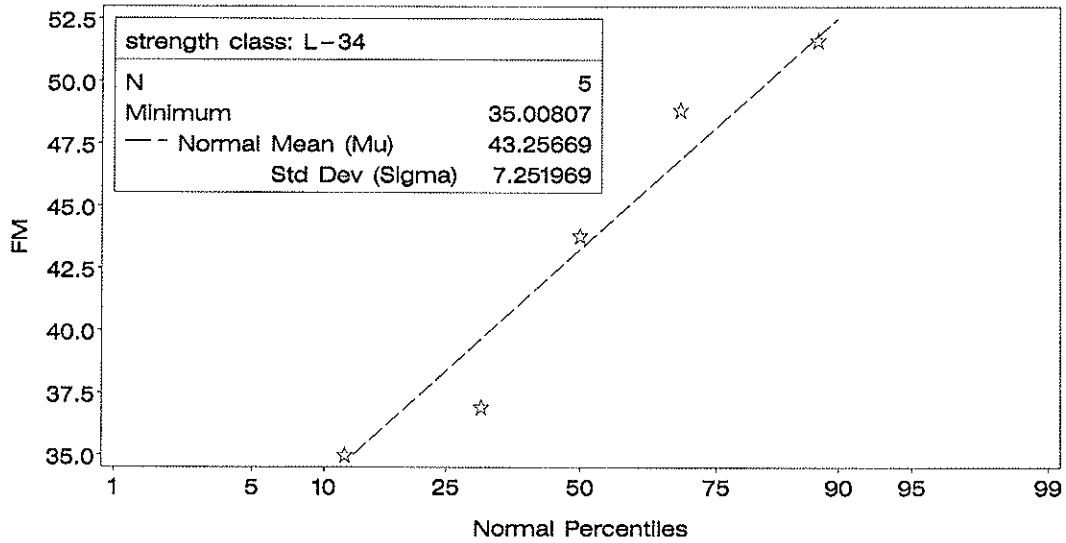
a)
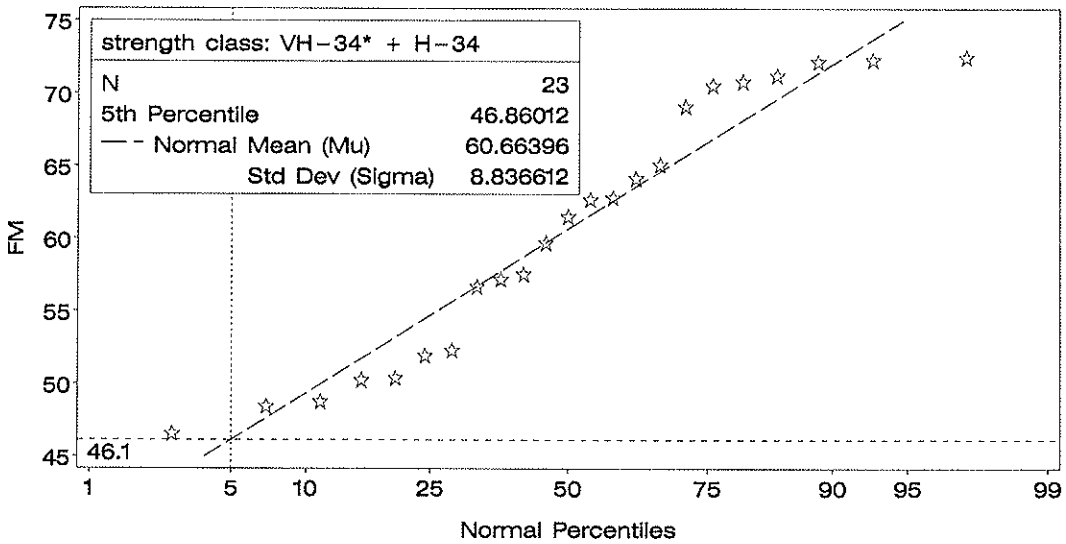
b)
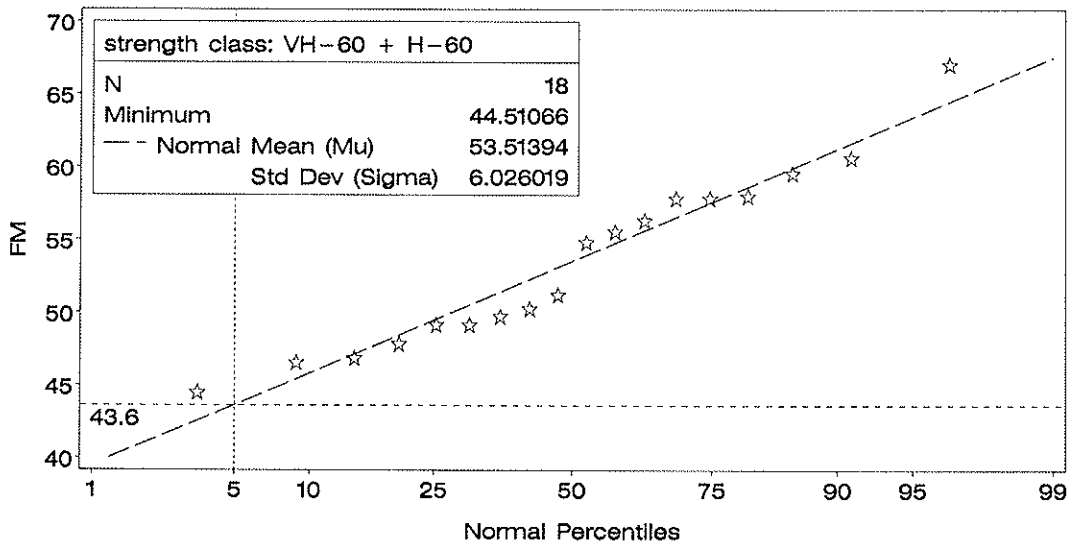
c)

Fig. 2   experimental data versus fitted normal density function;
strength class L-34 (a), VH-34 + H-34 (b) and VH-60 + H-60 (c)
*A poorly manufactured finger joint in the outermost lamella caused a strength
value of 32,7 N/mm². Hence this value is disregarded.

3

2.2 Calculation model

The calculation model is divided into a simulation and a finite element programme. The simulation programme works similarly as the real glulam production. A continuous lamella is generated consisting of simulated boards and finger joints. The mechanical properties are determined in steps of 150 mm. The autocorrelation of the mechanical properties is taken into account. The results are boards of low up to high quality. The activation of different density functions which describe the structural properties of the boards enables the simulation of a grading process according to the scheme in Table 1 as well as the grading proposals in Table 4 with regard to practical application. In general beams with combined lay-ups are simulated taking into account the economical use of the higher grade boards. The beam bending strength and MOE are calculated using a commercial finite element programme. Fig. 3 shows the mechanical model. Instead of a load a stepwise displacement Δu is applied in the middle of the loading equipment. Hence the unknown ultimate load is the sum of the forces in the links. The ultimate load is achieved when a crack is modelled in the outermost lamination. In this way the test concerning the EN 408 is suitably substituted.
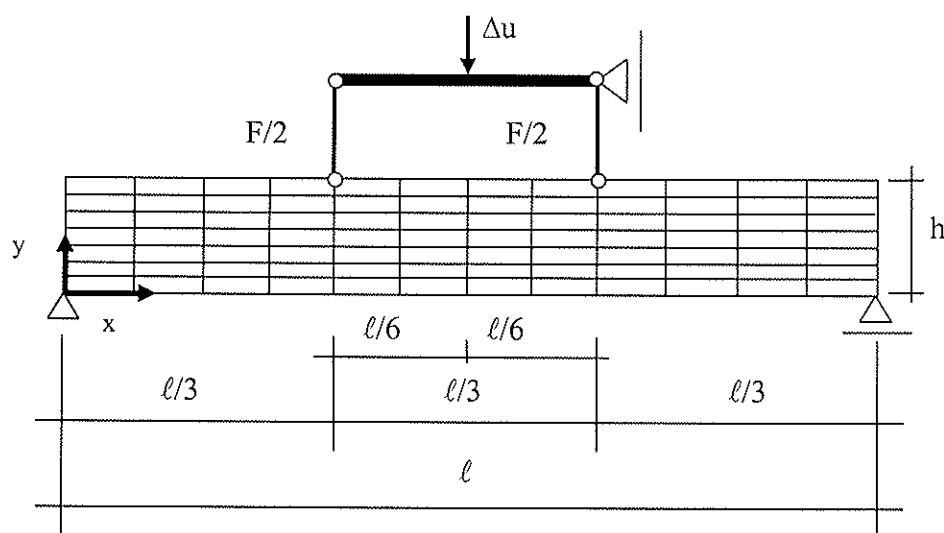
Fig. 3   Finite element model

2.3 Grading models

A large database describing the structural properties of the 1888 boards was used to develop the grading models. The mechanical grading using the dynamic MOE was only applied to simply and effectively divide the boards into classes to produce the combined test beams. Therefore it was not possible to produce multiple test series of beams considering different grading methods. This was performed with the calculation model taking into account the grades given in Table 4. The DEB value quantifies the single knot according to DIN 4074. More details concerning the determination of characteristic tensile strength of the boards as shown in the last column of Table 4 can be found in [3].

4

Table 4   Grades

No.	Model	knots	MOE (N/mm²)	characteristic tensile strength EN 408 (N/mm²)
1	LS10	DEB ≤ 0,33	-	22
2	LS13a	DEB ≤ 0,20	-	27
3	LS13b	DEB ≤ 0,042	-	31
4	MSa	DEB ≤ 0,20	$15000 < E_{dyn}$	40
5	MSb	DEB ≤ 0,042	$15000 < E_{dyn}$	48

2.4 Bending tests on finger joints

108 bending tests on finger joints manufactured from visually graded boards were performed. A further 127 tests were carried out to study the influence of mechanical grading on the bending strength of finger joints. These specimens were manufactured in the laboratory from the undamaged parts of tested beams. The clearly defined lay-up of the beams, see Table 3, made it possible to assign the specimens to the grades of the connected boards. All the bending tests were conducted flat wise according to EN 408 with a span of 15 times the height. The 5th percentile is 55,5 N/mm² in case of visual grading (Fig. 4 a). No increase of bending strength between grades 4 and 5 can be observed. Therefore the 127 specimens belonging to grades 4 and 5 were merged. The 5th percentile amounts to 68,8 N/mm² (Fig. 4 b). In terms of technical feasibility mechanical grading of grades 4 and 5 allows a 5th percentile value exceeding 70 N/mm². The continuous distribution of the experimental data is confirmed by the fitted lognormal curve in Fig. 4 a and b. A comparison of both visual and mechanical grading is depicted in Fig. 5.
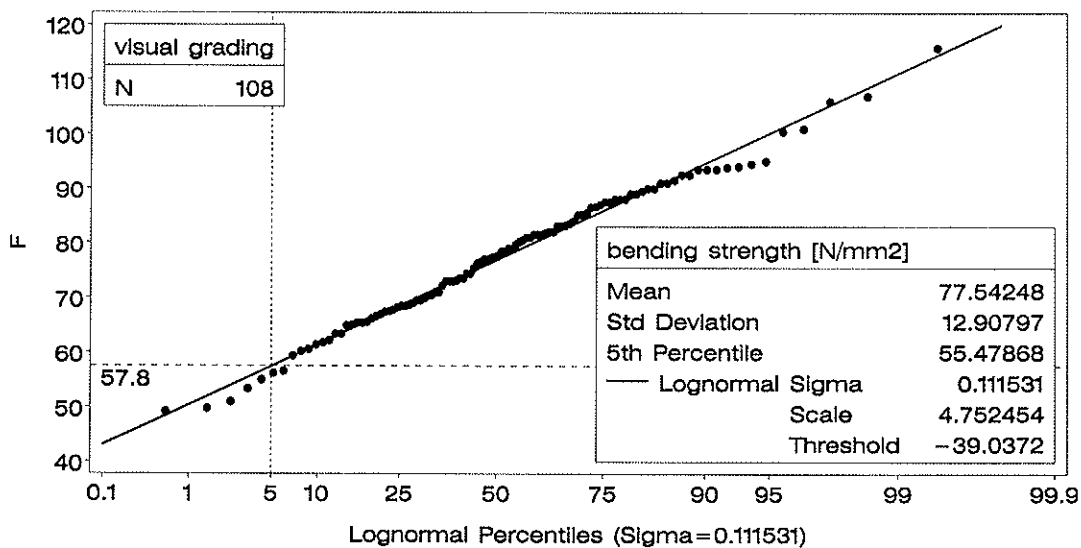
a)

Fig. 4   Experimental data versus fitted lognormal density function; visual grading (a)
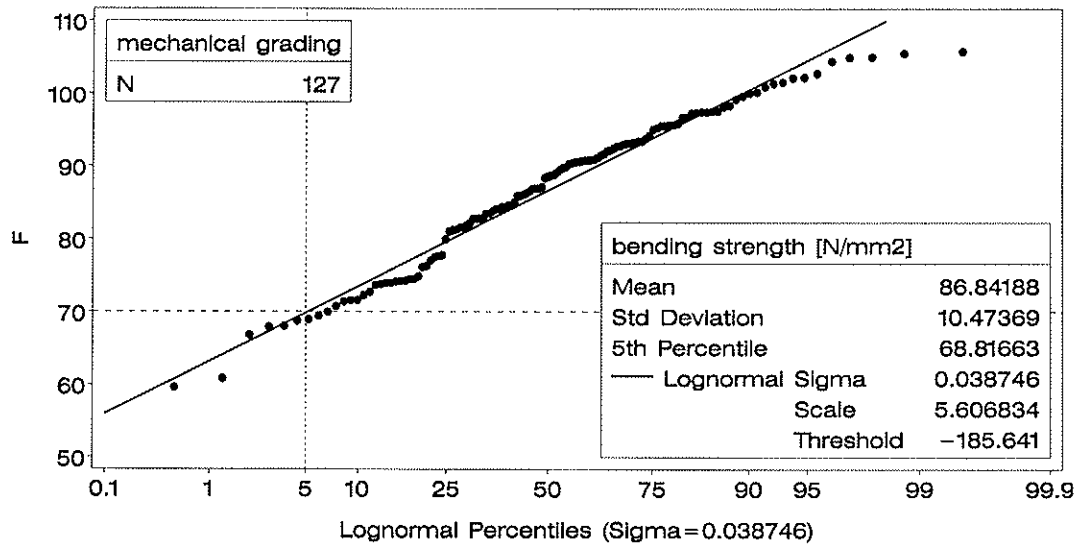
b)

Fig. 4   (Continuation) experimental data versus fitted lognormal density function; mechanical grading (b)
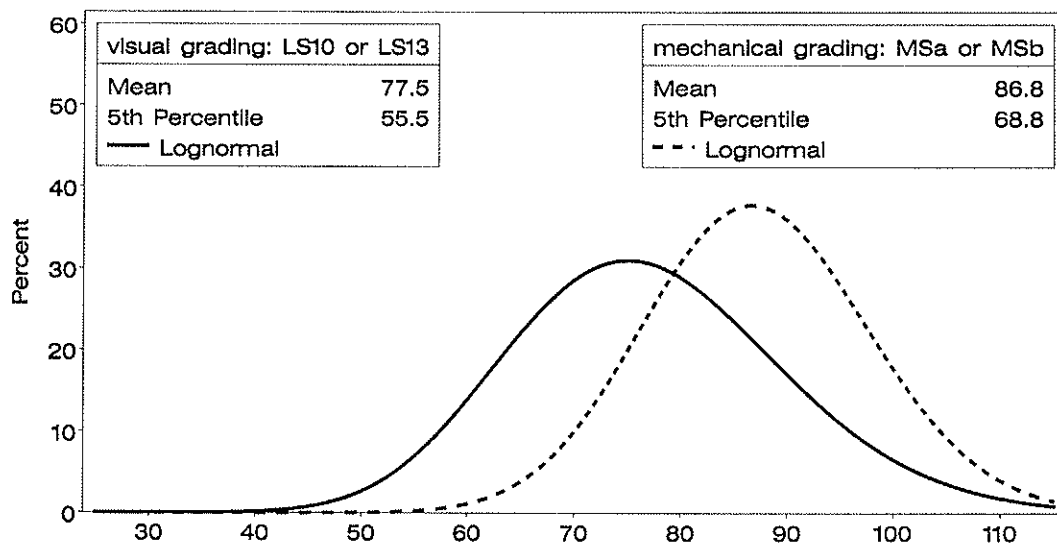
Fig. 5   lognormal density curve of finger joint bending strength (N/mm²); visual grading in comparison with mechanical grading

3   Strength classes

3.1   Proposals for strength classes

The influence of the grading method can be demonstrated in two ways. 1.: Fig. 6 displays the classification depending on grading model and variable finger joint bending strength. 2.: Using the data shown in Fig. 6 together with the characteristic tensile strength of boards as shown in Table 4, equation (1) can be derived. In this equation the characteristic glulam bending strength (= $f_{m,g,k}$) is calculated from both the characteristic tensile strength of the boards (= $f_{t,l,k}$) and the characteristic finger joint bending strength (= $f_{m,j,k}$). Considering the upper limits of the characteristic finger joint bending strength two further equations can be derived. Incorporating the values of 56 N/mm² (visual grading) and 70 N/mm² (mechanical grading) in equation (1) leads to the equations (2) and (3). The beech glulam design

6

proposals in comparison with the current model in EN 1194 referring to softwood, see equation (4), are shown in Fig. 7. There, the model according to equation (3) seems to be an adequate continuation of the model according to equation (4).
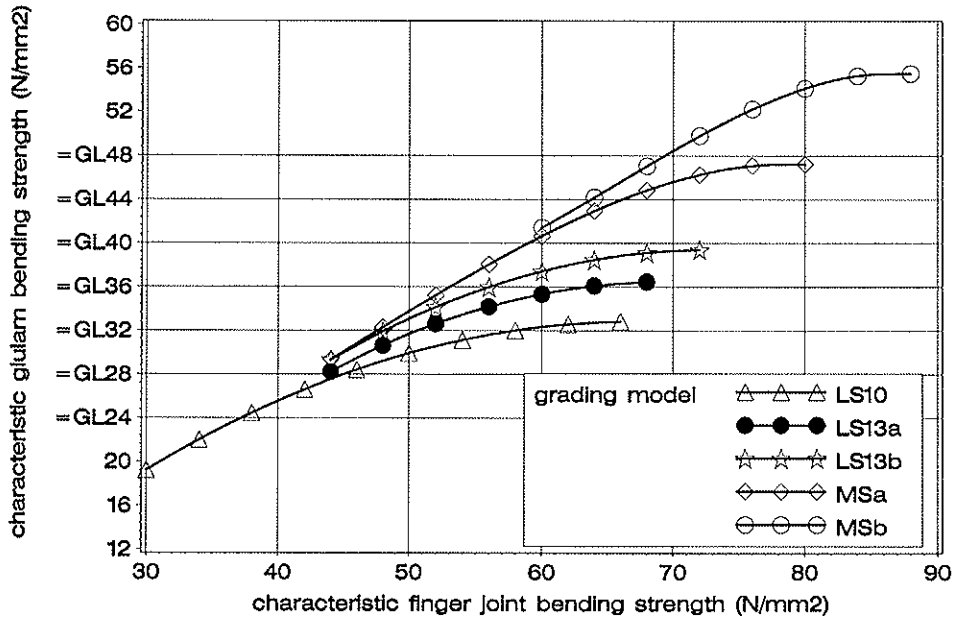
Fig. 6   Characteristic bending strength of glulam depending on characteristic finger joint bending strength
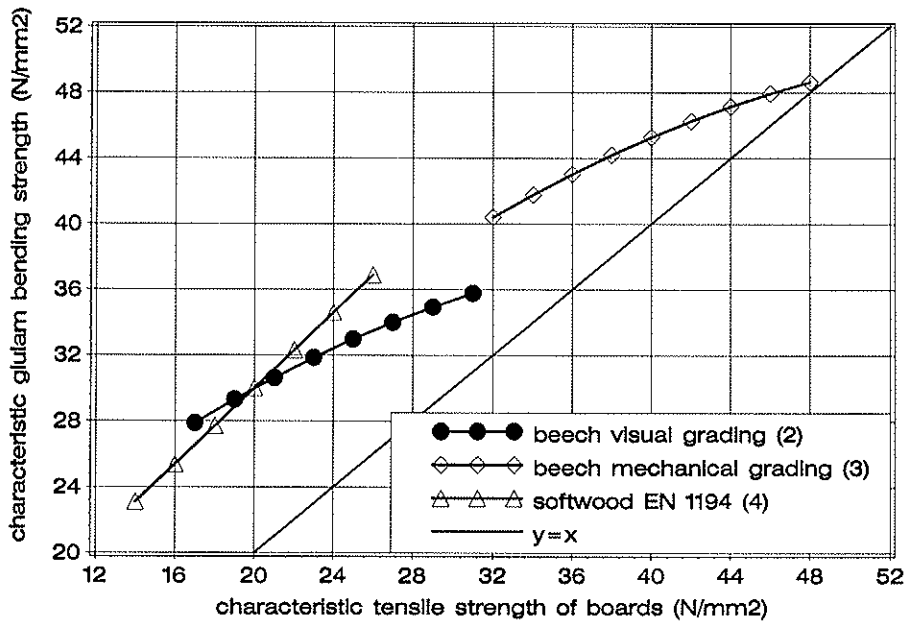
Fig. 7   Design models in comparison

$$f_{m,g,k} = -2,87 + 0,844 \cdot f_{m,j,k} - 0,0103 \cdot f_{m,j,k}^2$$
$$-0,192 \cdot f_{t,l,k} - 0,0119 \cdot f_{t,l,k}^2 + 0,0237 \cdot f_{m,j,k} \cdot f_{t,l,k} \tag{1}$$

$$f_{m,g,k} = 12,0 + 1,13 \cdot f_{t,l,k} - 0,0119 \cdot f_{t,l,k}^2 \tag{2}$$

$$f_{m,g,k} = 5,66 + 1,47 \cdot f_{t,l,k} - 0,0119 \cdot f_{t,l,k}^2 \tag{3}$$

$$f_{m,g,k} = 7 + 1,15 \cdot f_{t,l,k} \qquad (4)$$

3.2 Size effect

It is expected that the length of boards or the size of the beam, respectively, affects the characteristic bending strength of the beams. Assuming that the mean length of boards of about 2600 mm keeps constant, the influence of beam size on the bending strength is studied using the calculation model. The result of the study is shown in Fig. 8. Therein the beam height was varied from 300 mm up to 1500 mm in steps of 300 mm. The regression curve describing the height factor (= k_h) was calculated from a total of 6400 single calculations. During the calculations the relation of beam height and beam span is 1/18. The thickness of lamellae is 30 mm and the width 100 mm. The low influence of board width on the beam strength is reported in [1]. The value of the exponent (= 0,143) in equation (5) is very close to the value used in DIN 1052 (= 0,14). In EN 1194 an exponent of 0,10 is assumed. Since no further decrease in bending strength above h = 1200 mm was observed in the simulations, the decrease in bending strength is limited to 10 %. Consequently, equation (6) describes the size effect.
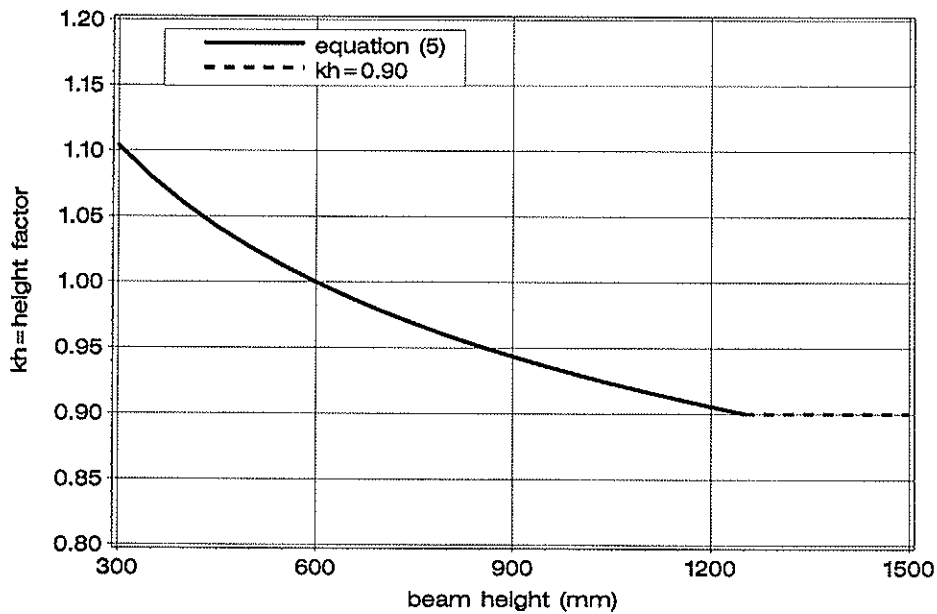
Fig. 8   Size effect

$$k_h = \left(\frac{600}{h}\right)^{0,143} \qquad (5)$$

$$k_h = \begin{cases} 1,10 & h < 300\,\text{mm} \\ \left(\dfrac{600}{h}\right)^{0,14} & 300 \leq h \leq 1200\,\text{mm} \\ 0,90 & h > 1200\,\text{mm} \end{cases} \qquad (6)$$

4 Conclusions

Table 5 gives a survey of the results. The most important findings are:

- Using beech glulam, it is possible to establish three further strength classes exceeding the strength class GL36. The maximum increase of bending strength is 33% comparing GL48 with GL36.

- The proposed strength grading techniques provide a remarkable 5th percentile MOE value of 12700 N/mm² and 14700 N/mm², respectively. The low difference between the mean values concerning GL36 made of softwood and GL48 made of beech could be extended by higher dynamic MOE limits for beech lamellae.

- Visual grading enables glulam producers to offer GL36.

- The increase in bending strength with decreasing beam height is as expected. Beam heights exceeding 600 mm cause a reduction of bending strength up to 10%.

- Further investigations are necessary to provide for factors from which more characteristic values can be calculated.

Table 5   Strength and stiffness values and requirements; reference beam height 600 mm

	GL28c	GL32c	GL36c	GL40c	GL44c	GL48c
strength values (N/mm²)						
$f_{m,k}$	28	32	36	40	44	48
stiffness values (N/mm²)						
$E_{0,mean}$	13500	13500	13500	15100	15100	15100
$E_{0,05}$	12700	12700	12700	14700	14700	14700
requirements outer zone 1						
DEB	≤0,33	≤0,20	≤0,042	≤0,20	≤0,20	≤0,042
E_{dyn}	-	-	-	>15000	>15000	>15000
$f_{m,j,k}$	≥45	≥50	≥56	≥59	≥66	≥70
requirements inner zone 2						
DEB	≤0,50	≤0,50	≤0,50	≤0,50	≤0,50	≤0,50
E_{dyn}	-	-	-	>14000	>14000	>14000

9

5 References

[1] Blaß HJ, Denzler JK, Frese M, Glos P, Linsenmann P (2004). Biegefestigkeit von Brettschichtholz aus Buche – Bending strength of beech glulam (only available in German). Band 1 der Reihe Karlsruher Berichte zum Ingenieurholzbau. Universitätsverlag Karlsruhe

[2] Görlacher R (1990). Klassifizierung von Brettschichtholzlamellen durch Messung von Longitudinalschwingungen - Grading of laminates by measuring longitudinal vibrations (only available in German). Karlsruhe, Universität (TH). Dissertation

[3] Frese M, Blaß HJ (2005/2006) Characteristic bending strength of beech glulam. Submitted for publication in Materials & Structures. Rilem France

DIN 1052, Ausgabe August 2004. Entwurf, Berechnung und Bemessung von Holzbauwerken – Allgemeine Bemessungsregeln und Bemessungsregeln für den Hochbau – Design of timber structures – General rules and rules for buildings (only available in German)

EN 1194, Ausgabe April 1999. Brettschichtholz – Festigkeitsklassen und Bestimmung charakteristischer Werte – Glued laminated timber - Strength classes and determination of characteristic values

DIN 4074, Ausgabe Juni 2003. Sortierung von Holz nach der Tragfähigkeit, Teil 5: Laubschnittholz – Strength grading of wood - Part 5: Sawn hardwood (only available in German)

EN 408, Ausgabe April 1996. Bauholz für tragende Zwecke und Brettschichtholz – Bestimmung einiger physikalischer und mechanischer Eigenschaften – Structural timber and glued laminated timber – Determination of some physical and mechanical properties

INTERNATIONAL COUNCIL FOR RESEARCH AND INNOVATION IN BUILDING AND CONSTRUCTION

WORKING COMMISSION W18 - TIMBER STRUCTURES

SHEAR STRENGTH OF GLUED LAMINATED TIMBER

H Klapp

H Brüninghoff

Bergische Universität Wuppertal

GERMANY

Presented by H Brüninghoff

P Kuklik commented on the detail of the connector at the support and commented that the changes in moisture in the connection may have caused tension perpendicular to grain stresses. Brüninghoff responded that the beam is free at the upper 2/3 portion and cracks outside the bolt area were also found. Density difference between adjacent ply may be an issue. A Ranta-Maunus asked about the weather information during failure. Brüninghoff responded that during winter the beam surface may have a 9% mc and 10% 5 cm deep from the surface. The climatic condition in the facility is quite stable.

G Schickhofer commented decrease in shear strength was found with increase in tension strength in previous work and micro and macro defects influence shear strength. Annular ring influence was found by Glos and Denzler. There is also knot effect. The work used data from small clear specimens which is not realistic for glulam. Brüninghoff agreed that more test on glulam may be appropriate. P Glos commented that EN 408 is not a good test and does not fit to solid timber. However in this case the failure indicate failure in wood along the glue line and does not have dowel effect; therefore, the data are good. P Glos also commented this is good work. S Thelandersson agreed with P Glos's comments in general. He mentioned also that one needs to define shear strength at the end of the beam where drying stresses may occur. This is an important point when evaluating this aspect in the lab.

R Steiger commented that this should be included in Eurocode 5 and ask what should be done from other country point of view. H Blass responded that Germany will take action. F Lam mentioned size effect for shear is in the Canadian code. A Ranta-Maunus commented that this has not been an issue in Nordic countries but will consider this information. A Buchanan suggested that may be a step function type approach can be used. F Lam commented this is the mention in Canada where beam larger than a certain size will have shear strength reduced according to size. H Blass said that the alternative can also be considered where beams smaller than a certain size will be allowed a larger shear strength.

Shear strength of glued laminated timber

H. Klapp, H. Brüninghoff

Lehr- und Forschungsgebiet Baukonstruktionen und Holzbau

Bergische Universität Wuppertal, Germany

1   Introduction

The current knowledge in timber research gives no applicable computation method for the shear bearing capacity of glued laminated timber beams. The dependence of the shear strength of the lamination tensile strength, set in EN 1194 [1], could not be confirmed by the tests of Schickhofer in Graz [2], so that in the new German standard DIN 1052 [3] instead a constant value of 3,5 N/mm² was set. This value was determined from the test results computationally as five percent quantile, whereby it is to be stated that about 10 percent of all test results fell below the strength of 3,5 N/mm². In the context of statistics, this doesn't seem to be alarming. But a negative influence of the volume on the shear bearing capacity is to be assumed as in the case of the likewise brittle transverse tension failure. The tests mentioned were conducted on comparatively small beams, so that lower shear strengths for dimensions of practical use can be supposed.
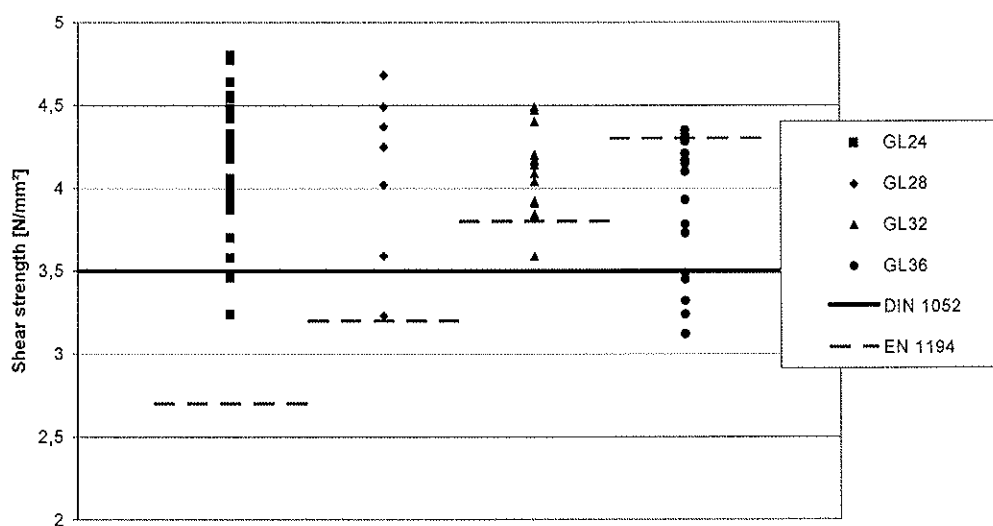
Fig. 1.1:   Comparison of the shear strengths from tests of Schickhofer [2] and current standards.

In view of this uncertainty concerning the shear strengths as well as the current cases of damage, there is an urgent need for further research. However larger test series with practical dimensions are costly in terms of resources and labour. For this reason the alternative solution of a simulation model, which considers the varying material properties, was selected.

2 Simulation model

2.1 Fundamental assumptions

The simulation model is based on the assumption that the shear strength of glued laminated timber depends on the properties of the laminations. In contrast to EN 1194 [1] a dependence not on the tensile strength is supposed, but on shear strength. Furthermore brittle fracture behaviour is applied by assuming failure as soon as the shear strength of the lamination is reached. According to this the shear strength of a glulam beam can be easily determined by comparing the shear stresses of the laminations with the corresponding shear capacities with consideration of the varying properties.

In the face of this simple failure criterion it is obvious that the quality of the results depends on an appropriate choice of the laminations shear strength. Shear tests (EN 408 [4]) on 272 timber specimens were carried out by Glos and Denzler [5] and the following findings can be pointed out:

> The shear strength depends slightly on the density

> An influence of knots on the shear strength could not be determined

> Higher values for shear strength in higher strength classes could not be confirmed

According to this it is not necessary to distinguish between strength classes. The tests of Glos and Denzler [5] as well as tests of Spengler [6] on timber laminations lead to a mean value of 5,3 N/mm² and a 5%-quantile of 3,8 N/mm². With application of these values and the normal distribution a good accordance with the test results of Glos and Denzler can be achieved (Fig. 2.1).
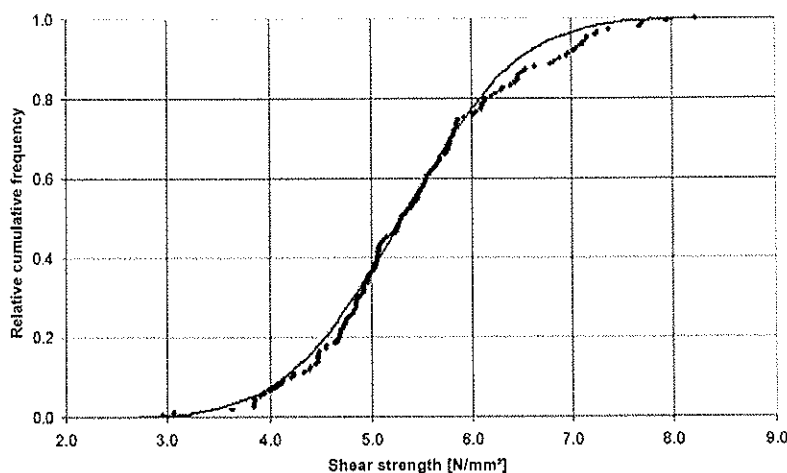
Fig. 2.1: Comparison of normal distribution and tests [5]

2

2.2 Simulation of the cross section

With the determined strength distribution the simulation includes the following steps:

1. The cross section is divided into laminations with a depth of 35 mm.

2. For each lamination, a shear strength is randomly assigned based on the normal distribution

3. According to its position the shear stress for each lamination is determined. The maximum value is set to 1 N/mm². Apart from that any stress distribution of the cross section can be applied in the model.

4. For every lamination the quotient of its shear strength and stress is computed.

5. The smallest quotient is determined. This value represents the smallest shear stress located at the maximum stress of the cross section, which causes a failure.

Obviously the influence of the depth but not the influence of the length is taken into account, so that only the depth effect can be analysed with the mathematical model so far.
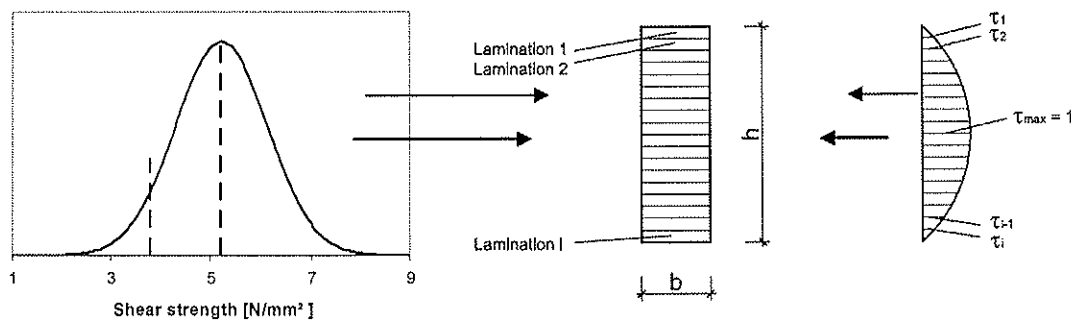
Fig. 2.2:   Assignment of strength and shear stress of the laminations

Because of the strength distribution of the laminations numerous simulations of the same cross section are needed to get the distribution of its load capacity. With this distribution the characteristic shear strength and the correlation with the depth can be determined. In order to check the quality of the simple simulation model, it has to be compared first of all with the test results of Schickhofer [2]. The influence of the depth and the mathematical description will be mentioned in the following chapter.
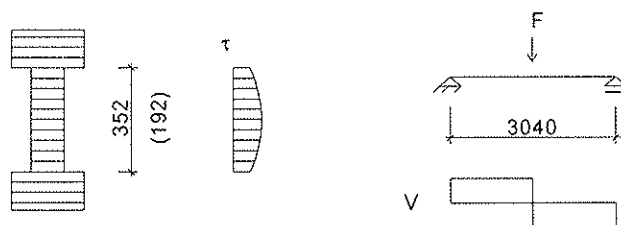
Fig. 2.3:   Test configuration of Schickhofer [2]

3

Tests on glulam beams with I-cross section and three point load were conducted by Schickhofer [2]. The cross section was selected to reach a shear failure rate and to avoid bending failure. All the shear failures in the tests were located in the web so that only a rectangular cross section with the shear stress distribution of the web needs to be simulated. The simulation model is compared with 64 test results and a web depth of 352 mm and a mean value of 6 tests on beams with a web depth of 192 mm.
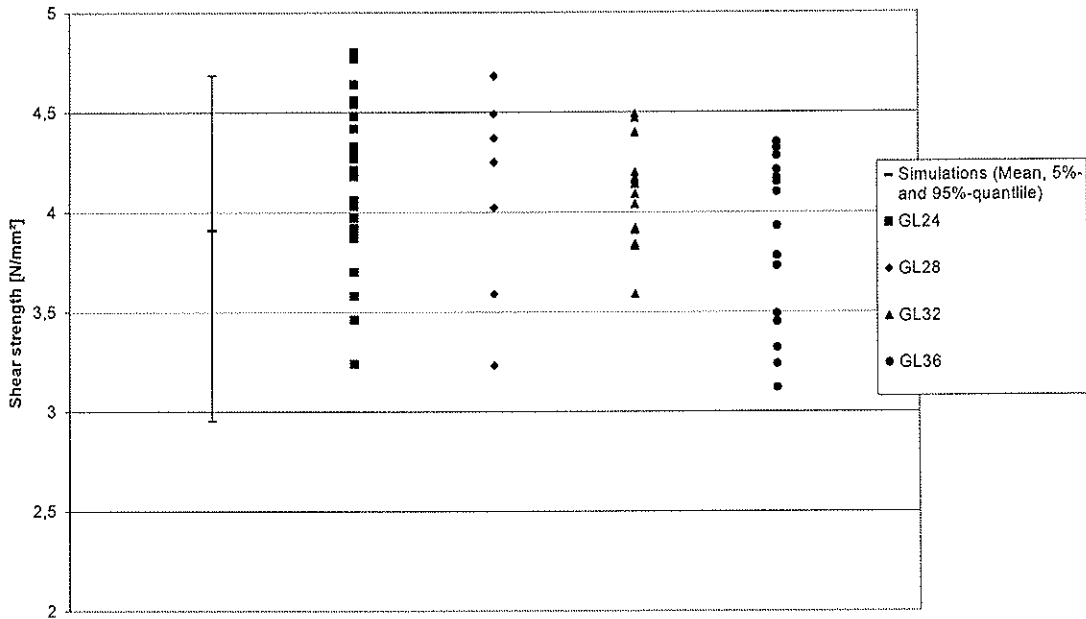
Fig. 2.4:   Comparison of simulations and tests by Schickhofer [2] with a web depth of 352 mm
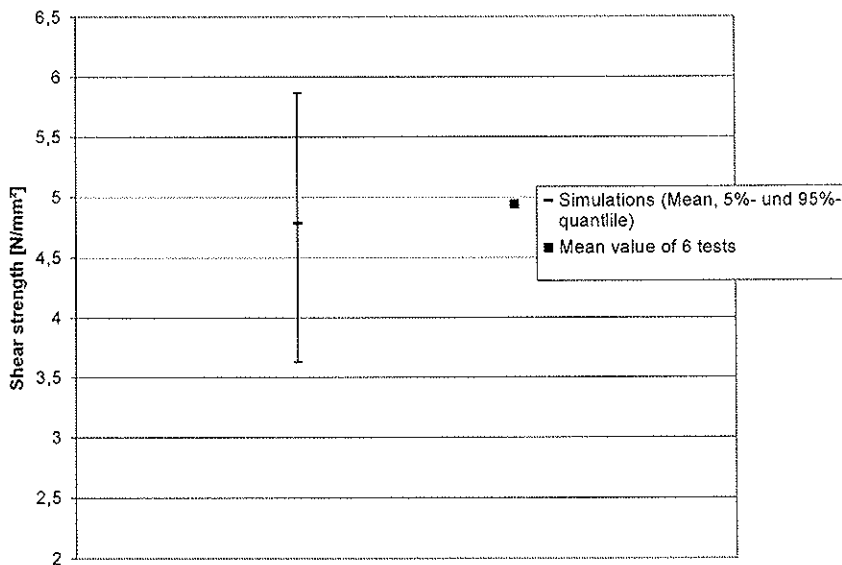
Fig. 2.5:   Comparison of simulations and tests by Schickhofer [2] with a web depth of 192 mm

4

The comparison shows a persuasive accordance of simulation and tests. In particular the influence of depth on the shear strength seems to be appropriately estimated.

2.3 Simulation of the cross section and length

The main cause of the length influence on the results can be seen in the fact, that several boards with differing properties are located within a lamination. Hence it is not sufficient to examine the cross section as done before - the whole beam must be simulated with varying properties.

The density varies only slightly within timber boards, so that it can be assumed that the shear strength also varies little. It is sufficient to pick randomly one shear strength out of the normal distribution and use this one for the entire board. But it is important to arrange these in the beam in a reasonable way. The assumptions of previous research projects, which successfully used similar simulation models, are adopted to build up the structure. For example the proportion of boards which are shortened because of knots or similar imperfections is set to 50%. The length of a board is randomly determined from one of the distributions for shortened or not shortened boards (Tab. 2.1).

Tab. 2.1:   Distribution of board length

	Board		mean [m]	standard deviation [m]	COV [%]
Larsen [7]	Shortened	b=100mm	4,30	0,71	17
		b=150mm	4,62	0,67	15
Ehlbeck/ Colling [8]	Not shortened		2,15	0,50	23

The results of simulations with the extended model are compared again with the results by Schickhofer (Fig. 2.6). The difference between these and the previous simulations is very small, which was expected. Schickhofer's test specimens were only 3 m long so that only a few boards in the laminations are needed to build the model. A slight underestimation of the test results can be explained by idealising the shear force distribution in the model. While in the model a constant value for shear force is used, the test specimens are loaded with plates which rounds off the shear force distribution.

Altogether the assumptions of the simulation model cause an influence of the volume on the shear strength of glued laminated beams. A bigger volume is linked to a bigger amount of boards, which raises the probability of a very low shear strength in the beam. The accordance of the simulation and the test results is convincing and enables us to research the volume effect in the following.
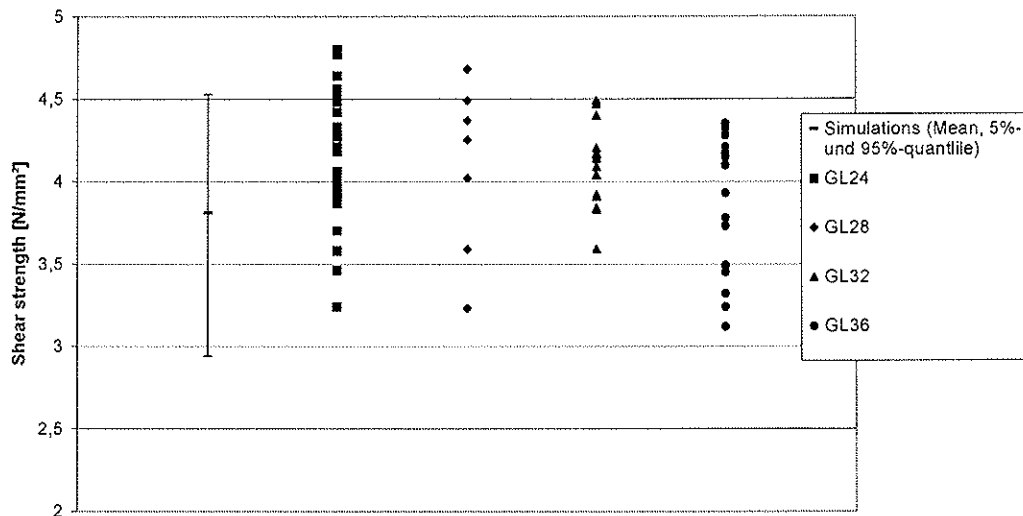
Fig. 2.6:   Comparison of simulations and tests by Schickhofer [2] with a web depth of 352 mm

3   Approximation for the Results of Simulation

3.1   Weibull's Theory

Colling [9] shows how to consider the influence of volume on the shear strength. In the following we will compare Weibull distribution results with those obtained from simulations, whether or how the shear strength capacity of glued laminated timber could be described well.

The survival probability of members with brittle failure may be characterized approximately by a two parameter Weibull's distribution (Colling [9])

$$1 - S = e^{\left(-\int_V \left(\frac{\sigma}{\sigma_0}\right)^k dV\right)} \quad \text{with} \quad k \cong \frac{1,15}{v} \tag{3.1}$$

In this are σ_0 and k two parameters of the Weibull-distribution and v the coefficient of variation received out of test results. The stress distribution can be showed by the maximum value of the shear stress and the function of distribution in length and depth direction of the beam, if the shear stresses are constant over the width as given.

$$\sigma = \sigma_{max} \cdot f(x) \cdot f(y) \tag{3.2}$$

Herewith is

6

$$\int_V \left(\frac{\sigma}{\sigma_0}\right)^k dV = V \cdot \left(\lambda_L \cdot \lambda_H \cdot \frac{\sigma_{max}}{\sigma_0}\right)^k \qquad (3.3)$$

With the coefficient of fullness

$$\lambda_L = \left[\int_0^1 f^k(\varepsilon)d\xi\right]^{\frac{1}{k}} ; \quad \varepsilon = x/l$$

$$\qquad (3.4)$$

$$\lambda_H = \left[\int_0^1 f^k(\xi)d\xi\right]^{\frac{1}{k}} ; \quad \xi = y/h$$

For two beams of the same probability of failure the following relationship will be received:

$$\frac{\tau_1}{\tau_2} = \frac{\lambda_{L,2}}{\lambda_{L,1}} \cdot \frac{\lambda_{D,2}}{\lambda_{D,1}} \cdot \left(\frac{V_2}{V_1}\right)^{1/k} \qquad (3.5)$$

Weibull's parameter k could in principle be defined approximately by use of the coefficient of variation. The simulations bring a COV of $v = 0,14$ and a calculated value of $k = 8,3$ ($1/k = 0,12$). Fig 3.1 shows that the function between the COV and the parameter k has only a small slope for $k = 8,3$. A small mistake would have a big influence for the parameter k. Therefore it is necessary to adjust the value k by test results.
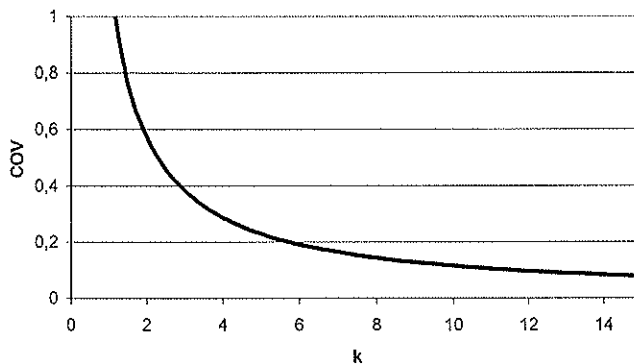
Fig 3.1: Approximation $k = \dfrac{1.15}{v}$

7

3.2 The Effect of Depth

A cross section model, in which the depth is varied, is used. A characteristic shear strength capacity for each depth is obtained by simulations. All cross sections have the same stress distribution and the same probability of failure on the basis of five percent quantiles. Length and width of the beams are neglected. Equation (3.5) is reduced to

$$\frac{\tau_1}{\tau_2} = \frac{\lambda_{L,2}}{\lambda_{L,1}} \cdot \frac{\lambda_{D,2}}{\lambda_{D,1}} \cdot \left(\frac{V_2}{V_1}\right)^{1/k} = \left(\frac{h_2}{h_1}\right)^{1/k} \tag{3.6}$$

For the comparison of simulations and of calculations on the basis of Weibull's theory all results are related to the smallest beam considered.
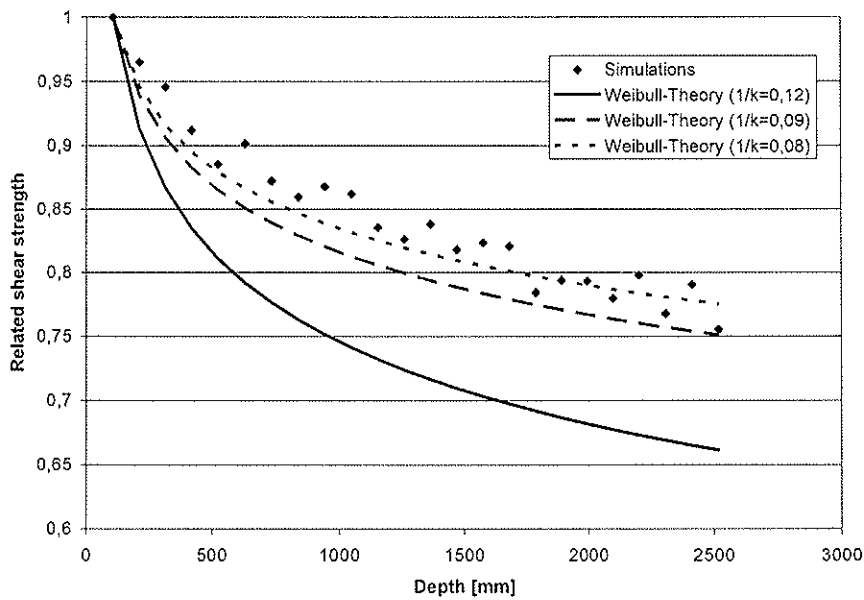
Fig. 3.2:   Related shear strength as a function of beam depth and Weibull's exponent 1/k

The calculated exponent of 0,12 does not describe the depth effect in a satisfying way as supposed, whereas exponents of 0,08 or 0,09 lead to reasonable approximations.

3.3 The Effect of Length

The effect of length is investigated in the same way as the effect of depth. The lengths are varied assuming a constant depth of 600 mm. The results are related to the shortest calculated beam of 2000 mm. The symbols of depth h in equation (3.6) are to be substituted by the length ℓ.
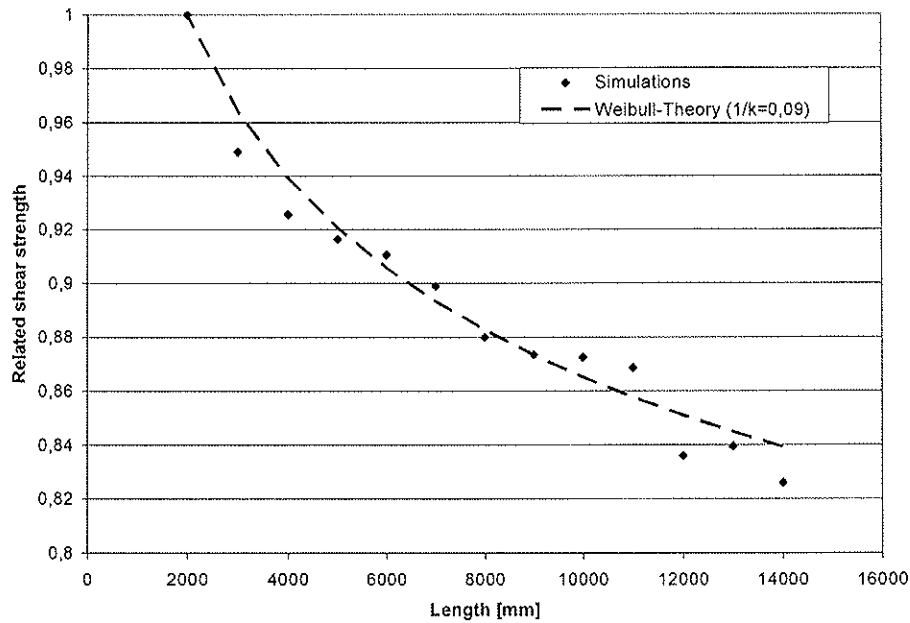
Fig. 3.3:   Related shear strength as a function of beam length

Weibull's equation with an exponent $1/k = 0,09$ fits the results of simulation calculation in a satisfactory way.

3.4   Influence of Stress Distribution

The influence of stress distribution is taken into account by the fullness parameters λ_H and λ_L, determined in accordance with equation (3.4). Theses coefficients have for the most unfavourable case of constant stresses over the depth and the length the value of 1.0. As an alternative to the use of Weibull's equations the coefficients are simulated for identical beams with varying stress distribution. The fullness parameters are received by the quotient of the simulated shear strength of a beam with constant stress distribution and the shear strength of beams with any stress distribution.

The depth factor λ_H is calculated to 0.89 and simulated to 0.90. The use of $\lambda_H = 0.90$ seems to be reasonable.

For the length factor λ_L it is of special interest to regard a uniformly loaded beam, which has a v-shaped line of shear force. The length factor λ_L is calculated to 0.80 and simulated to a mean value of 0.95. The difference appears because the shear strength has been assumed to be constant over the length of the boards for the simulation. Only the maximum shear stress of a board is checked against the shear strength. Therefore the result corresponds to a beam with a constant shear force over the length of a board. If one lamination is built up by three to five boards, each with constant shear strength over the length then $\lambda_L = 0.95$ is calculated and a correspondence with the simulations is made. But for long beams with numerous boards within a lamination the fullness parameter will be smaller than 0.95 but in any case bigger than 0.80.

9
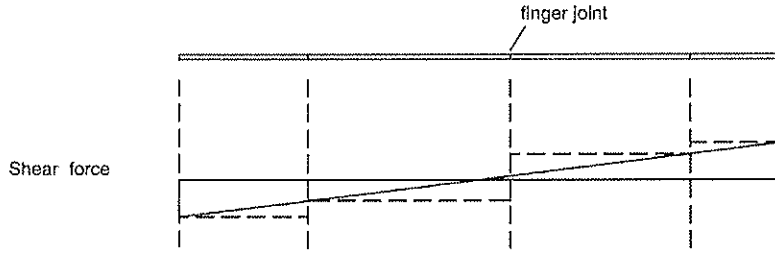
Fig. 3.4: In sections constant shear force assumed in the simulation model for uniformly loaded beams

4   Design Suggestion

A proposal for a design method is made and checked with numerous simulation calculations. The shear strength capacity of any beam may be compared to that of a reference beam by the change of equation (3.5) to

$$f_{v,k} = k_L \cdot k_H \cdot \left(\frac{h_0 \cdot l_0}{h \cdot l} \right)^{0,09} \cdot f_{v,k,0} \tag{4.1}$$

The reference beam is chosen with dimensions $h_0 = 600$ mm and $l_0 = 6000$ mm. The stress distribution in the cross section is parabolic. The uniformly loaded beam has a simulated characteristic shear strength of $f_{v,k,0} = 2,89$ N/mm². Weibull's exponent is proposed to be $1 / k = 0.09$. The coefficients to take into account the stress distribution are received as the quotient of the fullness parameters of the reference beam and any beam.

$$k_L = \frac{\lambda_{L,0}}{\lambda_L} \quad \text{and} \quad k_H = \frac{\lambda_{H,0}}{\lambda_H} \tag{4.2}$$

For a constant shear force over the length $k_L = 0.95$ and a constant shear stress in the cross section $k_H = 0.9$ is proposed.

The equation (4.1) is proved by simulations varying the depths and the lengths of the beams. Furthermore there are checked 60 different geometries with lengths between 2000 and 15000 mm and depths between 200 and 2500 mm. Beams with constant and with v-shaped shear force have been investigated.

The figures 4.1 and 4.2 show the result of the simulations and the plotted design proposal. The correlation is good. For the uniformly loaded beams the deviations from the design line are a little bit higher than for beams with a constant shear force. This could be improved by a higher number of simulations.

10
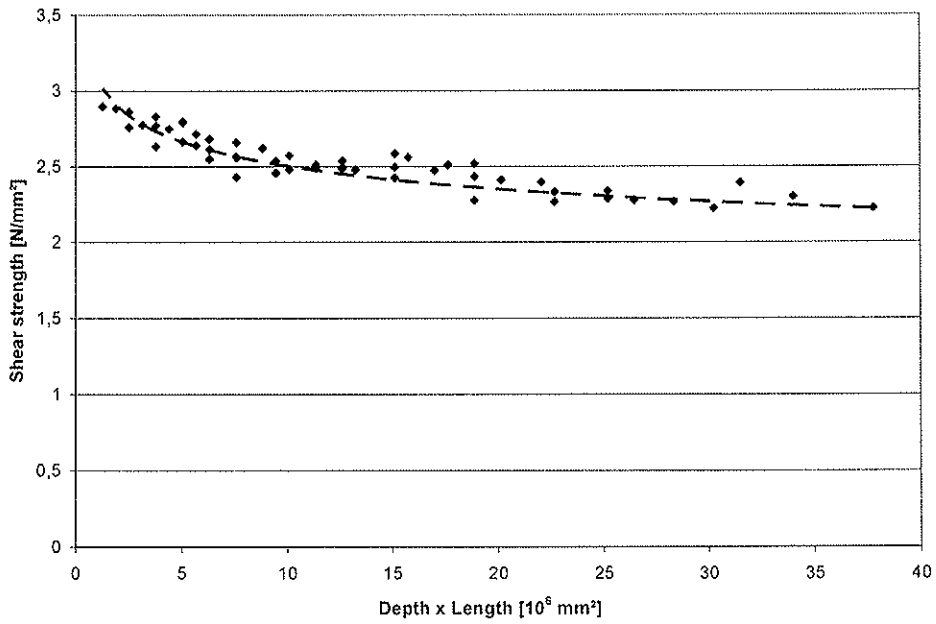
Fig. 4.1:   Maximum shear strength as a function of the stressed area, beams with constant shear force
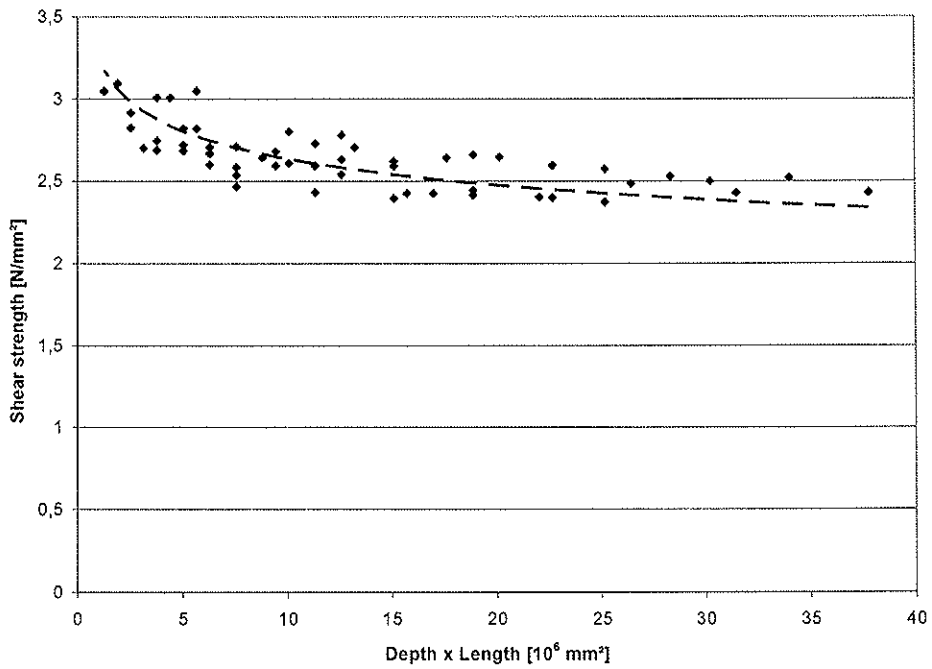
Fig. 4.2:   Maximum shear strength as a function of the stressed area, beams uniformly loaded

11

5 Conclusions

A mathematical model was used to simulate the shear strength capacity of glued laminated timber beams. The varying properties of the material and the influence of different dimensions were introduced. Good correspondence between the results of simulation and tests made in Graz were found. These tests by Schickhofer [2] have been made with relatively small specimens. Assuming that the simulation procedure developed here is correct a high influence of volume effect is given on the bearing capacity of big glulam beams. This effect has not been taken into account in the present European standards. Big glulam beams are overestimated in their real bearing capacity.

Based on a large amount of simulations in this study a design method is proposed, which improves the current rules and is easily to handle in practice. Caused by the assumptions of the model it is possible that the proposed method is conservative. A brittle failure of the beams was assumed and a rearrangement of shear forces in load bearing areas was not taken into account.

Some further simulation calculations have been made with different coefficients of variation (COV). The characteristic strength was adjusted; the other results did not change in principle. It is recommended to perform more tests with glulam beams to get a reliable shear strength for a reference beam. As alternative the shear strength of laminations could be defined, serving as a basis for further simulations.

6 Literature

[1]   EN 1194: Timber Structures – Glued laminated timber – Strength classes and determination of characteristic values, April 1999

[2]   Schickhofer, G.: Determination of Shear Strength Values for GLT using Visual and Machine Graded Spruce Laminations, CIB-W18-Meeting, Paper 34-12-6, Venice, Italy, August 2001

[3]   DIN 1052: Design of timber structures - General rules and rules for buildings, August 2004

[4]   EN 408: Timber structures - Structural timber and glued laminated timber - Determination of some physical and mechanical properties, August 2003

[5]   Glos, P., Denzler, J.K.: Kalibrierung der charakteristischen Schubfestigkeits-kennwerte für Vollholz in EN 338 entsprechend den Rahmenbedingungen der nationalen Sortiernorm, Technische Universität München, Bericht Nr. 04502, August 2004

[6]   Spengler, R.: Festigkeitsverhalten von Brettschichtholz unter zweiachsiger Beanspruchung – Ermittlung des Festigkeitsverhaltens von Brettlamellen aus Fichte durch Versuche. Sonderforschungsbereich 62, Heft 62. Laboratorium für den konstruktiven Ingenieurbau (LKI) Technische Universität München, 1982

[7]   Larsen, H.J.: Strength of Glued Laminated Beams, Part 2 (Properties of Glulam Laminations), Report No. 8004, Institute of Buildung Technology and Structural Engineering, Aalborg University, Aalborg, Dänemark, 1980

[8]   Ehlbeck, J. / Colling, F.: Biegefestigkeit von Brettschichtholz in Abhängigkeit

von Rohdichte, Elastizitätsmodul, Ästigkeit und Keilzinkungen der Lamellen, der Lage der Keilzinkungen sowie von der Trägerhöhe, Teil A: Karlsruher Untersuchungen, Forschungsbericht der Versuchsanstalt für Stahl, Holz und Steine, Abt. Ingenieurholzbau, Universität Karlsruhe, 1986

[9]   Colling, F.: Influence of volume and stress distribution on the shear strength and tensile strength perpendicular to grain CIB-W18-Meeting, Paper 19-12-3, Florence, Italy, 1986

INTERNATIONAL COUNCIL FOR RESEARCH AND INNOVATION
IN BUILDING AND CONSTRUCTION

WORKING COMMISSION W18 - TIMBER STRUCTURES

A NUMERICAL INVESTIGATION ON THE SPLITTING STRENGTH OF BEAMS LOADED PERPENDICULAR-TO-GRAIN BY MULTIPLE DOWEL-TYPE CONNECTIONS

M Ballerini

M Rizzi

University of Trento

Department of Mechanics & Structural Engineering

ITALY

Presented by M Ballerini

A. Jorissen asked and received explanation from M Ballerini about the form of Figure 8 in the paper. M Yasumura said similar work in pure tension was done previously and it will be interesting to compare results. He also questioned that since there is no shear between the two dowels, how can one explain the results. H Blass agreed that the shear force in that area is zero, however the Eurocode is derived from the single dowel case. M Ballerini mentioned that data is not available for his case and should look into whether it is conservative. H Blass mentioned that Eurocode is not meant to address the two dowels case. M Yasumura mentioned that if the spacing between the dowels is big enough cracks will propagate in each dowel. One has to be careful when applying Eurocode 5.

A numerical investigation on the splitting strength of beams loaded perpendicular-to-grain by multiple dowel-type connections

Marco Ballerini, Mirko Rizzi

University of Trento, Department of Mechanics & Structural Engineering, Italy

Abstract: The paper presents a numerical study on the splitting strength of timber beams loaded perpendicular-to-grain by dowel-type connections. The aim of the parametric numerical investigation is to find out the influence of main connections parameters on beams splitting strength.
The analyses are carried out in the framework of Linear Elastic Fracture Mechanics (LEFM). They are performed on beams loaded at mid-span by both single and multiple dowel connections. The strength of beams is derived by means of stress intensity factors (SIFs) at the crack tips in mode I and II through the classical Wu's fracture criterion.
The main investigated parameters are the connection width (l_r), the connection depth (h_m), and the number of rows of fasteners (n); they are analysed for different beam heights (h) and for different distances of the furthest row of fasteners from loaded edge (h_e).
The numerical results are compared with relationships embodied in a new semi-empirical prediction formula – based on a statistical survey on experimental data – recently developed by the author.
The first part of the paper presents shortly the new semi-empirical prediction formula and its prediction ability. The second part of the paper reports the main results of the parametric numerical analyses and their comparison with the effect assumed by the semi-empirical prediction formula. Finally, the strength of a beam with a complex connection is numerically investigated and the result compared with the experimental data and the predicted value.

1 INTRODUCTION

In the design of connections which transfer forces to timber elements in direction perpendicular-to-grain it should be carefully taken into account the splitting strength of beams rather than the one connections. Indeed, it is well known that the formation and the propagation of a crack along the grain of timber elements is a possible failure mechanism which can lead to ultimate loads considerably lower than the ones of connections.
This is particularly true when the distance from the beam loaded edge of the furthest row of fasteners (h_e) is small compared to the beam height (h).
Due to this reason connections which transfer forces perpendicular-to-grain should be placed far from the beam loaded edge or properly reinforced as suggested by Blass & Bejtka in [1].

The prediction of the splitting strength of timber beams loaded perpendicular-to-the-grain is a difficult task since it is influenced by a large number of parameters.
They are the height (h) and the thickness (b) of beams and, in the case of dowel-type connections, the distance of the furthest row of fasteners from the beam loaded edge (h_e), the height (h_m), the width (l_r), the number of rows (n) and the number of columns (m) of connections.

The splitting strength of beams loaded perpendicular-to-grain by dowel-type connections can be predicted theoretically, semi-empirically and numerically.
The most important theoretical prediction formula has been developed by T.A.C.M. van der Put in [2]. In his work, by means of an energetic approach in the framework of Linear Elastic Fracture Mechanics (LEFM), he developed a formula which is actually assumed as basis for design in the new European code for timber structures EN 1995-1-1:2004 [3].

At the class of semi-empirical prediction formula belong the ones developed by Ehlbeck, Görlacher & Werner in [4] and recently by Ballerini in [5].

The one of Ehlbeck, Görlacher & Werner is based on both empirical and theoretical considerations according to both experimental results and Weibull's failure theory; this prediction formula, with some little changes essentially due to simplification intentions, is actually embodied in the new German design standard for timber structures DIN 1052:2004 [6].

The one of Ballerini has been recently developed on the basis of both a statistical survey of experimental data available from literature (628 test results) and on the main results of theoretical and numerical works. The formula assumes the soundness of the van der Put LEFM energetic approach but, differently from that, it takes into account the effect of connections geometry as clearly shown up by tests results.

The prediction of splitting failure loads of timber beams can be profitably pursued also with numerical approaches. Although actually there are no prediction formulas based on numerical results, it has been widely demonstrated that it is possible with numerical analyses in the framework of Linear Elastic Fracture Mechanics (LEFM) found the failure loads of beams loaded by single-dowel connections (Ballerini & Bezzi [7], Acler [8]) and by multiple-dowel connections (Borth & Rautenstrauch [9]).

The paper follows the above mentioned numerical approach to determine the failure loads of beams loaded at mid-span by single-dowel and by multiple-dowel connections when crack propagation occurs.

It illustrates the main results of a still in progress parametric numerical investigation on the splitting strength of beams loaded by dowel-type connections with different geometry.

The investigated parameters are the connection width (l_r), the connection depth (h_m), and the number of rows of fasteners (n); they are analysed for different beam heights (h) and for different distances of the furthest row of fasteners from loaded edge (h_e).

The analyses are carried out in the framework of Linear Elastic Fracture Mechanics (LEFM) by means of the commercial FE program ANSYS 8.0. The strength of beams is derived for different values of the crack lengths by means of the evaluation of the stress intensity factors (SIFs) for unit load at the crack tips (in mode I and II) via the classical Wu's fracture criterion [10]. The crack length is assumed to be line with the furthest row of fasteners from loaded edge. The splitting failure load is the maximum value of curve F-a (failure load – half crack length). The length at which the load is maximum identifies the critical crack length; up to the critical crack length the crack propagation is stable, over this value the crack propagation is instable.

The main aim of the analyses is to obtain the influence of the investigated connection parameters: the width (l_r), the depth (h_m) and the number of rows of fasteners (n). As a consequence the results allow to verify the consistency of the semi-empirical prediction formula proposed by the author [5]. When possible the numerical results are compared with the experimental data available from literature.

The first part of the paper presents synthetically the semi-empirical prediction formula developed by Ballerini [5.] The second part of the paper shows the main results of the on going numerical analyses. Initially, the results of beams loaded by single-dowel connections are illustrated and compared with the ones reported in [7, 8]. Successively, the outcomes of the analyses on beams loaded by 1 row of 2 fasteners with different spacing (l_r), and the ones on beams loaded by a column of fasteners with different total connection height (h_m) and/or different number (n) of fasteners, are shown. The numerical results are compared with the values of the prediction formula and, when possible, with the experimental data.

Finally, the results for a beam loaded with a more complex connection is illustrated and compared directly with test data and prediction formula values.

2   THE NEW SEMI-EMPIRICAL PREDICTION FORMULA

This chapter gives a short description of the semi-empirical prediction formula developed by Ballerini in [5]. The purpose of this presentation is to facilitate the following comparison with the numerical results. The prediction formula is based on the experimental data available in literature. A total amount of 628 test results on beams loaded by dowel-type connections at mid-span or at one end have been considered; the specimens were simply supported or cantilevered beams.
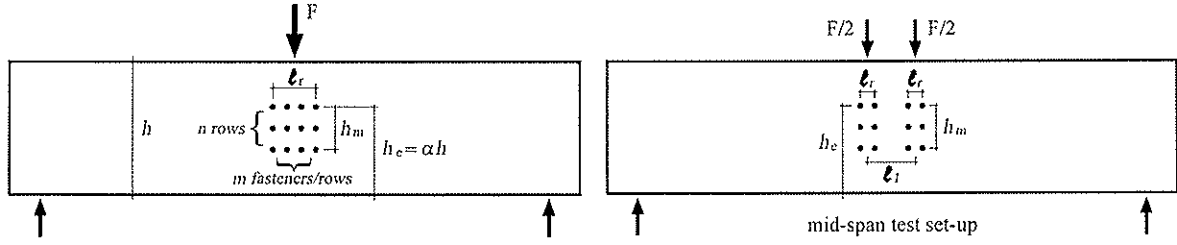
Figure 1 – Parameters of connections geometry in case of compact connections (left) and for connections made with two cluster of fasteners (right).

The beams parameters (b, h) and the ones of the connections geometry (α, h_m, l_r, l_1, n and m), see figure 1, have been investigated essentially in the following ranges:

b = 40÷200 mm; h = 88÷1200 mm;
α = 0.10÷0.75; h_m = 0÷90 mm (some data with 200 and 500 mm);
n = 1÷6; l_r = 0÷200 mm (some data 320, 420, 700 mm);
m = 1÷4 (some data 5, 10); l_1 = 0÷240 mm (some data up to 784 mm).

The majority of the experimental specimens had connections made with dowel fasteners (10÷30 mm); nevertheless, some specimens had used nail connections (4, 6 mm) or ring connectors (Appel ring, 65 mm in diameter).

Experimental results have shown that tests characterized by α values up to 0.7 fail by splitting of beams due to the propagation of a crack in line with the furthest row of fasteners.

With respect to the splitting strength, the following main outcomes can be driven:

(1) it is proportional to the beams thickness but influenced not-linearly by the beams height;

(2) it depends greatly by the distance from the loaded edge of the furthest row of fasteners;

(3) it is considerably influenced from the other connections parameters (h_m, l_r, l_1, n and m);

(4) it seems not influenced by type and size of fasteners and also by beams slenderness (L/h).

On the basis of the reported results, a prediction formula able to take into account the effect of the main parameters on the splitting strength of beams loaded by both single-dowel and multiple-dowel connections has been developed.

It has been derived initially for the case of single dowel connections, in this case only b, h, and α (or $h_e = \alpha h$) are significant parameters, and successively extended to cases of connections made with 1 row and with more row of fasteners (for further details see [5]).

According to Larsen's suggestions, the prediction formula can be written as follows:

$$F_{u,pre} = 2b \cdot 14 \cdot \sqrt{\frac{h_e}{1-\alpha^3}} \cdot f_w \cdot f_r \tag{1}$$

$$f_w = 1 + 0.75 \cdot \frac{l_r + l_1}{h} \leq 2.0 \tag{2}$$

$$f_r = 1 + 1.75 \frac{n \cdot h_m / 1000}{1 + n \cdot h_m / 1000} \tag{3}$$

Equations (2) and (3) represent respectively the effect of the connections width (l_r and l_1) and the one of connections height (h_m and n). Equation (1) without terms f_w and f_r predicts the basic splitting strength of beams loaded by single-dowel connections.

On the basis of the recorded coefficient of variation (cov ≅ 0.20, see ref. [5]), the following expression for the characteristic splitting strength can be derived:

$$F_{R,k} = 2b \cdot 9 \cdot \sqrt{\frac{h_e}{1-\alpha^3}} \cdot f_w \cdot f_r \tag{4}$$

Figures 2, left and right, reports respectively the prediction capability of eq. (1) and the ratios $F_u/F_{R,k}$ versus the non dimensional parameter α. From the first graph it is easy to appreciate the

3
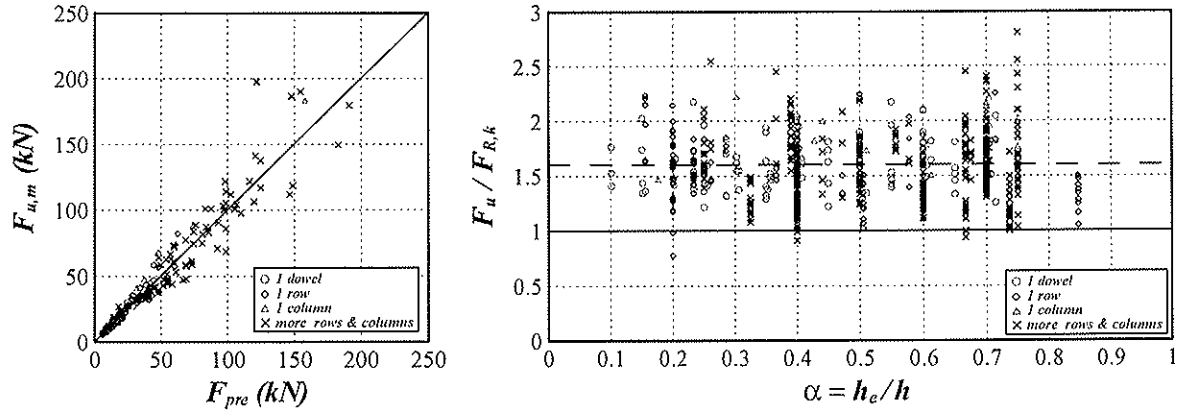
Figure 2 – Average splitting failure loads versus predicted values (left); ratios of failure loads with respect to predicted characteristic values versus α (right).

good prediction ability on the whole load range; from the latter one it is possible to notice no residual effect of α, moreover it is also detectable that the average strength is about 1.6 times the characteristic one and that quite all data have a strength lower than 2.5 times the predictable characteristic value.

3   PARAMETRIC NUMERICAL ANALYSES

The numerical analyses have been performed by means of the commercial FE program ANSYS 8.0 in the framework of Linear Elastic Fracture Mechanics (LEFM).

The splitting failure loads of beams have been derived for each crack length through the classical Wu's fracture criterion; to this aim, for each crack length, the stress intensity factors in mode I and mode II for unit load (k_I and k_{II}) have been computed on the basis of numerical results.

The stress intensity factors have been evaluated by means of different calculation techniques: the crack opening displacement method COD (developed by Chen & Kuang [11] and recently by Guinea, Planas & Elices [12]), and the virtual crack closure integral method; for further details see ref. [7]. Since both evaluation techniques give about the same results, only the stress intensity factors evaluated with the COD method are reported in the following.

The analyses, actually still in progress, have been carried out in plane stress conditions. Cracks have been assumed to be line with the furthest row of fasteners from loaded edge. The beam has been modeled with the following orthotropic parameters: E_x = 11000 MPa, E_y = 890 MPa, G_{xy} = 760 MPa, v_{xy} = 0.37.

Far away from crack tips, rectangular CPS8 and triangular CPS6 elements (continuous plane stress 8-nodes or 6-nodes elements) with size ranging from 0.5 to 10 mm have been used. The crack tips have been modelled with 16 collapsed CPS8 quarter point elements. At the connection, contact surfaces CONTACT 48 have been used between the beam elements and the dowel ones with a friction coefficient of 0.1. A typical mesh details at crack tips and at the dowel/beam contact is shown in figure 3.

The analyses have been performed on beams with single-dowel connections (only for comparison purposes), on beams loaded by a connection made with 1 row of two fasteners and on beams with connections made with 1 column of different fasteners. In this latter case, the analyses have been carried out for a unit vertical displacement of fasteners.

In the following the three set of analyses will be presented separately.

3.1   Analyses on beams with single-dowel connections

The analyses on beams loaded by single dowel connections have been performed only to tests the results provided by FE program ANSYS 8.0 with respect to those supplied by the more renowned FE program ABAQUS. Indeed, the splitting strength of 200 and 400 mm high beams has been already

4
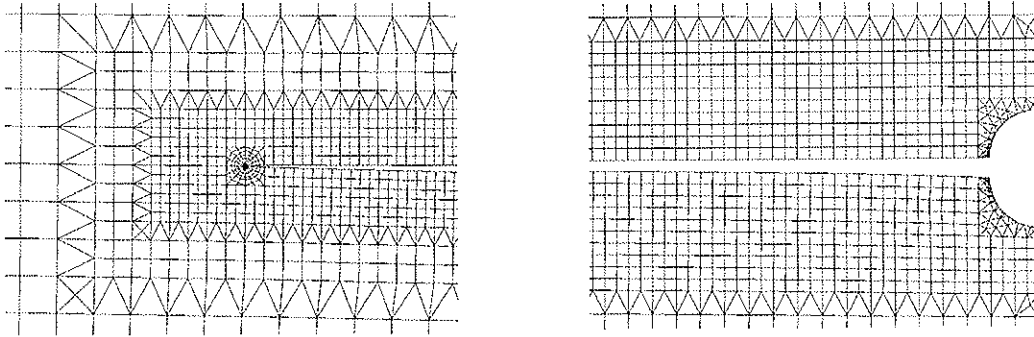
Figure 3 – Mesh details at crack tips (left) and at the dowel/beam contact

investigated in [7] and [8] with the FE program ABAQUS 6.2. In current research, only 200 mm high beams with values of α ranging from 0.2 to 0.8 have been considered.

The numerical results are summarized in figures 4-6. Figure 4 reports the stress intensity factors for unit load and for different α values. From the figure it is possible to notice a good agreement for the stress intensity factors in mode I while a lower agreement is detectable among the stress intensity factors in mode II. Figure 5 shows the numerical failure loads derived via the Wu criterion; also in this case a good agreement between the results of the two FE program is evident due to the fact that stress intensity factors in mode II have a limited effect in Wu's criterion. Finally, figure 6 illustrates the numerical (both FE programs), the experimental and the predicted failure loads versus α. From figure 6 it is possible to notice a good agreement between test data and both numerical/predicted values for α ratios lower than 0.5; for larger α values, it is apparent that only predicted values are again in good agreement while both numerical curves tend to overestimate tests data.
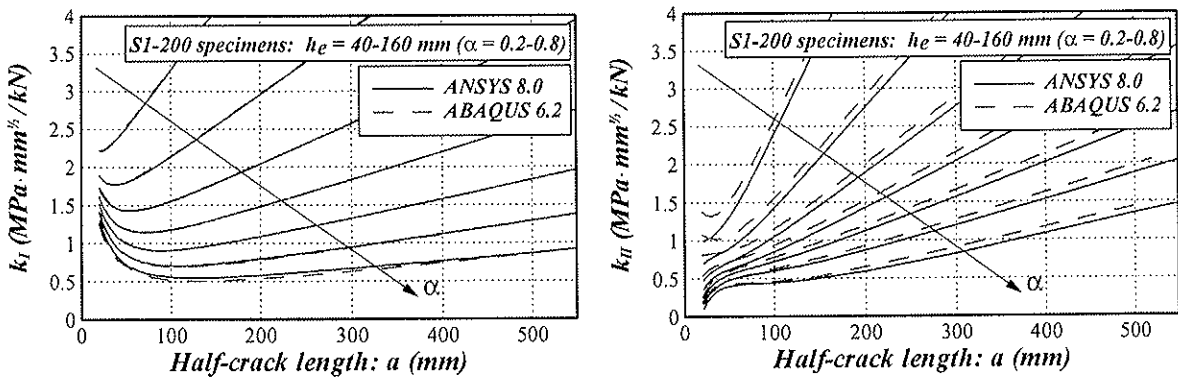
Figure 4 – Comparison between K_I (left) and K_{II} (right) values for unit load computed with ANSYS 8.0 and ABAQUS 6.2 FE programs.
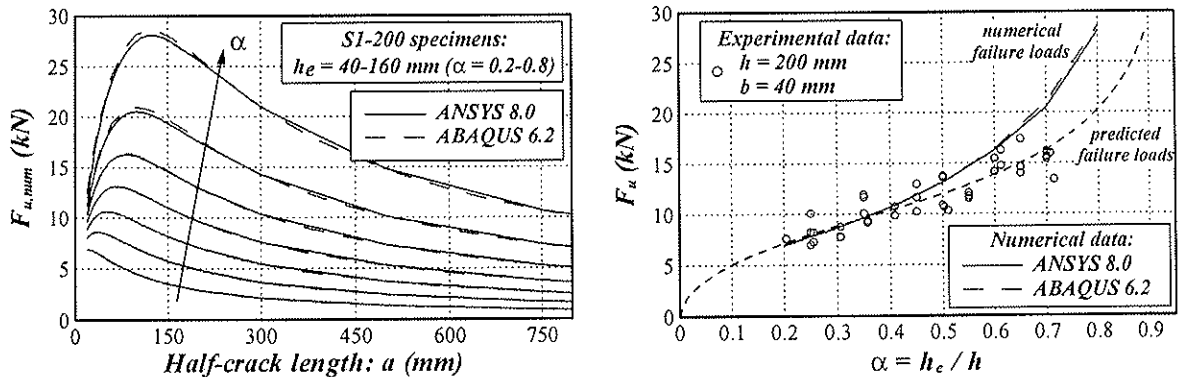
Figure 5 – Numerical failure loads evaluated on the basis of numerical SIFs by mean of Wu fracture criterion.
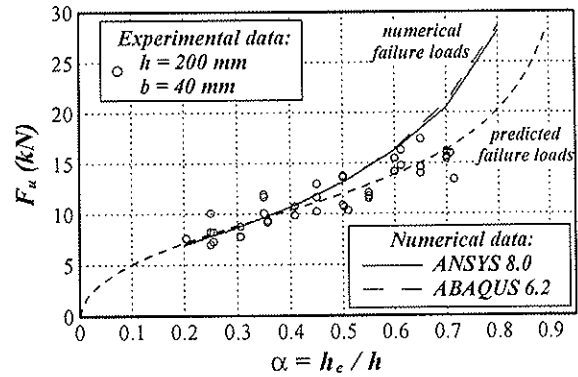
Figure 6 – Failure splitting loads versus α : experimental data, numerical values and predicted values.

5

3.2 Analyses on beams with connections made with 1 row of 2 fasteners

The analyses performed on specimens loaded by connections made with 1 row of 2 fasteners (in line with grain direction) characterized by different values of connections width (l_r), have been carried out to get the influence of connections width on the overall splitting strength of beams. This influence is accounted by the semi-empirical prediction formula by means of the corrective factor f_w (see eq. (2)).

The parametric investigation has taken into account 2 beam sizes (120 and 240 mm), 3 different α values (0.23 – 0.47 – 0.7 for 120 mm high beam and 0.12 – 0.23 – 0.47 for the 240 mm high one) and 7 values of the connection width l_r (0 – 10 – 19 – 38 – 76 – 152 – 304 mm). The beam size of 120 mm and the connection with investigated, have been selected to compare the numerical results with test data provided by Möhler & Lautenschläger (serie C) [13].

The typical FE mesh adopted for these analyses is illustrated in figure 7 left; figure 7 right shows the σ_{22} stress contours close to maximum numerical load.

The numerical splitting failure load as a function of half-crack length (a) are summarized in figure 8; the reported values of half-crack length are the distances from mid-span of the crack tip nearest to beam end.

Each curve plotted in graphs of figure 8, is the result of an automated crack propagation procedure based on Wu's crack propagation criterion. The procedure can be synthetically described as follows: (1) the stress intensity factors at both crack tips (the one in the direction of beam end and the one in the direction of beam mid-span) are evaluated in each analysis; (2) the minimum load which satisfy the Wu's crack propagation criterion is determined; (3) for the next analysis, the crack is opened in the direction at which the Wu's criterion is activated. Consequently, each curve is the result of about 100 analyses.

The fracture toughness in mode I used in Wu's criterion is the one obtained for the specimens with single-dowel connections; it is $K_{IC} = 0.493$ MPa·m$^{\frac{1}{2}}$ (K_{IIC}/K_{IC} has been fixed equal to 3) and is in line with literature data for spruce [14].

From graphs of figure 8 it is possible to notice a general great effect of connection width l_r on the splitting strength of beams. Indeed, a great increase in strength it is evident up to the complete opening of the crack in between of fasteners. After this, the failure loads severely decrease up to about the values of beams loaded with single-dowel connections.

The maximum splitting load, which corresponds to the beginning of the instable crack propagation, is usually reached before the complete development of the crack in between the two fasteners.

This general trend is not true when the connection width is small compared to beam height h and to parameter α. Indeed, it is clearly detectable that splitting failure loads of specimens with small l_r values are lower than the ones of corresponding specimens with single-dowel connection especially when α and h increase.

The above considerations are more evident in graphs of figure 9 where the strength increase for the investigated specimens are plotted with respect to the connection width l_r and to the ratio l_r/h.

From the right graph it is possible to notice that the maximum strength increase is greatly influenced by the α values. It is of about 100% for α values up to 0.233, of about 80% for $\alpha = 0.467$, and of about 55% for $\alpha = 0.7$. The maximum increment is reached when the ratio l_r/h is greater than 1.25. The shape of the increment for l_r/h values lower than 1.25 is greatly affected by α values and in less amount by beam height h. Particularly, as above mentioned, it is evident the lack of strength increase for ratios l_r/h lower than 0.16 when α is greater than about 0.45.
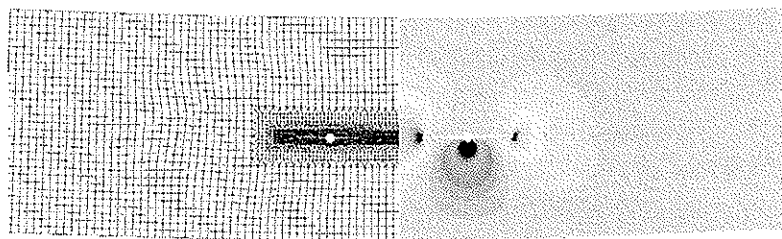
Figure 7 – FE mesh for the analyses of specimens with 1 row of two dowels and different connection width l_r (left); σ_{22} stress contours close to maximum load (right).
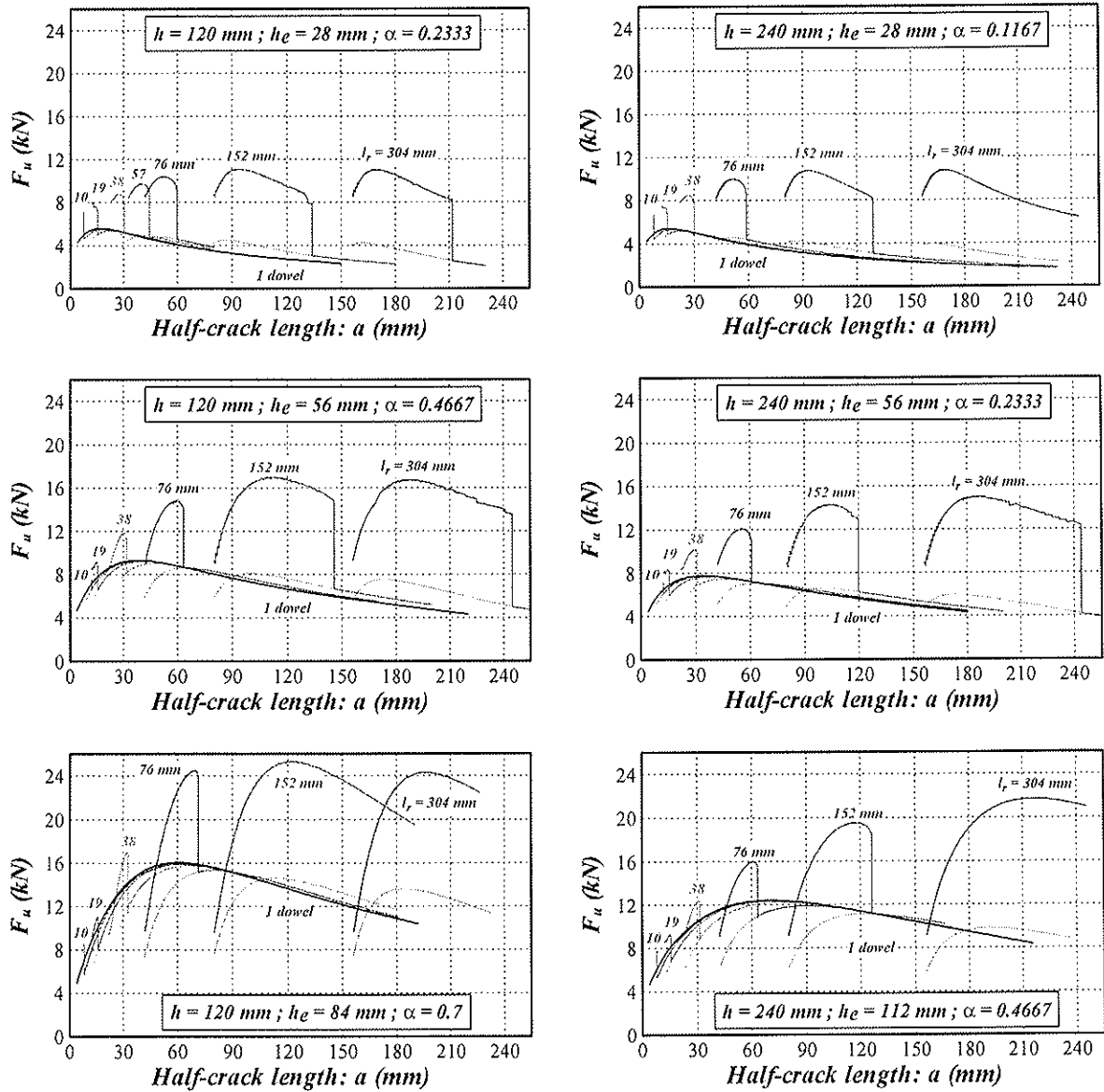
Figure 8 — Numerical failure splitting loads of beams loaded at mid-span by connections made with 2 fasteners at different spacing (l_r) versus half-crack length (half distance between furthest crack tips).
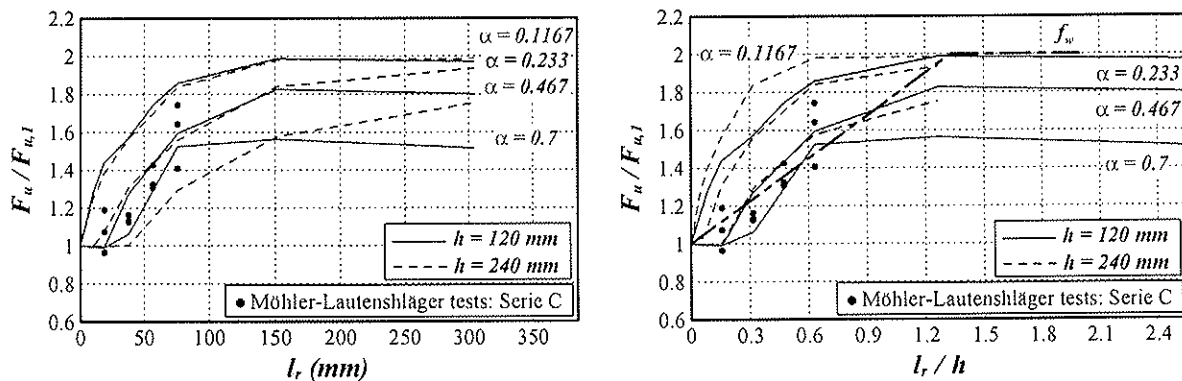
Figure 9 — Strength increase of specimens with 1 row of 2 fasteners as a function of the connection width l_r (left) and the ratio l_r/h (right).

On the same graphs the experimental results of Möhler and Lautenschläger, serie C tests (h=120mm, h_e = 28 mm, α = 0.233), are reported. From graphs it is apparent a quite large overestimation of experimental results even if the general trend is in accord. The right graph reports also the corrective factor f_w of the semi-empirical prediction formula (eq. (2)); although it doesn't take into account the effect of α, it is in good agreement both with test results and with the upper limit for the maximum strength increase.

3.3 Analyses on beams with connections made with 1 column of fasteners

These analyses have been carried out to evaluate the influence of parameters linked to connection depth: h_m and n. These parameters are taken into account by the semi-empirical prediction formula in the corrective factor f_t (eq. (3)).

For this parametric investigation, 180 mm high beams loaded at mid-span by connections made with 1 column of fasteners have been considered. The investigated parameters are: the number of fasteners in column (n = 2, 3, 4, and 5), the connection depth (h_m ranging from 19 to 76 mm), and 3 different α values (α = 0.37, 0.47, 0.58). As above already mentioned, the stress intensity factors have been computed imposing the same transversal displacement at all fasteners.

The numerical results are summarized in figures 10 and 11. In the first figure, the left graph reports the failure loads of beams loaded by a connection made with 1 column of 2 fasteners for different h_m and α values. The right graph shows the failure loads of specimens loaded by 3 different set of connections made with 1 column of fasteners; each set has constant h_m value (and consequently constant α value) and different number of fasteners.

From both graphs of figure 10 it is apparent that strength increases both with the connection depth h_m and also with the number of fasteners in column. Differently from the case of the connection width where two different cracks generate an abrupt change in beam strength when join together, these parameters
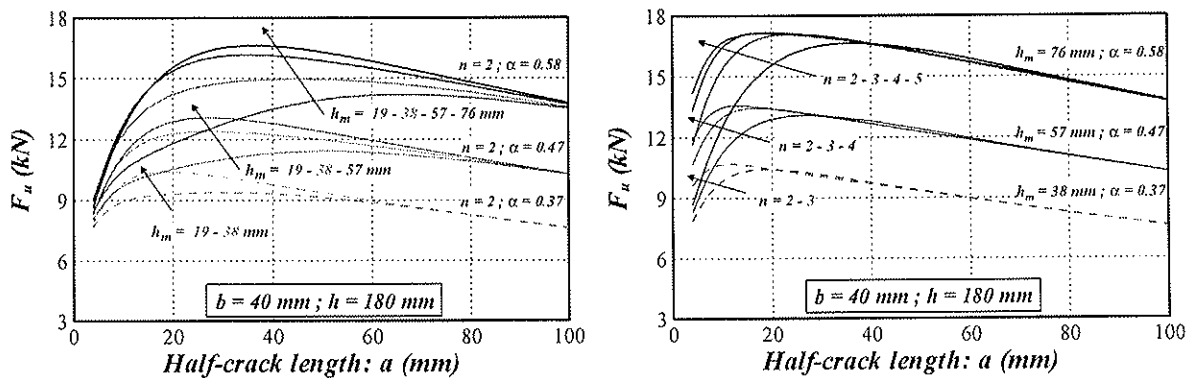
Figure 10 – Numerical failure loads vs half-crack length of specimen with 1 column of fasteners: 2 fasteners with different h_m (left); various number of fasteners with constant h_m (right).
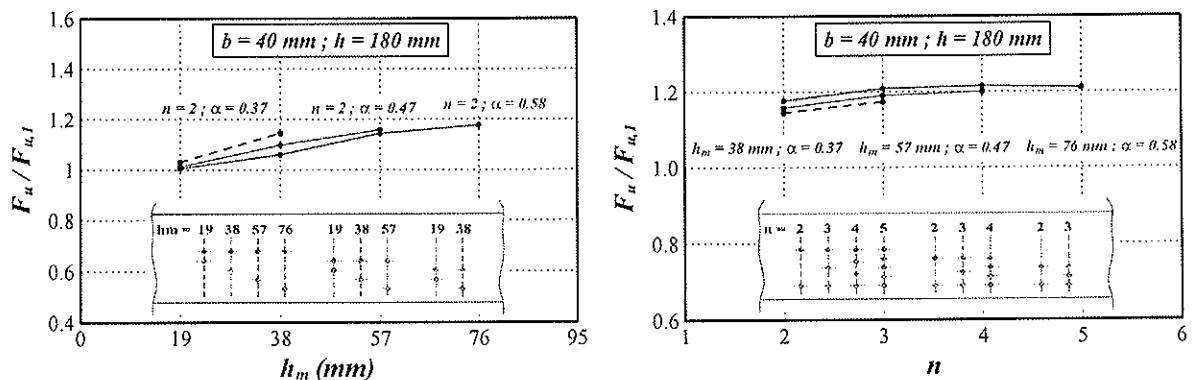
Figure 11 – Influence on strength of: connection height h_m for different α values and n=2 (left); the number of fasteners in 1 column n for different h_m and α values (right).

8

don't affect so greatly the curves F-a. The change in strength is associated to a decrease of the value of the critical half-crack length in the case of constant h_m (right graph), while it is only quite true for the case of connections made with 2 fasteners (left graph).

The graphs of figure 11 show the strengths increase for both set of analyses. From the left graph it is possible to notice the limited effect of connection depth h_m for different α values and for $n = 2$. The maximum increment is of about 20%, it grows up quite linearly with h_m and for same h_m is lower for higher α values. From the right graph it is evident the very limited effect of n; it is quite detectable up to a value of $n = 3$ while it seem quite negligible for higher n values.

The detected effects of both h_m and n highlights a quite large discrepancy between the numerically evaluated effects and the corrective factor f_r of the semi-empirical prediction formula calibrated on the basis of experimental data.

4   A CASE STUDY

To verify the possibility of the numerical prediction of the splitting failure load of beam loaded by a more realistic dowel-type connection, the specimen V11 of the Möhler and Siebert experimental research [15] has been investigated.

The specimen is a glulam beam with a size of 100 by 600 mm, loaded at mid-span by a connection made with 4 rows of 3 dowels (of 16 mm in diameter) and the following connection parameters: $\alpha = 0.5$, $l_r = 205$ mm, $h_m = 240$ mm.

The FE mesh (only half specimen has been modeled) together with σ_{22} stress contours at a load level close to maximum failure load is reported in figure 12.

Figure 13 reports the F-a curve together with the experimental and predicted splitting failure loads.

As expected, the curve drops dramatically when the tips of both cracks in the direction of mid-span join together. The maximum splitting load is reached when the tips of cracks in direction of beam ends are about 130 mm from mid-span.

Comparing the experimental, the numerical and the predicted failure loads, it is evident that in this case there is a good agreement between the 3 values.

Figure 12 – FE mesh and σ_{22} stress contours (2 separate cracks) for specimen V11 of Möhler & Siebert experimental research.
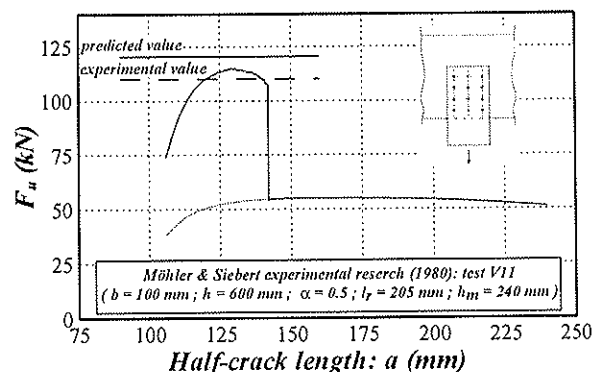
Figure 13 – Test V11: comparison between the numerical failure load, the experimental and the predicted ones.

5   CONCLUSIONS

A parametric numerical investigation on the splitting strength of beams loaded by different multiple-dowel connections has been presented in its main aspects. The aim of the numerical parametric study is the investigation of the effect of connections geometrical parameters on the overall splitting strength of beams. For comparison purpose, a recently derived semi-empirical formula based on both numerical and experimental results has been shortly illustrated.

Although the analyses are still in progress, from the intermediate results the following outcomes can be driven:

- numerical analyses on beams loaded by single-dowel connections tends to overestimate the strength of specimens characterized by α values greater than 0.5;
- the analyses on beams loaded by connections made with 1 row of 2 fasteners have highlighted the large strength increase due to parameter l_r. The analysis of numerical results has stress out that the strength increase is essentially a function of l_r/h, the maximum increase is equal to 100% and that parameter α plays a non secondary role. The numerical results are partially in accord with the proposed corrective factor f_w of the semi-empirical formula while are quite not in good agreement with test results;
- the analyses on beams with 1 column of fasteners have shown the limited effect of parameters h_m and n on the ultimate loads. This result it is not in accord with the corrective factor f_r of the semi-empirical formula which is based on test results;
- on contrary, the numerical analysis on specimen V11 (which represents a more realistic connection) has shown the good prediction ability of both numerical approach and prediction formula.

From the above considerations, it is evident that to better understand the effect of different connection parameters, more numerical investigations are necessary especially to get out the effect of α on f_w. Moreover the effect of m and l_1 should be investigated.

References

[1] Blass, H.J. and Bejtka, I., "Reinforcements perpendicular to grain using self-tapping screws", in Proceedings of 8th World Timber Engineering Conference, WCTE 2004, Lahti, Finland, June 2004.

[2] T.A.C.M. van der Put, "Tension perpendicular to the grain at notches and joints", in Proceedings of CIB-W18 Conference, paper 23-10-1, Lisbon, Portugal, Sept. 1990.

[3] EN 1995-1-1: 2004, "Eurocode 5 - Design of timber structures. Part 1-1: General rules and rules for buildings", CEN/TC 250/SC5, 2004-11-01.

[4] Ehlbeck, J., Görlacher, R. and Werner, H., "Determination of perpendicular-to-grain tensile stresses in joints with dowel-type fasteners: a draft proposal for design rules", in Proceedings of CIB-W18 Conference, paper 22-7-2, Berlin, German Democratic Republic, Sept. 1989.

[5] Ballerini, M., "A new prediction formula for the splitting strength of beams loaded by dowel-type connections", in Proceedings of CIB-W18 Conference, paper 37-7-5, Edinburgh, Scotland, Aug. 2004.

[6] DIN 1052:2004-08, "Design of timber structures – General rules and rules for buildings", DIN, Germany, 2004.

[7] Ballerini, M. and Bezzi, R., "Numerical LEFM analyses for the evaluation of failure loads of beams loaded perpendicular-to-grain by single-dowel connections", in Proceedings of CIB-W18 Conference, paper 34-7-6, Venice, Italy, Aug. 2001.

[8] Acler, W., "A numerical study on the splitting strength of beams loaded perpendicular-to-grain by single-dowel connections: influence of geometrical and mechanical parameters", (in Italian), Degree Thesis, University of Trento, Italy, Oct. 2002.

[9] Borth, O. and Rautenstrauch, K., "Estimation of the load-carrying capacity of perpendicular-to-grain bolted timber connections by fracture criterion in the framework of LEFM", in Proceedings of the International RILEM Symposium on "Joints in Timber Structures", Stuttgart, Germany, Sept. 2001.

[10] Wu, E.M, "Application of fracture mechanics to anisotropic plates", *ASME Journal of Applied Mechanics – Series E*, 34 (4) (1967) 967-974.

[11] Chen, L.S. and Kuang, J.H., "A displacement extrapolation method for two-dimensional mixed-mode crack problems", *Engineering Fracture Mechanics*, 46 (5) (1993) 735-741.

[12] Guinea, G.V., Planas, J. and Elices, M., "K_I evaluation by the displacement extrapolation technique", *Engineering Fracture Mechanics*, 66 (2000) 243-255.

[13] Möhler, K. and Lautenschläger, R., "Large perpendicular-to-grain connections in glulam beams", (in German), Forschungsbericht des Lehrstuhls für Ingenieurholzbau und Baukonstruktionen, Universität Karlsruhe, 1978.

[14] Valentin, G.H., Boström, L., Gustafsson, P.J., Ranta-Maunus, A. and Gowda, S., "Application of fracture mechanics to timber structures, RILEM state-of-the-art-report", VTT – Technical Research Centre of Finland, Research Notes 1262, Espoo, Finland, 1991.

[15] Möhler, K. and Siebert, W., "Design of perpendicular-to-grain joints for loads suspending for glulam or timber beams", (in German), Forschungsbericht des Lehrstuhls für Ingenieurholzbau und Baukonstruktionen, Universität Karlsruhe, 1980.

INTERNATIONAL COUNCIL FOR RESEARCH AND INNOVATION
IN BUILDING AND CONSTRUCTION

WORKING COMMISSION W18 - TIMBER STRUCTURES

A PROBABILISTIC FRAMEWORK FOR THE RELIABILITY ASSESSMENT OF CONNECTIONS WITH DOWEL TYPE FASTENERS

J Köhler

Swiss Federal Institute of Technology ETH, Zurich

SWITZERLAND

A probabilistic framework for the reliability assessment of connections with dowel type fasteners

Jochen Köhler

Swiss Federal Institute of Technology ETH, Zurich, Switzerland

1 Introduction

For timber structures, the structural performance depends to a considerable part on the connections between different timber structural members; connections can govern the overall strength, serviceability and fire resistance. Assessments of timber structures damaged after extreme events as storms and earthquakes often point to inadequate connections as the primary cause of damage (Foliente (1998)). Despite their importance codes and regulations for the design of timber connections, however, are not based on a consistent basis compared to the design regulations of timber structural components.

In the daily practice the engineering codes and regulations form the premises for the use of timber as a structural material. Code regulations in North America, Australia and Europe are based on the limit states design (LSD) approach which is implemented via load and resistance factor design (LRFD) formats. Originally, LRFD methods where converted as so called "soft conversions" of allowable stress design (ASD), the design method which was commonly used in code regulations before LRFD was introduced and which is usually based to a major part on experience, tradition and judgment. In the last decade this situation was changed by the use of structural reliability concepts as the basis of design of timber members. This progress was possible by means of collecting a huge amount of experimental data to characterize the statistical variation in timber material properties which facitilitates the formulation of probabilistic models for the behaviour of timber structural members. The resistance factors for members are calibrated employing probability based calibration techniques e.g. in Foschi et al. (2000) and Svensson and Thelandersson (2003). Therefore the design of structural members is based on the same consistent foundation as for other building materials as concrete or steel.[1] Codes for timber connections have been adjusted in recent years to reflect additional data and information on connections (see e.g. in Blass et al. (1999) and Jorissen (1998)), but reliability based design for joints is not yet implemented in the code formats. LRFD for joints is in general still soft-converted from the traditional ASD format (Smith and Foliente (2002)).

Explanations for this imbalance in advancement of design provisions for members and connections can be found in the relative simplicity of characterising mechanical behaviour

---

[1] Note that this is only the case for very general design situations, i.e. situations comparable to laboratory conditions in regard to the way and time of loading, surrounding climate and member size. Deviations from these conditions are not yet considered in a consistent manner.

of members, as compared to connections. A diversity of connections types is used in practise and these types have infinite variety in arrangement. This usually precludes the option of testing large numbers of replicas for a reliable quantification and verification of statistical and mechanical models.

For commonly used connections, a distinction is made between carpentry joints and mechanical joints that can be made from several types of fasteners. An overview of timber connections can be found in the literature, e.g. in Thelandersson and Larsen (2003). The mechanical joints are divided into two groups depending on how they transfer the forces between the connected members. The main group corresponds to the joints with dowel type fasteners. Connections with dowels, nails, screws and staples belong to this group. The second type includes connections with fasteners such as split-rings, shear-plates and punched metal plates in which the load transmission is primarily achieved by a large bearing area at the surface of the members.

In the course of this paper it is discussed how a probablilistic model for connections can be derived. It is focused on connections with dowel type fasteners, more precicely on timber to timber double shear parallel loaded connections with single dowel type fasteners.

2 The resistance of connections with a single dowel type fastener

2.1 Calculation framework

A model for the estimation of the load bearing capacity or resistance R of dowel type fastener connections is presented. The model framework is equivalent to the model used in the present version of Eurocode 5 (ENV 1995-1 (2004)). It is focused on parallel loaded double shear timber to timber connections as illustrated in Figure 1.
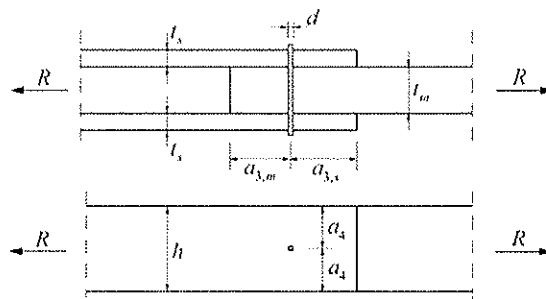
Figure 1   Example of a single fastener connection loaded parallel to the grain in tension.

Two side members and one middle member with member thickness t_s and t_m respectively are connected. The diameter of the fastener is specified by d. The end distance of the side members and the middle member is specified by $a_{3,s}$ and $a_{3,m}$. The side members and the middle member have the height h. The distance between the side edge and the fastener is defined by a_4.

The load carrying capacity of a single dowel type fastener connection is derived from the so-called Johansen equations (Johansen (1949)). The way these equations are presented in

European Codes was originally derived by Meyer (1957). For double shear connections 4 different failure modes are recognized as illustrated in Figure 2.
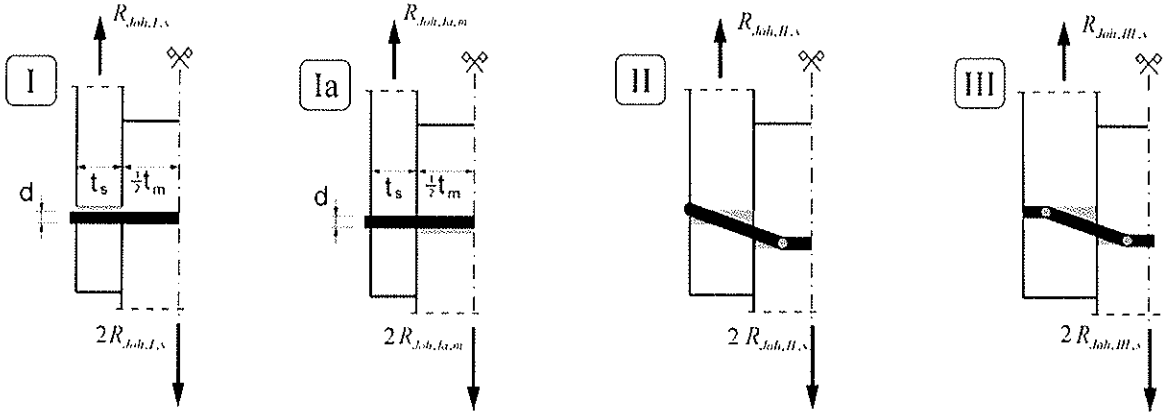
Figure 2   Johansen failure modes for double shear connections.

The resistance per shear plane R of each failure mode is given as in Equation (1) - (4).

$$R_{Joh,I,s} = t_s \, d \, f_{h,s} \tag{1}$$

$$R_{Joh,Ia,m} = \frac{1}{2} t_m \, d \, f_{h,m} \tag{2}$$

$$R_{Joh,II,s} = -\frac{t_s \, d \, f_{h,s} \, f_{h,m}}{2 f_{h,s} + f_{h,m}} + \frac{1}{2} \sqrt{ \left(\frac{2 d \, t_s \, f_{h,s} \, f_{h,m}}{2 f_{h,s} + f_{h,m}} \right)^2 + \frac{4 \left(t_s^2 \, d \, f_{h,s} + 4 M_y \right) d \, f_{h,s} \, f_{h,m}}{2 f_{h,s} + f_{h,m}} } \tag{3}$$

$$R_{Joh,III,s} = \sqrt{ \frac{4 M_y \, d \, f_{h,s} \, f_{h,m}}{f_{h,s} + f_{h,m}} } \tag{4}$$

The parameters used in Equations (1) – (4) are:

$t_s \, / \, t_m$ the side/middle member thickness $[\mathrm{mm}]$,

d the diameter of the fastener $[\mathrm{mm}]$,

$f_{h,s} \, / \, f_{h,m}$ the embedding strength of side/middle member $[\mathrm{MPa}]$,

M_y the yield moment of fastener $[\mathrm{Nmm}]$.

$R_{Joh,I,s}$, $R_{Joh,II,s}$, $R_{Joh,III,s}$ is the load carrying capacity in $[\mathrm{N}]$ of a side member according to failure modes I, II and III respectively (see Figure 2). $R_{Joh,Ia,m}$ is the load carrying capacity in $[\mathrm{N}]$ of the middle member according to failure mode Ia.

Beside the diameter of the fastener d and the member thickness t_s and t_m the geometry of the connection is specified by minimum values for the end distances a_3 and a_4. These values intend to provide that failure is governed by a failure mode described by the Johansen equations. The material parameters entering the Johansen equations are the embedding strength of the timber material f_h and the plastic yield capacity in bending

M_y. The embedding strength f_h is modelled as a function of the timber density ρ and the diameter of the fastener d as:

$$f_h = 0.082(1 - 0.01d)\rho \tag{5}$$

The plastic yield capacity M_y is modelled as a function of the ultimate yield capacity in tension f_u and the fastener diameter d as:

$$M_y = 0.3f_u d^{2.6} \tag{6}$$

2.2 The EC 5 design format

The design equation according to the EC 5 can be given as, e.g.:

$$G = zk_{mod}R_c / \gamma_m - (\gamma_G G_c + \gamma_Q Q_c) = 0 \tag{7}$$

z is a design variable,

k_{mod} is the composite modification factor taking into account deviations from normal load and climate conditions[2] during the service life,

R_c is the characteristic value for the resistance,

G_c is a characteristic value for the permanent load,

Q_c is a characteristic value for the variable load,

γ_m is the partial safety factor for the resistance,

γ_G is the partial safety factor for the permanent load,

γ_Q is the partial safety factor for the variable load.

The characteristic resistance of the dowel type fastener connection R_c is assigned based on Equations (1)-(6). The 5%-fractile values of the probability distribution functions of the timber density ρ_k and the ultimate yield capacity $f_{u,k}$ are used as material input parameters for Equations (5) and (6). The dowel diameter d and timber member thickness t_s and t_m are assumed to be exactly known values. The characteristic resistance of the connection $R_c = R_{single,EC}$ is the minimum of the characteristic resistances associated with the 4 Johansen failure modes (Equations (1)-(4)) as:

$$R_{single,EC} = 2\min\left(R_{Joh,I,s}, R_{Joh,II,s}, R_{Joh,III,s}, R_{Joh,Ia,m}\right) \tag{8}$$

As for structural timber elements the partial safety factor for the resistance (Equation (7)) is specified by $\gamma_m = 1.3$. In the EC 5 the modifications factor k_{mod} is specified for discrete load and climate exposures. Within this study k_{mod} is set to one.

2.3 The probabilistic model

For the probabilistic model an equivalent calculation framework than in the EC5 is utilized. The embedding strength and the yield capacity in bending are modelled with

---

[2] Normal load and climate conditions, here, are defined according ISO 8375, i.e. constant climate with 65% rel. humidity and 20°C and a load duration equivalent to 5 +/- 2 minutes.

Equation (5) and (6) respectively. The timber density and the steel yield capacity in tension are introduced as random variables. The connection is modelled as a system of the different failure modes according to Johansen. It is assumed that the modes I and Ia are brittle and the failure modes II and III are ductile. Furthermore, both side members are considered separately. The interaction of the different failure modes as illustrated in Figure 3 can be obtained.
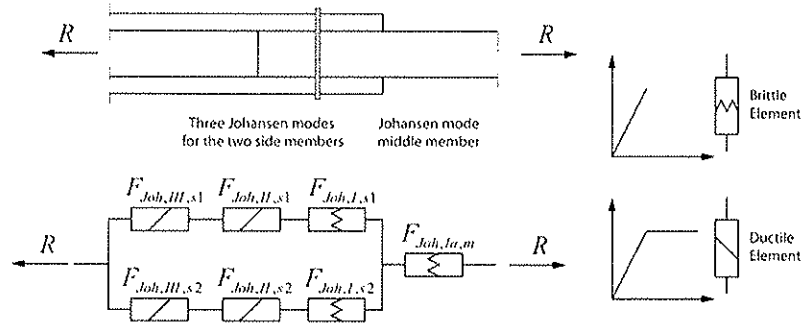
Figure 3   Interaction of failure modes

The componental failure events F associated with the different failure modes are indicated in Figure 3. System failure SF is related to the following combination of componental failure events:

$$SF = F_{Joh,I,s1} \cup F_{Joh,I,s2} \cup F_{Joh,Ia,m} \cup \left(F_{Joh,II,s1} \cap F_{Joh,II,s2} \right) \cup \left(F_{Joh,III,s1} \cap F_{Joh,III,s2} \right)$$
$$\cup \left(F_{Joh,II,s1} \cap F_{Joh,III,s2} \right) \cup \left(F_{Joh,III,s1} \cap F_{Joh,II,s2} \right) \tag{9}$$

According to Equation (9) system failure occurs when one of the side members follows the failure mode I, the middle member follows the failure mode Ia or the side members are following both a failure mode II or III.

The governing combination of failure modes for the determination of the single fastener connection strength R_s is quantified according a set of limit state functions as:

$$g_1 = 2zR_{Joh,I,s1}M - G - Q = 0$$
$$g_2 = 2zR_{Joh,I,s2}M - G - Q = 0$$
$$g_3 = 2zR_{Joh,Ia,m}M - G - Q = 0$$
$$g_4 = z\left(R_{Joh,II,s1} + R_{Joh,II,s2} \right)M - G - Q = 0$$
$$g_5 = z\left(R_{Joh,III,s1} + R_{Joh,III,s2} \right)M - G - Q = 0 \tag{10}$$
$$g_6 = z\left(R_{Joh,II,s1} + R_{Joh,III,s2} \right)M - G - Q = 0$$
$$g_7 = z\left(R_{Joh,III,s1} + R_{Joh,II,s2} \right)M - G - Q = 0$$

with

z is a design variable,

R is the resistance according to a Johansen failure mode,

G is the permanent load,

Q is the variable load,

5

M is the model uncertainty.

In Equation (10) the index m specifies the middle member, $s1$ and $s2$ the side members. The failure probability P_f can be estimated according to

$$P_f = P\left(\bigcup_{i=1}^{7} g_i \le 0\right)$$

(11)

The failure probability can be evaluated according to e.g. first or second order reliability method (FORM/SORM see e.g. Ditlevsen and Madsen (1996)). The equivalent reliability index β_E is defined as:

$$\beta_E = -\Phi\left(P_f\right)$$

(12)

2.4   Example 1

A calculation for the reliability of single dowel type fastener connections is exemplified. The EC 5 design format as presented in Section 2.2 is applied to specify the design variable z. The modification factor is set equal to unity. The probability of failure is estimated using the framework presented in Section 2.3. The software Strurel (1999) is utilized for the reliability calculation with the First Order Reliability Method (FORM) as the solution strategy.

The input variables are described as:

	timber density $\rho\left[kg/m^3\right]$	yield capacity $f_u\left[MPa\right]$	permanent load $G\left[N\right]$	variable load $Q\left[N\right]$	model uncertainty $M\left[-\right]$
distribution	Normal	Lognormal	Normal	Gumbel	Lognormal
mean value	450	427	1000	1200	1
st. dev.	45	17	100	480	0.1
COV	0.1	0.04	0.1	0.4	0.1
fractile	5%	5%	50%	98%	-
char. value	376	400	1000	2444	-
par. safety fac.	$\gamma_m = 1.3$		$\gamma_G = 1.35$	$\gamma_Q = 1.5$	-

geometry	member thickness	fastener diameter	fastener placing
	$t_m = 2t_s$	$d = 12mm$	$a_3 = 7d; a_4 = 3d$

The motivation of this example is to investigate the behaviour of the presented model in a reliability analysis. What is the effect of the model assumptions; especially the assumptions according to the system interactions in the probabilistic part of the model? Or, how sensitive is the result to possible quantification errors of the basic variables of the model? It is underlined that there is no attempt to quantify the nominal reliability of dowel type fastener connections.

To investigate different cases, i.e. different dominant failure scenarios a parameter study upon $t_m = \left[24mm, 160mm\right]$ is carried out.

2.4.1   Results

The equivalent reliability index β_E (Equation (12)) for different values for the middle member thickness t_m is calculated. For means of comparison β_E-values for two alternative system model assumptions are also considered; assuming that all Johansen failure modes

are brittle and assuming that all Johansen failure modes are ductile (both in contrast to the assumptions Figure 3 and Equation (9), brittleness for Johansen I and Ia and ductile behaviour for Johansen II and III).
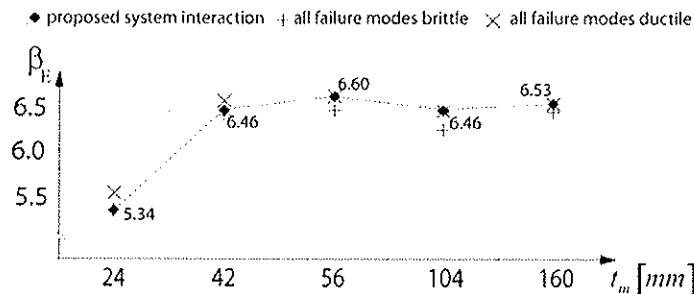
Figure 4   The equivalent reliability index (Equation(12)) for different middle member thickness. The results of the proposed system are compared with the results of two alternative system model assumptions.

The β_E-values range from 5.34 to 6.6 which is equivalent to a failure probability of 4.8E-8 and 2E-11 respectively. The results according to the alternative system model assumptions are in the same order of magnitude.

In Figure 5 the componental (failure mode) sensitivities τ_j are illustrated. τ_j can be seen as an indicator of the importance of a particular failure mode. E.g. for $t_m = 24mm$ the brittle failure modes I and Ia are relevant for the reliability calculation; for $t_m = 56mm$ exclusively failure mode II is relevant.

Ia	0.6	0.3	0.0	0.0	0.0
I	2x0.6	2x0.3	0.0	0.0	0.0
II	0.0	0.8	1.0	0.5	0.0
II/III	0.0	0.0	0.0	0.7	0.0
III	0.0	0.0	0.0	0.6	1.0
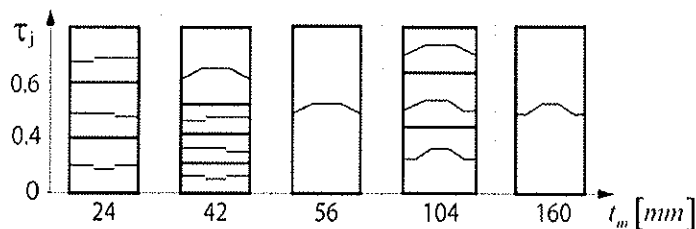
Figure 5   The componental (failure mode) sensitivities τ_j for different middle member thickness.

In Figure 6 the α - values, or sensitivity factors, of the basic variables are illustrated. The sensitivity factors are a measure for the relative importance of the uncertainty in the (stochastic) basic variable on the reliability index, (Madsen et al. (1986)). It can be seen that the uncertainty associated with the model uncertainty M and the variable load Q is dominating the result of the reliability calculation.

7

$|\alpha_i|$

<table>
<tr><td></td><td>· 0.68</td><td>·· 0.68</td><td>× 0.69</td><td>× 0.69</td><td>·0.69</td><td>• M</td></tr>
<tr><td></td><td>• 0.52</td><td>• 0.59</td><td>• 0.68</td><td>• 0.65</td><td>•0.65</td><td>■ P_m</td></tr>
<tr><td></td><td></td><td></td><td></td><td></td><td></td><td>G</td></tr>
<tr><td>0.3</td><td>• 0.29</td><td>▮ 0.26
0.23</td><td>0.15</td><td>0.16</td><td>0.19
0.14</td><td>f_e</td></tr>
<tr><td></td><td>0.14
0.00</td><td>0.14
0.06</td><td>■ 0.14
0.10</td><td>■ 0.14
0.09</td><td>■0.13
•0.08</td><td>• P_t</td></tr>
<tr><td>0</td><td>24</td><td>42</td><td>56</td><td>104</td><td>160</td><td>t_m [mm]</td></tr>
</table>
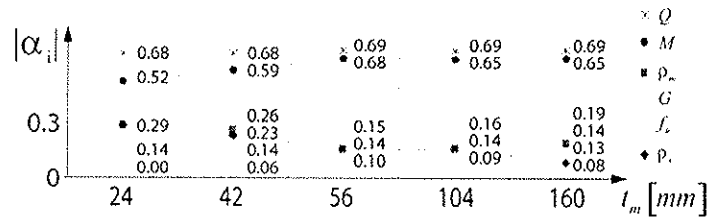
Figure 6   The sensitivity factors α_i for the basic variables for different middle member thickness.

2.4.2 Discussion

Cases with different relevant failure mode combinations are considered. For all combinations it can be observed that the variables model uncertainty M and the variable load Q are dominating the result of the reliability calculation. The evaluated β_E-values are significantly larger than usual target reliability indices (β_{target} = 4.2 according to the recommendations of JCSS (2001)). A possible reason for this could be the inappropriate quantification of the model uncertainty. Considering all the model assumptions integrated into the model a large variation of the model uncertainty could be imagined. The possible sources of model uncertainty are briefly dicussed next:

- Resistance is modelled as a consequence of the embedding strength of the timber and the plastic bending capacity of the fastener. Other possible effects on the resistance of dowel type connections are not considered.

- The embedding strength is defined as e.g. in EN 383. This standard defines the embedment strength as the highest embedment stress within 5 mm displacement for both parallel and perpendicular to grain tests. Regression rules (associated with uncertainties) are evaluated based on these test data (Leijten et al. (2004), Whale and Smith (1986)). Further, the embedding stress strain relationship according to the Johansen equations is idealized with a ideal rigid-plastic model, which obviously does not reflect the real behaviour.

- The plastic bending capacity of the fastener is estimated by Equation (6), which is derived by Blass et al. (2001). The parameters 0.3 and 2.6 are found by applying an iterative procedure, estimating the activated plastic capacity for different geometrical configurations and for an assumed strength criterion of 15mm relative displacement in the connection. In fact and as shown in Jorissen (1998) the ultimate relative displacement could be less than 15mm.

- The system assumptions (Figure 3 and Equation (9)) are idealisations and associated with uncertainties.

- The statistical modelling of the material properties, the timber density and the ultimate fastener capacity in tension is associated with model uncertainties.

Because of the high importance of the model uncertainty in reliability evaluation (Figure 6) and the several sources of uncertainty the model uncertainty is assessed based on observations from experiments.

8

2.5 Quantification of the Model Uncertainty M

The model uncertainty M can be quantified by comparing model predictions and measurements from experiments. In the JCSS Probabilistic Model Code (JCSS (2001)) the model uncertainty is (among other formulations) given as:

$$Y = Mf\left(X_1...X_n\right)$$ (13)

with

Y	the structural performance,
$f(.)$	the model function,
M	the model uncertainty,
X_i	the basic variables.

In this case the model uncertainty can be quantified as a log-normal distributed random variable M with the realizations m according to Equation (14).

$$m = \frac{y}{f(\mathbf{x})}$$ (14)

If the mean value of M is not equal to 1 the model is biased.

Under consideration of a comprehensive data base, published in Jorissen (1998), the model uncertainty is assessed. Double shear timber to timber connections are loaded parallel to the grain in tension and compression. The fasteners are bolts without nuts. Teflon layers between the timber members minimise the friction between the members. The motivation for these tests is to investigate the Johansen failure modes under additional consideration of a splitting mode. Undesired side effects as an axial tension force components in the fastener (rope effect) and friction between the timber members are aimed to be minimised by having no nuts on the bolts and by introducing the Teflon layers respectively. The number of observations is $N = 90$, the dowel diameter is $d = [10.65;11.75]$ mm (sold as M12), the middle member thickness is $t_m = [24;48;72]$, the side member thickness $t_s = [12;24;36;59]$ the end distance is $a_3 = 7d$ and the height is $h = 6d$. Material is north european spruce, visual graded according to the Dutch class B, defined in NEN 5466 [5], which, according to EN 1194 [6], corresponds to the European strength class C24. The sample characteristics for density ρ are the mean value $m = 454$ and the standard deviation $s = 45$, both in $\left[kg/m^3\right]$; the number of density measurements is $N = 270$.

Within the experiments, the following quantities were measured:

- The density of each side and middle member: ρ_{s1}, ρ_{s2} and ρ_m.
- The load carrying capacity: R
- The relative end-displacement, i.e. the relative displacement at failure: Δ.

Based on the model presented, assessments for the load carrying capacity of the test specimen are performed. Therefore, the measured timber densities are used together with the assumed ultimate tension strength of the fastener material and the specified geometry as input parameters for the presented model. As in Jorissen (1998), the ultimate tension strength f_u of the fastener material is approximated by $f_u = 400$ MPa.

The model assessments are compared with the observations from the experiments in Figure 7; the different failure modes according to Johansen are indicated. Predictions of the load bearing capacity according the Johansen equation for failure mode I (Equations (1) and (2)) are always larger than the load bearing capacity observed from the experiments and are therefore on the unsafe side. Mode II and III model calculations are consistently lower than the real capacity of these connections.

The model uncertainty is quantified according Equation (14) and is presented in Table 1. In Table 1 a distinction is made also between the different Johansen equations which were found to be relevant within the model calculations.
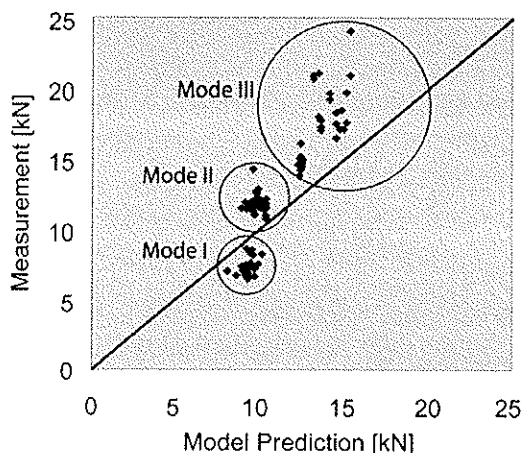
Figure 7   Comparisons of model predictions and test observations. The Johansen failure modes are indicated.

Table 1   Model uncertainties for the strength estimation of single dowel type fastener connections as lognormal random variables.

	Mean	St.dev
entire model	1.117	0.240
Joh I	0.802	0.061
Joh II	1.202	0.080
Joh III	1.278	0.131

By inspecting Figure 7 together with Table 1 it can be concluded that it makes no reason to assess a general model uncertainty for the models of all Johansen modes together. The predictive characteristic of the Johansen models is rather distinct. When Johansen Equations *I* or *Ia* are relevant the model is overpredicting failure loads which is a rather adverse characteristic. Johansen Equations *II* and even more *III* are underpredicting the observed failure loads. The standard deviations for the model uncertainties are decreasing from Mode *I* over *II* to *III*.

The results have to be seen in the light that the test results referred to are not representative for connections in real structures.

3 Model verifications

3.1 Embedding Strength

In the presented model the embedding strength is evaluated based on the density and the diameter of the fastener according to Equation (5). A recent study published in Leijten et al. (2004) points to an alternative formulation for the embedding strength. The study is founded upon on the analysis of data bases from several research projects and suggests a formulation based on the timber density ρ and the diameter of the fastener d as:

$$f_h = A\rho^B d^C \tag{15}$$

A, B, C are the model parameters which are quantified as $(A, B, C) = (0.097, 1.066, -0.253)$ for dowels (pre-drilled), softwood and parallel to the grain loading. In Leijten et al. (2004) the uncertainty associated with the formulation in Equation (15) is quantified. This is not followed further here.

3.2 Splitting mode

In Jorissen (1998) a model based on fracture mechanical considerations is proposed to cover the splitting failure mode. According to Jorissen (1998) the splitting load bearing capacity of a member can be estimated as:

$$R_{splitt,i} = t_i \sqrt{\frac{G_{c,i} E_{0,i} d(2h - d)}{h}} \tag{16}$$

with

$G_{c,i}$ the mixed mode fracture energy according to Peterson (1995) loading parallel to the grain $[\text{N/mm}]$,

d the diameter of the dowel type fastener $[\text{mm}]$,

$E_{0,i}$ the modulus of elasticity parallel to the grain $[\text{MPa}]$,

h the member width $[\text{mm}]$,

t_i the member thickness $[\text{mm}]$,

m the number of rows (perpendicular to the grain),

$R_{splitt,i}$ the load bearing capacity $[\text{N}]$.

The mixed mode fracture energy according Peterson (1995) is a function of the ratio between tension strength perpendicular to the grain and shear strength $f_{t,90}/f_v$, the ratio between the MOE perpendicular to the grain and the MOE parallel to the grain E_{90}/E_0, the fracture energy opening mode G_{Ic} and the fracture energy sliding mode G_{IIc}.

If the parameters are quantified as $f_{t,90}/f_v = 0.6$, $E_{90}/E_0 = 0.03$, $G_{Ic} = -162 + 1.07\rho$, $G_{IIc} = 3.5 G_{Ic}$ the mixed mode fracture energy G_c can be estimated as a function of the density ρ as:

$$G_c = 0.0013\rho - 0.1918 \quad \left[\frac{Nmm}{mm^2} \right] \tag{17}$$

3.3 Factor for the rope effect

The model predictions for semi rigid and slender fasteners (Johansen Modes II and III) are consistently lower than the real capacity of these connections. According to the Johansen model the load bearing capacity of a dowel type connection R is exclusively governed by the embedding resistance of the timber f_h and the plastic moment capacity of the fastener M_y. Other effects than friction between the timber side and middle members are not considered by the model. The reason for the special test configuration in Jorissen (1998) is to exclude these side effects as good as possible and to focus on the Johansen mechanisms. However, the consistent underestimation of the load bearing capacity by the model provokes a deeper thought in regard to what is modelled and what is really observed.

Friction might occur between bolt shaft and timber and this effect might increase the load bearing capacity. This effect might be proportional to the normal force between shaft and timber and might also be different for the case of two plastic hinges (Mode II) and four hinges (Mode III) in the fastener (Figure 2). The model could be refined by introducing the two factors $k_{f,II}$ and $k_{f,III}$ as:

$$R_{Joh,II,s} = k_{f,II} \left[-\frac{t_s \, d \, f_{h,s} \, f_{h,m}}{2 f_{h,s} + f_{h,m}} + \frac{1}{2} \sqrt{\left(\frac{2d \, t_s \, f_{h,s} \, f_{h,m}}{2 f_{h,s} + f_{h,m}} \right)^2 + \frac{4 \left(t_s^2 \, d \, f_{h,s} + 4 M_y \right) d \, f_{h,s} \, f_{h,m}}{2 f_{h,s} + f_{h,m}}} \right] \quad (18)$$

$$R_{Joh,III,s} = k_{f,III} \sqrt{\frac{4 M_y \, d \, f_{h,s} \, f_{h,m}}{f_{h,s} + f_{h,m}}} \quad (19)$$

The factors are quantified by simple least squares technique minimising the difference between model calculation and observation to $k_{f,II} = 1.19$ $k_{f,III} = 1.29$ for the verified model.

3.3 Effect of model verifications

In Figure 8 the effect of the possible model verifications is illustrated. The major change for Johansen failure modes II and III is goverened by the friction factors derived in Equations (18) and (19). These factors are fitted according to the considered data set and are not representing a general phenomenon. Referring to the special test arrangement it could be argued that the effect of friction is higher in real dowel type fastener connections due to the absence of Teflon layers between the timber members. The effect of the alternative formulation for the embedding strength (Equation (15)) for Johansen mode II and III is comparably minor.

A quite interesting fact is that by applying the verified model in the calculations Johansen failure mode I and Ia are never relevant. They are entirely replaced by the splitting mode. The model predictions according to the splitting mode are accurate considering that the parameters of that model are derived independently from the data set considered for the comparison.
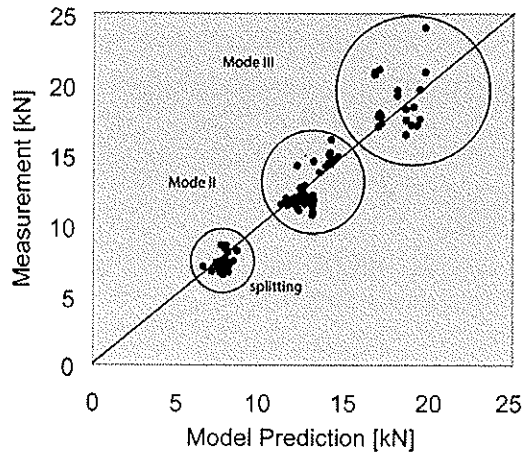
Figure 8   Comparisons of model predictions and test observations. The Johansen failure modes II and III (modified Equations (18) and (19)) and the splitting mode (Equation (16)) are indicated.

4   Summary and conclusions

A probabilistic modelling framework for the load bearing capacity of single dowel type fastener connections is derived based on the design framework utilized in the present version of the Eurocode 5. Reliability analysis for connections with different fastener slenderness ratio is performed and the following conclusions can be drawn:

- The reliability index is an order of magnitude too high.

- System model assumptions have minor consequence on the result of the reliability calculation.

- The relative importance of the basic variables is quantified by sensitivity factors. The model uncertainty and the variable load are found to be most relevant.

Based on these findings the model uncertaintainty is quantified based on test data of connections. The following can be observed:

- The parameters of the model uncertainty are considerably different for cases where different Johansen failure modes are relevant.

- Especially the model bias is different for different failure modes.

Model verifications are proposed, whereas the introduction of an additional spitting mode and the utilisation of an alternative embedding strength model where derived independently of the considered data set. Friction factors for Johansen modes II and III are introduced. It is found that:

- A significant model improvement is reached by introducing the splitting mode.

- A minor improvement is reached by using the alternative embedding strength model.

- The improvement which is obtained by introducing friction factors has to be seen conditional on the data base which is considered.

13

References

Blass H.J., Bienhaus A. and Krämer V. (2001) Effective bending capacity of dowel-type fasteners. *Proc. PRO 22, Int. RILEM Symposium on Joints in Timber Structures*. pp. 71-88.

Ditlevsen O. and Madsen H.O. (1996). Structural Reliability Methods. Wiley, Chichester, UK.

EN 1995-1-1 (2004), Eurocode 5: Design of timber structures; part 1-1: general rules and rules for buildings. Comité Européen de Normalisation, Brussels, Belgium, 2004.

EN 383. Timber Structures; test methods; determination of embedding strength and foundation values for dowel type fasteners. Comité Européen de Normalisation, Brussels, Belgium, 1993.

Foliente, G.C. (1998). Design of timber structures subjected to extreme loads. *Prog. Struct. Eng. Mater.*, 1(3), pp. 236-244.

Foschi, R.O. (2000). Reliability applications in wood design. *Prog. Struct. Eng. Mater.*, 2(2), pp. 238-246.

Johansen, K.W. (1949). Theory of timber connections. *International Association of Bridge and Structural Engineering, Publication No. 9*:pp. 249-262, Bern, Switzerland.

Joint Committee of Structural Safety (JCSS, 2001). *Probabilistic Model Code,* Internet Publication: www.jcss.ethz.ch.

Jorissen, A. (1998). *Double shear timber connections with dowel type fasteners.* PhD-Thesis, Delft University Press, Netherlands.

Leijten, A., Köhler, J., Jorissen, A.J.M. (2004). Review of probability data for timber connections with dowel type fasteners. *Proc. Of the 37th CIB W18 meeting*, Edinburgh, UK, Paper 37-7-6.

Madsen H.O., Krenk S. and Lind N.C. (1986). Methods of Structural Safety. Prentice-Hall, Eaglewood Cliffs, NJ, USA.

Meyer, A. (1957). Die Tragfähigkeit von Nagelverbindungen bei Statischer Belastung. *Holz als Roh- und Werkstoff.* 15(2), pp. 96-109.

NEN 5466. *Kwaliteitseisen voor hout (KVH 1980).* Houtsoort Europees vuren (in Dutch). Quality requirements for timber. Species European spruce. Netherlands Normalisatie Instituut, Delft, Netherlands, 1983.

Smith, I. and Foliente, G.C. (2002). Load and Resistance Factor Design of Timber Joints: International Practice and Further Direction. *Journal of Structural Engineering, ASCE.* 128(1), pp. 48-59.

Strurel (1999). *Structural reliability analysis program system.* Comrel 7.0 & Sysrel 9.6. RCP Consulting, Munich.

Svensson, S. and Thelandersson, S. (2003). Aspects on reliability calibration of safety factors for timber structures. *Holz als Roh- und Werkstoff.* 61 pp. 336-341.

Whale, L.R.J. and Smith, I. (1986). The derivation of design clauses for nailed joints in Eurocode 5, *Proc. of the 19th CIB W18 meeting*, Paper 19-7-6.

INTERNATIONAL COUNCIL FOR RESEARCH AND INNOVATION
IN BUILDING AND CONSTRUCTION

WORKING COMMISSION W18 - TIMBER STRUCTURES

LOAD CARRYING CAPACITY OF CURVED GLULAM BEAMS REINFORCED WITH SELF-TAPPING SCREWS.

J Jönsson

S Thelandersson

Lund University

SWEDEN

Presented by F J Jönsson

H Blass asked if decrease of splitting was observed when reinforcement was present. J Jönsson answered only without reinforcement cases were tested. A Buchanan received clarification that the double pitched fasteners were considered and questioned whether regular screws would work. A Ceccotti commented that well design beam with regular reinforcement should also work. A. Jorissen asked whether both FEM and design code based calculations were made. J Jönsson answered only FEM calculations were made.

Load Carrying Capacity of Curved Glulam Beams Reinforced with Self-tapping Screws.

Johan Jönsson, Sven Thelandersson
Division of Structural Engineering
Lund University, Lund, Sweden

Abstract

The aim of this research was to determine the load carrying capacity of curved glulam beams reinforced perpendicular to grain and subjected to climate induced internal stresses. The self-tapping screws used as reinforcement prevents the glulam to split along the grain causing failure perpendicular to grain. Different tests were performed; specimens seasoned in dry and moist climate, specimens exposed to single climate change and reinforced specimens seasoned in a dry and moist climate. Specimens without reinforcement where tested to failure and then reinforced and tested again. From the tests it can be concluded that reinforcement improves the capacity of the beam in some cases up to 50% compared to unreinforced beams. The effect of moisture gradients on the capacity is significant and the worst case is when the beams are in a moistening phase.

1 Introduction

The weakest link in timber structures is often the tensile strength perpendicular to grain; hence understanding the mechanism behind tensile stresses perpendicular to grain is crucial. These stresses are caused not only by external forces such as dead weight, wind- and snow load but also by climate changes inducing eigenstresses. According to Ranta-Maunus (2003), moisture action should be treated as a variable load to be combined with other load effects i.e. should not be treated as a strength reducing effect. In Jönsson (2004) a large number of tests were performed on glulam, to study the influence of natural climate change on the stress distribution. In some cases the stress levels locally exceeded the characteristic value for several weeks. The fact that moisture induced stresses is more or less always present means that commonly used design criteria are associated with large uncertainty. The interaction between moisture induced stresses and stresses induced by external force was investigated experimentally by Jönsson and Thelandersson (2003), who found a significant influence on the capacity in glulam both in a positive and negative way. In the case when the specimens are in a moistening phase and subjected to external force the stresses in the inner part are added leading to a very non-uniform stress distribution resulting in lower tensile capacity.

To avoid failure perpendicular to grain in timber structures such as pitched, curved and end-notched beams and in beams with holes the use of reinforcement is often necessary. Typically, reinforcement is arranged with bolts or glued in rods e.g. for pitch-cambered beams, see e.g. Blass and Steck (1999) and Blass and Laskewitz (2002). In Kasal and Heiduschke (2004) glued in glass-fibre composite tubes were used to reinforce small glulam-arches. Another approach is presented in Dahlblom et al. (1993) where fibre reinforcement glued on the surface of curved glulam beams was used.

2 Material and Methods

The glulam elements used in the test are shaped as a curved beam with cross-section 90x280 mm² see Figure 1. They were manufactured from standard lamellas 45x95 mm² of Norway spruce, which were cut and planed to size 20x90 mm², see Figure 2. The glulam beams were manufactured by Moelven Töreboda Limträ AB, and taken directly from the production line. The position of the reinforcing screws in the curved part can be seen in Figure 1. Screws made by SFS Intec AG (WT-T-8.2x300) were used. The screws have two thread segments, each 135 mm long, with different thread leads, which give a prestressing effect. The screws are placed in a zigzag pattern along the beam with a lateral displacement equal to 1/3 of the beam width.
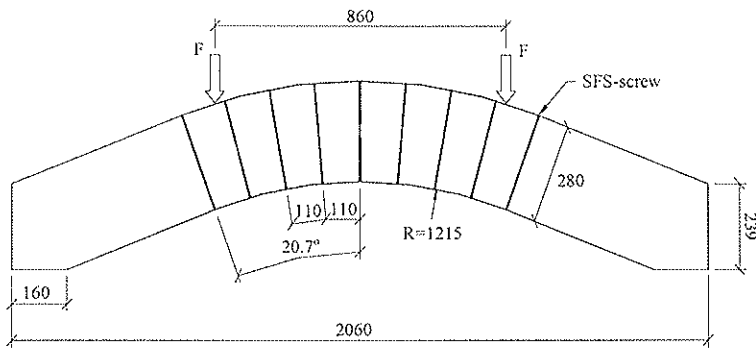
Fig. 1. *The geometry of the beam used in the test.*
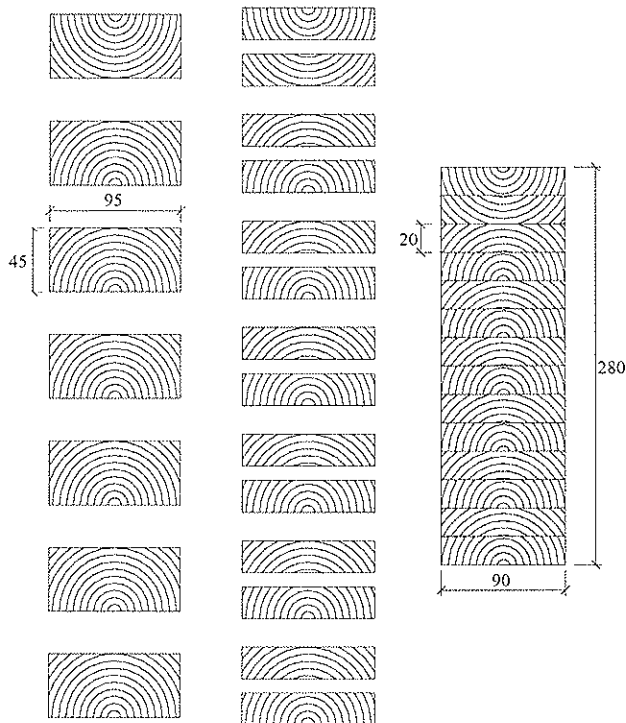
Fig. 2. *Lamellae, sawing pattern and cross section.*

The criterion for choosing the distance between the screws was selected to achieve a uniform stress distribution perpendicular to grain in the curved part during loading i.e. the stress between and near the screws should not differ too much.

2

This was examined using FE-analysis where the whole structure, shown in Figure 1, was modeled. A parameter study was conducted concerning the distance between screws and the interaction between screws and wood.

A 2-D linear elastic anisotropic model in transversal and longitudinal direction was used in a commercial finite element program, ANSYS. The material properties are taken from Dinwoodie (2000), where the modulus of elasticity in the transverse and longitudinal direction are set to 430 and 10700 MPa respectively, the shear modulus to 620 MPa and Poisson's ratio to 0.03. The interaction between wood and screws is modeled with linear elastic springs acting in the transverse direction. The modulus of elasticity in the screw is 210000 MPa.

Analyses showed that the stresses perpendicular to grain in the curved part of the beam become reasonably uniform if the distance between screws is selected to 110 mm. The results from this case can be seen in Figure 3, where the stresses perpendicular to grain, σ_{90}, are shown for an applied load F=100 kN and spring stiffness 48 MN/m (SFS Intec AG, 2003).

The stresses are approximately equal between and near the screws as can be seen Figure 3. Figure 3 also shows the reduction of the stress perpendicular to grain due to the screws. The maximum stress was reduced from 1.51 to 0.97 MPa by reinforcing the beam. It could also be concluded that increasing the spring stiffness above 48 MN/m did only influence the stress distribution marginally.

This study indicates that the distance between the screws should be approximately 40% of the cross-section height, i.e. 110 mm, to achieve a uniform stress distribution along the curved part.
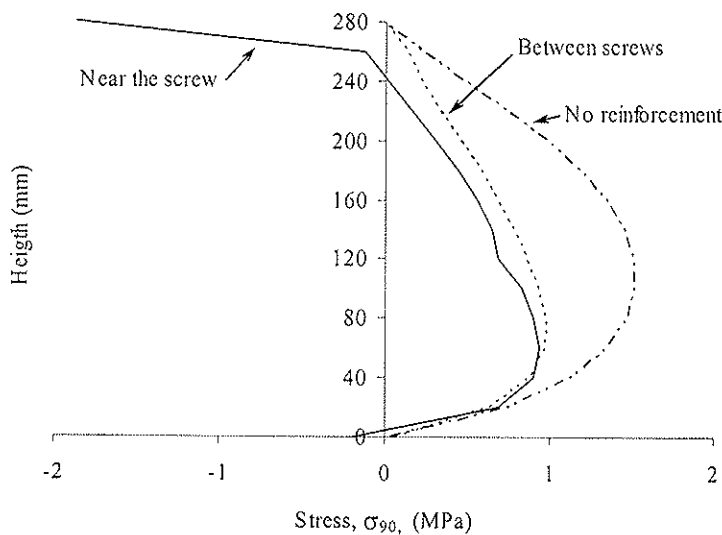
Fig. 3. *Distribution of stress perpendicular to grain near the screw, between two screws and stress distribution without screws. External force 100 kN, spring stiffness 48 MN/m and distance between screws 110 mm.*

2.1 Test program

The test program was divided into three different types of tests A, B and C (Table 1). One half of the specimens were seasoned in RH 40% and the other half in 80%. In A and B the beams were tested in a seasoned state. In test B the beams were reinforced. In test type C the specimens are affected by internal stresses perpendicular to grain due to climate change. These stresses as well as moisture distribution and the effect on the capacity due to eigenstresses are known from a previous study presented in Jönsson (2004) and Jönsson & Thelandersson (2003) where the same test program was used.

After failure of the non-reinforced beams (A and C) they were tested again after reinforcing, to investigate the effect on capacity due to cracking prior to reinforcing.

Table 1. *Test program.*

Test type	Seasoned in relative humidity	Climate exposure	Total number of specimens	Days of testing
A	40%	-	8[1,3]	-
	80%	-	8[1,3]	-
B	40%	-	8[2]	-
	80%	-	8[2]	-
C	40%	80%	7[1]	1,3,5,7,11,24,38
	80%	40%	7[1]	1,3,5,6,11,24,38

1 Tested without reinforcement and tested again after failure with reinforcement.
2 Reinforced prior to test.
3 Half of the beams were reinforced in the curved part and the other half along the whole beam.

The beams were tested in a hydraulic testing machine (MTS). Two concentrated loads, 860 mm apart, were applied as shown in Figure 1. The loading was made with a constant displacement rate of 3 mm/min leading to failure in 5 to 10 minutes. During testing the beam was braced against lateral deflection at the apex of the beam. The beam and the yoke (transferring the load from MTS to the beam) were both applied on a fixed knife support on one side and roller support on the other side.

The maximum tensile stress perpendicular to grain in curved beams are calculated according to

$$\sigma_{90} = \frac{3M}{2r_{mean}bh}$$

where M is the applied constant moment, r_{mean} the mean radius of the curved beam and b,h width and height of the beam

3 Results and Discussion

Type A, seasoned in RH 40 and 80%, not reinforced
The fracture mode for this type of beams is predominantly tension perpendicular to grain. The fracture is localised in the lower part of the beam approximately one third from the lower edge of the beam. The crack follows a specific lamellae and ends approximately where the curvature ends. As shown in Figure 4, test results indicate a linear relationship between force and displacement. The average fracture loads for beams seasoned in RH 40 and 80% are 120 and 107 kN respectively; implying 12% higher strength for the beams seasoned in the dry climate, see Table 2. The stiffness of the beams seasoned in RH 80% is 80% of that for beams seasoned in RH 40%.
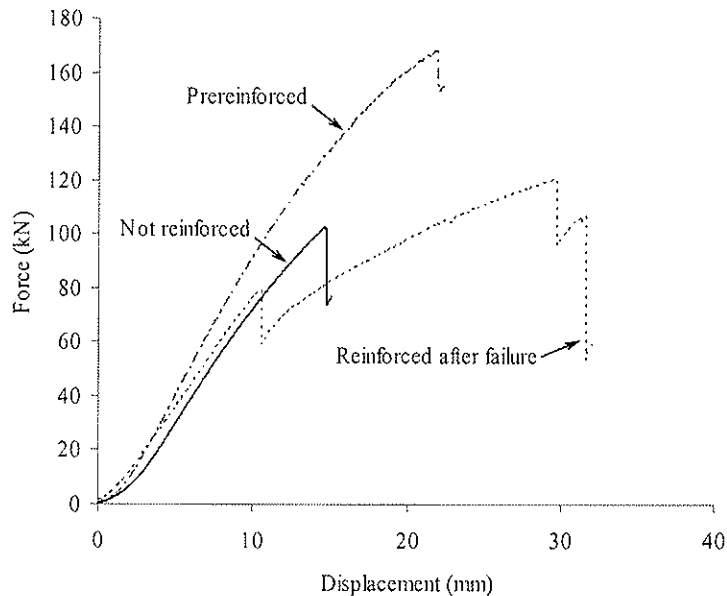
Fig. 4. *Typical force-displacement diagram, prereinforced, not reinforced and reinforced after failure and tested again. Seasoned in RH 80% and distance between screws 110mm.*

3.1 Type A, seasoned in RH 40 and 80%, reinforced after fracture

Regardless if the reinforcement is limited to the curved part or along the whole beam, the initial fracture mode is always shear failure at the end of the beam, see Figure 5. The shear failure is initiated by the pre-existing crack. The stiffness of the beams (RH 80%) is the same as in the previous test (not reinforced). For the beams at RH 40% the stiffness after failure is approximately 90% compared to the unreinforced beams. The stiffness decreases after the first shear failure which occurs at 70-80% of the maximum load for the unreinforced beam; however the deformation capacity is approximately doubled, see Figure 4. After the shear failure which often occurs at both ends the beam performs as two parts connected with the screws. When the beam reaches maximum load the lower lamellae of the top part is torn apart in a flexural type failure. The remaining load carrying capacity is surprisingly high and in all cases the test was terminated before a total collapse, the large deformation is a limit.

The maximum capacity was increased compared to the unreinforced beams. The largest effect by the reinforcement can be seen on the beams seasoned in RH 80%. In this case a 20% increase in strength was found. The corresponding increase for the other group seasoned in RH 40% was 10%.

Reinforcement along the whole beam did not influence the maximum load capacity. It merely restricted the shear deformation of the upper part of the beam. It can also be concluded that the capacity is marginally higher for the beams seasoned in the dry climate compared to the ones seasoned in the moist climate.
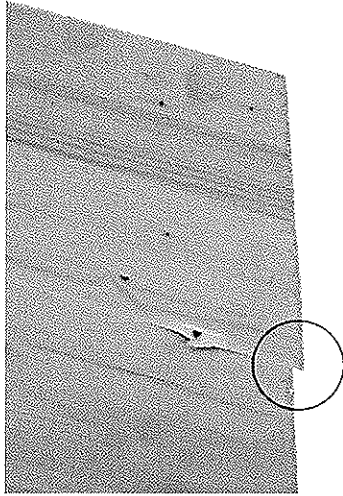
Fig.5. *Shear failure at the end of the beam.*

Table 2. *Results.*

	F_{mean} (kN)	cov (%)	σ_{mean} (MPa)	Ratio[1]
A-40 Not reinforced	120	15	1.37	1
A-40 Reinforced	131	5	1.50	1.11
B-40 Prereinforced	169	13	1.93	1.43
C-40-80 Not reinforced	100	20	1.15	-
C-40-80 Reinforced	131	18	1.50	-
A-80 Not reinforced	107	10	1.22	1
A-80 Reinforced	128	7	1.46	1.21
B-80 Prereinforced	160	3	1.83	1.50
C-80-40 Not reinforced	125	13	1.43	-
C-80-40 Reinforced	124.1	19	1.42	-

1 Ratio between F_{mean} for reinforced and not reinforced beams.

3.2 Type B, seasoned in RH 40 and 80%, prereinforced

These test showed the same behaviour as the previous type (*Type A, not reinforced*) i.e. linear relationship between force and displacement and a brittle type failure, see Figure 4. However in most of the cases, the beams failed in shear instead of tension failure perpendicular to grain. In one test there was a knot formation at the lower edge in the middle of the beam causing flexural failure, which led to lower capacity compared to other beams. The stiffness is the same as for the unreinforced beams. The maximum capacity is increased by 40-50% compared to the unreinforced beams; the largest effect can be seen for the beams seasoned in the moist climate. There is a small difference between the maximum capacity for the beams seasoned in a dry and moist climate, only 6% in favour for the dry beams. The shear failure occurring at the end of the beams is a failure mode related to this particular test setup. Therefore it can be concluded that effectiveness of the reinforcement is probably larger than the 50% improvement observed in these tests.

3.3 Type C. Single climate change, RH 40 to 80% and RH 80 to 40%

Figure 6 shows the maximum stress at failure for the two groups of specimens. It can be seen that the specimens in a drying phase is stronger than the specimens in a moistening phase. This behaviour is known from previous tests conducted on glulam cross-sections in tension, see Jönsson and Thelandersson (2003), also shown in Figure 6. The fracture mode was the same as in *Type A, not reinforced* expect for two occasions, day 7 and 11 marked with a circle, changed to failure in shear i.e. the strength perpendicular to grain is not the limiting

6

factor. As a reference, the mean values of the seasoned specimens are also plotted. It can be observed that immediately after changing climate, the capacity for the moistening specimens decrease compared to the seasoned specimens in RH 40%. This difference in capacity can be explained by the interaction between moisture and externally induced stresses. In the case of moistening the stresses are added in the inner part leading to a very non-uniform distribution of stress across the width of the specimen, leading to lower maximum capacity. In the opposite case with drying, the combined stresses lead to a more uniform stress distribution i.e. no stress peaks, which increase the capacity.

The influence of reinforcement after failure shows that the largest effect in capacity was in the moistening group with a 30% increase. For the specimens subjected to drying there was no increase, see table 2.
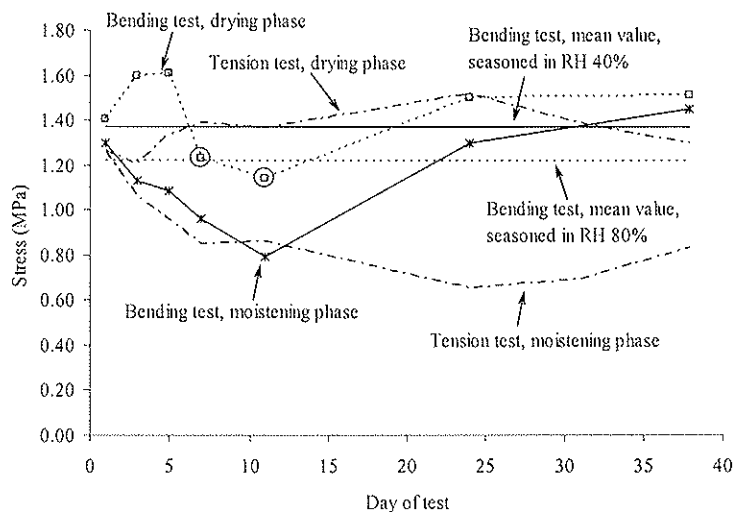
Fig. 6. *Stress perpendicular to grain in bending and tension versus day of test for specimens in a drying and moistening phase and seasoned in RH 40 and 80%. The results from the tension tests are results from a previous study, Jönsson and Thelandersson (2003)*

4 Conclusions from the tests

The tests conducted in this study were made to investigate the effect of reinforcement and climate induced internal stresses perpendicular to grain on the capacity in curved glued laminated beams. The following conclusions can be made

– According to FE-analysis the distance between the screws should be approximately 40% of the cross-section height i.e. 110 mm to obtain a uniform stress distribution in the curved part of the beam.

– The capacity is increased by 10-20% when reinforcing the beams after failure and tested again. The stiffness is also in the same order of magnitude and the deformation capacity is increased by approximately a factor 2

– Reinforcing prior to test increased the capacity with 40-50% and the stiffness was the same as for the unreinforced beams.

– The capacity with respect to perpendicular to grain failure is affected by moisture gradients. If the beam is in a moistening phase the capacity is almost halved compared to the mean value of the seasoned specimen.

- Beams subjected to climate change display larger variability in capacity than seasoned specimens.

- Regarding the test set up, it can be concluded that due to the short span the dominating fracture mode after reinforcing (both before and after testing) is shear. This is no problem in real structures where larger structures are used and most likely the ultimate failure for reinforced structures should be in bending, i.e. perpendicular to grain failure can probably be avoided by reinforcement of the type investigated here.

5 Concluding remarks

Due to the fact that climate induced stresses almost always are present in wood, the question is in what way to take them into consideration when designing structures? One possible solution is to assume that there is no strength in wood when it comes to tensile stress perpendicular grain (compare reinforced concrete). This means that different reinforcement methods have to be used, such as self tapping screws, glued in rods, fully threaded bars, nail plated fasteners, glued on plywood or glass fibres etc. Perhaps new technology and how to think when reinforcing members and structures should be developed and used. This way of thinking should probably lead to greater safety due to the fact that there is a "buffer in strength" in wood itself and the ductility is enhanced. In some cases the cross-section area could be made smaller without decreasing the load-carrying capacity, for instance in curved glulam beams.

Another approach should be to consider these stresses as a new load case combined with other loads such as wind, snow or serviceability loads. If so, there are some questions to be asked. Is it possible to add a prescribed value of moisture induced stress to be used for all structures, or should there be different values depending on size, annual ring pattern, moisture exposure, whether the surface is coated or not etc.? There is also a problem finding out in what way it is reasonable to combine loads. For instance, should maximum moisture induced stress be combined with snow or wind. If this is the case what should the combination factors be?

A third alternative would be to decrease the design strength in wood but this approach would probably leave no or very little strength left. So this alternative is basically the same as the first proposal.

The most reasonable and safe alternative is the first alternative where reinforcement such as self-tapping screws is used. When using this concept three different criteria has to be checked to evaluate the minimum distance between the screws 1) the withdrawal strength in the screw/wood 2) the tensile strength in the screw 3) and to achieve a uniform stress distribution near and between the screws.

The withdrawal strength is closely related to where the crack is developed. According to earlier discussion the maximum stress perpendicular to grain evolves approximately one third from the lower edge of the beam, but due to the variation in wood a shorter anchorage length should be used. The centre between screws can be evaluated according to

$$F_w = sb\sigma_{90} = \pi d l_a f_k$$

where F_w is the withdrawal capacity, s is the centre between the screws, b the cross-section width of the beam, σ_{90} the tensile stress perpendicular to grain, d the nominal diameter of the screw, l_a the anchorage length and f_k the characteristic withdrawal strength.

In the second case, when the beam cracks the cross-section is only held together by the screws, the centre between screws can be evaluated according to

$$F_k = sb\sigma_{90} = \frac{\pi d^2}{4} f_{uk}$$

where F_k is the tensile capacity and f_{uk} the characteristic ultimate strength.

In the last case the position of the screws should be such that a fairly uniform stress distribution perpendicular to grain between and the near the screws should be attained. According to FE- analysis the distance between the screws in *this case* should be approximately 40% of the beam height. A more thorough investigation should be carried out where parameters such as geometry (curved, tapered, pitched and pitched cambered), curvature, load configuration and distance between screws should be investigated to see the effect on the stress distribution perpendicular to grain.

6 References

Blaß, H.J., Steck, G. 1999. Perpendicular to the grain reinforcements of timber. Proceedings, Pacific Timber Engineering Conference, Rotorua, New Zealand, ISSN 1174-5096, 107-113.

Blaß, H.J., Laskewitz, B. 2002. Axiale Kraftverteilung in der Bewehrung von Satteldachträgern mit gekrümmtem Untergurt aus Brettschichtholz. Bautechnik 79 (7), S. 446-454

Dahlblom, O., Enquist, B., Gustafsson, P.J., Knudsen, R., Larsen, H.J., Ormarsson, S., Traberg, S. 1993. Fibre reinforcement of glulam: Summary and reports 1-7. Lund University, Div. of Structural Mechanics, Report TVSM-7083.

Dinwoodie, J.M. 2000. Timber: its Nature and Behaviour. Second edition, E & FN Spon, New York

Jönsson, J. 2004. Internal stresses in the cross-grain direction in glulam induced by climate variations. Structural Engineering, Lund Institute of Technology, Holzforschung *58*, 154-159.

Jönsson, J., Thelandersson, S. 2003. The effect of moisture gradients on the strength perpendicular to grain in glulam. Holz Roh- Werkst. *61*, 342-348.

Kasal, B., Heiduschke, A. 2004. Radial reinforcement of curved glue laminated wood beams with composite materials. Forest Products Journal, Vol. 54, No. 1, 74-79.

Ranta-Maunus, A. 2003. Effects of climate and climate variations on strength. *In*: Timber Engineering. S. Thelandersson, H.J. Larsen. Wiley & Sons Ltd, England. pp. 153-167.

SFS Intec AG, Fasteningsystems. 2003. Untersuchungsbericht, Nr. 173975/03-3, Labor-Nr.:2007/03-271.

INTERNATIONAL COUNCIL FOR RESEARCH AND INNOVATION
IN BUILDING AND CONSTRUCTION

WORKING COMMISSION W18 - TIMBER STRUCTURES

SELF-TAPPING SCREWS AS REINFORCEMENTS IN CONNECTIONS WITH DOWEL-TYPE FASTENERS

I Bejtka

H J Blaß

Universität Karlsruhe

GERMANY

Self-tapping screws as reinforcements in connections with dowel-type fasteners

I. Bejtka, H.J. Blaß

Lehrstuhl für Ingenieurholzbau und Baukonstruktionen

Universität Karlsruhe, Germany

1   Introduction

Connections with dowel-type fasteners are often used to transfer loads between timber members. Here, the load-carrying capacity, which can be calculated according to Johansen´s yield theory, is limited by the embedding strength of the timber, by the yield moment of the dowel-type fasteners and finally by the geometry of the connection.

The spacing of dowel-type fasteners affects the splitting tendency of timber in the connection area. The splitting tendency increases with decreasing fastener spacing parallel to the grain and hence decreases the effective number of fasteners n_{ef}. Splitting may be prevented by reinforcing the connection area and, consequently, the effective number n_{ef} of fasteners increases. Self-tapping screws with continuous threads represent a simple and economic reinforcement method. The screws are placed between the dowel-type fasteners, both perpendicular to the dowel axis and to the grain direction.

In connections with sufficient reinforcement between the dowels, the timber does not split and the effective number n_{ef} equals the actual number n of dowels.

Timber splitting is prevented, when the axial load-carrying capacity R_{ax} of each screw is larger than 30% of the lateral load-carrying capacity R per shear plane of each dowel [1]. The lateral load-carrying capacity R can be calculated according to Johansen´s yield theory. The axial load-carrying capacity R_{ax} of the screws may e.g. be calculated according to [2].

Furthermore, by placing the screws in contact with the dowel-type fasteners (Fig. 1), the load-carrying capacity and the stiffness of a connection increases.
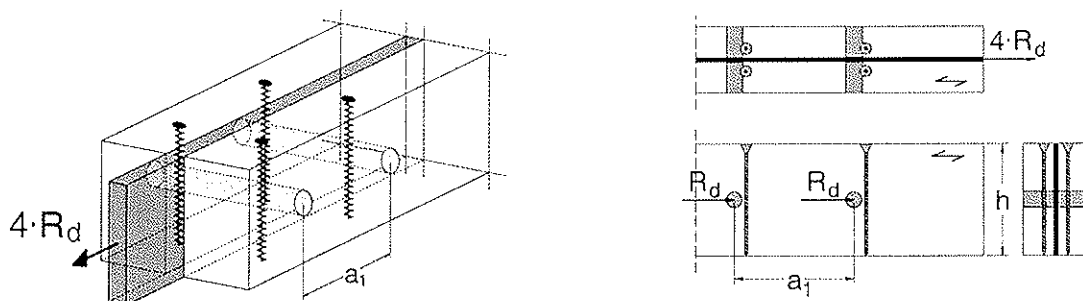
Fig. 1: Reinforced connection using self-tapping screws placed in contact with the dowels

Both effects – preventing splitting and increasing the load-carrying capacity by placing the screws in contact with the dowels – may cause an increase of up to 120% of the load-carrying capacity compared to non-reinforced connections (Fig. 2).
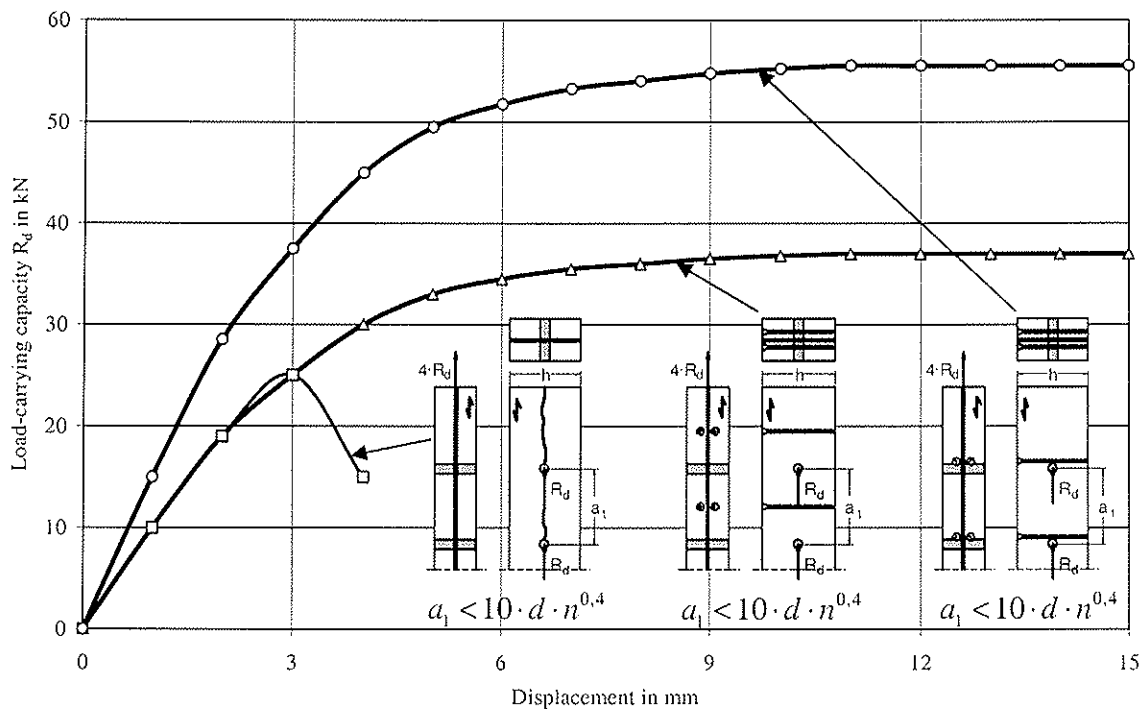
Fig. 2: Typical load-displacement-curves of non-reinforced and reinforced connections

A calculation model as an extension of Johansen´s yield theory and based on theoretical and experimental studies is presented.

2 Calculation model for the extended Johansen´s yield theory

2.1 Assumptions

The load-carrying capacity for reinforced connections is derived on the basis of the same assumptions as Johansen´s yield theory. The screws, placed in contact with the dowel-type fasteners, perpendicular to the dowel axis and to the grain direction (Fig. 1), are loaded just as the dowels themselves perpendicular to their axis. One of the basic assumptions in Johansen´s yield theory is an ideal rigid-plastic material behaviour of the timber in embedding and of the fastener in bending. Under this assumption, screws as reinforcements loaded perpendicular to their axis also show an ideal rigid-plastic load-carrying behaviour (Fig. 3).

Consequently, the screw only moves in force direction, when the dowel load component F_{VE} reaches the load-carrying capacity R_{VE} of the screw. In this case, the screw represents a "soft" support. Alternatively, for $F_{VE} < R_{VE}$, the screw does not move and represents a rigid support for the dowel. This consideration leads to four sub-failure modes for each failure mode in timber-to-timber connections and two sub-failure modes for each failure mode in steel-to-timber connections in Johansen´s yield theory. Subsequently, the sub-failure modes for reinforced steel-to-timber and timber-to-timber connections are presented.

2
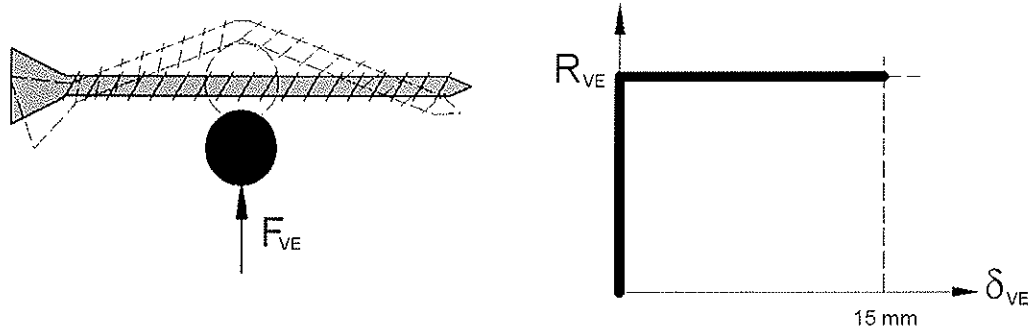
Fig. 3: Assumed load-carrying behaviour of a screw as reinforcement loaded perpendicular to the axis

2.2 Reinforced steel-to-timber connections

As an example for the derivation of all failure modes, the load-carrying capacity for a reinforced steel-to-timber connection with an inner steel plate and with two plastic hinges (failure mode 3) per shear plane is derived. The load-carrying capacity for the corresponding non-reinforced connection (right side in Fig. 4) is derived from the force and moment equilibrium in the shear plane (see equation (1)).
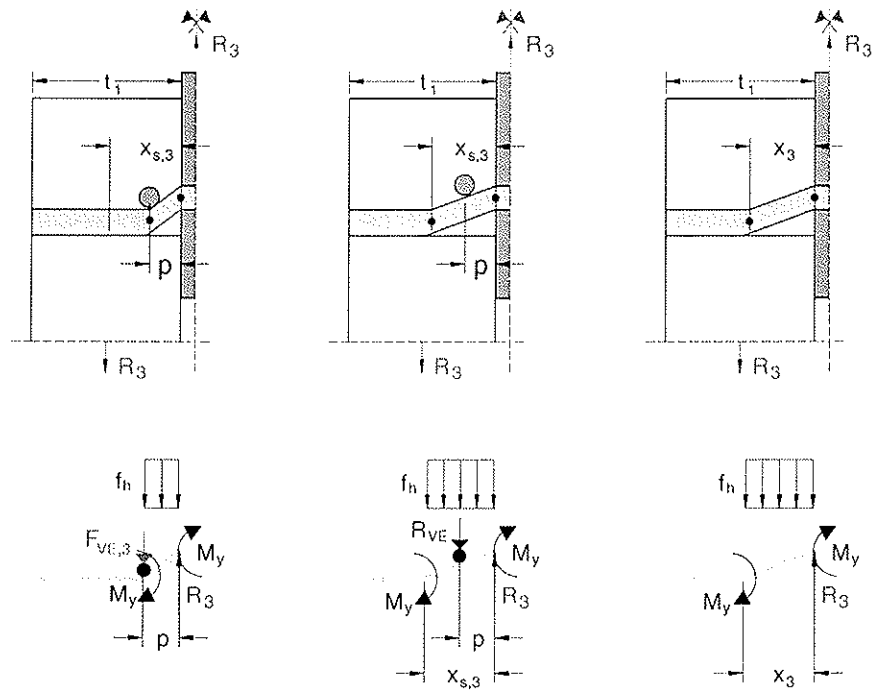
Fig. 4: Reinforced connection with sub-failure mode "rigid", reinforced connection with sub-failure mode "soft" and non-reinforced connection (from left to right side)

$$R_3 = \sqrt{2} \cdot \sqrt{2 \cdot M_y \cdot f_h \cdot d} \tag{1}$$

The distance x_3 between the shear plane and the plastic hinge is given in equation (2).

$$x_3 = \sqrt{\frac{4 \cdot M_y}{f_h \cdot d}} \tag{2}$$

3

By placing the screws in contact with the dowel in-between the shear plane and the plastic hinge for a non-reinforced connection ($p < x_3$) and taking into consideration the load-carrying behaviour of the screw (Fig. 3), two sub-failure modes for failure mode 3 can occur (left and middle side in Fig. 4).

Sub-failure mode "rigid" appears for $F_{VE,3} < R_{VE}$. R_{VE} is the lateral load-carrying capacity of the screw. $F_{VE,3}$ can be derived from the force and moment equilibrium in the shear plane for the left system in Fig. 4 (eq. (3)).

$$F_{VE,3} = \frac{2 \cdot M_y}{p} - \frac{f_h \cdot d \cdot p}{2}$$ (3)

In this case, the load-carrying capacity R_3 is derived as:

$$R_3 = \frac{2 \cdot M_y}{p} + \frac{f_h \cdot d \cdot p}{2}$$ (4)

In the case of $F_{VE,3} \geq R_{VE}$ the load-carrying capacity of a reinforced connection is derived from the force and moment equilibrium in the shear plane for the middle system in Fig. 4 (sub-failure mode "soft") as:

$$R_3 = R_{VE} + \sqrt{2} \cdot \sqrt{f_h \cdot d \cdot \left(2 \cdot M_y - R_{VE} \cdot p\right)}$$ (5)

Recapitulating, the load-carrying capacity for Johansen's failure mode 3 for a reinforced steel-to-timber connection can be calculated as follows:

For $p \geq x_3$ no reinforcement occurs. The load-carrying capacity for failure mode 3 is calculated according to eq. (1).

For $p < x_3$ the reinforcement increases the load-carrying capacity. For $F_{VE,3} < R_{VE}$ the load-carrying capacity is calculated according to eq. (4), for $F_{VE,3} \geq R_{VE}$ according to eq. (5). $F_{VE,3}$ for failure mode 3 is calculated using eq. (3).

Similarly, the load-carrying capacities of the other two failure modes for reinforced steel-to-timber connections with an inner steel plate are derived. Therewith, the load-carrying capacity for reinforced steel-to-timber connections with an inner steel plate can be calculated as follows.

$$R = \min\{R_1, R_2, R_3\}$$ (6)

with

$$R_1 = f_h \cdot d \cdot t_1 + R_{VE}$$ (7)

$$R_2 = f_h \cdot d \cdot t_1 \cdot \left[\sqrt{2 + \frac{4}{t_1^2} \cdot \frac{M_y}{f_h \cdot d}} - 1\right] \qquad \text{for } p \geq x_2$$ (8)

$$R_2 = \frac{M_y}{p} + f_h \cdot d \cdot t_1 \cdot \left[\frac{t_1}{2 \cdot p} + \frac{p}{t_1} - 1\right] \qquad \text{for } p < x_2 \text{ and } R_{VE} > F_{VE,2}$$ (9)

$$R_2 = R_{VE} + f_h \cdot t_1 \cdot d \cdot \left[\sqrt{2 + \frac{4}{t_1^2} \cdot \left(\frac{M_y - R_{VE} \cdot p}{f_h \cdot d}\right)} - 1\right] \qquad \text{for } p < x_2 \text{ and } R_{VE} \leq F_{VE,2}$$ (10)

4

$$\text{with } F_{VE,2} = \frac{M_y}{p} + \frac{f_h \cdot d}{p} \cdot \left[\frac{t_1^2}{2} - p^2 \right] \qquad \text{and } x_2 = \sqrt{\frac{t_1^2}{2} + \frac{M_y}{f_h \cdot d}} \qquad (11)$$

$$R_3 = \sqrt{2} \cdot \sqrt{2 \cdot M_y \cdot f_h \cdot d} \qquad \text{for } p \geq x_3 \qquad (12)$$

$$R_3 = \frac{2 \cdot M_y}{p} + \frac{f_h \cdot d \cdot p}{2} \qquad \text{for } p < x_3 \text{ and } R_{VE} > F_{VE,3} \qquad (13)$$

$$R_3 = R_{VE} + \sqrt{2} \cdot \sqrt{f_h \cdot d \cdot \left(2 \cdot M_y - R_{VE} \cdot p\right)} \qquad \text{for } p < x_3 \text{ and } R_{VE} \leq F_{VE,3} \qquad (14)$$

$$\text{with } F_{VE,3} = \frac{2 \cdot M_y}{p} - \frac{f_h \cdot d \cdot p}{2} \qquad \text{and } x_3 = \sqrt{\frac{4 \cdot M_y}{f_h \cdot d}} \qquad (15)$$

Fig. 5 shows the reinforcing effect as a R over R_{VE} diagram for a steel-to-timber connection with a 16 mm steel dowel, for an embedding strength $f_h = 30$ N/mm^2, a yield moment $M_y = 246$ Nm, a timber member thickness $t_1 = 60$ mm and a distance p = 20 mm.
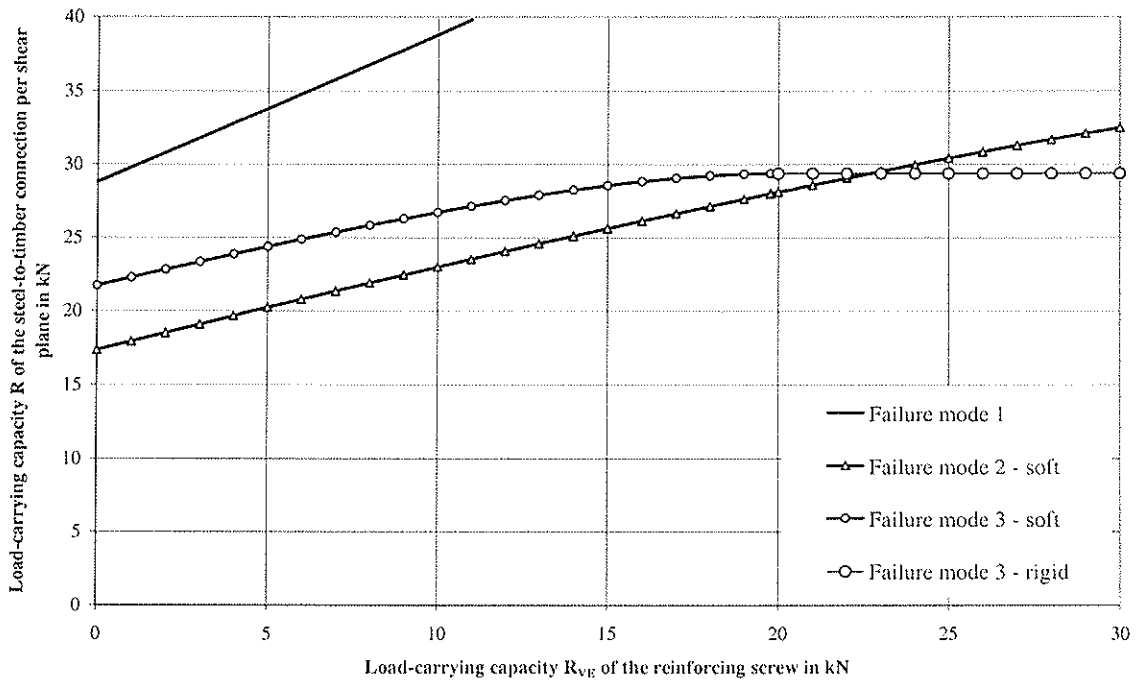
Fig. 5: Load-carrying capacity R for a steel-to-timber connection depending on R_{VE}

For $R_{VE} = 0$ the load carrying capacity R is equal to the load-carrying capacity for a non-reinforced connection (R = 17,4 kN). Here, failure mode 2 with one plastic hinge per shear plane occurs. With increasing load-carrying capacity R_{VE} of the screw, the load-carrying capacity R of the steel-to-timber connection increases. For $R_{VE} = 22,6$ kN the load-carrying capacity R reaches the maximum value of about R = 29,4 kN which is equal to an increase of about 69%. Due to the fact that for even higher values of R_{VE} sub-failure mode "rigid" occurs, a further increase is not possible.

2.3 Reinforced timber-to-timber connections

Compared to reinforced steel-to-timber connections, the calculation model for reinforced timber-to-timber connections is more complicated. In addition to the presented sub-failure modes "rigid" and "soft", two further sub-failure modes "rigid-soft" and "soft-rigid" for each Johansen's failure mode occur. These additional sub-failure modes occur, when the load-carrying capacities for the reinforcements $R_{1,VE}$ and $R_{2,VE}$ or/and the load components $F_{1,VE}$ and $F_{2,VE}$ in both timber members are not equal. $R_{1,VE} \neq R_{2,VE}$ or/and $F_{1,VE} \neq F_{2,VE}$, when the timber density ρ in both timber members is not equal.

As an example for the derivation of all failure modes, the load-carrying capacity for a reinforced timer-to-timber connection with two plastic hinges per shear plane (failure mode 3) is derived. All possible sub-failure modes for Johansen's failure mode 3 are shown in Fig. 6.
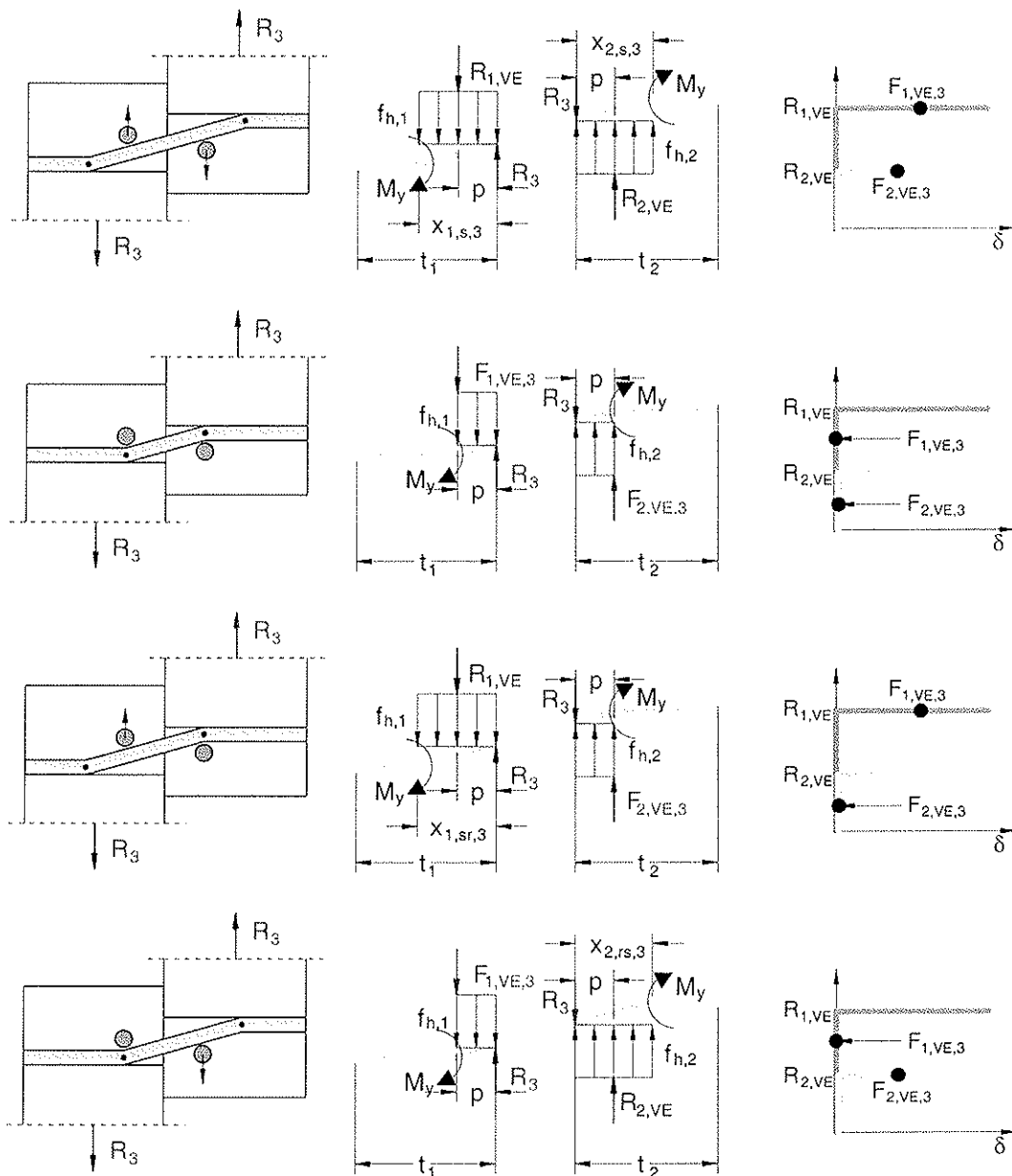
Fig. 6: Reinforced timber-to-timber connection with sub-failure modes "soft", "rigid",
"soft-rigid" and "rigid-soft" for Johansen's failure mode 3 (from top to bottom)

The load-carrying capacity for the non-reinforced connection is derived from the force and moment equilibrium in the shear plane as:

$$R_3 = \frac{\sqrt{2 \cdot \beta}}{\sqrt{1 + \beta}} \cdot \sqrt{2 \cdot M_y \cdot f_{h,1} \cdot d} \tag{16}$$

The distances $x_{1,3}$ and $x_{2,3}$ between the shear plane and the plastic hinges for a non-reinforced connection are:

$$x_{1,3} = \sqrt{\frac{2 \cdot \beta}{1 + \beta}} \cdot \sqrt{\frac{2 \cdot M_y}{f_{h,1} \cdot d}} \qquad\qquad x_{2,3} = \frac{\sqrt{2}}{\sqrt{\beta \cdot (1 + \beta)}} \cdot \sqrt{\frac{2 \cdot M_y}{f_{h,1} \cdot d}} \tag{17}$$

Further on applies:

$$\beta = \frac{f_{h,2}}{f_{h,1}} \qquad\qquad \psi = \frac{R_{2,VE}}{R_{1,VE}} \tag{18}$$

By placing the screws in contact with the dowels in-between the shear plane and the plastic hinges of a non-reinforced connection ($p < x_{1,3}$ and $p < x_{2,3}$) and taking into consideration the ideal rigid-plastic load-carrying behaviour of the screw loaded perpendicular to the axis, four sub-failure modes for Johansen's failure mode 3 occur (Fig. 6).

Sub-failure mode "rigid" appears for $F_{1,VE,3} < R_{1,VE}$ and $F_{2,VE,3} < R_{2,VE}$. $R_{i,VE}$ are the load-carrying capacities of the screws in both timber members. $F_{1,VE,3}$ and $F_{2,VE,3}$ are derived from the force and moment equilibrium in the shear plane for the sub-failure mode "rigid" as:

$$F_{1,VE,3} = \frac{M_y}{p} - \frac{f_{h,1} \cdot d \cdot p}{4} \cdot (3 - p) \qquad\qquad F_{2,VE,3} = \frac{M_y}{p} - \frac{f_{h,1} \cdot d \cdot p}{4} \cdot (3 \cdot \beta - 1) \tag{19}$$

In this "rigid" case, the load-carrying capacity R_3 is derived as:

$$R_3 = \frac{M_y}{p} + \frac{f_{h,1} \cdot d \cdot p}{4} \cdot (1 + \beta) \tag{20}$$

The load-carrying capacity for the sub-failure mode "soft" is derived from the force and moment equilibrium in the shear plane as:

$$R_3 = R_{1,VE} \cdot \frac{(\beta + \psi)}{(1 + \beta)} + \sqrt{\frac{2 \cdot \beta}{1 + \beta}} \cdot \sqrt{f_{h,1} \cdot d \cdot \left(2 \cdot M_y - R_{1,VE} \cdot p \cdot (1 + \psi)\right) - \frac{R_{1,VE}^2 \cdot (\psi - 1)^2}{2 \cdot (1 + \beta)}} \tag{21}$$

This sub-failure mode appears for $p < x_{1,s,3}$ and $p < x_{2,s,3}$ (Fig. 6). The distances $x_{1,s,3}$ and $x_{2,s,3}$ can be derived from the force and moment equilibrium in the shear plane for the sub-failure mode "soft". Taking into account the assumption $p < x_{1,s,3}$ and $p < x_{2,s,3}$, following precondition for sub-failure mode "soft" is derived:

$$R_{1,VE} \le Z_3 = \min \left\{ \begin{array}{c} \dfrac{M_y}{p} - \dfrac{f_{h,1} \cdot d \cdot p}{4 \cdot \beta} \cdot (1 + \beta) \\[3mm] \dfrac{M_y}{p} - \dfrac{f_{h,1} \cdot d \cdot p \cdot \beta}{4} \cdot (1 + \beta) \end{array} \right\} \qquad \text{for } \psi = 1 \tag{22}$$

7

$$R_{1,VE} \leq Z_3 = \min \left\{ \begin{array}{l} \dfrac{f_{h,1} \cdot d \cdot p}{(\psi-1)^2} \cdot \left[\sqrt{(1+\psi)^2 \cdot (\beta^2 + \beta) - 4 \cdot \beta \cdot \psi^2 + \dfrac{4 \cdot \beta \cdot (\psi-1)^2 \cdot M_y}{p^2 \cdot d \cdot f_{h,1}}} \atop -(\beta-1) \cdot \psi - \beta - 1 \right] \\[6mm] \dfrac{f_{h,1} \cdot d \cdot p}{(\psi-1)^2} \cdot \left[\sqrt{(2+\psi) \cdot (\beta+1) \cdot \psi + 1 - 3 \cdot \beta + \dfrac{4 \cdot (\psi-1)^2 \cdot M_y}{p^2 \cdot d \cdot f_{h,1}}} \atop -(\beta+1) \cdot \psi + \beta - 1 \right] \end{array} \right\} \tag{23}$$

for $\psi \neq 1$

The load-carrying capacity for the sub-failure mode "soft-rigid" is derived from the force and moment equilibrium in the shear plane as:

$$R_3 = R_{1,VE} + f_{h,1} \cdot d \cdot \left[\sqrt{(1+\beta) \cdot p^2 - \dfrac{4 \cdot R_{1,VE} \cdot p - 4 \cdot M_y}{f_{h,1} \cdot d}} - p \right] \tag{24}$$

This sub-failure mode appears for $F_{1,VE,3} \cdot \psi > F_{2,VE,3}$ and for $Z < R_{1,VE} \leq F_{1,VE,3}$. Those ancillary conditions can be derived in the same way from the force and moment equilibrium in the respective shear plane.

For $F_{1,VE,3} \cdot \psi \leq F_{2,VE,3}$ and for $Z < R_{1,VE} \leq F_{2,VE,3}/\psi$ sub-failure mode "rigid-soft" appears. The load-carrying capacity for this sub-failure mode is derived from the force and moment equilibrium in the respective shear plane as:

$$R_3 = R_{1,VE} \cdot \psi + f_{h,1} \cdot d \cdot \left[\sqrt{(1+\beta) \cdot \beta \cdot p^2 - \dfrac{4 \cdot \beta \cdot (R_{1,VE} \cdot \psi \cdot p - M_y)}{f_{h,1} \cdot d}} - p \cdot \beta \right] \tag{25}$$

Similarly, the other five Johansen's failure modes for reinforced timber-to-timber connections are derived.

Therewith, the load-carrying capacity for a reinforced timber-to-timber connection can be calculated as follows.

$$R = \min \left\{ R_{1a}, R_{1b}, R_{1c}, R_{2a}, R_{2b}, R_3 \right\} \tag{26}$$

with

$$R_{1a} = f_{h,1} \cdot d \cdot t_1 + R_{1,VE} \tag{27}$$

$$R_{1b} = \beta \cdot f_{h,1} \cdot d \cdot t_2 + \psi \cdot R_{1,VE} \tag{28}$$

$$R_{1c} = \dfrac{f_{h,1} \cdot d \cdot t_1}{(1+\beta)} \cdot \left[\sqrt{\beta + 2 \cdot \beta^2 \cdot \left(1 + \dfrac{t_2}{t_1} + \dfrac{t_2^2}{t_1^2}\right) + \beta^3 \cdot \dfrac{t_2^2}{t_1^2}} - \beta \cdot \left(1 + \dfrac{t_2}{t_1}\right) \right] \quad \begin{array}{l} \text{for } p \geq x_{1,1c} \\[2mm] \text{or/and } p \geq x_{2,1c} \end{array} \tag{29}$$

$$R_{1c} = \dfrac{f_{h,1} \cdot d \cdot t_1}{2} \cdot \left[(\beta+1) \cdot \dfrac{p}{t_1} - 1 - \beta \cdot \dfrac{t_2}{t_1} + \left(1 + \beta \cdot \dfrac{t_2^2}{t_1^2}\right) \cdot \dfrac{t_1}{2 \cdot p} \right] \tag{30}$$

for $p < x_{1,1c}$ and $p < x_{2,1c}$ and for $R_{1,VE} > F_{1,VE,1c}$ and $R_{1,VE} > \dfrac{F_{2,VE,1c}}{\psi}$

$$R_{1c} = R_{1,VE} \cdot \frac{(\psi + \beta)}{(1+\beta)} + \frac{f_{h,1} \cdot d \cdot t_1}{(1+\beta)}$$

$$\cdot \left[\sqrt{ \begin{array}{c} \beta + 2 \cdot \beta^2 \cdot \left(1 + \frac{t_2}{t_1} + \frac{t_2^2}{t_1^2}\right) + \beta^3 \cdot \frac{t_2^2}{t_1^2} - \frac{R_{1,VE}^2 \cdot \beta \cdot (\psi - 1)^2}{t_1^2 \cdot d^2 \cdot f_{h,1}^2} \\ - \frac{2 \cdot R_{1,VE} \cdot \beta \cdot p \cdot \left(2 \cdot (1+\beta) \cdot (1+\psi) + \frac{t_1}{p} \cdot (1-\psi) \cdot \left(\beta \cdot \frac{t_2}{t_1} - 1\right)\right)}{f_{h,1} \cdot d \cdot t_1^2} \end{array}} - \beta \cdot \left(1 + \frac{t_2}{t_1}\right) \right] \qquad (31)$$

for $p < x_{1,1c}$ and $p < x_{2,1c}$ and for $R_{1,VE} \le Z_{1c}$

$$R_{1c} = R_{1,VE} + f_{h,1} \cdot d \cdot t_1$$

$$\cdot \left[\sqrt{2} \cdot \sqrt{ 2 \cdot \frac{p^2}{t_1^2} \cdot (1+\beta) + 2 \cdot \frac{p}{t_1} \cdot \left(1 - \beta \cdot \frac{t_2}{t_1}\right) + \left(1 + \beta \cdot \frac{t_2^2}{t_1^2}\right) - \frac{4 \cdot R_{1,VE} \cdot p}{t_1^2 \cdot d \cdot f_{h,1}} } - 2 \cdot \frac{p}{t_1} - 1 \right] \qquad (32)$$

for $p < x_{1,1c}$ and $p < x_{2,1c}$ and for $F_{1,VE,1c} > \dfrac{F_{2,VE,1c}}{\psi}$ and $Z_{1c} < R_{1,VE} \le F_{1,VE,1c}$

$$R_{1c} = R_{1,VE} \cdot \psi + f_{h,1} \cdot d \cdot t_1 \cdot \left[\sqrt{2 \cdot \beta} \cdot \sqrt{ \begin{array}{c} 2 \cdot \frac{p^2}{t_1^2} \cdot (1+\beta) - 2 \cdot \frac{p}{t_1} \cdot \left(1 - \beta \cdot \frac{t_2}{t_1}\right) \\ + 1 + \beta \cdot \frac{t_2^2}{t_1^2} - \frac{4 \cdot R_{1,VE} \cdot \psi \cdot p}{t_1^2 \cdot d \cdot f_{h,1}} \end{array}} - \beta \cdot \left(\frac{t_2}{t_1} + 2 \cdot \frac{p}{t_1}\right) \right] \qquad (33)$$

for $p < x_{1,1c}$ and $p < x_{2,1c}$ and for $F_{1,VE,1c} \le \dfrac{F_{2,VE,1c}}{\psi}$ and $Z_{1c} < R_{1,VE} \le \dfrac{F_{2,VE,1c}}{\psi}$

With

$$x_{1,1c} = \frac{t_1}{2 \cdot (1+\beta)} \cdot \left[\sqrt{\beta + 2 \cdot \beta^2 \cdot \left[1 + \frac{t_2}{t_1} + \left(\frac{t_2}{t_1}\right)^2\right] + \beta^3 \cdot \left(\frac{t_2}{t_1}\right)^2} + 1 - \beta \cdot \frac{t_2}{t_1} \right] \qquad (34)$$

$$x_{2,1c} = \frac{t_1}{2 \cdot \beta \cdot (1+\beta)} \cdot \left[\sqrt{\beta + 2 \cdot \beta^2 \cdot \left[1 + \frac{t_2}{t_1} + \left(\frac{t_2}{t_1}\right)^2\right] + \beta^3 \cdot \left(\frac{t_2}{t_1}\right)^2} - \beta \cdot \left(1 - \beta \cdot \frac{t_2}{t_1}\right) \right] \qquad (35)$$

$$F_{1,VE,1c} = \frac{f_{h,1} \cdot d \cdot t_1}{2} \cdot \left[(\beta - 3) \cdot \frac{p}{t_1} + 1 - \beta \cdot \frac{t_2}{t_1} + \left(1 + \beta \cdot \frac{t_2^2}{t_1^2}\right) \cdot \frac{t_1}{2 \cdot p} \right] \qquad (36)$$

$$F_{2,VE,1c} = \frac{f_{h,1} \cdot d \cdot t_1}{2} \cdot \left[(1 - 3 \cdot \beta) \cdot \frac{p}{t_1} - 1 + \beta \cdot \frac{t_2}{t_1} + \left(1 + \beta \cdot \frac{t_2^2}{t_1^2}\right) \cdot \frac{t_1}{2 \cdot p} \right] \qquad (37)$$

9

$$Z_{1c} = \min \left\{ \begin{array}{l} \dfrac{f_{h,1} \cdot d}{(\psi-1)^2} \cdot \left[\begin{array}{l} (t_1 - t_2 \cdot \beta - 2 \cdot p) \cdot (1-\psi) - 2 \cdot p \cdot \beta \cdot (1+\psi) + \sqrt{2 \cdot \beta} \\ \sqrt{\begin{array}{l} 2 \cdot p^2 \cdot (\psi+1)^2 \cdot (1+\beta) + t_1^2 \cdot (\psi-1)^2 \cdot \left(1 + \beta \cdot \dfrac{t_2^2}{t_1^2}\right) \\ +2 \cdot p \cdot t_1 \cdot (1-\psi^2) \cdot \left(\beta \cdot \dfrac{t_2}{t_1} - 1\right) - 8 \cdot \psi^2 \cdot p^2 \end{array}} \end{array} \right] \\[3em] \dfrac{f_{h,1} \cdot d}{(\psi-1)^2} \cdot \left[\begin{array}{l} (t_1 - t_2 \cdot \beta - 2 \cdot p) \cdot (1-\psi) + 2 \cdot p \cdot \beta \cdot (1-\psi) - 4 \cdot \psi \cdot p \\ + \sqrt{2} \cdot \sqrt{\begin{array}{l} 2 \cdot p^2 \cdot \psi \cdot (\psi+2) \cdot (1+\beta) + 2 \cdot p^2 \cdot (1 - 3 \cdot \beta) \\ + 2 \cdot p \cdot (1-\psi^2) \cdot (\beta \cdot t_2 - t_1) + (\psi-1)^2 \cdot (t_1^2 + \beta \cdot t_2^2) \end{array}} \end{array} \right] \end{array} \right\} \qquad (38)$$

for $\psi \neq 1$

$$Z_{1c} = \min \left\{ \begin{array}{l} \dfrac{f_{h,1} \cdot d}{2 \cdot \beta} \cdot \left[(t_1 - t_2 \cdot \beta) - p \cdot (\beta+1) + \dfrac{t_1^2}{2 \cdot p} \cdot (\beta-1) + \dfrac{(\beta \cdot t_2 + t_1)^2}{4 \cdot p} \right] \\[1.5em] \dfrac{f_{h,1} \cdot d \cdot \beta}{2} \cdot \left[(t_2 \cdot \beta - t_1) - p \cdot (\beta+1) + \dfrac{t_2^2}{2 \cdot p} \cdot (1-\beta) + \dfrac{(\beta \cdot t_2 + t_1)^2}{4 \cdot p \cdot \beta} \right] \end{array} \right\} \qquad (39)$$

for $\psi = 1$

$$R_{2a} = \dfrac{f_{h,1} \cdot d \cdot t_1}{(2+\beta)} \cdot \left[\sqrt{2 \cdot \beta \cdot (1+\beta) + \dfrac{4 \cdot \beta \cdot (2+\beta) \cdot M_y}{f_{h,1} \cdot d \cdot t_1^2}} - \beta \right] \qquad \begin{array}{l} \text{for } p \geq x_{1,2a} \\ \text{or/and } p \geq x_{2,2a} \end{array} \qquad (40)$$

$$R_{2a} = \dfrac{f_{h,1} \cdot d \cdot t_1}{4} \cdot \left[(\beta+2) \cdot \dfrac{p}{t_1} - 2 + \dfrac{t_1}{p} \right] + \dfrac{M_y}{2 \cdot p} \qquad (41)$$

for $p < x_{1,2a}$ and $p < x_{2,2a}$ and for $R_{1,VE} > F_{1,VE,2a}$ and $R_{1,VE} > \dfrac{F_{2,VE,2a}}{\psi}$

$$R_{2a} = R_{1,VE} \cdot \dfrac{(2 \cdot \psi + \beta)}{(2+\beta)}$$

$$+ \dfrac{f_{h,1} \cdot d \cdot t_1}{(2+\beta)} \cdot \left[\sqrt{\begin{array}{l} 2 \cdot \beta \cdot (1+\beta) - \dfrac{2 \cdot R_{1,VE}^2 \cdot \beta \cdot (\psi-1)^2}{t_1^2 \cdot d^2 \cdot f_{h,1}^2} \\ - \dfrac{4 \cdot R_{1,VE} \cdot \beta \cdot \left(\dfrac{p}{t_1} \cdot (1+\psi) \cdot (2+\beta) + \psi - 1\right)}{f_{h,1} \cdot d \cdot t_1} + \dfrac{4 \cdot \beta \cdot (2+\beta) \cdot M_y}{f_{h,1} \cdot d \cdot t_1^2} \end{array}} - \beta \right] \qquad (42)$$

for $p < x_{1,2a}$ and $p < x_{2,2a}$ and for $R_{1,VE} \leq Z_{2a}$

10

$$R_{2a} = R_{1,VE} + f_{h,1} \cdot d \cdot t_1 \cdot \left[\sqrt{(2+\beta) \cdot 2 \cdot \frac{p^2}{t_1^2} + 2 + 4 \cdot \frac{p}{t_1} - \frac{(8 \cdot R_{1,VE} \cdot p - 4 \cdot M_y)}{t_1^2 \cdot f_{h,1} \cdot d}} - 2 \cdot \frac{p}{t_1} - 1 \right] \tag{43}$$

for $p < x_{1,2a}$ and $p < x_{2,2a}$ and for $F_{1,VE,2a} > \dfrac{F_{2,VE,2a}}{\psi}$ and $Z_{2a} < R_{1,VE} \le F_{1,VE,2a}$

$$R_{2a} = R_{1,VE} \cdot \psi$$
$$+ f_{h,1} \cdot d \cdot t_1 \cdot \left[\sqrt{(2+\beta) \cdot \beta \cdot \frac{p^2}{t_1^2} + \beta - 2 \cdot \beta \cdot \frac{p}{t_1} - \frac{\beta \cdot (4 \cdot R_{1,VE} \cdot \psi \cdot p - 2 \cdot M_y)}{t_1^2 \cdot f_{h,1} \cdot d}} - \beta \cdot \frac{p}{t_1} \right] \tag{44}$$

for $p < x_{1,2a}$ and $p < x_{2,2a}$ and for $F_{1,VE,2a} \le \dfrac{F_{2,VE,2a}}{\psi}$ and $Z_{2a} < R_{1,VE} \le \dfrac{F_{2,VE,2a}}{\psi}$

$$x_{1,2a} = \frac{t_1}{2 \cdot (2+\beta)} \cdot \left[\sqrt{2 \cdot \beta \cdot (1+\beta) + \frac{(2+\beta) \cdot \beta \cdot 4 \cdot M_y}{t_1^2 \cdot f_{h,1} \cdot d}} + 2 \right] \tag{45}$$

$$x_{2,2a} = \frac{t_1}{\beta \cdot (2+\beta)} \cdot \left[\sqrt{2 \cdot \beta \cdot (1+\beta) + \frac{(2+\beta) \cdot \beta \cdot 4 \cdot M_y}{t_1^2 \cdot f_{h,1} \cdot d}} - \beta \right] \tag{46}$$

$$F_{1,VE,2a} = \frac{f_{h,1} \cdot d \cdot t_1}{4} \cdot \left[(\beta - 6) \cdot \frac{p}{t_1} + 2 + \frac{t_1}{p} \right] + \frac{M_y}{2 \cdot p} \tag{47}$$

$$F_{2,VE,2a} = \frac{f_{h,1} \cdot d \cdot t_1}{4} \cdot \left[(2 - 3 \cdot \beta) \cdot \frac{p}{t_1} - 2 + \frac{t_1}{p} \right] + \frac{M_y}{2 \cdot p} \tag{48}$$

$$Z_{2a} = \min \left\{ \begin{array}{l} \dfrac{f_{h,1} \cdot d}{(\psi-1)^2} \cdot \left[\begin{array}{l} (2 \cdot p - t_1 - \beta \cdot p) \cdot (\psi - 1) - 2 \cdot p \cdot \beta \\ + \sqrt{\begin{array}{l} \beta \cdot p^2 \cdot (\psi+1)^2 \cdot (2+\beta) + 2 \cdot p \cdot t_1 \cdot \beta \cdot (\psi^2 - 1) \\ + \beta \cdot t_1^2 \cdot (\psi-1)^2 - 8 \cdot \beta \cdot \psi^2 \cdot p^2 + \dfrac{2 \cdot \beta \cdot (\psi-1)^2 \cdot M_y}{f_{h,1} \cdot d} \end{array}} \end{array} \right] \\[3em] \dfrac{f_{h,1} \cdot d}{(\psi-1)^2} \cdot \left[\begin{array}{l} (2 \cdot p + t_1 + \beta \cdot p) \cdot (1 - \psi) - 4 \cdot p \\ + \sqrt{2} \cdot \sqrt{\begin{array}{l} p^2 \cdot (\psi+1)^2 \cdot (2+\beta) + 2 \cdot p \cdot t_1 \cdot (\psi^2 - 1) \\ + t_1^2 \cdot (\psi-1)^2 - 4 \cdot \beta \cdot p^2 + \dfrac{2 \cdot (\psi-1)^2 \cdot M_y}{f_{h,1} \cdot d} \end{array}} \end{array} \right] \end{array} \right\} \tag{49}$$

for $\psi \neq 1$

$$Z_{2a} = \min \left\{ \begin{array}{l} \dfrac{f_{h,1} \cdot d}{4 \cdot p \cdot \beta} \cdot \left[(\beta - 1) \cdot t_1^2 + 4 \cdot p \cdot t_1 - 2 \cdot p^2 \cdot (2+\beta) \right] + \dfrac{M_y}{2 \cdot p} \\[1.5em] \dfrac{f_{h,1} \cdot d}{8 \cdot p} \cdot \left[t_1^2 - 2 \cdot p \cdot \beta \cdot t_1 - p^2 \cdot \beta \cdot (2+\beta) \right] + \dfrac{M_y}{2 \cdot p} \end{array} \right\} \text{ for } \psi = 1 \tag{50}$$

11

$$R_{2b} = \frac{f_{h,1} \cdot d \cdot t_2}{(2 \cdot \beta + 1)} \cdot \left[\sqrt{2 \cdot \beta^2 \cdot (1+\beta) + \frac{4 \cdot \beta \cdot (2 \cdot \beta + 1) \cdot M_y}{f_{h,1} \cdot d \cdot t_2^2}} - \beta \right] \qquad \begin{array}{l} \text{for } p \geq x_{1,2b} \\ \\ \text{or/and } p \geq x_{2,2b} \end{array} \tag{51}$$

$$R_{2b} = \frac{f_{h,1} \cdot d \cdot t_2}{4} \cdot \left[(2 \cdot \beta + 1) \cdot \frac{p}{t_2} + 2 \cdot \beta \cdot \left(\frac{t_2}{2 \cdot p} - 1 \right) \right] + \frac{M_y}{2 \cdot p} \tag{52}$$

for $p < x_{1,2b}$ and $p < x_{2,2b}$ and for $R_{1,VE} > F_{1,VE,2b}$ and $R_{1,VE} > \dfrac{F_{2,VE,2b}}{\psi}$

$$R_{2b} = R_{1,VE} \cdot \frac{(2 \cdot \beta + \psi)}{(2 \cdot \beta + 1)}$$
$$+ \frac{f_{h,1} \cdot d \cdot t_2}{(2 \cdot \beta + 1)} \cdot \left[\sqrt{\begin{array}{c} 2 \cdot \beta^2 \cdot (1+\beta) - \dfrac{2 \cdot R_{1,VE}^2 \cdot \beta \cdot (\psi - 1)^2}{t_2^2 \cdot d^2 \cdot f_{h,1}^2} + \dfrac{4 \cdot \beta \cdot (2 \cdot \beta + 1) \cdot M_y}{f_{h,1} \cdot d \cdot t_2^2} \\ - \dfrac{4 \cdot R_{1,VE} \cdot \beta \cdot \left(\dfrac{p}{t_2} \cdot (1+\psi) \cdot (2 \cdot \beta + 1) + \beta - \psi \cdot \beta \right)}{f_{h,1} \cdot d \cdot t_2} \end{array}} - \beta \right] \tag{53}$$

for $p < x_{1,2b}$ and $p < x_{2,2b}$ and for $R_{1,VE} \leq Z_{2b}$

$$R_{2b} = R_{1,VE} + f_{h,1} \cdot d \cdot t_2 \cdot \left[\sqrt{(1 + 2 \cdot \beta) \cdot \frac{p^2}{t_2^2} + \left(1 - 2 \cdot \frac{p}{t_2} \right) \cdot \beta - \frac{(4 \cdot R_{1,VE} \cdot p - 2 \cdot M_y)}{t_2^2 \cdot f_{h,1} \cdot d}} - \frac{p}{t_2} \right] \tag{54}$$

for $p < x_{1,2b}$ and $p < x_{2,2b}$ and for $F_{1,VE,2b} > \dfrac{F_{2,VE,2b}}{\psi}$ and $Z_{2b} < R_{1,VE} \leq F_{1,VE,2b}$

$$R_{2b} = R_{1,VE} \cdot \psi + f_{h,1} \cdot d \cdot t_2 \cdot$$
$$\left[\sqrt{\beta} \cdot \sqrt{(1 + 2 \cdot \beta) \cdot 2 \cdot \frac{p^2}{t_2^2} + \left(1 + 2 \cdot \frac{p}{t_2} \right) \cdot 2 \cdot \beta - \frac{4 \cdot (2 \cdot R_{1,VE} \cdot \psi \cdot p - M_y)}{t_2^2 \cdot f_{h,1} \cdot d}} - \beta \cdot \left(1 + 2 \cdot \frac{p}{t_2} \right) \right] \tag{55}$$

for $p < x_{1,2b}$ and $p < x_{2,2b}$ and for $F_{1,VE,2b} \leq \dfrac{F_{2,VE,2b}}{\psi}$ and $Z_{2b} < R_{1,VE} \leq \dfrac{F_{2,VE,2b}}{\psi}$

With

$$x_{1,2b} = \frac{t_2}{1 + 2 \cdot \beta} \cdot \left[\sqrt{2 \cdot \beta^2 \cdot (1+\beta) + \frac{(1 + 2 \cdot \beta) \cdot \beta \cdot 4 \cdot M_y}{t_2^2 \cdot f_{h,1} \cdot d}} - \beta \right] \tag{56}$$

$$x_{2,2b} = \frac{t_2}{2 \cdot \beta \cdot (1 + 2 \cdot \beta)} \cdot \left[\sqrt{2 \cdot \beta^2 \cdot (1+\beta) + \frac{(1 + 2 \cdot \beta) \cdot \beta \cdot 4 \cdot M_y}{t_2^2 \cdot f_{h,1} \cdot d}} + 2 \cdot \beta^2 \right] \tag{57}$$

$$F_{1,VE,2b} = \frac{f_{h,1} \cdot d \cdot t_2}{4} \cdot \left[(2 \cdot \beta - 3) \cdot \frac{p}{t_2} + 2 \cdot \beta \cdot \left(\frac{t_2}{2 \cdot p} - 1 \right) \right] + \frac{M_y}{2 \cdot p} \tag{58}$$

$$F_{2,VE,2b} = \frac{f_{h,1} \cdot d \cdot t_2}{4} \cdot \left[(1 - 6 \cdot \beta) \cdot \frac{p}{t_2} + 2 \cdot \beta \cdot \left(\frac{t_2}{2 \cdot p} + 1 \right) \right] + \frac{M_y}{2 \cdot p} \tag{59}$$

$$Z_{2b} = \min \left\{ \begin{array}{l} \dfrac{f_{h,1} \cdot d}{(\psi - 1)^2} \cdot \left[\begin{array}{l} (p + \beta \cdot t_2 - 2 \cdot \beta \cdot p) \cdot (\psi - 1) - 4 \cdot p \cdot \beta + \sqrt{2} \\[4pt] \sqrt{\begin{array}{l} \beta \cdot p^2 \cdot (\psi + 1)^2 \cdot (2 \cdot \beta + 1) + 2 \cdot p \cdot t_2 \cdot \beta^2 \cdot (1 - \psi^2) \\[4pt] + \beta^2 \cdot t_2^2 \cdot (\psi - 1)^2 - 4 \cdot \beta \cdot \psi^2 \cdot p^2 + \dfrac{2 \cdot \beta \cdot (\psi - 1)^2 \cdot M_y}{f_{h,1} \cdot d} \end{array}} \end{array} \right] \\[30pt] \dfrac{f_{h,1} \cdot d}{(\psi - 1)^2} \cdot \left[\begin{array}{l} (2 \cdot p \cdot \beta - \beta \cdot t_2 + p) \cdot (1 - \psi) - 2 \cdot p \\[4pt] + \sqrt{\begin{array}{l} p^2 \cdot (\psi + 1)^2 \cdot (2 \cdot \beta + 1) + 2 \cdot \beta \cdot p \cdot t_2 \cdot (1 - \psi^2) \\[4pt] + \beta \cdot t_2^2 \cdot (\psi - 1)^2 - 8 \cdot \beta \cdot p^2 + \dfrac{2 \cdot (\psi - 1)^2 \cdot M_y}{f_{h,1} \cdot d} \end{array}} \end{array} \right] \end{array} \right\} \tag{60}$$

for $\psi \ne 1$

$$Z_{2b} = \min \left\{ \begin{array}{l} \dfrac{f_{h,1} \cdot d}{8 \cdot p \cdot \beta} \cdot \left[\beta^2 \cdot t_2^2 - 2 \cdot p \cdot \beta \cdot t_2 - p^2 \cdot (2 \cdot \beta + 1) \right] + \dfrac{M_y}{2 \cdot p} \\[12pt] \dfrac{f_{h,1} \cdot d}{4 \cdot p} \cdot \left[4 \cdot p \cdot \beta^2 \cdot t_2 - 2 \cdot p^2 \cdot \beta \cdot (2 \cdot \beta + 1) + t_2^2 \cdot \beta \cdot (1 - \beta) \right] + \dfrac{M_y}{2 \cdot p} \end{array} \right\} \tag{61}$$

for $\psi = 1$

The load-carrying capacity R_3 for failure mode 3 is calculated according to the equations (16) to (25).

Fig. 7 shows the reinforcing effect as a R over $R_{1,VE}$ diagram for a timber-to-timber connection with a 16 mm dowel, for an embedding strength $f_{h,1} = 26$ N/mm^2, a yield moment $M_y = 246$ Nm, timber member thicknesses $t_1 = 60$ mm and $t_2 = 80$ mm and for a distance p = 15 mm ($\beta = 1,2$; $\psi = 1,1$).

For $R_{1,VE} = 0$ the load carrying capacity R is equal to the load-carrying capacity for a non-reinforced connection (R = 12,4 kN). Here, failure mode 2a with one plastic hinge in the right timber member occurs. With increasing load-carrying capacity $R_{1,VE}$ (and $R_{2,VE}$) of the screws, the load-carrying capacity R of the timber-to-timber connection increases. For $R_{1,VE} = 15,3$ kN and $R_{2,VE} = \psi \cdot R_{1,VE} = 16,8$ kN the load-carrying capacity R reaches the maximum value of R = 19,8 kN which corresponds to an increase of about 60%. Due to the fact that for higher values of R_{VE} sub-failure mode "rigid" occurs, a further increase is not possible for this configuration.
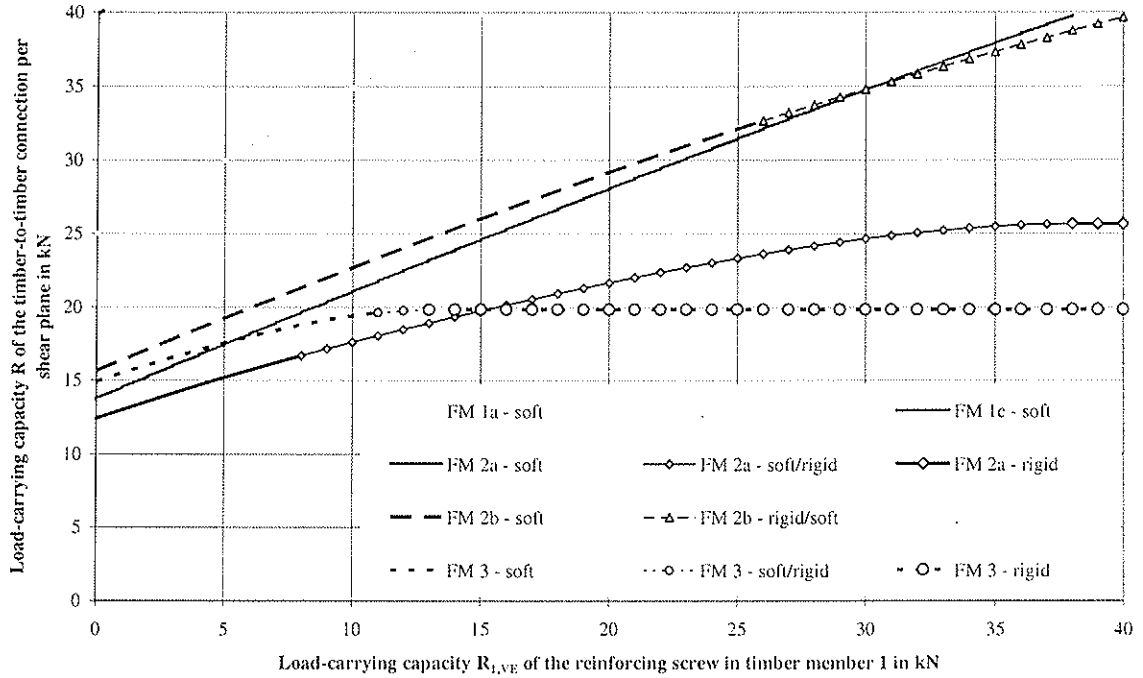
Fig. 7: Load-carrying capacity R of a timber-to-timber connection depending on $R_{1,VE}$

2.4 Load-carrying capacity of the reinforcements

The load-carrying capacity R of reinforced connections is calculated depending on the load-carrying capacity $R_{i,VE}$ of the reinforcing screws. $R_{i,VE}$ is derived and calculated according to Johansen's yield theory as for steel-to-timber connections with inner steel plates. For the case of one dowel-type fastener being reinforced by one screw (Fig. 8), the load-carrying capacity R_{VE} follows as:
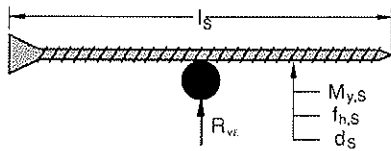
$$R_{VE} = \min\{R_{A1}, R_{A2}, R_{A3}\} \qquad (62)$$

Fig. 8: One dowel-type fastener reinforced by one screw

$$R_{A1} = f_{h,S} \cdot d_S \cdot l_S \qquad (63)$$

$$R_{A2} = f_{h,S} \cdot d_S \cdot l_S \cdot \left[\sqrt{\frac{16 \cdot M_{y,S}}{f_{h,S} \cdot d_S \cdot l_S^2} + 2} - 1 \right] \qquad (64)$$

$$R_{A3} = 4 \cdot \sqrt{M_{y,S} \cdot f_{h,S} \cdot d_S} \qquad (65)$$

Six possible failure modes must be taken into consideration when two adjacent dowel-type fasteners are reinforced by one screw (Fig. 9).

14
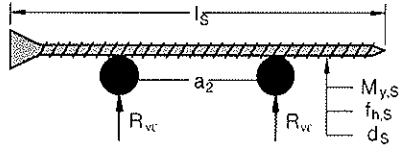
$$R_{VE} = \min\{R_{B1}, R_{B2}, R_{B3}, R_{B4}, R_{B5}, R_{B6}\} \tag{66}$$

Fig. 9: Two dowel-type fasteners reinforced by one screw

$$R_{B1} = 0,5 \cdot f_{h,S} \cdot d_S \cdot l_S \tag{67}$$

$$R_{B2} = \frac{f_{h,S} \cdot d_S \cdot l_S}{2} \cdot \left[\sqrt{\frac{16 \cdot M_{y,S}}{f_{h,S} \cdot d_S \cdot l_S^2} + 2 \cdot \left(\frac{a_2}{l_S} - 1\right)^2} + 2 \cdot \frac{a_2}{l_S} - 1 \right] \tag{68}$$

$$R_{B3} = \frac{f_{h,S} \cdot d_S \cdot a_2}{2} + \sqrt{2} \cdot \sqrt{2 \cdot M_{y,S} \cdot f_{h,S} \cdot d_S} \tag{69}$$

$$R_{B4} = 4 \cdot \sqrt{M_{y,S} \cdot f_{h,S} \cdot d_S} \tag{70}$$

$$R_{B5} = \frac{f_{h,S} \cdot d_S \cdot l_S}{2} \cdot \left[\sqrt{\frac{16 \cdot M_{y,S}}{f_{h,S} \cdot d_S \cdot l_S^2} + 2 \cdot \left(\frac{a_2}{l_S} - 1\right)^2} + 4 \cdot \sqrt{\frac{M_{y,S}}{f_{h,S} \cdot d_S \cdot l_S^2} + \frac{a_2}{l_S} - 1} \right] \tag{71}$$

$$R_{B6} = \frac{f_{h,S} \cdot d_S \cdot l_S}{2} \cdot \left[\sqrt{\frac{8 \cdot M_{y,S}}{f_{h,S} \cdot d_S \cdot l_S^2} + \left(\frac{a_2}{l_S} - 1\right)^2} - \frac{a_2}{l_S} + 1 \right] \tag{72}$$

If more than two dowel-type fasteners are reinforced by one screw, the load-carrying capacity R_{VE} can be derived by combining eq. (62) with eq. (66).

2.5 Tests

In order to confirm the extended Johansen´s yield theory for reinforced connections, tests with reinforced and non-reinforced steel-to-timber and timber-to-timber connections were performed. For each test series five reinforced and five non-reinforced specimens were tested. All parameters and test results are summarised in Table 1. The specimen notation is displayed in column one. Reinforced and non-reinforced steel-to-timber connections with inner steel plates, two shear planes and dowels as fasteners are listed in lines one to six. In the following four lines reinforced and non-reinforced steel-to-timber connections with outer steel plates, two shear planes and bolts as fasteners are shown. The following lines contain the main parameters for further timber-to-timber connections. Columns five to nine contain the connection geometry and the parameters of the dowel-type fasteners. The properties of the reinforcements are described in column ten to fifteen. In column sixteen the average load-carrying capacity per shear plane and dowel-type fastener for each test series is shown.

15

Table 1: Specimens parameters and test results

Specimen	Number of specimens n [-]	Type [-]	mean density ρ [kg/m³]	Dowel-type fasteners					Reinforcements						load-carrying capacity R_VM [kN]
				t_1 [mm]	t_2 [mm]	d [mm]	M_y [Nm]	number of dowels perpendic./parallel to grain	d_s [mm]	l_s [mm]	distance p [mm]	a_2 [mm]	R_{VE} [kN]	number of screws [-]	
S-2-8-0	5	T-S-T	412	60		8	51,2	2 / 1	-	-	-	40	-	-	7,65
S-2-8-1	5	T-S-T	425	60		8	51,2	2 / 1	7,5	130	15	40	7,21	1	9,33
S-1-16-0	5	T-S-T	406	60		16	164	1 / 1	-	-	-	-	-	-	16,1
S-1-16-1	5	T-S-T	416	60		16	164	1 / 1	7,5	130	15	-	9,26	1	22,6
S-1-24-0	5	T-S-T	396	60		24	553	1 / 1	-	-	-	-	-	-	32,0
S-1-24-2	5	T-S-T	407	60		24	553	1 / 1	7,5	130	15	-	9,13	2	53,5
B-2-8-0	5	S-T-S	397	60		8	36,7	2 / 1	-	-	-	40	-	-	6,38
B-2-8-2	5	S-T-S	401	60		8	36,7	2 / 1	7,5	130	15	40	6,77	2	12,6
B-1-20-0	5	S-T-S	411	60		20	573	1 / 1	-	-	-	-	-	-	16,9
B-1-20-2	5	S-T-S	414	60		20	573	1 / 1	7,5	130	15	-	9,22	2	31,2
H-24-0	5	T-T	412	50	50	24	553	1 / 2	-	-	-	-	-	-	13,1
H-24-1	5	T-T	409	50	50	24	553	1 / 2	7,5	180	15	-	9,15	1	19,1
H-16-0	5	T-T	415	40	40	16	164	2 / 2	-	-	-	60	-	-	7,6
H-16-1	5	T-T	399	40	40	16	164	2 / 2	7,5	180	15	60	9,01	1	11,5
H-20-0	5	T-T-T	392	100	60	20	320	2 / 2	-	-	-	60	-	-	19,6
H-20-1	5	T-T-T	403	100	60	20	320	2 / 2	7,5	180	15	60	9,07	1	24,5
H-30-0	5	T-T-T	415	100	100	30	1080	1 / 2	-	-	-	-	-	-	34,9
H-30-1	5	T-T-T	408	100	100	30	1080	1 / 2	7,5	180	15	-	9,14	1	42,3

The expected load-carrying capacities for each test series were calculated using the average timber density, fastener yield moment and the connection geometry. The comparison between test results and calculated load-carrying capacities is shown in Fig. 10.
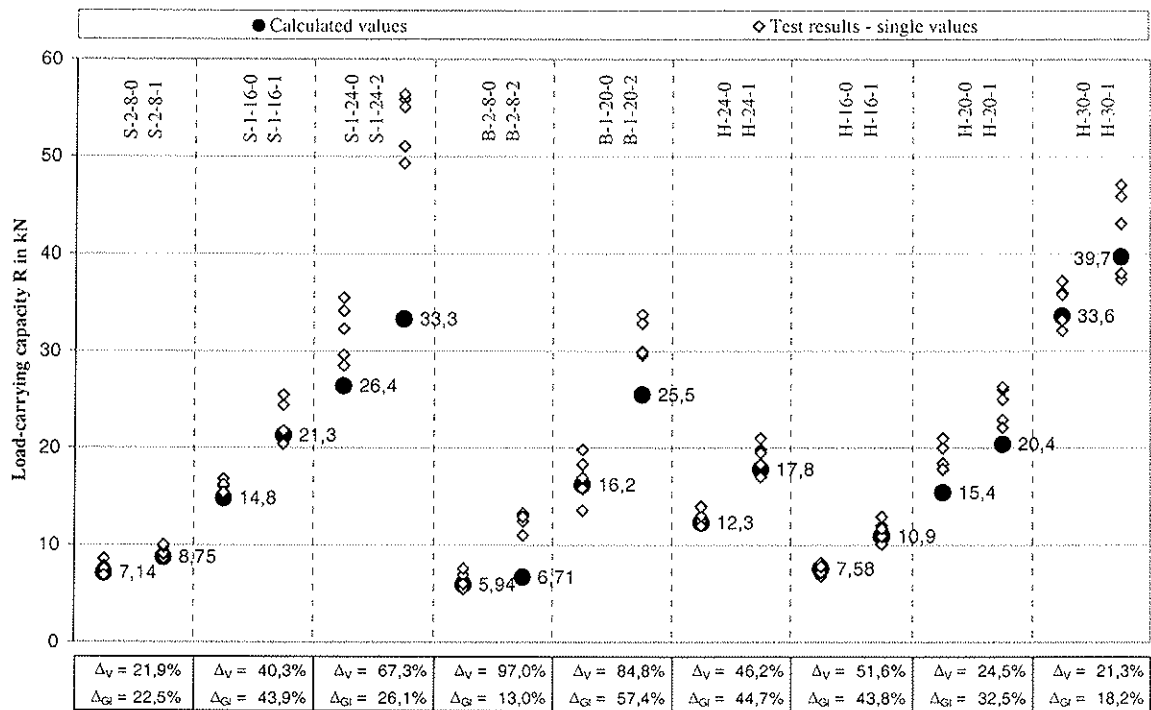
Fig. 10: Comparison between test results and calculated load-carrying capacities

On the left side in each column the load-carrying capacities of non-reinforced connections are shown. The load-carrying-capacities of geometrically identical reinforced connections are displayed on the right side. In the bottom line the calculated increases Δ_{Gl} and Δ_v reached in tests compared to non-reinforced connections are displayed. For the test series in column 1, 2, 6 to 9, the calculated increases are similar to the increases reached in tests. For

16

the test series in column 3 to 5, the increase reached in tests are clearly larger than the calculated increases. The reason for this discrepancy is the number of the reinforcements for each dowel-type fastener. In the latter, each dowel-type fastener was reinforced by two parallel screws. The presented calculation model is valid for connections reinforced with one screw per one or two dowels. This particular case with two screws per dowel can be derived similarly to the presented calculation model or conservatively be handled with the presented method.

An opened steel-to-timber connection is shown in Fig. 11. On the left side the non-reinforced connection S-2-8-0 and on the right side the reinforced connection S-2-8-1 is displayed. The load-carrying capacities reached in tests and even the failure modes were calculated using the extended Johansen´s yield theory.
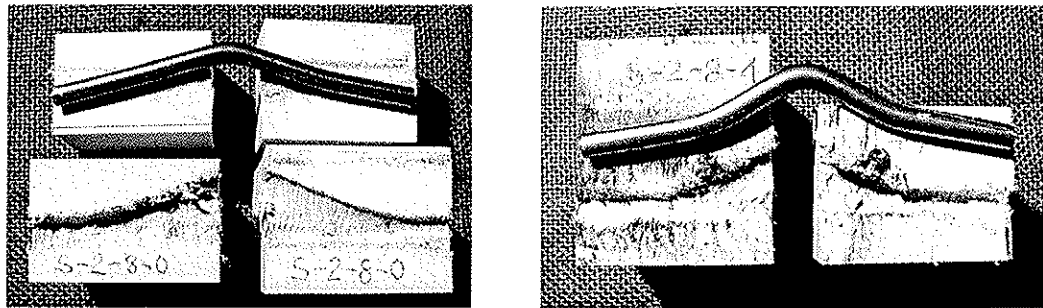
Fig. 11: Left: non-reinforced connection S-2-8-0 – Right: reinforced connection S-2-8-1

In Fig. 12 two opened reinforced steel-to-timber connections S-1-24-2 and S-1-16-1 as well as a non-reinforced connection S-1-16-0 are displayed. In both pictures the sub-failure mode "soft" dominates the failure.
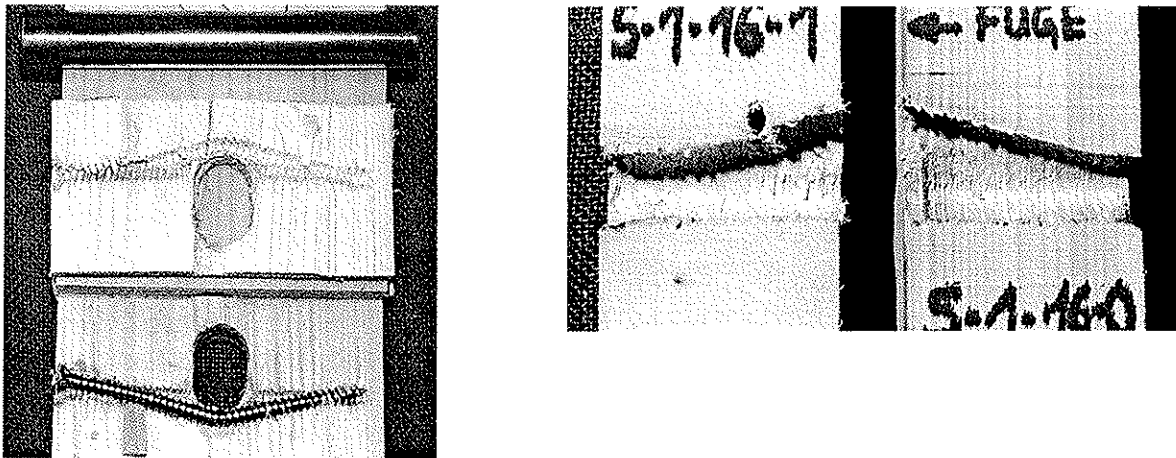
Fig. 12: Left: reinforced connection S-1-24-2 – Right: reinforced and non-reinforced connection S-1-16-1 and S-1-16-0

For numerous reinforced connections a parameter study was performed. The influence of the ratio of the reinforcement diameter d_S to the dowel diameter d on the increase of the load-carrying capacity was studied. Thereby all parameters plausible for practical application were varied. Depending on the diameter d_S of the reinforcement and on the diameter d of the dowel, the increase due to the reinforcement is shown in Fig. 13. In this comparison the influence of brittle timber splitting was not taken into account ($n = n_{ef}$).
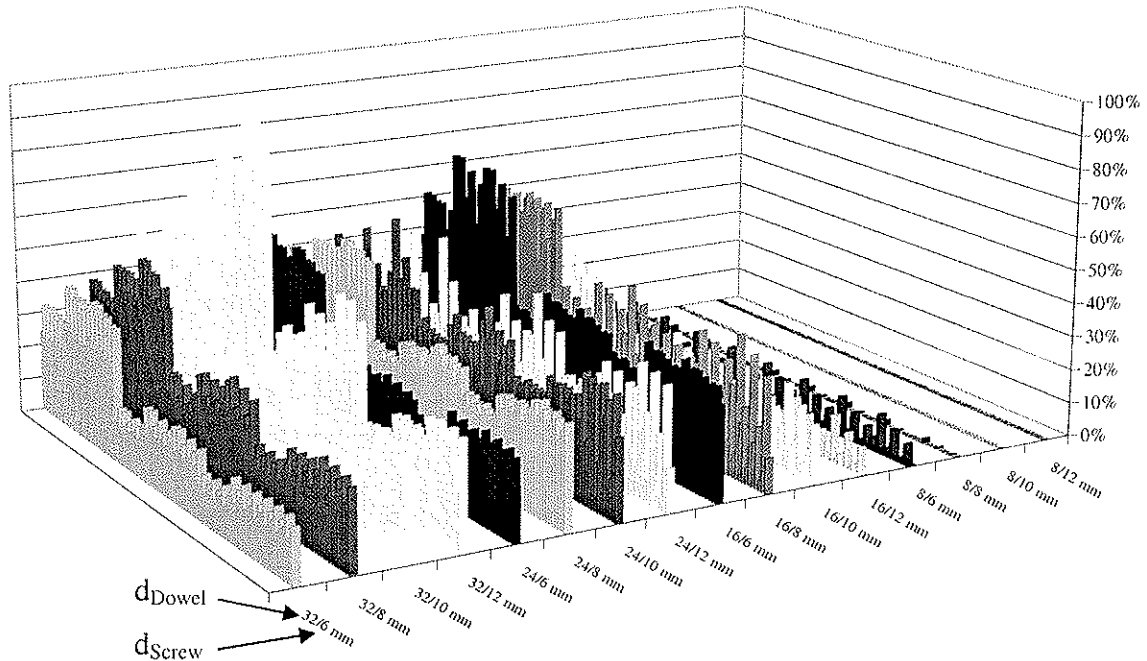
Fig.13: Increase of the load-carrying capacity for a reinforced connection compared to a non-reinforced connection without taking into account the timber splitting

Considering this parameter study, the largest increase can be reached in connections with dowel-type fasteners with a large diameter d. The largest reinforcement effect was reached in connections with dowel-fasteners with 32 mm diameter. Further on, the largest increasing effect can be reached for a ratio of the screw diameter d_S to the dowel diameter d of about d_S / d = 0,35 to 0,40. The largest increase was calculated to about 80%. Here again, the brittle splitting behaviour was not taken into account (n = n_{ef}).

3 Summary

Self-tapping screws with continuous thread represent a simple and economic method to reinforce connections where the timber is prone to splitting. In connections with sufficient reinforcement between the dowels, the timber does not split and the effective number n_{ef} equals the actual number n of dowels. Furthermore, by placing the screws in contact with the dowel-type fasteners, the load-carrying capacity and the stiffness of a connection increases.

A calculation model based on Johansen's yield theory was developed. Depending on the embedding strength of the timber, the yield moment of the dowel-type fasteners, the geometry of the connection and finally on the load-carrying capacity of the reinforcements, the load-carrying capacity of reinforced connections can be calculated.

This reinforcing method causes an increase of the load-carrying capacity up to 80% compared to non-reinforced connections with a ductile load-carrying behaviour. Compared to non-reinforced connections with a brittle load-carrying behaviour (n_{ef} < n), the method shows an increase of the load-carrying capacity of up to 120%.

Both values were verified by tests.

4 References

[1] Schmid, M. (2002). Anwendung der Bruchmechanik auf Verbindungen mit Holz. 5. Folge – Heft 7. Berichte der Versuchsanstalt für Stahl, Holz und Steine der Universität Fridericiana in Karlsruhe (TH):

[2] Blaß, H.J.; Ehlbeck, J.; Kreuzinger, H.; Steck, G. (2002). Entwurf, Berechnung und Bemessung von Holzbauwerken, BEKS 1-16 und Anhänge (13.07.2002); In: Ingenieurholzbau – Karlsruher Tage 2002; Bruderverlag; Universität Karlsruhe (TH)

[3] Bejtka, I. (2005). Verstärkung von Bauteilen aus Holz mit Vollgewindeschrauben. Band 2 der Reihe Karlsruher Berichte zum Ingenieurholzbau. Herausgeber: Universität Karlsruhe (TH), Lehrstuhl für Ingenieurholzbau und Baukonstruktionen, Univ.-Prof. Dr.-Ing. H.J. Blaß. ISSN 1860-093X,ISBN 3-937300-54-6

INTERNATIONAL COUNCIL FOR RESEARCH AND INNOVATION
IN BUILDING AND CONSTRUCTION

WORKING COMMISSION W18 - TIMBER STRUCTURES

THE YIELD CAPACITY OF DOWEL TYPE FASTENERS

A Jorissen

Eindhoven University of Technology and SHR Timber Research

A Leijten

Delft University of Technology

THE NETHERLANDS

Presented by A Jorissen

H Larsen pointed out that the bending case should not be an issue as this can be explained by the strain hardening of the fastener. A Jorissen responded that strain hardening is not an issue in small diameter bolts. H Larsen disagrees and further pointed out that the 3 point bending testing is no good. A Leijten mentioned that in the tension test no yielding was seen. They are aware of the material outside is different from the core material; however, no one would consider it as a non homogeneous material. H Blass pointed out that the statement of no shear force in the bending test is wrong. J W van de Kuilen mentioned the difference between model and experiment is the straining. C Ni received clarification that shear strength varies with diameter.

The yield capacity of dowel type fasteners

André Jorissen, Eindhoven University of Technology and SHR Timber Research
Ad Leijten, Delft University of Technology
The Netherlands

Since the load carrying capacity of connections with dowel type fasteners is determined using the so-called Johansen equations, the yield capacity of the dowel type fasteners is mostly of importance. Some years ago there was a discussion within CIB-W18 about the yield capacity of dowel type fasteners with diameters larger than 12 mm; Jorissen et al. [5] and Blaβ et al. [6]. It was found, that the yield capacity of those fasteners cannot be determined according to EN 409, where a bending test up to a bending angle of 45 degrees is prescribed; an angle of 45 degrees cannot be reached for "large" diameters.

Based on this discussion, equation (1) was introduced in Eurocode 5 for bolts and dowels.

$$M_{y;Rk} = 0,3 f_{u,k} d^{2,6}$$ (1)

Where:

$M_{y;Rk}$ is the characteristic value for the yield capacity, in Nmm
$f_{u,k}$ is the characteristic tensile strength, in N/mm^2
d is the bolt diameter, in mm

More recently, equation (1) has also entered Eurocode 5 for the determination of the yield capacity of dowel type fasteners with thin diameters like nails and staples. Whether this is correct is discussed in this paper.

Load carrying capacity of connections with dowel type fastener loaded in shear

As known the load carrying capacity of connections with metal dowel type fasteners in shear mostly depend on the material properties of both the wood and the fastener. Johansen [1] derived some equations based on the equilibrium of the fastener with which the load carrying capacity of timber to timber connections can be determined. He assumed equal properties of the timber elements ($f_{h;s} = f_{h;m} = f_h$) and elastic behaviour of the fastener material., which results, for example, in a failure load according to equation (2) for the failure mechanism shown in figure 1.

$$F = 0,5 d f_h t_s + \frac{2 M_y}{t_s}$$ (2)

With:

d fastener diameter [mm]
t_s thickness of the timber side member [mm]
f_h embedment strength of the timber middle member [N/mm^2]

M_y fastener elastic capacity in bending $= \frac{\pi}{32} d^3 f_e$

[Nmm] according to figure 2.
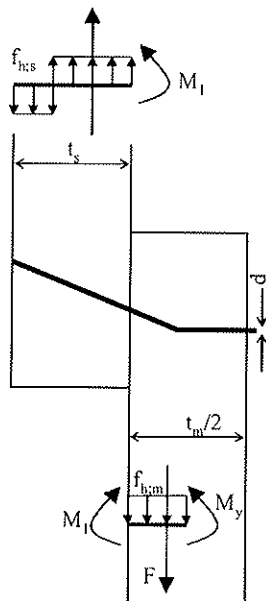
Figure 1: Failure mechanism leading to equations (2) and (3)

1

$$M_y = \frac{\pi}{32} d^3 f_e \qquad (3)$$

With $f_e = 0{,}6 \ f_u$ (see figure 4)
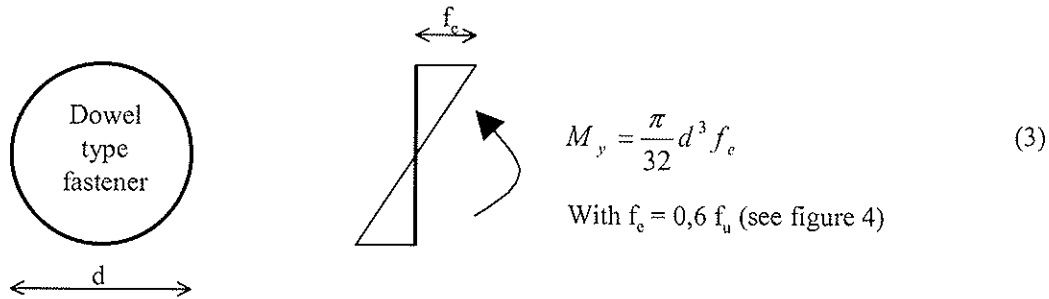
Figure 2:   Elastic fastener bending capacity used by Johansen [1].

Meyer [2] extended the Johansen theory by assuming different properties of the timber elements and plastic behaviour of the fastener material. As a consequence equation (2) changes into equation (4), corresponding to the same failure mechanism described by equation (2).

$$F = -\frac{dt_s f_{h,s} f_{h,m}}{2 f_{h,s} + f_{h,m}} + \sqrt{\left(\frac{dt_s f_{h,s} f_{h,m}}{2 f_{h,s} + f_{h,m}}\right)^2 + \frac{\left(t_s^2 df_{h,s} + 4M_y\right) df_{h,s} f_{h,m}}{2 f_{h,s} + f_{h,m}}} \qquad (4)$$

With: d   fastener diameter [mm]
          t_s thickness of the timber side member [mm]
          $f_{h,s}$ embedment strength of the timber side member [N/mm²]
          $f_{h,m}$ embedment strength of the timber middle member [N/mm²]
          M_y fastener yield capacity in bending = ... [Nmm] according to figure 3.

$$M_y = \frac{1}{6} d^3 f_e \qquad (5)$$
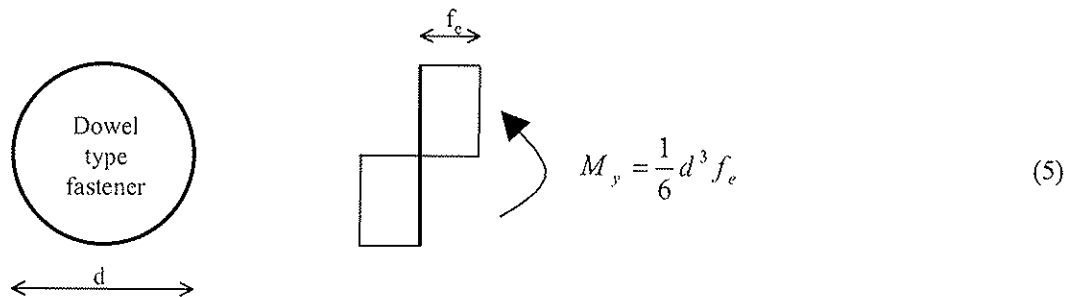
Figure 3:   Plastic fastener bending capacity used by Meyer [2].

As can be read from the title of the work of Meyer [2], the theory was originally meant for nailed connections.

The yield capacity in bending

As described, Johansen originally used the elastic bending capacity. Using the full plastic yield capacity, as Meyer suggested, results in higher and more realistic values for the calculated load carrying capacity. Both the elastic and the full plastic bending capacity depend on the yield strength f_e which is for mild steel defined in figure 4.
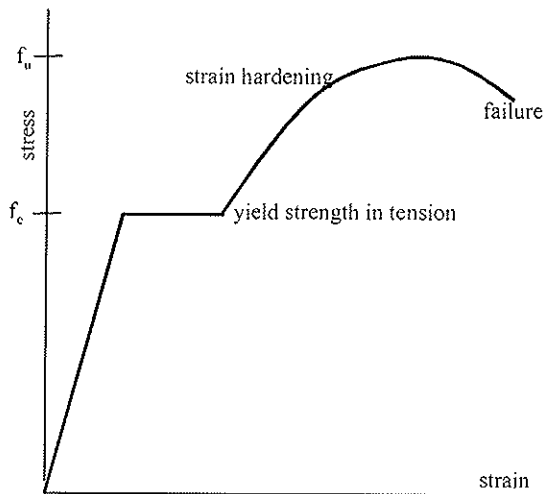
Figure 4: Stress-strain relationship for mild steel in tension.

Based on the stress-strain relationship for mild steel in tension, the yield strength in bending was defined according to equation (6) while the yield capacity in bending was calculated according to equation (5).

$$f_e = 0{,}8 f_u \qquad (6)$$

Substitution of equation (6) in equation (5) results in equation (7).

$$M_y = 0{,}133 f_u d^3 \qquad (7)$$

This is, at a characteristic level, directly comparable to equation (1).

The full plastic or yield moment in bending M_y of nails, 2,0 mm < d < 8,0 mm, can also be determined by carrying out tests as described in EN 409 [3]. According to this standard the nail should be subjected to a four-point bending test as shown in figure 5.
The yield moment M_y is defined as the bending moment at maximum load or at an angle $\alpha = 45°$, whichever is the lesser.

During tests on (multiple) bolted connections with, mostly, bolts M12, carried out between 1994 and 1998, and reported in [4], it was observed that the bending angle of 45°, prescribed for nails in EN 409 [3], was never reached. If "large" diameters are bent to an angle of 45°, part of the cross section will be hardened and the yield bending capacity will therefore be overestimated. Furthermore, if a bending angle of 45° is never reached, the "yield" moment M_y to be substituted in e.g. equation (5) is overestimated, which consequently leads to an overestimation of the calculated load carrying capacity. This was reported earlier in [5], in which it was reported that the yield capacity in bending for larger diameters is only 60% to 70% of the value determined according to EN 409.
Further research was carried out at Karlsruhe university and reported at CIB W18 in 2000 [6], which also contains results of bending tests carried out by Scheer, Peil and Nölle [7]; they report that, due to a low bending angle ($\approx 10°$ as also reported in [5]), $f_e = 0{,}67 f_u$, which results, together with equation (5), in equation (8) for "large" diameters.

3
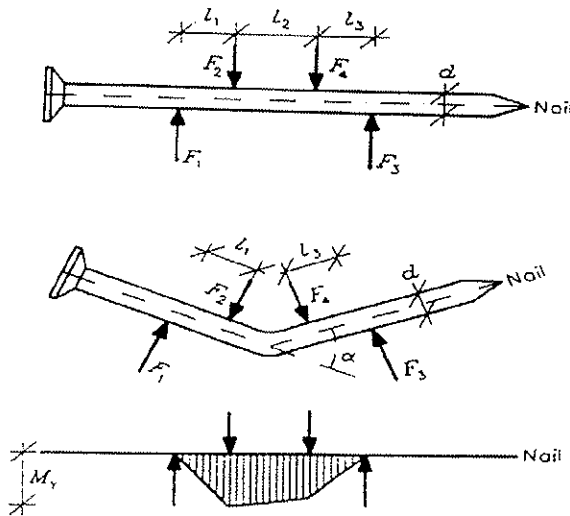
Figure 5:   Nail loading, nail deformation and bending moments according to the tests
             described in EN 409 [3].
             Remark: Since F_2 and F_4 may differ, the midsection may also be affected to shear. Since
                     the loads are perpendicular to the fastener axis tensile forces are avoided.

$$M_y = 0,112 f_u d^3 \tag{8}$$

Eurocode 5 disregards the differences between "small" and "large" diameters. The yield moment
M_y is calculated according to equation (1) regardless of the diameter.

Experimental data according to EN 409

In order to verify some equations given above, recently some experiments, listed in table 1, on
small diameter dowel type fasteners, nails, according to EN 409 [3] were carried out at
Eindhoven University of Technology. Simultaneously, three point bending tests were carried out
at the Structural Function of the Research Institute for Sustainable Humanosphere in Kyoto.

To meet the requirements from EN 409 special equipment, shown in figure 6, was built.
According to the geometry of this apparatus, the maximum bending moment in the nail can be
calculated according to equation (9).

$$M_y = (l_2 + l_4) * F_{reaction} \tag{9}$$

Table 1:   Experiments. according to EN 409

nail diameter	number of tests	
[mm]	bending	Tension
3,0	15	10
4,0	15	10
5,0	15	10

4
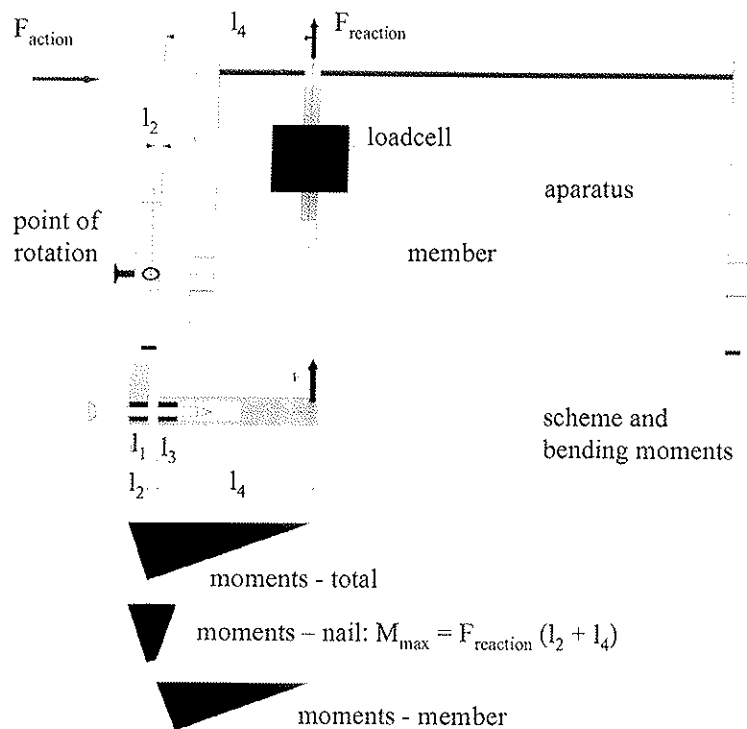
Figure 6:   Nail bending apparatus.
Remark: The shear force in the fasteners equals $F_{reaction}$.
The (axial) tensile forces in the fastener are avoided.

Additionally, the tensile strength was determined according to EN 10002-1 [8].
The results of the tensile tests carried out in Eindhoven, obtained from tests carried out on specimen shown in figure 7, are given in tables 2 and 3.

Table 2:   Individual tensile tests.

test	d = 3,0 mm $d_r = \dfrac{\sum_{i=1}^{3} d_i}{3}$ mm	$f_u = \dfrac{F_u}{\frac{\pi}{4}d_r^2}$ N/mm^2	d = 4,0 mm $d_r = \dfrac{\sum_{i=1}^{3} d_i}{3}$	$f_u = \dfrac{F_u}{\frac{\pi}{4}d_r^2}$ N/mm^2	d = 5,0 mm $d_r = \dfrac{\sum_{i=1}^{3} d_i}{3}$	$f_u = \dfrac{F_u}{\frac{\pi}{4}d_r^2}$ N/mm^2
1	2,55	801,46	3,45	487,93	4,41	578,25
2	2,47	872,38	3,44	612,31	4,40	579,63
3	2,53	794,08	3,43	597,48	4,40	563,18
4	2,47	815,58	3,45	519,83	4,41	559,52
5	2,51	920,62	3,44	595,41	4,40	526,00
6	2,44	828,70	3,45	594,85	4,41	565,87
7	2,54	892,29	3,44	577,11	3,39	583,00
8	2,45	804,34	3,43	697,91	4,42	567,09
9	2,48	892,08	3,44	607,47	4,41	564,23
10	2,50	810,80	3,44	602,73	4,41	580,74
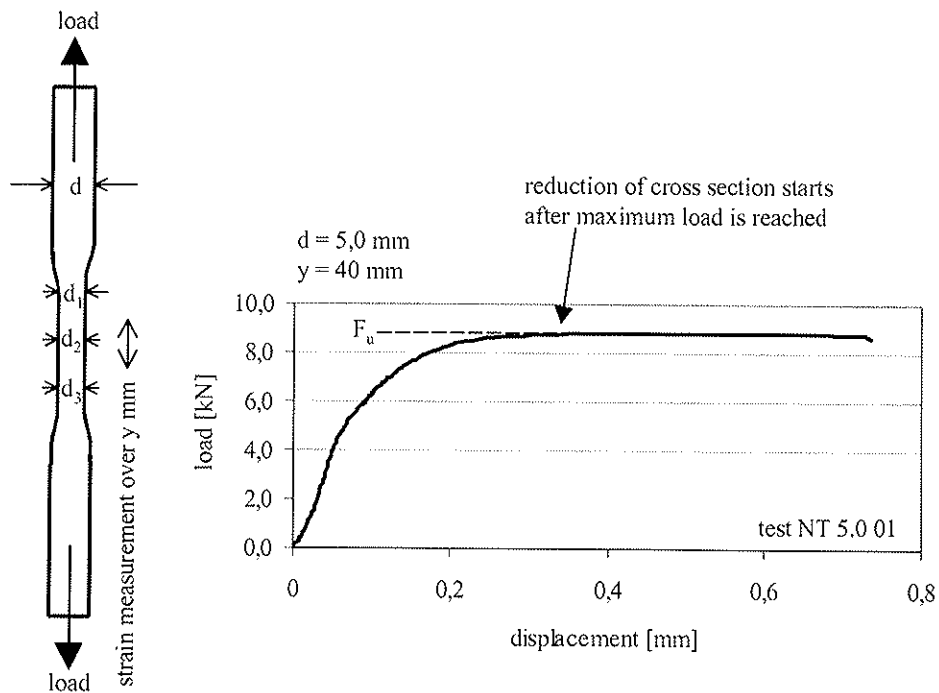
Figure 7: Test specimen for the nail tensile tests and a typical load displacement curve.

Table 3: Tensile tests; average and coefficient of variation.

	d = 3,0 mm	d = 4,0 mm	d = 5,0 mm
Average f_u [N/mm²]	843	579	567
Coefficient of variation [%]	5,50	7,16	2,94

The results of the bending tests, obtained from tests carried out with the apparatus shown in figure 6, are given in tables 4 to 6.

Table 4: Nails d = 5 mm in bending. Load applied with the apparatus shown in figure 6.

d [mm]	l_1 [mm]	l_2 [mm]	l_3 [mm]	l_4=10l_1 [mm]	F [N]	M [Nmm]; Eq. (9)	c.o.v.	M [Nmm] caracteristic	
5,0	20,1	10,0	20,1	200	82,1	17241,0			
5,0	20,1	10,0	20,1	200	79,6	16716,0			
5,0	20,1	10,0	20,1	200	80,1	16821,0			
5,0	20,1	10,0	20,1	200	81,1	17031,0			
5,1	20,1	10,0	20,1	200	71,5	15015,0			
5,0	20,1	10,0	20,1	200	84,0	17640,0			
5,0	20,1	10,0	20,1	200	79,4	16674,0			
5,0	20,1	10,0	20,1	200	82,2	17262,0			
5,0	20,1	10,0	20,1	200	81,9	17199,0			
5,0	20,1	10,0	20,1	200	79,8	16758,0			
5,1	20,1	10,0	20,1	200	77,5	16275,0			
5,0	20,1	10,0	20,1	200	79,2	16632,0			
5,0	20,1	10,0	20,1	200	79,8	16758,0			
5,0	20,1	10,0	20,1	200	83,0	17430,0			
5,0	20,1	10,0	20,1	200	79,9	16779,0			
				average	16815,4	3,64	15687,0		
			f-u =	567,0	N/mm2	eq. (1)	10535,3		
			f-u;k =	534,8	N/mm2	eq. (3)	3937,9	Original Johansen	
						eq. (7)	8891,3		
						eq. (8)	8155,9		

6

Table 5: Nails d = 4 mm in bending. Load applied with the apparatus shown in figure 6.

d [mm]	l_1 [mm]	l_2 [mm]	l_3 [mm]	$l_4=10l_1$ [mm]	F [N]	M [Nmm]; Eq. (9)
4,0	20,0	10,0	20,0	200	49,8	10458,0
4,1	20,0	10,0	20,0	200	39,7	8337,0
4,1	20,0	10,0	20,0	200	45,8	9618,0
4,0	20,0	10,0	20,0	200	39,6	8316,0
4,0	20,0	10,0	20,0	200	40,1	8421,0
4,1	20,0	10,0	20,0	200	46,7	9807,0
4,0	20,0	10,0	20,0	200	48,3	10143,0
4,0	20,0	10,0	20,0	200	47,1	9891,0
4,0	20,0	10,0	20,0	200	49,2	10332,0
4,0	20,0	10,0	20,0	200	47,2	9912,0
4,0	20,0	10,0	20,0	200	40,5	8505,0
4,0	20,0	10,0	20,0	200	42,1	8841,0
4,1	20,0	10,0	20,0	200	53,4	11214,0
4,0	20,0	10,0	20,0	200	48,8	10248,0
4,0	20,0	10,0	20,0	200	42,4	8904,0

	F [N]	
average		9529,8
f-u =	579,0	N/mm2
f-u;k =	500,0	N/mm2

c.o.v.	M [Nmm] characteristic	
10	7847,7	
eq. (1)	5513,8	
eq. (3)	1885,0	Origional Johansen
eq. (7)	4256,0	
eq. (8)	3584,0	

Table 6: Nails d = 3 mm in bending. Load applied with the apparatus shown in figure 6.

d [mm]	l_1 [mm]	l_2 [mm]	l_3 [mm]	$l_4=10l_1$ [mm]	F [N]	M [Nmm]; Eq. (9)
3,0	10,0	6,0	10,0	100	45,2	4791,2
3,0	10,0	6,0	10,0	100	51,0	5406,0
3,0	10,0	6,0	10,0	100	50,0	5300,0
3,0	10,0	6,0	10,0	100	47,3	5013,8
3,0	10,0	6,0	10,0	100	45,6	4833,6
3,0	10,0	6,0	10,0	100	43,1	4568,6
3,0	10,0	6,0	10,0	100	44,5	4717,0
3,0	10,0	6,0	10,0	100	45,5	4823,0
3,0	10,0	6,0	10,0	100	46,0	4876,0
3,1	10,0	6,0	10,0	100	47,8	5066,8
3,0	10,0	6,0	10,0	100	49,1	5204,6
3,0	10,0	6,0	10,0	100	48,7	5162,2
3,0	10,0	6,0	10,0	100	44,8	4748,8
3,0	10,0	6,0	10,0	100	50,2	5321,2
3,1	10,0	6,0	10,0	100	50,1	5310,6

	F [N]	
average		5009,6
f-u =	843,0	N/mm2
f-u;k	754,0	N/mm2

c.o.v.	M [Nmm] characteristic	
5,1	4539,6	
eq. (1)	3935,6	
eq. (3)	1199,2	Origional Johansen
eq. (7)	2707,6	
eq. (8)	2280,1	

The test results show that, fortunately, the tested yield capacity for nails with d = 3,0 mm, d = 4,0 mm and d = 5,0 mm is higher than the calculated values according to equations (1), (7) and (8).

Experimental data determined by three-point bending

Before the EN 409 was published researchers determined the yield bending moment by simple three point bending tests. They concluded that the resulting data was unreliable. Only recording the force and mid span displacement ignores the effect that the support forces become inclined

7

compared to the initial vertical direction. This leads to conservative values for the bending moment. The three point bending tests, carried out at the laboratories of Structural Function of the Research Institute of Sustainable Humanosphere (RISH), Kyoto University, Japan, are not corrected for this effect.

All tests were carried out displacement controlled. The yield moment is taken as the maximum value until a rotation angle of 45^0 is attained. The nail is simply regarded as a beam on two supports with a mid span load. The determination of the tensile strength was identical as given above.

Table 7: Experiments performed in Japan.

Nail diameter [mm]	Number of tests	
	bending	tensile
2.8	17	10
3.4	17	10
4.2	17	10
5.2	17	21

The results of the tensile tests are presented in Tables 8

Table 8: Individual tensile test, Japan.

nominal	Nail	tensile	nail	tensile	nail	tensile	nail	tensile
	2.8	stress	3.4	stress	4.2	stress	5.2	stress
No.	mm	N/mm2	mm	N/mm2	mm	N/mm2	mm	N/mm2
1	2,7	906	3,37	814	4,16	638	5,15	774
2	2,68	962	3,32	831	4,14	659	5,16	793
3	2,7	897	3,37	824	4,18	660	5,19	776
4	2,71	795	3,38	788	4,17	689	5,16	799
5	2,71	890	3,36	810	4,17	642	5,19	814
6	2,69	798	3,37	812	4,17	647	5,17	798
7	2,72	896	3,37	805	4,15	682	5,18	791
8	2,73	933	3,36	804	4,18	639	5,16	811
9	2,71	836	3,37	821	4,15	673	5,15	809
10	2,72	825	3,37	833	4,15	660	5,19	809
11							5,17	804
12							5,18	794
13							5,15	813
16							5,18	807
17							5,21	794
18							5,18	796
19							5,19	802
20							5,17	818
21							5,18	794
Mean								
[N/mm2]	2,71	**874**	3,36	**814**	4,16	**659**	5,17	**800**
Cov [%]	0,37	4,67	0,24	1,53	0,16	2,76	0,00	1,04

8

The differences between the mean tensile strength of the different diameters is considerably. The minimum tensile strength required in Eurocode 5 is $f_{u,k}$ = 600 N/mm^2 and is not fulfilled by all nails.

A summary of the yield moment data of this data set is given in Table 9

Table 9: Yield moment determined with three point bending tests, Japan

span [mm]	30		50		70		100	
	nail	bending	nail	bending	nail	Bending	nail	bending
nominal	2,8	moment	3,4	moment	4,2	moment	5,2	moment
No.	[mm]	Nmm	[mm]	Nmm	[mm]	Nmm	[mm]	Nmm
1	2,73	3522	3,37	5849	4,17	9142	5,17	19785
2	2,72	3568	3,37	5964	4,17	8545	5,17	19940
3	2,71	3633	3,38	5851	4,16	8913	5,17	19845
4	2,69	3352	3,39	5933	4,16	8799	5,17	19753
5	2,7	3613	3,36	5905	4,18	8573	5,17	19503
6	2,71	3369	3,37	5913	4,16	9175	5,17	19953
7	2,69	3214	3,37	5853	4,17	9237	5,17	19498
8	2,71	3647	3,38	5943	4,16	8757	5,17	19933
9	2,71	3721	3,37	5940	4,18	8587	5,17	19988
10	2,71	3297	3,37	5956	4,16	8738	5,17	19443
11	2,71	3714	3,36	5836	4,16	9006	5,17	19315
12	2,7	3744	3,38	5960	4,17	8799	5,17	19423
13	2,72	3630	3,37	5739	4,17	8517	5,17	19665
14	2,71	3594	3,38	5910	4,16	9086	5,17	19745
15	2,71	3635	3,37	6158	4,17	8503	5,17	19733
16	2,71	3310	3,36	5966	4,17	8969	5,17	19753
17	2,71	3599	3,37	6034	4,17	8983	5,17	19638
Mean	2,71	**3539**	3,37	**5924**	4,17	**8843**	5,17	**19700**
Cov [%]	0,37	4,67	0,24	1,53	0,16	2,76	0,00	1,04

Discussion

For 5 mm nails the experimental data show, that the actual full plastic bending capacity, reached within the bending angle of the nail α = 45° (see figure 5), is lower than obtained with Eq. (1), which is part of Eurocode 5. Fortunately, this is not automatically on the unsafe side since the directly from tests obtained values for the yield capacity is higher. However, Eq. (1) was derived for diameters larger than 8 mm and, as shown in figure 8, the values for the yield capacity for smaller diameters obtained by calculation according to Eq. (1) are higher than the values obtained with the assumption of full plasticity: Eq. (7).

The bending angle of 45 degrees is never reached for large diameters due to strain hardening. Strain hardening for small diameters is of less influence compared to large diameters. However, when bending up to 45 degrees strain hardening will occur in small diameters as well and the resistance is higher than calculated with the full plastic capacity. This might explain the higher values obtained by experiment compared to the values obtained by calculation.
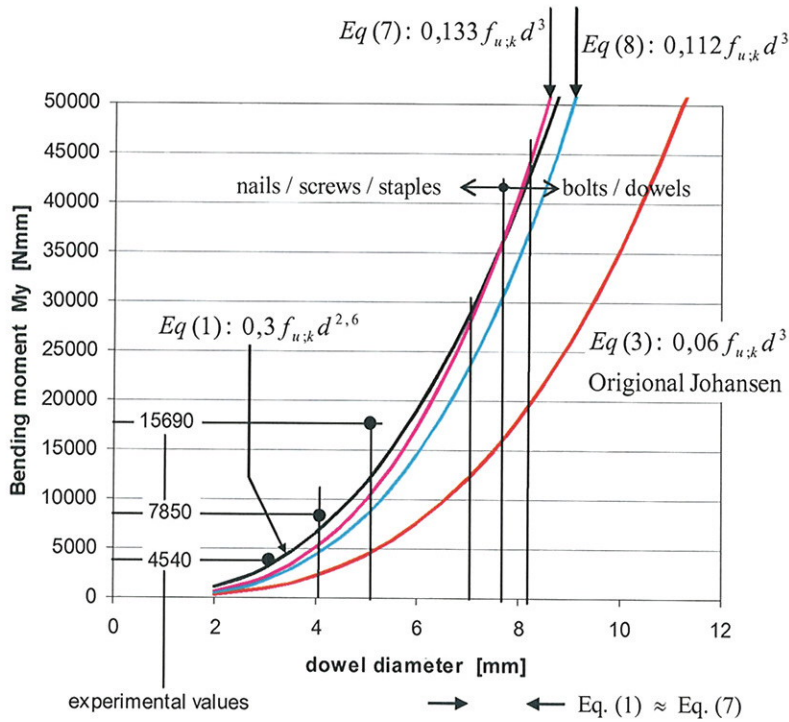
Figure 8: Calculated results according the equations mentioned in this paper; $f_{u;k} = 600$ N/mm^2.

The value inserted for the fastener yield capacity affects the calculated load carrying capacity if modes II and III, defined in figure 9, are governing. The load carrying capacity is affected most for failure mode III, for which the load carrying capacity is given by equation (10).
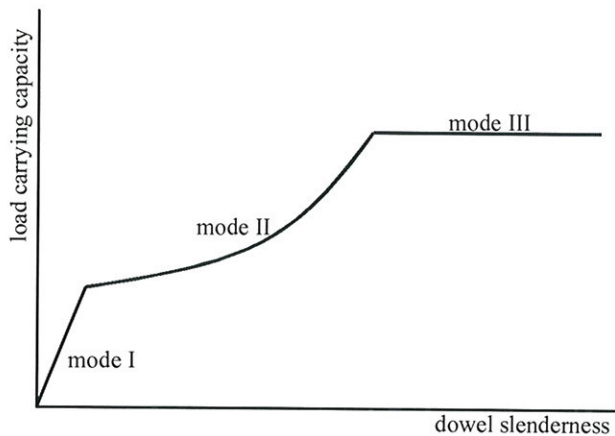
Figure 9:   Failure modes of single dowel type fastener connections.

$$F = \sqrt{\frac{2 M_y f_{h;s} f_{h;m}}{f_{h;s} + f_{h;m}}} \qquad (10)$$

From equation (10) it is clear that an overestimation of the yield capacity M_y of 20%, which, regarding figure 8, might be a realistic value, results in an overestimation of the load carrying capacity of about 10%.

In addition to figure 8 it can be seen from figure (10), that the ratio between the experimental data (yield moment) and the calculated values according to equation (1), which is in Eurocode 5, is the lowest of all.
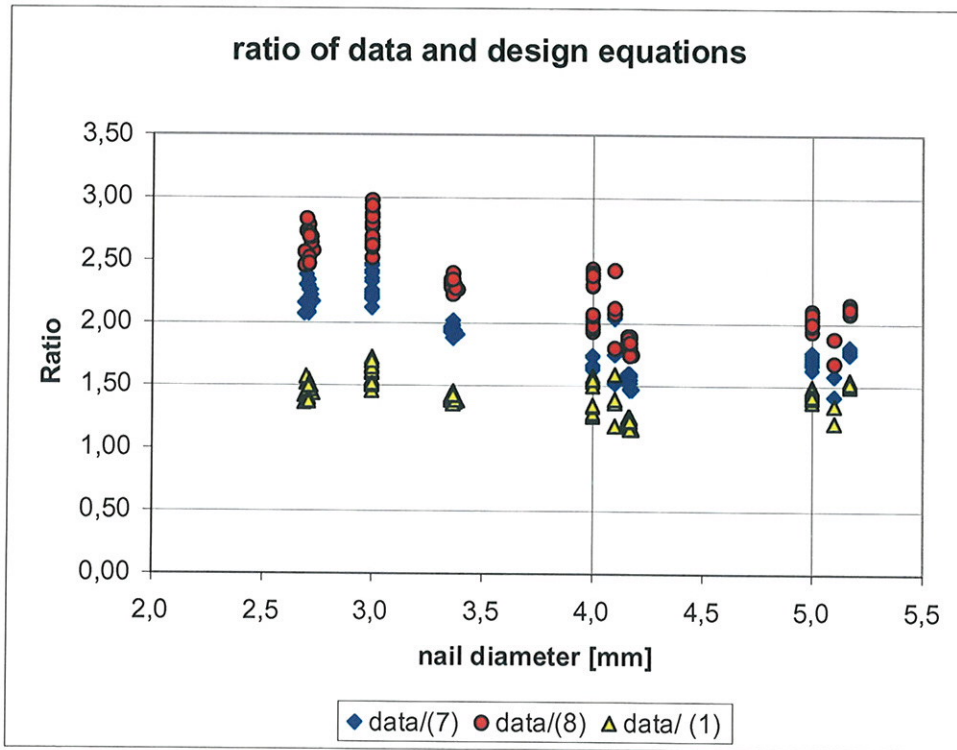
Figure 10: Comparison of experimental data and design yield moment equations based on a tensile strength of 600 N/mm².

  Remark: data/(7) experimental data devided by the calculated yield moment according to equation (7)

       data/(8) experimental data devided by the calculated yield moment according to equation (8)

       data/(1) experimental data devided by the calculated yield moment according to equation (1)

By taking the ratio of the maximum bending moment and the tensile strength of both EN409 and three point bending tests a comparison is given in Figure 11. This ratio is believed to rule out any differences in steel quality between the test in Eindhoven and Kyoto. The figure shows that the three point bending result in a conservative estimation of the maximum bending capacity as expected.
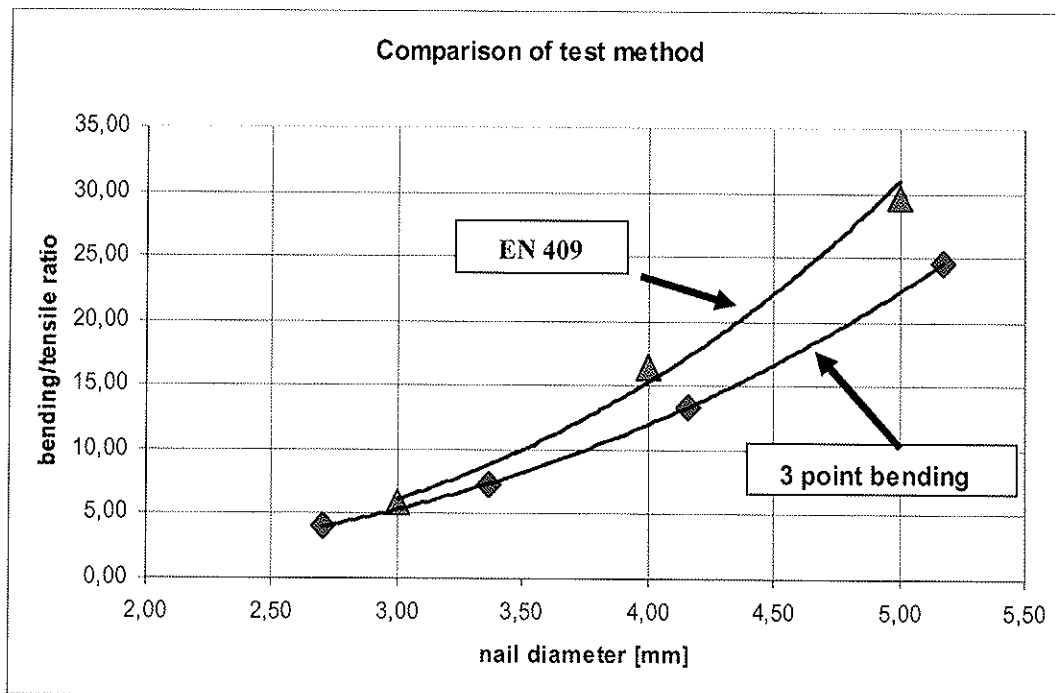
Figure 11: Comparing the EN409 method with the three point bending test. The latter is performed without correction of the bending moment for the rotation of the nail axes.

Conclusion and suggestion for code modification

Since the values for the yield capacity obtained directly from tests are higher than the values obtained whichever equation mentioned in this paper, it is not on the unsafe side to use Eq. (1) for small diameter dowel type fasteners as well.

Driven by the idea to keep it as simple as possible, we like to suggest to keep Eq. [1] into Eurocode 5 for all diameters.

Acknowledgement

References

[1]   Johansen, K.W. *Theory of timber connections*. International Association of Bride and Structural Engineering, Publication 9:249-262,1949.

[2]   Meyer, Adolf. *Die Tragfähigkeit von Nagelverbindungen bei statischer Belastung*. Holz als Roh- und Werkstoff, 15 Jg. Heft 2, S. 96-109, 1957.

[3] EN 409, Timber structures – Test methods – Determination of the yield moment of dowel type fasteners – Nails, CEN, Brussels, 2003.

[4] Jorissen, Andre. Double *shear timber connections with dowel type fasteners*, ISBN 90-407-1783-4, Delft University Press, Delft, 1998.

[5] Jorissen, Andre and Blass, Hans Joachim. *The fastener yield strength in bending*. CIB W18 31-7-6, Savolinna, Finnland 1998.

[6] Blass H.J., Bienhaus A., Krämer V. *Effective Bending Capacity of Dowel-Type Fasteners*. CIB W18 33-7, Delft, The Netherlands, 2000.

[7] Scheer J., Peil U., Nölle, H. *Schrauben mit planmäßiger Biegebeanspruchung*, Stahlbau 57, 1988, S. 237-245.

[8] EN 10002-1, Metallic materials – Tensile testing – Part 1: Method of test (at ambient temperature), CEN, Brussels, 1990.

INTERNATIONAL COUNCIL FOR RESEARCH AND INNOVATION
IN BUILDING AND CONSTRUCTION

WORKING COMMISSION W18 - TIMBER STRUCTURES

NAILS IN SPRUCE

SPLITTING SENSITIVITY, END GRAIN JOINTS AND WITHDRAWAL STRENGTH

.

A Kevarinmäki

VTT Technical Research Centre of Finland

FINLAND

Presented by A Kevarinmäki

H Blass asked about the splitting sensitivity study where the nails were driven at 19% mc and wondered if 12% mc be a less favourable condition. A Kevarinmäki responded that they believe drying after nailing is more critical. H Blass questioned the low density of the timber used and commented that the proposal is independent of the strength class. A Kevarinmäki responded that high density pieces also show similar results. B Leicester commented that the end grain test apparatus may create friction from induced side pressure that could bias the results. M Schmidt questioned about hammer versus nail gun. A Kevarinmäki responded that hammer were used while ensure nail head is flushed with timber surface. A Leijten asked why withdrawal strength goes down with decrease in mc. A Kevarinmäki responded that as mc increase wood swells and increase the gripping on the nail. H Larsen commented about the relationship between the test standard and Eurocode 5. Standard should test at RH of 65%. If the standard is changed, it would invalidate past results. Correction to Eurocode 5 is the way to go. S Thelandersson commented that cyclic of climatic conditions should be considered. A Kevarinmäki responded that this information will be available in long term loading.

Nails in spruce - splitting sensitivity, end grain joints and withdrawal strength

Ari Kevarinmäki

VTT Technical Research Centre of Finland

1 Introduction

The new Eurocode 5 (EN 1995-1-1:2004) allows the national choices for the rules for nails in end grain and for the rules of timber thickness and edge distance of nailed joints with the species sensitive to splitting. Spruce (*Picea abies*) is named as an example of species sensitive to splitting. The experimental research (VTT 2004) was done for the justification of these national choices and for the development of the next version of Eurocode 5.

The withdrawal strength of nails was also studied (Kevarinmäki 2005). In Finland, the withdrawal failures of machine driven nails have caused several collapsing of secondary structures of ceilings in public buildings.

2 Nailing tests of timber thickness and edge distance

The nailing tests for spruce (*Picea abies*) were done with two kind of the test pieces: crossed timber joint (90°) and splice joint (0°) as are shown in Figure 1 and 2 (VTT 2004). Parameters for the thickness of the headside timber (t) and edge distances (a_4) and the number of joints in each test series are shown in Table 1. The timber pieces had been selected with the density criteria of $\rho_\omega > 380$ kg/m^3 with $\omega \approx 15$ %. Before fabrication of the test specimens the timber material was conditioned in RH 85%. During the nailing, the moisture content of timber was about $\omega = 19$ %. After the test specimens were fabricated they were stored in climate room of RH 40 % and T 20 °C for ten to twelve weeks.

The smooth square nails, 2,8x75, 3,4x100 and 5,1x150 (mm) were hammered in the "diagonal" position as shown in Figure 3. Most of nails were hammer on the sapwood side (Figure 3). The nails in a row parallel to the grain were staggered perpendicular to grain by the nail diameter $1d$. Nails spacing parallel to grain was $a_1 = 10d$ or for $d = 5,1$ mm $a_1 = 12d$ and perpendicular to grain $a_2 = 5d$ according to the minimum values in EC5.

The number and length of the headside splits of timber members were measured both after the fabrication of test specimens and after the storage in RH 40%. Splits were also documented for the loading test specimens of splitting sensitive joints presented in Chapter 3. The cracking results of altogether 2282 nails have been reported in VTT 2004 with the information of the moisture contents, timber density and split lengths. The summary of the cracking results is presented in Appendix of this paper. The presented split percents have been calculated dividing number of cracks by the number of nails.

Table 1   Series of nailing tests. Number of joints in each test series.

Test series [1]	Thickness of the headside member t and edge distance a_4		
	N: $t = 7d$, $a_4 = 5d$	M: $t = 10d$, $a_4 = 7d$	S: $t = 14d$, $a_4 = 10d$
AFT	6	6	-
AFC	6	6	6
ABT	6	6	6
DFT	6	6	-
DFC	6	6	6
DBT	4	4	4
EFT	6	6	-
EFC	6	6	6
EBT	6	6	6

[1] 1. letter shows dimensions of nails: A = 2,8x75, D = 3,4x100 and E = 5,1x150.

    2. letter shows type of joint: F = cross joint 2x2 nails and B = splice joint (4 or 5)x6 nails.

    3. letter shows end distance of nails: T = tension joint $a_3 = 15d$ and C = compression $a_3 = 10d$
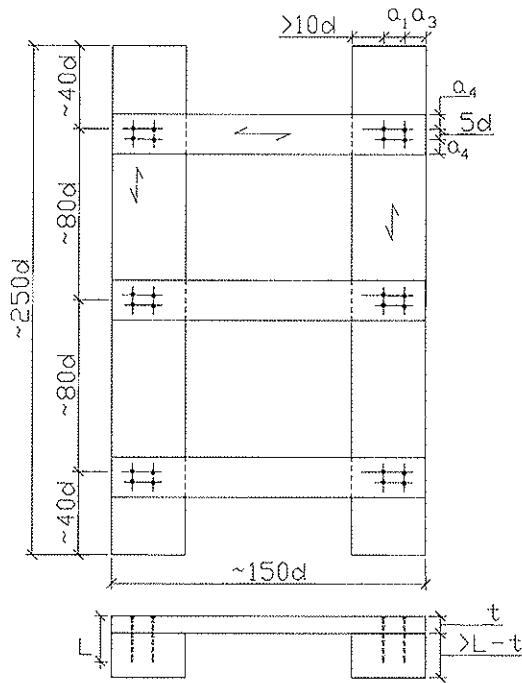
Figure 1   Test specimen of cross joints (_F_-series 90°). Each of test specimens had six similar joints (1 test series = 1 test specimen).
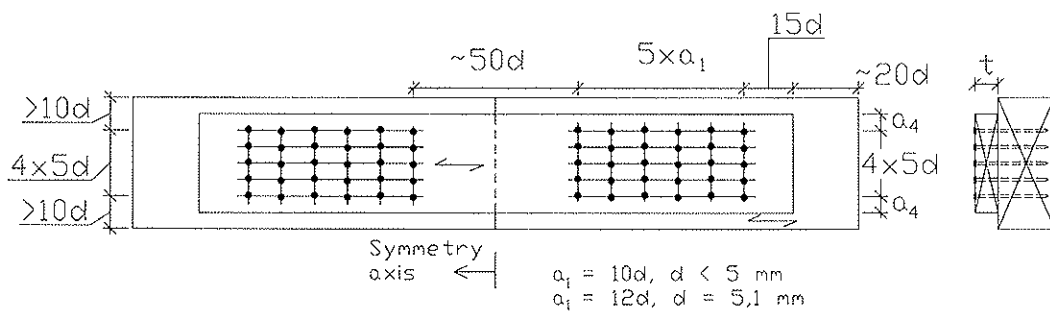
Figure 2   Test specimen of splice joints (_B_-series, 0°). Note, when $d = 5,1$ mm, number of nails in a row perpendicular to grain was four (4).

2
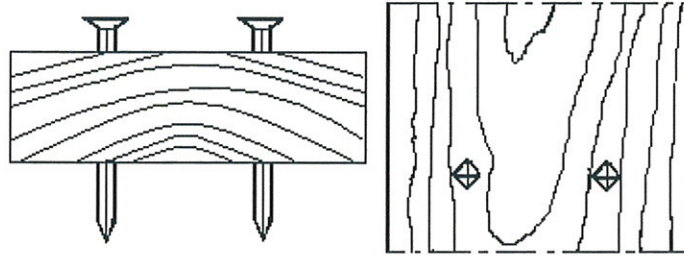
Figure 3   Position of the nails in the tests.

Figure 4   Examples on the biggest cracks of the nailing test specimens.

The main part of documented splits was short ($< 3d$) and fine cracks, like a hair. Only in some cases split lengths more than $3d$ was found (see Figure 4). Drying down from 19 % moisture content to 10 % increased the split lengths as average less than 10 %, so that greater amount of lengthening occurred with the highest density of timber. The most of the splits were formed immediately during nailing. The drying of wood did not have noteworthy influence to the number of the splits, especially when density was less than 460 kg/m^3. The cracking results were very similar with the results of corresponding nailing tests of pine (*Pinus sylvestries*) presented by Niskanen (1959).

The number of fine cracks was generally highest with N -series (thin timber and small edge distance) and smallest with S -series (thick timber and longest edge distance). After the drying phase the average spitting percentage was 16 % with N-series nails while it was 11 % for M-series and 7 % for S-series. However, when the split length of at least $3d$, there were no significant difference between the different test series of timber thickness and edge distances.

3 Loading tests of splitting sensitive joints

The tests consisted both compression and tension tests (VTT 2004). The test specimens were according to EN 1380 and the loading process was according to EN 26891. The timber material was selected and conditioned and the test specimens were fabricated similarly as the nailing test specimens of Chapter 2. After the nailing, the test specimens of H-series were stored first in the climate room of RH 40 % for five weeks and then in the moisture of RH 65 % for four weeks before loading tests. Test specimens of G-series were conditioned to RH 65% directly after nailing.

The dimensions of the test specimens are shown in Table 2 and Figures 5 and 6. The smooth square nails, 2,8x75, were hammered in. The nails in a row parallel to the grain were staggered perpendicular to grain by the nail diameter $1d$. The thickness of the centre member t_2 was selected so that $t_2 = l_p + 12$ mm (12 mm $\approx 4d$), when l_p is the pointside penetration. Nails spacings $a_1 = 10d$ (parallel to grain) and $a_2 = 5d$ (perpendicular to grain) and the end distances a_3 were minimum values according to EC5. The thickness of the headside timber (t_1) and the edge distances (a_4) were variables alike with the nailing test specimens. Splits of timber were documented after fabrication and just before the loading test. The summary of splitting results has been presented in Appendix.

Table 2   Test specimens of loading test series of splitting sensitive joints.

series	n	moisture cycles	test	a_3 (mm)	t_1 (mm)	a_4 (mm)
G-NC	10	RH85 => RH65	compression	28	20	14
G-NT	5	RH85 => RH65	tension	42	20	14
H-NC	5	RH85 => RH40 => RH65	compression	28	20	14
G-MC	10	RH85 => RH65	compression	28	28	20
G-MT	5	RH85 => RH65	tension	42	28	20
H-MC	5	RH85 => RH40 => RH65	compression	28	28	20
G-SC	5	RH85 => RH65	compression	28	40	28
G-ST	5	RH85 => RH65	tension	42	40	28
H-SC	5	RH85 => RH40 => RH65	compression	28	40	28
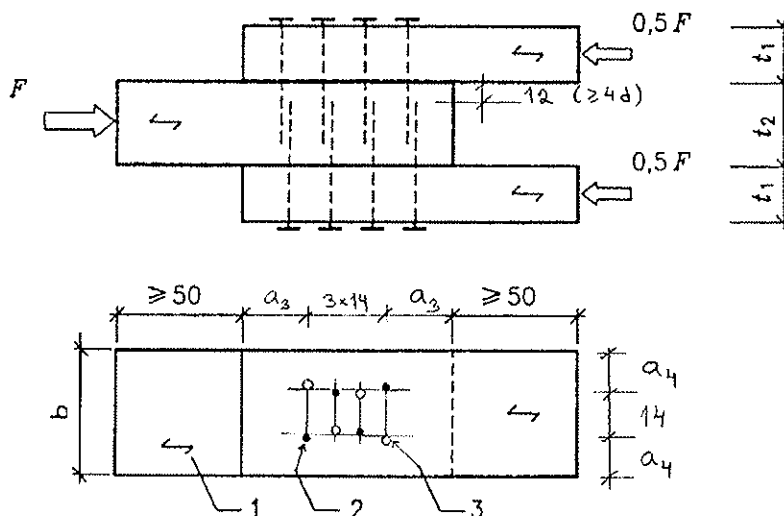
Figure 5   Compression test specimens. 1 = Grain direction, 2 = Nail head and 3 = Nail point. Nail was 2,8x75, square smooth shank.
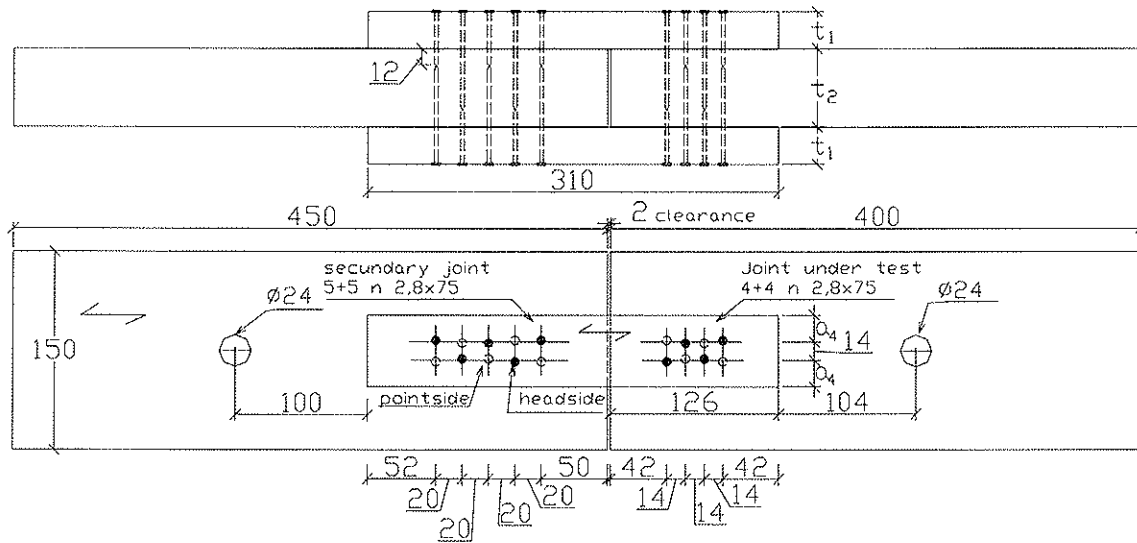
Figure 6   Tension test specimens.

Mean values of the test results are shown in Table 3. The individual test results with the calculated load-carrying capacities of EC5 are presented in Figure 7. There was no significant difference between compression and tension test results. The drying cycle of H-series test specimens did not have an influence to the load-carrying capacity of the joints.

All the test results of N series (thin timber) exceeded clearly the calculated capacities, when the calculations were done by the EC5 method with the measured density values of the actual test specimens (failure mode d: one hinge yielding of nail). With the thicker timber (M and S series) some F_{15} values were slightly smaller than the calculated capacities with the actual density values, but on average the calculation method of EC5 corresponded very well with the test results of M and S series (failure mode f: yielding by two hinges).

Table 3   Mean results of the loading tests.

Test series	ρ_{outer} kg/m^3	ω %	F_{15} kN	cov %	F_{max} kN	cov %	M.o.F
G-NC	440	15.2	8.28	5.4	8.66	5.8	d [1]
G-NT	434	15.5	7.92	5.0	8.20	7.3	d [1]
H-NC	451	13.3	8.75	2.1	8.98	3.8	d [1]
G-MC	401	15.0	7.95	4.2	8.56	3.6	f
G-MT	458	15.3	7.94	3.6	8.66	3.8	f
H-MC	406	13.3	8.05	2.6	9.04	7.7	f
G-SC	417	14.6	8.13	2.6	8.33	4.0	f
G-ST	437	15.2	8.11	2.0	8.25	2.9	f
H-SC	413	13.2	8.36	3.4	8.52	3.1	f

[1] Timber failure occurred in some test pieces after displacement of 15 mm.

5
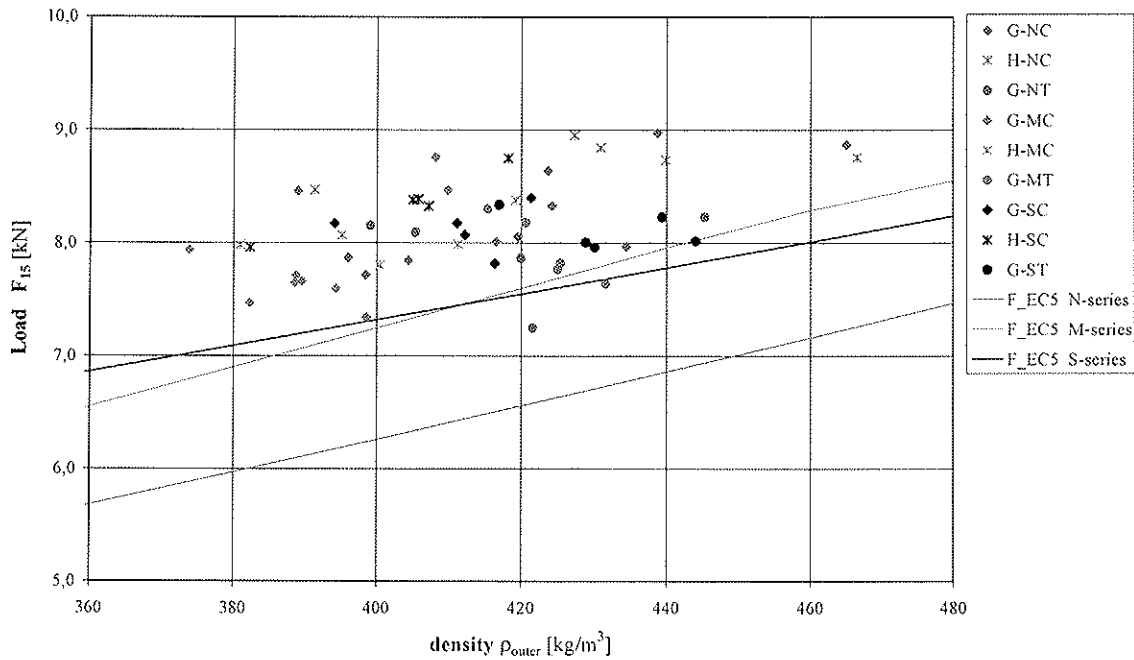
Figure 7   Test results and the load-carrying capacities F_{EC5} calculated according to Eurocode 5 using measured ρ_{outer} as ρ_k for both timber members ($f_{h,1} = f_{h,2}$).

4   Loading tests of smooth nails in end grain

The lateral load-carrying tests of nails in end grain of Nordic spruce (*Picea abies*) were done according to EN 26891 (VTT 2004). The timber pieces were selected in accordance with the method 1 in EN 28970 with the required characteristic density value of timber ρ_k = 350 kg/m^3 (strength class C24). The dimensions of the test specimens are shown in Figure 8. The square smooth shank nails, 3,4x100, were hammered in. The nails in a row parallel to the grain were staggered perpendicular to grain by the nail diameter $1d$. The nail spacing $a_1 = 10d$ (parallel to grain) and $a_2 = 5d$ (perpendicular to grain). In the end grain member, the edge distance of loaded end $a_4 = 7d$, and for the unloaded edge distance $a_4 = 5d$. The pointside penetration of the nails was $10d = 34$ mm. Spacings and edge distances for nails were the minimum values of Eurocode 5.
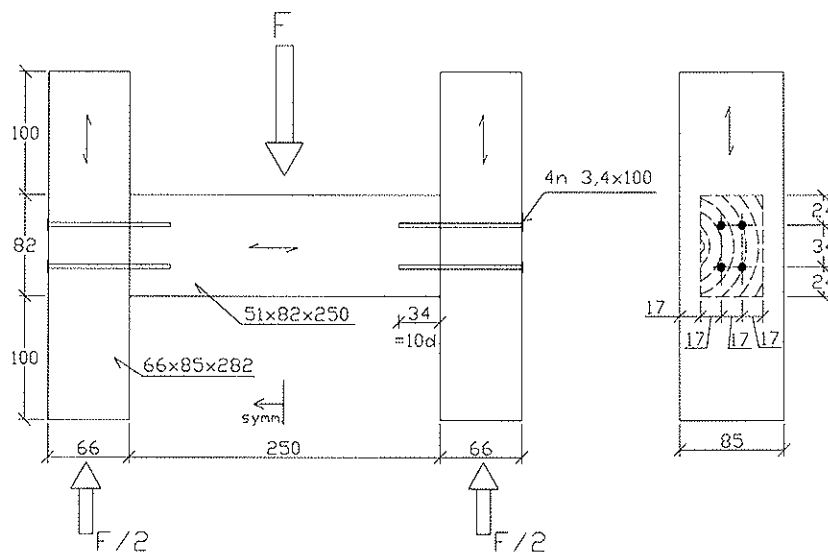
Figure 8   Test specimen for smooth nails in end grain (dimensions in mm).

6

After the test specimens were fabricated using timber stabilized to RH 85 % they were stored in climate room of RH 40 % for 40 days. At that time moisture content of timber was about 10 %. Then the test specimens were conditioned to RH 65 % before testing. The loading was done by compression as shown in Figure 8. The deformations were measured between timber members from the both joints of the test specimens.

The mean values of test results of five similar test specimens are shown in Table 4 where also the characteristic load carrying capacity of EC5 is presented ($F_{EC5,k}/3$) for timber density $\rho_k = 350$ kg/m^3. According to EC5 the smooth nails may be used in end grain for the secondary structures if it is allowed in the National annex. Then the design values of the load-carrying capacity should be taken as 1/3 of the values for nails installed at right angles to the grain.

The failure mode of all the joints was yielding of the nail in the point side timber (failure mode d of EC5). All the cases, the final failure load was not reached until the joint slip was more than 15 mm. There was a crackle sound after loading of 4,5 kN in all test pieces. In some cases the timber splitting failure of the end grain member occurred, when the joint slip value of 15 mm had been exceeded.

Table 4 Mean results of the end grain joint tests and calculated comparison values.

ρ kg/m^3	moisture cycles	ω %	F_{15} kN	cov %	F_{max} kN	cov %	$F_{test,k}$ [1] kN	$F_{EC5,k}/3$ kN
364	RH85 => RH40 => RH65	12,9	**6,52**	11,3	6,77	10,8	5,11	2,75

[1] $F_{test,k} = F_{15} - 1,92*v$; where v is the standard deviation.
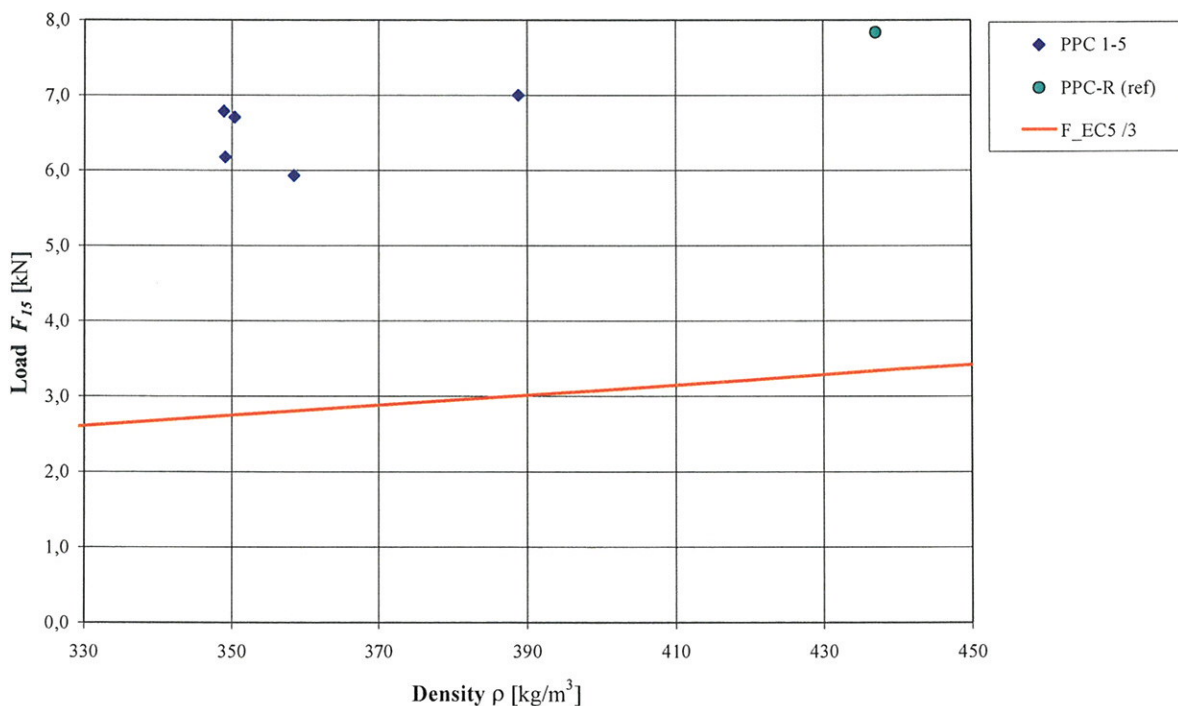
Figure 9 Test results (F_{15}) of end grain joints and capacity according to EC5.

7

5 Withdrawal strength of machine driven nails

The withdrawal strength of nails used in pneumatic nailing machine was studied (Kevarinmäki 2005). Five different nails were tested with the penetration length of $l_p = 18d$. The tests were carried on using Norway spruce (*Picea abies*) wood in three different moisture contents and two different density classes. One hundred short-term withdrawal strength tests were carried out according to EN 1382 (Table 5). In addition 15 long-term tests were done ($\leq$ 560 days) in cyclic humidity conditions under load levels of 50–80 %.
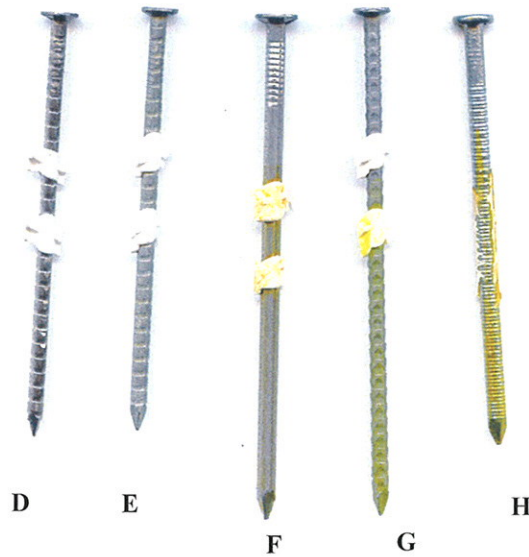
Figure 10   Tested machine driven nails.

Table 5   Results of the short-term test. ω is the moisture content in testing. $f_{1,mean}$ is tested withdrawal strength according to EN 1382. $f_{ax,cal}$ is calculated according to EN 1995-1-1 by the equation of smooth nails with the density of test specimen ρ_{RH65} ($f_{ax,cal} = 20 \times 10^{-6} \rho^2$).

Test series	Nail	d (mm)	Moisture nailing => conditioning	ρ_{RH65} (kg/m³)	ω (%)	$f_{1,mean}$ (N/mm²)	cov (%)	$f_{ax,cal}$ EC5 (N/mm²)
AK-D	Jaggen, bright	2,8	RH65=>RH65	373	13,7	5,53	10,0	2,78
AK-E	Jaggen, hdg	2,8	RH65=>RH65	373	13,7	9,80	15,4	2,78
AK-F	Smooth, bright	3,1	RH65=>RH65	373	13,7	7,17	9,2	2,78
AK-G	Glue-tipped, hdg	2,8	RH65=>RH65	373	13,7	9,41	16,0	2,78
AK-H	Ringlock, hdg	3,1	RH65=>RH65	373	13,7	5,56	19,4	2,78
AR-F	Smooth, bright	3,1	RH65=>RH65	476	14,1	9,81	7,4	4,53
AR-H	Ringlock, hdg	3,1	RH65=>RH65	476	14,1	8,70	12,1	4,53
BK-F	Smooth, bright	3,1	RH85=>RH40	355	10,6	2,80	5,7	2,52
BK-G	Glue-tipped, hdg	2,8	RH85=>RH40	356	10,8	6,33	10,8	2,52
BK-H	Ringlock, hdg	3,1	RH85=>RH40	356	10,8	3,72	7,9	2,52
CK-F	Smooth, bright	3,1	RH65=>RH85	359	15,2	7,19	18,0	2,58
CK-G	Glue-tipped, hdg	2,8	RH65=>RH85	359	15,2	9,27	7,5	2,58
CK-H	Ringlock, hdg	3,1	RH65=>RH85	360	15,2	5,73	25,7	2,59

The withdrawal strength of plain shank nails of Eurocode 5 is well on the safe side when compared to the results of the tests done according to EN 1382. It is observed however, that if the connection dries after nailing, the withdrawal strength decreases considerably. In realistic test conditions, where the nailing is done on wood conditioned to RH85% (external dry) and the connection is tested after conditioning to RH40% (internal dry), the withdrawal strength of plain shank nails was only 39 % of the strength based on EN 1382 of connections conditioned to RH65% before nailing and then directly tested. With the tested profiled nails the corresponding reduction factor was average 67 %.

In the long-term tests, the most of failures occurred during the short-term increase phase of load with the load levels of 68–81% (see Figure 11). This demonstrated that the previous loading history decreased the withdrawal strength of nails in cyclic humidity conditions.
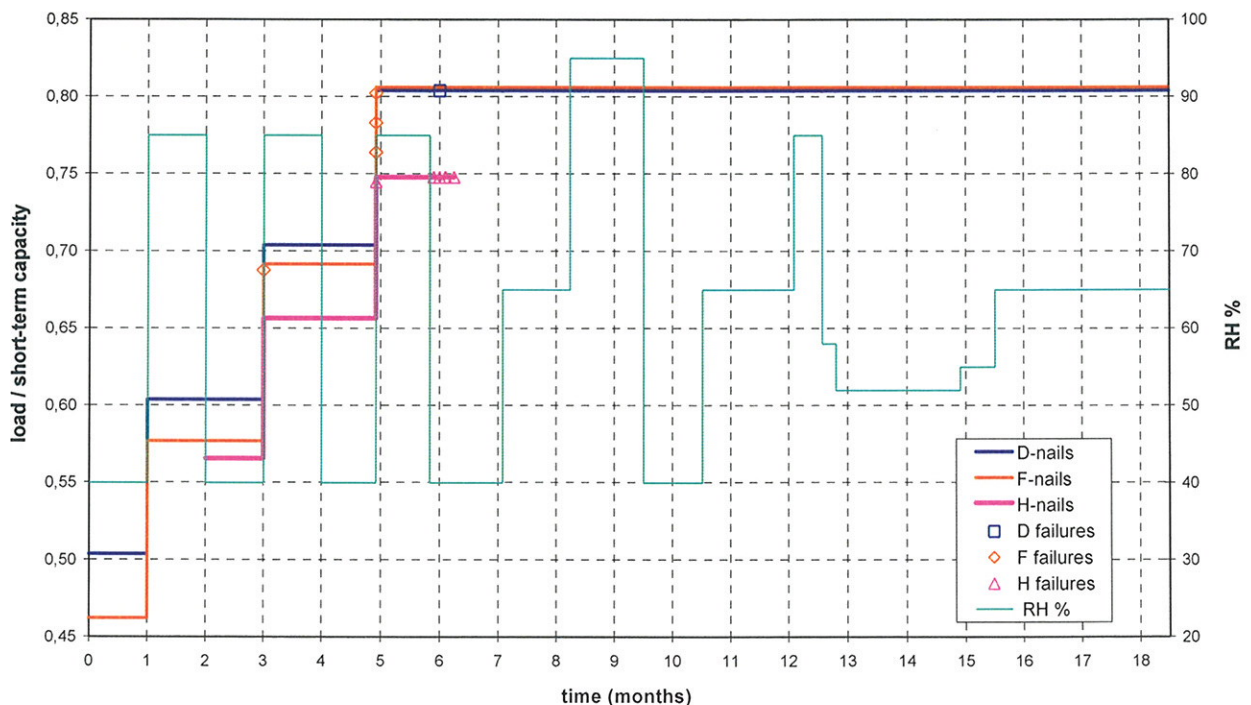
Figure 11   Moisture and loading cycles and the failure times in long-term tests.

6   Conclusions

Splitting sensitivity of spruce

The clause 8.3.1.2(7) of Eurocode 5 (EN 1995-1-1) given for timber of species especially sensitive to splitting is recommended to omit at all or to limit only for the silver fir (*Abies alba*) and Douglas fir by National annexes. With the Nordic spruce, the allowed minimum thickness of timber for nailed connections without predrilled holes may be safely defined as for the common species of timber: $t_{min} = \max(7d; (13d-30)\rho_k/400)$. The general minimum value of edge distance $a_4 = 5d$ may be also safely used for the nails hammered into the Nordic spruce without predrilled holes.

For the next version of Eurocode 5, the clause 8.3.1.2(7) shall be corrected: spruce should be eliminated from the list of species of sensitive to splitting and the real splitting sensitivity of silver fir (*Abies alba*) and Douglas fir should be verified. The rules given for "timber of species especially sensitive to splitting" seems to be over-conservative: the minimum timber thickness or the minimum edge distance is required to double.

Nails in end grain

In National annexes, the clause 8.3.1.2(3) of Eurocode 5 (EN 1995-1-1), "Smooth nails in end grain should not be consider capable of transmitting lateral forces", should be recommended to replaced by clause 8.3.1.2(4). The clause 8.3.1.2(4) with the limitation of the load-carrying capacity of nails in end grain to 1/3 of the values for nails installed at right angles to the grain may be safely applied.

Long-term lateral load-carrying capacity tests of nails in end grain should be done for the future development of Eurocode 5. According to the results of short-term tests, the lateral load-carrying capacity for nails in end grain may be increased at least to 1/2 from 1/3 of the values for nails installed perpendicular to the grain. Also the exceptional and unclear rule for the restriction on use of smooth nails only for secondary structures given in EN 1995-1-1:2004 should be cancelled from the next versions of Eurocode 5.

Withdrawal strength

It is proposed that the test standard for withdrawal strength EN 1382:1999 is modified so that the conditioning of wood is done to RH85% before nailing and after it is conditioned to RH40% before testing at a temperature of 20°C. This requirement could also be mentioned in the product standard for nails EN 14592. In case the nail type specific withdrawal capacity is determined according to EN 1382:1999 conditioned to RH65%, the experimental withdrawal strength $f_{ax,k}$ should be reduced by a factor of 0,4 for plain shank nails and at least by a factor of 0,7 for profiled nails.

The reduction of the short-term withdrawal strength due to the previous long-term loading should be taken into account in design. The next version of Eurocode 5 (EN 1995-1-1) could be supplemented for example as follows: In case the share of the permanent and long-term loads is over 1/3, the withdrawal capacity of nails is calculated with a modification factor k_{mod} equal or lower than 0,7 ($k_{mod} \leq 0,7$).

7   References

EN 1380. 1999. Timber structures - Test methods - Load bearing nailed joints. CEN.

EN 1382. 1999. Timber Structures - Test methods - Withdrawal capacity of timber fasteners. CEN.

EN 1995-1-1. 2004. Eurocode 5 - Design of timber structures - Part 1-1: General - Common rules and rules for buildings. CEN.

EN 26891. 1991. Timber structures - Joints made with mechanical fasteners - General principles for determination of strength and deformation characteristics. CEN.

EN 28970. 1992. Timber structures. Testing of joints made with mechanical fasteners. Requirements for wood density. CEN.

Kevarinmäki, A. 2005. Withdrawal strength of machine driven nails. VTT Working Papers 27. Espoo, Finland. 36 p. http://www.vtt.fi/inf/pdf/workingpapers/2005/W27.pdf

Niskanen, E. 1959. Investigations on cracking, splitting and strength of nailed timber joints. VTT Report series I - Wood 8. Helsinki, Finland. 78 p.

prEN 14592. 2002. Timber structures - Fasteners - Requirements. CEN

VTT. 2004. Research Report No. RTE 3198/04: Experimental study of nailed joints. VTT Building and Transport, Espoo, Finland. 33 p.

APPENDIX: Summary of the cracking results of splitting test specimens measured after drying phase.
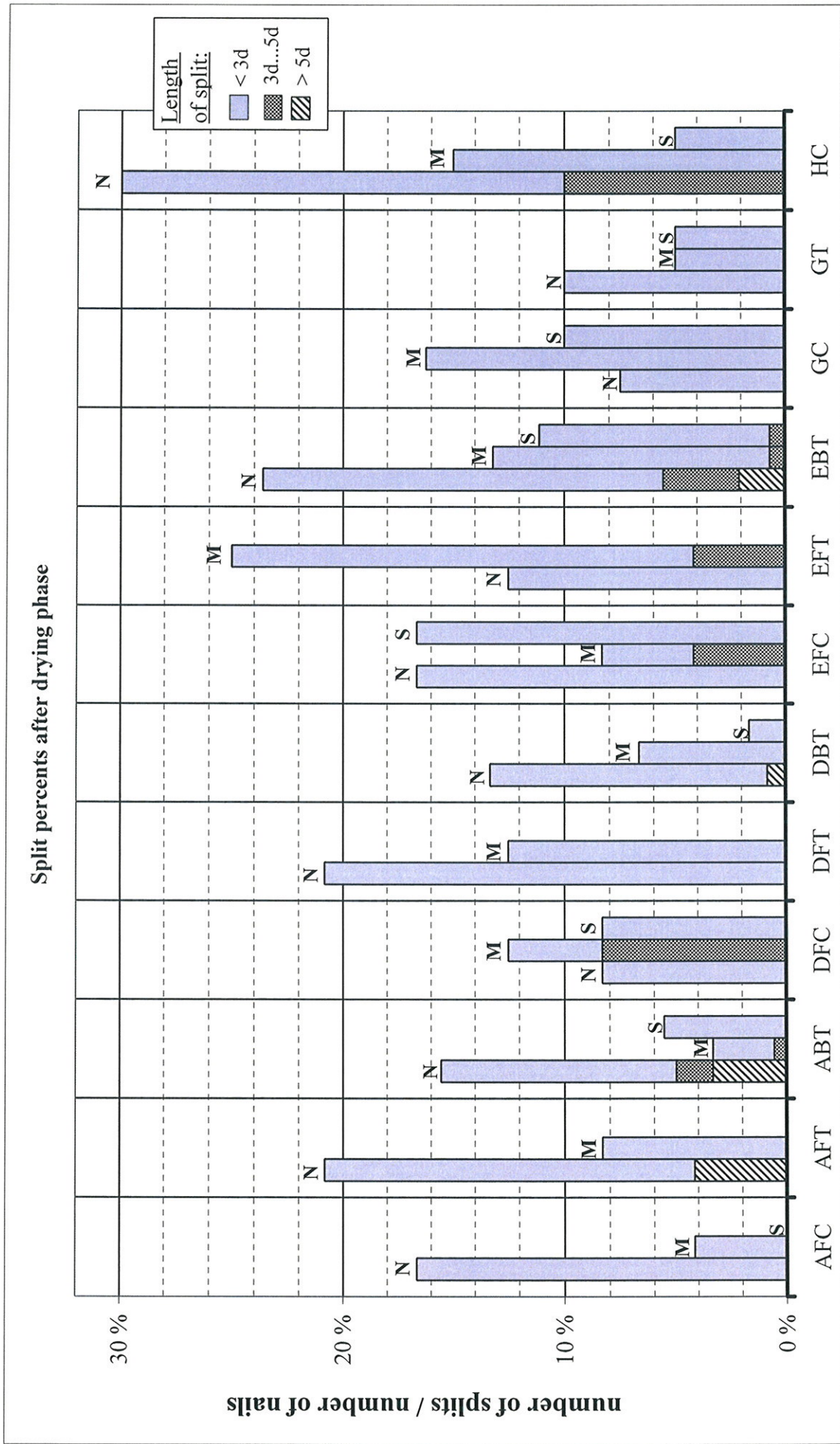
Split percents after drying phase

Length of split:
- <3d
- 3d...5d
- >5d

number of splits / number of nails

Categories: AFC, AFT, ABT, DFC, DFT, DBT, EFC, EFT, EBT, GC, GT, HC

INTERNATIONAL COUNCIL FOR RESEARCH AND INNOVATION
IN BUILDING AND CONSTRUCTION

WORKING COMMISSION W18 - TIMBER STRUCTURES

DESIGN OF TIMBER CONNECTIONS WITH SLOTTED-IN STEEL PLATES AND SMALL DIAMETER STEEL TUBE FASTENERS

.

B Murty

I Smith

A Asiz

University of New Brunswick, Fredericton

CANADA

Presented by A Asiz

H Blass commented that the oval cross section of the fastener under load would change the yield moment. A Asiz stated more test will come to confirm this. M Popovski asked about cyclic testing and behaviour in heavy timber. A Asiz said it would be interesting to consider cyclic testing and heavy timber is more appropriate. F Lam asked whether heavy timber would be tested. A Asiz agreed. F Lam also commented the lack of restraint in the tube compared to Delft's expansion tube. The tube can slide out of the connection and the behaviour between this and the original system is different. A Jorissen questioned and received clarification on figures in table for modification factor in relationship with numbers in the Table. A Leijten commented that the commercial application of the tube type connection is interesting and Delft's experience would be important.

Design of Timber Connections with Slotted-in Steel Plates and Small Diameter Steel Tube Fasteners

Bona Murty, Ian Smith and Andi Asiz
University of New Brunswick, Fredericton, Canada

1   Introduction

Finding combinations of member materials and fasteners that produce ductile timber connection responses is challenging and research toward that end is being conducted by the authors. Others have pursued the same aim but their techniques resulted in solutions that are labour intensive and also expensive in other ways, e.g. involving localised reinforcement of the members and grouting the fasteners in with epoxy [5]. The approach taken here is to use 3 mm thick steel plate link-elements that slot into ends of wood members and circular cross-section steel tubes of relatively small external diameter (up to 12.7 mm), Figure 1. Solid *spruce* and *Laminated Strand Lumber* (*LSL*) were used as representative diverse 'wood' member materials. *LSL* is an advanced type of engineered wood product common in North America. While *spruce* is splitting prone, *LSL* is not. Tested connection arrangements had one or two slotted-in link-elements and one or four tube fasteners. Specimens were subjected to axial tensile static load until failure. Ductile load-deformation responses were expected to occur through combinations of wood crushing beneath fasteners, bending induced plastic hinges in fasteners, and plastic distortion of fastener cross-sections. Distortion of fastener cross-sections was the result of them being hollow, with the extent of those distortions controlled by the ratio of inner and outer tube diameters and the yield stress. Especially in cases where the fasteners were not slender, that mechanism compensated for loss of the other sources of ductility.

The remainder of this paper is focussed on test and results, examination of the acceptability of closed form Johansen type yield models for design level predictions of strengths of connections with small diameter steel tube fasteners [6], and the format of design rules. Yield models, or *European Yield Models (EYM)* as North Americans like to call them, are very widely accepted for making strength predictions for connections with dowel fasteners. However, *EYM* as currently implemented in many national and model international timber design codes, e.g. [4], can over predict a connection's capacity by a considerable margin. Errors occur mostly when failure is due to splitting of the wood member(s), rather than creation of plastic hinges in fasteners and localised crushing of members by fasteners. Further, it is erroneous to suppose that if codes specify use of large fastener spacings and large fastener end distances then splitting of members can be reliably avoided.

2   Test program

2.1   Specimens

The nature of specimens and test arrangements are shown schematically in Figure 1. All wood materials were pre-conditioned in an environmental chamber at 20°C/65%RH for two weeks prior to manufacture of specimens. The 'wood' members were cut from billets of *LSL* and *spruce*. The *spruce* was visually inspected to ensure that cut pieces were free from major

defects. Wood members had the size of 38 mm x 86 mm x 460 mm, with the long axis parallel to the strong axis of material symmetry (parallel to grain in the case of *spruce*). Steel plate 3 mm thick (Grade A36), and steel tubes with 6.35 mm, 9.52 mm and 12.70 mm outside diameters (Grade A179) were used to create plate link-elements and fasteners respectively. The fasteners were cut from lengths of seamless cold-drawn low-carbon steel heat-exchanger and condenser tube [1], which is cheap and widely available. Figures 2 (schematic) and Figure 3 (photograph) show unassembled specimen components. For connections using one link-element, the plate was placed in a pre-cut slot located coincident with the wide middle plane of the wood member. For connection using two link-elements, the plates were placed in pre-cut slots, one slot located 12.5 mm below each wide surface of the wood member. Steel tubes fitted tightly in predrilled holes oriented normal to the plane(s) of the link-element(s). Fastener spacing and end distances, Figure 2, were those typically used for steel bolts [4]. For the connection with one link-element, there were sets of specimens representing single and multiple (four) fastener arrangements (*patterns 1 & 2*). For the connections using two link-elements only the four fastener arrangement was investigated (*pattern 2*). There were 6 replicates of each specimen type, resulting in 54 *LSL* specimens and 54 *spruce* specimens.
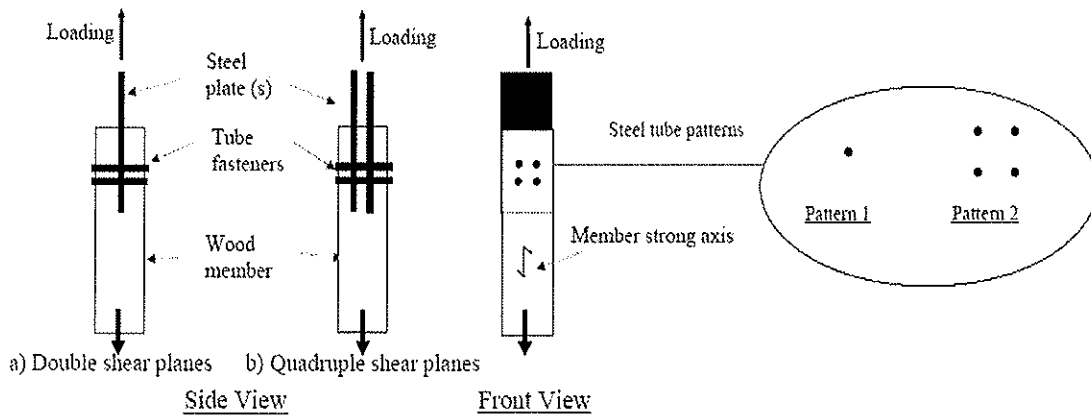
Figure 1. Specimen arrangement (half-joint test)

Pattern 1   *Pattern 2*
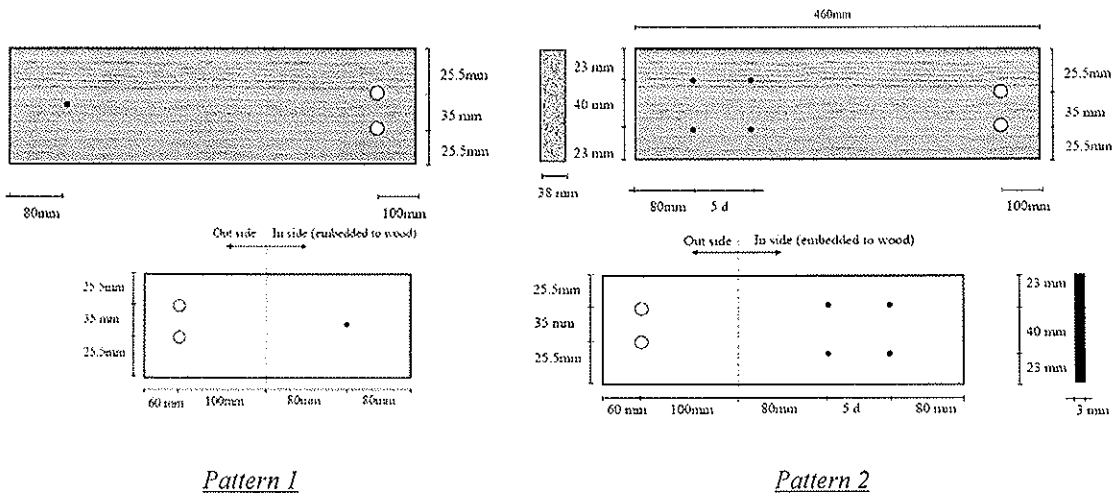
Figure 2. Plate and member geometries
(upper diagrams: members, lower diagrams: link-elements)

2

All connections were tested in axial tension under displacement control at a rate intended to attain the maximum load in about 0.1 hours. Test practices were based on requirements of ASTM D 5652-95 [2]. Two LVDT's were used to measure slip of the link-element(s) relative to the wood member, Figure 4.
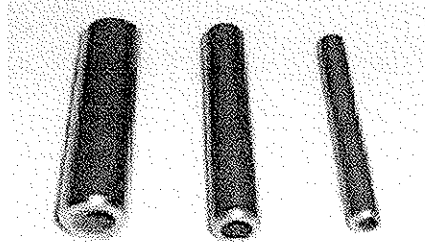
Figure 3. Steel tube fasteners with 12.70 mm, 9.52 mm and 6.35 mm outside diameters
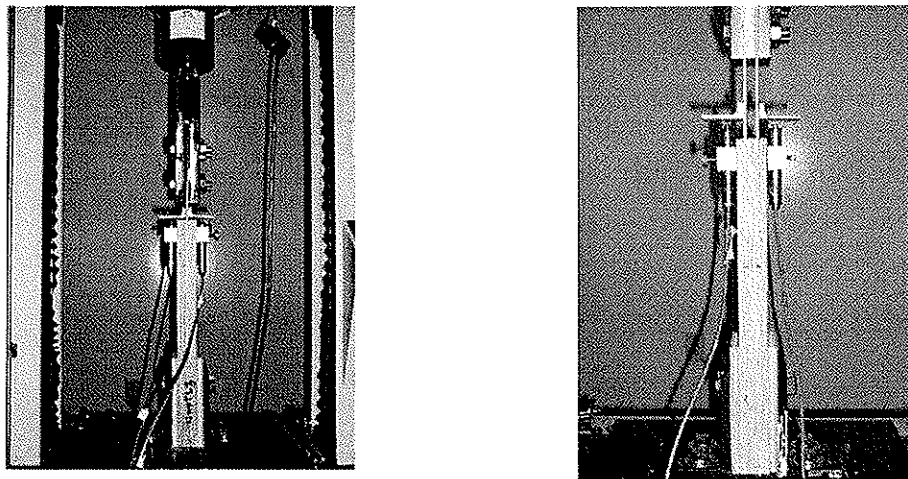
Figure 4. Specimens under test
(left: one link-element, right: two link-elements)

2.2 Test results

2.2.1 One link-element connections

2.2.1.1 LSL connections

Table 1. Average maximum (peak) loads for *LSL* connections with one link-element

Number of fasteners	Maximum load, kN (according to fastener diameter)		
	6.35 mm	9.52 mm	12.70 mm
1	5.43	10.5	18.4
4	24.0	45.1	64.4

All *LSL* connections failed in a ductile manner with crushing in the *LSL* by fasteners and yielding in the fasteners, Figure 5, with fasteners exhibiting large levels of slip, Figure 6. Average ductility ratios were in the order of 6. The strength of four-fastener connections was about four times the strength of similar single-fastener connections. This implies *pattern 2* arrangements shared the load evenly between fasteners at failure, in contrast with what is implied by earlier tests on connections employing solid bolts in solid wood members [5].

3

Figure 6 shows a typical set of load-slip curves for single link-element *LSL* connections, based on six test replicates. It is clear from the figure that variability in responses is small between replicates. This and the lack of visible member splitting are highly suggestive indications that failure characteristics of the steel fasteners dominated the failure mechanisms. There is apparently no need for design rules to discount the capacity per fastener in multiple steel tube fastener connections in *LSL* members. Undoubtedly this also applies to tube fastener connections in some other engineered wood materials (those where wood veneers, wafers or strands reinforce each other through effects of cross-lamination).
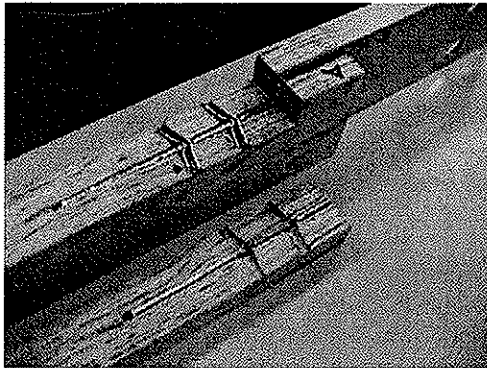
Figure 5. Typical failed *LSL* connection
with one link-element
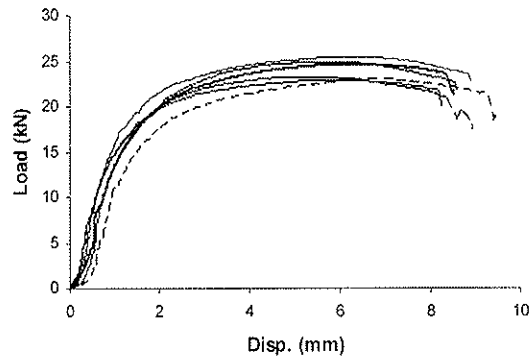
Figure 6. Load-slip (displacement) curves for
LSL connections with one link-element and
four 6.35 mm fasteners

2.2.1.2 *Spruce connections*

Table 2. Average maximum (peak) loads for *spruce* connections with one link-element

Number of fasteners	Maximum load, kN (according to fastener diameter)		
	6.35 mm	9.52 mm	12.70 mm
1	4.44	12.0	13.8
4	16.5	35.1	39.3
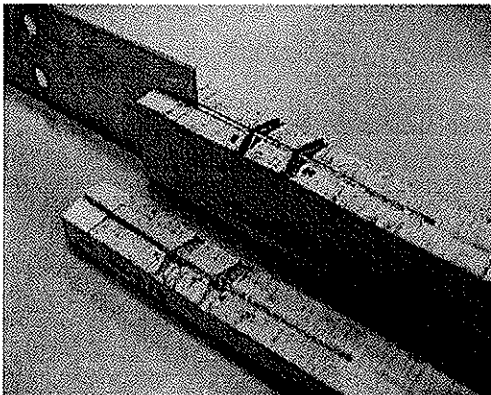
Figure 7. Typical failed *spruce*
connection with one link-element
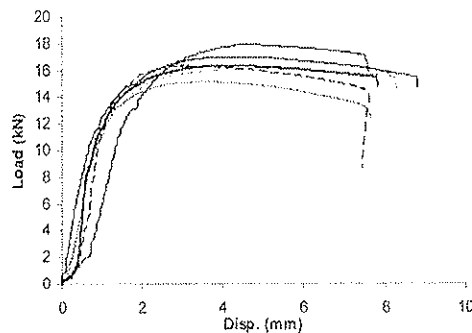
Figure 8. Load-slip (displacement) curves for
spruce connections with one link-element and
four 6.35 mm fasteners

4

The typical failure mechanism for the fasteners is shown in Figure 7. All *spruce* connections failed in an apparently ductile manner, Figure 7, but there was some evidence of post-peak softening in the load carrying capability associated with cracking, Figure 8. Average ductility ratios were in the order of 3. The relatively low ductility ratios are attributed to creation of small splits (cracking) beneath the fasteners at about the yield load. This was most obvious for connections with 12.70 mm fasteners, as one would expect. This reflects that *spruce* has relatively low fracture resistance (much lower than for *LSL*). Although the strength of connections with four 6.35 mm fasteners was about four times the strength of similar single-fastener connections, the strengths of connections with four 9.52 or 12.70 mm fasteners were only about three times those for similar single-fastener connections. As illustrated by the sets of load-slip curves in Figure 8, although variability in strength between replicates was greater than for *LSL* connections (compare with curves in Figure 6), it was not large. Proneness to member splitting indicates that for *spruce* connections the behaviour characteristics of both the members and fasteners have strong influence on overall connection behaviour, and capacity. This is the same as for connections with solid steel bolts in solid wood members [5]. Clearly, there is need for design rules to recognize that, unless very small diameter steel tube fasteners are used ($\leq$ 6.35 mm outside diameter), the strengths of connections in solid wood members are not directly proportional to the number of fasteners.

2.2.2 Two link-element connections

2.2.2.1 LSL connections

Table 3. Average maximum (peak) loads for *LSL* connections with two link-elements and four tube fasteners: and comparison with results for connections with one link-element

Number of link-elements	Maximum load, kN (according to fastener diameter)		
	6.35 mm	9.52 mm	12.70 mm
2	34.9	57.4	66.9
1	24.0	45.1	64.4
% difference[1]	31	22	3.7

[1] (difference ×100) ÷ (two link-element value)
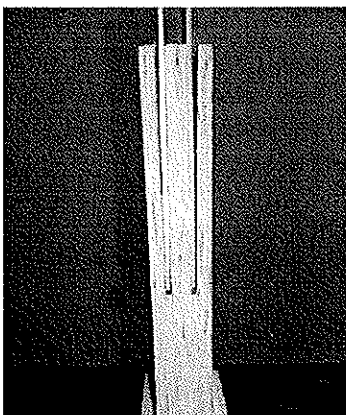
Figure 9. Typical failed *LSL* connection with two link-elements
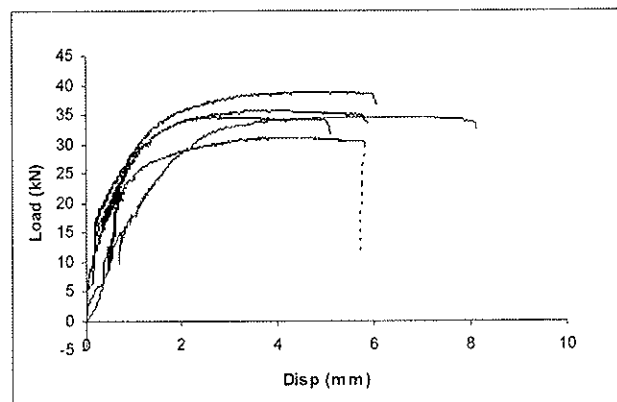
Figure 10. Load-slip (displacement) curves for *LSL* connections with two link-elements and four 6.35 mm fasteners

As seen from the comparison with Table 3, the gain in connection strength due to use of two instead of one link element is inversely proportional to the fastener diameter, with a

5

negligible gain in strength when 12.7 mm diameter fasteners are employed. This is because when there is only one link-element slender, small diameter, fasteners develop plastic hinges, but when there are two link-elements fasteners the fasteners are not prone to development of plastic hinges. Strengths of all two link-element connections approached the theoretical maximum peak strength, i.e failure simply involved cross-section distortion of fasteners and localised crushing of the wood member by fasteners. Even using multiple fasteners the high fracture resistance of the *LSL* prevented premature splitting failure of members, as typically occurred in solid wood members. All the two link-element *LSL* connection specimens exhibited distinctly ductile failures. There was a tendency toward peeling away of outer layers of the member, Figure 9, because of bending deflection in outer cantilevered sections of fasteners. Ductility rations were high despite the absence of plastic hinges (in the order of 5 or greater), Figure 10.

2.2.2.2 Spruce connections

Table 4. Average maximum (peak) loads for *spruce* connections with two link-elements and four tube fasteners: and comparison with results for connections with one link-element

Number of link-elements	Maximum load, kN (according to fastener diameter)		
	6.35 mm	9.52 mm	12.70 mm
2	29.5	43.6	47.8
1	16.5	35.1	39.3
% difference[1]	44	20	18

[1] (difference ×100) ÷ (two link-element value)
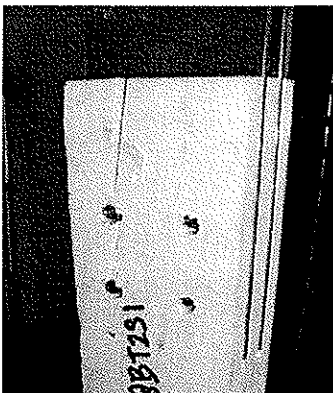
Figure 11. Typical failed *spruce* connection with two link-elements
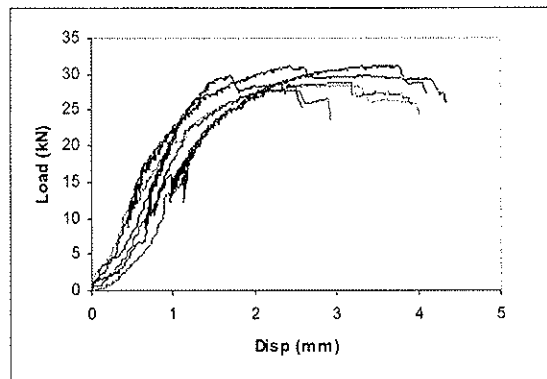
Figure 12. Load-slip (displacement) curves for *spruce* connections with two link-elements and four 6.35 mm fasteners

As seen from the comparison in Table 4, the gain in connection strength due to use of two instead of one link element is inversely proportional to the fastener diameter. For *spruce* connections, unlike *LSL* connections, there were substantial strength gains for all of the tested fastener diameters. Failure modes for two link-element connections involved wood splitting, Figure 11, but this did not mean that there was no ductility in the responses, Figure 12. However ductility ratios were in the order of ≤ 5. As illustrated by a comparison of results in Figures 8 and 12, use of two link-elements rather than one led to relatively higher variability in connection strengths and reflects the proneness of *spruce* member to splitting. For *spruce* connections substantial capacity gains from using two link-elements are offset by losses in

6

ductility and lowered repeatability in strengths. From a design perspective neither of these features would suggest the particular solid wood (*spruce*) connection detail is a good choice when either seismic or strong wind events are likely to be the governing loading scenario, if structural systems employing them are unable to develop alternative primary load paths.

3   *European Yield Model* predictions

The key issue in application of the *European Yield Model (EYM)* in design is that the modelling approach is only strictly appropriate to multiple fastener connections if they exhibit ductile failure and the maximum load is linearly proportional to the number of fasteners. For simplicity, in this paper consideration is restricted to applying *EYM* equations to double shear (one link-element) *LSL* and *spruce* connections with steel tube fasteners. However the conclusions are equally valid for quadruple shear connections -- two link-elements, because either case can result in any of the three possible *EYM* failure mechanisms (actual or extensions of Modes I to III in Figure 13) governing.

Parameters entering *EYM* calculations are member thicknesses, fastener plastic moment capacity (section modulus × yield strength), and embedment strengths of members. Figure 13 defines the possible yield failure modes, based on double shear connections, and key geometric notation. Because it was not observed in tests, the simplifying assumption that the fastener will not crushing the steel plate member (link-element) can be applied. Following essentially the notation of Pedersen et al [7], the *EYM* equations (1) to (3) apply.

Mode I   Mode II   Mode III
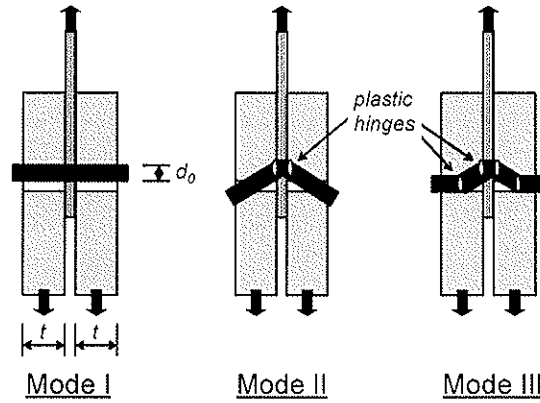
Note: All failures are symmetric.

Figure 13. EYM modes for a wood – steel plate – wood connection

$$
(1) \qquad\qquad\qquad\quad td_o f_h \qquad\qquad\quad \text{for } t < \sqrt{\dfrac{2M_y}{d_o f_h}} \qquad\qquad \text{Mode I}
$$

$$
(2) \qquad F_y = \min \left\{ \left(\sqrt{2 + \dfrac{4M_y}{t^2 d_o f_h}} - 1\right) td_o f_h \quad \text{for } \sqrt{\dfrac{2M_y}{d_o f_h}} \le t < \sqrt{\dfrac{16M_y}{d_o f_h}} \quad \text{Mode II} \right.
$$

$$
(3) \qquad\qquad\quad \sqrt{4M_y d_o f_h} \qquad\qquad \text{for } t \ge \sqrt{\dfrac{16M_y}{d_o f_h}} \qquad\qquad \text{Mode III}
$$

where: F_y = the maximum load (failure capacity) per shear plane for a one fastener connection, t = thickness of the wood side pieces, d_o = outside fastener diameter, M_y = plastic moment capacity of the fastener, f_h = embedment strength of the wood member (bearing pressure to crush the wood). Under double shear the total connection yield capacity is 2 F_y per fastener.

The plastic moment capacity for a circular tube fastener is:

$$(4) \qquad M_y = \frac{f_y (d_o^3 - d_i^3)}{6}$$

where: f_y = yield strength of the fastener and d_i = inside fastener diameter.

Based on equation (4), the plastic moment capacities for the three sizes of fasteners were calculated to be 4.81 x 10^3 Nmm, 18.7 x 10^3 Nmm and 43.1 x 10^3 Nmm for fasteners with 6.35 mm, 9.52 mm and 12.70 mm outside diameters respectively. These estimates are based on yield strength f_y = 180 MPa [1]. Average embedment strengths of LSL and spruce were measured and found to be 50 MPa and 34 MPa respectively [8]. Using these component properties, the appropriate d_o and taking t = 17.5 mm, connections strengths predicted based on equations (1) to (3). Table 5 lists EYM predictions of single fastener connection strengths and compares those with average test strengths. Overall it can be concluded that the EYM is reasonably accurate and errs on the safe side. It is therefore a reliable basis for design level predictions of tensile strengths (maximum sustainable loads) of wood connections employing slotted-in steel plate link-element(s) and a single small diameter steel tube fastener. This holds irrespective of whether the wood member is made of an easily split material like solid wood or a hard to split materials like LSL.

Table 5. EYM predicted maximum (peak) loads for LSL and spruce connections with one link-element and one tube fastener: and comparison with test results, kN

Fastener diameter (mm)	LSL member		spruce member	
	EYM	Test	EYM	Test
6.35	4.95	5.43	3.85	4.44
9.52	9.69	10.5	7.44	12.0
12.70	15.5	18.4	12.3	13.8

4 Discussion and application of findings

As proven previously [9], it not reliable to presume that just because single fastener connections fail in a ductile manner similar multiple fastener connections will also exhibit ductility prior to failure. This is because single fastener connection tests can never simulate fastener interaction in multiple fastener patterns. For dowel fastener tension connections, effects of fastener interactions on connection strength can be characterised by any arrangement with two or more fasteners in a row [9]. Ongoing research at The University of New Brunswick (UNB) is addressing prediction of how fastener pattern, spacing and the loaded end distance (tension connections) influence the extent of fastener interactions [8].

Deductions based on previous and current work at UNB point toward the possibility of quite simple treatment of multiple fastener connections by design by codes. Tentatively, it seems that if the ductility ratio estimated from tests on single fastener connections is ≥ 5, it can be assumed that the connection strength is linearly proportional to the number of fasteners. Also,

8

tentatively, if the ductility ratio estimated from single fastener connection tests is in the order of ≤ 3, it can be assumed for multiple fastener arrangements that the connection strength is about 0.7 × *EYM* strength per fastener × number of fasteners. These tentative 'rules' are premised on use of traditional spacing and end distance rules for bolts.

Although during design it is simple to predict the *EYM* strength and the *EYM* failure mode for a single fastener connection, it is not easy to predict the ductility ratio. However, test data suggests the existence of a relationship between predicted *EYM* failure modes and ductility ratios. That relationship leads to the very practical design equation:

(5) $$P = n_{no.\_fast.} n_{no.\_shear-planes} K_{mat.} K_{no.\_fast.\_per\_row} F_y$$

where: $n_{no.\_fast.}$ = total number of fasteners, $n_{no.\_plane}$ = number of shear planes per fastener, F_y = maximum load per shear plane for a one fastener connection (minimum value from equations (1) to (3)). The modification factors $K_{mat.}$ and $K_{no.\_fast.\_per\_row}$ both depend on the level of ductility that the type of connection is capable of achieving, Table 6.

Table 6. Tentative modification factors for design of tension connections with dowel type fasteners, based on equation (5)[1]

Characterisation of wood member failure	EYM mode	Modification factor for type of wood member material $K_{mat.}$	Modification factor for number of fasteners per row $K_{no.\_fast.\_per\_row.}$[2]	
			1	≥ 2
Splitting (e.g. solid wood)	I	0.9	1.0	0.7
	II	0.9	1.0	0.8
	III	0.9	1.0	0.9
Non- splitting (e.g. *LSL*)	I	1.0	1.0	1.0
	II	1.0	1.0	1.0
	III	1.0	1.0	1.0

[1] Assumes a concentrically loaded wood member. Presently values in the table are based on both analysis of data and expert judgement. Ongoing studies at UNB are intended to refine the concepts, and values in the table.
[2] Number of fasteners arranged in a line(s) parallel to the member axis.

What is discussed here is only one component of a broad initiative in Canada aimed at achieving rational and consistent code provisions. The companion paper "New generation of timber design practices and code provisions linking system and connection design" [3] discusses the broader initiative. Although not discussed here, the caveat to using *EYM* strengths (or any other predictions) as reliable design capacities for connections is that structural systems must be capable of allowing a level of deformation in connection, prior to global system failure, sufficient to realise the ascribed design connection resistance.

5 Conclusions

Small diameter steel tube fasteners are an effective means of achieving strong and ductile structural wood connections. This is especially true if steel tube fasteners are used in conjunction with slotted-in steel plate link-elements, and join members manufactured from one of the newer generation of engineered wood materials (e.g. *Laminated Strand Lumber*).

Closed form yield models appear to yield acceptable design level predictions of the tensile strengths of axially loaded connections with a single small diameter steel tube fastener. This is irrespective of whether the wood member(s) is made from an easily split material like solid wood or a split resistant engineered wood material. Multiple fastener connections in split resistant engineered wood materials have maximum strengths that can sensibly be regarded as linearly proportional to the number of fasteners. However, for multiple fastener connections in easily split materials (solid wood) their strength per fastener needs to be discounted by a considerable amount (by at least 30 percent). A major question is how to develop relatively accurate but simple design rules that recognise all the behavioural characteristics of connections employing dowel type fasteners. Fortunately it appears that appropriate and simple design rules are possible. Current Canadian work on this should interest the international timber design code writing community as well as the domestic code writers.

Acknowledgement

References

[1] ASTM. 1990. Standard specification for seamless cold-drawn low-carbon steel heat-exchanger and condenser tubes. Designation A 179/ A 179M-90a, American Society for Testing and Materials, West Conshohocken, PA, USA.

[2] ASTM. 2000. Standard test methods for bolted connections in wood and wood based products. Designation D 5652-95, American Society for Testing and Materials, West Conshohocken, PA, USA.

[3] Asiz, A. and Smith, I. 2005. New generation of timber design practices and code provisions linking system and connection design. Working Commission W18-Timber Structure, International Council for Building Research Studies and Documentation, Karlsruhe, Germany, (in press).

[4] CSA. 2001. Engineering design in wood. CSA Standard O86-01, Canadian Standards Association, Toronto, ON, Canada.

[5] Guan, Z.W. and Rodd, P.D. 2000. A three-dimensional finite element model for locally reinforced timber joints made with hollow dowel fasteners. Canadian Journal of Civil Engineering, 27: 785-797.

[6] Johansen, K.W. 1949. Theory of timber connections. International Association for Bridge and Structural Engineering, 98: 249-262.

[7] Pedersen, M.U., Clorius, C.O., Damkilde, L., Hoffmeyer, P., and Esklidsen, L. 1999. Dowel type connections with slotted-in steel plates. Working Commission W18-Timber Structure, Paper 32-7-8, International Council for Building Research Studies and Documentation, Rotterdam, The Netherlands.

[8] Smith, I. and Asiz, A. 2004 (October). Design method for connections in engineered wood product, Progress Report to Natural Resources Canada, University of New Brunswick, Fredericton, NB, Canada.

[9] Tan, D. and Smith, I. 1999. Failure in-the-row model for bolted timber connections. ASCE Journal of Structural Engineering, 125(7): 713-718.

INTERNATIONAL COUNCIL FOR RESEARCH AND INNOVATION
IN BUILDING AND CONSTRUCTION

WORKING COMMISSION W18 - TIMBER STRUCTURES

DESIGN SPECIFICATIONS FOR THE DURABILITY OF TIMBER

R H Leicester,

C-H Wang

M . Nguyen

G C Foliente

CSIRO Manufacturing & Infrastructure Technology, Melbourne

AUSTRALIA

Presented by R H Leicester

S. Thelandersson asked how to generalize the findings on the building envelope study. B Leicester responded that in total 44 houses in two or three groups were considered. It was tried to use climatic information outside to predict the mc in the wall cavity. Wall cavity details are important. Knowledge on building physics needs to be used.

Design Specifications for the Durability of Timber

R.H. Leicester, C-H. Wang, M. Nguyen and G.C. Foliente
CSIRO Manufacturing & Infrastructure Technology, Melbourne, Australia

Abstract

In the development of prediction models for the durability of timber construction, data was obtained from several sources. These include basic physics and biology, field tests on small clear wood and steel specimens, field tests on full size structures, in-service structures and expert opinion. This paper provides a discussion on the role played by these various sources of information, and also procedures for drafting rules for engineering design codes.

1. Introduction

During the past 8 years, there has been a major national undertaking sponsored by the Forestry and Wood Products Research and Development Corporation, to develop procedures for engineering the durability of timber construction in Australia. In this project, consideration was given to attack by decay fungi, termites, marine borers and corrosion agents. The construction environments considered included in-ground, in sea water, exposed outdoors and within a building envelope. Figure 1 shows the type of predictions that are made with the models developed.

(a) Attack by decay fungi, marine borers and corrosion

(b) Attack by termites
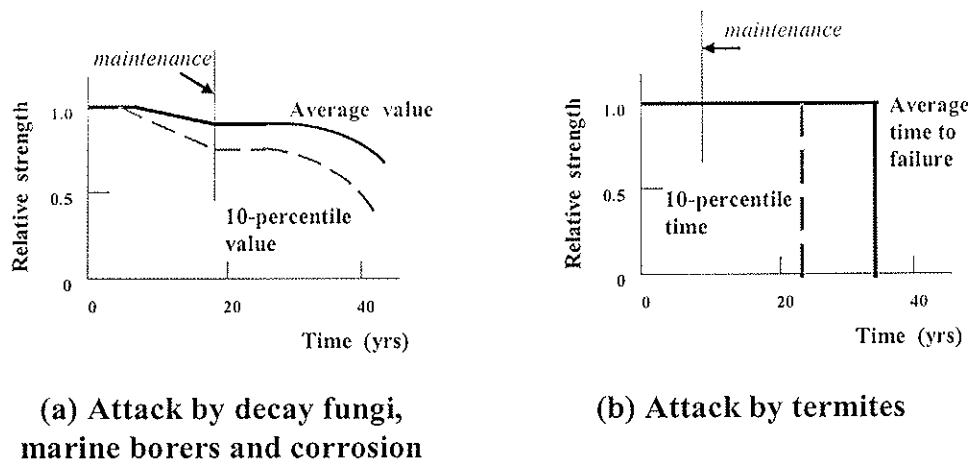
Figure 1. Examples of performance predictions.

The final outcomes of the project will include user-friendly software and a draft engineering design code. It is the purpose of this paper to discuss the process of developing design rules for the code. The concepts proposed for this procedure are simple, but they are complex to apply [10].

The proposed format for the design load capacity M_{design} is given by

$$M_{design} = k_{durability} \, M_o \qquad (1)$$

where M_o is the design capacity specified in the Australian Standard AS 1720.1 [12] when durability considerations are ignored, and $k_{durability}$ is a factor to account for durability effects.

M_{design} will be evaluated from

$$M_{design} = 0.9 \, M_{mean} \, \exp(-0.6 \, \beta \, V_M) \qquad (2)$$

Where M_{mean} and V_M are the mean value and coefficient of the load capacity M, and β is a safety index. The use of equation (2) has been discussed in a previous paper Leicester [3] and is derived from the discussion by Ravindra and Galambos [1].

The coefficient of variation V_M is obtained from

$$V_M^2 = V_o^2 + V_{durability}^2 \qquad (3)$$

where V_o and $V_{durability}$ denote the coefficients of variation of M_o and $k_{durability}$ mentioned in equation (1).

An idealised application of this procedure has been given in a previous paper [4].

The term $V_{durability}^2$ may be taken to be given by

$$V_{durability}^2 = V_{model}^2 + V_{env}^2 + V_{pattern}^2 + V_{rate}^2 \qquad (4)$$

where $V_{model}^2, V_{env}^2, V_{pattern}^2$ and V_{rate}^2 are coefficients of variation related to the uncertainty in modelling, the structural environment, the attack pattern and the attack rate respectively.

The difficulty in applying these probabilistic concept lies in the complexity of durability phenomena and the variety of sources from which data has been obtained. The following is a discussion on these matters.

2. Models

A list of the durability models developed are shown in Table 1. Details of the models used currently exist in laboratory reports, available on request, and some have been published in conference and workshop proceedings [5,6,7,8,9].

Table 1. List of models

Attack mechanism	Environment
Decay fungi	In-ground Exposed Building envelope
Termites	Building envelope
Marine borers	Coastal waters
Corrosion	Exposed Building envelope

Climate factors required for the modelling include rainfall, temperature, relative humidity, wind speed and direction, solar radiation, sea-state activity, sea-water temperature and salinity. Information on distance from the coast and sources of industrial pollution are also required. Combining this data with factors related to structure location, shelter effects, and details of building construction, procedures were developed to predict significant local attack parameters such as of surface wetness, rainfall penetration, wood timber moisture content and airborne salt. Elements of the building envelope investigated are shown in Figure 2a.

(a) Basic elements

(b) Shelter from the rain, sun and wind

(c) Mode of rainwater penetration
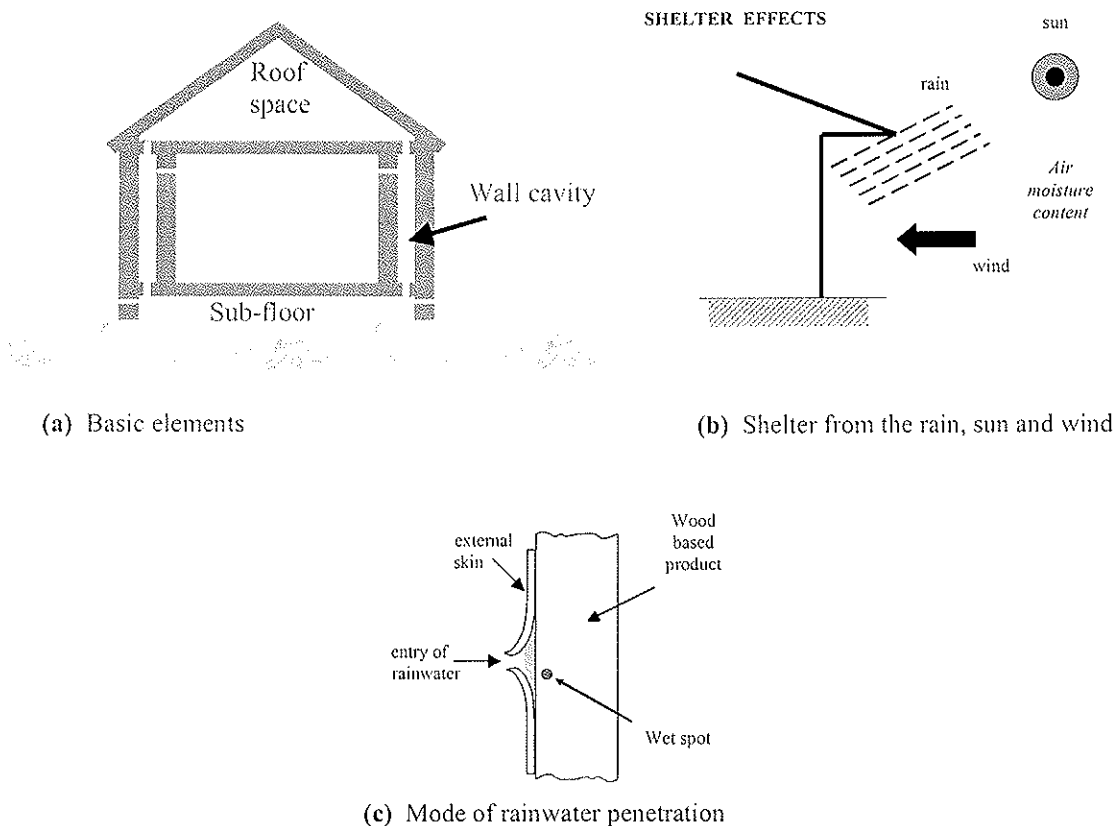
Figure 2. The building envelope.

3

3. Data Sources

Within the time frame allocated for the project, it was not feasible to set up long term experiments and so it was necessary to make use of existing data. The sources of this data were as follows:

- Fundamental building physics and biology, and laboratory studies
- Field tests of small clear specimens
- Field tests of full size structural members
- In-service structures
- Expert opinion

The use of this data will be discussed in the following sections. A summary of the number of samples obtained from the field data is given in Table 2. As far as possible, the locations of the field data sources were chosen so as to cover the climate range of Australia, Figure 3.

Table 2. Summary of the sources of data

Investigation	Number of data items		In-service studies
	Field studies		
	Small clears	Full size	
In-ground decay	5000	60	230
Exposed decay	4000	-	1800
Marine borer attack	2600	-	4500
Termite attack	-	-	5000*
Corrosion	700	-	20
Building microclimate	-	1	44*
number of houses			

(a) In-ground stakes   (b) Exposed L-joints and panels
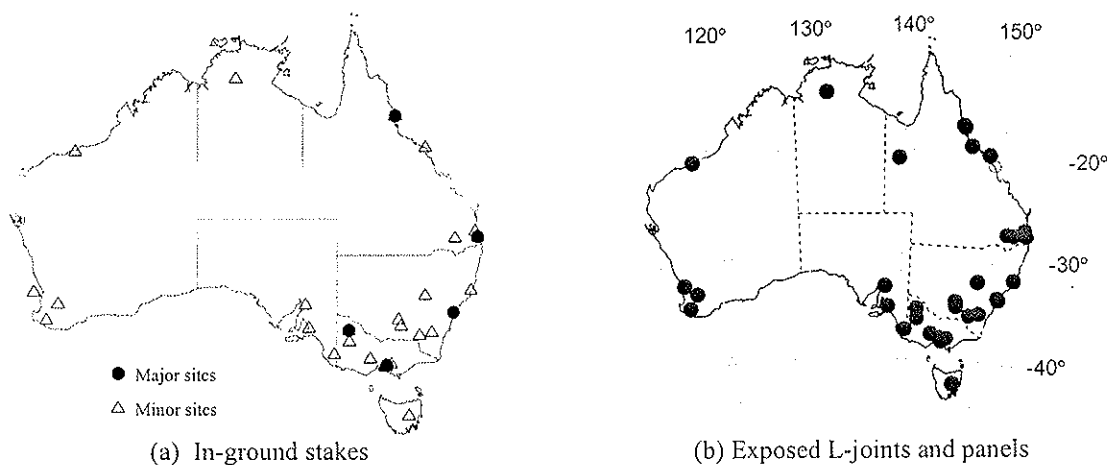
Figure 3. Examples of locations of test sites.

4. Basic Physics and Biology

Basic physics [1,2,13,14], was used to develop models for building microclimate, soil moisture and shelter effects. In modelling the effects of shelter, Figure 2(b), it was found necessary to use relatively sophisticated assessments of raindrop size, surface sorption and solar radiation models. Basic physics has also been used to assess the time of moisture content exceeding 30%, such as that in a building envelope as shown in Figure 2(c).

As an example of the use of basic biology, Figure 5 shows a method of using the mean value of data scatter to force-fit a relationship that has a form in accordance with the expectations of biological decay [15].

| (a) individual sites | (b) average for all sites |
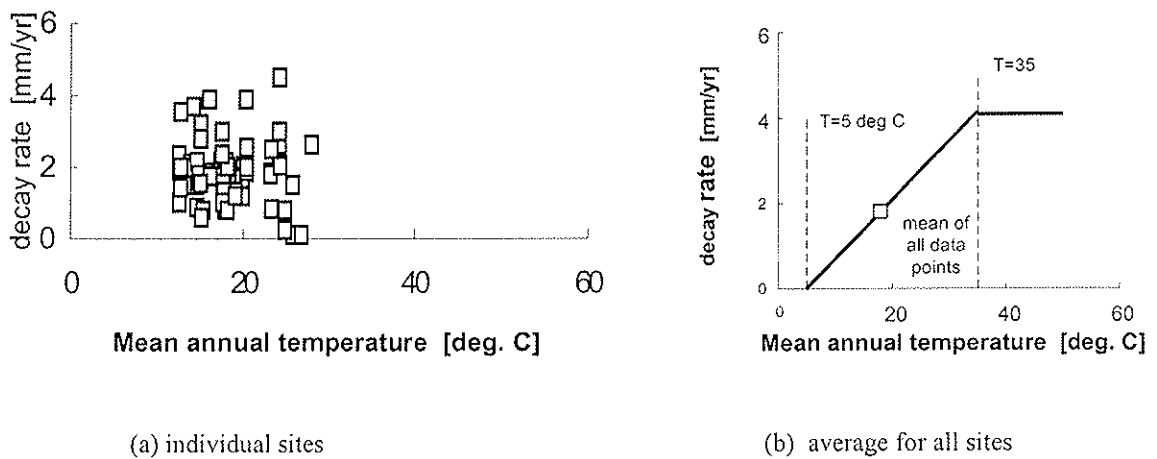
Figure 4. Measured rates of decay for exposed timber.

5. Field Studies Using Small Clear Specimens

Examples of specimens used to obtain small clears data are shown in Figure 5. These were placed around Australia as indicated in Figure 3. The duration of the field tests at the time of this project were about 31 years for in-ground wood stakes, 11 years for exposed wood L-joints and panels, 4 years for panels in sea-water and 2 years for metal coupons.

About 80 species of timber were studied and the climate of the test locations ranged from tropical to cool temperate. A typical example of measured data is shown in Figure 6(a). For practical purposes, it was decided to group the timber into four durability classes and to group the climate classifications into a few zones. In addition, the decay was idealised so that it could be described in terms of a single parameter as shown in Figure 67(b). The field studies using small clears have provided good value for the project.
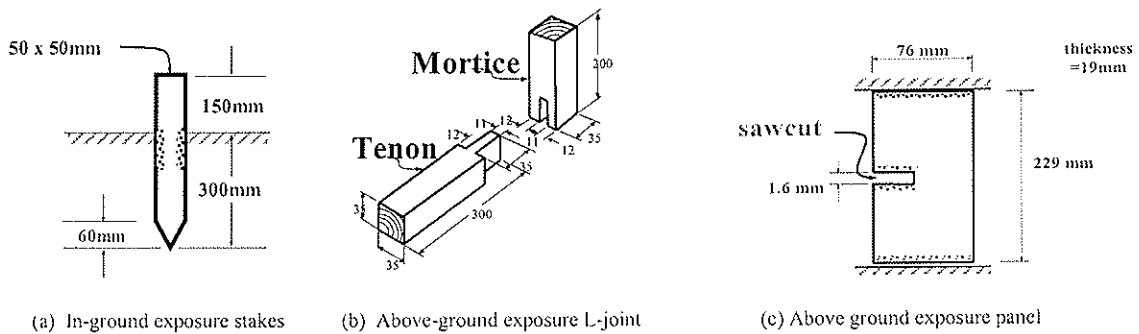
(a) In-ground exposure stakes   (b) Above-ground exposure L-joint   (c) Above ground exposure panel

Figure 5. Examples of standard test specimens for assessing the durability of timber.
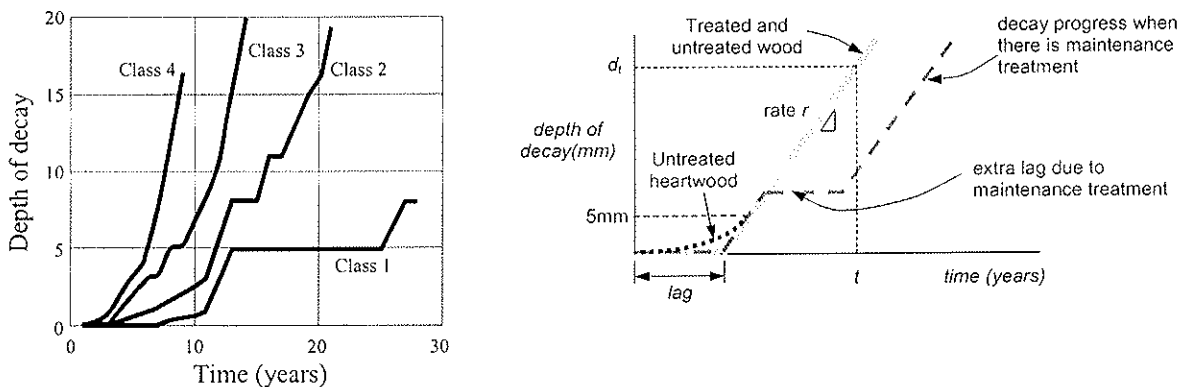
(a) Measured 50-percentile values of
    decay of untreated in-ground stakes
    at Sydney; Classes 1–4 refer to
    durability classes

(b) The idealised decay relationship

Figure 6. Decay of in-ground stakes

6. Field Studies Using Full Size Specimens

There is always some question as to how the data from small clear specimens should be used to assess the performance of full size timber members. For a start, it is uncertain as to whether decay in a full size member should be considered as the average of several stakes or as a weakest-link phenomenon. For the case of preservative treated round poles it was found that the performance of the outer perimeter was considerably better than would have been predicted by small clear specimens and in fact even the performance of untreated inner core wood appeared to be improved.

Study of full size timber is also essential to discover the attack pattern. As an example, Figure 7 shows idealised attack patterns to be found in in-ground rectangular sections.

(a) untreated hardwood, $D \leq 150$mm   (b) untreated hardwood, $D \geq 150$mm   (c) treated softwood

☐ Sound wood   ☐ Decayed wood
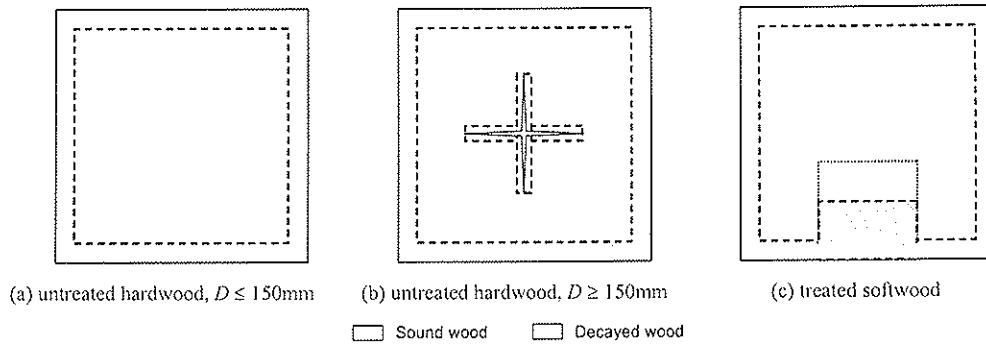
Figure 7. Typical in-ground decay patterns of square section timber

7.   In-Service Structures

An example of data obtained from in-service structures is shown in Figure 8. The data from such structures is essential for calibrating the prediction models. Unfortunately, not only is it expensive to obtain such data, but complete data sets that include all the requisite parameters such as in-service life, timber species, treatment, maintenance etc are not usually available.
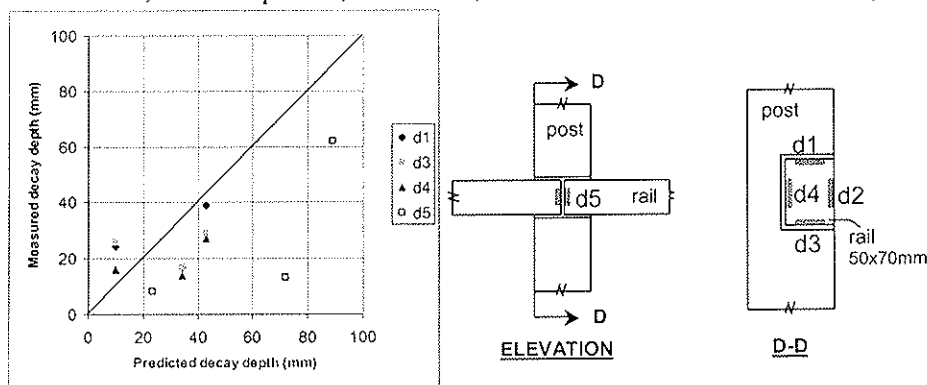
Figure 8. Data from in-service timber fences, Melbourne, Australia.

8.   Expert Opinion

A useful procedure was developed for capturing expert opinion in quantified form. As an example, consider the derivation of a model to predict the time t for a termite to travel 20 m to a house. The expert is first asked to identify the important parameters for this prediction. He is also asked to state the importance of the influence of these parameters. Each parameter is then subdivided in a number of (descriptive) classes that range from the smallest to the greatest hazard situation. For the case of three parameters and five classes, the estimate of time t is taken to be given by

$$t = A(1 + k_a\, I_a j)\,(1 + k_b\, I_b j)\,(1 + k_c\, I_c j) \tag{5}$$

7

where the subscripts a, b and c refer to the three parameters , I is the importance rating of the parameter, j is tied to the assessment attitude of the expert, k takes on the value 2, 1, 0, -1, -2 depending on the hazard class and A is a random variable.

If the expert is asked to make an estimate of the typical (or mean value of) t for two scenarios, usually with all $k = 2$ and all $k = -2$, then equation (5) can be used to provide A_{mean} and j and a prediction of t_{mean} will be possible for any input values of k. If in addition, the expert is willing to give an estimate of t_{min}, the fastest time for t, and assuming that these are one standard derivation from the mean values, then a coefficient of variation cov(A) can be deduced.

The advantage of the above procedure is that the expert need only make quantitative guesstimates for two particular cases for which he has had experience or for which case study data is available.

An obvious use of experts is to have them operate the prediction software and then to let it be known where modifications are required so that the software predictions conform with their experience. An example that occurred was for a recommendation for changes to be made to the climate zone map for in-ground decay as illustrated in Figure 9.

(a) hazard map based on meteorological information

(b) map with decay hazard zones modified according to expert opinion
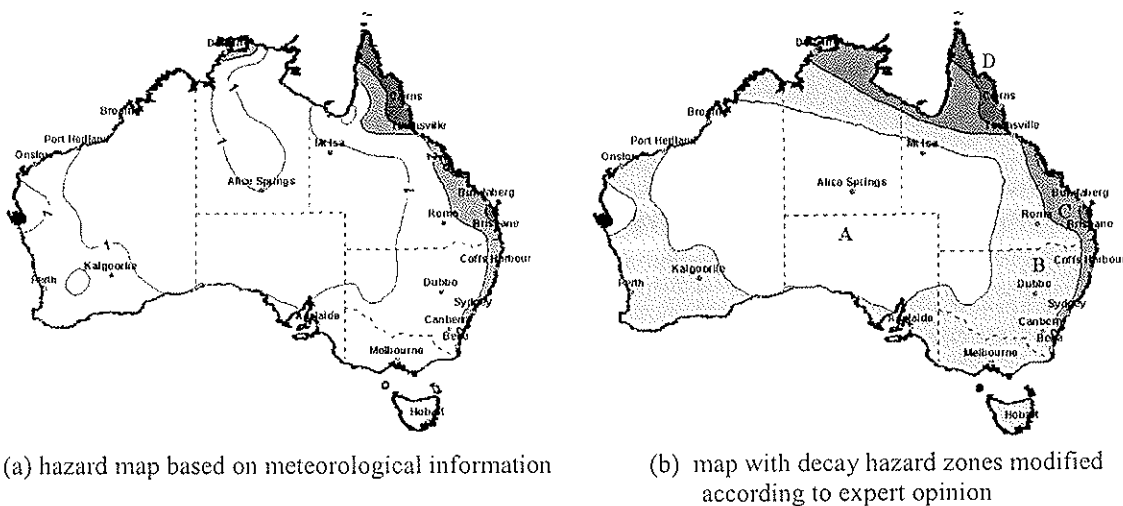
Figure 9. Hazard maps for in-ground decay of timber (zone D is the zone of highest risk).

9. Conclusion

There are several reasons as to why the formal application of Bayesian procedures is not suitable for application to the durability model. One reason is that the models are highly nonlinear and complex. Another reason is that the in-service data required for use in such a procedure is usually not completely defined.

The current procedure is to use an "evidence-based" approach, i.e. to ensure that the models comply with all the data sources mentioned including that of expert opinion. Another possibility is to develop models that focus on high risk performance rather than mean values.

The suitable choice of a reliability index β to be used in equation (2) is an interesting topic for investigation.

10. Acknowledgments

11. References

[1] American Society of Heating, Refrigeration and Air-Conditioning Engineers Inc (2005). *Fundamentals*. ASHRAE Handbook, Atlanta, GA.

[2] Jury, W.A. and Horton, R. (2004). *Soil Physics*. Sixth Edition, John Wiley & Sons Inc, New Jersey, 370 pages.

[3] Leicester, R.H. (1987). Load factors for proof and prototype testing. *Proc. 1st National Structural Engineering Conference*, Institution of Engineers, Melbourne, Australia, August, 2, 546–550.

[4] Leicester, R.H., Wang, C-H. and Foliente, G.C. (2001). A probabilistic decay attack model of timber in-ground. *Proc. ICOSSAR 8th International Conference of Structural Safety & Reliability*, Newport Beach, CA.

[5] Leicester, R.H. (2001). Engineered durability for timber construction. *Progress in Structural Engineering & Materials*, 2(3), 1–12.

[6] Leicester, R.H., Wang, C-H, Nguyen, M.N., Thornton, J.D., Johnson, G., Gardner, D., Foliente, G.C., MacKenzie, C. (2003). An engineering model for the decay of timber in-Ground contact". *The 34th Annual Conference of the International Research Group on Wood Preservation (IRG)*, Brisbane, Australia, May 2003.

[7] Leicester, R.H., Foliente, G.C., Wang, C-H., Nguyen, M., Wang, X, MacKenzie, C., Thornton, J.B. and Cause, M. (2004). Structural durability of exposed timber. *Proc. Woodframe Housing Durability and Disaster Issues*, Forest Products Society, Las Vegas, USA, 4–6 October, 277–283.

[8] Leicester, R.H., Wang, C-H., and Cookson, L. (2004). A probabilistic model for termite attack on housing in Australia. *Proc. Woodframe Housing Durability and Disaster Issues*, Forest Products Society, Las Vegas, USA, 4–6 October, 169–182.

[9] Leicester, R.H., Ganther, W., Seath, C.A., Wang, C-H., Nguyen, M., Foliente, G.C., Cole, I. and MacKenzie, C. (2004). Australian houses: Monitoring and predicting microclimate and the durability of the building envelope. *Proc. Woodframe Housing Durability and Disaster Issues*, Forest Products Society, Las Vegas, USA, 4–6 October, 9–18.

[10] Leicester, R.H., Foliente, G.C., Wang, C-H., Nguyen, M and Cookson, L. (2004). Modelling the uncertainty of biological attacks on timber construction. *Proc. Risk 2004 Engineering Conference, Risk 2004*, Risk engineering Society, Engineers Australia, Melbourne, 8–9 November, Paper 228.

[11] Ravindra, M.K. and Galambos, T.V. (1978). Load resistance factor design for steel. *Journal of the Structural Division, Proc. ASCE 104*, ST9, September, 1331–1354.

[12] Standards Australia (1997). AS 1720.1: Australian Standard – Timber Structures – Part 1: Design Methods. Standards Australia, Sydney, 181 pages.

[13] Trechsel, H.R. (ed.) (1997). *Moisture Control in Buildings*. ASTM MNL 18, PA, 485 pages.

[14] Trechsel, H.R. (ed.) (2001). *Moisture Analysis and Condensation Control in Building Envelopes*. ASTM MNL 40, PA, 192 pages.

[15] Zabel, R.A. and Morrell, J.J. (1992). *Wood Microbiology–Decay and Its Prevention*. Academic Press Inc, New York, 476 pages.

INTERNATIONAL COUNCIL FOR RESEARCH AND INNOVATION
IN BUILDING AND CONSTRUCTION

WORKING COMMISSION W18 - TIMBER STRUCTURES

CONSIDERATION OF MOISTURE EXPOSURE OF TIMBER STRUCTURES AS AN ACTION

.

M Häglund

S Thelandersson

Division of Structural Engineering

Lund University

SWEDEN

Presented by S Thelandersson

A Ranta-Maunus commented that the model to moisture load on structure in future is important. For example dry period followed by wet period will be important to consider moisture load. J W van de Kuilen commented that their data agree with the Swedish findings and this is a good start. S Thelandersson responded that building physicists think that this is too simple as microclimatic condition rather than the macroclimatic conditions is important. The building physicists' approach is too complicated. A Ceccotti stated that this work is very important. The 5% mc change is a compromise to calculate the consequence. If 20% is used then every timber member may crack. Creep and mechano-sorptive effects are good things in this case as it can relax the stress built up in timber. J Köhler and S Thelandersson initiated a discussion on how to integrate the moisture load model in design with respect to load duration. V Rajcic asked how to introduce the concept in code? S Thelandersson responded that it would be nice to treat this from the external load perspective. Curved beams and notched beams cases are particularly influenced by mc. Reduced strength is also an option. A Ranta-Maunus stated that it is more important to consider moisture as a load otherwise the strength may be zero. A Jorissen commented that the effect of this may be more on the serviceability rather than strength issue.

Consideration of moisture exposure of timber structures as an action

Martin Häglund, Sven Thelandersson
Division of Structural Engineering, Lund University, Sweden

1. Introduction

Moisture exposure is a very significant factor for serviceability as well as load bearing capacity of structural timber elements and systems. Not only the moisture content level but also the variation of the moisture content is of great importance for the performance of timber structures and engineering wood products. One critical factor is varying relative humidity in the ambient air, and thus non-uniform moisture content in wood cross sections. External and internal restraint of hygro-expansion will then create stresses mainly perpendicular to grain. Such stresses may cause cracks, reducing the load bearing capacity of the individual timber element and thus the whole structure (see e.g. Gustafsson et al (1998) and Morlier & Ranta-Maunus (1998) concerning the significance of perpendicular to grain stresses and related failure modes). Experiments performed on glulam subject to natural sheltered outdoor climate conditions have shown that climate variations can induce significantly high stresses (in addition to stresses from applied loads) in the range of two thirds of the characteristic strength value (Aicher et al 1997), or even higher (Jönsson 2004).

Determination of moisture content profiles due to natural moisture content variations is hence important in order to better understand and quantify how these variations affect timber. Today's design codes use service classes to account for moisture induced effects, but since the class selection is only based on anticipated equilibrium levels, the nature of timber exposed to moisture is not fully reflected. In order to improve design codes, it has been proposed that instead of using strength reduction factors, induced moisture stresses may be treated as an ordinary design load to be combined with effects from other loads (for example snow and wind load). This is also discussed and suggested in Ranta-Maunus (2003). For this purpose, a moisture exposure model that reflects the nature of the variations—the dynamics—of moisture in the ambient air is desired. The model should also include temperature, since this is needed for conversion of outdoor moisture levels to corresponding indoor levels. Moisture transport in wood can be modelled as a diffusion process to describe how penetration effects depend on temporal variation in relative humidity, RH. For example, Arfvidsson (1998) showed that the penetration depth (here defined as the depth where RH differs 1%) in the tangential direction for a semi-infinite solid spruce element exposed to diurnal, rectangular cycling between 50% and 95% RH is about 10 mm, whereas an annual cycling increased the penetration depth approximately ten times. The exact figures are of course highly dependent on what moisture transport model being used and its related parameters, but it demonstrates the transient properties of wood. In reality, however, the relative humidity varies irregularly with occasional large differences in magnitude from day to day.

In this paper, a general and possible approach to describe moisture exposure based on real recorded data is proposed. Specifically, the methodology is applied for climate data at two locations in Sweden, Stockholm and Sturup in southern Sweden. Moisture distributions in both time and space are calculated with a 2-D finite element program. Selected results on the

response of timber subject to naturally varying climate at different climatic locations are presented. The obtained results may be used as a basis for code specification of moisture effects with targeted reliability levels.

2. Modelling of climate exposure

Time series representing instant values of temperature, T, and relative humidity, RH, at geographically different locations in Sweden were obtained from the Swedish Meteorological and Hydrological Institute (SMHI). The data record encompassed approximately 25 to 40 consecutive years starting in the beginning of the 60s with observation intervals between 3 and 12 hours depending on location. The raw data were transformed to time series of daily averages of T and RH. One reason for this is that the hygroscopic response of timber is highly time dependent and thus fast changes (e.g. hourly) will hardly affect wood products with dimensions used in practice. Locations Stockholm and Sturup are addressed in this paper.

Modelling of moisture exposure generally involves temperature, relative humidity and vapour concentration. Since the vapour concentration was not given in the time series, it must be calculated from

$$v = \varphi v_{sat}(T),$$

Eq. (1)

where v is the vapour concentration, φ is the relative humidity and $v_{sat} = v_{sat}(T)$ is the vapour concentration at saturation point. v_{sat} changes with temperature T according to a physically determined relation. The three above-mentioned quantities, i.e., temperature, relative humidity and vapour concentration, are stochastic processes with random patterns as illustrated for Stockholm from 1981 to 1984 in Fig. 1 (left plots). A simple model could be obtained by randomly selecting e.g. temperatures and vapour concentrations from the measured empirical distributions. This approach, however, does not take into account the persistence of the climate, or the correlation between the stochastic variables. Instead, by using time series analysis, it is possible to model the characteristics of the recorded observations in a more adequate way. One general and frequently used process is the linear ARMA(p,q) process, where ARMA stands for Auto Regressive Moving Average. The process can also be extended with an external part, as shown in Eq. (2), in order to consider influence from other quantities. It is then called an ARMAX(p,r,q) process.

$$\underbrace{y(t) + \sum_{i=1}^{p} a_i y(t-i)}_{\text{AR part}} = \underbrace{\sum_{i=0}^{r-1} b_i u(t-i)}_{\text{external input}} + \underbrace{\sum_{i=1}^{q} c_i e(t-i) + e(t)}_{\text{MA part}}.$$

Eq. (2)

$y(t)$ is the modeled quantity e.g. temperature, $u(t)$ is the external input and $e(t)$ represents the innovations which are assumed to be white noise and uncorrelated with past values $y(t-1)$, $y(t-2)$, $y(t-3)$... etc; t is discrete and represents days; a_i, b_i and c_i are constants. A more detailed and general introduction to time series analysis can be found in e.g. Olbjer et al (2002) and Brockwell and Davis (1996).

To simulate the climate as an ARMAX process the original time series has to be decomposed into seasonal variations and random variations, according to

$$y(t) = F(y^{\circ}(t)) - d(t)$$

Eq. (3)

where $y(t)$ is the obtained stationary process, $y^{\circ}(t)$ is the original time series, F is a suitable transformation function considering varying variance, and $d(t)$ is a deterministic function describing seasonal variations of $F(y^{\circ})$. By visual inspection, the temperature and the vapour
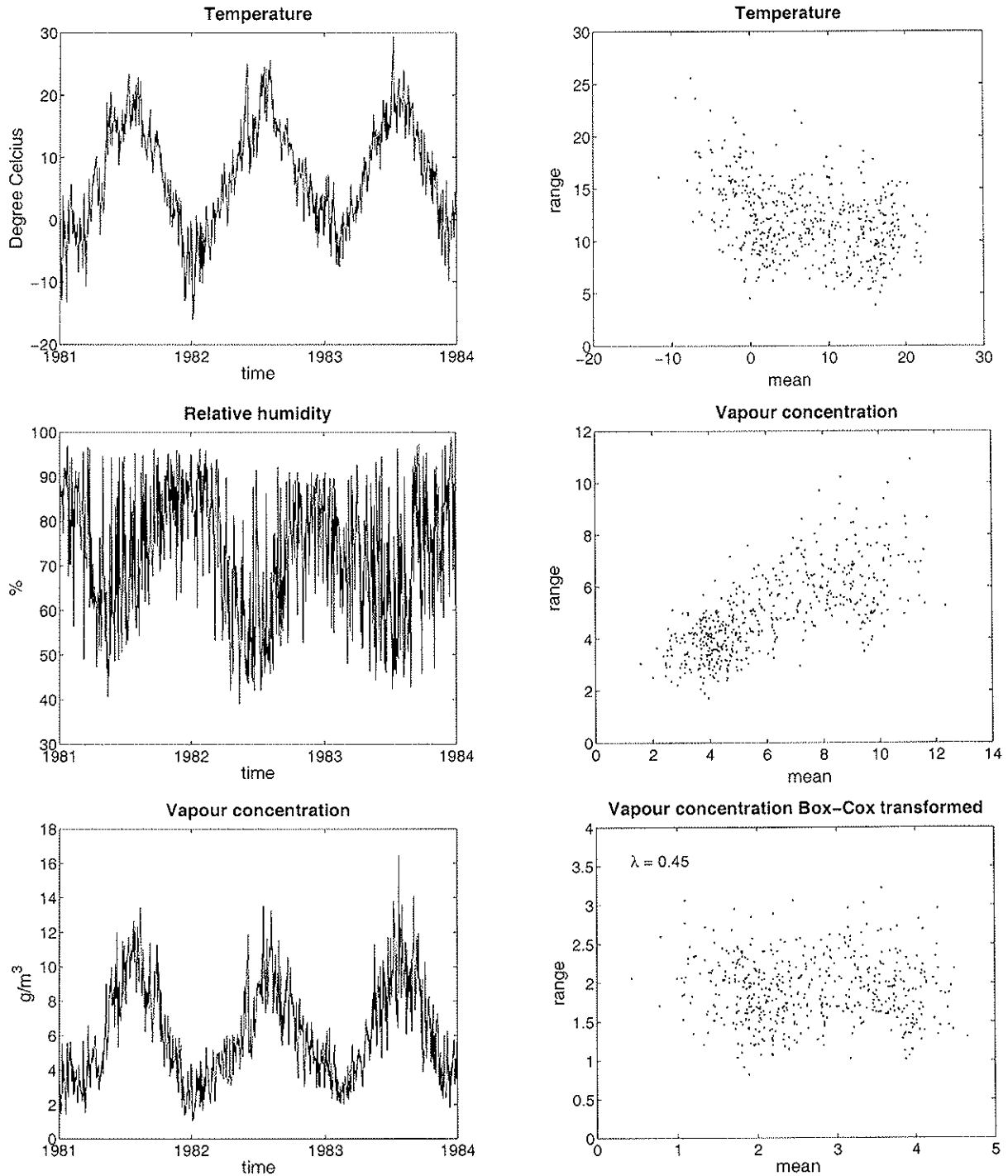
Fig. 1. A sample of the time series from Stockholm (left plots) and range-mean plots for the temperature and the vapour concentration (right plots).

concentration seemed to be the best candidates to model; the relative humidity displays changes that are more irregular and is also bounded by the interval 0 to 100 %. The decomposition was done in two steps. First, by making range-mean plots for intervals of 30 days for temperature and vapour concentration (shown in Fig. 1, right plots), it was found that the variance is fairly constant for temperature as a function of mean temperature, but not for vapour concentration (the range represents the difference of max and min during a period). This problem, however, was circumvented through a so called Box-Cox transformation, see Eq. (4), where F is used to indicate the connection to Eq. (3). This transformation produces

uniform variance and λ=0.45 was found to give a good result. Secondly, the seasonal variations were removed by fitting a periodic function described by Eq. (5). The assumed result of the transformation is a zero-mean, stationary time series.

$$F(y^\circ) = ((y^\circ)^\lambda - 1)/\lambda; \quad \lambda \neq 0,$$

Eq. (4)

$$d(t) = C_0 + C_1 \cos(2\pi t / \tau) + C_2 \sin(2\pi t / \tau),$$

Eq. (5)

where C_0, C_1 and C_2 are constants and the period τ = 365.25 days (considering leap year).

A more detailed description of the time series modelling and the methods used to identify the parameters in Eqs. (2), (4) and (5) can be found in Häglund et al (2005).

3. Modelling of moisture transfer in wood cross sections

Moisture transport in wood is commonly described by a diffusion process that, even though it is not capable of in detail describing the complex internal moisture transport in wood, is used for engineering purposes and found to produce reasonably accurate results below the fibre saturation point. By Fick's first law the moisture flow vector $\mathbf{q}$ [kg/(m^{2}s)] is expressed as

$$\mathbf{q} = -D_\phi grad\,\phi$$

Eq. (6)

for any chosen moisture state variable ϕ, e.g. relative humidity φ [%] or moisture content w [kg/m^3], with corresponding diffusion coefficient $D_\phi = D_\phi(\phi)$. Although wood as a material is neither perfectly homogeneous, nor isotropic, it is rational to treat it as isotropic in the transversal directions. Experiments on Nordic softwood have shown that the diffusion coefficients are practically the same in the tangential and the radial direction (Rosenkilde and Arfvidsson 1997, Hedenblad 1996). This is also commented by Hukka (1999). (Note that the moisture transport in the longitudinal direction is very different.) Under assumption of flow continuity and no internal moisture production, the continuity equation for an isotropic material in two dimensions can be expressed as

$$\frac{\partial w}{\partial t} = \frac{\partial}{\partial x}\left(D_\phi \frac{\partial \phi}{\partial x}\right) + \frac{\partial}{\partial y}\left(D_\phi \frac{\partial \phi}{\partial y}\right)$$

Eq. (7)

for Cartesian principal axes x and y and where w is the moisture content and t is time. It would be convenient to use $\phi = \varphi$ since the boundary conditions are based on varying RH. Nevertheless, because the diffusion coefficient curve for RH typically is very steep near 100%, numerical problems may occur and affect the solution. The moisture state parameter used here is the so called Kirchhoff potential, ψ [kg/(m·s)], defined as

$$\psi = \int_{\phi_{ref}}^{\phi} D_\phi(\phi)d\phi$$

Eq. (8)
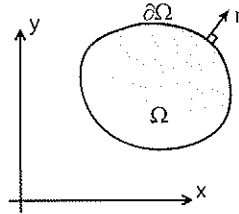
where ϕ_{ref} represents a reference moisture state which can be chosen arbitrarily and be expressed in any moisture state parameter. Eq. (7) can then be written as

$$\frac{\partial w}{\partial t} = \frac{\partial w}{\partial \psi}\frac{\partial \psi}{\partial t} = C_\psi(\psi)\frac{\partial \psi}{\partial t} = \frac{\partial^2 \psi}{\partial x^2} + \frac{\partial^2 \psi}{\partial y^2}$$

Eq. (9)

since from Eq. (8) $D_w = d\psi / dw$ (for $\phi = w$) and thus $D_\psi = 1$; $C_\psi(\psi)$ [s/m^2] is known as the moisture capacity. Further explanation and details on the Kirchhoff potential can be found in e.g. Arfvidsson (1998) and Claesson (1997). In addition to the internal moisture transport,

there is a resistance against moisture transport at the surface between air and the wood material. For a 2-dimensional diffusion problem, the governing equations may be expressed as

$$C_\psi(\psi)\frac{\partial\psi}{\partial t} - \left(\frac{\partial^2\psi}{\partial x^2} + \frac{\partial^2\psi}{\partial y^2}\right) = 0 \quad \text{in the domain } \Omega$$

$$\mathbf{q}_n = \beta_\psi(\psi_s - \psi_{eq}) \qquad \text{on the boundary } \partial\Omega \qquad\qquad \text{Eq. (10a-b)}$$

where $\mathbf{q}_n$ is the moisture flux normal to the surface [kg/(m^{2}s)], $\beta_\psi = \beta_\psi(\psi)$ is the mass transfer coefficient, and ψ_s and ψ_{eq} are the Kirchhoff potentials at the surface and at equilibrium in the ambient air, respectively. Once boundary conditions are specified, ψ can be solved using a finite element program. Moreover, because a cross-section of a rectangular beam is double symmetric, it is only necessary to model one quarter of the section and thus save both calculation time and memory usage. An illustration of the procedure is shown below in Fig. 2 together with a 2D FEM model.

beam   cross-section   model after using symmetry   mesh grid
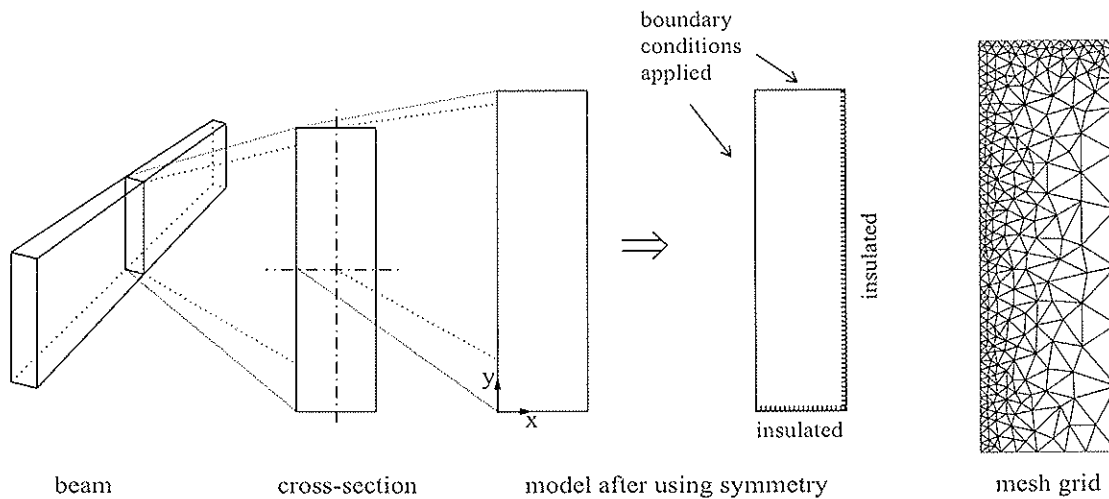
Fig. 2. Illustration showing usage of a doubly symmetric beam cross-section together with applied mesh grid for the upper right quarter of a glulam beam. The mesh is finer at the non-insulated boundaries in order to prevent numerical errors and convergence problems due to steep moisture gradients near the surface.

The calculations were run on Femlab, a commercial multi-physics finite element program, using triangular Lagrange elements (quadratic with 6 nodes). The initial moisture content was set to the average of the boundary conditions over the calculation time.

Material data were obtained from measurements presented in Hedenblad (1996). Relations between RH and the Kirchhoff potential ψ as well as RH and moisture content w [kg/m^3] were determined for spruce from southern Sweden under absorption at a temperature around 20°C. The radial moisture transport properties were approximately the same as the tangential ones. The obtained data is shown in Fig. 3, where the circles represent digitized points from hardcopy figures and the lines fitted polynomials. Since the Kirchhoff potential only was presented for RH levels above 35%, it was assumed that the curve could be approximately linearly extrapolated down to 0% (Arfvidsson, 2004). Possible hysteresis effects are neglected, i.e. the w vs. RH curve represents the average of the desorption and absorption

curves. The moisture capacity $C_\psi(\psi)$ was determined on the basis of the measured relations $w = w(\phi)$ and $\psi = \psi(\phi)$.
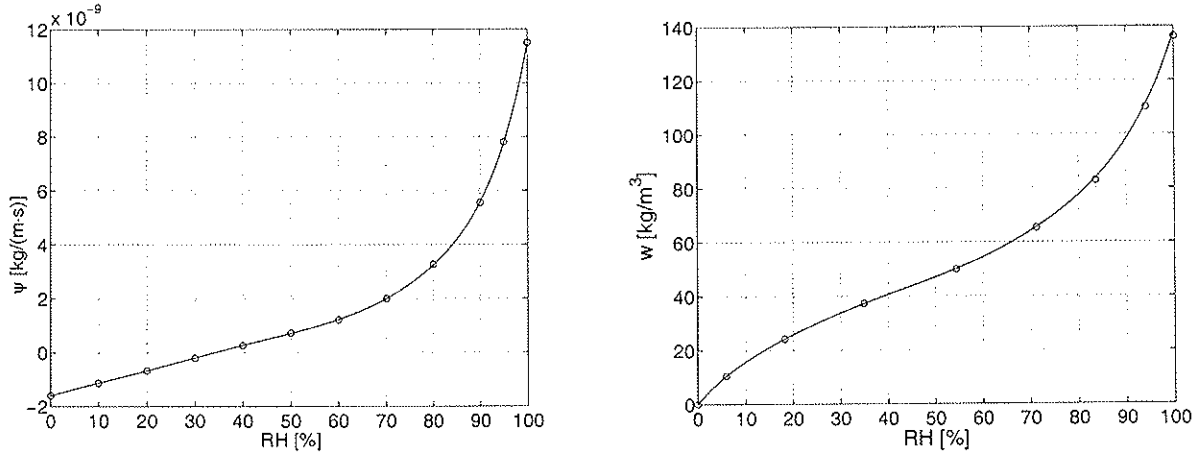
Fig. 3. Relations between RH, moisture content and the Kirchhoff potential for spruce in the tangential direction. Circles ('o') represent digitized points from hardcopy figures; lines are fitted polynomial functions.

4. Results from simulations of moisture action

The stochastic process model for temperature and vapour concentration described in section 2 was used to simulate the annual maxima for relevant climatic parameters for the south Swedish location, Sturup. Simulations were made for a 1000 year sequence and cumulative distributions (CDF) for annual maximum and minimum values are shown in Fig. 4. Figure 4a shows CDF:s for maximum and minimum of outdoor temperatures (daily averages). Corresponding CDF:s for outdoor relative humidity are shown in Fig. 4b, together with indoor values based on the somewhat unrealistic assumption that indoor and outdoor vapour concentrations are equal. This assumption implies that effects of indoor moisture production, air conditioning systems and micro climate effects are neglected, so that the indoor relative humidity ϕ_{indoor} can be determined as

$$\phi_{indoor} = min(v_{outdoor} / v_{sat}(20°C), 100\%) \qquad \text{Eq. (13)}$$

where $v_{outdoor}$ is the vapour concentration outdoors and $v_{sat}(20°C)$ is the saturation vapour concentration at 20 °C, which is the assumed indoor temperature.

The minimum indoor RH values obtained under this assumption are very low. It is seen that the average of annual minima is of the order 10 %. It is not realistic to assume that the indoor moisture production is zero at the same time as these extreme values occur. A more realistic estimate can be found if the increase in vapour concentration due to indoor moisture production is set to the representative value $3g/m^3$, Nevander & Elmarsson (1981). The CDF for indoor relative humidity under this assumption can also be seen in Fig. 4b, in comparison with the case where the indoor moisture production is zero. It is obvious that this effect is very significant.

a) b)
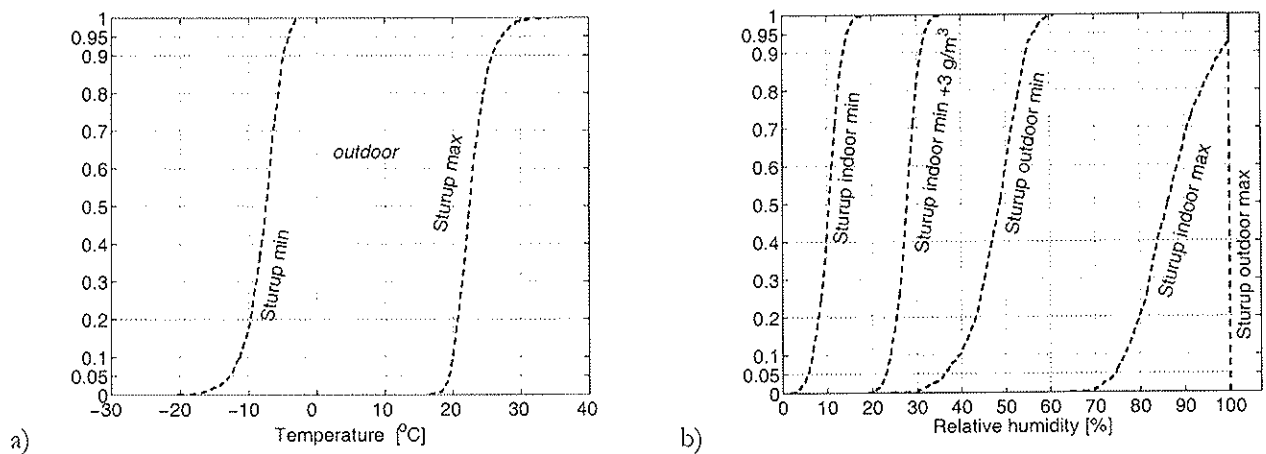
Fig. 4. Cumulative distribution functions (CDF) of annual minimum and maximum of temperature and relative humidity for Sturup. The added vapour concentration due to indoor moisture production is set to 3 g/m³.

To investigate if the stochastic process model gives reasonable results, the simulated relative humidities are compared with the distribution of annual minima for outdoor RH obtained from the original data. This is shown in Figure 5, where the original data from Stockholm is also displayed. It can be concluded that the stochastic process seem to represent the data in a reasonable way, although the results at the tails of the distribution might be uncertain.
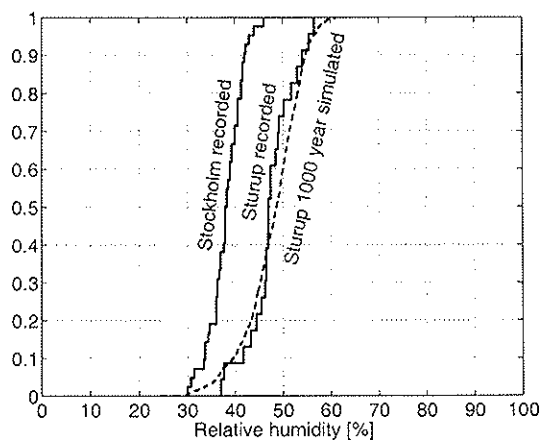
Fig. 5. CDFs of annual minimum of relative humidity based on original data from Stockholm and Sturup, and a 1000 year simulation sequence for Sturup.

From the results in Figs. 4 and 5, percentiles corresponding to return periods of 50 years and 5 years were estimated. These are shown in Table 1. Results for a 5 year return period are represented quite well by the model, whereas comparisons with the original data indicates that the data for 50 year return periods should be interpreted with care. The results represent daily average values. Wood panels and products with cross dimensions of the order 10 mm can be assumed to reach nearly equilibrium within the time span of one day when exposed from both sides. The corresponding moisture content levels in (kg/kg) which can be reached in wood products with small dimensions were derived for the different cases and are displayed in

Table 1. To estimate design moisture movements in wood it is of interest to estimate a design value of maximum variation in moisture content (MC). It is proposed here that this should be based 5 year return values since this information usually concerns the serviceability limit state. This moisture content range Δu (% by weight) for "daily average" values of MC is also displayed in Table 1. It is seen that Δu is of the order 20-25 %, which is much higher than expected. Surprisingly, the value is similar for outdoor (service class 3) and indoor conditions (service class 1).

Table 1. Moisture exposure characteristics for Sturup and Stockholm. Min and max represent annual values occurring in average every 50 years/5 years. Moisture content is based on assumed equilibrium with daily average RH. ($\rho_{dry} \approx 430$ kg/m³). v_{MP} is the increment in vapour concentration due to indoor moisture production (MP).

		Sturup				Stockholm
		Simulated as ARMAX process			Original data	Original data
		Outdoor	Indoor $v_{MP}=0$	indoor $v_{MP}=3$g/m³	Outdoor	Outdoor
Temperature [°C]	min	-15/-10	20.0/20.0		-20/-12	-24/-17
	max	29/25			25/24	29/26
Relative humidity [%]	min	33/43	4/8	22/26	37/44	30/36
	max	100/100	100/94.1	100/100	100/100	100/100
Moisture content [%] (equilibrium with daily average RH)	min	8/10	2/3	6/7	9/10	8/9
	max	32/32	32/26	32/32	32/32	32/32
Moisture content range Δu, 5 year return period, %		±22	±23	±25	±22	±23

5. Results from simulations of moisture distributions in timber cross section

For larger cross sections the variation in moisture content can be expected to be much lower due to the slow moisture response of the material. By diffusion calculations with natural moisture variations as input it is possible to determine and quantify for example moisture penetration and moisture gradients within timber elements. Results from calculations of penetration (based on outdoor RH time series from Stockholm) in a beam with cross section 90x270 mm for 3 and 43 years are shown in Figs. 6 and 7, respectively. The calculation was made under the assumption that surface resistance can be neglected, which is on the safe side regarding maximum moisture penetration. It is interesting to note the low-pass filter properties that timber elements hold. Rapid, daily changes are damped out fast, whereas annual variations have an evident penetrating effect. A closer inspection also reveals that the annual variations in the middle of the beam are phase-shifted as compared to variations at the surface (the boundary). This is best seen for the 3 year simulation (Fig. 6). Also note that the difference between the two lines indicating the extremes of the varying moisture profile
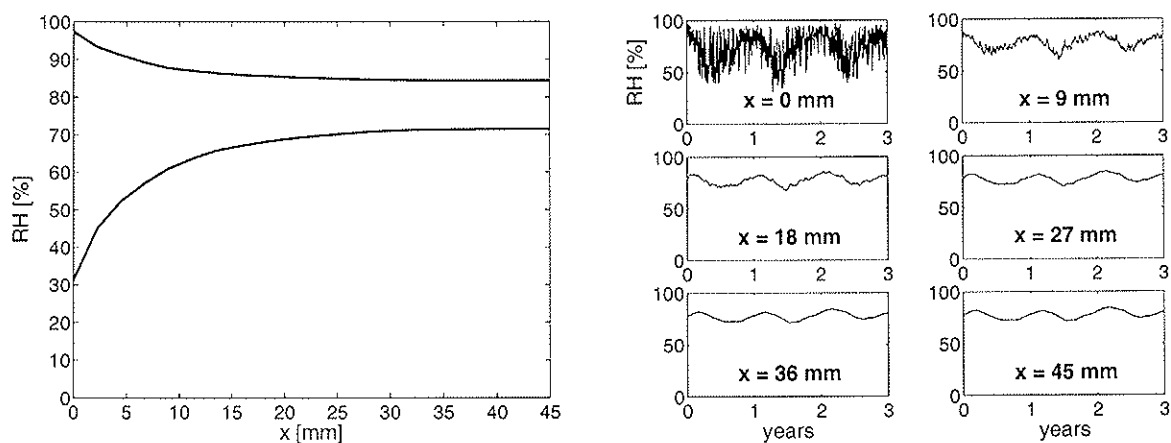
Fig. 6. Results from penetration depth calculations based on a 3 year long simulation sequence recorded in Stockholm (1961-1963). The left plot shows the extremes of the varying moisture profile, and the right plot shows the variation in time at different positions in the cross-section (position 'x' refers to the lower insulated boundary line shown in Fig. 2, i.e. x = 0 is in the lower left corner of the shaded quarter).
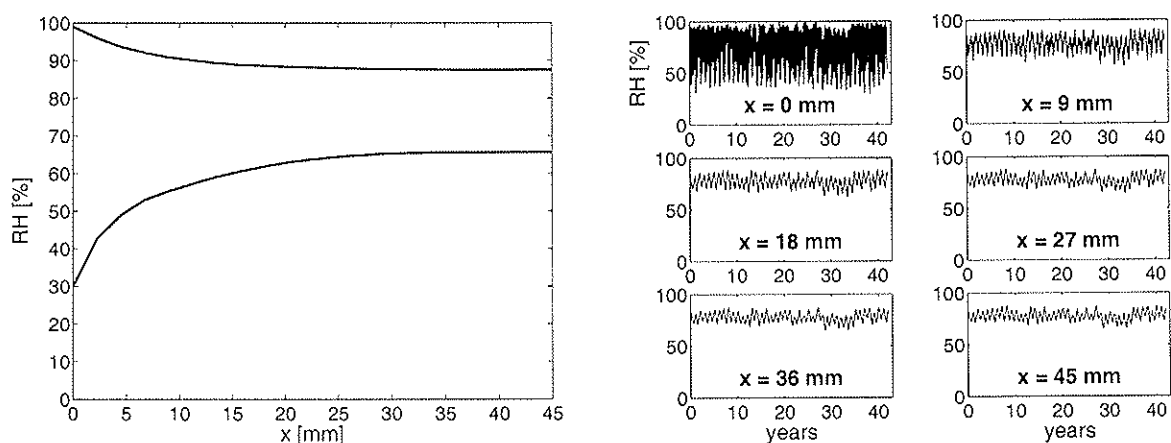
Fig. 7. Results from penetration depth calculations based on a 43 year long simulation sequence recorded in Stockholm (1961-2003). The left plot shows the extremes of the varying moisture profile, and the right plot shows the variation in time at different positions in the cross-section (position 'x' refers to the lower insulated boundary line shown in Fig. 2, i.e. x = 0 is in the lower left corner of the shaded quarter).

increases with the simulation time. This is reasonable since the longer the simulation sequences are, the higher the probability is for "extreme" boundary conditions to occur (for example several consecutive days with RH levels close to 100%).

The moisture content range Δu (in percentage units averaged over cross section) was calculated from the results in Figs. 6 and 7 to 7% and 10 % for simulations over 3 and 43 years respectively. This can be compared with recommendations given in the Swedish manual for glulam, Limträhandbok (2001), which states that Δu can be taken to 8-10 % for unprotected structures outdoor. This is in good accordance with the results obtained here. But the same source also states that for structures indoor as well as outdoor under shelter, Δu is in the interval 3-5 %. The results in the present paper indicate that this figure is too low. This will be further investigated in coming research, but it can already be estimated that the results

for indoor conditions can be expected to of the same order as for outdoor conditions, i.e. Δu= 7-10%. Note that Δu is the predicted difference between maximum and minimum MC, but that the time average of MC is significantly lower indoors than outdoors.

6. Discussion and conclusions

The results presented in this paper are part of an ongoing research, which has the goal to characterize moisture as an action on timber structures. The results so far indicate that it is possible to make statistical estimates of moisture effects in terms of annual extremes, from given input of recorded meteorological data. This is consistent with modern safety concepts. A time series methodology has been employed, by which synthetic sequences of temperature and relative humidity can be generated. Simulated sequences may be used for probabilistic investigations of the response of timber structures to varying climate, for refined definitions of service classes and for calibration of climate related factors in timber design codes.

The following conclusions can be made from the research so far

- Extreme values of relative humidity indoors (service class 1) seem to be more severe than is usually anticipated, which means that the risk for adverse effects of moisture exposure can be significantly higher than normally conceived in design.

- The moisture content variation (difference between maximum and minimum MC, defined as 5 year return value) is of the same order of magnitude for indoor conditions and for outdoor conditions.

- Very low humidity levels with high shrinkage can cause problems from the point of view of serviceability, especially for wood products and panels with small cross dimensions. This problem is seldom recognized in design.

- The stochastic process model developed can be used to simulate climatic exposure as sequences of daily averages. The prediction from this model of extreme values with return periods of the order 5 years seems to be reliable. For lower probabilities the values produced by the process model are uncertain.

- Considering moisture exposure on timber structures with normal dimensions, however, extreme values of daily average humidity will be damped out by the slow moisture transfer in wood. The stochastic process model can be expected to give reasonable results in such cases.

- For timber structures with larger dimensions, swift changes at the boundary are damped out fast and leave the inner parts of a cross section unaffected, whereas slow changes, as annual variations, affect the whole beam. Timber performs as a low-pass filter, allowing low frequencies to pass but filter out higher ones.

For handling of moisture effects in design of timber structures it is proposed that guidelines and principles are developed to determine consistent design values for

- Expected variation between maximum and minimum moisture content averaged over cross sections to be able to determine moisture movements with adequate reliability.

- Expected spatial variation of moisture content within cross sections to predict strength reduction due to moisture induced eigenstresses for failure modes perpendicular to grain.

References

Aicher S, Dill-Langer G. (1997). Climate induced stresses perpendicular to the grain in glulam. Otto Graf Journal, 8:209-227.

Arfvidsson, J. (1998). Moisture Transport in Porous Media. Report TVBH-1010 (Doctoral thesis), Div. of Building Physics, Lund University, Lund, Sweden.

Arfvidsson, J. (2004). Personal Communication. Lund, Sweden.

Brockwell PJ. and Richard A D. (1996). An introduction to time series and forecasting. New York: Springer.

Claesson J. Mathematical Modelling of Moisture Transport. COST Action E8, International Conference on Wood-Water Relations 1997.

Gustafsson PJ, Hoffmeyer P and Valentin G. (1998). DOL behaviour of end-notched-beams. Holz als Roh- und Werkstoff, 56:307-317.

Hedenblad, G. (1996). Material data for Moisture Transport Calculations, (in Swedish). T19:1996, ISBN 91-540-5766-3, Swedish Council for Building Research, Stockholm.

Hukka, A. (1999). Diffusion and Mass Transfer Coefficient of Nordic Softwoods. Holzforschung 53 No. 5 534-540.

Häglund M., Isaksson, T., Holst J. (2005). Time series modelling of moisture exposure on timber. Submitted to J. of Building and Environment.

Jönsson J. (2004). Internal stresses in the cross-grain direction in glulam induced by climate variations. Holzforschung, 58:154-159.

Limträhandbok, (2001). Nordic design manual for glulam. (In Swedish). Svenskt Limträ AB, Stockholm, Sweden.

Morlier P and Ranta-Maunus A. (1998). DOL effect of different sized timber beams. Holz als Roh- und Werkstoff, 56:279-284.

Nevander LE., Elmarsson B. (1981). Fukthandboken. (Moisture design manual). Svensk Byggtjänst, Stockholm, Sweden

Olbjer L, Holst U, and Holst J. (2002). Tidsserieanalys. (Time series analysis). Div. of Mathematical Statistics, Lund University.

Ranta-Maunus A. (2003). Effects of Climate and Climate Variations on Strength. In: Thelandersson S, Larsen HJ. editors. Timber Engineering, Wiley, Ch. 9 pp. 153-167.

Rosenkilde, A. and Arfvidsson, J. (1997). Measurement and Evaluation of Moisture Transport Coefficients During Drying of Wood. Holzforschung 51 No.4 372-380.

INTERNATIONAL COUNCIL FOR RESEARCH AND INNOVATION
IN BUILDING AND CONSTRUCTION

WORKING COMMISSION W18 - TIMBER STRUCTURES

BACKGROUND INFORMATION ON ISO STANDARD 16670
FOR CYCLIC TESTING OF CONNECTIONS

E Karacabeyli

Forintek Canada Corporation, Vancouver

CANADA

M Yasumura

Department of Forest Resources Science, Shizuoka University

JAPAN

G C Foliente

CSIRO Manufacturing & Infrastructure Technology, Highett,

AUSTRALIA

A Ceccotti

Consiglio Nazionale della Ricerche, Florence

ITALY

Presented by E Karacabeyli

A Ceccotti stated that the EN12512 was written by a very small group. One can use ISO results to transfer to CEN standard which is used to support Eurocode 8 (yielding and ductility factors). M Yasumura stated that in Japan this is also used for shear walls. Japan has her own protocol which is similar but different. The question is how to adapt international standard to national standards. E Karacabeyli suggested testing according to both protocols.

A Leijten asked about equivalent damping ratio in the CEN standard is for the linear range only. No information on equivalent damping ratio for the non linear range. Is there any info in the ISO standard that can consider this. Chun Ni commented that connections and shear walls are tested using this standard and no nail fatigue breaking was observed. F. Lam asked whether it is true that nail fatigue was not observed. E Karacabeyli responded that some nail fatigue failures are seen. This is also seen in walls subjected to multiple shake table tests.

A Leijten commented on the basis of loading cycle determination of the nail slip. In ASTM the determination of yielding slip is different. ISO does not define yield displacement. You can use EN standards to get yield displacement later. A Ceccotti stated that ductility definition is important. One must take into account calculation design code which is a national issue. The choice of not defining yield displacement is a good one.

P Quenneville stated provisions to test asymmetric loading is needed. E Karacabeyli stated that this is provided in the standard.

Background Information on ISO Standard 16670

for Cyclic Testing of Connections

E. Karacabeyli[1], M. Yasumura[2], G.C. Foliente[3], A. Ceccotti[4]

[1]Forintek Canada Corporation, Western Laboratory
Vancouver, B.C. V6T 1W5, Canada
[2]Department of Forest Resources Science, Shizuoka University
Ohya, Shizuoka, 422, Japan
[3]CSIRO Manufacturing & Infrastructure Technology
Highett, Victoria, 3190, Australia
[4]Consiglio Nazionale della Ricerche via Madonna del Piano
Sesto Fiorentino I-50019 Florence, Italy

Abstract

ISO (International Organization for Standardization) Technical Committee on Timber Structures (ISO TC 165) convened in 1995 a working group (WG7) for the development of international standards for connections. As a first priority, the WG7 worked with a group of international experts and developed the ISO Standard 16670 "Timber Structures – Joints made with mechanical fasteners – Quasi-static reversed-cyclic test method" to provide a cyclic test method as a basis for derivation of parameters which are required in seismic design of timber structures. The cyclic test protocol in this standard was used in various research studies in testing of joints as well as shearwalls. In this paper, the basic features and application of the ISO 16670 are presented along with its differences with respect to other standards.

1   Introduction

International standards are needed to provide a consistent basis for performance of connections and shearwalls and exchange of technical information, and to facilitate cooperative efforts to develop analytical models and improved design procedures. In earlier workshops and meetings, where worldwide developments on seismic behaviour of timber structures were presented or reviewed and research needs identified (Gupta and Moss 1991; Foliente 1994), the need for an internationally accepted cyclic test protocol for timber systems has consistently been pointed out. Many experimental results have been reported where selection of loading histories and test details, and presentation of results were performed in a subjective or arbitrary manner, even when (*1*) the test objectives were the same, and (*2*) the tests were conducted in the same country (Foliente and Zacher 1994). Because this non-standardized approach limits the potential usefulness of the experimental database for development of models and design methods, various methods of seismic performance evaluation of timber joints have been developed and proposed. These include the proposals or draft standards by RILEM TC 109-TSA (1994), ASTM (Dolan 1994),

1

CEN (1995), Australia-New Zealand (SAA 1997) and the Structural Engineers Association of California (SEAOC) (Shepherd 1996).

Aware of these national and regional efforts and desiring to minimize the differences in these various standards, the ISO Technical Committee on Timber Structures (TC 165) convened Working Group 7 (WG 7) during its 1995 meeting in Paris, France to draft an ISO standard on cyclic testing of joints with mechanical fasteners. The members of the WG7 worked with over twenty international experts and developed the ISO Standard 16670 (2003). This paper presents key provisions of that standard. An extensive review of related literature and other proposed protocols, comments of experts around the world and results of laboratory tests were all considered in its development (Karacabeyli and Ceccotti 1996; Foliente 1996; Yasumura and Kawai 1997).

1.1   ISO 16670 Cyclic Test Schedule

The procedures to assess products on the basis of testing are key components of performance-based standards. The closer the test method approaches in-service conditions, the more useful the evaluated parameters will be for predicting performance. However, tests that approach in-service conditions are very costly; in practice, they can only be used to calibrate simpler procedures. Actual in-service loads acting on structures (Figure 1) are complex and stochastic in nature, but only simplified, repeatable loading regimes are specified in testing standards for practicality and consistency. This is acceptable as long as key features of the in-service loads that affect in-service performance are in one form or another incorporated in the simplified loading regime – e.g., low-cycle fatigue test for cyclonic winds and reversed cyclic test with increasing amplitude (to load the joint to inelastic range and eventually to ultimate capacity) for earthquakes.

Loading Type	Example of In-Service Load	Test Load
• Gravity (Dead and live)		
• Earthquake		
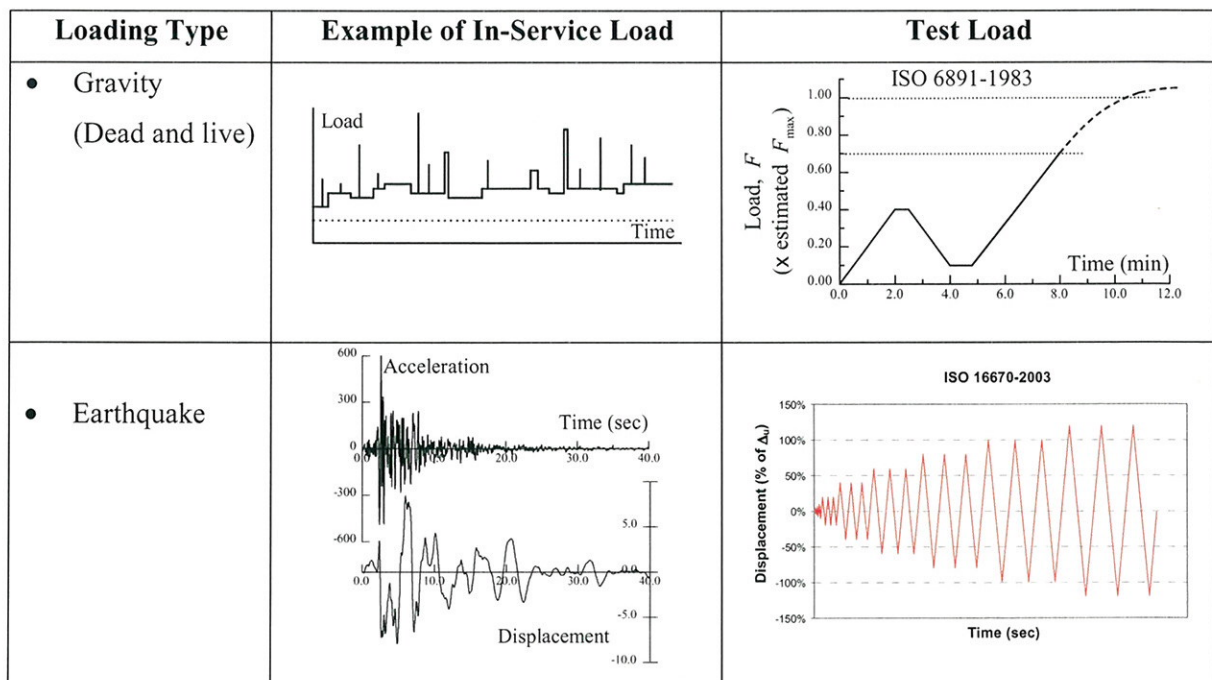
Figure 1:   Examples of in-service loads and proposed test loads (after Foliente and Leicester 1996)

A critical aspect of any cyclic test standard is the specification of the load history, which had been a topic of debate for some time (Foliente 1996). A unique loading history will

always be a compromise, but one that allows derivation of joint properties for design and/or analysis that are deemed conservative for most practical cases should be selected. To be effective, the cyclic test standard should include a basic loading history for general seismic evaluation. To accommodate special cases or test objectives, the standard should allow the use of other loading types but the response data measured should be consistent as much as possible with the requirements of the standard. It is ideal that the test protocol produce: (1) data that sufficiently describes the elastic and inelastic cyclic properties of the joints, and (2) typical failure mode that the joint is known to exhibit under earthquake loading. These are the intended objectives of the ISO Standard 16670.

To accomplish this, the ISO Standard 16670 requires both a static monotonic test and a cyclic test. The former is conducted on a matched group of specimens according to ISO Standard 6891 (ISO 1983) (with the exception of pre-loading; see Figure 1) to determine the average ultimate displacement v_u. If v_u is already known from a previous static test on a matched group of specimens, additional static testing is not required.

Unlike other cyclic test standards, the application of displacement cycles in the ISO 16670 is given in terms of fractions of the ultimate displacement. Other test procedures use the yield displacement, which is a fictitious parameter for most timber structures. A wide variety of methods to determine yield point in timber structures can produce a wide range of values of "yield displacement" (Chui et al. 1995, Karacabeyli and Ceccotti 1996; Foliente 1996; Yasumura and Kawai 1997; He et al. 1998). The definition and determination of ultimate displacement, on the other hand, are relatively straightforward (Figure 2), and less contentious. The "yield displacement" of the joint can still be obtained from the results of the ISO cyclic tests based on any given definition or method.
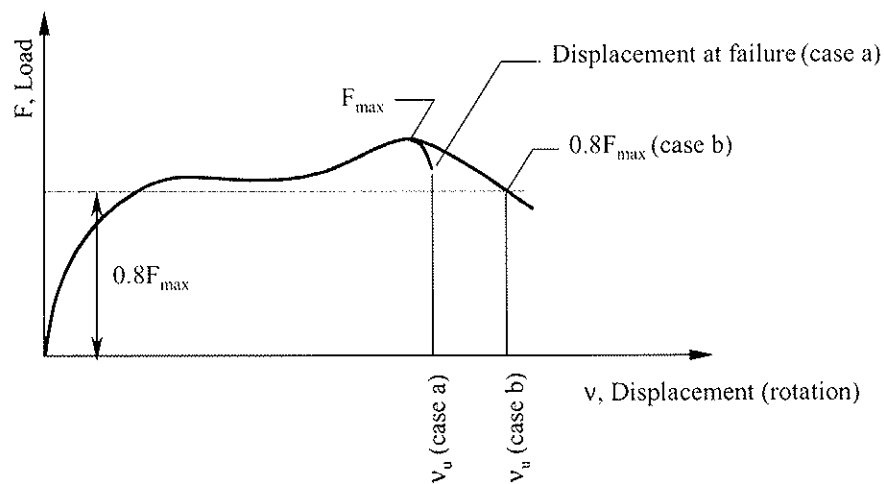
Figure 2: Definition of ultimate displacement: v_u corresponds to failure displacement [Case (a)], or displacement at 0.8 F_{max} [Case (b)], whichever occurs first in the test.

The ISO 16670 cyclic displacement schedule is graphically shown in Figure 1 and described in Table 1 which includes both the 1997 Draft ISO schedule as well as the 2003 ISO cyclic schedule as published in the ISO 16670. The ISO 16670 cyclic schedule is intended to provide a cyclic test method to develop the envelope (backbone or skeleton) curves. The method generates suitable data in the elastic and in-elastic ranges. In the elastic range, only one cycle is applied for each of the displacement levels (1.25%, 2.5%, 5%, 7.5%, and 10% of ultimate displacement). In the in-elastic range, the method generates three envelope curves which are evenly distributed along the displacement axis. These envelope curves may be used to determine impairment of strength, ductility and

yield displacement according to the definitions adopted in different jurisdictions. The initial cycles may be omitted or new cycles may be added between Stages 1 and 5, depending on the elastic stiffness of the joint or the accuracy of the measurement system, to obtain sufficient data in the elastic range. If needed (e.g., in analytical modelling), an additional cycle at a lower amplitude may be added at the end of the required cycles in Stages 6 to 10 (ISO 2003).

It is desirable to perform the reversed cyclic tests within a few minutes because earthquakes do not generally last more than one minute. The upper limit (10 mm/sec) was selected as the fastest rate which may be employed with the intention of avoiding dynamic effects to the test specimen. The lower limit (0.1 mm/sec) was selected as the lowest rate to accommodate the use of test equipment which have limitation in applying relatively high rates of displacements. The Standard allows the use of both velocity or frequency based test protocols.

Recommendations for cases for which a modified schedule would be more appropriate are also included in ISO 16670, and they are also given below. Details about test specimens (conditioning, form and dimension, sampling, number of replicates) and apparatus are given in the Standard.

1.2 Modification of ISO displacement schedule

The ISO 16670 displacement schedule could be modified in cases where:

- the behaviour of the joint is significantly different in two opposite directions. In this case, monotonic tests should be performed in both directions. The ultimate displacement in cyclic displacement schedule should then be determined for each direction based on their respective ultimate displacement obtained in monotonic tests;

- the joint exhibits in-elastic behaviour within five initial steps. In this case, (i) new single steps may be added to ensure a minimum of three steps for obtaining sufficient data within elastic range; and (ii) initial steps beyond elastic range should be repeated three times to generate three envelope curves;

- the amplitudes of the first and second steps are too small to be accurately applied. In this case, the first and second steps may be omitted;

- decreasing cycles are necessary (for example to generate suitable data for calibration of hysteresis models). In this case, application of single decreasing cycles before increasing to the next displacement cycle may be added to the displacement schedule.

- Specific earthquake or dynamic effects are studied (e.g. near-fault earthquake effects, cumulative damage effects, etc.).

- the joint-displacement increases at zero load at the beginning of the test due to fastener tolerance (e.g. bolted joints). In this case, this tolerance may be subtracted from measured displacement values when determining the amplitudes for cyclic displacement schedule.

1.3 Test Results

The ISO 16670 requires that the complete hysteretic response data (load-displacement or moment-rotation data) shall be plotted and stored for each test joint. The first, second and third envelope curves for the cyclic tests are established by connecting the points of

4

maximum load in the hysteresis plot in each slip level in the first, second and third reversed cycles, respectively. The maximum load values and their associated displacements obtained in the first five single reversed cycles are taken to be the same for all envelope curves. An example is given in Appendix A. In another table, the maximum load taken from the envelope curves F_{max}, ultimate displacement v_u and joint stiffness k are to be reported in both directions. The joint stiffness is calculated as follows:

$$k = (0.3 \, F_{max}) \, / \, (v_{0.40Fmax} - v_{0.10Fmax}) \tag{1}$$

where $v_{0.40Fmax}$ and $v_{0.10Fmax}$ are the displacements corresponding to 40% and 10% of F_{max}, respectively.

Table 1   Cyclic displacement schedules in the draft ISO (1997) and the ISO (2003)

Stage	Number of Cycles	ISO Draft (1997) Amplitude ($\times v_u$)	ISO (2003)[1] Amplitude ($\times v_u$)
1	1	2.5%	1.25%
2	1	5.0%	2.5%
3	1	7.5%	5.0%
4	1	10.0%	7.5%
5	1	12.5%	10%
6	3	25.0%	20%
7	3	50.0%	40%
8	3	75.0%	60%
9	3	100.0%[2]	80%
10	3	Increments of 25.0%[2]	100%[2]
11	3	-	Increments of 20%[2]

NOTES:

[1] Some of the initial steps (1.25% to 10%) may be omitted or repeated (or new steps may be added) depending on the stiffness of the joint or accuracy of the measurement system, as long as the principles given in the standard are satisfied. The standard also identifies cases where modification of the cyclic displacement schedule may be warranted.

[2] To be conducted only if necessary.

Measurement of other cyclic properties, such as yield displacement, ductility and impairment of strength, are not explicitly specified but can be determined from the envelope curves according to the definitions and methods given in national standards or building codes.

1.4   Application & Comparison with Other Standards

CEN (2001) standard EN 12512:2001 *Timber structures— Test methods — Cyclic testing of joints made with mechanical fasteners* is written as a support document to Eurocode 8 (2004), the calculation code for construction in seismic zone, enforced in Europe. It refers to the concept of "ductility" and gives a methodology for its calculation from tests results. A definition of "yielding" displacement is therefore given and the test protocol is based on this yielding displacement. Nevertheless CEN procedure can "read" the test results obtained by following ISO protocol and vice versa. In other words, the information obtained from a CEN cyclic test can provide the information the ISO procedure requires, and an ISO cyclic test can provide the information required by the CEN procedure (i.e.

ductility and ultimate displacement, impairment of strength per cycle and dissipated energy per cycle).

Typical hysteresis plots for nailed joints with plywood sheathing using the draft ISO 1997 test schedule and the draft CEN (1995) test schedule (later published as CEN (2001)) are shown in Figures 3a and 3b, respectively. Details about the joints are given by Yasumura and Kawai (1997). Although some differences in the response are observed in this figure, Table 2 shows that the average values of ultimate strength and displacement of six joints are reasonably close. Similar results were observed for nailed joints with oriented strand board (OSB) and gypsum board sheathing (Table 2).

The draft ISO 1997 cyclic test schedule has also been applied to wood shearwalls and results were compared with those obtained using the draft CEN and draft ASTM (which, at that time only included Sequential Displacement Method "SPD") schedules, and the calculated wall displacement response from six earthquake records as the input displacement (Karacabeyli and Ceccotti 1998). Among other results, it was observed that the energy demand of the draft ISO 1997 and CEN schedules is in the high end of the range of values from the six earthquakes while the energy demand of the SPD schedule is about two times that of the draft ISO and CEN schedules. A high number of nail fatigue failures were observed in walls tested using the SPD schedule; similar results have also been observed by those who used the proposed SEAOC procedure, which like the draft ASTM procedure, is based on SPD schedule. This type of failure has rarely been observed in damaged wood structures after earthquakes. An appropriate test procedure is one that induces a failure mode in the specimen that is similar to that observed under earthquake loading.

(a)   (b)
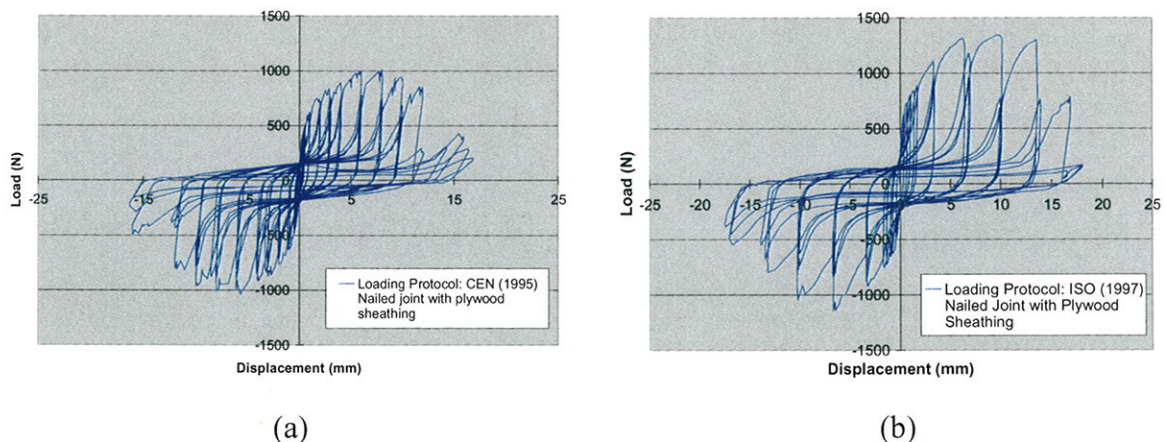
Figure 3: Typical hysteresis plots from cyclic tests of plywood-sheathed nailed joints following: (a) the draft CEN (1995) standard, and (b) draft ISO (1997) standard (tests conducted at Shizuoka University)

ISO Standard 16670 was published in 2003. Its cyclic displacement schedule has been included in the ASTM Standard E2126 (2002) for cyclic (reversed) load testing for shear resistance of walls for buildings. ASTM E2126 includes two other cyclic displacement schedules; one based on Sequential-Phased Displacement (SPD) procedure; and one based on the Consortium of Universities for Research in Earthquake Engineering (CUREE) basic loading schedule (Krawinkler et al 2000). This is a positive step towards acceptance of results obtained with different displacement schedules. It has been reported by Gatto and Uang (2003) that the results obtained on nailed shearwalls with ISO cyclic schedule were between those obtained with CUREE basic cyclic displacement schedule and SPD

schedule; the latter resulted in relatively low load carrying capacities for the joints due to excessive nail fatigue failures.

The draft ISO 1997 cyclic test schedule has also been applied to full-scale testing of an L-shaped one-storey woodframe building (Paevere et al. 2003). This test program provided useful insights in load distribution and re-distribution within light woodframe construction subject to lateral loads, validation data for lateral load design models or procedures (Kasal et al. 2004), and substantial data required for analytical modeling and performance analyses of woodframe buildings (Paevere 2002; Collins et al. 2005a; 2005b; Wang and Foliente 2005).

Table 2   Comparison of ultimate joint capacities based on the draft CEN (1995) procedure and the draft ISO (1997) procedure (tests conducted at Shizuoka University)

Sheathing Material	Draft CEN Procedure				Draft ISO 1997 Procedure			
	Ultimate Strength		Ultimate Displ.		Ultimate Strength		Ultimate Displ.	
	Ave.[1] (N)	COV[2]	Ave[1] (mm)	COV[2]	Ave.[1] (N)	COV[2]	Ave[1] (mm)	COV[2]
Plywood	907	0.12	15.0	0.16	879	0.16	14.0	0.14
OSB	872	0.09	16.2	0.22	903	0.04	16.3	0.10
Gypsum	282	0.12	14.3	0.32	269	0.04	14.3	0.12

[1] Based on six replicates
[2] COV is coefficient of variation (standard deviation/average).

2   Future Work

Using ISO 16670 and other relevant standards, the ISO TC 165 Working Group 7 is planning to develop a standard for static and cyclic testing of shearwalls. For development of seismic capacity design procedures for timber structures, information on "upper bound" characteristic values for the joints (e.g., 95th percentile values) are needed. Thus, consistent statistics-based procedures for establishing design values should be considered.

3   Conclusion and Recommendations

The background information and some key features of ISO Standard 16670 for cyclic testing of joints in timber structures under earthquake loads are presented. Because the standard was developed through international collaboration, it is used and referenced in many countries. The inclusion of ISO 16670 cyclic displacement schedule in the ASTM Standard 2126 (cyclic testing of shearwalls) is a positive step towards international harmonization. It is recommended that a similar step be considered by other national standards committees. It is also recommended that research studies include reference tests conducted with ISO 16670 schedule to enhance the comparability of results from other studies.

As performance-based engineering becomes more common in the design of structures, designers will increasingly rely on the performance data provided by testing, which reflects the demands from in-service conditions. International standards provide a consistent basis for performance comparison of systems and exchange of technical information, and facilitate cooperative efforts to develop analytical models and improved design procedures for timber construction.

7

4   Acknowledgements

5   References

ASTM 2002. Standard test methods for cyclic (reversed) load test for shear resistance of walls for buildings. ASTM E 2126. American Society of Testing and materials.

CEN. (1995). *Timber structures— Test methods — Cyclic testing of joints made with mechanical fasteners.* Draft EN TC 124.117. European Committee for Standardization, Brussels, Belgium.

CEN (2001). *Timber structures— Test methods — Cyclic testing of joints made with mechanical fasteners.* EN 12512:2001 European Committee for Standardization, Brussels, Belgium.

Collins, M., Kasal, B., Paevere, P. and Foliente, G.C. 2005a. "Three-dimensional model of light-frame wood buildings — I. Model formulation," *ASCE Journal of Structural Engineering,* in press.

Collins, M., Kasal, B., Paevere, P. and Foliente, G.C. 2005b. "Three-dimensional model of light-frame wood buildings — II. Experimental investigation and validation of the analytical model," *ASCE Journal of Structural Engineering,* in press.

Chui, Y., H., Smith, I., and Daneff, G. 1995. *On protocols for charactersing "Dynamic" properties of structural timber connections.* Proc. Of 7th Canadian Conference on Earthquake Engineering, Montreal, Canada. P: 617-624

Dolan, J.D. 1994. Proposed test method for dynamic properties of connections assembled with mechanical fasteners. *ASTM Journal of Testing and Evaluation,* 1994, 22(6), 542-547.

Eurocode 8 (2004). *Design of structures for earthquake resistance - Part 1: General rules, seismic actions and rules for buildings. Chapter 8, Specific rules for timber structures.* EN 1998-1:2004 European Committee for Standardization, Brussels, Belgium.

Foliente, G.C. (Ed.) (1994). *Analysis, Design and Testing of Timber Structures Under Seismic Loads.* Procs. Research Needs Workshop, University of California Forest Products Lab., Richmond, Calif.

Foliente, G.C. 1996. Issues in seismic performance testing and evaluation of timber structural systems. *Procs. Int'l. Wood Engineering Conference (IWEC '96),* Baton Rouge, Louisiana, USA, 1996, 1, 29-36.

Foliente, G.C. and E.G. Zacher. 1994. Performance tests of timber structural systems under seismic loads. *In* Foliente, G.C. (Ed.) *Analysis, Design and Testing of Timber Structures Under Seismic Loads.* Procs. Research Needs Workshop, Univ. of California Forest Products Lab., Richmond, Calif., 1994, 21-86.

Foliente, G.C. and R.H. Leicester. 1996. Evaluation of mechanical joint systems in timber structures. *Proceedings of the 25th Forest Products Research Conference,* CSIRO Division of Forestry and Forest Products, Clayton, Victoria, Australia, 1996, **1**, Paper 2/16, 8 pp.

Gatto, K., and Uang, C. 2003. *Effects of loading protocol on the cyclic response of woodframe walls.* J. of Struc. Eng. Vol. 129, No. 10. American Society of Civil Engineers.

Gupta, A.K. and P. Moss (Eds.). (1991). *Pros. Workshop on Full-Scale Behavior of Wood-Framed Buildings in Earthquakes and High Winds,* Watford, UK. North Carolina State University, Raleigh, No. Carolina.

He, M., Lam, F., and Prion, H. (1998). *Influence of cyclic test protocols on performance of wood-based shear walls.* Can. J. Civ. Eng., 25(3), 539-550.

ISO. (1983). *Timber structures – Joints made with mechanical fasteners – General principles for the determination of strength and deformation characteristics.* ISO 6891-1983 (E). International Organization for Standardization, Switzerland.

ISO. (2003). *Timber structures – Joints made with mechanical fasteners – Quasi-static reversed-cylic test method.* ISO 16670 The international Organization for Standardization, Genava. ISO (1997) is the 1997 draft version of this standard.

Karacabeyli, E. and A. Ceccotti. 1996. Quasi-static reversed-cyclic testing of nailed joints. *Procs. CIB W18 Meeting,* Bordeaux, France, 1996.

Karacabeyli, E. and A. Ceccotti. 1998. Nailed wood-frame shear walls for seismic loads: Test results and design considerations. *Procs. Structural Engineers World Congress (SEWC'98),* San Francisco, Calif., 1998.

Kasal, B., Collins, M., Paevere, P. and Foliente, G.C. 2004. "Design Models of Light-Frame Wood Buildings Under Lateral Loads." *ASCE Journal of Structural Engineering* 130(8): 1263-1271.

Krawinkler, H. Parisi, F., Ibarra, L., Ayoup, A., and Medina, R., 2000. Development of a Testing Protocol for Wood- Frame Structures, CUREE-Caltech Woodframe Project Report No. W-02. Stanford Univ., CA., USA.

Paevere, P. J. 2002. "Full-Scale Testing, Modelling and Analysis of Light-Frame Structures Under Lateral Loading." Ph.D. Thesis, Department of Civil and Environmental Engineering, The University of Melbourne, Parkville, Victoria, Australia.

Paevere, P.J., Foliente, G.C., Kasal, B. 2003. "Load distribution and load-sharing mechanisms in a one-story woodframe building." ASCE *Journal of Structural Engineering* 129 (9): 1275-1284

RILEM 109-TSA. 1994. Timber structures in seismic regions: RILEM State-of-the-art report. *Materials and Structures,* 1994, **27**, 157-184.

SAA. (1997). *Timber – Methods for evaluation of mechanical joint systems. Past 1: Static loading; Part 2: Cyclonic wind loading; Part 3: Earthquake loading.* Draft AS/NZS BBBB issued April 1997. Standards Association of Australia, Sydney.

Shepherd, R. 1996. Standardized experimental testing procedures for low-rise structures. *Earthquake Spectra,* 1996, **12** (1), 111-127.

Wang, C.-H. and Foliente, G.C. 2005. "Seismic reliability of low-rise, non-symmetric wood frame buildings," *ASCE Journal of Structural Engineering,* in press.

Yasumura, M. and N. Kawai. 1997. Evaluation of wood framed shear walls subjected to lateral load. *Procs. CIB W18 Meeting*, Vancouver, Canada, 1997.

Appendix A: Example of load-displacement curve and tabular form

Displacement (mm)
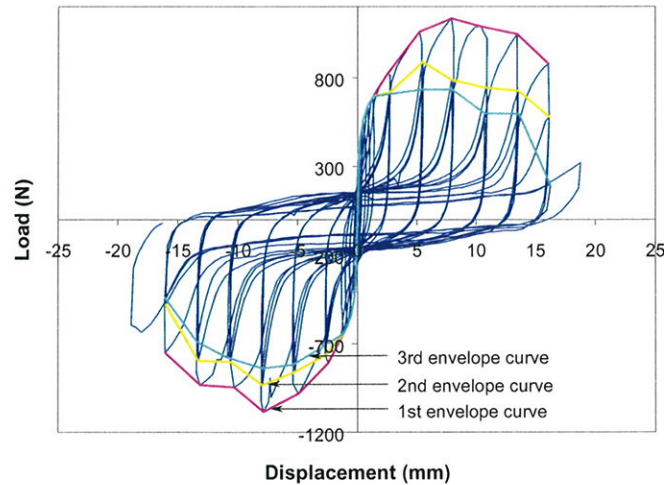
Figure A1   Envelope curves traced from hysteresis data.

Table A1   Tabulated values of points defining the envelope curves.

First envelope curve				Second envelope curve				Third envelope curve			
Positive		Negative		Positive		Negative		Positive		Negative	
mm	N	mm	N	mm	N	mm	N	mm	N	mm	N
0.2	448.4	-0.2	-360.2	0.2	448.4	-0.2	-360.2	0.2	448.4	-0.2	-360.2
0.4	524.3	-0.3	-450.8	0.4	524.3	-0.3	-450.8	0.4	524.3	-0.3	-450.8
0.5	563.5	-0.6	-543.9	0.5	563.5	-0.6	-543.9	0.5	563.5	-0.6	-543.9
0.9	646.8	-0.9	-600.3	0.9	646.8	-0.9	-600.3	0.9	646.8	-0.9	-600.3
1.3	695.8	-1.2	-641.9	1.3	695.8	-1.2	-641.9	1.3	695.8	-1.2	-641.9
2.5	818.3	-2.5	-808.5	2.7	717.9	-2.7	-764.4	2.7	708.1	-2.6	-705.6
5.2	1058.4	-5.0	-982.5	5.5	886.9	-5.3	-857.5	5.4	732.6	-5.4	-818.3
7.9	1131.9	-7.9	-1082.9	7.9	786.5	-8.0	-933.5	8.0	732.6	-8.0	-837.9
10.4	1087.8	-10.4	-945.7	10.8	742.4	-10.6	-801.2	10.7	597.8	-10.9	-776.7
13.5	1043.7	-13.2	-933.5	13.6	725.2	-13.3	-796.3	13.6	595.4	-13.4	-688.5
16.1	877.1	-16.1	-752.2	16.2	578.2	-16.0	-477.8	16.3	193.6	-16.1	-441.0

		Maximum Load (N)	Ultimate displacement (mm)
First envelope curve	Positive	1131.9	15.6
	Negative	-1082.9	-14.3
Second envelope curve	Positive	886.9	13.8
	Negative	-933.5	-13.7
Third envelope curve	Positive	732.6	13.7
	Negative	-837.9	-13.6

INTERNATIONAL COUNCIL FOR RESEARCH AND INNOVATION
IN BUILDING AND CONSTRUCTION

WORKING COMMISSION W18 - TIMBER STRUCTURES

TESTING & PRODUCT STANDARDS –

A COMPARISON OF EN TO ASTM, AS/NZ AND ISO STANDARDS

A Ranta-Maunus

VTT

FINLAND

V Enjily

BRE

UNITED KINGDOM

Presented by A Ranta-Maunus

B Leicester commented that in the ISO and AS/NZ standard there is an attempt to draft equivalence and harmonisation for different standards. In general the idea is to try to test against the load capacity of the material in service. Shear testing is an example. Similar issue is for tension. In AS/NZ in service length was developed. Studies indicate that although the N. American standard requires the position of worst defect within the test span, it is possible to obtain lower results with the AS/NZ standard because it is difficult to accurately identify the "worst defect". A Ranta-Maunus said that the Europeans should be more involved in ISO process.

H Larsen stated the paper partly on testing and partly on code values for timber. These values may not be linked. Bending test is important and may be an issue. He is not too happy with the choices European had to set up their test standard as there was pressure fitting to a large existing data base of BRE. Difference in test method is a big problem for example for compression perpendicular to grain tests. Big problem when tested according to testing standard and values in the code is much too high which led to changes in the values in the code. Pre-stress bridge deck and concentrated load from column to sill are two examples of different applications for this issue.

F Lam stated the harmonisation work in ISO addresses MOR, MOE and tension. This paper points out more work need to be done in the area of harmonisation in area of shear and other properties. E Karacabeyli brought up the issue of poles and simply supported structures. S Thelandersson sees this as the same problem with concrete when one wants to characterize certain properties. In timber this is bending. One must consider how to use these values such as shear and perpendicular to grain properties. May be factors are needed. For example compression perpendicular o grain strength can be based on density. H Larsen restated that there is a need to have the same test method. Values in the code may not be 100% based on testing. BJ Yeh stated European tension test have shorter gauge length than the N. American, why are the strength lower in Europe compared to N. America. A Ranta-Maunus said that this is H Larsen's point.

J Ehlbeck said that if the standards are not used why not get rid of them. We need to do something. P Kuklic stated designers have trouble with some of the values. H Blass concluded that competitive aspect is one of the key issues of the paper.

Testing & product standards

– a comparison of EN to ASTM, AS/NZ and ISO standards

Alpo Ranta-Maunus, VTT, Finland

Vahik Enjily, BRE, UK

1 Introduction

Introducing innovative timber products to the market currently entails longwinded test programmes which are generally replicated in various European and other countries depending on market potential. Often a wide variety of products remains unchanged or further developed to minimise development costs. This lengthy and costly process together with a wide range of co-referencing product standards is seen to stifle innovation of the timber products in construction which hinders the increased use of wood in construction.

The information on how to conduct and report the outcome of a test is not unified in simplified manner throughout European testing organisations. Reporting of the test outcome does often not account for the practical implications of the test result and does not relate to the performance of a product in its end use conditions. In addition, the information extracted from the test and its impact on product design are not addressed clearly. The information dwells on basic research where required but does not investigate the practical applications. In addition, outputs, results and implications of the tests are often not communicated in clear and concise language, putting forward ideas for development, which can be communicated effectively to the lay person as well as the professional. Consequently, knowledge of best use of standards with regard to product development to meet client needs is very limited.

European standards are a big step forward for European market but they need to be adjusted throughout Europe and implemented in an integrated and harmonised way. This paper tries to identify and examine briefly some of major test methods and results as an example of disparity with their parallel international standards which affect the design of new products.

1.1 Background

The slow and delayed uptake of wood products is often related to longwinded and complicated product specification and testing. To ensure a thriving and dynamic industry and implementing the benefits of wood, the development of structural wood products and their market introduction needs to be swift and cost effective. It is of greatest importance to

link product development and required testing into a design standardisation process. There are many adequate and necessary standards available in Europe but the link and optimisation of their use are lacking at present.

The current European standards have been produced over a decade or so by reputable and experienced people across Europe. They are useful tools and they must not be ignored but improved in line with the new developments in the market which are different with those a decade ago. Some industries, competing with the wood sector, have already analysed and rationalised their testing approaches. This can provide useful learning for the wood industry and can also allow examining the overall competitiveness of the industry, especially with regard to developing new products and systems based on standards for the wider market introduction.

1.2 Objectives of the paper

The main objective of this paper is to review briefly some of the testing standards as an example in order to highlight the differences which exist between European and International standards. A piece of timber, component or element should have the same characteristic properties no matter where in the world it has been tested. However, it seems that this is not the case at present.

The aim of this paper is to highlight works needed to overcome certain barriers caused by test and product standards. The paper also tends to highlight criteria needed for the industry and future use of wood in construction.

2.0 Review of the testing standards (Europe, ISO and national)

In this section a comparison of strength testing standards used in different continents is made. Special attention is paid to the conformity of the results, practicality, cost of testing, and relevance of the results in structural design. Determination of characteristic values for design strength are also compared.

2.1 Bending

Bending strength is commonly tested by using a similar procedure: edge wise bending by two point loads at a distance of 1/3 span from the supports (Fig. 1). Span width to beam depth ratio is practically the same in different standards. However, there are factors which cause deviation of results. Positioning of the specimen for loading is different. In Europe the anticipated weakest cross-section is positioned on the maximum loading area when possible, whereas on other continents the positioning is made randomly. This can affect maximum 30% difference in the characteristic values, depending on the quality of timber (Wang et al 2004, Leicester et al 1996). ISO 13910 Table A1 gives a ratio between characteristic values determined according to ISO 13910 and EN 384 procedure. The given ratio is from 1 to 1.3 depending on grade and dimension.
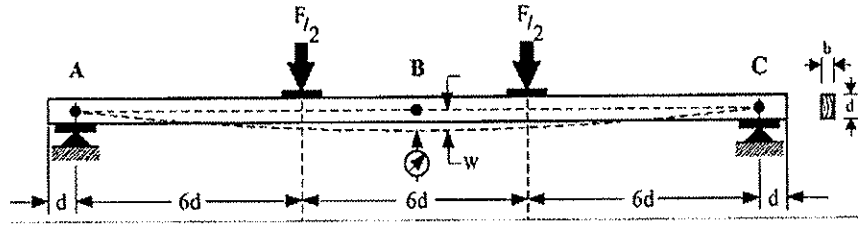
Figure 1. Bending test arrangement according to ISO/DIS 13910

In Europe the characteristic value given for strength classes refers to a reference size (beam depth or larger cross-sectional dimension in tension =150 mm) both in case of visually and machine graded timber. This is different from the other continents where the characteristic bending strength of machine graded timber is directly the value shown by the grade, not adjusted to any other size.

For modulus of elasticity two methods are standardised in Europe: local and global modulus of elasticity. Recently global modulus of elasticity is considered the standard value to be used in strength grading. When measurement of deflection is made on both sides of beam and global modulus is determined, standard deviation of results is minimised. The small contribution of shear deformation to deflection (4-5 %) can be tolerated as the result is relevant to the calculation of deflection of structures, where also the shear deformation is also neglected.

2.2 Tension

Length of tension test specimen, expressed as free space between grips, is the main variable in tension testing of structural size timber. Clear distance requirements are as follows:
ISO/DIS 13910 (see Fig. 2): 8 times width + 2 m
EN 408:   9 times width, at least
ASTM D4761:   25 times width
AS/NZS 4063:   7.5 times width + 2.25 m.
European test specimen is shorter and will therefore give higher strength values than longer specimens. Tension testing of sawn timber needs not be done regularly, because characteristic values of tension strength are given in standards based on bending strength.

Comparison of European, American and Australian characteristic tension strength values used in structural design is shown in Figure 3. EN and ISO uses a constant ratio of tension to bending strength (0.6), whereas the others have adopted a variable ratio. It is believed that tension to bending strength ratio is larger for higher grades, and it is known that tension strength of clear wood is higher than bending strength.
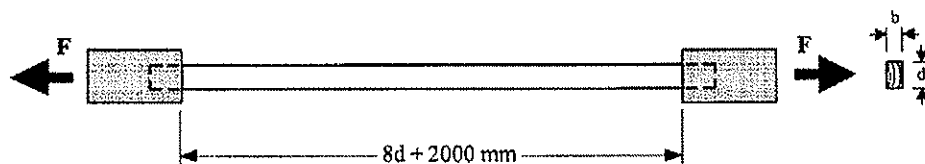
Figure 2. Configuration of tension test according to ISO/DIS 13910

3
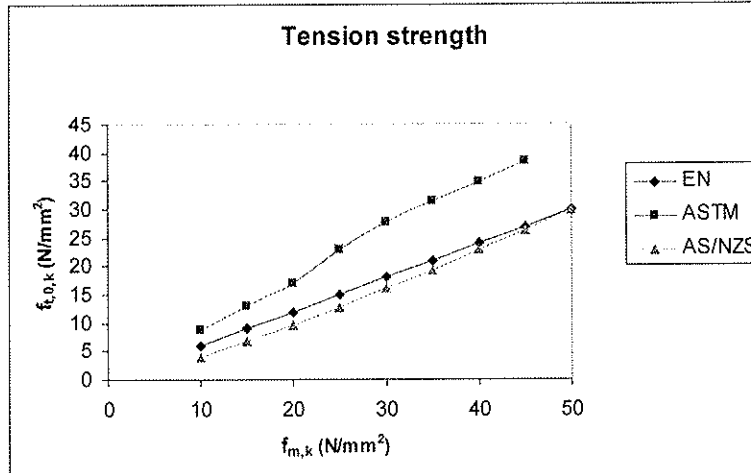
Figure 3. Characteristic tension strength as a function of characteristic bending strength as given in EN, ASTM and AS/NZ standards. ISO is identical to EN.

2.3 Compression

For testing of compression strength EN408 uses, and ASTM D4761 allows the use of a short test specimen which includes the anticipated weakest cross section. EN specimen shall have length of six times the smaller cross-sectional dimension and ASTM at least 2.5 times the larger cross-sectional dimension. ISO 13910 and AS/NZS 4063 use a long specimen, supported against lateral buckling.

The characteristic value of compression strength used in structural design is determined from characteristic bending strength by using different relations, which are illustrated in Figure 5.
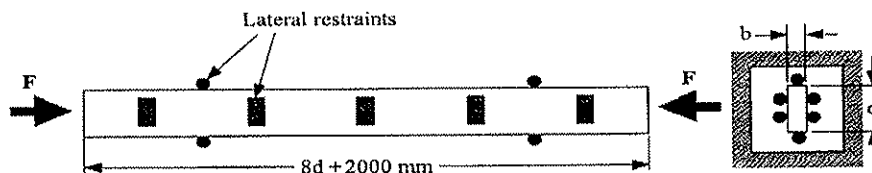
Figure 4. Configuration of compression test according to ISO/DIS 13910.
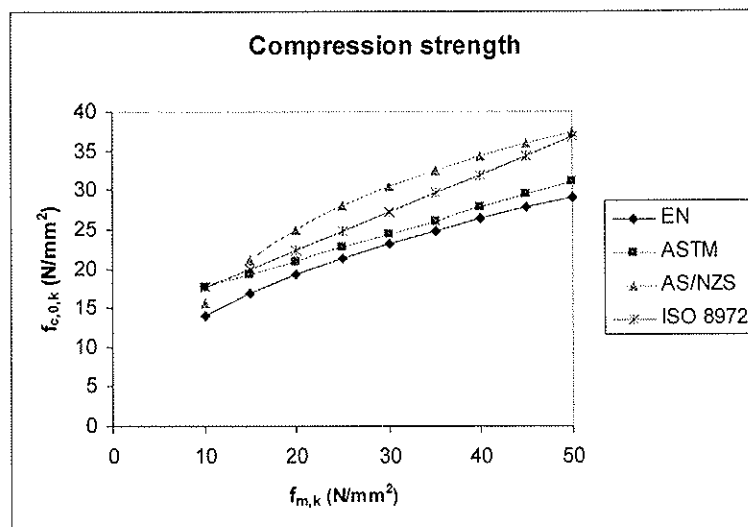
Figure5. Relation of compression strength and bending strength in standards.

4

2.4   Compression perpendicular to grain

According to EN408 test pieces are of size 45x90x70 for sawn timber and 250x100x200 for glulam. Full surface is loaded and compression strength is determined when plastic deformation is 1%.

ASTM D143 test specimen is of size 50x50x150 and is loaded in tangential direction on a third of the upper surface. Compression strength is determined when total deformation is 5%.

The two methods give obviously different results because of following reasons

- the size of test specimen is different
- compression force is loading the full or partial surface of specimen
- compression strength is defined when 1% vs. 5% deformation is achieved.

Characteristic values of sawn timber are calculated from bending strength or density as illustrated in Figure 6. ISO draft and especially AS/NZS give higher values than EN 384. When strength values are so different, also design codes must be different. When $f_{c,90,k}$ - values are used in design in accordance with EN1995-1-1, it is multiplied by a factor from 2 to 3 depending on the size of loaded area and dimensions of timber.
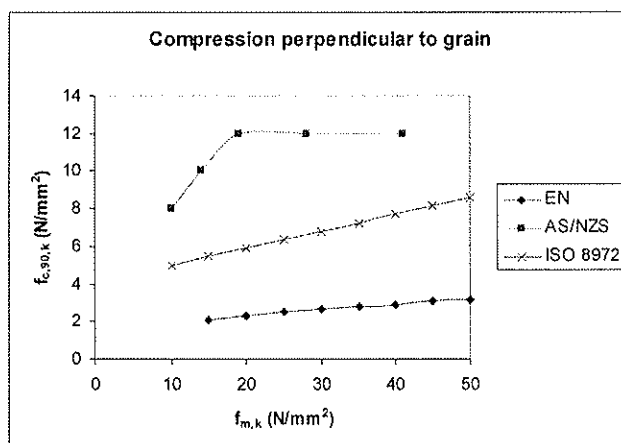
Figure 6. Characteristic compression strength perpendicular to grain as function of bending strength according to different standards.

2.5   Shear

Shear test of ISO 13910 is based on a short span 3-point bending test (l=6d) whereas EN408 uses a glued specimen for determination of shear strength, see Appendix 1. ASTM D143 uses a notched specimen of size 50x50x63 mm.

EN method gives lower values than ISO. Only few test results based on EN408 are published. German experiments give characteristic shear strength value of 3.8 MPa and COV = 0,20 for spruce from C18 to C30, on average (Glos et al 2003).

European specimen attempts to measure pure shear strength whereas many others use a beam specimen which is similar loading case as in beam structures. Beam specimen has not a pure shear stress but combination of shear and compression perpendicular to grain. However, the test is simple and directly relevant to structures. Pure shear strength values are used for analysis of dowel type connections in case of wood failure. An alternative

5

would be to use a plug shear type test specimen to produce data needed for plug shear or block shear analysis.

The characteristic values used in design are calculated from bending strength in several standards. These values are compared in Figure 7. European values are only a half of AS or ISO values.
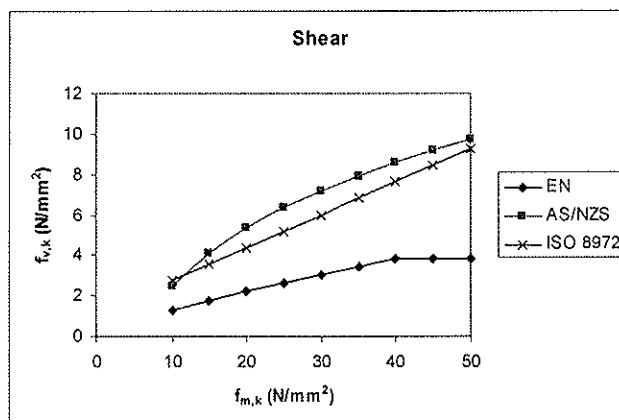
Figure 7. Illustration of characteristic shear strength given by ISO, AS/NZS and EN.

2.6 Tension perpendicular to grain

In EN408 the size of test piece in tension test perpendicular to grain is 45x180x70 in case of sawn timber and volume is $0{,}01m^3$ in case of glulam. Specimens are glued to steel plates at the ends to enable the gripping of specimen.
ISO/DIS 13910 uses bending test to measure tension strength perpendicular to grain.

2.7 Density measurement

According to ISO 13910 density measurement is based on weight of 10d long specimen of full cross-section of sawn timber and density is given at 12% moisture content. In EN 408 the density is determined from a full cross-section, close to fracture, free from knots and resin pockets. Perpendicular to grain-specimens are weighed prior to loading for determination of density.

3.0 Discussion

Some test methods used in Europe give lower strength values than those used by ISO or ASTM. This affects confusion in international trade and creates doubts that European species are weaker. The difference is most obvious in shear and compression perpendicular to grain values. International harmonisation of methods is needed also in bending tests, even if the difference is marginal in higher grades.

Apart from the test methods is the method of determination of characteristic values used in structural design. Characteristic values of different strengths are calculated from bending values in all standards. Accordingly, other than bending tests, are rarely needed or used. However, calculated characteristic values are given in line with the test method, and change of test method would result in a change in characteristic values, and possibly also in structural design code.

Bending tests are fairly similar on different continents. From European perspective two matters need consideration:

- size effect is not consistently considered in testing and design standards, and size effect in machine graded timber is an unnecessary complication
- European testing standard gives smaller strength values for lower grades than other standards which are based on random testing.

Tension test results obtained are in principle relevant for sawn timber used in trusses. For glulam these results are too low because the specimen is not kept straight during loading as it is when acting as a lamination in glulam. Because tension testing is used only for glulam lamellae, the testing standard should be developed to be more accurate for glulam.

European shear strength values are known to be unreasonably low, especially for lower strength classes. Because shear strength is not normally dimensioning sawn timber structures, not much attention is paid to this problem. The EN shear test method is expensive to use, because steel plates are glued on both sides of wood specimen. A simple beam type method should be adopted.

Compression perpendicular to grain values are needed for dimensioning of beams at supports. Present EN test method combined with complex calculation in design code is unnecessary complication and should be harmonised with ISO development.

Table 1 includes a summary of observations related to EN408 and EN384 which could be a motivation for future change.

Table 1. Evaluation of EN 408 / EN384

Test	Determination of characteristic strength for structural code (EN384)	Main problems in test method (EN408)
Bending strength	Biased method, weakest cross-section loaded which gives smaller values than other standards Confusing size effect /reference size	
Tension strength	Values conservative, lower than ISO and much lower than ASTM	- needed only for glulam but testing procedure has no direct relevance to glulam strength
Compression strength	Values lower than ISO	- different from ISO, ASTM
Compression perpendicular to grain	Values much lower than ISO or ASTM	- different from others and no direct relevance to structures
Shear strength	Values low	- expensive to use: gluing of wood to steel - no direct relevance to sawn timber structures

4.0 Conclusions and recommendations

7

By showing only a few examples in this paper, it is clear that there are many issues in our European test and product standards that need to be addressed in order to make wood as competitive as possible and support innovation. These will facilitate improvements to the industry by:

> Developing and introducing swift and cost effective products
> Eliminating longwinded test programmes, replicated in various European countries
> Unifying and simplifying information on how to conduct and report the outcome of a test for the practical applications of the test result and portraying the performance of a product in its end use conditions
> Obtaining safe performance figures using appropriate safety factors.

Developing superior competitive edges for timber buildings by means of product standardisation must be a key goal. This can be achieved by:

- *Performance testing standards*
  These test standards are numerous and replicated in each European country. The work will be required to accomplish an overview of relevant testing standards throughout Europe, establish framework of tests required to enable use of product system in construction industry.

- *Basic principles and philosophy of test approaches*
  The basic principles and philosophies underlying the testing standard have to be explored in order to identify problem areas in the testing approach, such as the applicability of the test output in a real end use condition of the product. This will need to be done on a large scale, as the procedures and requirements in each European country will need to be reviewed and examined. Testing techniques, such as full-scale testing should be examined in detail to optimise the use of safety factors for timber structures and components based on reliability theories.

- *Comparison of output performance*
  Establishing the output results from a test is obviously vital. Modification factors accounting for the numbers of tests and the method of accounting for safety factors, variability and treatment of extreme test results are needed.

- *Practical value of test output*
  Each test regime is to be assessed on the practical value of the result. End use conditions, loading and exposure scenarios need to be examined. The test and its result must provide performance data relevant to end use conditions without unduly high safety factors for extrapolating the test result to final applications.

- *Compatibility with EN 1995*
  Any test result and outcome needs to be compatible with EN 1995 and vice-versa. This is very important in order to endorse the design rules and thereby remove barriers to trade throughout the European market. In the long term the regulatory framework endorsed throughout Europe will be the single most important set of design rules.

- *Improvements*
  The information on how to conduct and report the outcome of a test should be unified in simplified manner. Reporting of the test outcome need to account for the practical implications of the test result and portray the performance of a product in its end use conditions. The information extracted from the test and its impact on product design should be addressed in clear language, dwelling on basic research where required but avoiding investigations remote from practical applications.

- *Reliability*

The reliability of the test output is of paramount importance. The tests undertaken on a product or system must produce reliable product and performance results and parameters. The number of tests and the test set-up need to be designed so as to ensure reliable performance data to be extracted from them. Only then are these results of value to the industry and their products. The test outcomes must be replicable and adequately portray the expected performance of the products. The number of tests and testing scenarios to be undertaken must reflect this aim. Safety is of paramount importance. Safe performance figures using appropriate safety factors must not be compromised but have to be optimised in order not to penalize timber construction. Guidance is needed for "Design by Testing" for EN1995-1-1as the guide in EN1990 is not sufficient for timber structures.

- *Reduce cost of testing and development of products*
  To ensure a thriving and dynamic industry the development of products and their market introduction needs to be swift and cost effective. In some areas new research might need to be undertaken or confirmation will need to be sought. These areas need to be identified and the appropriate measures taken.

References

Glos, Denzler, 2003, Characteristic Shear Strength Values Based on Tests according to EN 1193.CIB W 18/36-6-1.

Leicester, Breitinger, Fordham, 1996, Equivalence of in-grade testing standards, CIB W18/29-6-2. 1996

Wang, Barrett, Lam, He, 2004, Wood product test methods and stress class systems in the world. Proceedings of the 8th World Conference on Timber Engineering, Lahti, Finland, June 14-17, 2004. Vol. II, p 167-172. ISSN 0356-9403

AS/NZS 4063, Timber - Stress-graded - In-garde strength and stiffness evaluation

ASTM D 143-1994 Standard Methods of Testing, Small Clear Specimens of Timber

ASTM D 4761-96 Standard Test methods for Mechanical Properties of Lumber and Wood-Base Structural Material

EN 384 Structural timber. Determination of characteristic values of mechanical properties and density

EN 408 Timber structures. Structural timber and glued laminated timber. Determination of some physical and mechanical properties

EN 1193 Timber structures. Structural timber and glued laminated timber. Determination of shear strength and mechanical properties perpendicular to grain.

EN 1995-1-1, 2004, Eurocode 5 - Design of timber structures, Part 1-1: General rules and rules for buildings.

ISO/AWI 8972 Solid timber - Structural classes, draft standard.

ISO/DIS 13910, Structural timber - Characteristic values of strength-graded timber - Sampling, full size testing and evaluation. Draft standard 2003.

Shear strength testing

Various specimens are used for shear testing as illustrated in Figures A1...A4.
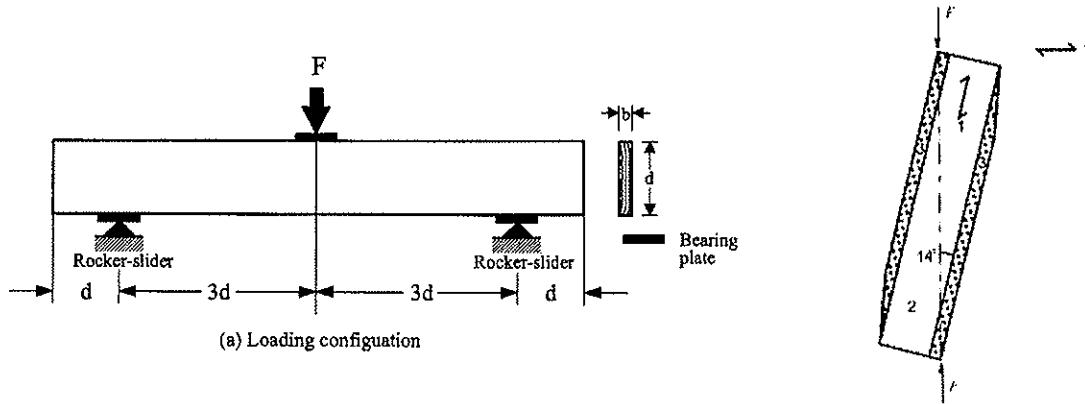
FigureA1. Shear test specimen of ISO 13910 (left) and EN 408 (right).
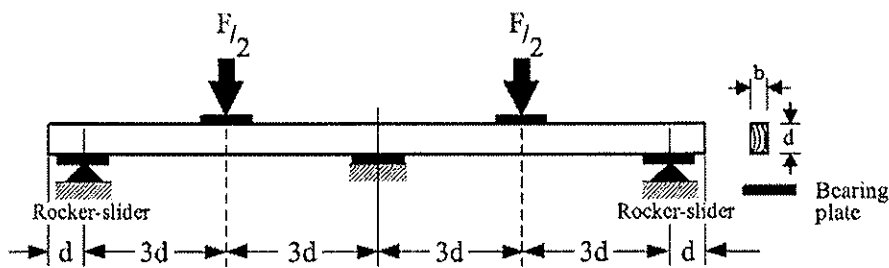
Figure A2. Double span shear test of ISO 13910.
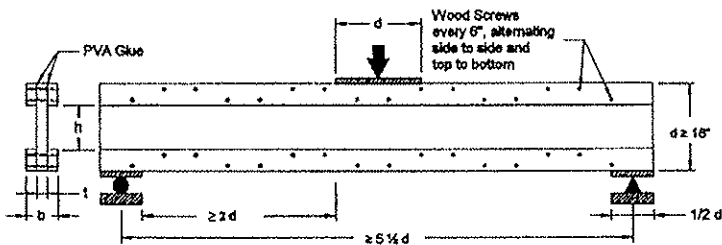
Figure A3. Shear test for structural-size PSL according to ASTM D 5456-03
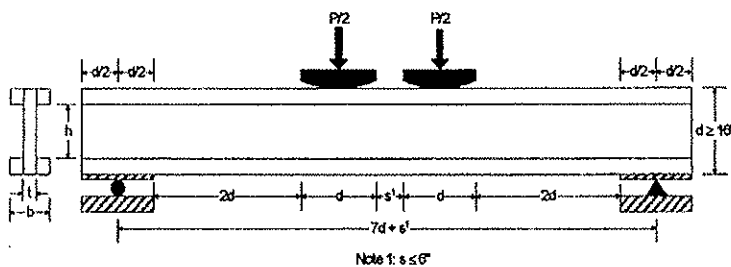
Figure A4. Shear test of structural size LVL according to ASTM D 5456-03

INTERNATIONAL COUNCIL FOR RESEARCH AND INNOVATION
IN BUILDING AND CONSTRUCTION

WORKING COMMISSION W18 - TIMBER STRUCTURES

FRAMEWORK FOR LATERAL LOAD DESIGN PROVISIONS FOR ENGINEERED WOOD STRUCTURES IN CANADA

M Popovski

E Karacabeyli

Forintek Canada Corp.

Vancouver

CANADA

Presented by M Popovski

A Ceccotti stated that the structural behaviour depends on joint behaviour and Eurocode 8 has three statements about this. A Buchanan stated that there is useful information in this paper from loading to response. A concern that specification of how to design a timber building is not well set. If all the information is to be considered, the chapter in the Canadian code will be huge. May be better to have principles rather than details in the code and give designers the freedom to provide the ductility etc. M Popovski said connection work will go into another chapter. Guidelines can be provided.

F Lam stated that the next code cycle in Canada just started. To make it into the code will probably require information in 3.5 years. He asked how much manpower and resources are needed to complete the work. M Popovski agrees the timing is tight and will start be looking at existing information. He will look for input from within Canada and other outside Canada.

B Dujic questioned about R factors and which joint will fail to dissipate energy. M Popovski stated that the factors come from committee input some have data some based on educated guesses. R factors depend on system.

R Steiger commented that forces of acceleration increase from 475 to 2500 years return. One should have concerns with existing building and may be reliability method is needed to help justify. E Karacabeyli stated that other part of the equation was also changed so that the final demand is not changed too much.

S Thelandersson stated from a non seismic country point of view capacity design concept is interesting to design robust building to promote ductility. The question becomes how to guarantee that the dowels are not too strong.

E Karacabeyli stated that in Canada small building in Part 9 and engineered building in Part 4 of the code where all material are to be treated at the same level. A Ceccotti stated that Eurocode 8 considered all these issues.

Framework for Lateral Load Design Provisions for Engineered Wood Structures in Canada

Marjan Popovski and Erol Karacabeyli

Forintek Canada Corp., Vancouver, British Columbia, Canada

1 Introduction

The main sources of lateral loads on buildings are either strong winds or earthquakes. Wind and earthquake loads, however, act in a different way on the building and impose different demands related to the strength, stiffness, and deformation properties of the building. For design purposes, a building subjected to wind loads is assumed to remain within the linear elastic range, so the stiffness and strength of the lateral load resisting system are of outmost importance. On the other hand, a building subjected to earthquake loads is expected to undergo non-linear deformations. Consequently, the seismic design process should consider a careful balance of the strength, stiffness, ductility, and energy dissipation properties of the lateral load resisting system of the structure.

Basic procedures for the design of buildings subjected to seismic and wind loads are provided in the national and international model building codes and material standards. At this point, the seismic and wind design provisions for engineered wood structures have to be improved to be competitive with those already available for structures built according to the other material standards. Design provisions are also needed to ensure that wood-based lateral load resisting systems can be combined with reinforced concrete and steel systems in hybrid structures. This paper proposes a framework for development of such enhanced lateral load design provisions for engineered wood structures in Canada.

2 Seismic design principles and building codes

The principles of the seismic design of buildings are incorporated in a unified and reasonably simple manner into many national and international codes and standards. The content of these codes and standards and how well they are implemented in design and construction significantly affects the performance of buildings during an earthquake. Most countries develop their own set of codes and standards. In Canada, for example, the National Building Code of Canada (NBCC, 1995) serves as a single model code, which can then be adopted by each province to become the legal building regulation within its jurisdiction. Other countries, such as the USA, have several building codes. In addition, regional and international codes have been developed, such as Eurocode 8 (prEN 1998-1), and that of the International Standards Organization - ISO 3010 (ISO, 2001). Some of the codes contain the particular seismic design information on timber structures (such as FEMA 368, chapter 12), while others just make a reference to the adequate wood design standard (such as the NBCC, which makes reference to CSAO86-01).

The fundamental aim of earthquake-resistant design according to most building codes is to provide structures with an acceptable level of safety for public use. This is achieved by

specifying design loads and detailing requirements so that the probability of building collapse or injury to people is acceptably low when the structure is subjected to a certain level of ground motion. For example, the NBCC uses the generally accepted approach that aims to minimize the probability of injury and loss of life by specifying design criteria according to which the structures should: (i) Withstand a minor earthquake without any damage; (ii) Resist a moderate earthquake without significant structural damage, but possibly with some non-structural damage; and (iii) Resist a severe earthquake without major failure or collapse. This approach aims to achieve a balance between the opposing requirements for safety and economy by prescribing minimum requirements for seismic design to prevent injury and death of people. This generally means prevention of collapse, but at the same time the structure may be severely damaged during an earthquake and may even have to be demolished. Thus under design objectives of life safety, if no deaths or serious injuries have occurred, such a situation could be viewed as a success. If operational readiness or immediate occupancy was the design objective, however, the same severe damage would not represent a satisfactory outcome. Similar type of objectives will form the basis of performance based seismic design that will be included in future building codes.

The most common design approach used in seismic design codes around the world is to convert the dynamic loads on buildings to equivalent static lateral loads. To obtain the equivalent static loads, the inertia forces generated during a linear elastic response of a structure with a given fundamental period, on a site with certain seismic hazard and soil conditions given by the design spectrum, are then reduced by force modification factors (e.g. R-factors in NBCC). The R-factors account for the energy absorption capacity of the structural system through damping and inelastic action during the load reversals. There is very little theoretical or experimental background for the numerical values of the R factors currently assigned to different structural systems in the codes. Consequently, the R-factors reflect the design and construction experience, along with the past performance of structures in major and moderate earthquakes, and considerable engineering judgment. Equivalent factors to the R-factors in Canada are the behaviour factor q in Eurocode 8, and the K_D factor in ISO 3010.

3 The new Canadian model code - NBCC 2005

The National Building Code of Canada (NBCC, 1995) is a model code that forms the basis for all the provincial building codes in the country. The next 2005 edition of NBCC will be published in an objective based format intended to allow more flexibility when evaluating "non-traditional" solutions. It is expected that such code will foster a spirit of innovation and create new opportunities for Canadian manufacturers. The 2005 version of NBCC includes considerable changes to how the earthquake forces are calculated. The main changes include the following (Heidebrecht, 2003):

- Seismic hazard is represented by Uniform Hazard Spectra (UHS) with 2% probability of exceedance in 50 years (2500 year return period), rather than PGA and PGV with 10% in 50 years (475 year return period);
- Explicit recognition of ductility and dependable over-strength of the structure through ductility (R_d) and over-strength (R_o) modification factors for various Seismic Force Resistant Systems (SFRS).
- Different formulas for calculating the initial period of the structure;
- Inclusion of period and site dependent effects of local soil conditions on the structural response for six categories of soil (A to F) through F_a and F_v factors;

- Recognition of elastic dynamic response analysis as the preferred approach for calculating the design forces on buildings;
- More thorough treatment of structural irregularities when calculating the seismic forces;
- Increase in storey drift limits for regular buildings from 2% to 2.5% of the storey height;

Introduction of factors R_o and R_d instead of only one R-factor is probably one of the most important changes in the 2005 edition of NBCC. Recent studies have shown that the R-factor is a function of many different parameters. Some parameters include the initial period of the structure, its ductility, the shape of the load deformation relationship, the degree of damping, the level of over-strength in the structure, characteristics of ground motion and of the P-Δ effects. From all these parameters, ductility and over-strength appear to have the largest impact on R-values (Mitchel et al., 2003). For those reasons, the 2005 edition of NBCC introduces two R-factors, an over-strength factor R_o and a ductility related factor R_d.

4 Referenced material design standards and their link to NBCC

Part 4 of the NBCC deals with structural design issues, including structural design for loads generated by winds and earthquakes. The NBCC makes references to four material design standards for further details about design of a particular structure and particular seismic force resisting systems (Figure 1). The design standards cited in NBCC include:
- Engineering design in wood – CSA O86-01 (CSA O86, 2001)
- Limit states design of steel structures – CSA S16-01 (CSA S16, 2001)
- Design of concrete structures – CSA A23.3-94 (CSA A23.3, 1994-R2000)
- Masonry design for buildings CSA S304.1-95 (CSA S304.1, 1995-R2001)
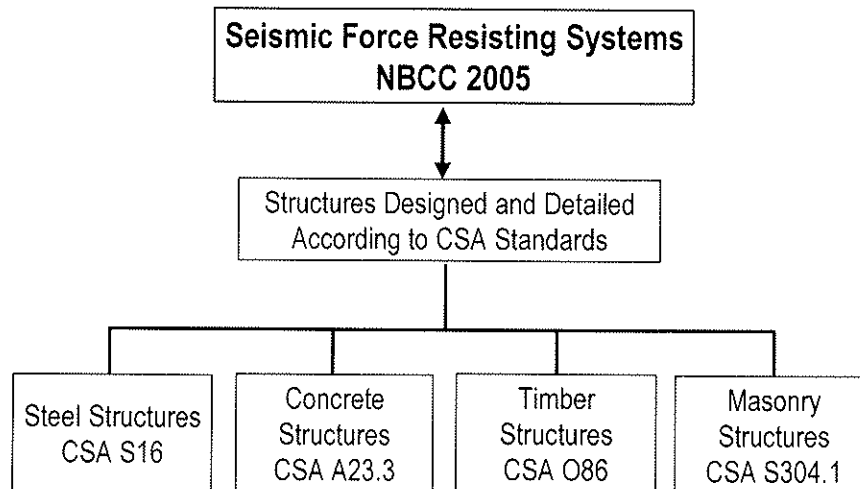
Figure 1. Links between the SFRS in NBCC and the referenced material standards

The links between the NBCC and the CSA standards for design of steel, concrete, timber, and masonry structures in the area of design of Seismic Force Resisting Systems (SFRS) are shown in Figure 1. The links can be summarized in two areas: (i) general design guidelines for ductile structures, and (ii) specific design guidelines for structures with defined ductility category in NBCC. For example Table 1 shows the R-factors that are

3

specified for reinforced concrete structural systems in the 2005 NBCC. The link of these SFRS to the adequate material design standard is made in Section 21 of CSA A23.3 under "Special provisions for seismic design". The section specifies detailed design guidelines for different lateral load resisting systems.

Table 1.   Force modification factors R_o and R_d for reinforced concrete structural systems as specified in the 2005 NBCC

Type of Seismic Force Resisting System (SFRS)	R_d	R_o
Ductile moment resisting frames	4.0	1.7
Moderately ductile moment resisting frames	2.5	1.4
Ductile coupled walls	4.0	1.7
Ductile partially coupled walls	3.5	1.7
Ductile shearwalls	3.5	1.6
Moderately ductile shearwalls	2.0	1.4
Conventional construction		
▪ Moment resisting frames	1.5	1.3
▪ Shearwalls	1.5	1.3
Other concrete SFRS not listed above	1.0	1.0

Similarly, for steel structures the link between the seismic force resistant systems specified in 1995 NBCC to the steel design standard - CSA S16-01 is made in Section 27 under "Seismic Design Requirements". Among others, this section contains the following subsections: (i) Ductile moment resisting frames R=5.0, including column design, beam and connection design; (ii) Moderately ductile moment resisting frames R=3.5; (iii) Limited-ductility moment resisting frames R=2.0, including column, beam and panel zone design; (iv) Moderately ductile concentrically braced frames R=3.0, including bracing members, brace connections, beams and columns; (v) Limited ductility concentrically braced frames R=2.0, including bracing members, brace connections; (vi) Ductile eccentrically braced frames R=4.0, including design of the brace and the link beam; (vii) Plate walls (steel shearwalls) R=5.0; (viii) Plate walls (steel shearwalls) R=2.0; and (ix) Conventional construction R=1.5. It is obvious that the design guidelines for steel structures are very detailed, even specifying the R-factor for each SFRS.

Table 2.   Force modification factors R_o and R_d for wood-based SFRS in 2005 NBCC

Type of Seismic Force Resisting System (SFRS)	R_d	R_o
Shearwalls		
▪ Nailed shearwalls – wood-based panels	3.0	1.7
▪ Shearwalls – wood-based and gypsum panels in combination	2.0	1.7
Braced or Moment resisting frames with ductile connections		
▪ Moderately ductile	2.0	1.5
▪ Limited ductility	1.5	1.5
Other wood-based SFRS	1.0	1.0

With the exception of shearwalls and diaphragms, however, details for other SFRS are not explicitly given in CSAO86-01, the standard for engineering design in wood. For example the 1995 NBCC states that nailed shear walls with plywood, waferboard or OSB panels

should be assigned an R-factor of 3.0, while concentrically braced timber frames or moment resistant frames with ductile connections should be assigned a factor of 2.0. Other timber structures with ductile connections are entitled an R-factor of 1.5. Neither NBCC nor its counterpart for timber design in Canada CSAO86-01, however, specify: (i) the specific seismic and wind design requirements for each of these systems, (ii) the ductility, strength and stiffness requirements for connections (and systems) to be classified as ductile, moderately ductile, or with limited ductility, (iii) the link between the information on the connection performance and its failure modes and corresponding system performance and failure modes. Similar remarks hold for the link of CSAO86 to the new 2005 edition of the NBCC, which introduces two force modification factors, an over-strength related factor R_o and a ductility related factor R_d (Table 2). Consequently, the Seismic Task Force of the CSAO86 Technical Committee on Engineering Design in Wood will be drafting a section on the lateral load design provisions for engineered wood structures in Canada.

5 Proposed framework for development of new design guidelines for LLRS in engineered wood construction

The framework presented here provides a viable path for the future design guidelines to be implemented in CSAO86 consistent with the existing SFRS already in place in the 2005 edition of NBCC, and the future editions of it. It is suggested that a new version of Section 9 be introduced in CSAO86 during the next code cycle, replacing the current section entitled "Shearwalls and Diaphragms". It is proposed that the new section be named "Lateral Load Resisting Systems" (LLRS) and should include the design guidelines on the LLRS subjected to wind and seismic loads. It is suggested that for the post 2005 editions of the NBCC, the wood-based LLRS be divided into three categories: (i) wood-frame systems, (ii) heavy timber frames, and (iii) hybrid systems (Figure 2). The wood-frame systems category should include nailed shearwalls with wood-based panels, shearwalls with wood-based and gypsum panels in combination, shearwalls with diagonally sheathed boards, tall walls, and other innovative wall solutions such as Midply walls. Heavy timber systems include various types of braced frames (concentrically braced timber frames, eccentrically braced timber frames, and knee-braced frames), moment resisting timber frames, and arches. The hybrid systems category should include dual systems (those that include two or more different wood-based lateral load systems), as well as concrete-wood, steel-wood, and masonry-wood hybrid systems. It should be noted, however, that changes to the framework presented in this paper are expected over time as the work on the topic intensifies.

For the next CSAO86 code cycle, it is suggested that the design guidelines on LLRS be directly linked to the systems already in place in the 2005 edition of NBCC. As a result of research projects on the seismic performance of wood shearwalls around the world and developed methodologies for assessment of the seismic design parameters for such systems (Ceccotti and Karacabeyli 2002), at this point only the design information for shearwalls and diaphragms in CSAO86 is linked to the structural systems mentioned in NBCC (link 1 in Figure 3). Other links need to be established in the future, including design solutions for the two ductility categories for braced and moment resisting frames, already mentioned in 2005 NBCC (link 2 in Figure 3). In other words, the section should clearly specify the ductility, strength and, if possible, stiffness requirements for systems to be classified as ductile, moderately ductile, or with limited ductility. Research information that can be used to fulfill some of the existing gaps regarding the seismic performance and design of braced timber frames with various connections is given in Yasamura, 1990 and Popovski, 2000.

5

Proposed Wood-Based Lateral Load Resisting Systems for NBCC 2010

Wood-frame Systems

- Nailed shearwalls with wood-based panels
- Shearwalls with wood-based and gypsum panels in combination
- Shearwalls with diagonally sheathed boards
- Tall walls
- Midply walls

Heavy Timber Systems

- Concentrically braced timber frames
- Eccentrically braced timber frames
- Knee-braced frames
- Moment resisting timber frames
- Arches
- Other systems

Hybrid Systems

- Wood–Wood (heavy timber and shearwalls)
- Concrete-Wood
- Steel-Wood
- Masonry–Wood

Figure 2. Categories of wood-based Lateral Load Resisting Systems suggested for future editions of NBCC

Seismic Force Resisting Systems NBCC 2005

Shearwalls
- Wood-Based
- Wood & Gypsum

Braced Frames

Moment Frames

Other Systems

Ductility Categories
- Moderately Ductile
- Limited Ductility

(1) (2) (3)

CSA O86 - Wood Structures
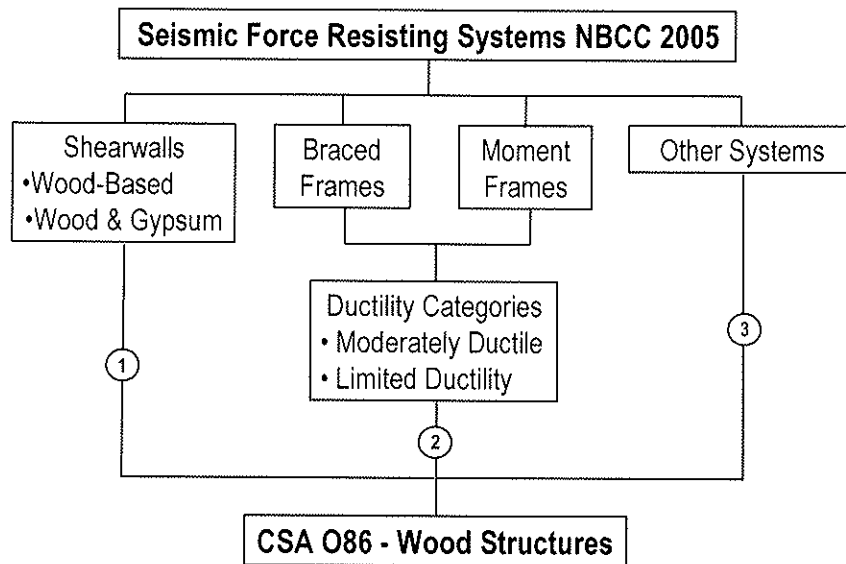
Figure 3. Current and future links between the Seismic Force Resisting Systems in CSAO86 and NBCC

Since the performance of connections and their failure modes directly influence the corresponding system performance and system failure modes, the information in the new Section 9 on LLRS should be closely linked to the information in Section 10 – Fastenings. It is suggested that the section on Fastenings be renamed to "Connections", raising the importance of the entire connection as a primary working unit within in the structural system. The Connections Section should include information on properties such as strength, ductility, ductility categories, and permissible failure modes for various types of loading, for various connections in wood and engineered wood products. Stiffness values for various connections are also of high importance, however, it will be difficult to

6

implement them during the next code cycle. This enriched Connections section with information on capacities and corresponding failure modes for various connections, will help establish capacity and performance-based design procedures for various LLRS in the future.

A hypothetical example on how the design information in both sections of CSAO86 (section 9 on LLRS, and section 10 on Connections) should be linked is shown in Figure 4. For example, some bolted connections with stocky bolts in glulam loaded parallel to grain may be treated as connections with ductility category of 2, and can thus satisfy the ductility demand for structural systems with limited ductility. On the other hand, connections with timber rivets subjected to bending moments (as expected in moment resistant connections) can be assigned a ductility category of 4, and can thus satisfy the structural demand of highly ductile structural systems.
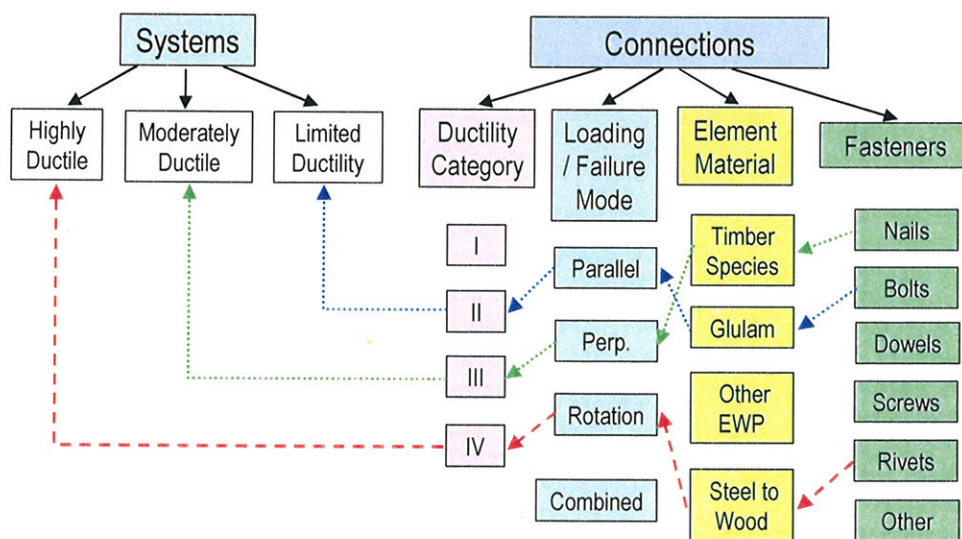
Figure 4. Examples of the proposed link of design information in CSAO86 between the Section on LLRS (section 9) and the Section on Connections (section 10)

Introduction of structural systems such as braced frames, moment resisting frames, tall walls, and some other innovative systems, may sometimes require use of proprietary engineered wood products and proprietary or innovative connections. Although the traditional focus of CSAO86 has been to include design methods applicable to buildings constructed with generic materials and fasteners, inclusion of design methods for proprietary materials and connections should be allowed. It should be noted, however, that there is a need for a consistent set of practices related to determination of factored (design) resistances of connections in generic and proprietary wood materials, and connections made with proprietary fasteners.

In the seismic design of structures in general, the concept of capacity design is of major importance. This design approach is based on the simple understanding of the way a structure sustains large deformations under severe earthquakes. By choosing certain modes of deformation, we can ensure that the brittle elements have the capacity to remain intact, while inelastic deformations occur in selected ductile elements. These ductile elements act as fuses or energy absorbers and help to reduce the force levels on the structure. It is important to have these ductile locations distributed in the structure at strategic locations so that the vital parts of the lateral resistant system are not destroyed during the seismic

7

response. Although this method has been used for a number of years in the design of reinforced concrete and steel structural systems, so far it has not been introduced to timber-based structural systems.

Capacity design can be introduced in the future design guidelines for wood-based structural systems in an explicit or implicit way. In either way, when adopted, certain issues have to be addressed. The failure of wood members in tension or bending is not favourable because of its brittle characteristics. Therefore, when applying the capacity design for wood structures, the potential of the wood to absorb energy in compression perpendicular to grain has to be exploited. The LLRS have to be designed using ductile connections that are weaker than the wood members they connect so the connections can fail before the structural members in the case of a strong seismic event (Popovski et al., 1999). In some current design practices for wood-based structural systems, the opposite is actually true. There is a tendency to produce over-designed connections in comparison to the members. Weaker ductile connections are also needed because they are the only significant sources of ductility and energy absorption in the system during the seismic response. The connection failure, however, should be of a controlled and predictable type, and eventual connection failure should not result in a structural collapse. The current design procedures, except for timber rivets, do not provide information on the intended failure mode of specific connections. Finally, the seismic design should assure existence of a number of different load paths in the structure able to transfer the inertial forces induced on the structure down to the foundation.
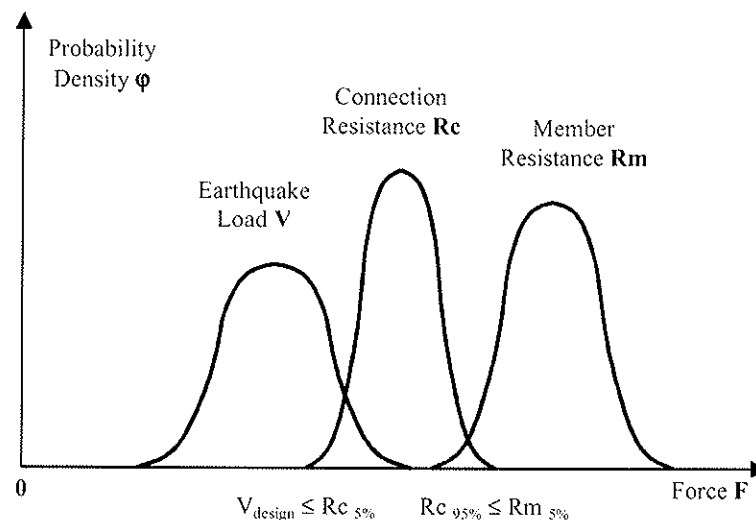
Figure 5. Graphical presentation of the logic behind the capacity design procedures

In cases when the design provisions for connections are more conservative than those for the wood members in a wood design standard, the capacity design concept might be difficult to apply without changing the philosophy for deriving the design values for both, the structural members and the connections (Chui Y. H. and Smith I., 1993). As shown in Figure 5, values for both lower and upper characteristic strength of connections is required for establishing the capacity design procedures. The capacities of properly designed connections can be less variable than those of the wood members they connect. In the case of engineered wood products, that difference will be much lower. By using a capacity design philosophy, connections with more uniform strength and consistent failure mode properties will lead to more economical design solutions for the structural systems.

8

When introducing a new section on seismic design of wood-based structural systems, it should be anticipated that the design practices on a system level in general would soon move toward performance-based procedures. Implementation of performance-based procedures for structural systems will require implementation of similar design procedures on a connection level, for which an evaluation protocol and general performance requirements for adequate connection and system behaviour should be developed.

The tendency to move from deterministic mechanics-based system and connection models to reliability-based ones should also be anticipated in the future. Although on numerous occasions it has been proven that mechanics-based models provide a good approximation of the average capacity and deformation of a structural system (or a connection), knowing the average properties will not be sufficient for deriving the design resistances. For reliability-based design, the variance (variability) of the characteristic resistances must also be known. In addition, the appropriate choice of the reliability indices for structural systems, members, and connections, has to be chosen to satisfy the design and performance-based requirements. The research work of Ceccotti and Foschi (1999) is an example of a reliability-based evaluation of the seismic design procedures for wood shearwalls according to NBCC.

Although numerous research activities in the field of wood-based lateral load resisting systems and connections have been conducted throughout the world, a significant amount of new, well coordinated, research is still needed, to fill the knowledge gaps that currently exist. A strong cooperation between researchers, the engineering community and regulatory representatives is vital for successful delivery and implementation of the design guidelines.

7 Conclusions

This paper proposes a framework for establishment of a new lateral load design section in the Canadian Standard for Engineering Design in Wood (CSAO86) to respond to the changes already in place in the 2005 edition of the National Building Code of Canada (NBCC). The proposed section includes subsections on structural systems such as shearwalls and diaphragms, heavy frames (braced and moment resisting frames), and hybrid (mixed) systems, with their appropriate R-factors. The information on structural performance of the lateral load resisting systems should be linked to the performance of connections used in such systems. In order to better quantify the connection behaviour, design provisions for brittle and ductile failure modes for connection under static and dynamic loads should be developed in the corresponding design section for connections. Based on the connection performance, the connection section should also establish ductility categories for connections. In principle, the design procedures should move towards adopting capacity design procedures for lateral load resisting systems. Finally, there should be an effort to find a way to implement innovative connection and structural system solutions in CSAO86. This will provide designers with more options regarding the structural system when designing engineered wood-based or hybrid buildings.

8 References

Ceccotti, A., Foschi, R. O. 1999. Reliability assessment of wood shear walls under earthquake excitation. Proceedings of the Third International Conference on Computational Stochastic Mechanics. Santorini, Greece.

Ceccotti, A., Karacabeyli, E. 2002. Validation of seismic design parameters for wood-frame shearwall systems. Canadian Journal of Civil Engineering. 29: 484-498.

Chui, Y.H., Smith, I. 1993. Proceedings of the Canadian Society for Civil Engineering, Annual Conference, Fredericton, N.B. 365-374.

CSA S304.1-95 R2001. Canadian Standards Association Standard S304.1 Masonry Design for Buildings (Limit States Design), CSA, Toronto, Ontario, Canada.

CSA A23.3-94 R2000. Canadian Standards Association Standard A23.3 - Design of Concrete Structures, CSA, Toronto, Ontario, Canada.

CSA O86-01. 2001. Canadian Standards Association Standard O86 - Engineering Design in Wood. CSA, Toronto, Ontario, Canada.

CSA S16-01. 2001. Canadian Standards Association Standard S16 - Limit States Design of Steel Structures, CSA, Toronto, Ontario, Canada.

EN 1995-1-1:2004. EUROCODE 5 - Design of Timber Structures, Part 1-1: General – Common Rules and Rules for Buildings. European Committee for Standardization, Brussels, Belgium.

FEMA-368, 2000. NEHRP Recommended Provisions for Seismic Regulations for New Buildings and other Structures. Part 1 Provisions. Federal Emergency Management Agency, Washington, DC.

Heidebrecht, A. C. 2003. Overview of seismic provisions of the proposed 2005 edition of the National Building Code of Canada. Canadian Journal of Civil Engineering. 30: 241-254.

ISO 3010. 2001. Basis for design of structures – Seismic actions on structures. An international standard, ISO, CEN European Committee for Standardization, Brussels, Belgium.

Mitchel, D., Trembley, R., Karacabeyli, E., Paultre, P., Saatcioglu, M., Anderson, D. 2003. Seismic force modification factors for the proposed 2005 edition of the National Building Code of Canada. Canadian Journal of Civil Engineering. 30: 308-327.

NBCC 1995. National Building Code of Canada. Canadian Commission on Building and Fire Codes, National Research Council of Canada, Ottawa, Ontario.

Popovski, M. 2000. Seismic performance of braced timber frames. A thesis submitted in partial fulfillment of the requirements the degree of Doctor of Philosophy, University of British Columbia, Canada.

Popovski, M., Prion, H. G. L., Karacabeyli, E. 1999. Braced timber frames as lateral load resistant system. Proceedings of PTEC'99 International Conference on Timber Engineering, Rotorua, New Zealand.

PrEN 1998-1:200X. EUROCODE 8. Draft 6, 2003. Design of structures for earthquake resistance, Part1: General rules, seismic actions and rules for buildings; European Committee for Standardization, Brussels, Belgium.

Yasumura, M. 1990. Seismic behaviour of braced frames in timber construction. Proceedings of meeting twenty-three of The International Council for Building Research Studies and Documentation, Working Commission W18A-Timber Structures. (23-15-4). Lisbon, Portugal.

INTERNATIONAL COUNCIL FOR RESEARCH AND INNOVATION
IN BUILDING AND CONSTRUCTION

WORKING COMMISSION W18 - TIMBER STRUCTURES

DESIGN OF SHEAR WALLS WITHOUT HOLD-DOWNS

Chun Ni

E Karacabeyli

Building Systems Department, Forintek Canada Corp.

CANADA

Presented by Chun Ni

B Dujic commented that the vertical acceleration from earthquake may counteract the downward force that you are counting on. C Ni responded that this was considered in another paper as wind uplift load. B Griffith agrees with the findings in general and questioned that the testing deals with long panels without openings and how to treat such cases in design. C Ni answered that the sections with opening are ignored. B Griffith questioned how the 0.6 to 2.4 m length to determine vertical load is applied to the shorter panels. C Ni responded that the effective length is set no longer than wall height.

Design of Shear Walls Without Hold-Downs

Chun Ni and Erol Karacabeyli

Building Systems Department, Forintek Canada Corp., Canada

Abstract

Hold-down connections are often used to resist the uplift loads induced by wind or earthquake loads in wood-frame construction. When there is excess amount of walls available to resist these lateral loads, hold-down connections, are not always used in conventional wood-frame construction, particularly at the end of wall segments near door and window openings. In earlier editions of Canadian Standard for Engineering Design in Wood (CSA O86) and in other design codes, hold-down (or tie-down) connections were required, in designing wood-frame nailed shear walls, at the ends and around openings of a shear wall to provide restraint against overturning moment. To provide guidance for the design of shear walls without hold-downs, a mechanics-based approach was developed and implemented in the 2001 edition of the CSA O86. In this paper, this mechanics-based approach is presented. Implementation of the mechanics-based method with complete load path in the CSA O86 is also discussed.

1   Introduction

Nailed shear walls are the primary vertical structural elements to resist lateral loads in platform-frame wood construction. In designing shear walls, hold-down (or tie-down) connections are often used to resist the uplift loads induced by wind or earthquake loads in wood-frame construction. For example, in earlier editions of Canadian Standard for Engineering Design in Wood (CSA O86), lateral load capacities were provided only for those shear walls where hold-down connections are used or dead loads are sufficient to prevent overturning moment.

Hold-down connections, on the other hand, are not always used in conventional wood-frame construction. In such case, if dead loads are not sufficient to prevent the overturning moment, nails along the bottom plate at the tension end take the uplift forces due to the overturning moment, and as a result the lateral load capacity of the shear wall is reduced. Because of this, there is a need to quantify the effect of overturning restraints on the lateral load capacity of a shear wall without hold-downs. Ni et al. (2000, 2002a & 2002b) and Källsner et al. (2001, 2002, 2004a and 2004b) have independently developed a mechanics-based approach to account for the effects of uplift restraint on the performance of shear walls. In this paper, this mechanics-based approach and comparison to test results are presented. Implementation of the mechanics-based method with complete load path in the CSA O86 is also discussed. This method may also be instrumental in refining current design methodologies for shear walls in other wood design codes.

2   Mechanics-Based Method

Figure 1 shows a shear wall with partial uplift restraints (force P). For studs where two panels meet, with the assumption that the forces from nails on either side of the gap act vertically and opposed to each other, the studs work only as splice plates that transfer the shear from one panel to another through the nail joints. Because the nail forces from adjacent panels "cancel each other", no appreciable axial force would be generated in the studs. However, the nail forces at the end studs do not "cancel out" so the end studs must carry the resulting axial force that must be transferred to the foundation. For an end stud under compression, the force is directly supported by foundation. For an end stud in tension without a hold-down connection, the force is resisted by nail joints attaching the edge of the panel to the bottom plate. Assuming that the shear wall reaches its lateral load capacity when all nails along the bottom plate reach their own load capacity C_N, based on force equilibrium, the following equations can be obtained:
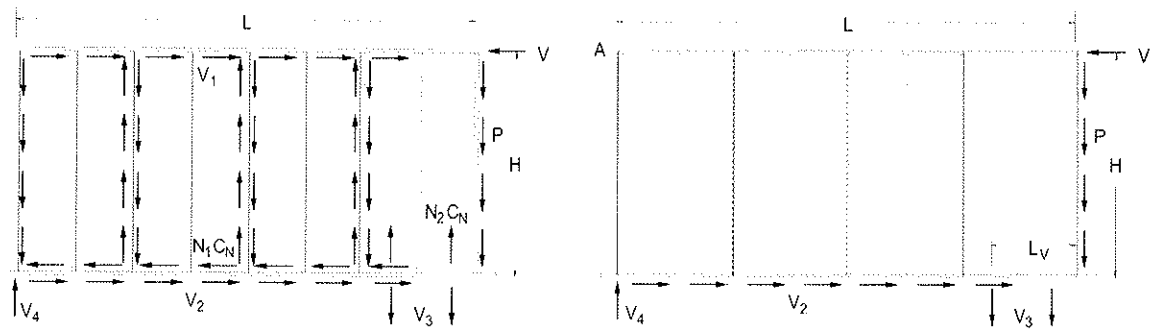
| a) Forces on wood frame members | b) External forces on wall segment |

Figure 1   A simplified model for shear walls without overturning restraints

$$V_2 = N_1 C_N \tag{1}$$

$$V_3 = N_2 C_N \tag{2}$$

$$V_2 H = V_3 (L - \frac{L_v}{2}) + PL \tag{3}$$

where

H -- height of the wall

L -- length of the wall

L_v -- length of bottom plate where the nails are required to resist the vertical tension force

N_1 -- number of nails resisting lateral load along bottom plate

N_2 -- number of nails resisting vertical tension force along bottom plate over length L_v

C_N -- lateral load capacity of a single nailed joint

P -- uplift restraint force on the end stud of a shear wall segment

For a shear wall segment in a given storey, the uplift restraint force, P is the resultant of the following forces: a) resultant vertical force from upper storeys (negative if it is a net uplift force); b) forces due to dead weight, corner framing or sheathings above and below openings in that storey.

Assuming N is the total number of nails along the bottom plate, then the N_1, N_2, and L_v have the following relations

$$N_1 + N_2 = N \tag{4}$$

$$\frac{L - L_v}{N_1} = \frac{L_v}{N_2} = \frac{L}{N} \tag{5}$$

Based on the Equations 1, 2, and 5, Equation 3 can be rewritten as

$$N_1 H = N_2 (L - \frac{N_2}{2N} L) + \frac{PL}{C_N} \tag{6}$$

Assuming M is the total number of nails along the end stud of a particular shear wall segment, then $M \cdot C_N$ would be the unbalanced uplift force at the wall's shear capacity, and parameter $\phi = \frac{P}{MC_N}$ can be defined as an uplift restraint effect. Parameter ϕ will equal 1.0 if the uplift restraint is large enough to prevent the end stud uplift at the ultimate shear wall capacity.

Let $\alpha = \frac{N_1}{N}$, $\beta = \frac{N_2}{N}$, and $\gamma = \frac{H}{L}$, where parameter α is the ratio of the lateral load capacity of walls with partial uplift restraint compared to the capacity of walls with full uplift restraint. Parameter γ is the aspect ratio of the shear wall segment. Equation 6 can be rewritten as

$$\alpha \gamma = \beta (1 - \frac{1}{2} \beta) + \phi \gamma \tag{7}$$

Since $\alpha + \beta = 1$ (Equation 4), α is then obtained from Equation 7 as

$$\alpha = \sqrt{1 + 2\phi\gamma + \gamma^2} - \gamma \tag{8}$$

Figure 2 shows the effect of uplift restraint on the lateral load capacity of a wall, based on Equation 8. It is clear that both the aspect ratio and the uplift restraint influence the lateral load capacity of shear wall. The shorter the shear wall, the greater the influence from uplift restraint.

3
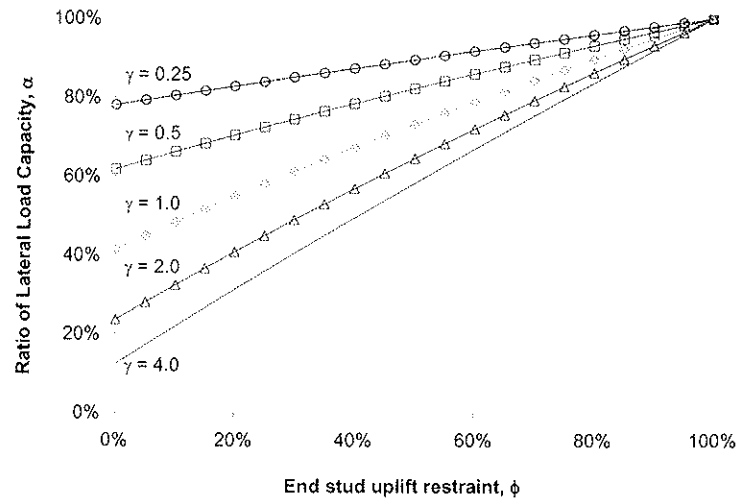
Figure 2   Effect of uplift restraint on the lateral load capacity of a shear wall

3   Verification of Mechanics-Based Method

3.1   Tests of Shear Walls

Two groups of full-scale shear walls were tested under monotonic and reversed cyclic tests. The details of the shear walls can be found in (Ni and Karacabeyli 2000). The testing program was designed to evaluate the effect of shear wall length and vertical load on the performance of shear walls without hold-downs. Shear wall frames were constructed using NLGA No. 2 and better grades of Spruce-Pine-Fir 38mm × 89mm (2 in × 4 in) lumber for the wall studs, and 1650f-1.5E MSR 38mm × 89mm (2 in × 4 in) lumber for the top and bottom plates. Stud members were spaced at 400mm on center. Canadian Softwood Plywood (CSP), 9.5mm thick, was used for the sheathing panels. The sheathing panels were connected to the framing members with 8d common nails at nail spacing of 150 mm around the panel perimeter, and 300 mm elsewhere. Conditioning and testing were performed at ambient laboratory conditions where average oven-dry moisture content of both lumber and the plywood were approximately 9%. The average oven-dry relative density of the lumber was approximately 0.44.

The bottom plates of the walls were attached to the foundation using 12.7 mm (1/2 inch) diameter anchor bolts spaced at 406 mm on center. The distance between the center of the first anchor bolt and the outer edge of the wall was 203 mm. The same anchorage was used between the double top plates and the load spreader. The walls with hold-down connections used commercially available hold-downs attached to the double end studs with two 15.9 mm (5/8 inch) diameter bolts, and to the foundation with one 15.9 mm (5/8 inch) bolt.

Test results are summarized in Tables 1 and 2. As expected, the ultimate unit lateral load capacities were similar for shear walls with different wall lengths when hold-downs were installed. The ultimate unit lateral load capacity was found strongly influenced by the wall

4

aspect ratio (height/length) when the shear walls were built without hold-downs and tested without vertical load. The unit lateral capacity varies inversely with the wall aspect ratio. The end studs of the walls with no hold-downs and vertical loads almost completely separated from the bottom plate at large displacements. Without hold-downs, the lifting force strove to draw the panel apart from the bottom plate and force the nails to act almost perpendicular to the edge of the panel. This redistribution of the nail forces resulted in a lower load capacity for the shear wall.

Table 1 A summary of test results of shear walls with different wall lengths.

Wall length (m)		With hold-down				Without hold-down		
		No. of Tests	P_{max} [1] (kN/m)	Δ_u [2] (mm)	K [3] (kN/m/mm)	No. of Tests	P_{max} [1] (kN/m)	Δ_u [2] (mm)	K [3] (kN/m/mm)
1.22	Ramp	2	8.5	114	0.428	2	2.9	46	0.491
	1st [4]	2	8.7	99	0.425	2	3.0	39	0.524
	3rd [5]		7.2	87	0.546		2.5	43	0.615
2.44	Ramp	2	8.9	85	0.899	2	5.0	31	0.773
	1st [4]	2	8.7	71	0.878	2	5.1	28	0.818
	3rd [5]		6.9	57	0.993		4.2	28	0.944
4.88	Ramp	2	7.4	106	0.861	2	6.9	46	0.925
	1st [4]	2	8.3	73	1.058				
	3rd [5]		6.6	59	1.206				
4.88	Ramp	1	9.1	77	0.598	1	5.8	44	0.544
	1st [4]	1	8.0	50	0.913	1	5.3	38	0.638
	3rd [5]		6.6	40	0.882		4.6	31	0.721

Note: No vertical load applied.

[1] P_{max} is the average value of maximum unit lateral load.

[2] Δ_u is the average value of ultimate displacement, which is defined as the displacement at 80% of maximum load on the descending portion of the load-displacement curve.

[3] K is the average value of the secant stiffness between 10% and 40% of the maximum load.

[4] Average of the first envelope in the reversed cyclic test.

[5] Average of the third envelope in the reversed cyclic test.

Table 2 A summary of test results of 2.44 m shear walls with different vertical loads.

Vertical load [1] (kN/m)	With hold-down				Without hold-down			
	No. of Tests	P_{max} (kN/m)	Δ_u (mm)	K (kN/m/mm)	No. of Tests	P_{max} (kN/m)	Δ_u (mm)	K (kN/m/mm)
0.0	2	8.7	88	0.560	2	4.6	43	0.628
4.6					2	7.0	85	0.507
9.1					2	7.4	103	0.521
13.7					2	8.5	109	0.511
18.2	2	9.0	107	0.640	2	8.7	111	0.568

[1] Constant vertical loads were applied by two hydraulic actuators, at a distance of 609 mm from the edge of the wall, as point loads on the load spreader which was attached to the double top plates.

The ultimate displacements of shear walls were also greatly influenced by the hold-downs. For shear walls without hold-downs, the ultimate displacement was less than 50% of the ultimate displacement reached by a shear wall with hold-downs. This negative impact on ultimate displacement however was compensated by the vertical loads which had a large influence on the unit lateral load capacity of shear walls without hold-downs. By applying a vertical load of 18.2 kN/m, which was sufficient to resist the overturning moment, the shear wall was able to reach its full lateral load capacity. Without the vertical load, the unit lateral load capacity of the 2.44 m shear wall was only about 50% of the capacity of shear

wall with hold-downs. With a vertical load of 4.6 kN/m, the unit lateral load capacity of a 2.44 m shear wall reached to 80% of its full capacity. The rate of increase in lateral load capacity decreased as the applied vertical loads increased. The ultimate displacement follows a similar trend as the lateral load capacity.

3.2   Test Results Versus Predictions

Comparison of the lateral load capacities obtained from the tests and mechanic-based method is presented in Figure 3. Predictions based on mechanics-based method are in reasonable agreement with the test data. For all the cases, the mechanics-based method is more conservative than the test results. For walls tested under reversed cyclic loads, the prediction applies to both first and third (stabilized) envelope curves.

a) Shear walls with different wall lengths   b) Shear walls with different vertical loads
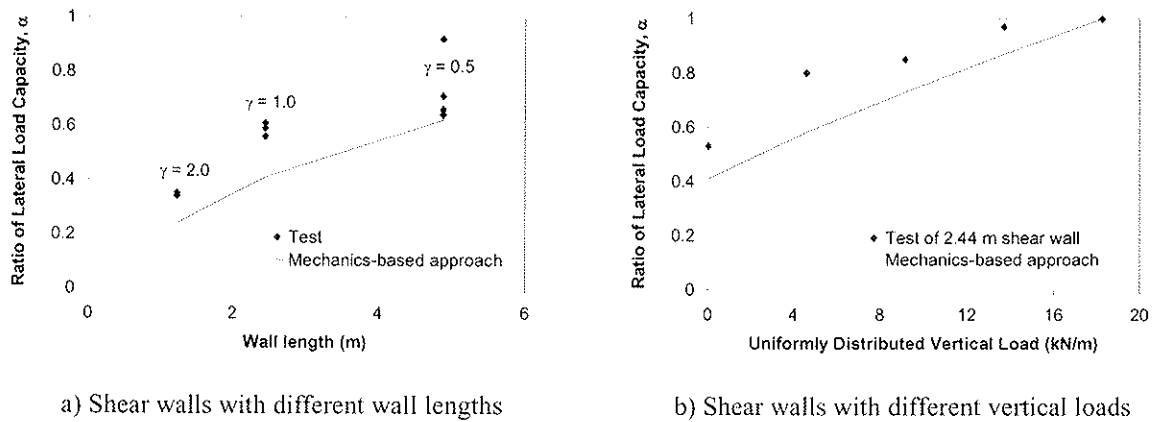
Figure 3   Comparison of measured and calculated lateral load capacities of shear walls

4   Code Implementation

The mechanics-based method presented in this paper has been implemented in the 2001 edition of the Canadian wood design code CSA O86-01 (Canadian Standard Association 2001). By introducing the ratio of the lateral load capacity, α, in Equation 8 as Hold-down Effect Factor J_{hd}, the lateral load capacity of a shear wall, either with or without hold-downs, can be calculated. For shear walls with hold-down connections designed to resist the uplift forces due to over-turning, the J_{hd} factor is considered as being unity. For shear walls without hold-down connections, the J_{hd} factor is determined by

$$J_{hd} = \sqrt{1 + 2\frac{P}{V_{hd}} + \left(\frac{H}{L}\right)^2} - \left(\frac{H}{L}\right) \leq 1.0 \qquad (9)$$

where:

P   = factored uplift restraint force, which is the sum of resultant force from upper story (negative if it is a net uplift force) and forces due to dead weight in the storey of analysed shear walls;

V_{hd} = factored shear resistance of the shear wall calculated with J_{hd} = 1.0;

H   = height of shear wall segment;

6

L   = length of shear wall segment.

To illustrate how to calculate the J_{hd} factor and the load path for shear walls between stories, an example of typical shear walls in a two-storey building is provided in Figure 4. In this example, hold-down connections are not used in both the shear walls in the first and second storeys. The overturning restraints due to sheathing above and below the openings are ignored. The lateral load capacity is determined as the sum of the lateral load capacities of full-height shear wall segments. This is compatible with traditional engineering approach for calculating the lateral load capacities of shear walls with openings.

$$P_{top21} = q_2 \frac{L_1}{2} + q_2 \frac{L_3}{2}$$

$$P_{21} = P_{top21} + q_{w2} \frac{L_1}{2}$$

$$R_{21} = F_{21} \frac{H+h_2}{L_1} - P_{21}$$

$$P_{top22} = q_2 \frac{L_2}{2}$$

$$P_{22} = P_{top22} + q_{w2} \frac{L_2}{2}$$

$$R_{22} = F_{22} \frac{H+h_2}{L_2} - P_{22}$$

$$P_{top11} = q_1 \frac{L_1}{2} + q_1 \frac{L_3}{2} - R_{21}$$

$$P_{11} = P_{top11} + q_{w1} \frac{L_1}{2}$$

$$R_{11} = F_{11} \frac{H+h_1}{L_1} - P_{11}$$

$$P_{top12} = q_1 \frac{L_2}{2} - R_{22}$$

$$P_{12} = P_{top12} + q_{w1} \frac{L_2}{2}$$

$$R_{12} = F_{12} \frac{H+h_1}{L_2} - P_{12}$$
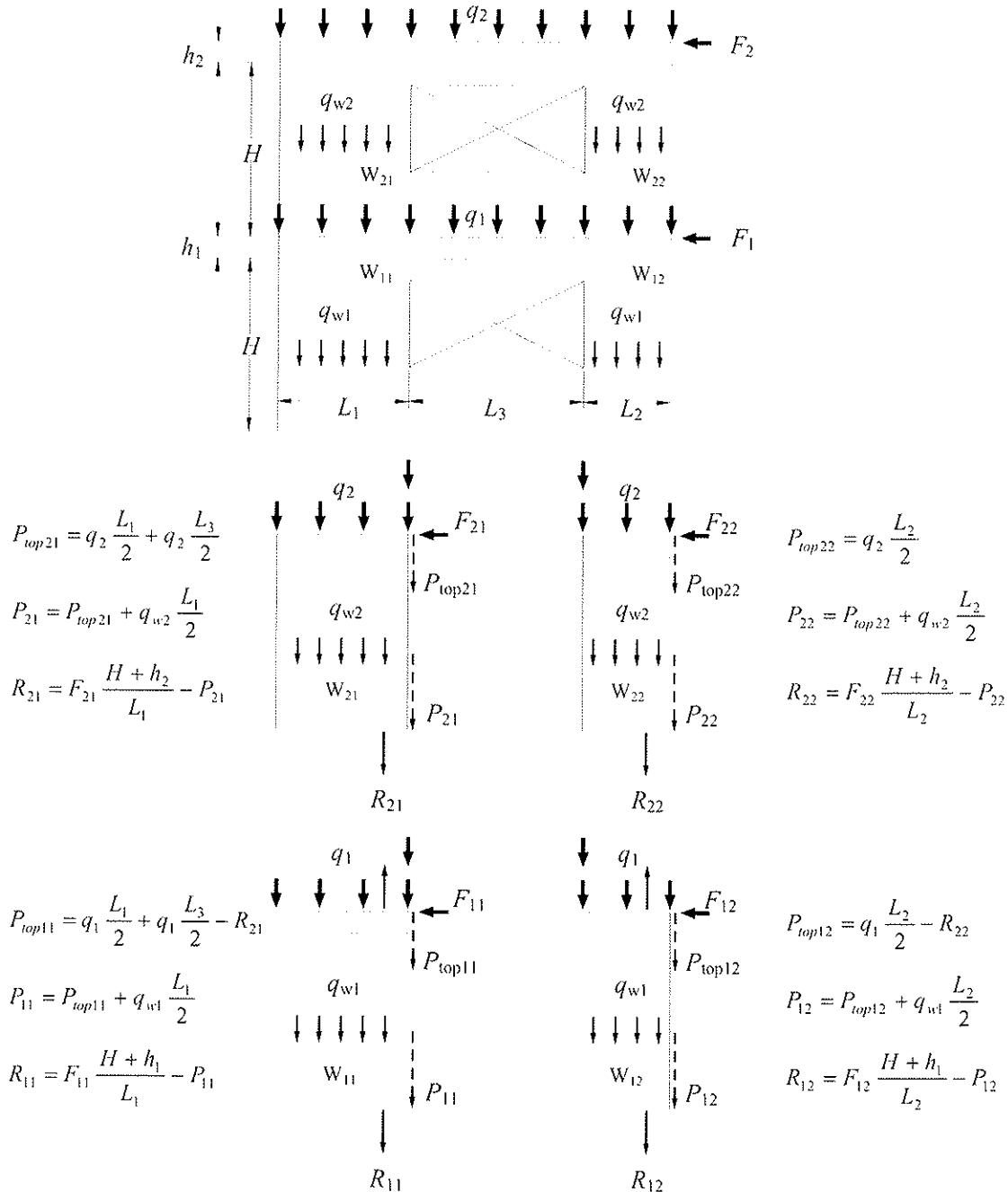
Figure 4   Load path diagram of multi-story shear walls

7

In this example, it is assumed that the factored lateral load exerted to each wall segment is proportional to the factored shear resistance of that shear wall segment. Therefore, the factored uplift restraint forces in wall segments 1 and 2 of the second storey are respectively

$$P_{21} = q_2 \frac{L_1}{2} + q_2 \frac{L_3}{2} + q_{w2} \frac{L_1}{2} \qquad (10)$$

$$P_{22} = q_2 \frac{L_2}{2} + q_{w2} \frac{L_2}{2} \qquad (11)$$

The resultant overturning forces in wall segments 1 and 2 are respectively

$$R_{21} = F_{21} \frac{H + h_2}{L_1} - P_{21} \qquad (12)$$

$$R_{22} = F_{22} \frac{H + h_2}{L_2} - P_{22} \qquad (13)$$

Where factored dead loads are not sufficient to prevent overturning, anchorage on the bottom plate within 300 mm from both ends of the shear wall segment is required to transfer the uplift force to the top plate of the shear wall below.

The factored uplift restraint forces and factored overturning forces in wall segments 1 and 2 of the first storey can be similarly derived. Where factored dead loads are not sufficient to prevent overturning, anchorage on the bottom plate within 300 mm from both ends of the shear wall segment is required to transfer the uplift force to the foundation.

For shear walls with partial restraints, formulae for determination of displacements were developed and can be found in Ni and Karacabeyli (2004).

5   Discussion

5.1   Seismic Force Modification Factor

In the National Building Code of Canada (NBCC, 1995), the seismic force modification factor, R, is assigned a value of 3.0 for nailed wood shear walls where hold-downs are used or dead loads are sufficient to prevent overturning moment. This factor is primarily used to characterize the ability of the structure to undergo deformations beyond yielding. For shear walls with no hold-downs, it is noticed from the shear wall tests that the ultimate displacement of the shear wall without vertical loads is only about 50% of the displacement of the shear wall with hold-downs. This indicates that a lower force modification factor for such walls should be used. However, with a vertical load of 4.6 kN/m that counteracts approximately 25% of the overturning moment, the displacement of the shear wall was able to reach 80% of the ultimate displacement of a fully restrained

shear wall. Therefore, in order to use R of 3.0, it is recommended that the uplift restraint force should counteract at least 25% of the overturning moment.

5.2 Determination of Uplift Restraint Force

In calculating the J_{hd} factor, there is a question of how much of the dead load applied along the shear wall and transverse walls could be counted as uplift restraint force. Studies conducted by Andreasson (2000) provide some insight on this issue. Depending on the in-plane stiffness of the shear wall, the uplift restraint force is the dead load over somewhat between half the stud spacing and half the wall length (Figure 5). Similarly, where dead load is applied on transverse wall, the uplift restraint force is the dead load over somewhat between half the stud spacing and half the wall length to the stud to which shear wall is connected (Figure 6).
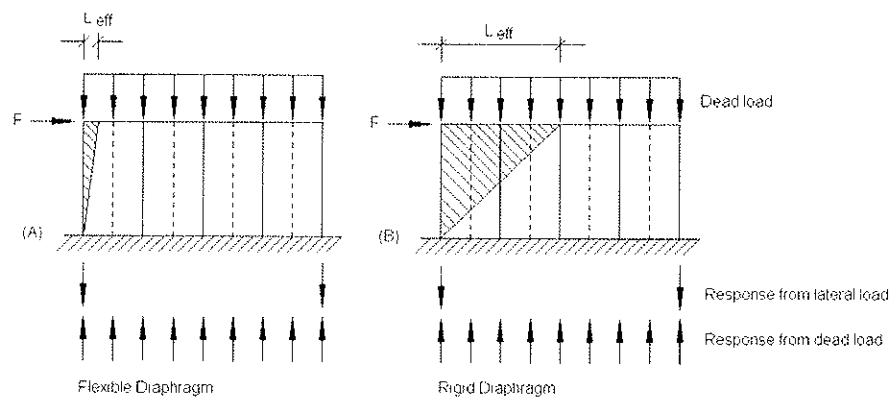
Figure 5   Distribution of dead load if the wall is regarded as: a) flexible, and b) rigid reproduced from (Andreasson 2000)
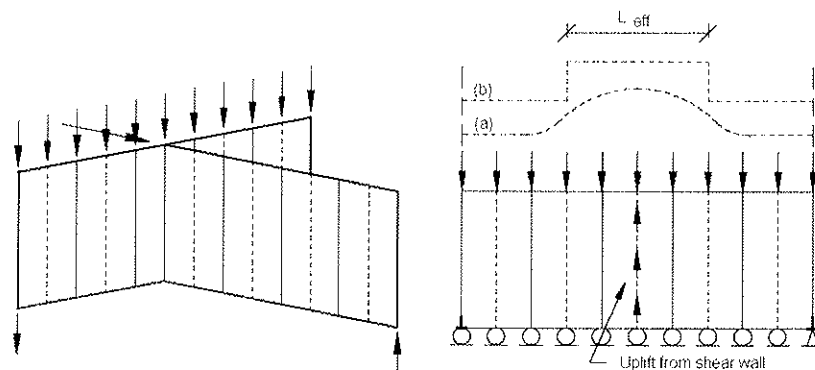
Figure 6   Distribution of dead load of a transverse wall reproduced from (Andreasson 2000)

6   Conclusion

A mechanics-based method to quantify the effect of overturning restraints on the lateral load capacity of a shear wall without hold-downs is presented. Predictions based on the mechanics-based method are in reasonable agreement with the test data. For all the cases,

9

predictions based on the mechanics-based method are conservative when compared to the test results.

Implementation of the mechanics-based method with complete load path in the CSA O86 is also discussed. By taking into consideration of dead load and shear walls without hold-downs, the design provisions give engineers more options in the design of shear walls. As it is compatible with traditional shear wall design methodology, it is easier for design professionals to use the new method. This method will also shed light on explaining the superior performance of small wood buildings in past earthquakes, and on refining current design methodologies for shear walls in other wood design codes.

References

Andreasson, S., 2000. Three-dimensional interaction in stabilisation of multi-storey timber frame building systems. Report TVBK-1017, Division of Structural Enineering, Lund University, Sweden.

CSA, 2001. Engineering Design in Wood. Standard CSA O86-01, Canadian Standards Association, 178 Rexdale Boulevard, Etobicoke, Ont.

Källsner, B., Girhammar, U.A., Wu, L., 2001. A simplified plastic model for design of partially anchored wood-frame shear walls. Proceedings CIB-W18 Meeting, Venice, Italy, 34-15-1.

Källsner, B., Girhammar, U.A., Wu, L., 2002. A plastic design model for partially anchored wood-frame shear walls with opening. Proceedings CIB-W18 Meeting, Kyoyo, Japan, 35-15-2.

Källsner, B., Girhammar, U.A., 2004a. A plastic lower bound model for design of wood-frame shear walls. Proceedings 8th World Conference on Timber Engineering 2004, Lahti, Finland, June 14-17, 2004.

Källsner, B., Girhammar, U.A., 2004b. Influence of framing joints on plastic capacity of partially anchored wood-framed shear walls. Proceedings CIB-W18 Meeting, Kyoyo, Japan, 36-15-1.

NBCC, 1995. National Building Code of Canada. Institute for Research in Construction, National Research Council of Canada, Ottawa, Ont.

Ni, C., Karacabeyli, E., 2000. Effect of overturning restraint on performance of shearwalls. Proceedings 6th World Conference on Timber Engineering, Whistler Resort, British Columbia, Canada, Paper 2-3-1.

Ni, C., Karacabeyli, E., 2002a. Nailed shearwalls under simultaneous uplift and lateral loads. Proceedings of World Conference on Timber Engineering 2002, Shah Alam, Malaysia, August 12-15, 2002.

Ni, C., Karacabeyli, E., 2002b. Capacity of shear wall segments without hold-downs. Wood Design Focus, Vol. 12, No. 2, p.10-17.

Ni, C., Karacabeyli, E., 2002b. Deflections of Nailed Shearwalls and Diaphragms. Proceedings 8th World Conference on Timber Engineering 2004, Lahti, Finland, June 14-17, 2004.

INTERNATIONAL COUNCIL FOR RESEARCH AND INNOVATION
IN BUILDING AND CONSTRUCTION

WORKING COMMISSION W18 - TIMBER STRUCTURES

PLASTIC DESIGN OF PARTIALLY ANCHORED WOOD-FRAMED WALL DIAPHRAGMS WITH AND WITHOUT OPENINGS

B Källsner

SP Swedish National Testing and Research Institute
School of Technology and Design, Växjö University

U A Girhammar

Department of Applied Physics, Umeå University

SWEDEN

Presented by B Källsner

J Leskelä asked how to control deflection with the use of plastic method. B Källsner said that deflection calculation methods are needed. B Dujic received clarification about the source of the contact force being that of the panels. F Lam received confirmation that drift limits are not in Eurocode and confirmed that this is desirable. F Lam stated that deflection method is then needed.

A Buchanan stated that the last two papers deal with two similar topics but with different approach. The Canadian method deals with commonly built structures and looks into understanding the details about the forces. Europe seems to go the other way with a complicated design method. NZ uses the capacity design principle by identifying and designing the fuses accordingly.

B Griffith commented that in practice timber designers need something simple, safe and workable. Maximize analysis tool to allow competitiveness of timber frame. A Buchanan stated that the difference may be between large displacement of earthquake load and serviceability concerns. E Karacabeyli stated that in Ni's study the openings in wall issues were verified against test data.

Plastic design of partially anchored wood-framed wall diaphragms with and without openings

Bo Källsner
SP Swedish National Testing and Research Institute, Stockholm, Sweden
School of Technology and Design, Växjö University, Sweden

Ulf Arne Girhammar
Department of Applied Physics, Umeå University, Sweden

Abstract

In the European timber design code, Eurocode 5, two parallel methods for design of wood-framed wall diaphragms are given. In order to get rid of this situation a unified design method is needed.

This paper gives a theoretical and experimental background to a plastic design method that can serve as a basis for a new code proposal. The principle of the design method has previously been presented for walls without openings. In this paper the methodology is extended to wall diaphragms including openings and the method is also presented in a more straightforward format. Conducted experiments show good agreement between measured and calculated load-carrying capacity.

1   Introduction

1.1   Background

In the European timber design code, Eurocode 5, two parallel methods for design of wood-framed wall diaphragms are given. In the first method the leading stud is assumed to be fully anchored to the substrate. In the second method the bottom rail is assumed to be anchored to the substrate. The first method has a theoretical background while the second method is mainly experimentally based.

Design of wood-framed wall diaphragms has been the topic in a suite of papers published in the last years by Källsner et al (2001, 2002, 2004a, 2004b) and Girhammar et al (2004). All these papers were based on the principles of a so called plastic lower bound method (Neal, 1979). In this method a force distribution is chosen within the structure that fulfils the conditions of force and moment equilibrium for all parts of the structure studied.

In Källsner et al (2001 and 2002) the method was applied on wall diaphragms without and with openings, respectively. A more condensed form of the theory for wall diaphragms without openings was presented in Källsner et al (2004a) and comparisons with test results were shown in Girhammar et al (2004).

In Källsner et al (2004b) the influence of the framing joints (stud-to-rail joints) was studied. An alternative design method was here presented in which the full vertical shear capacity of the wall is utilised, disregarding that the conditions of equilibrium are not always fulfilled. This method results in load-carrying capacities that are equal to or slightly higher than capacities obtained by the more complicated plastic lower bound method. The

1

great advantage of the method is that the load-carrying capacity can be determined in a simple straightforward process.

1.2 Objective

The overall purpose of the research project is to develop an analytical design method that can be used for design of wood-framed wall diaphragms.

The objective of this paper is to demonstrate that the theory developed in Källsner et al (2004b) can be presented in a simpler format and that the theory also can be applied to walls with openings.

2 Plastic design method

2.1 Walls without openings

2.1.1 Vertical point loads

In order to explain the structural behaviour a wall configuration according to Figure 1 will be studied. The wall is subjected to vertical point loads V_i at the top of each stud and a horizontal load H along the centre of the top rail. The length of the wall is l and the spacing of the studs is s. The width and height of the full format sheets are denoted by b and h, respectively. The bottom rail is assumed to be fully anchored to the substrate by screws or other mechanical fasteners. The studs are not assumed to have any tie-downs. The influence of tie-downs can be taken into account considering them as external point loads. The forces acting on the wall in the ultimate limit state are assumed to be distributed according to the lower part of Figure 1. The forces acting along the bottom of the wall are shown in a section immediately above the bottom rail and represent the forces in the sheathing-to-timber joints. These forces are assumed to act either perpendicular or parallel to the bottom rail. The plastic capacity per unit length of these joints is denoted by f_p and it is assumed that plasticity has been attained along the entire bottom rail. The μ factor opens for the possibility of using reduced strength properties when the fastener forces act perpendicular to the edges of the sheets and the frame members.

The wall is separated into two fictitious segments with the lengths l_1 and l_2. The length l_1 is determined from the condition that the plastic shear capacity $f_p h$ is assumed to be attained in this vertical section of the wall, i.e.

$$\sum_{i=0}^{n} V_i + \mu f_p l_1 = f_p h \tag{1}$$

Introducing the notation

$$\kappa_1 = \sum_{i=0}^{n} \frac{V_i}{f_p h} \tag{2}$$

the length l_1 is obtained from equation (1) as

$$l_1 = \frac{h}{\mu}(1 - \kappa_1) \tag{3}$$

2
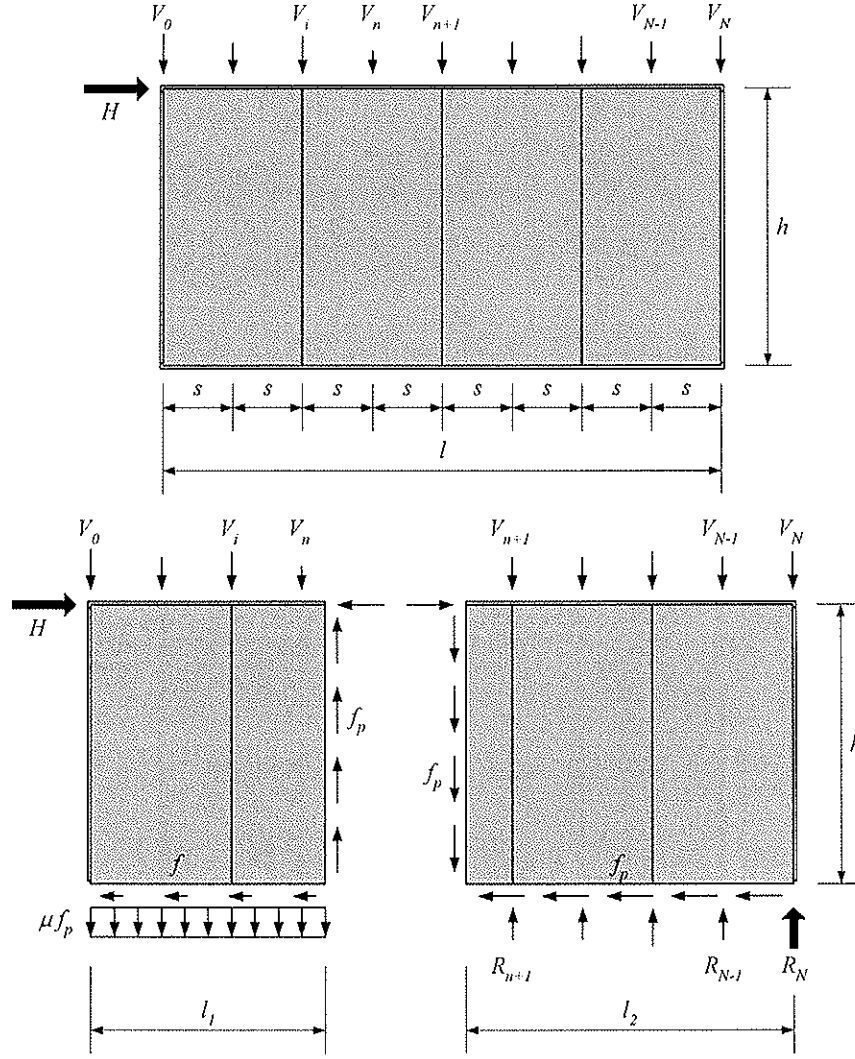
Figure 1. Forces acting on a wall diaphragm with fully anchored bottom rail but without tie-downs. The plastic capacity has been attained in the section l_1 from the leading stud.

There are two occasions when equation (1) is not fulfilled. The first one occurs when the vertical force on the leading stud $V_0 > f_p h$, corresponding to the conditions of a fully anchored wall. In this case we find

$$l_1 = 0 \qquad (4)$$

The second occasion occurs when the left side of equation (1) does not attain the full vertical plastic capacity $f_p h$ of the wall. In this case l_1 is obtained as

$$l_1 = l \qquad (5)$$

Considering the assumed force distribution along the bottom of the left wall segment we realise that the resulting force from μf_p and f is formally too high to be transferred only by the sheathing-to-timber joints. However, f can be motivated by two reasons. The first one is that the load-carrying capacity of the stud-to-rail joints along the bottom of the wall element has not been taken into account. This was demonstrated in Källsner et al (2004b) where it was concluded that all stud-to rail joints in the centre of the sheets of segment 2 and all stud-to-rail joints of segment 1 could be used for this purpose. These forces can be transferred to the left wall segment via contact forces between the sheets at the bottom rail.

These contact forces are not shown in Figure 1. Another reason to accept a certain force f is that the sheathing-to-timber joints in fact can be used for a certain degree of horizontal force transfer without causing large reductions in vertical force transfer. For example a horizontal force $f = 0.3 f_p$ will reduce the vertical force transfer μf_p by less than 5 %.

Denoting the horizontal force transferred to the left wall segment by H_1, a moment equation with respect to segment 1 around its lower right corner gives

$$H_1 h - \mu f_p l_1 \frac{l_1}{2} - \sum_{i=0}^{n} V_i (l_1 - is) = 0 \qquad (6)$$

Introducing the notations

$$\alpha_1 = \frac{l_1}{h} \qquad (7)$$

$$\beta_1 = \sum_{i=0}^{n} \frac{V_i}{f_p h} \frac{l_1 - is}{l_1} \qquad (8)$$

the horizontal force H_1 is obtained from equation (6) as

$$H_1 = f l_1 = (\frac{1}{2} \mu \alpha_1 + \beta_1) f_p l_1 \qquad (9)$$

Within segment 2 the wall is subjected to a pure plastic shear flow f_p, corresponding to the conditions of a fully anchored wall segment, resulting in the horizontal force

$$H_2 = f_p l_2 \qquad (10)$$

The resulting capacity of the two wall segments is obtained as

$$H = H_1 + H_2 = (\frac{1}{2} \mu \alpha_1 + \beta_1) f_p l_1 + f_p l_2 \qquad (11)$$

The stabilising effect of the vertical loads V_1, V_2 ... V_N is sometimes fairly small and can be neglected. The expression for the factors β_1 and κ_1 are then given as

$$\beta_1 = \kappa_1 = \frac{V_0}{f_p h} \qquad (12)$$

2.1.2 Vertical distributed load

In order to obtain somewhat simpler design equations the vertical point loads acting on the vertical studs can often, as a good approximation, be replaced by a single point load V acting on the leading stud and a distributed load q_V acting on all the studs according to Figure 2 . Using the same design method as in section 2.1.1, the horizontal capacity H of the wall is given as

$$H = H_1 + H_2 = (\frac{1}{2} \gamma \mu \alpha_1 + \beta_1) f_p l_1 + f_p l_2 \qquad (13)$$

$$l_1 = \frac{h}{\gamma \mu} (1 - \kappa_1) \qquad (14)$$

$$\alpha_1 = \frac{l_1}{h} \qquad (15)$$

4

$$\beta_1 = \kappa_1 = \frac{V}{f_p h} \qquad (16)$$

$$\gamma = 1 + \frac{q_V}{\mu f_p} \qquad (17)$$
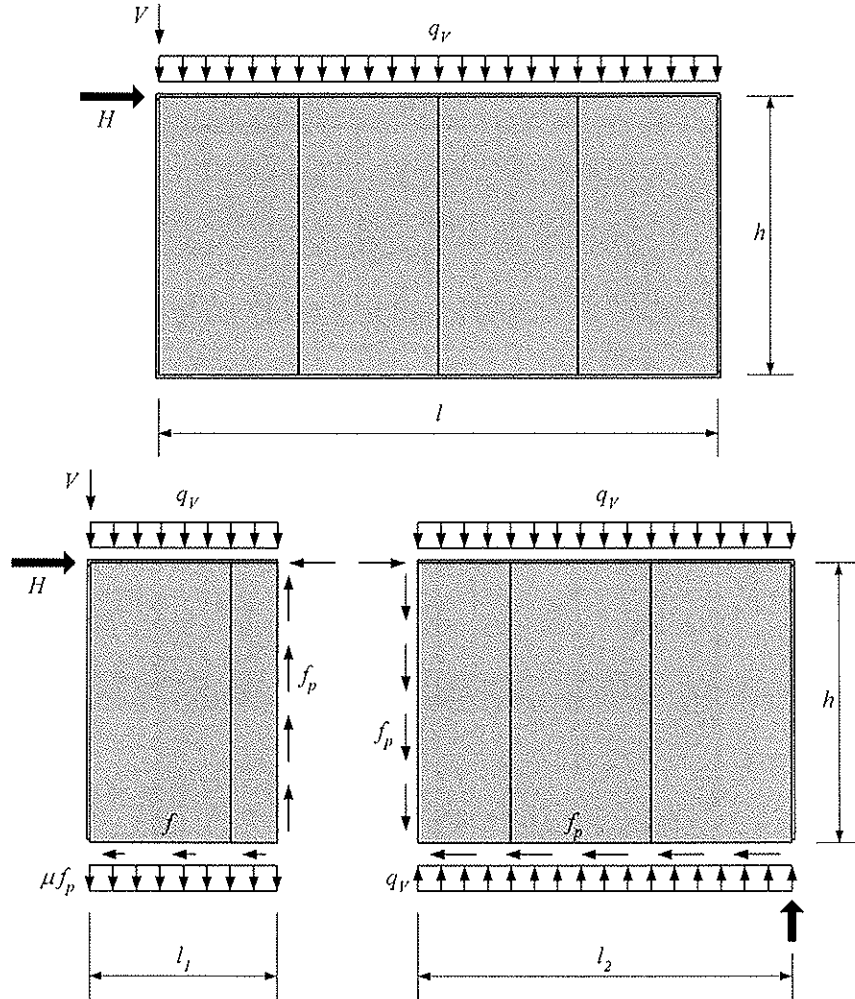
Figure 2. Forces acting on a wall diaphragm with fully anchored bottom rail but without tie-downs. The plastic capacity has been attained in the section l_1 from the leading stud.

2.2 Walls with openings

2.3.1 Windward side of opening

We will now study the wall configuration in Figure 3 where a wall segment of low depth h_l has been added on the leeward side of the wall. As in section 2.1.1 it is assumed that the wall part of full depth can be separated into two segments where the left segment can be treated as partially anchored while the right side can be treated as fully anchored. It is further assumed that a contact force H_w is transferred from the low wall segment via segment 2 to segment 1. By studying the moment equilibrium of the low wall segment, assuming that the plastic shear flow f_p has been attained, this contact force is determined to

$$H_w = f_p l_w \qquad (18)$$

5
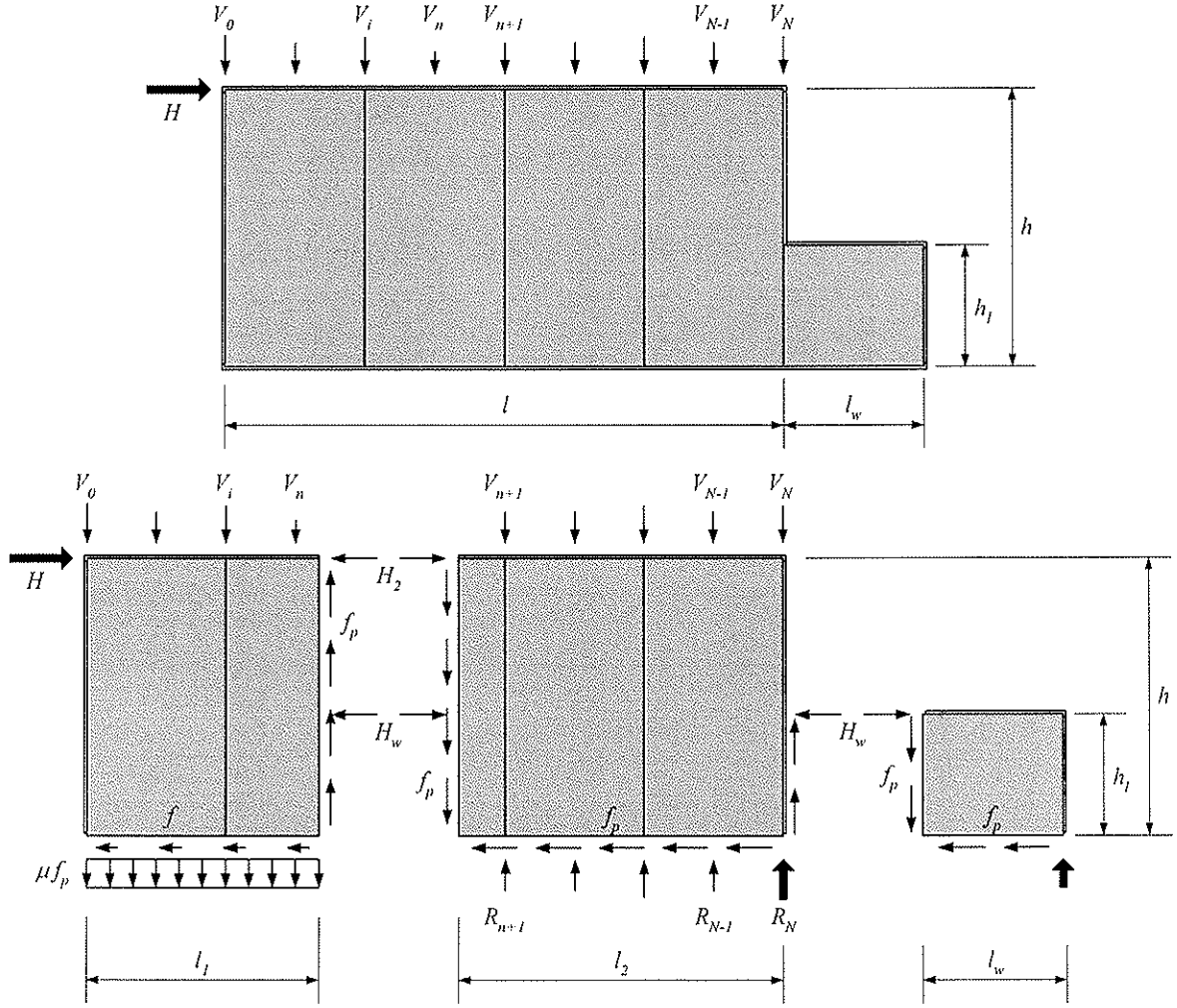
Figure 3. Forces acting on a wall diaphragm with fully anchored bottom rail but without tie-downs. The plastic capacity has been attained in the section l_1 from the leading stud.

A moment equation with respect to wall segment 1 around its lower right corner gives

$$H_1 h - \mu f_p l_1 \frac{l_1}{2} - \sum_{i=0}^{n} V_i (l_1 - is) - H_w h_l = 0 \qquad (19)$$

Using the notations according equations (7) and (8) the horizontal force H_1 acting on wall segment 1 is obtained as

$$H_1 = (\frac{1}{2} \mu \alpha_1 + \beta_1) f_p l_1 + \frac{h_l}{h} f_p l_w \qquad (20)$$

So far it has not been checked that the force H_1 can be transferred along the top rail to wall segment 1, i.e.

$$H_1 \leq f_p l_1 \qquad (21)$$

Adding the contribution of segment 2 finally gives the capacity of the wall as

$$H = \min \begin{cases} (\frac{1}{2} \mu \alpha_1 + \beta_1) f_p l_1 + \frac{h_l}{h} f_p l_w + f_p l_2 \\ f_p l \end{cases} \qquad (22)$$

6

If the length l in Figure 3 is small it might occur that the plastic shear flow f_p is not attained until within the low segment. This load case is shown in Figure 4 where it is assumed that the plastic shear flow is attained in the vertical section at the distance l_1 from the leading stud. The length l_1 is determined from the condition

$$\sum_{i=0}^{n} V_i + \mu f_p l_1 = f_p h_l \tag{23}$$

Using the notation

$$\kappa_{low} = \sum_{i=0}^{n} \frac{V_i}{f_p h_l} \tag{24}$$

the length l_1 is obtained as

$$l_1 = \frac{h_l}{\mu} (1 - \kappa_{low}) \tag{25}$$
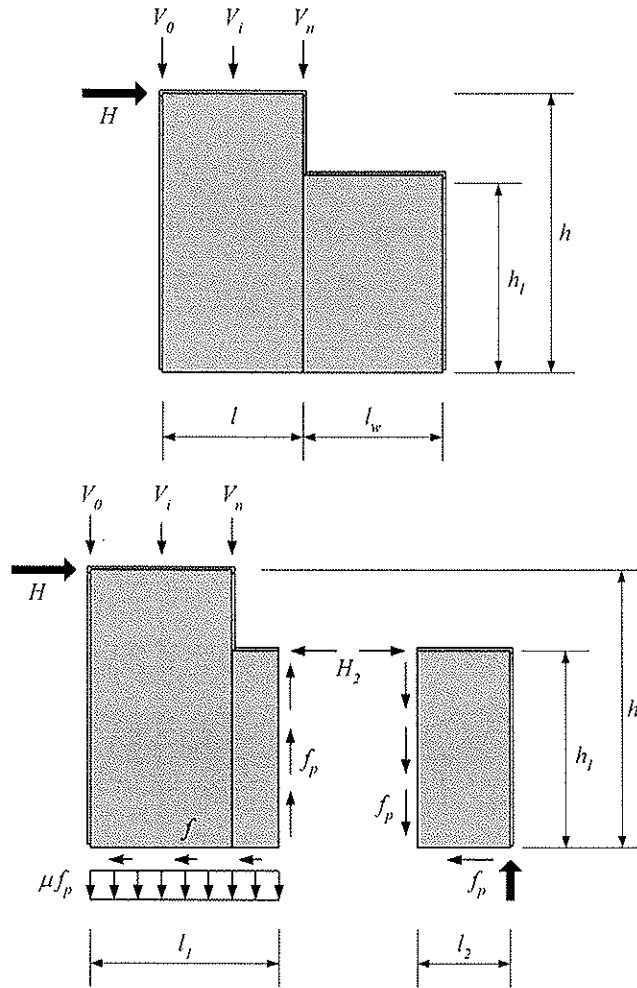
Figure 4. Forces acting on a wall diaphragm with fully anchored bottom rail but without tie-downs. The plastic capacity has been attained in the section l_1 from the leading stud.

Since the right part of the low wall segment is subjected to a pure shear flow f_p we find that

$$H_2 = f_p l_2 \tag{26}$$

A moment equation with respect to the left part of the wall gives

$$Hh - \mu f_p l_1 \frac{l_1}{2} - \sum_{i=0}^{n} V_i (l_1 - is) - H_2 h_l = 0 \tag{27}$$

Using the previous notations for α_1 and β_1 the capacity of the wall is determined to

$$H = (\frac{1}{2}\mu\alpha_1 + \beta_1)f_p l_1 + \frac{h_l}{h} f_p l_2 \tag{28}$$

2.3.2 Leeward side of opening

The capacity of the wall to the right of the opening can be determined studying the equilibrium of the wall part in Figure 5. The same methodology as in section 2.1.1 is used.
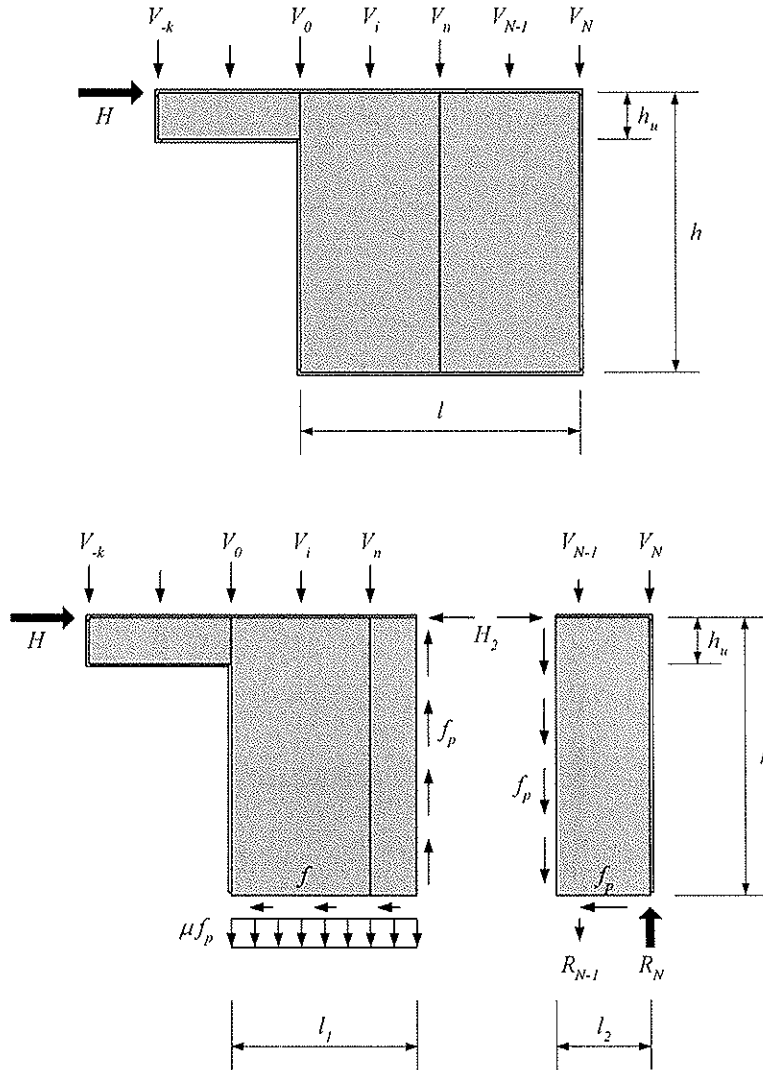
Figure 5. Forces acting on a wall diaphragm with fully anchored bottom rail but without tie-downs. The plastic capacity has been attained in the vertical section shown.

First of all it must be checked that the sum of the vertical forces acting on the cantilever is not higher than the shear capacity of the cantilever, i.e.

8

$$\sum_{i=-k}^{-1} V_i \leq f_p h_u \tag{29}$$

The capacity of the wall is obtained as in section 2.1.1 to

$$H = H_1 + H_2 = \min \begin{cases} (\frac{1}{2}\mu\alpha_1 + \beta_1)f_p l_1 + f_p l_2 \\ f_p l \end{cases} \tag{30}$$

but with the difference that the forces acting on the cantilever are included in the factors κ_1 and β_1 i.e.

$$\kappa_1 = \sum_{i=-k}^{n} \frac{V_i}{f_p h} \tag{31}$$

$$\beta_1 = \sum_{i=-k}^{n} \frac{V_i}{f_p h} \frac{l_1 - is}{l_1} \tag{32}$$

3　Comparison with test results

In this section the results from testing of two types of wall diaphragms including openings (Figure 6) will be reported. The sheathing material in all tests consisted of 8 mm hardboard (wet process fibre board, HB.HLA2, supplier Masonite AB). The size of the sheets was 1200 x 2400 mm and the dimension of the frame members 45 x 120 mm. Only one side of the timber frame was sheathed. For the sheathing-to-timber connections, annular ringed shank nails of dimension 50 x 2.1 mm were used. The distances between the fasteners were 100 mm along the perimeter of the sheets and 200 mm along the vertical centre lines of the sheets. The nominal edge distance was 11.25 mm along the vertical studs and 22.5 mm along the bottom and top rails. For each framing joint two annular ringed shank nails of dimension 90 x 3.1 mm were used. These nails were applied in the grain direction of the vertical studs. For details, see Risberg et al (2005).
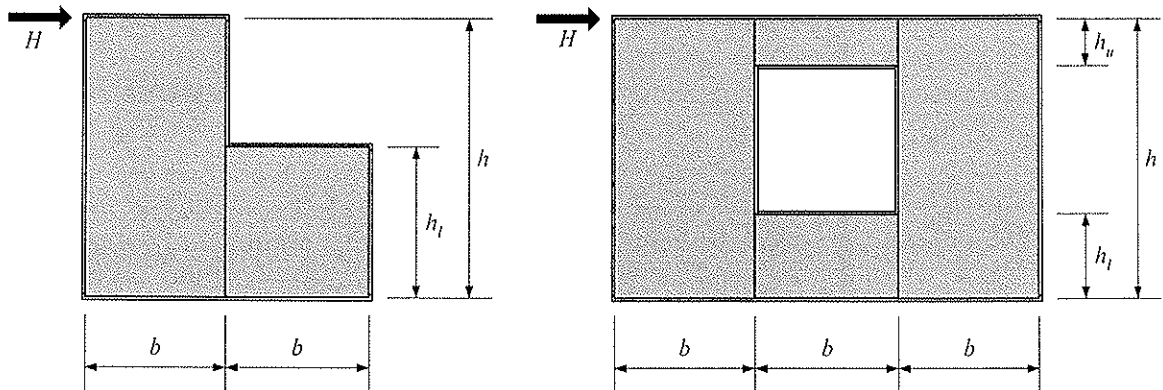
Figure 6. Wall diaphragms tested (type 1 to the left, type 2 to the right).

A specification of wall diaphragms tested is given in Table 1. In test series 1 the load was applied diagonally corresponding to the conditions of fully anchored leading stud. In all other test series the load was applied horizontally. All tests were performed under deformation control with a constant horizontal rate of 8 mm/min corresponding to a time to failure of about 5 minutes. The bottom rail was prevented from vertical uplift by

mechanically fixed steel plates between the studs and from horizontal slip by a stop at the trailing stud.

Table 1. Specification of wall diaphragms tested. Measured and calculated load-carrying capacities.

Test series	Type of specimen	h_l/h	h_u/h	Number of tests	H_{meas} [kN]	H_{th} [kN]	H_{meas}/H_{th}
1	1 *	1		4	29.9	29.9 (2.00 f_pb)	1.00 ref.
2	1	0		4	3.8	3.7 (0.25 f_pb)	1.02
3	1	0.25		3	6.7	7.5 (0.50 f_pb)	0.90
4	1	0.5		4	10.5	11.2 (0.75 f_pb)	0.94
5	1	0.75		4	13.1	14.0 (0.94 f_pb)	0.93
6	1	1		4	13.9	15.0 (1.00 f_pb)	0.93
7	2	0.5	0	4	20.8	22.4 (1.50 f_pb)	0.93
8	2	0.25	0.25	4	21.2	22.4 (1.50 f_pb)	0.95
9	2	0	0.5	4	21.4	18.7 (1.50 f_pb)	1.15

* Fully anchored wall diaphragm

The results from testing of the various wall configurations are summarised in Table 1. The measured load-carrying capacities H_{meas} represent mean values. The theoretical capacities H_{th} (given within parenthesis in the second last column) have been determined using the plastic design method described in chapter 2. For test series 2-6 equation (22) has been used. For test series 7-9 the capacity has been determined adding the contributions from equations (22) and (30). The numerical values given for H_{th} have been obtained by using test series 1 as a reference for determination of the plastic capacity f_pb. From test series 1 we obtain f_pb = 14.95 kN. This reference test was conducted in an earlier separate test series. The sheathing-to timber fasteners of test series 1 were taken from a different batch than the rest of the test series.

From the last columns of Table 1 we see that, by using the fully anchored wall as a reference for determination of the plastic shear flow, the theoretical capacity of the walls with openings is in general somewhat overestimated. This is reasonable since in the calculation of the theoretical capacity for series 1 (2.00 f_pb) we have not considered the positive effect from the framing joints between the vertical studs and the top and bottom rails. Another interesting observation is that the theoretical capacity of test series 9 is somewhat underestimated. This is probably a consequence of the assumptions made in section 2.3.2 where no bending moments are transferred along the left side of the cantilever arm. In test series 9, the depth h_u is fairly large which might cause this kind of moment transfer.

4 Conclusions

An analytical plastic model for design of partially or fully anchored wood-framed wall diaphragms is presented. The model can only be applied on wall diaphragms where the sheet material is fixed by mechanical fasteners to the timber members and where these sheathing-to-timber joints show plastic behaviour. The model covers only static loads in the ultimate limit state.

10

The basic idea of the method is that the full vertical shear capacity of the wall diaphragm is utilised, disregarding that the conditions of equilibrium are not always fulfilled. It has previously been shown that the method gives a load-carrying capacity that is equal to or slightly higher than the capacity obtained by means of a more complicated plastic lower bound method.

Some tests of wall diaphragms with openings have been conducted where the bottom rail was fixed to the substrate. The test results indicate good agreement between measured and calculated load-carrying capacities.

The plastic design method may serve as a basis for a new revised design method in Eurocode 5.

5   Acknowledgement

We gratefully acknowledge received opinions from Dr. Bob Griffiths and Prof. Hans Blass during the development of the design principles and the assistance of Mr Håkan Risberg, M.Sc., and Mr Patrik Viberg, B.Sc., who performed the tests at Umeå University.

6   References

prEN 1995-1-1, Eurocode 5 – Design of timber structures – Part 1-1: General – Common rules and rules for buildings, December 2003.

Girhammar U.A., Källsner B.: Tests on partially anchored wood-framed shear walls. *Proceedings 8th World Conference on Timber Engineering*, Lahti, Finland, June 14-17, 2004.

Källsner B., Girhammar U.A., Wu L., A simplified plastic model for design of partially anchored wood-framed shear walls, *Proceedings CIB-W18 Meeting*, Venice, Italy, 2001.

Källsner B., Girhammar U.A., Wu L., A plastic design model for partially anchored wood-framed shear walls with openings, *Proceedings CIB-W18 Meeting*, Kyoto, Japan, 2002.

Källsner B., Girhammar U. A.: A plastic lower bound method for design of wood-framed shear walls. *Proceedings 8th World Conference on Timber Engineering*, Lahti, Finland, June 14-17, 2004a.

Källsner B., Girhammar U.A., Influence of framing joints on plastic capacity of partially anchored wood-framed shear walls, *Proceedings CIB-W18 Meeting*, Edinburgh, UK, 2004b.

Neal B.G., *Plastic Methods of Structural Analysis*, 2nd edition, London,1978.

Risberg H., Viberg P., Testing of partially anchored wood-framed shear walls with openings (in Swedish), Umeå University, Department of Applied Physics & Electronics, Civil Engineering, Report 2005:01, Umeå, Sweden, 2005.

INTERNATIONAL COUNCIL FOR RESEARCH AND INNOVATION
IN BUILDING AND CONSTRUCTION

WORKING COMMISSION W18 - TIMBER STRUCTURES

RACKING OF WOODEN WALLS EXPOSED TO DIFFERENT BOUNDARY CONDITIONS

B Dujic

R Zarnic

University of Ljubljana, Faculty of Civil Engineering and Geodesy
SLOVENIA

S Aicher

MPA University Stuttgart (Otto-Graf-Institute)
GERMANY

Presented by B Dujic

B Griffith received confirmation that the boundary condition as vertical load was applied to the frame. E Karacabeyli asked whether buckling was observed when heavy vertical load was applied. B Dujic responded that buckling was not observed.

H Blass asked whether much of the capacity of the nail was used up to carry the heavy vertical load. B Dujic responded that special hardware was provided to ensure the vertical load went directly to the studs. C Ni questioned whether the stiff upper boundary is reality for the case where the wall only has floor not another wall on top. B Dujic said that stiff floor is very common in Europe.

BJ Yeh commented in their work a 5% to 10% difference can be observed when a stiff loading beam was used in 2x4 wall tests. M Yasumura stated that in Japan hold downs at 4 corners are used to get the shear capacity. Other tests are used to develop information for the joints to develop calculation information for design.

E Karacabeyli stated that in terms of loading bar more effects were noted when walls have openings. V Rajcic commented in European system very stiff floor can result from concrete floors.

Racking of Wooden Walls exposed to Different Boundary Conditions

Bruno Dujic

University of Ljubljana, Faculty of Civil and Geodetic Engineering, Ljubljana, Slovenia

Simon Aicher

MPA University Stuttgart (Otto-Graf-Institute), Stuttgart, Germany

Roko Zarnic

University of Ljubljana, Faculty of Civil and Geodetic Engineering, Ljubljana, Slovenia

1 Introduction

Post earthquake observations of damaged wooden houses and the analysis of experimentally tested structural elements have developed the worldwide knowledge about the response of wooden buildings on earthquake and strong wind. One of the major problems of understanding is related to boundary conditions and the influence of vertical loading on building elements. Learning from experimental and on-site observations, researchers have developed different test protocols and test set-ups trying to simulate the natural behavior of buildings as realistically as possible. Some of these efforts are reflected in codes and standards.

Eurocode 5 (ENV 1995-1-1:1993) introduces two methods for the determination of the racking strength of cantilever wall diaphragms: i) an analytical approach and ii) an experimental approach using a test protocol according to EN 594. Both approaches are related exclusively to timber frame walls with sheathing plates. However, the current construction practice introduces many other types of wall diaphragms. Among them, very popular are one or multi-layer boards or perforated glued panels and braced walls with different diagonal strengthenings.

The Eurocode 5 calculation procedure is based on lower value of plastic capacity of the fasteners which connect the sheathing plates to the timber frame. The approach can estimate only the racking strength of panels having wood based sheathing plates where frame studs are fully restrained. In the cases of partially anchored studs and low magnitudes of vertical loading, the calculation may result in values that significantly overestimate the load-bearing capacity [4, 5]. The testing procedure according to EN 594 requires a partially anchored wall that does not necessarily represent the actual wall diaphragm used for construction of wooden buildings. The EN 594 load protocol does not use the cyclic horizontal load to simulate the earthquake loading. It is obvious that both analytical and experimental methods addressed in Eurocode 5 need to be upgraded.

The experimental investigations on the racking behavior of different types of wall diaphragms recently carried out at University of Ljubljana justify the need for further development of test protocols and analytical methods. The above commented influences of boundary conditions and vertical load should be properly taken into account. In this paper

the experimentally obtained responses of wall panels exposed both to the EN 594 protocol and to cycling loading are presented. Three different cases of boundary conditions that may occur in real structures were applied and the magnitude of the constant vertical load was varied.

The intention of the presented research results is to support the discussion about potential needs for further development of relevant codes including Eurocode 5.

2 Description of test approach

2.1 Boundary conditions

Following the experiences obtained from testing of masonry panels, a universal shear wall test set-up was developed and installed at Faculty for Civil and Geodetic Engineering of the University of Ljubljana in 1999. The main idea of the new device was to use a gravity load induced by ballast as a constant vertical load and a displacement controlled hydraulic actuator as a driver of the cyclic horizontal load. The main challenge was to simulate realistic boundary conditions that may occur during the action of an earthquake. In reality, the boundary conditions may change during an earthquake excitation because of the changes of the building characteristics due to the development of damages. Therefore, the testing device should allow the altering of boundary conditions from one test run to another. Following this idea, the set-up can be easily adapted to various boundary conditions applied to tested panels.

Basically, three major cases of boundary conditions are most likely to appear in reality:

- **shear cantilever mechanism** where one edge of the panel is supported by the firm base while the other can freely translate and rotate (Case A, Figure 1)

- **restricted rocking mechanism** where one edge of the panel is supported by the firm base while the other can translate and rotate as much as allowed by the ballast that can translate only vertically without rotation (Case B, Figure 1)

- **shear wall mechanism** where one edge of the panel is supported by the firm base while the other can translate only in parallel with the lower edge and rotation is fully constrained (Case C, Figure 1)

In Cases A and B the panel is exposed to constant vertical load in every stage of the cycling excitation or horizontal deformation induced along the upper edge where the ballast is acting. In Case C the vertical load increases when the panel wants to uplift due to displacements along the upper horizontal edge. The advantage of the herein proposed testing procedures for Cases A or B is avoiding the boundary conditions of Case C. However, the main problem of the protocol proposed by ASTM E72 is obvious in Case C because of vertical constraining of the upper edge of the test specimen [9].

In practice, Case A represents mostly the behavior of narrow panels and panels located in attics and vertically loaded only by flexible roof constructions. Case B is typical for panels carrying the floor construction above it and Case C is the typical case of infill of a stiff surrounding frame.

Case A
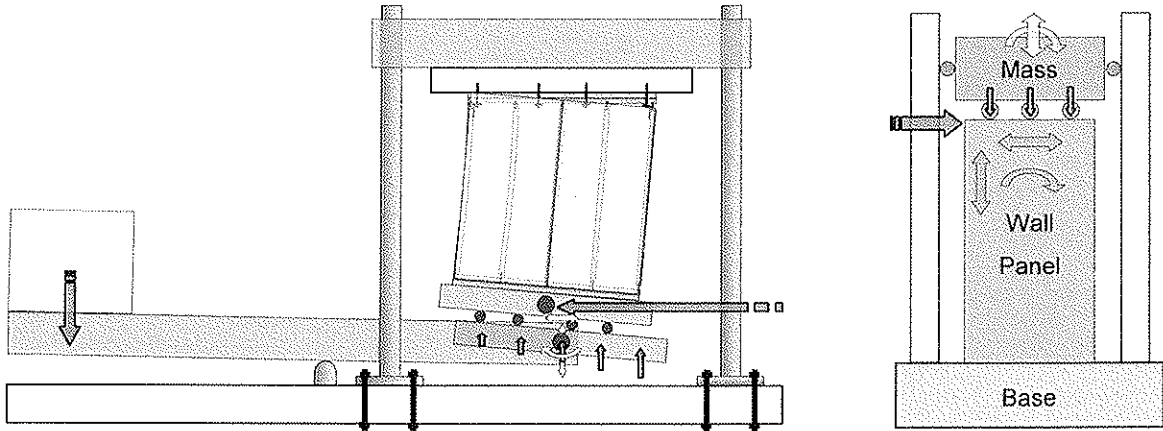
Case B
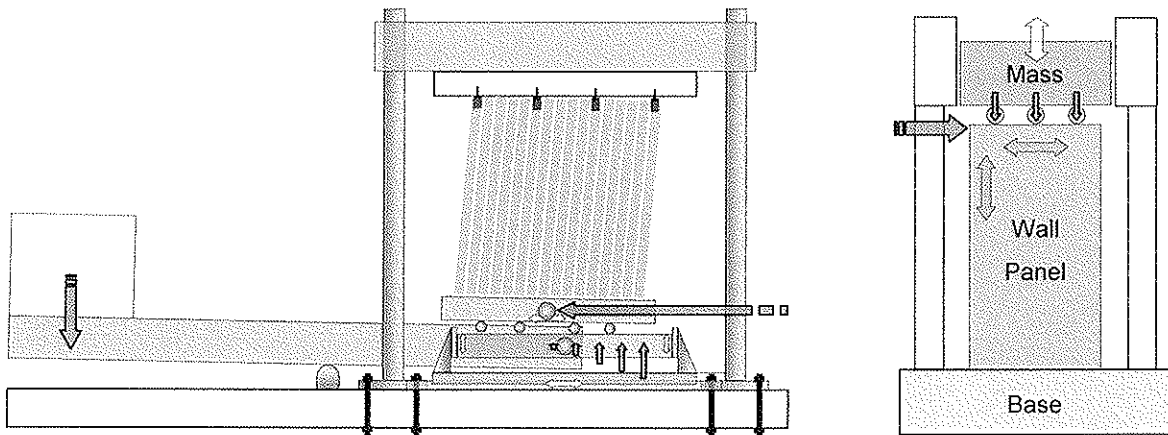
Case C
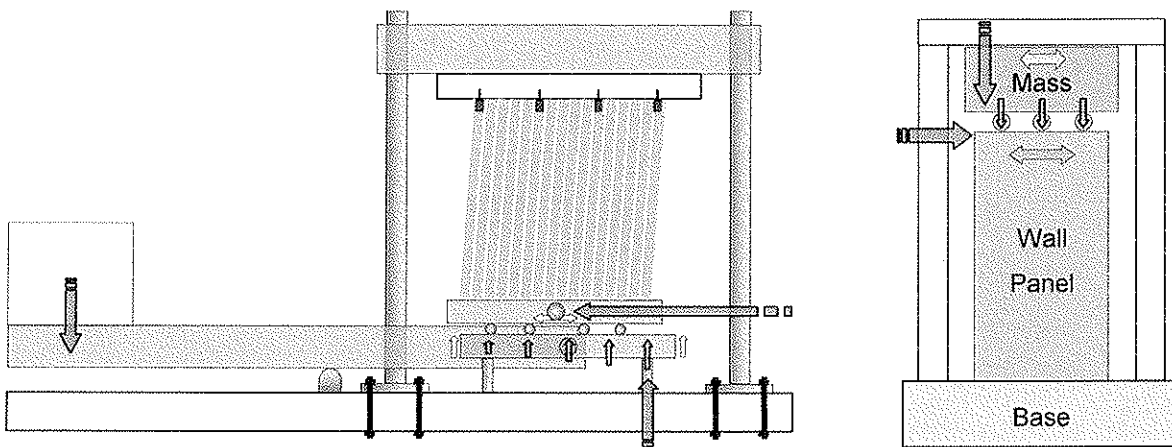
Figure 1: Three different boundary conditions presented in the developed and installed setup at UL FGG and on schematic sketches.

2.2 Test setup

The construction of the set-up enables testing of panels simulating all three above described cases of boundary conditions. The horizontal load is applied by successively inducing displacements along the free edge of the specimen. The specimens (4) are turned upside-down and supported along the upper edge by a steel frame structure to make the application of gravity load by ballast easier. The test set-up is composed of six major parts, marked in Figure 2 by numbers 1 to 6. The pair of lever beams (1) follows the vertical deformation of the specimen, while constant vertical load induced by counterbalance acts on the specimen. The horizontal displacement is applied along the lower horizontal edge of the specimen by a single displacement-controlled actuator (5) that moves the roller beam (3). The beam rolls along the supporting beam (2), hinged between the pair of lever beams. During the testing, the lower edge of the panel is supported by a hinged (2) and horizontally movable mechanism (3), which allows its free horizontal movement and rotation (boundary condition of Case A). Rotation of the supporting beam (2) can be constrained by both vertical side and horizontal sliding supports (6) that allow only its vertical translation. The sliding supports enable the simulation of the boundary conditions of Case B. Further alternation of the setup by blocking the movement of the supporting beam in one direction (7) gives the boundary conditions of Case C.
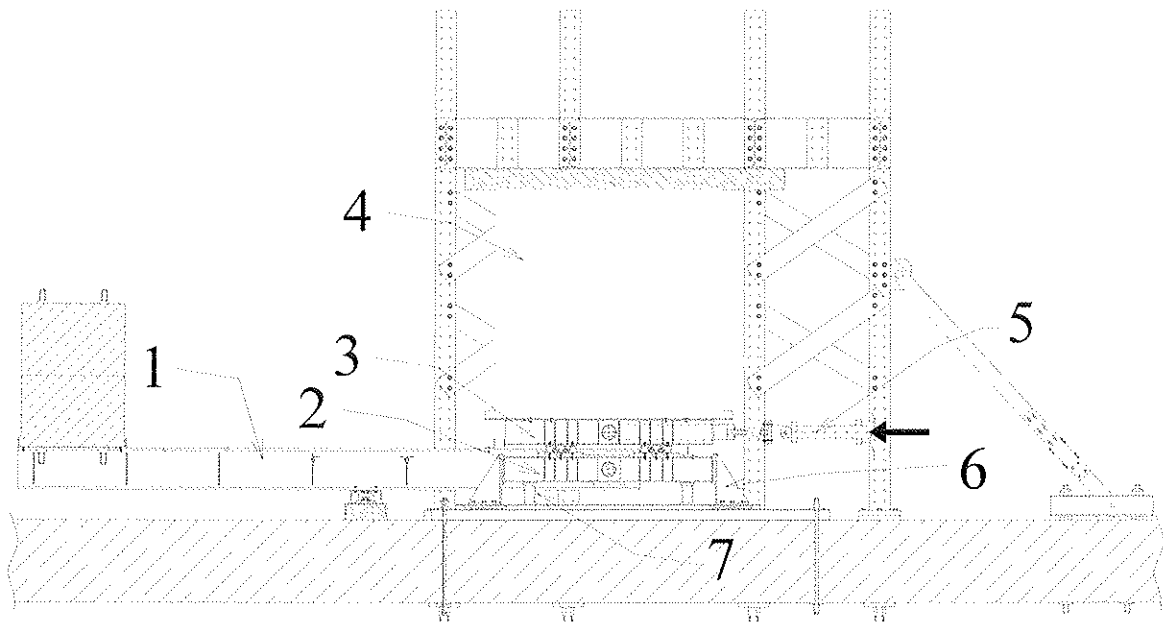
Figure 2: Longitudinal cross-section of the set-up for testing wall panels at different boundary conditions.

The set-up is calibrated for vertical and horizontal load. The measuring of strains of the upper flanges of lever beams in the cross-section above the lever support enables the control of the vertical load acting on the tested specimen. The horizontal action of the hydraulic actuator is controlled by data acquisition and actuator control system by Röell/Amsler. The capacity of the test set up is 500kN of constant vertical load provided by ballast and 250kN of horizontal load in a displacement range of ± 200mm.

3 Testing procedures and panel responses

Well known critics of ASTM E 72 [10] speak of the importance of proper boundary conditions to be used for realistic testing of panels. The European test standard EN 594 offers a step forward in the improvement of the testing procedure. However, it does not solve the problem of taking into account the above described realistic boundary conditions in a proper way. The EN 594 procedures assume partial anchoring of the panels along the bottom rail, which is not the case in many systems that are presently on the market. Bottom rail anchoring is not an appropriate solution in earthquake prone areas where the stud anchoring gives higher earthquake resistance to the entire building. Therefore, the testing method should cover most of the possible cases that may appear on the market. Beside this, EN 594 does not cover loadings that may occur in earthquake prone areas, because it takes into account only a monotonous racking load.

The main goal of this paper is to demonstrate the variety of testing possibilities using the herein proposed testing approach with adaptable boundary conditions and different loading protocols from simple monotonous to more complex cyclic ones. Cyclic testing can be carried out following the EN 12512:2001, ISO 16670:2003 protocol or any other protocol. Using the above described set-up, various configurations of wooden walls anchored with different anchors and exposed to different vertical loads and boundary conditions were tested.

Two different types of wooden walls were tested: timber-framed walls with OSB sheathing and solid cross-laminated wooden walls. The test protocol included in both cases boundary conditions of Case A and B, three levels of vertical load and two patterns of horizontal load: monotonous according to EN 594 and cyclic according to ATC [1]. The first tests started in 1999 and the last were finished recently this year.

The response of the tested wooden walls does not depend only on the boundary conditions and the magnitude of vertical load, but mostly on the configuration and mechanical properties of the constituent elements and the assembly as a whole. However, ignoring the influence of different boundary conditions and the level of vertical load may lead to misinterpretation of the observed response. In Figure 4 three different patterns of wall behavior are presented: shear, rocking and combined shear – rocking response. All of them can develop under boundary conditions of shear cantilever mechanism (Case A). The behavior depends on the shear stiffness of the wall diaphragm as a whole, the magnitude of vertical load and the layout and mechanical characteristics of the anchors. The shear response develops either if the panel is flexible in shear or if the magnitude of the vertical force is relatively high. The rocking response is typical for weakly anchored stiff panels or for a low level of vertical loading. Combined behavior can be observed in most cases of realistic behavior of panels where different combinations of panel stiffness, anchoring and vertical load take place.

The response of panels tested with Case A boundary conditions represents the conservative behavior. If the same panel is exposed to other boundary conditions (Cases B or C), the response values of rocking and combined shear-rocking may be higher than the values observed using Case A conditions. The reason therefore is the lowering of the tensile forces developed in the vertical edges of the panel, consequently lowering the tensile loading of anchors. Testing under conditions of Case B is justified only when the behavior of the panel in the real building is governed by an in and out of plane stiff floor diaphragm (composite wood-concrete or solid wood slab). Testing under conditions of Case C is

suitable for panels designed to act as frame infill, panels with glued-in-rods or for highly vertically loaded walls in the lowest story of multistory buildings.

Timber framed panels

Solid wooden laminated panels

Rocking response of walls	Combined shear - rocking response of wall	Shear response of walls
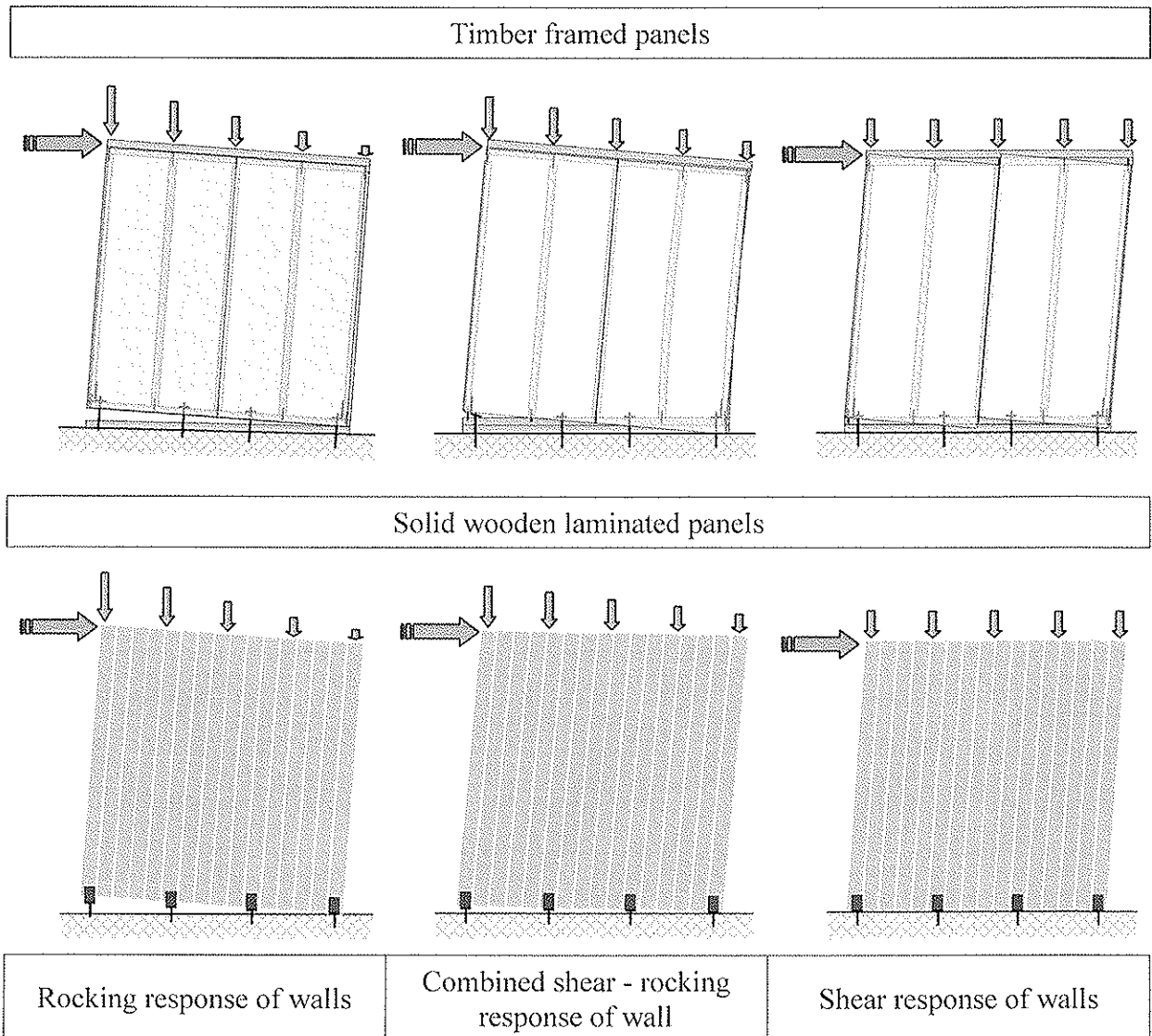
Figure 3: Typical responses of wooden wall panels exposed to combined vertical and horizontal load.

The published results of testing under conditions of Case C can not be considered applicable to most realistic cases and may lead to serious mistakes if used in the design of structures. Due to the underestimation of the importance of the boundary conditions the load bearing capacity of the panels is extremely overestimated, especially when the panels are loaded with vertical loads of low intensity or when the panels are weakly anchored. However, at present the majority of known tests in Europe and hereon based expertises and technical approvals are based on Case C conditions. Presently, in the framework of the research cooperation between University of Ljubljana (FGG) and University of Stuttgart (Otto-Graf-Institute) on cyclic and dynamic behaviour of shear walls with fiber gypsum panels, the effect of boundary conditions represents one of the parameters investigated in depth.

4 Influence of loading protocol

The complete information about the mechanical characteristics of wooden wall panels and their anchoring can be obtained from responses both to monotonous and cyclic loading with proper combination of vertical forces (Figure 4). The protocol of EN 594 covers sufficiently the monotonous loading of wall panels. Unfortunately, the protocol of EN 12512 covers only cyclic testing of particular joints made with mechanical fasteners, which is an insufficient tool for the evaluation of the behavior factor "q" needed for the design of earthquake resistant buildings. On the other hand, the ISO 16670 standard also addresses only the joints but the proposed protocol can be also used for the testing of wooden wall diaphragms. The reason therefore is that ultimate joint displacement is used instead of yield slip (EN 12512) which is difficult to define. Since the ISO protocol is based on ultimate displacement, it can forward a behavior factor "q" as addressed in Eurocode 8.

It is obvious that there is a need for the development of an integral European standard that would cover both monotonous and cyclic testing of wall diaphragms. The new standard should also include the criteria for the determination of limitations of inter-story drifts according to the concept of performance-based earthquake engineering design.
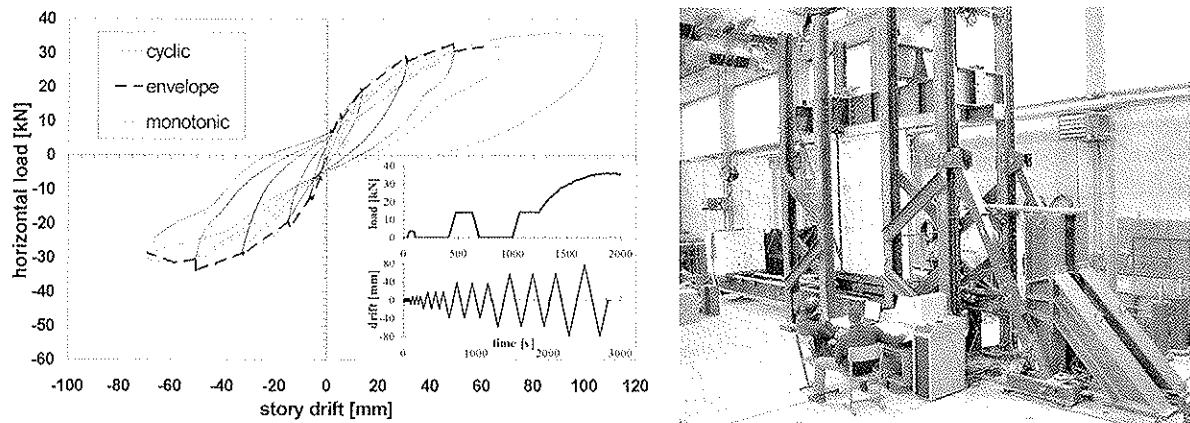
Figure 4: Comparison of monotonic and cyclic response of wall panels (length of 244 cm) vertically loaded with 51 kN in the set up installed at UL FGG.

The comparison of the responses of wooden panels subjected to cyclic and monotonous loading (Figure 4) illustrates well the importance of cycling testing. In the case presented in the diagram the load carrying capacity of the panel exposed to cyclic loading was 15% lower than the resistance of the panel exposed to monotonous loading. The cyclic response shows higher initial stiffness due to hardening of the fasteners exposed to low-cycle fatigue and lower ductility (down to 50% of the ductility reached by monotonous loading). Therefore, earthquake design of wooden buildings can not be properly performed without data obtained from cyclic testing of panels exposed to different intensities of vertical load.

The graphs in Figure 5 reveal the influence of vertical load intensity both on the load carrying capacity and the type of response mechanisms, as discussed above and presented in Figure 3. In the case of timber frame panels the rocking mechanism was observed at the lowest magnitude of vertical load and the shear mechanism at the highest magnitude of vertical load. The boundary conditions were of Case A at all vertical load intensities. In the case of low vertical load, the anchorage system increases the racking resistance of the wall. Fully anchored framed panels with tie-downs at the leading stud have higher lateral resistance and load carrying capacity than partially anchored walls. At the magnitudes of the total vertical load above 50 kN (20 kN per meter length of the wall) the anchorage

7

system did not significantly influence the lateral resistance of the shear wall. In this case the shear mechanism was developed.

| Timber framed panels | Solid wooden panels |
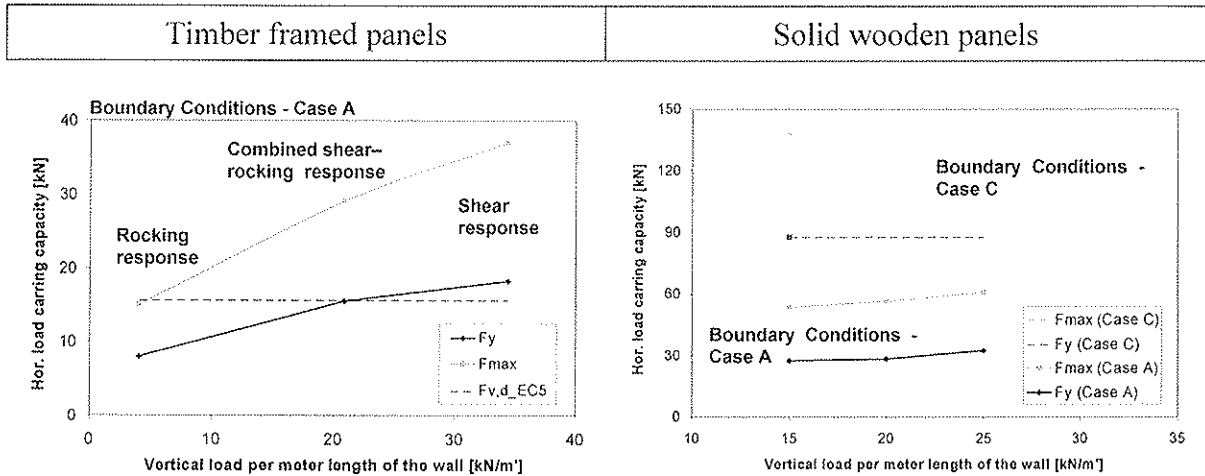
Figure 5: Influence of vertical load intensity on load carrying capacity of wooden panels at a length of 244 cm.

In the case of much stiffer solid wooden panels the shear mechanism did not develop, despite the varying of boundary conditions from Case A to Case B. It was reached when boundary conditions were set to Case C.

5 Concluding remarks

The importance of a proper taking into account of the boundary conditions and of the influence of vertical and type of horizontal loading is evident from the comparison of the behavior of differently tested panels. There is a need for further development of standard protocols for wooden wall diaphragms used for structures located in earthquake prone areas. New standards should implement the concept of performance-based earthquake engineering design to obtain experimental data needed for the evaluation of the behavior factor "q" and to set the values of story drifts defining the limit states of the story base shear diagram.

6 References

[1]   Applied Technology Council (ATC), 1994. Tests of Narrow Plywood Shear-Wall Panels. Redwood City, CA: Applied Technology Council.

[2]   ASTM E 564 - 95. Standard Practice for Static Load Test for Shear Resistance of Framed Walls for Buildings. Annual Book of ASTM Standards. ASTM, Philadelphia, PA: 556-559.

[3]   ASTM E 72 - 95. Standard Test Methods of Conducting Strength Tests of Panels for Building Construction. Annual Book of ASTM Standards. ASTM, Philadelphia, PA: 392-402.

[4]   Dujic, B., 2001 "Experimental Supported Modeling of Response of the Timber-Framed Wall Panels to Horizontal Cyclic Load", Ph.D. thesis (in Slovenian), Faculty of Civil and Geodetic Engineering, University of Ljubljana, Slovenia.

[5]   Dujic, B., Zarnic R., 2002. "Influence of Vertical Load on Lateral Resistance of Timber-Framed Walls", Proceedings of CIB-W18/35-15-4, Kyoto, Japan.

[6]   EN 12512:2001. Timber structures - Test methods – Cyclic Testing of Joints made with Mechanical Fasteners. CEN, European Committee for Standardization, Brussels.

[7]   EN 594:1995, Timber structures - Test methods - Racking strength and stiffness of timber frame wall panels, CEN, European Committee for Standardization, Brussels.

[8]   ENV 1995-1-1:1993. Eurocode 5 – Design of timber structures – Part 1-1: General rules and rules for buildings, CEN, European Committee for Standardization, Brussels.

[9]   Girhammar, U. A., Wu, L., Källsner, B., 2002. "On Test Methods for Determining Racking Strength and Stiffness of Wood-Framed Shear Walls", Proceedings CIB-W18, paper 35-15-1, Kyoto, Japan.

[10]   Griffiths, D. R., 1984. "Determining the Racking Resistance of Timber Framed Walls", Proceedings of the Pacific Timber Engineering Conference, Auckland, New Zealand, Vol. I, pp. 504-512.

[11]   ISO 16670:2003. International Standard, Timber structures – Joints Made with Mechanical Fasteners – Quasi-Static Reversed-Cyclic Test Method. First edition 2003-12-15.

[12]   prEN 1998-1:2003. Eurocode 8: Design of structures for earthquake resistance, Part 1: General rules, seismic action and rules for buildings, CEN, European Committee for Standardization, Brussels.

INTERNATIONAL COUNCIL FOR RESEARCH AND INNOVATION
IN BUILDING AND CONSTRUCTION

WORKING COMMISSION W18 - TIMBER STRUCTURES

A PORTAL FRAME DESIGN FOR
RAISED WOOD FLOOR APPLICATIONS

T G Williamson

Z A Martin

Borjen Yeh

APA - The Engineered Wood Association

U.S.A.

Presented by B Yeh

F Lam received clarification that the load deflection curves are obtained from sequential loading test. F Lam commented that although cost saving is an issue, the application of through bolts to connect inter storey and the use of the existing anchor bolts for hold down should not be too costly. BJ Yeh responded that the builders may build thousands of homes per year and they want the lowest cost option. Anchor bolts can be hidden which may be an issue for inspection.

E Karacabeyli commented that this help address the soft storey issues. He asked whether reference tests with full hold-down or through rods were performed. BJ Yeh responded that this was not directly done but the high end restraint information on reference wall has the hold downs installed.

A Portal Frame Design for
Raised Wood Floor Applications

Thomas G. Williamson, P.E.
Zeno A. Martin, P.E.
Borjen Yeh, Ph.D., P.E.
APA - The Engineered Wood Association, U.S.A.

Abstract

The performance of narrow shear walls or bracing segments without hold-downs has been recognized by the International Residential Code (IRC) in the U.S. by setting a maximum aspect ratio of 6:1 in the 2004 code change cycle. The background information supporting the code change has been presented (Williamson and Yeh, 2004). However, due to the lack of test data on raised wood floors at that time, the U.S. building codes restrict this application to construction on rigid foundations, such as a concrete foundation, stem wall, or slab.

In order to address the raised floor issue such as occurs in basement or crawl space construction and in second or third level floors, a research project was conducted by APA - The Engineered Wood Association in late 2004 on narrow shear walls constructed on the top of a raised wood floor assembly without hold-downs. A total of 12 full-scale cyclic shear wall tests were conducted in this study. Several different raised floor configurations were first tested to determine the difference between engineered-wood raised floors using I-joists and solid-sawn raised floors, and to evaluate the effect of joist orientation relative to the braced wall segment. The wall heights tested were 2438 mm (8 feet) and each total wall segment was 3658 mm (12 ft) long. The SEAOSC (1997) cyclic load protocol was used in this test program.

1. Introduction

Unlike many other countries, in the U.S., wood framing is the dominant type of construction for new homes. With housing starts of approximately 2 million units per year, this represents a huge market for wood products. In recent years new home construction has seen an increasing trend toward 2 and 3 story construction with a high percentage of narrow wall segments due to the demand by architects and owners for maximum window areas. This report presents test data for a wood portal frame design with no hold-down devices built on top of a raised wood floor as would be typical for 2 and 3 story construction, intended for use in a fully sheathed structures.

The 2003 International Residential Code (IRC, Section R602.10.5) permits a 4:1 aspect ratio wood structural panel braced wall segment if a) the structure is fully sheathed with wood structural panels and b) openings next to such segments are limited to 0.65 times the story height. These 4:1 aspect ratio segments can be used in any of 3 stories. There are no specific hold-down requirements in the IRC for this 4:1 aspect ratio wall segment, except a corner framing detail is specified at corners. Thus, in actual field applications, the fully sheathed perpendicular walls and dead loads would provide the end restraint for this 4:1 aspect ratio wall segment rather than hold-down devices.

Using this IRC 4:1 aspect ratio wall segment as a currently acceptable baseline, tests were conducted on a 406 mm (16-in.)-wide portal frame design (6:1 aspect ratio) with similar end restraint as the IRC 4:1 aspect ratio wall segment to investigate if such an alternate narrow wall segment would provide equal or better performance when built on a raised wood floor. Similar comparative testing has been done with wall segment elements built on a steel test frame (rigid foundation) and results showed the 6:1 aspect ratio portal frame designs perform approximately equal to or better than the IRC 4:1 aspect ratio wall segment (APA, 2003).

2. Materials and Test Assemblies

Table 1 summarizes details of each test.

Table 1. Raised floor wall testing description

Wall Test[1]	Degree of End Restraint	Wall Segment Type	Joist Depth (mm)	Rim Joist Type	Joist Type	Joist Orientation[2]	Connection of Braced Wall to Raised Floor[3]
RF1	High	R602.10.5	302	28.6 mm OSB	PRI-20	Perp.	see footnote 3
RF2	High	R602.10.5	302	PRI-20	PRI-20	Perp.	see footnote 3
RF3	High	R602.10.5	286	2x12	2x12	Perp.	see footnote 3
RF4	High	R602.10.5	302	PRI-20	PRI-20	Parallel	see footnote 3
RF5	High	R602.10.5	286	2x12	2x12	Parallel	see footnote 3
RF6	Low	R602.10.5	302	PRI-20	PRI-20	Parallel	see footnote 3
RF7	Low	Portal Frame	302	PRI-20	PRI-20	Parallel	see footnote 3
RF8	Low	Portal Frame	302	PRI-20	PRI-20	Parallel	2 LTP4 at each wall segment[3]
RF9	Low	Portal Frame	302	PRI-20	PRI-20	Parallel	302 mm OSB overlap with rim joist[3]
RF10	Low	Portal Frame	286	2x12	2x12	Parallel	235 mm OSB overlap with rim joist[3]
RF11	Low	R602.10.5	302	PRI-20	PRI-20	Parallel	see footnote 3
RF12	High	Portal Frame	302	PRI-20	PRI-20	Parallel	2 LTP4 at each wall segment(3)

(1) Wall tests RF4 and RF5 were built with 8d box nails, all others 8d common. RF9, RF10, and RF12 had an unblocked sheathing joint near wall mid height.
(2) Joist orientation relative to wall segment; either parallel, or perpendicular.
(3) All tests had sole plate to rim joist connection with 3-16d @ 406 mm o.c. at braced wall segment per IRC Table R602.3(1), plus additional connection as noted.

2.1 Wall Segments

For the wall framing, dry 38.1 mm x 88.9 mm (2x4) No. 2 Douglas-fir (DF) lumber was used. The header was built up using two lumber 38.1 mm x 286 mm (2x12) No. 2 DF members, with an 11.9 mm (15/32-in.) OSB spacer used on the backside of the 2x12's to create a header surface that was flush with the 2x4 framing. APA Rated Sheathing oriented strand board (OSB) with a thickness of 9.5-mm (3/8-in.) and a span rating of 24/0, Exposure 1, was used for all wall sheathing. Nails used for attaching wall sheathing to framing were 8d common (3.3 mm diameter x 63.5 mm long), except two tests (as noted, RF4 and RF5) were built with 8d box nails (2.9 mm x 63.5 mm). Nails used for stitch nailing of the double end studs were 10d common (3.8 mm x 76.2 mm), spaced 610

mm (24 in.) o.c., per code. Nails used for attaching the sole plate to the raised floor were 16d sinkers (3.8 mm x 82.5 mm).

Hold-down devices were used in some tests. . The tests using hold-down devices were intended to simulate the case with a high degree of end restraint, such as that provided by the fully sheathed return wall, header, and dead weight from above. The hold-down devices used were Simpson Strong Tie PHD5's attached to a single 2x4 that was nailed to the wall framing with 16-16d sinker nails.

A Simpson Strong Tie LSTA 24 strap (31.7 mm wide x 610 mm long, 20-gage steel) was used in the portal frame tests to provide vertical continuity and resistance to loads normal to the sheathing surface, and to provide some reinforcement for lateral loadings.

2.2 Raised Floor Assemblies

The raised floor assemblies were built with a continuous No. 2 DF 2x4 bottom plate. The rim joist was either 28.6 mm (1-1/8-in.) APA OSB Rim Board, a No. 2 DF 2x12 joist, or a PRI-20 I-joist. The PRI-20 I-joist had a 44.4-mm (1-3/4-in.) wide x 33.3-mm (1-5/16-in.) thick flange, with a 9.5-mm (3/8-in.) OSB web. When the solid-sawn 2x12 rim joists were used, the same material was used for the floor joists. When engineered wood products were used as the rim joist, PRI-20 I-joists were used for the floor joists. APA Rated Sheathing OSB with a thickness of 9.5 mm (3/8-in.), with a span rating of 24/0, Exposure 1, was used for the wall portion of the raised floor. APA Rated Sheathing OSB with a thickness of 18.2 mm (23/32-in.), with a span rating of 48/24, Exposure 1, was used for all floor sheathing.

Nails used for attaching wall sheathing to rim joist, rim joist to sill plate, and rim joist to joist (where applicable) were 8d common (3.3 mm diameter x 63.5 mm long). Four 1/2-in.-diameter sill bolts with 50.8 mm x 50.8 mm x 4.8 mm (2-in. x 2-in. x 3/16-in.) plate washers were used to fasten the sill plate to the test frame. Placement of the sill anchorage is shown in Figure 1.
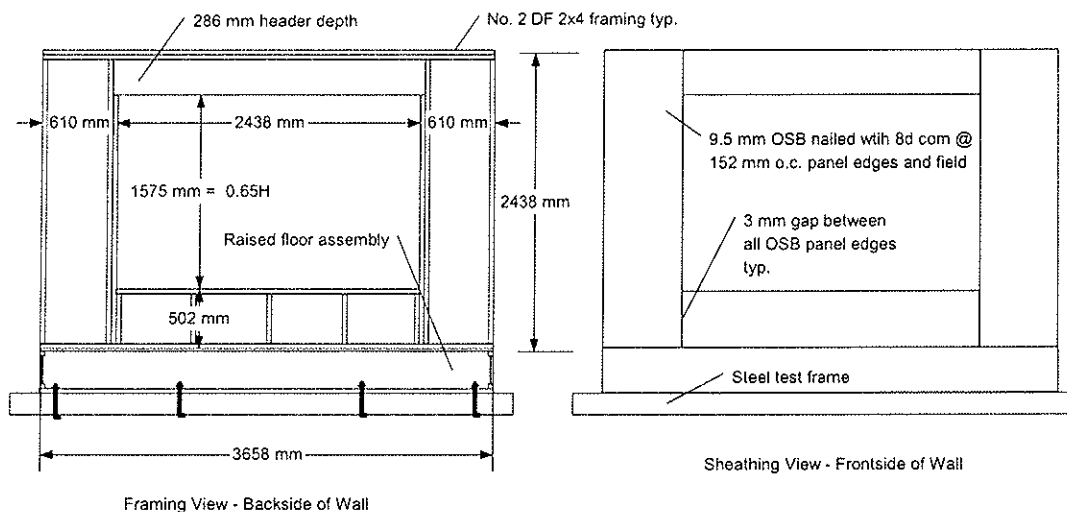
Figure 1. **Wall construction details for the 4:1 aspect ratio walls segments used as the baseline**

Figure 1 shows the typical R602.10.5 wall segment test specimen with a low degree of end restraint. This R602.10.5 wall segment is currently permitted in the IRC and is considered the baseline in this test program. The raised floor assembly with perpendicular joists had joists spaced 610 mm (24 in.) o.c. perpendicular to the rim joist. The raised floor assembly with parallel joists had the outer joist spaced 406 mm (16 in.) o.c. parallel to the rim joist.

Figure 2 shows the typical portal frame built on top of the raised floor assembly, where two LTP4 plates are used in addition to the 3-16d sinker nails to connect the wall segment to the raised floor.
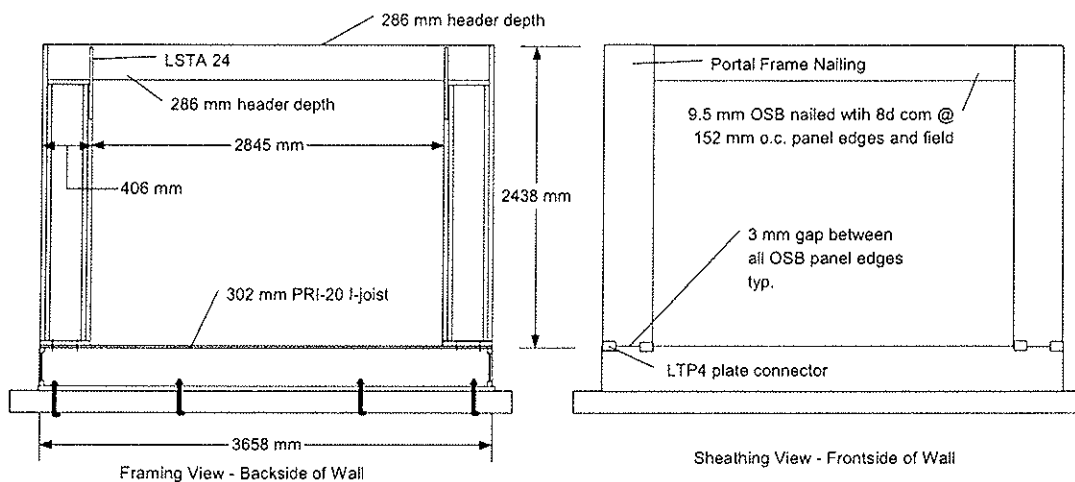
Figure 2. **Wall construction details for the 6:1 aspect ratio portal frame wall segments**

For the low degree of end restraint condition, only the minimum anchor bolts, placed as shown in Figures 1 and 2 were used to restrain the assembly from uplift. For the high degree of end restraint condition, a single 2x4 attached to the wall with 16-16d sinkers was used and this 2x4 was connected to a Simpson PHD5 hold-down. Complete details with figures have been published (APA, 2004).

Tests RF1-RF5 were conducted to determine effect of different raised floor configurations and establish which to use as the worst case for subsequent testing. A high degree of end restraint was used in Test RF1-RF5 to force the highest loads possible on the raised floor and wall assembly. The test results for the parallel and perpendicular joist orientation were very close to each other, but the parallel joist case was slightly more critical. By inspection, the parallel joist case provides less material to resist compressive forces due to the wall racking. Therefore, the remaining tests (RF6 – RF12) were conducted with the parallel joist orientation. Tests RF6 and RF11 established the baseline for a low degree of end restraint. Tests RF7-RF10, with a low degree of end restraint, were of different portal frame-wall-segment to raised-floor connections. Previous testing (APA, 2003) has shown that the critical relative performance comparisons between the portal frame and baseline occur for the low degree of end restraint condition.

4

3. Test Set-Up and Procedure

For the portal frame tests, load was applied to the walls via a load head beam-to-header connection using five 19 mm x 152 mm (3/4-in. x 6-in.) lag screws evenly spaced along the length of header. For the 4:1 aspect ratio wall segment tests, a combination of similarly sized bolts and lag screws were used. The OSB sheathing was free to rotate in that the OSB sheathing was neither bearing on the foundation frame nor on the load beam above. A 3.2-mm (1/8-in.) gap was left as spacing between adjacent OSB panels. Walls were tested both with a high degree of end restraint and a low degree of end restraint to investigate the range of response expected for a segment which does not require hold-down devices, but which does have some degree of end restraint provided by the surrounding structure.

4. Test Results

A summary of the test results is shown in Tables 2 and 3 and Figures 3 and 4. The test results in Table 2 are the absolute average values of the positive and negative displacement excursions.

Table 2. Summary of test results (data is average of +/- excursions)

Degree of End Restraint	Wall Type	Wall Test	Load (kN) at		Maximum	
			6.1 mm	12.2 mm	Load (kN)	Defl. (mm)
Low	R602.10.5	RF6	2.24	3.57	10.07	83.2
	R602.10.5	RF11	1.94	3.19	9.96	92.6
	Portal Frame	RF7	2.18	3.73	8.06	69.8
	Portal Frame	RF8	2.58	4.40	10.07	75.6
	Portal Frame	RF9	2.54	4.42	11.00	76.8
	Portal Frame	RF10	2.77	4.74	10.18	62.5
High	R602.10.5	RF1	3.93	6.00	14.14	57.2
	R602.10.5	RF2	3.85	6.34	13.69	62.5
	R602.10.5	RF3	4.12	6.59	13.77	68.7
	R602.10.5	RF4	3.63	5.54	12.39	56.1
	R602.10.5	RF5	3.91	6.16	12.43	61.4
	Portal Frame	RF12	3.78	6.51	16.78	85.1

Table 3. Ratio of average portal frame tests results divided by baseline tests results

Degree of End Restraint	Wall Comparison Between	Load (kN) at		Maximum	
		6.1 mm	12.2 mm	Load (kN)	Defl. (mm)
Low	RF7/(ave. of RF6&11)	1.04	1.10	0.80	0.79
	RF8/(ave. of RF6&11)	1.23	1.30	1.00	0.86
	RF9/(ave. of RF6&11)	1.21	1.31	1.10	0.87
	RF10/(ave. of RF6&11)	1.32	1.40	1.02	0.71
High	RF12/RF4	1.04	1.18	1.35	1.52
	RF12/(ave. of RF1,2,3,4& 5)	0.97	1.06	1.26	1.39

5
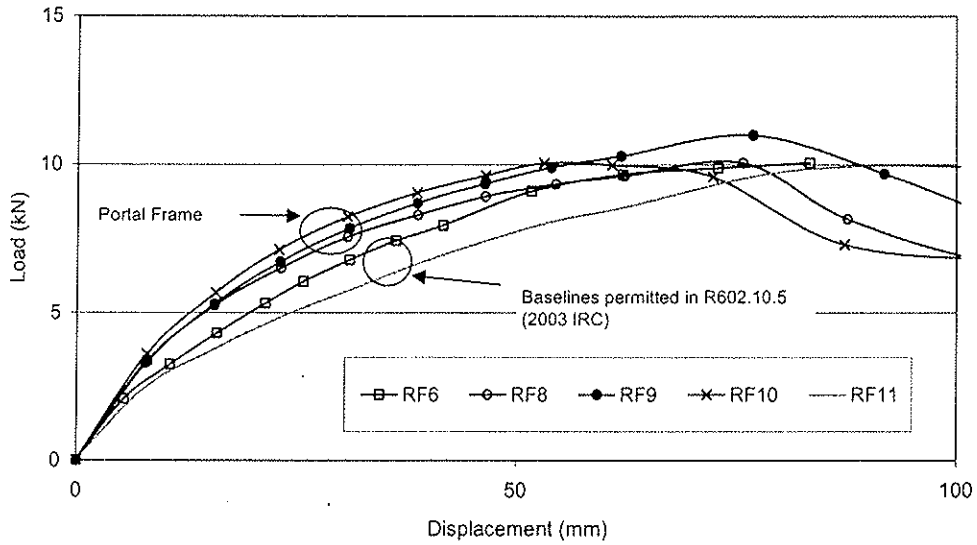
Figure 3. Backbone curve summary – positive and negative excursions averaged for tests with a low degree of end restraint (Test RF7 is omitted for clarity)
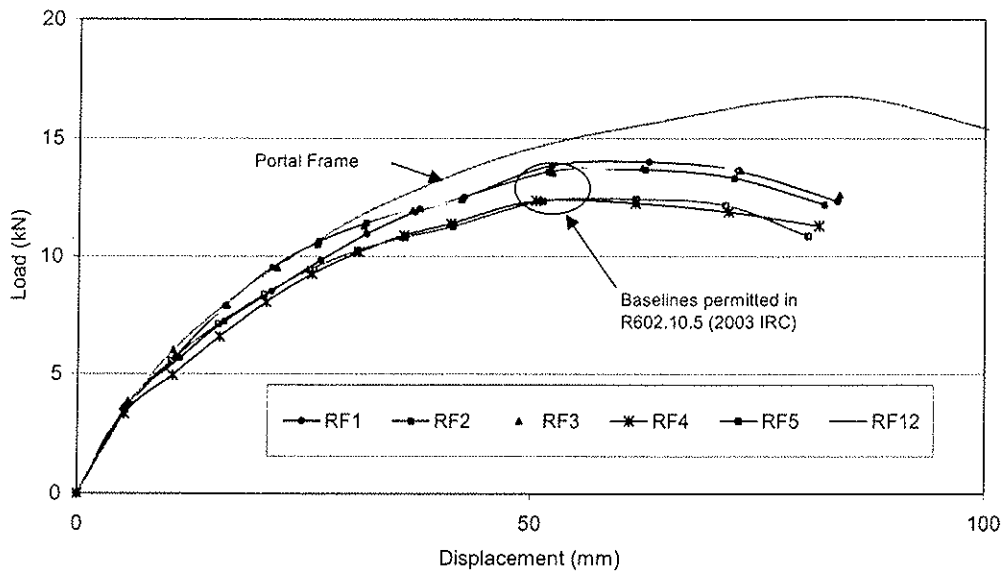
Figure 4. Backbone curve summary – positive and negative excursions averaged for tests with a high degree of end restraint

4.1 Failure Modes

All of the raised floor tests had the wall segment, rather than the raised floor segment, dominate the failure. R602.10.5 wall segments had classic shear wall failure mechanisms where the failure was dominated by the nailed connection of the sheathing to the framing.

Some nail fatigue was observed in these wall tests as is common for wood structural panel shear wall tests conducted with the SPD (SEAOSC, 1997) load protocol.

The portal frame wall failure region was more concentrated at either the wall connection to the raised floor or the sheathing overlapping the header, or both. In some tests the OSB failed in bending (tension) where it overlaps the header, as previously reported (APA, 2003). Almost all metal strap components failed in fatigue before the 72 cycles of the SPD protocol were finished, as is typical of these strap components subjected to the SPD (SEAOSC, 1997) load protocol.

4.2 Portal Frame vs. Existing Bracing Comparison

As shown in Table 3 by ratios greater than 1 (or within a few percent, e.g. 0.97) all portal frame test results except RF7 (a design that will not be recommended) had better stiffness and maximum load capacity compared to the existing bracing permitted in R602.10.5. The deflection at peak load for the portal frames was less than the existing permitted bracing for the low degree of end restraint walls, but higher for the high degree of end restraint walls. The high degree of end restrain condition is believed to be more representative of actual end use conditions because perpendicular walls, finishes, and dead weight will all add a degree of end restraint. For the high degree of end restraint, the portal frame has equal or better performance characteristics by every measure.

5. Comparison to Previous Testing

The testing described in this report was similar to previous testing (APA, 2003) in that the purpose was to make relative performance comparisons between portal frame bracing and existing permitted bracing. However, in this report, all relative comparisons were made for wall segments built on top of a raised wood floor assembly. Note that the raised floor portal frames had a different bottom of wall attachment to the "foundation" as described, and RF9, RF10 and RF12 had an unblocked panel edge at mid-height of the wall segment. Comparisons of tests results between wall segments built on a rigid foundation to those built on a raised floor show that
- The raised floor reduces wall stiffness but not ultimate strength, and
- The effect of the raised floor is not as significant as is the degree of end restraint applied to wall segments.

6. Conclusions

Portal frame wall segments having a 6:1 aspect ratio wall segment, whether built on a rigid foundation or a raised floor foundation, have comparable performance to the 24-in. braced wall segments currently permitted by code (see 2003 IRC, Section R602.10.5) built on the same.

7. References

APA, 1999. Preliminary Testing of Wood Structural Panel Shear Walls Under Cyclic (Reversed) Loading. APA Research Report 158. APA-The Engineered Wood Association. Tacoma, WA, USA.

APA, 2003. Testing a Portal Frame Design for Use as Bracing in Fully Sheathed Structures. APA-Report T2003-48. APA-The Engineered Wood Association. Tacoma, WA, USA.

APA, 2004. A Portal Frame Design on Raised Wood Floors for Use as Bracing in Fully Sheathed Structures. APA-Report T2004-38. APA-The Engineered Wood Association. Tacoma, WA, USA.

COLA-UCI, 2001. Report of a Testing Program of Light-Framed Walls with Wood-Sheathed Shear Panels. Final Report to the City of Los Angeles Department of Building Safety by SEAOSC, COLA-UCI Light Frame Test Committee, and the Department of Civil and Environmental Engineering at the University of California, Irvine, USA.

ICC, 2004. Supplement to the International Codes. International Code Council. Country Club Hills IL, USA.

IRC, 2003. International Residential Code for One and Two Family Dwellings. International Code Council. Country Club Hills IL, USA.

SEAOSC, 1997. *Standard method of cyclic (reversed) load test for shear resistance of framed walls for buildings.* Structural Engineers Association of Southern California, Whittier, CA, USA.

Williamson, T., Yeh, B. 2004. Narrow Shear Walls -- A Portal Frame Solution. Proceedings of the 8th World Conference on Timber Engineering, Lahti, Finland.

INTERNATIONAL COUNCIL FOR RESEARCH AND INNOVATION
IN BUILDING AND CONSTRUCTION

WORKING COMMISSION W18 - TIMBER STRUCTURES

LINEAR ELASTIC DESIGN METHOD FOR TIMBER FRAMED CEILING, FLOOR AND WALL DIAPHRAGMS

J Leskelä

Finnish Forest Industries Federation

FINLAND

Presented by J Leskelä

M Yasumura asked whether deflection or capacity is of interest and how to define capacity. J Leskelä responded that they are both considered. The capacity is based on the code equations based on exceeding the strength of the fasteners. H Larsen liked the conclusion that more research is needed and commented that since the work is based on design method, verification of such methods is needed. H Larsen further pointed out that design methods always have safety factors and asked if the level of deformation is known? J Leskelä responded that the level of deformation is not done in this exercise and commented that there is a need to do more tests. B Källsner stated that he has test results from the 80's and the method seems to be quite good. Nailing along the edge of sheathing with small spacing may lead to problems. H Larsen further questioned why one cannot use the plastic model if the elastic model can be used.

Linear elastic design method for timber framed ceiling, floor and wall diaphragms

Jarmo Leskelä

Finnish Forest Industries Federation

Abstract

The objective of the paper is to present linear elastic hand calculation design method for timber framed ceiling, floor and wall diaphragms developed in author's licentiate's thesis.

Fastening lay-out contributes significantly to the calculatory racking capacity and horizontal deflection of ceiling, floor and wall diaphragms. Fastening lay-out depends on the orientation of panels and frame members and on the spacing of frame members. The panels should be orientated parallel to the frame members in order to maximise the racking capacity and to minimise the horizontal deflection of blocked and unblocked diaphragms.

Further research is recommended to experimentally analyse the fastening lay-out's contribution to the racking capacity and the horizontal deflection of unblocked ceiling, floor and wall diaphragms.

1   Introduction

1.1   Background

Most of the existing hand calculation design methods for timber framed ceiling, floor and wall diaphragms do not take the horizontal deflection of diaphragms into account or do not consider fastening lay-out's contribution to the performance of diaphragms. These may lead to an inaccurate design of diaphragms.

1.2   Objective

The objective of the paper is to present linear elastic hand calculation design method for timber framed ceiling, floor and wall diaphragms developed in author's licentiate's thesis.

Simplified analysis for roof, floor and wall diaphragms given in Eurocode 5 is reviewed. Equations for wall diaphragm unit given in STEP 3 method are extended to wall diaphragms and further to ceiling and floor diaphragms. Factors taking into account the fastening lay-out are tabulated for the most typical combinations of dimensions of a panel and spacing of fasteners.

Fastening lay-out's contribution to the racking capacity and the horizontal deflection of ceiling, floor and wall diaphragms is evaluated by comparing the calculation results of different lay-outs. The accuracy of calculations is enabled by cancelling the material properties causing inaccuracy.

1.3   Limitations

The method covers static wind loaded rectangular and non perforated ceiling, floor and wall diaphragms composed of wood-based panels mechanically fastened to frame members.

2   Review

2.1   Horizontal deflection

Eurocode 5 analysis (EN 1995-1-1) does not take the horizontal deflection of roof, floor and wall diaphragms into account, as shown in Figure 2.1. It is assumed that the fasteners in panel to frame connection behave completely plastic in shear, which may lead to unlimited deformations.
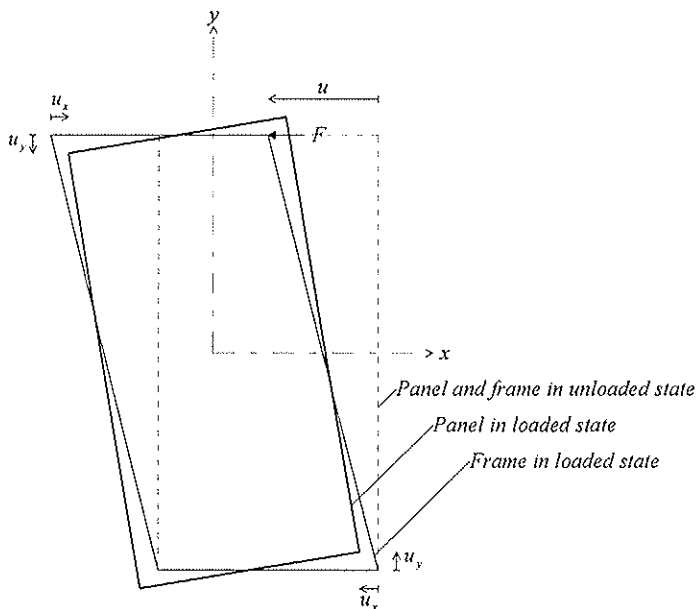
Figure 2.1: Horizontal deflection of diaphragm unit

STEP 3 method (Källsner&Lam 1995) does not provide equations for ceiling and floor diaphragms.

2.2   Fastening lay-out

Eurocode 5 analysis does not consider fastening lay-out's contribution to the racking capacity and the horizontal deflection of ceiling, floor and wall diaphragms. It is assumed that the diaphragms are blocked (fasteners along the perimeter of each panel), as shown in Figure 2.2, and the shear forces are uniformly distributed to the fasteners. The assumption restricts the applicability of the method, since the ceiling, floor and crossing stud wall diaphragms are often unblocked (fasteners along the width or height direction of each panel only), as shown in Figure 2.3. In addition, the unsupported edges of panels are not usually connected to each other by battens, as assumed, but by tongue and groove joints or just by butt joints. Consequently, there is not always mechanical connection between the unsupported edges of panels.

2
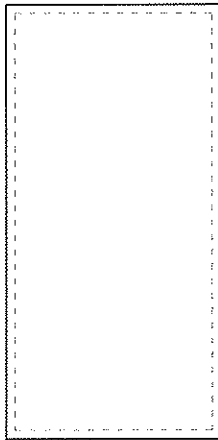
Figure 2.2: Blocked diaphragm unit
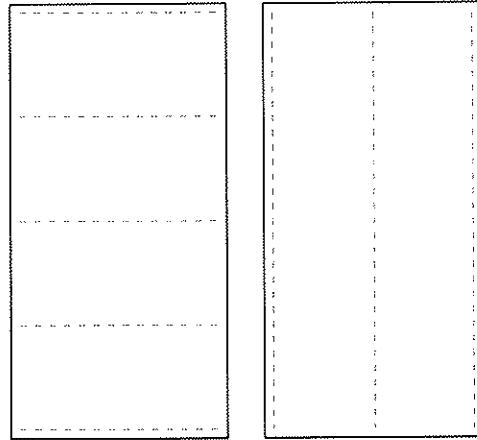
Figure 2.3: Unblocked diaphragm unit

STEP 3 method is applicable to unlimited number of fastening lay-out assumptions.

3   Design method

Author's method is based on the STEP 3 method, the elastic model and the following assumptions:

- panels are rigid in bending and in tension but linear elastic in shear
- frame members (battens, joists, studs, plates) are rigid and hinged to each other, thus no deformations of frame members occur
- fasteners in panel to frame connection are linear elastic in shear until failure
- spacing of fasteners is constant along different frame members
- edge distance and spacing of fasteners are sufficient, thus no brittle failures occur
- there is no direct contact between the adjacent panels and between the panel and the adjacent structure, thus the panels are subjected to shear forces of fasteners only
- displacements are small compared with the width and the height of a panel
- end studs of wall diaphragms are fully anchored to the transversal load-bearing walls or to the floor diaphragm below or to the foundation, thus no uplifts of studs occur
- bottom plates of wall diaphragms are fully anchored to the floor diaphragm below or to the foundation, thus no slips of plates occur
- ceiling, floor and wall diaphragms have stiffness on their planes only

3.1   Wall diaphragm units

Wall diaphragm unit, shown in Figures 3.1 and 3.2, is composed of a panel mechanically fastened to frame members (studs, plates). Width of a panel is B, height H, thickness t and shear modulus G. Spacing of fasteners is s and slip modulus K. Horizontal load F is subjecting to the top of a wall diaphragm unit. Wall diaphragm unit is behaving as an elastic cantilevered deep I-beam on its plane transferring horizontal force F to the foundation and vertical forces N to the end studs of a wall diaphragm unit.
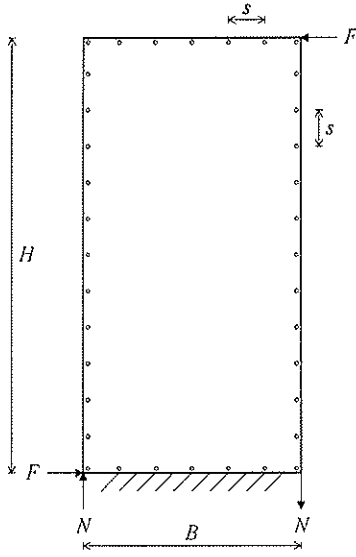
Figure 3.1: Orientation of a panel transversal
to the load direction
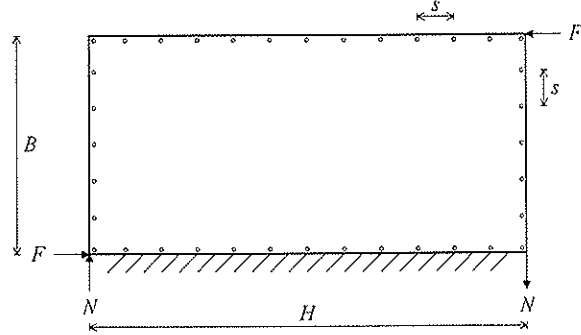
Figure 3.2: Orientation of a panel parallel
to the load direction

Maximum shear force F_{max} of fasteners in the corners of a panel is given by

$$F_{max} = \alpha HF \qquad \text{(orientation of a panel transversal to the load direction)} \qquad (3.1a)$$

$$F_{max} = \alpha BF \qquad \text{(orientation of a panel parallel to the load direction)} \qquad (3.1b)$$

and horizontal deflection u at the top of a wall diaphragm unit by

$$u = \left(\beta \frac{H^2}{K} + \frac{H}{tBG} \right) F \qquad \text{(orientation of a panel transversal to the load direction)} \qquad (3.2a)$$

$$u = \left(\beta \frac{B^2}{K} + \frac{B}{tHG} \right) F \qquad \text{(orientation of a panel parallel to the load direction)} \qquad (3.2b)$$

where

$$\alpha = \sqrt{ \left(\frac{x_{max}}{\sum\limits_{i=1}^{n} x_i^2} \right)^2 + \left(\frac{y_{max}}{\sum\limits_{i=1}^{n} y_i^2} \right)^2 } \qquad (3.3)$$

$$\beta = \frac{1}{\sum\limits_{i=1}^{n} x_i^2} + \frac{1}{\sum\limits_{i=1}^{n} y_i^2} \qquad (3.4)$$

x_{max} is the x-co-ordinate $(B/2)$ for individual fastener in the corner of a panel [mm]

y_{max} is the y-co-ordinate $(H/2)$ for individual fastener in the corner of a panel [mm]

$\displaystyle\sum_{i=1}^{n} x_i^2$ is the sum of the squared x-co-ordinates for n number of fasteners $[mm^2]$

$\displaystyle\sum_{i=1}^{n} y_i^2$ is the sum of the squared y-co-ordinates for n number of fasteners $[mm^2]$

Tension and compression forces N are resisted by the end studs and are given by

$$N = \frac{H}{B} F \qquad\qquad \text{(orientation of a panel transversal to the load direction)} \qquad (3.5a)$$

$$N = \frac{B}{H} F \qquad\qquad \text{(orientation of a panel parallel to the load direction)} \qquad (3.5b)$$

3.2   Wall diaphragms
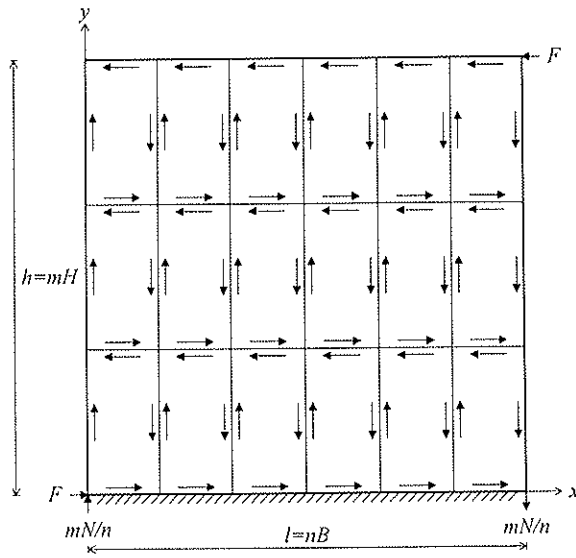
Figure 3.3: Number of diaphragm units in width and height direction

Wall diaphragm, shown in Figure 3.3, is composed of n number of diaphragm units in width direction and m number of diaphragm units in height direction. Width of a wall diaphragm is l and height h. Horizontal load F is uniformly distributed to the top of a wall diaphragm. Wall diaphragm is behaving as an elastic cantilevered deep I-beam on its plane transferring horizontal force F to the foundation and vertical forces mN/n to the end studs of a wall diaphragm.

Maximum shear force F_{max} of fasteners in the corners of panels is given by

$$F_{max} = \frac{\alpha H F}{n} \qquad\qquad \text{(orientation of panels transversal to the load direction)} \qquad (3.6a)$$

$$F_{max} = \frac{\alpha B F}{n} \qquad\qquad \text{(orientation of panels parallel to the load direction)} \qquad (3.6b)$$

Horizontal deflection u at the top of a wall diaphragm is the sum of deflections of diaphragm units in height direction and is given by

5

$$u = \left(\beta\frac{H^2}{K} + \frac{H}{tBG}\right)\frac{mF}{n} \quad \text{(orientation of panels transversal to the load direction)} \quad (3.7a)$$

$$u = \left(\beta\frac{B^2}{K} + \frac{B}{tHG}\right)\frac{mF}{n} \quad \text{(orientation of panels parallel to the load direction)} \quad (3.7b)$$

Studs and plates fastening the adjacent panels are subjected to each other compensating vertical and horizontal forces N/n and F/n. Tension and compression forces mN/n are resisted by the end studs and are given by

$$\frac{mN}{n} = \frac{mHF}{nB} \quad \text{(orientation of panels transversal to the load direction)} \quad (3.8a)$$

$$\frac{mN}{n} = \frac{mBF}{nH} \quad \text{(orientation of panels parallel to the load direction)} \quad (3.8b)$$

3.3 Ceiling and floor diaphragms

Ceiling or floor diaphragm, shown in Figure 3.4, is composed of n number of diaphragm units in width direction and $2m$ number of diaphragm units in length direction. Width of a ceiling or floor diaphragm is d and length L. Horizontal load w is uniformly distributed to the plane of a ceiling or floor diaphragm. Ceiling or floor diaphragm is behaving as an elastic simply supported deep I-beam on its plane transferring horizontal loads $F=Lw/2$ to the tops of wall diaphragms below.
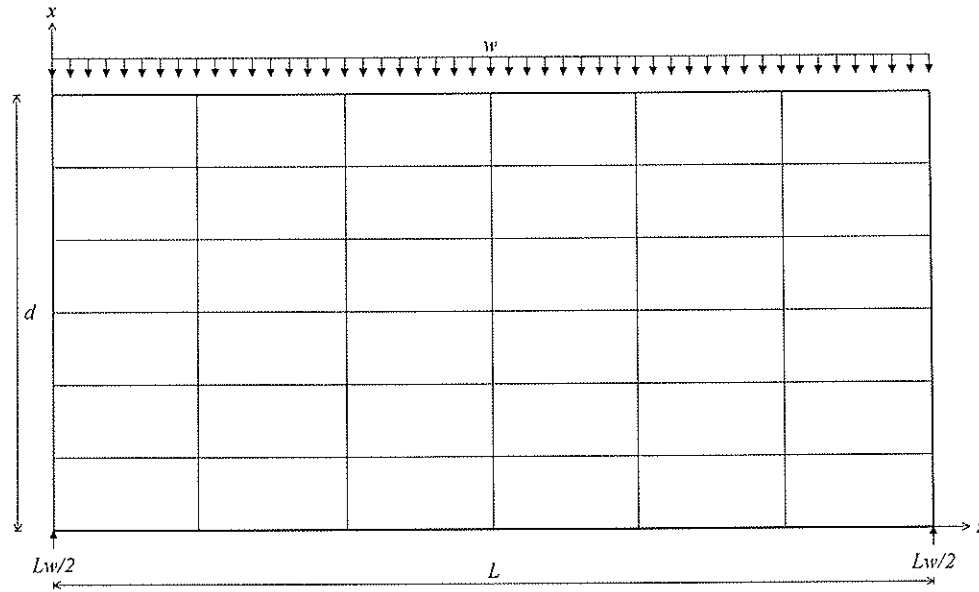
Figure 3.4: Ceiling or floor diaphragm

Maximum bending moment M_{max} and shear force V_{max} are given by

$$M_{max} = \frac{L^2 w}{8} \quad (3.9)$$

$$V_{max} = \frac{Lw}{2} \tag{3.10}$$
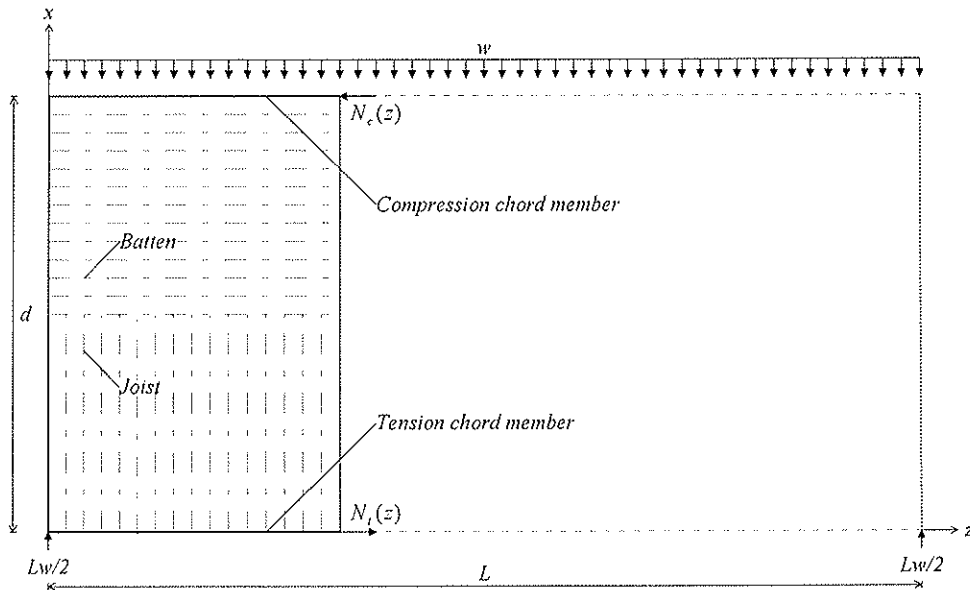
Figure 3.5: Bending moment distribution of a ceiling or floor diaphragm

Tension $N_t(z)$ and compression forces $N_c(z)$ are resisted by the tension and compression chord members. Maximum tension and compression force N_{max} is given by

$$N_{max} = \frac{M_{max}}{d} = \frac{L^2 w}{8d} \tag{3.11}$$
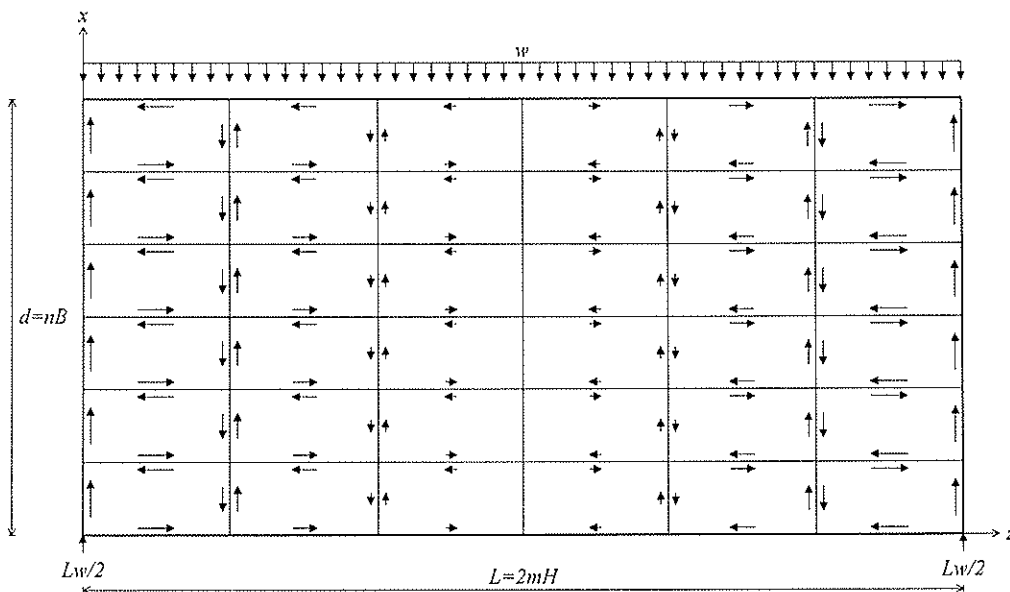
Figure 3.6: Shear force distribution of a ceiling or floor diaphragm

Shear forces $V(z)$ are resisted by the sheathing and are distributed to the symmetrical halves of a ceiling or floor diaphragm in accordance with Chapter 3.2. When determining

7

shear forces of fasteners in ceiling or floor diaphragm, the maximum value of shear force V_{max}/n subjecting to the diaphragm unit is used.

$$\frac{F}{n} = \frac{V_{max}}{n} = \frac{Lw}{2n} \tag{3.12}$$

Maximum shear force F_{max} of fasteners in the corners of panels locating at the ends of a ceiling or floor diaphragm is given by

$$F_{max} = \frac{\alpha HLw}{2n} \qquad \text{(orientation of panels transversal to the load direction)} \tag{3.13a}$$

$$F_{max} = \frac{\alpha BLw}{2n} \qquad \text{(orientation of panels parallel to the load direction)} \tag{3.13b}$$
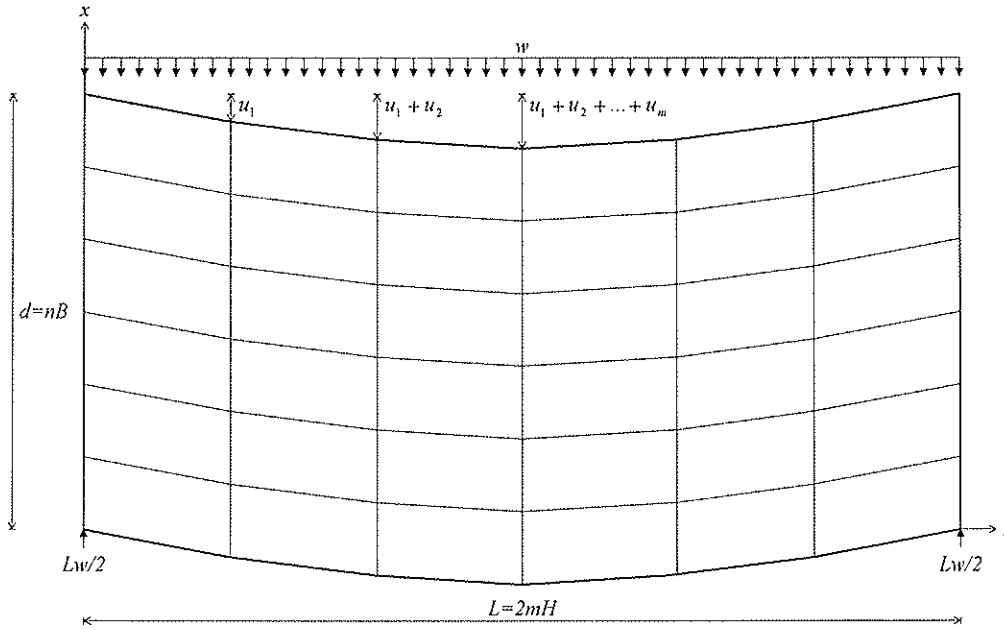
Figure 3.7: Shear deformation of panels

When determining deflection of a ceiling or floor diaphragm, the mean value of shear force V_{mean}/n subjecting to the diaphragm unit is used.

$$\frac{F}{n} = \frac{V_{mean}}{n} = \frac{Lw}{4n} \tag{3.14}$$

Horizontal deflection u at the mid length of a ceiling or floor diaphragm is given by

$$u = \left(\beta \frac{H^2}{K} + \frac{H}{tBG} \right) \frac{mLw}{4n} \qquad \text{(orientation of panels transversal to the load direction)} \tag{3.15a}$$

$$u = \left(\beta \frac{B^2}{K} + \frac{B}{tHG} \right) \frac{mLw}{4n} \qquad \text{(orientation of panels parallel to the load direction)} \tag{3.15b}$$

8

3.4 Fastening lay-out

Factors α and β taking into account the fastening lay-out are tabulated and given in Table 3.1 for the most typical combinations of dimensions of a panel and spacing of fasteners.
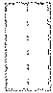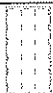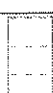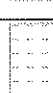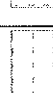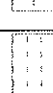
Fastening lay-out	Dimensions of a panel	B*H=1200mm*2400mm		B*H=1200mm*2700mm	
	Spacing of fasteners	Factor α $[*10^{-5}/mm]$	Factor β $[*10^{-8}/mm^2]$	Factor α $[*10^{-5}/mm]$	Factor β $[*10^{-8}/mm^2]$
1)	s=75mm	2,722	5,017	2,409	4,336
	s=100mm	3,626	6,684	3,210	5,778
	s=150mm	5,428	10,00	4,805	8,648
2)	s=75mm	2,592	4,817	2,297	4,175
	s=100mm	3,458	6,425	3,064	5,568
	s=150mm	5,189	9,639	4,597	8,351
3)	s=75mm	2,341	4,357	2,071	3,771
	s=100mm	3,128	5,821	2,766	5,036
	s=150mm	4,709	8,759	4,162	7,573
4)	s=75mm	2,105	3,920	1,859	3,387
	s=100mm	2,817	5,244	2,486	4,528
	s=150mm	4,253	7,914	3,749	6,826
5)	s=75mm	9,053	16,57	8,983	16,14
	s=100mm	11,45	20,99	11,35	20,43
	s=150mm	15,52	28,55	15,38	27,74
6)	s=75mm	6,898	12,73	6,824	12,35
	s=100mm	8,732	16,14	8,631	15,64
	s=150mm	11,87	21,99	11,71	21,26
7)	s=75mm	5,584	10,35	5,512	10,01
	s=100mm	7,074	13,13	6,976	12,68
	s=150mm	9,630	17,90	9,479	17,25
8)	s=75mm	4,054	7,538	3,989	7,262
	s=100mm	5,141	9,566	5,053	9,206
	s=150mm	7,012	13,06	6,878	12,54
9)	s=75mm	3,185	5,931	3,129	5,702
	s=100mm	4,042	7,530	3,966	7,231
	s=150mm	5,521	10,29	5,404	9,856
10)	s=75mm	3,468	6,189	2,944	5,159
	s=100mm	4,536	8,120	3,863	6,785
	s=150mm	6,559	11,80	5,617	9,909
11)	s=75mm	2,888	5,273	2,476	4,432
	s=100mm	3,785	6,923	3,254	5,833
	s=150mm	5,490	10,08	4,744	8,528
12)	s=75mm	2,473	4,555	2,131	3,846
	s=100mm	3,243	5,983	2,802	5,063
	s=150mm	4,713	8,715	4,092	7,407

Table 3.1: Factors taking into account the fastening lay-out

4   Calculatory comparison between the fastening lay-outs

Fastening lay-out's contribution to the racking capacity and the horizontal deflection of ceiling, floor and wall diaphragms is evaluated by comparing the calculation results of different lay-outs. The accuracy of calculations is enabled by cancelling the material properties causing inaccuracy.

4.1   Ceiling and floor diaphragms

Unblocked ceiling or floor diaphragm with size of $d*L=4800mm*9600mm$, shown in Table 4.1, is composed of sixteen number of diaphragm units. Panels are mechanically fastened to frame members (battens or joists). Dimensions of a panel are $B*H=1200mm*2400mm$. Spacing of frame members is $B/4=300mm$, $B/3=400mm$ or $B/2=600mm$. Spacing of fasteners is $s=75mm$, $s=100mm$ or $s=150mm$. Panels are orientated transversal (a) or parallel (b) to the load direction. Frame members are orientated transversal (battens) or parallel (joists) to the load direction. Fasteners are laid-out as type 7 to 12.
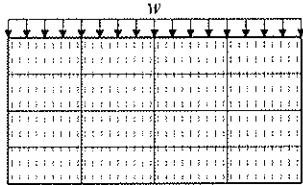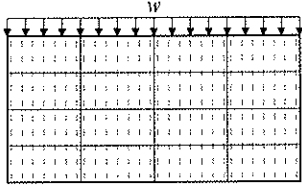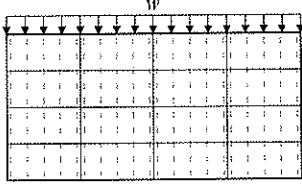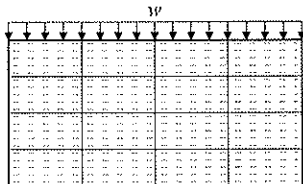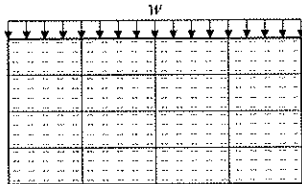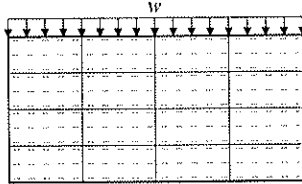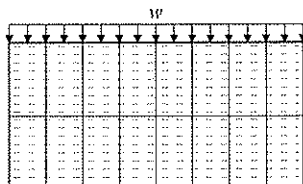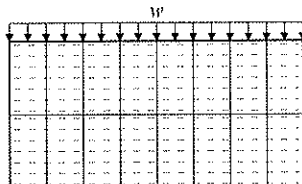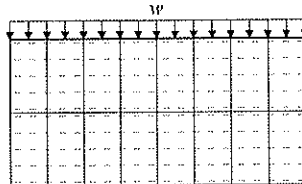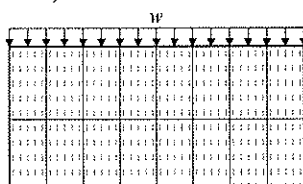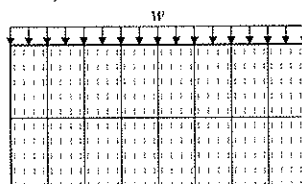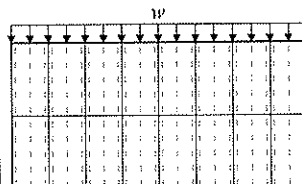
Spacing of frame members		
$B/4=300mm$	$B/3=400mm$	$B/2=600mm$
9a)	8a)	7a)
12a)	11a)	10a)
9b)	8b)	7b)
12b)	11b)	10b)

Table 4.1:   Fastening lay-out of a ceiling or floor diaphragm

Racking capacity R and horizontal deflection u are calculated in accordance with equations 3.13 and 3.15. Constant terms and material properties are cancelled. Calculation results are given in Figures 4.1 to 4.4.

Comparison shows that the fastening lay-out contributes significantly to the calculatory racking capacity and horizontal deflection of ceiling and floor diaphragms. Fastening lay-out depends on the orientation of panels and frame members and on the spacing of frame members.

Orientation of panels and frame members

By changing the orientation of panels from transversal to parallel to the frame members, the racking capacity of unblocked diaphragm may increase even 47 to 61 % and the horizontal deflection decrease even 34 to 40 %, as shown in Figures 4.1 and 4.2.
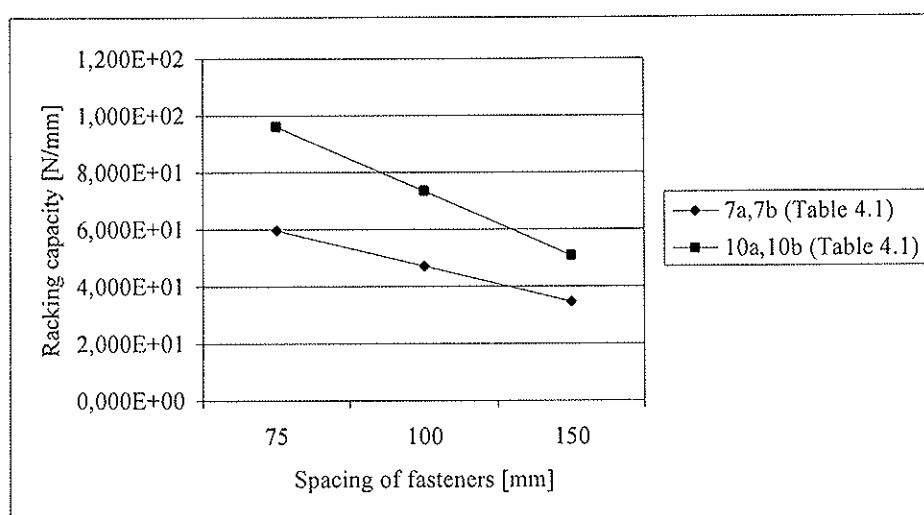
Figure 4.1: Orientation of panels contribution to the racking capacity of a ceiling or floor diaphragm
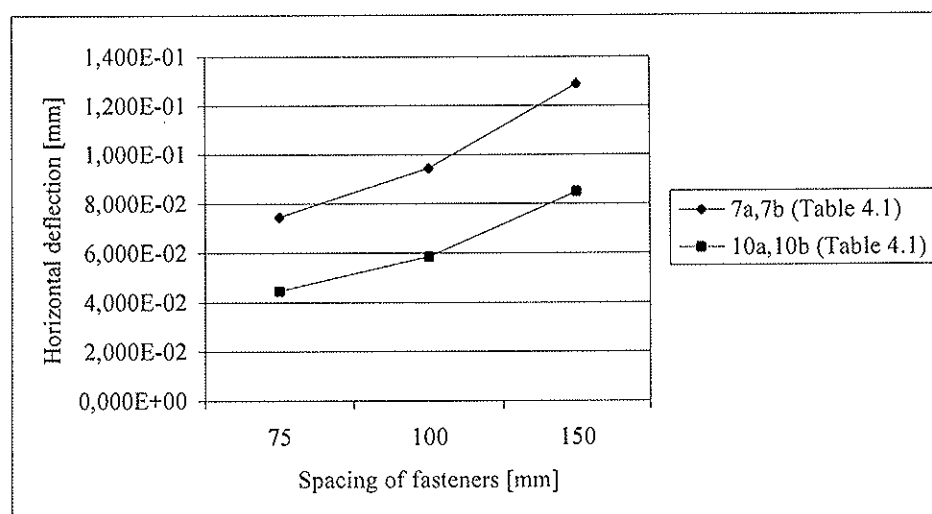
Figure 4.2: Orientation of panels contribution to the horizontal deflection of a ceiling or floor diaphragm

The panels should thus be orientated parallel to the frame members in order to maximise the racking capacity and to minimise the horizontal deflection of unblocked diaphragm. Consequently, the ceiling panels should be orientated parallel to the battens and the floor panels parallel to the joists.

Changing orientation of panels does not contribute to the racking capacity and the horizontal deflection of diaphragm at all, if the fastening lay-out maintains within the arbitrary size of rectangular diaphragm.

<u>Spacing of frame members</u>

By changing the spacing of frame members from 600*mm* to 400*mm* or 300*mm*, the racking capacity of unblocked diaphragm may increase even 37 to 75 % and the horizontal deflection decrease even 27 to 43 %, as shown in Figures 4.3 and 4.4.
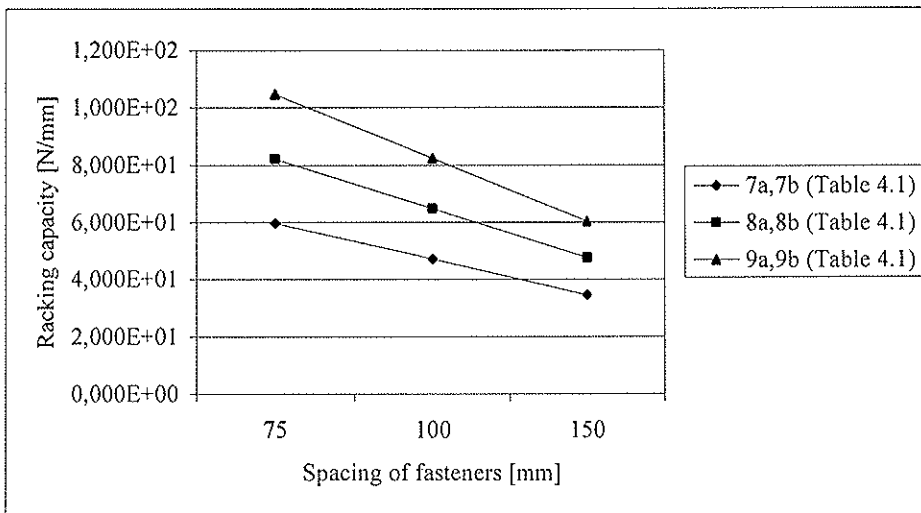
Figure 4.3: Spacing of frame members contribution to the racking capacity of a ceiling or floor diaphragm
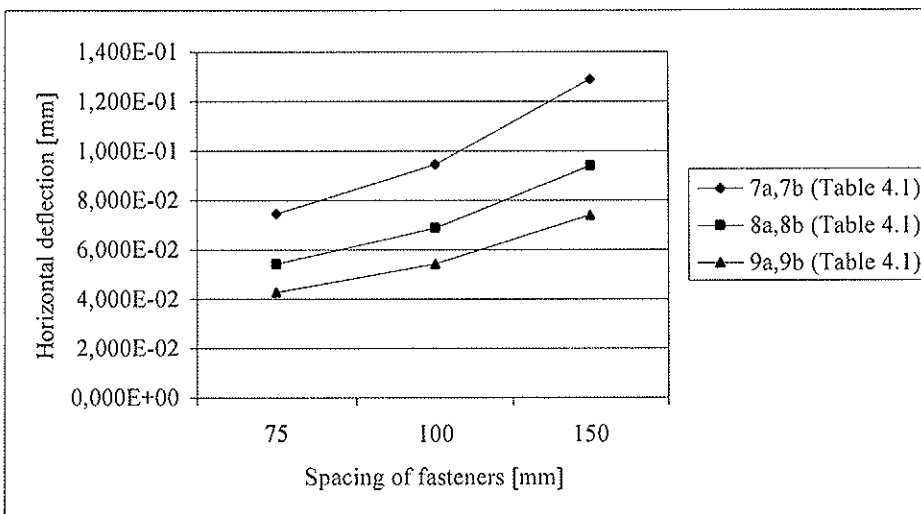
Figure 4.4: Spacing of frame members contribution to the horizontal deflection of a ceiling or floor diaphragm

The spacing of frame members should thus be as dense as possible in order to maximise the racking capacity and to minimise the horizontal deflection of unblocked diaphragm.

4.2   Wall diaphragms

Blocked or unblocked wall diaphragm with size of $l*h$=4800mm*2400mm, shown in Table 4.2, is composed of four number of diaphragm units. Panels are mechanically fastened to frame members (studs and plates or crossing studs). Dimensions of a panel are $B*H$=1200mm*2400mm. Spacing of frame members is $B/4$=300mm, $B/3$=400mm or $B/2$=600mm. Spacing of fasteners is s=75mm, s=100mm or s=150mm. Panels are orientated transversal (a) or parallel (b) to the load direction. Frame members are orientated transversal (studs) or parallel (plates and crossing studs) to the load direction. Fasteners are laid-out as type 2 to 4 and 7 to 12.

Spacing of frame members		
$B/4$=300mm	$B/3$=400mm	$B/2$=600mm
4a) F	3a) F	2a) F
9a) F	8a) F	7a) F
12b) F	11b) F	10b) F

Table 4.2:   Fastening lay-out of a wall diaphragm

Racking capacity R and horizontal deflection u are calculated in accordance with equations 3.6 and 3.7. Constant terms and material properties are cancelled. Calculation results are given in Figures 4.5 to 4.8.

Comparison shows that the fastening lay-out contributes significantly to the calculatory racking capacity and horizontal deflection of wall diaphragms. Fastening lay-out depends on the orientation of panels and frame members and on the spacing of frame members.

Orientation of panels and frame members

By changing the orientation of panels from transversal to parallel to the frame members and by blocking the diaphragm, the racking capacity of unblocked diaphragm may increase even 86 to 115 % and the horizontal deflection decrease even 46 to 53 %, as shown in Figures 4.5 and 4.6.
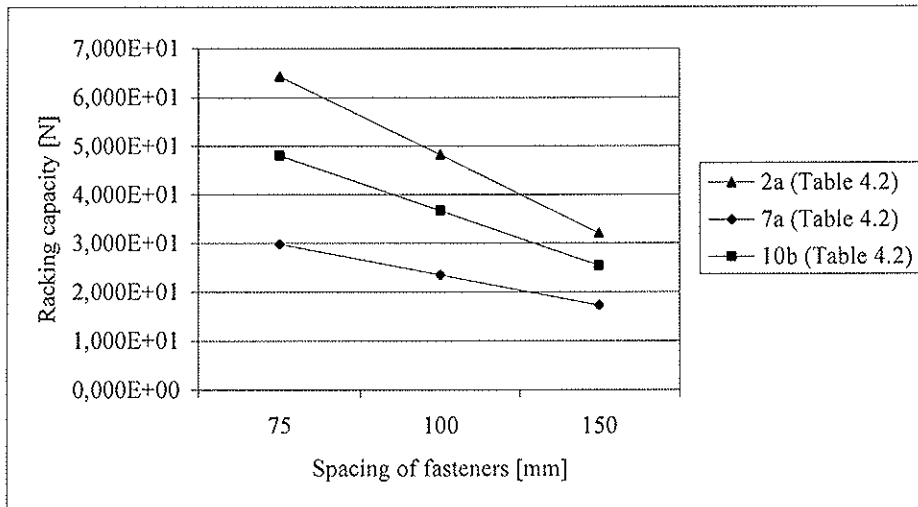
Figure 4.5: Orientation of panels contribution to the racking capacity of a wall diaphragm
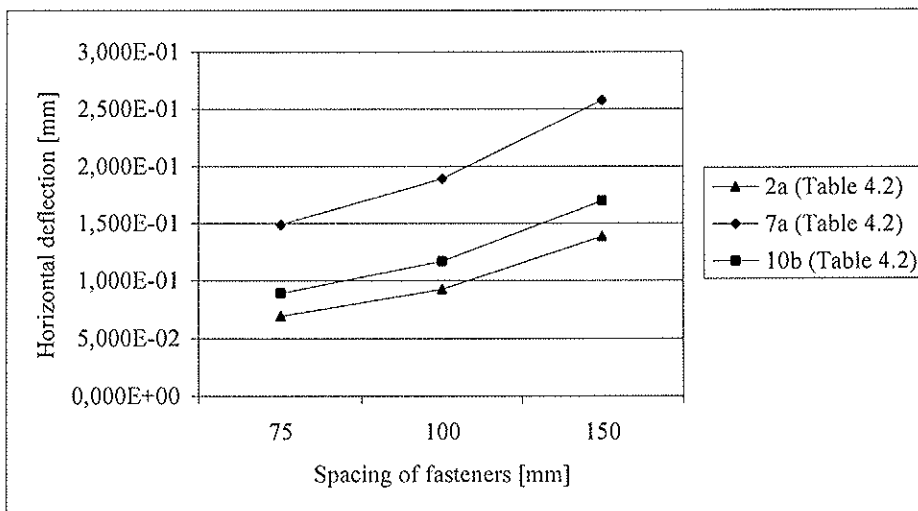
Figure 4.6: Orientation of panels contribution to the horizontal deflection of a wall diaphragm

The panels should thus be orientated parallel to the frame members in order to maximise the racking capacity and to minimise the horizontal deflection of blocked and unblocked diaphragms. Consequently, the stud wall panels should be orientated parallel to the studs and the crossing stud wall panels parallel to the crossing studs.

Spacing of frame members

By changing the spacing of frame members from 600mm to 400mm or 300mm, the racking capacity of blocked diaphragm may increase only 10 to 23 % and the horizontal deflection decrease only 9 to 19 %, as shown in Figures 4.7 and 4.8.
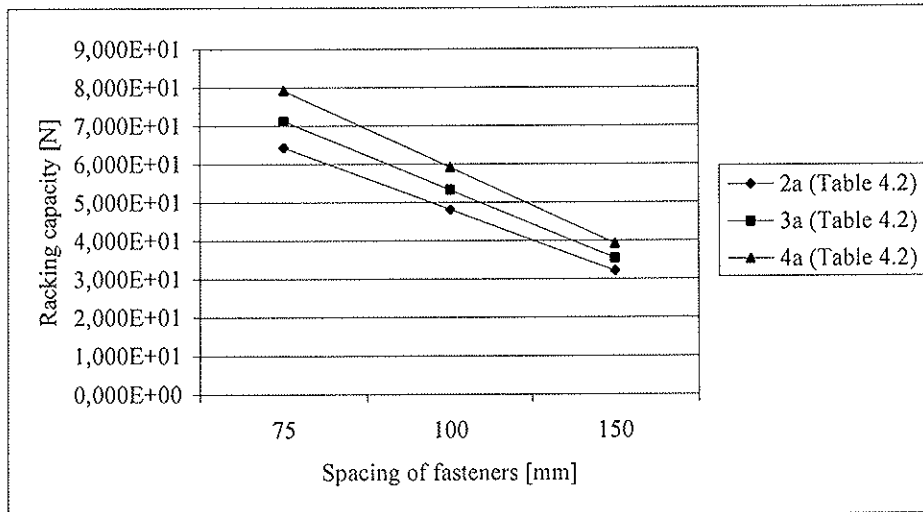
Figure 4.7: Spacing of frame members contribution to the racking capacity of a wall diaphragm
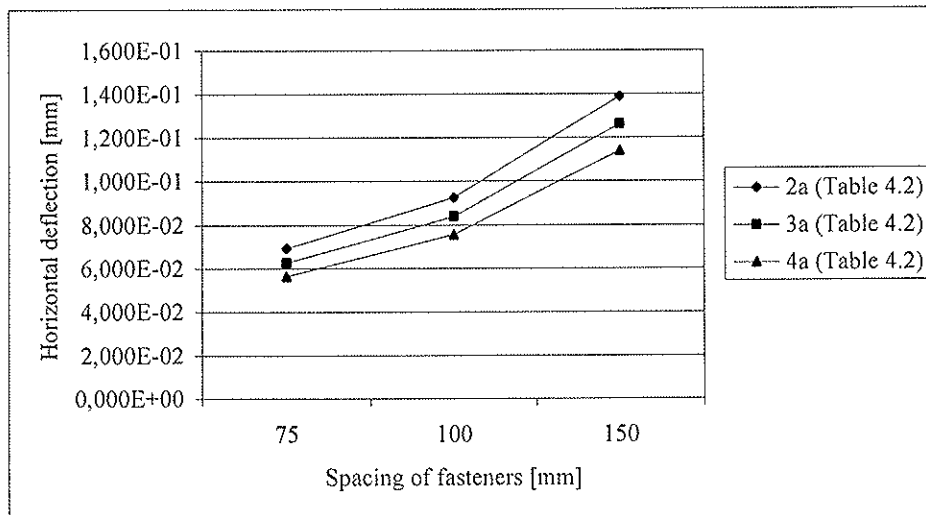
Figure 4.8: Spacing of frame members contribution to the horizontal deflection of a wall diaphragm

5 Conclusions

Further research is recommended to experimentally analyse the fastening lay-out's contribution to the racking capacity and the horizontal deflection of unblocked ceiling, floor and wall diaphragms.

References

EN 1995-1-1 Eurocode 5 - Design of timber structures - Part 1-1: General - Common rules and rules for buildings, 2004.

Källsner B. & Lam F. (1995) STEP 3 Lecture 15, Diaphragms and shear walls, 1995.

Leskelä J. (2005) Linear elastic design method for timber framed ceiling, floor and wall diaphragms, Helsinki University of Technology, Licentiate's Thesis, 2005.

INTERNATIONAL COUNCIL FOR RESEARCH AND INNOVATION
IN BUILDING AND CONSTRUCTION

WORKING COMMISSION W18 - TIMBER STRUCTURES

A UNIFIED DESIGN METHOD FOR THE RACKING
RESISTANCE OF TIMBER FRAMED WALLS
FOR INCLUSION IN EUROCODE 5

B Griffiths

V Enjily

Centre for Timber Technology and Construction, BRE

UK

Hans Blass

Blass and Eberhart

GERMANY

Bo Källsner

Swedish Institute for Wood

SWEDEN

Presented by R Griffiths

BJ Yeh stated in US the concept of relying on vertical load for uplift restraint is questioned as the load may not be there with wind uplift as an example. R Griffiths responded that in the case of 1 to 2 story building this is not an important issue. For 4 to 5 storey buildings the dead load is significant and should be considered.

E Karacabeyli asked whether ductility is considered in terms of comparisons. R Griffiths responded that for the large scale building test in the UK. Very high stiffness ~ 7 to 10 times design level was observed. In testing work he found this if brittle failure can be avoided then the timber frame is ductile. F Lam commented that stiffness and ductility should not be mixed as ductility is the ability of the system to carry load under large deformation. R Griffiths agreed.

A Unified Design Method for the Racking Resistance of Timber Framed Walls for Inclusion in Eurocode 5

Bob Griffiths
Centre for Timber Technology and Construction, BRE, UK
Vahik Enjily
Centre for Timber Technology and Construction, BRE, UK
Hans Blass
Blass and Eberhart, Germany
Bo Källsner
SP Swedish National Testing and Research Institute and Växjö University, Sweden

1   Introduction

A recent European research programme sponsored by Wood Focus OY identified a need for a unified approach in Europe to the design of timber framed walls for racking resistance. Such an approach should improve on and thereby make redundant current design methods viz.
- Methods A and B in Eurocode 5 (Ref a)
- Methods 6.1 and 6.2 in BS 5268 (Refs b and c).

Work by Källsner et al (Refs d and e) was effective in linking the principles underlying the different design approaches and, following a number of early drafts, the method presented herein was proposed. It is written so as to be a direct substitution of Methods A and B in EC5 hence the numbering of the sections. It is not viewed as a final draft since the detailed development and checks were cut short by the time scale of the research programme. However the effectiveness of the method was checked by trials on a number of hypothetical wall units the results of which are reported.

The authors hope that the design approach will attract comment and development that could be incorporated prior to submission for adoption by both Code bodies in order that Europe should have a single design approach supported by all parts of the timber frame industry because it offered advantages over existing methods. Although not an objective of the research programme, the new approach can be more easily used with other similar frame type or sandwich panel systems.

2   Background

The pan European project sponsored by Wood Focus OY was entitled "The Influence of the National Standard and EN1995-1-1 on Competitiveness of Wood in Construction:- Design of Wall Diaphragms" (Ref f). It brought together designers and researchers throughout Europe specialising in timber frame wall design. Their principal objectives were:

1. To investigate the different thinking throughout Europe with regard to the assessment of wall racking resistance in timber frame houses

1

2. To identify the principal differences in design approaches and the impact of those differences on performance

3. To put forward measures that would help unify the approach to design and would therefore break down any barriers to free trade in Europe caused by dependence on one or other design method

4. If successful, to present proposals for similar projects where fair trade might be hindered either by poor or ineffective drafting of the Eurocode or an unnecessary reliance on national standards

Wall racking was seen as a prime example where the differences in national approaches had not been resolved through the introduction of EC5 and there remained a desire in different countries to maintain their own approach to design and legislation which could adversely effect free trade. Potentially, this action could compromise the use of timber as a building solution in what is a high volume end use. Furthermore, wall racking was typical of peripheral areas of design in the Eurocode which although important from a commercial viewpoint were rather specialised and had been dealt with unsuccessfully by the code drafting committee.

The project developed through a number of separate tasks leading to the development of the Unified Design Method. The significant findings are recorded below.

2.1   Review of Design Methods

Design methods from Austria, France, Germany, Sweden, Switzerland and the UK were reviewed. All except the UK method aligned with Method A in EC5 although not all were in limit state format. In later comparison work factors were applied to working stress designs to allow direct comparison. Although unique, the UK method was more detailed. It had been introduced to enable the use of low rise timber frame and had developed to cover multi storey design and commercial and industrial applications.

2.2   Whole House Design

Two designs typical of high volume construction in the UK were checked structurally by German and UK engineers using their national DIN and BS codes together with Eurocode 5. Both designs gave problems due to the layout of walls and the openings required. Discussing the designs three conclusions were drawn:

1. It would appear that in Germany deflection is largely ignored and that very strong anchorages are required by design but are probably not utilised in practice. Whereas in the UK, anchorage is largely ignored and deflection is critical to many design although it is believed not to be a problem in practice.

2. The "Helmdon" house was satisfactory using the UK code and could be proven by EC5 if similar allowances were made for wind shielding, use of brickwork and plasterboard. However these opportunities are not available to designers through the Eurocode and so the design could not be made acceptable unless
   i)   German values for nail shear performance in plasterboard were used.
   ii)   structural sheathing boards were used on internal walls.

3. Differences in national wind codes affected loading and could have implications on wall design

3   Wall Design to Current Codes

The early work had shown that the design of whole houses was too complex to enable a simple comparison of wall racking design methods. Discussion had also shown that specification and sizing of timber in designs in different countries had little relevance to the design method but were based on: tradition, availability of materials and most importantly the sector of the housing market that was being targeted. The target market greatly affected quality levels and consequently were more strongly allied to cost than design method. Requirements for special housing features created specific problems for some designs, which could not be resolved by changing the design method.

In the UK, timber frame was commonly competing in the low cost, high volume estate market. Here the cost of land and client desire for detached accommodation leads to narrow properties with openings often concentrated in the shorter walls. Wind normal to the longer walls creates a significant racking force and there is too little full height wall in the shorter walls to resist the load. All the design methods had difficulty with such designs but the UK allows other factors to mitigate the problem;
- i)   wind shielding by masonry outer leaf walls
- ii) racking resistance of masonry
- iii) a racking allowance for plasterboard

The easiest way to provide additional design strength to these houses would be to be less conservative in the structural use of plasterboard.

Larger houses presented fewer problems as there were more full height walls available to resist the load in proportion to the increase in load. Where larger buildings were subdivided into units either as terraced houses or blocks of flats the larger building footprint improved strength so long as there was structural continuity between units. The UK design method again offered a significant benefit by defining party walls which could be considered fully structural although clad only in plasterboard.

The suitability of timber frame for flats had led to the opportunity to consider taller buildings with more storeys of timber frame. Each storey added considerably to the racking load at the vulnerable ground floor level. However, separating walls between units gave strength and stiffness along with lift shafts and stair wells. Where the walls were too imperforate as a result of client needs for doors and windows the ground floor could be replaced by alternative structural forms and this is often done to enable taller buildings. Here the problems facing the timber frame are less likely to relate to racking resistance but are poorly covered by all European codes. Design factors will be fire, differential movement and disproportionate collapse (Ref g)

It was decided that the major issue that still needed to be resolved, simply because it polarised the European timber frame industry, was the method for determining racking resistance. Earlier work had shown that;
- i)   all the mainland Europe design approaches were related to Method A of Eurocode 5,
- ii) the UK approach in BS5268 Section 6.1 and 6.2 was unique but was well used and proven over a wider range of structures

iii)   Method B in Eurocode 5 which had attempted to resolve the differences had misinterpreted some significant factors.
iv)   neither of the main methods was complete in its coverage of design issues.
v)   both designs had some particularly good features, worth building on.
vi)   neither design method was straight forward and simple to operate.

As a result of these findings the work programme was changed slightly to compare the performance of the available design methods and, later, any new proposal through the assessment of a range of standard wall configurations and variables which covered the significant wall and material design factors. More details are given in the main report (Ref f).

Direct comparison of the design methods are shown in Figures 1 and 2. The results are broken up into three groups covering:

1. The 2.4m walls; Panel number10, 9 and 8
2. The 7.2m walls with or without windows; Panel number 7, 6, 5, 4 and 1
3. The 7.2m walls with a patio door opening in different positions within the panel; Panel number 2 and 3

The first group shows the effect of two similar width but different height openings on a short length of wall. The second group demonstrates the progressive reduction in strength as the number of openings increase and also allows comparison of a 7.2m plain wall with a 2.4m plain wall (Results 1 and 8). The third group shows the impact of one large opening in a 7.2m wall and the effect of the location of the opening.

From the results it is clear that the traditional French and German methods are similar and the later German method includes the change to limit state principles. These methods all have the same basis as Method A in EN1995-1-1. However the European code produces higher design values because a special 1.2
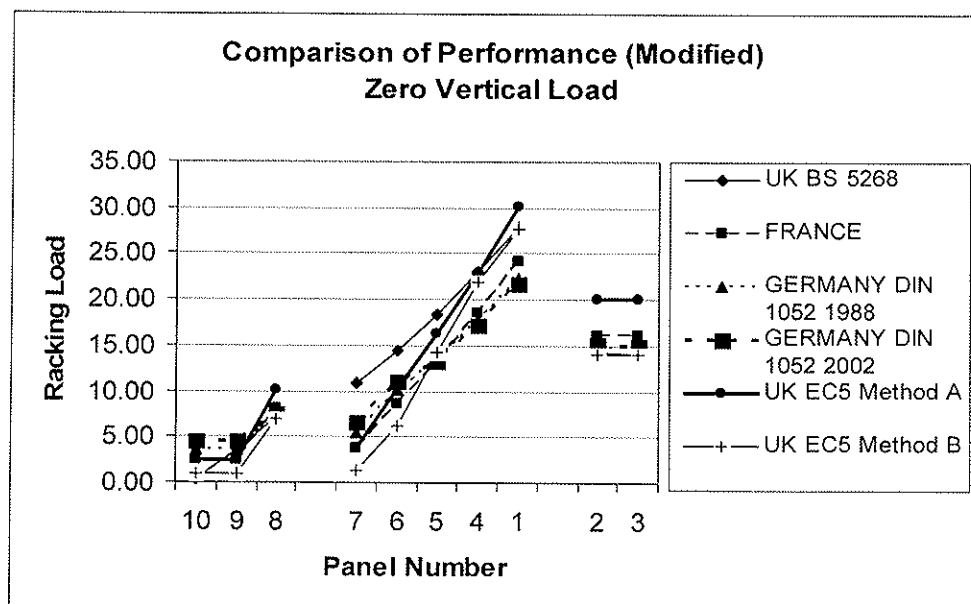
Figure 1:   Comparison of Current Design Methods at Zero Vertical Load

4

enhancement factor is allowed for use with all nail shear values. This factor had been included by the Code drafting committee as the number of nails included in a panel justified a mean performance value rather than a 5 percentile characteristic value.

All four methods require the leeward stud in a full length wall unit to be held down to the foundation which could be taken as equivalent to applying vertical load. The UK BS5268 method is closer to zero vertical load conditions with only the bottom rail fixings acting against board rotation as well as resisting horizontal sliding. The five methods are compared in Figure 1 where they are classified as zero vertically loaded.

The high performance of the UK design method is clear; noting that it requires no additional hold down. The explanation for this is that the values have been based on test performance rather than analysis linked to a fundamental nail property. In this situation secondary factors such as shear in frame fixing nails contribute to horizontal resistance. Figure 2 details the performances where vertical load is added and allowed to enhance racking performance. The approaches for BS5268 Section 6.1 and Method B of EN1995-1-1 are directly comparable and may also be compared with the zero vertical load cases for the same methods and the fundamental EN1995-1-1 Method A.
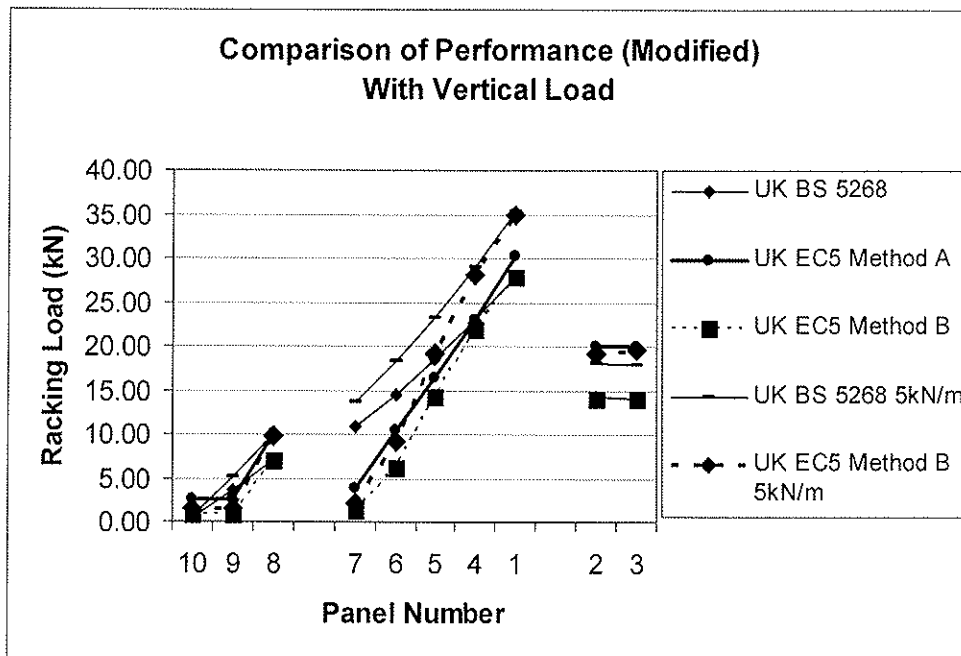
Figure 2:   Comparison of Current Design Methods at 5kN/m Vertical Load

The trial walls were used to generate a further comparison, between Method A and B of EN1995-1-1. Performance differences for singly sheathed plain wall panels are shown in Figure 3 for three different conditions of vertical load. Method A gives higher results than Method B at zero vertical load regardless of length. As vertical load increases so too does the benefit from using Method B, but for short walls Method A will always be better. As both methods sum the individual performances of full height wall lengths to determine overall racking resistance, it is clear that Method A will normally yield better results unless there are significant proportions of the wall which are full height and longer than say 2.4m. The lower the vertical load, the greater the length will need to be. To have any possibility of advantage, Method B would need to incorporate the BS 5268

5

approach, or similar, for openings, otherwise it must be viewed as an unrealistic alternative to Method A since it is much more complex and in normal circumstances gives reduced performance.

Method B / Method A Performance v Length For Fully Sheathed Walls at 3 Vertical Loads
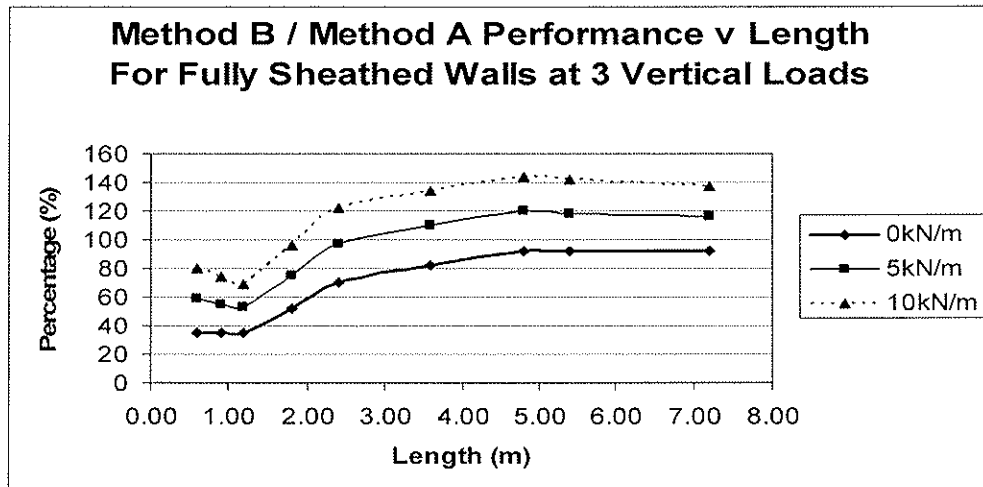
Figure 3: Comparison of EN1995-1-1 Methods A and B for Vertical Load and Length

The comparison examples highlight the differences between the two methods particularly at extremes, such as long length, short length, high vertical load etc. However for more practical situations where the full height lengths of wall units are quite short, say between 1.2 and 2.4m the differences in design performance are likely to be relatively small. The following conclusions can then be drawn:

1. EN1995-1-1 Method A is more easy to use and relates to readily available component design values. The most important being the lateral design capacity of an individual fastener.
2. The summation of performance for full height wall panels is easier to use than to consider the reduction effect of openings on a full length wall however the Method A approach to window openings is unnecessarily conservative.
3. There need be no requirement to include anchor straps to provide stability in a wall panel.
4. Vertical load, and implied vertical load, either from holding down straps or the resistance gained from return walls will contribute to racking resistance.
5. Design performance will be affected by a number of secondary factors such as:
   i)   The performance attributable to semi-structural materials such as plasterboard.
   ii).   The use of other components in the house structure to either reduce the applied load (i.e. wind shielding) or contribute to the resistance of the structure.
   iii). The additional performance achieved by considering the building as a three dimensional entity rather than resolving forces to allow a two dimensional approach to behaviour.
6. Neither method has either the rigour or accuracy to put it above the other.
7. Both methods were based on either specialist or limited design needs and are less suited to the expanding use of timber in Europe where there is a need for a harmonisation of approach.

6

At this stage in the project it was seen as important to introduce a third approach taking the better parts of previous designs and develop them for modern building requirements.

4 Unified Design Method (Method C)

The new approach was named to show its development within EN1995-1-1 and its principal aim which is to provide a single design approach which through its acceptability and benefits is the first choice for all designers in Europe.

Method C was developed through two different strands of work which were linked to achieve a balance between:

    i)   Practical efficiency and detail
    ii)   Cost implications related to design spending
    iii)   Theoretical accuracy and rigour

Firstly, the format for the design method was developed through the learning achieved in the early stages of the project and was based heavily on the best features of EN1995-1-1 Method A and BS5268: Section 6.1. Secondly, advantage was taken of parallel research headed up by Bo Källsner who developed an approach to cover the use of vertical load within the format of the EN1995-1-1 Method A design.

The proposed Unified Design Method offers a greater degree of detail than the current Method A and it relates to basic design principles on which different countries can overlay their approaches to the use of more controversial secondary design factors, notably the use of plasterboard and brickwork, in the overall performance of the building. The code format for the Unified Design Method for Timber Frame Wall Diaphragms for EN1995-1-1 is included as Appendix A

4.1 Basic Principles for Method C

The key principles are developed from EN1995-1-1 Method A. Firstly, related to plain walls:

1. Design is strength based
2. Shear resistance is based on the performance of the fasteners connecting the sheathing material to the bottom rail
3. The full length of wall is broken into full height wall components
4. Components are discounted if their aspect ratio is too narrow (i.e. length is less than a quarter of the height). This minimises problems of low stiffness.

The method retains the 1,2 enhancement factor for nail shear but would limit its use to proven material combinations. The Method proposes rules to cover combinations of sheathings and makes an allowance for indirect transfer of shear from board, through fastenings, to the stud and then to the bottom rail through the frame joint. It includes an approach for dealing with plasterboard which at best is semi structural in use but which in reality contributes greatly to wall stiffness and strength. Views on the use of plasterboard are varied and often polarised and therefore its use may need to be dealt with through the use of National Annexes.

The design method does not give guidance regarding connections between the bottom rail and the foundations. It is assumed that the bottom rail is rigidly fixed to the foundations. Thus the connection should be designed for sliding and overturning. The latter will however be affected by vertical forces as noted in the investigation.

The second area of major importance is in dealing with openings. Here a totally new approach is recommended:

1. Small openings are allowed in wall components without loss of performance
2. Larger openings are responsible for breaking up full length walls into full height wall components.
3. The soffit wall under a window opening to the leeward side of a level may contribute to racking resistance depending on its length, height and the length of the preceding plain wall.
4. Door units, which by definition have no soffit, cannot provide any additional racking resistance.

The third factor of importance relates to vertical restraint and introduces the principal changes from Method A:

1. Vertical restraint to wall components will affect their racking resistance
2. Restraint can be provided by:
   - i). holding downs normally attached to the panel studs
   - ii). vertical load
   - iii). reaction from the wall(s) fixed to the windward edge of the panel, these can be acting either in the same plane or as a return wall.

A fully restrained wall will behave as one designed to Method A but with enhancement due to the window openings etc. Restraint can be from a combination of the factors noted above. If there is insufficient vertical restraint to motivate the full racking resistance then some of the fastenings contributing to racking resistance must be re-assigned to prevent overturning with a subsequent reduction in racking performance.

4.2   Theoretical Background

The theoretical basis for dealing with limited vertical restraints is provided in papers by Källsner (References d and e). Here a plastic lower bound approach is used to show that if the bottom rail is fully anchored but no tie down is provided for the leading stud then the sheathing to timber bottom rail fastenings at the windward end of the wall component can work with the compressive forces carried down the leeward stud to produce a restoring moment resisting the moment induced by the racking force. The remaining fastenings in the bottom rail resist shear. Equations are developed balancing shear against rotation, related to fastener spacing and performance, from which the shear capacity can be calculated. The work has been developed to cover other methods of providing partial restraint and to analyse window openings.

In other areas of the Design Method and particularly those concerned with load spread an empirical approach is necessary. Such interpretation has been done conservatively and can be related back to test information and standard principles.

5   Validating Design Method C

Trials have been carried out on the current version of Method C, using the ten standard panels to compare it with the other test methods. The results are shown in Table 1.

WALL PERFORMANCE COMPARISONS (UNIFIED METHOD)

Restraint Case	Racking Load in kN when $F_{f,Rd/s}$ = 4.6 kN/m									
Wall Number	10	9	8	7	6	5	4	1	2	3
Zero										
Base	0.69	1.26	5.52	3.05	6.35	12.67	20.98	27.59	12.41	11.04
Windows	0.69	2.41	5.52	12.24	16.04	19.09	24.62	27.59	12.41	11.04
Windows and return	2.07	6.09	9.66	14.54	18.33	21.39	26.92	31.73	15.17	15.17
5kN/m Vert load only (base)	1.44	2.64	9.89	6.36	12.58	19	26.81	33.11	19.24	19.77
Full effect (v+w+r)	2.82	7.47	11.04	17.85	22.46	24.44	29.11	33.11	21.60	20.92
$\Sigma F_{i,v,Rd}$ (Full Restraint)	5.52	10.12	11.04	26.67	28.97	28.51	30.81	33.11	22.07	22.07

Table 1:   Comparison of Method C Racking Design Loads (kN) for Standard Panels Showing the Influence of Design Components

All the values are derived for nail shear performance ($F_{f,Rd}/s$) of 4.60 kN/m. This figure represents a 12mm oriented strand board with 3.0mm diameter nails at 150mm centres and includes k_{mod} for short term loading plus the special factors outlined in the Design Method. A number of different situations have been trialled to show the impact of the different restraint situations. Referring to Table 1 and Figure 4 they are as follows:

- **Base:** covers the bottom rail fixings only with no allowances made for any form of vertical restraint. Here, in comparison with EN1995-1-1 Method A, some fixings are lost as they are needed to resist uplift but other fixings are added as a result of the added contribution of the window soffits.

- **Windows:** introduces the first component of vertical restraint due to the panel attached to the windward edge of the full height wall component and in the same plane as the wall. This must be a window opening; a fully sheathed panel would have added to the length of the component and a door panel currently allows no transfer of vertical force. The improvement is marked particularly in practical panels where only short lengths of full height wall are available due to the frequent inclusion of openings.

- **Windows and Return Walls:** this adds the contribution of a return wall at the windward end of the total wall. The return effect will normally depend on the length of full height wall adjacent to the racking wall. The connections between the return wall and racking wall would also need to be checked and could be critical to load transfer. In the example the maximum effect is used which is based on the wall height and a spread of h/2. The return improved the performance of all walls and the improvement was greater, the longer the full height wall component attached to the return.

- **Vertical loads only:** after removing the window and return effects a 5kN/m top load was added to the wall. This improves the capacity of each full height component. In this example a simple approach is taken whereby the load applied to the windward edge of the wall component is determined from the vertical load intensity x half the full height wall length.

- **Full effect (vertical load + windows + return):** this is the maximum restraint condition for the vertical load case and the panel configurations stipulated.

9

- $\Sigma F_{i,v,Rd}$: this case shows the maximum racking resistance available when full vertical restraint is provided. It is noticeable that in short lengths of full height wall the vertical load contribution is small and the return/window effect is no more than a 50% contribution hence racking capacity can be improved by anchorage which would normally be provided by holding down straps. In the longer walls the vertical load is a significant influence.
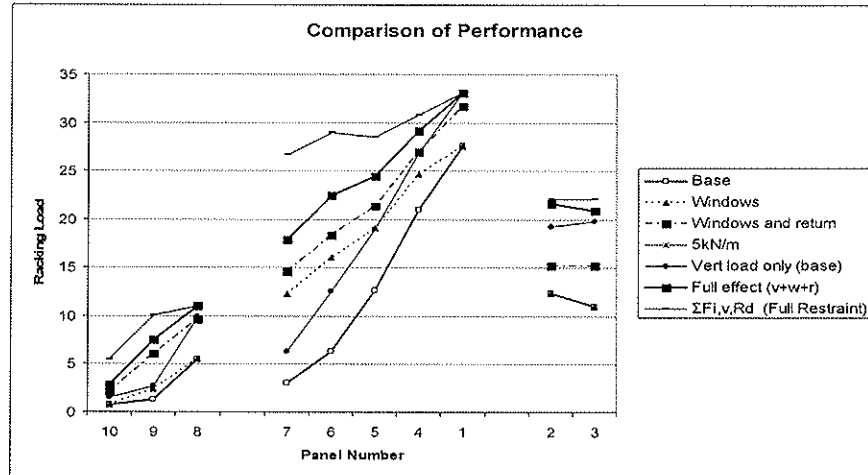
Figure 4: The Influence of Method C Design Components on Racking Performance Based on Standard Panel Design Values

In Table 2, the Method C results are compared with those for current design methods. At zero vertical load as seen in Figure 5, the practical situation is where the window and end return effects are taken into account. Here Method C compares well with BS5268 and in particular has a similar behaviour pattern regarding openings. The improved overall performance is due to the enhancement factors for nail shear including that for the stud/bottom rail shear. The improvement over EN1995-1-1 Method A for panels with window openings is marked and is significant to design but in panels with door openings the new method shows less improvement since door panels offer only little vertical restraint.

WALL PERFORMANCE COMPARISONS (Modified)
Working Stress values enhanced by factor of 1.5

Design Method	Racking Load in kN when $F_{(Rd)_s}$ = 4.6 kN/m									
Wall Number	10	9	8	7	6	5	4	1	2	3
UK BS 5268	0.44	3.63	7.06	10.84	14.37	18.41	22.94	27.98	14.22	14.13
FRANCE	2.45	2.45	8.03	3.68	8.67	13.16	18.45	24.06	16.05	16.05
GERMANY DIN 1052 1988	3.60	3.60	7.50	5.40	10.05	13.50	17.70	22.35	14.85	15.00
GERMANY DIN 1052 2002	4.40	4.40	7.50	6.60	11.10	13.30	17.30	21.80	15.10	15.00
UK EC5 Method A	2.52	2.52	10.04	3.78	10.36	16.32	22.90	30.12	20.08	20.08
UK EC5 Method B	0.88	0.88	7.01	1.32	6.25	14.28	21.98	27.77	14.13	14.03
UK BS 5268 5kN/m	0.62	5.13	9.99	13.71	18.20	23.30	29.04	35.42	18.00	17.90
UK EC5 Method B 5kN/m	1.48	1.48	9.79	2.22	9.09	19.08	28.13	34.84	19.20	19.52
Zero										
Base	0.69	1.26	5.52	3.05	6.35	12.67	20.98	27.59	12.41	11.04
Windows	0.69	2.41	5.52	12.24	16.04	19.09	24.62	27.59	12.41	11.04
Windows and return 5kN/m	2.07	6.09	9.66	14.54	18.33	21.39	26.92	31.73	15.17	15.17
Vert load only (base)	1.44	2.64	9.89	6.36	12.58	19	26.81	33.11	19.24	19.77
Full effect (v+w+r)	2.82	7.47	11.04	17.85	22.46	24.44	29.11	33.11	21.60	20.92
$\Sigma F_{i,v,Rd}$ (Full Restraint)	5.52	10.12	11.04	26.67	28.97	28.51	30.81	33.11	22.07	22.07

Table 2: Comparison of Method C Racking Design Loads With Current Methods
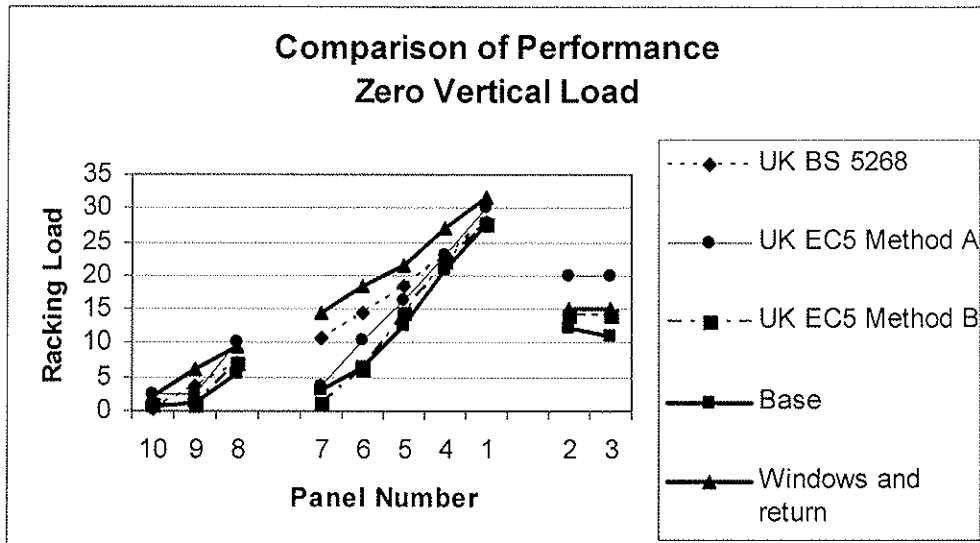
Figure 5: Comparison of Method C with Current Designs for Zero Vertical Load

The same trends are seen at 5kN/m vertical loading in Figure 6. There is only small improvement in large plain wall performance since these walls require only minimal restraint to gain maximum racking capacity. The results are better than Method A once more because the nail shear value includes a factor for stud nail shear. However, the improvement for walls with windows is enormous. The vertical load shows maximum benefit in walls with doors where it can be a major contributor to vertical restraint.
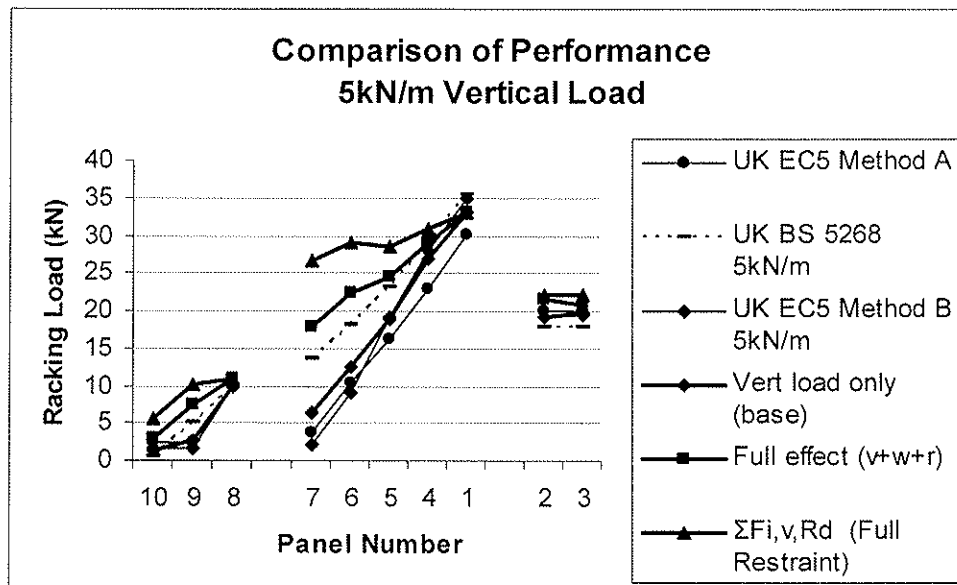
Figure 6: Comparison of Method C with Current Designs for 5kN/m Vertical Load

11

6. Conclusions

1. This project offered the opportunity for a more in depth study which evaluated similarities and differences in national and Eurocode approaches and built on them to derive a unified design approach that should find favour with the major protagonists.

2. With regard to timber frame walls it was quickly found that timber frame housing sold into different markets in different countries and that the market requirements were likely to have a much greater influence on the design of a building and the use of materials than the approach to design for wall racking.

3. The contributors to this project were specialists in the field of wall racking, representing wide experience in the two design approaches both from a practical and a regulatory viewpoint. Having identified the weaknesses in both methods and requirements that could in relative safety be discarded, they were able to call on recent research material which provided the key to unifying the methods. As a consequence the programme was able to progress to a higher goal and has developed a design method known as the Unified Design Method, for obvious reasons, which should be seen as sufficiently close to both original approaches, whilst omitting their weaknesses, so as to obtain acceptance by all parties. The method also takes advantage of other research which has demonstrated the large reserves of inbuilt strength in timber frame construction in order to justify increased levels in performance compared with both previous methods. As a consequence the outcome of this work will improve the opportunities for timber frame against its competitors.

4. Overall the results show the Unified Design Method (Method C) is capable of performing well in all the critical areas. Its use will significantly improve racking design values especially for typical walls with many openings where the short lengths of full height wall mean the current Method A is extremely conservative.

5. Unified Design Method (Method C) has been written in such a way that it could immediately be substituted into EN1995-1-1 to replace the current design methods A & B. Subsequent changes are envisaged in the detail only, covering:
   i).   Fastener shear values
   ii).   Allowable spread of racking load into window soffits
   iii). Extent of vertical restraint from adjacent windward edge wall component
   iv).   Extent of zone of influence for vertical load

   These factors are more subjective in nature and it is therefore important that the design proposal is judged by a wider audience than the authors.

6. The method leaves open the debate on whether or not to include brick shielding and the racking contribution of brick and plasterboard. It is recommended that these factors be addressed in National Annexes.

7. REFERENCES

a) CEN, EN1995-1-1 Design of timber structures, Part 1-1 General- Common rules and rules for buildings, 2004

b) British Standards Institution, BS5268 Structural use of timber, Part 6, Code of practice for timber frame walls Section 6.1, Dwellings not exceeding four storeys, London, UK, 1996

c) British Standards Institution, BS5268 Structural use of timber, Part 6, Code of practice for timber frame walls Section 6.2, Buildings other than dwellings not exceeding four storeys, London, UK, 2001

d) Kallsner B. and Girhammar U., A plastic lower bound method for the design of wood-framed shear walls, Proc WCTE 2004, Lahti, FINLAND, 2004

e) Girhammar U. and Kallsner B., Tests on partially anchored shear walls, Proc WCTE 2004, Lahti, FINLAND, 2004

f) Enjily V, Griffiths D.R. and Blass H Final Report:- The influence of the national standards and EN1995-1-1 on competitiveness of wood in construction-design of wall diaphragms. BRE client report 223-024, BRE Garston, UK, April 2005.

g) Grantham R., Enjily V. Multi-storey timber frame buildings – a design guide, BR454, BRE, UK, 2003

Appendix A   EN1995-1-1 Unified Design Method for Timber Frame Wall Diaphragms

A.1   Notation

$F_{v,Ed}$	Applied racking force.
$F_{v,Rd}$	Total racking resistance of full wall length.
$F_{i,v,Rd}$	Racking resistance of full height wall component, i.
$F_{f,Rd}$	Lateral design capacity of an individual fastener contributing to racking resistance in the wall components.
s	Fastener spacing
h	height of wall
l_i	Length of full height wall component
$l_{i,ef}$	Effective length of full height wall component allowing non contributory length (normally due to narrow sheathing board) and for racking contribution from leeward, or following, part height component.
l_{ss}	Width of full height sheet where width is less than h/4.
$l_{w,ss}$	Width of window soffit sheet where width is less than h/4.
l_{wi}, h_{wi}	Dimensions of window soffit where the unit follows the full height wall component, i, and can therefore contribute to its racking resistance.
l_o, h_o, d_o	dimensions of small openings within a full height wall component which do not affect its racking resistance.
l_{eo}, h_{eo}	clear distances between small openings and edges of full height wall components.
$k_{i,w}$	Modification factor for wall i if the total resistance to uplift is less than the standard requirement.
$R_{i,v}$	Total resistance to uplift at the windward, or leading, edge of full height wall component, i.
$R_{v,con}$	Shear capacity of the connections linking wall components.
$R_{i,wall}$	Contribution to uplift resistance from wall component attached to the windward or leading edge of full height wall component, i. This can be either in line with i or a return wall.
$R_{i,hd}$	Contribution to uplift resistance from hold down attaching the windward or leading edge of full height wall component, i, to the next level of structure below
$R_{i,wr,ll}$	Contribution to uplift resistance from windward reaction of live loads on wall component i.
l_{rw}	length of full height return wall connected to full height component i.

A.2   Draft clauses for inclusion in EN1995-1-1 replacing clauses 9.2.4.2 and 9.2.4.3

9.2.4.2 Simplified analysis of wall diaphragms (unified method):
(1) This method applies to all wall panels that are adequately held down to the foundations or lower storey walls either by tie downs or base rail connections. The method covers only the racking resistance of the wall units and separate checks must be

14

made to ensure the tie downs and connections to the wall units are adequate in resisting sliding and overturning.

(2) The design load carrying capacity $F_{v,Rd}$ (the design racking resistance) under a force $F_{v,Ed}$ acting at the top of a cantilevered wall secured against uplift (by anchors or vertical load or bottom rail hold down or any combination) and sliding should be determined using the following simplified method of analysis for walls made up of one or more full height wall units, as shown in Figure 9.5.

Full height wall components

Full length of wall between returns
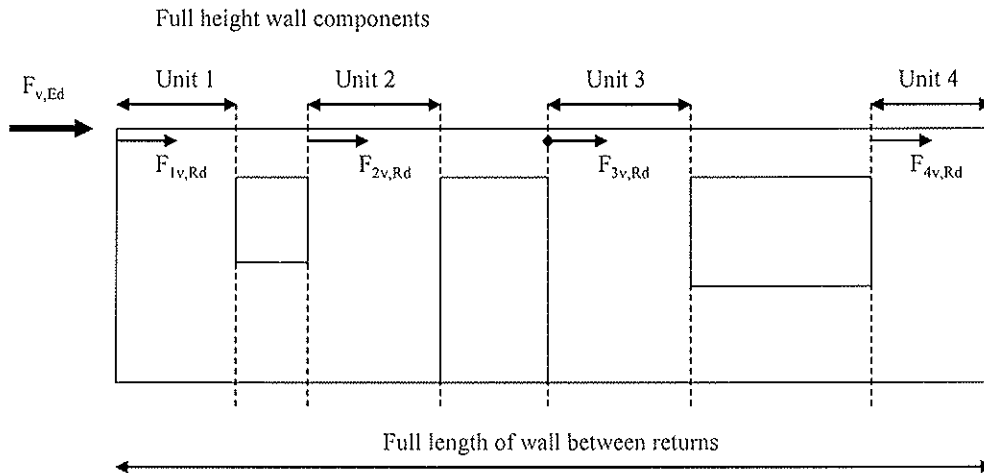
Figure 9.5 **Showing how a building wall is broken into full height wall components for design. These units are independent of manufactured component joints and sheathing joints**

(3) For a wall made up of several full height wall units the design racking load carrying capacity should be calculated from:

$$F_{v,Rd} = \Sigma \, F_{i,v,Rd}$$

Where

$F_{i,v,Rd}$ is the design racking load carrying capacity of the wall panel in accordance with 9.2.4.2 (5).

(4) Small openings may be allowed within a full height wall unit if the following conditions, illustrated in figure 9.6, are met:

    (i)   the opening does not exceed 300mm in both length or height if the opening is fully framed.

    (ii)   the opening does not exceed 150mm in both length and height or 200mm in diameter if the opening is unframed.

    (iii)   the edge distance from the opening to any edge of the wall unit is at least the maximum dimension of the opening.

    (iv)   only one such opening is allowed in each unit.
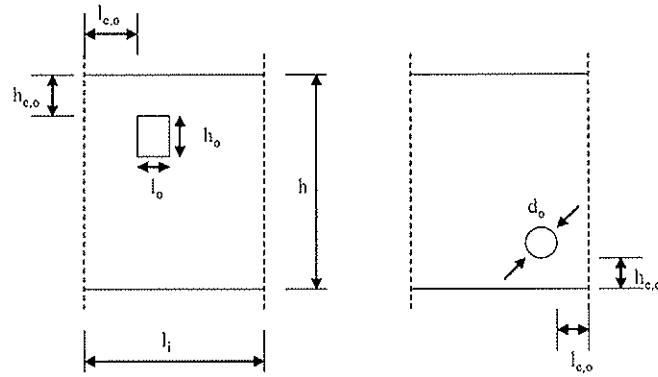
Figure 9.6: **Allowable openings in full height walls**

(5) The design racking load carrying capacity of each full height wall unit, $F_{i,v,Rd}$ is given by:

$$F_{i,v,Rd} = (F_{f.Rd} / s) * l_{i,ef} * k_{i,w}$$

Provided that the fastener spacing is constant along the perimeter of each sheet and that intermediate supports include fasteners at no greater than twice the spacing or 300mm, whichever is smaller.

Where;

$F_{f.Rd}$ is the lateral design capacity of an individual fastener

S is the fastener spacing

$l_{i,ef}$ is the effective length of the unit as detailed in 9.2.4.2(11)

$k_{i,w}$ is a modification factor taking into account wall length, the vertical load on the wall, the hold down restraint on the wall and the windward loading condition as detailed in 9.2.4.2(12)

Structural wall components may be sheathed on either one or both sides, A sheathing is a structural sheet material which through its fastenings contributes to the racking resistance of the wall. Normally it will be an approved grade of wood based material such as plywood, OSB, particle board or fibreboard where the strength and durability of the board have been proven. For internal faces of walls, materials such as plasterboard may contribute to racking performance if approved fastener design values are available for the board. The total contribution of these boards should not exceed 35% of the applied racking load at any given floor level.

(6) For fasteners along the edges of an individual sheet, the fastener design load carrying capacity $F_{f.Rd}$ may be increased by a factor of 1,2 over the corresponding value given in Section 8. In determining the fastener spacing in accordance with the requirements of Section 8, the edges may be assumed to be unloaded.

The 1,2 factor and the use of the rope effect in determining $F_{f.Rd}$ may only be included for wood based sheet materials approved for use as an external sheathing for timber frame walls such as appropriate grades of plywood, OSB, particleboard or fibreboard.

16

(7) The fastener design load carrying capacity $F_{f,Rd}$ may be increased by a further factor of 1,1 to take account of frame joints if;

- the stud spacing is less than 650mm
- the joint consists of at least two nails of at least 3.8mm diameter with a point side penetration of at least 50mm
- the wall is designed as sheathed on one side (single sheathing) only.
- the sheathing must be of approved grades of plywood, OSB, particleboard or fibreboard

(8) For wall units with sheathing on both sides the following rules apply;

- If the sheets and fasteners are of the same type and dimension then the total racking load carrying capacity of the wall should be taken as the sum of capacities of the individual sheets
- If different sheets or fastenings are used then the contribution of the weaker sheathing should be reduced to 65% of its individual racking load capacity.

(9) Shear buckling of the sheet may be disregarded, provided that $b_{net}/t \leq 100$
Where:

b_{net} is the clear spacing between studs
t is thickness of the sheet.

Sheets should be supported internally. This will be adequate if studs are spaced no further apart than 650mm otherwise horizontal supports will be required. For internal members to provide support the spacing of fasteners should not be greater than twice the spacing of fasteners along the edge of the sheet.

(10) In contact areas between vertical studs and horizontal timber members, compression stresses perpendicular to the grain should be verified in the timber members.

(11) The effective length of wall unit takes account of the extra racking resistance achieved if the unit continues under a window at the leeward edge and the reduced resistance if sheathing widths are too small. Based on Figure 9.7 it is determined as:

$$l_{i,ef} = \quad l_i - \Sigma l_{ss} + \min\{h_{w,i}, l_{w,i} - \Sigma l_{w,ss}\}$$

Where:

$h_{w,i}$ is the height of the window soffit on the leeward side
$l_{w,i}$ is the window length on the leeward side
l_{ss} and $l_{w,ss}$ are widths of sheet less than h/4
$$l_{i,ef} = \quad l_i + \min\{h_{w,i}, l_{w,i}\} - \Sigma L_{ss}$$

Loaded/windward edge | Leeward edge

l_{ss}

$F_{iv,Ed}$

Sheeting Joints

l_{ss} represents a sheet length less than h/4 within l_i

$l_{w,ss}$ represents a sheet length Less than h/4 within $l_{w,i}$

$l_{w,ss}$

h

$h_{w,i}$

45° max spread

l_i | $l_{w,i}$
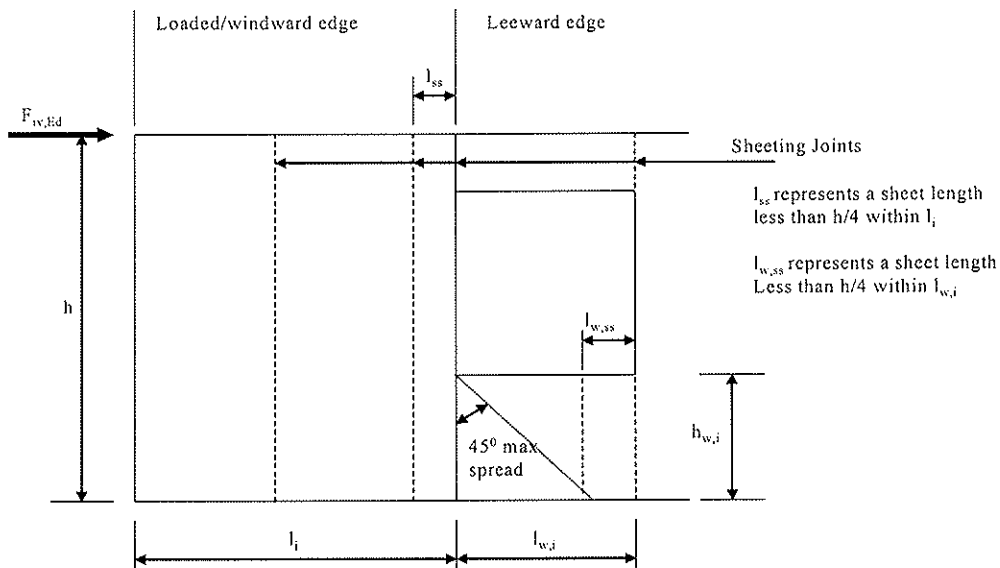
Figure 9.7:   **Determination of the effective length of a full height wall unit**

(12) The modification factor $k_{i,w}$ is determined by the anchorage of the wall unit which affects its shear resistance.

For a fully anchored wall unit,
$$k_{i,w} = 1$$

This condition is fulfilled if :
$$R_{i,v} > (F_{f,Rd} / s) * h$$

Where:

$R_{i,v}$ is the vertical restraint and is determined from the capacity of the anchorage of the leading stud, the resulting vertical load on the leading stud and the contribution from walls fixed to the leading stud, as shown in figure 9.8 such that:
$$R_{i,v} = R_{i,hd} + R_{i,wr,dl} + R_{i,wall}$$

$R_{i,hd}$ = the characteristic load carrying capacity of the leading stud anchorage to the foundations or the storey below

$R_{i,wr,dl}$ = the reaction on the windward edge of wall unit i to the favourable vertical dead loads applied to the wall unit as shown in figure 9.9

$R_{i,wall}$ = the minimum of the connection capacity between the racking wall and the windward return wall ($R_{v,con}$) and the hold down afforded by the base connections of either the return wall or windward wall unit as shown in Figure 9.10

18
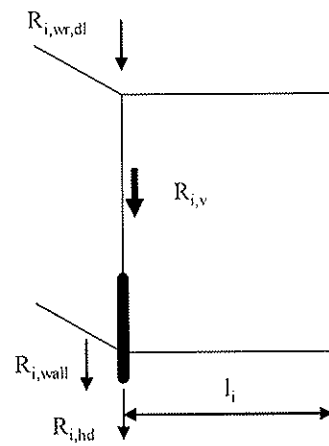
$$R_{i,v} = R_{i,hd} + R_{i,wr,dl} + R_{i,wall}$$

Figure 9.8   Vertical restraint $R_{i,v}$
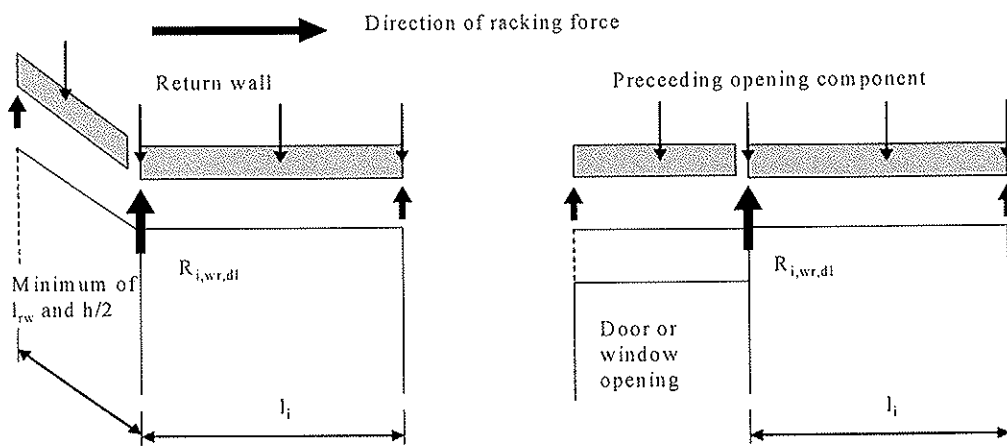
$R_{i,wr,dl}$ is the reaction on the windward end of wall unit l_i to the favourable vertical dead loads on the wall panel and either the return wall or the preceeding door or window opening

Figure 9.9:   Vertical load component $R_{i,wr,v}$

19

Return wall   Door opening   Window opening

R_{wall} is minimum of
$(F_{f,Rd}/s)*h/2$ or
$(F_{f,Rd}/s)*l_{rw}$ or
$R_{v,con}$

R_{wall} is zero

R_{wall} is minimum of
$(F_{f,Rd}/s)*h_w/2$ or
$R_{v,con}$

$R_{v,con}$ is the shear capacity of the
Connections linking the two walls
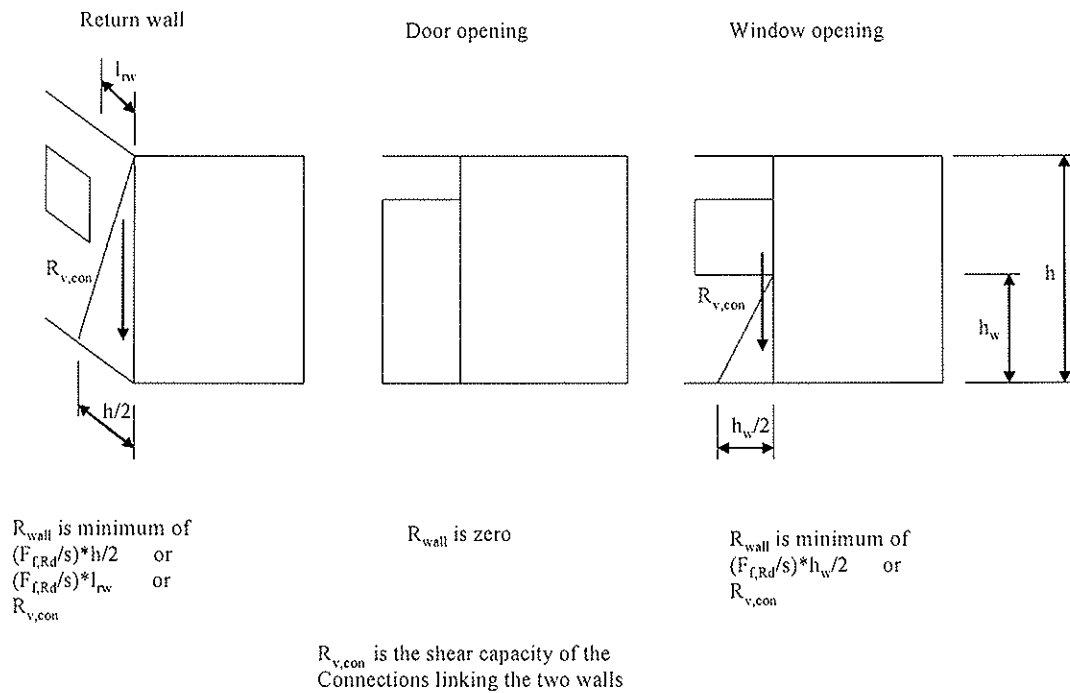
Figure 9.10:   **Vertical load component R_{wall}**

If:

$$R_v < (F_{f,Rd} / s) *(h-l_i),$$

Then

$$k_{i,w} = 0,5 \cdot \alpha + \beta$$

Where

$$\alpha = l_i / h$$
$$\beta = R_v / (F_{f,Rd} / s) *h$$

Otherwise

$$k_{i,w} = 1 - \frac{(1-\beta)^2}{2 \cdot \alpha}$$

....

The text for the wall racking method in Eurocode 5 ends here. Other parts of the document such as fastener values are used in design however they may also apply limitations to the design. It is recommended that factors such as design values for plasterboard and masonry and allowances for brick shielding are covered by National Annexes.

INTERNATIONAL COUNCIL FOR RESEARCH AND INNOVATION
IN BUILDING AND CONSTRUCTION

WORKING COMMISSION W18 - TIMBER STRUCTURES

FIRE BEHAVIOUR OF MULTIPLE SHEAR STEEL-TO-TIMBER CONNECTIONS WITH DOWELS

C Erchinger

A Frangi

Institute of Structural Engineering, ETH Zurich

A Mischler

University of Applied Science, HSR, CH-8640 Rapperswil

SWITZERLAND

Presented by C Erchinger

J König commented that he is happy about the work as the data is very good input to Eurocode 5; however, the idea of doubling is for end distance and not for member thickness and this would explain the findings. Also the one parameter exponential function is intended to yield conservative results. A two parameter function may be tried and may be more realistic. He asked whether additional models will be considered. C Erchinger responded that only 2 parameter model will be considered for now.

H Blass commented that 2 parameter model should not be fitted through one data point. J König said additional points are available and agreed that these points should not be too closely grouped.

A Buchanan received confirmation that longer BSB (plain) dowels were used in the extra thick specimens and commented that shorter dowel can also be considered so that there is no heat flux through the dowel. He further asked whether Johansen yield model were tried for both cold and hot dowel and whether bending of dowel in the fire case was observed. C Erchinger confirmed that some dowels were bent. A Frangi stated the yield theory was tried but did not give good match. The key is the change to wood failure mode in high temperature.

V Rajcic asked whether different configurations will be tried. C Erchinger confirmed that tests are finished and want to work on FEM. J König added that each configuration gives a different K and a lot of work is needed. A Buchanan stated data using LVL is available and will offer results.

Fire behaviour of multiple shear steel-to-timber connections with dowels

Carsten Erchinger, Andrea Frangi

Institute of Structural Engineering, ETH Zurich, CH-8093 Zurich, Switzerland

Adrian Mischler

University of Applied Science, HSR, CH-8640 Rapperswil, Switzerland

1   Introduction

In recent years, the load-carrying capacity of multiple shear steel-to-timber connections with slotted-in steel plates and steel dowels has been thoroughly investigated at the Swiss Federal Institute of Technology in Zurich (ETH) [1,2]. Besides of a high load-carrying capacity and a ductile failure mode, the advantage of this connection is the protection of the slotted-in steel plates against fire. Therefore, a high fire resistance may be achieved.

In the last couple of years, many countries have started to introduce performance based fire regulations or liberalized the use of timber for buildings. These regulations open the way for new applications, in particularly for an extended use of timber structures in multi-storey buildings.

The fire behaviour of steel-to-timber connections was experimental analysed with an extensive programme sponsored by the Swiss Agency for the Environment, Forests and Landscape [3]. The connections were tested with different timber thicknesses and different end distances of the fasteners. In addition to the unprotected connections some connections were tested protected by timber boards or gypsum plasterboards. The fire tests were completed by a series of tests at normal temperature.

Eurocode 5, part 2 (EN 1995-1-2) [4] gives design rules for symmetrical three-member connections made with nails, bolts, dowels, split-ring connectors, shear-plate connectors or toothed plate connectors. Besides simplified rules, the fire resistance of unprotected and protected connections can be calculated according to the "Reduced Load Method". The parameter k describing the exponential functions was determined for different connections using available test results. For steel-to-timber connections with dowels a value of k is only given for a diameter greater or equal than 12 mm. On the other hand, no value is given for multiple shear steel-to-timber connections with smaller diameters as tested in the ongoing research project.

Based on the main results of the fire tests, the paper analyses the efficiency of different strategies in order to increase the fire resistance of the connection. Further, particular attention is given to the comparison between test results and the design rules given in EN 1995-1-2. Based on the test results, the parameter k is calculated and compared to other connections to improve the design rules in EN 1995-1-2 for this connection type.

2 Experimental Investigations

2.1 Overview and test results

The connections were tested in tension parallel to the grain direction of the timber member. During the fire tests, the connections were loaded with a constant static load level ($0.3 * F_{v,R}$, $0.15 * F_{v,R}$ or $0.075 * F_{v,R}$), where $F_{v,R}$ is the average measured load-carrying capacity of the connections based on 5 tests performed at normal temperature according to EN 26891 [5]. In the fire rests the following test parameters were varied:

- load level
- diameter of the steel dowels (6.3 and 12 mm)
- number and configuration of the steel dowels (9 x 2, 9 x 3, 3 x 3 and 4 x 2)
- timber cover of the connection
- protection of the connection with timber boards or gypsum plasterboards

The timber cross-section was 200 x 200 mm including two or three slotted-in steel plates. For the connection D 01.2 the thickness of the outer timber members was increased by 40 mm up to 77 mm as well as the edge and end distances were increased by 40 mm to 60 and 83 mm, respectively.

The fire tests were carried out on the small furnace (1.0 x 0.8 m) at the Swiss Federal Laboratories for Materials Testing and Research (EMPA) in Dübendorf according to EN 1363-1 [6]. Table 1 gives an overview of the 18 fire tests. More details concerning the material properties and geometry of the test specimens, the test programme and the test arrangement as well as comments to the test results are published in [7].

Table 1   Overview of the fire tests and failure times

Connection	Load level [kN]	Test number	Failure time [minutes]	Remarks
D 01.1	$0.3 * F_{v,R} = 145$	1	32.0	200 x 200 mm, GL 24h, 9 x 2 steel dowels diameter dowels: d = 6.3 mm, 3 steel plates
		2	34.0	
	$0.15 * F_{v,R} = 72$	1	38.0	200 x 200 mm, GL 24h, 9 x 2 steel dowels diameter dowels: d = 6.3 mm, 3 steel plates
		2	34.5	
	$0.075 * F_{v,R} = 36$	1	41.5	200 x 200 mm, GL 24h, 9 x 2 steel dowels diameter dowels: d = 6.3 mm, 3 steel plates
		2	41.0	
D 01.2	$0.3 * F_{v,R} = 173$	1	73.0	280 x 280 mm, GL 24h, 9 x 2 steel dowels diameter dowels: d = 6.3 mm, 3 steel plates
		2	73.0	
D 01.3	$0.3 * F_{v,R} = 145$	1	72.0	Same as D 01.1; connection protected by 27 mm thick timber boards
		2	57.0	
D 01.4	$0.3 * F_{v,R} = 145$	1	60.5	Same as D 01.1; connection protected by 15/18 mm thick gypsum plasterboards
		2	61.0	
D 02.1	$0.3 * F_{v,R} = 188$	1	30.5	200 x 200 mm, GL 36h, 9 x 3 steel dowels diameter dowels: d = 6.3 mm, 3 steel plates
		2	32.0	
D 03.1	$0.3 * F_{v,R} = 69$	1	32.0	200 x 200 mm, GL 24h, 3 x 3 steel dowels diameter dowels: d = 6.3 mm, 3 steel plates
		2	33.0	
D 04.1	$0.3 * F_{v,R} = 124$	1	34.5	200 x 200 mm, GL 24h, 4 x 2 steel dowels diameter dowels: d = 12 mm, 2 steel plates
		2	35.0	

In all fire tests an increased charring was observed on the upper and lower side of the timber. After the fire tests, the steel dowels located close to the edges of the timber

2

members were completely embedded in charred wood. However, the char-layer did not fall into the furnace so that the slotted-in steel plates were not exposed directly to the fire during the experimental tests. In the following the efficiency of the different test parameters to increase the fire resistance is analysed.

- *Load level:*

All unprotected connections tested under a constant static load of 0.3 * $F_{v,R}$ showed failure times between 30.5 and 35 minutes. A reduction of the load level to 0.15 * $F_{v,R}$ and 0.075 * $F_{v,R}$ (connection D 01.1) led only to an increased failure time of about 3 and 8 minutes, thus the load level seems not to be a relevant parameter in order to increase the fire resistance.

- *Diameter, number and configuration of the steel dowels:*

A reduction (connection D 02.1) or increase (connection D 03.1) of the number of dowels as well as an increase of the diameter from 6.3 to 12 mm (connection D 04.1) did not significantly increase the fire resistance. A variation of the number or diameter of the fasteners improved the fire resistance of max. 2 minutes. Independent from the failure mode it can be expected that the fire resistance of unprotected multiple shear steel-to-timber connections with slotted-in plates and dowels loaded with 0.3 * $F_{v,R}$ is around 30 minutes.

- *Timber cover of the connection:*

The increase of the timber cover of the slotted-in steel plates as well as of the end distance by 40 mm (connection D 01.2), the fire resistance of the connection type D 01.2 reached more than 70 minutes, thus showing a much higher fire resistance in comparison with the other tested connections.

- *Protected connections:*

The connections D 01.3 (27 mm timber board protection) and D 01.4 (gypsum plasterboard protection, 18 mm in test 1 and 15 mm in test 2) reached a fire resistance of around 60 minutes. Therefore, the protection of the connections led to an increased fire resistance of about 25 minutes. This corresponds for the 27 mm thick timber board to an improvement of the fire resistance of about 1 mm for 1 mm timber protection.

2.2 Residual cross-section

The residual cross-section of the test specimens was surveyed by laser-scanning as shown in figure 1, left. With this method it is possible to generate three-dimensional models of the
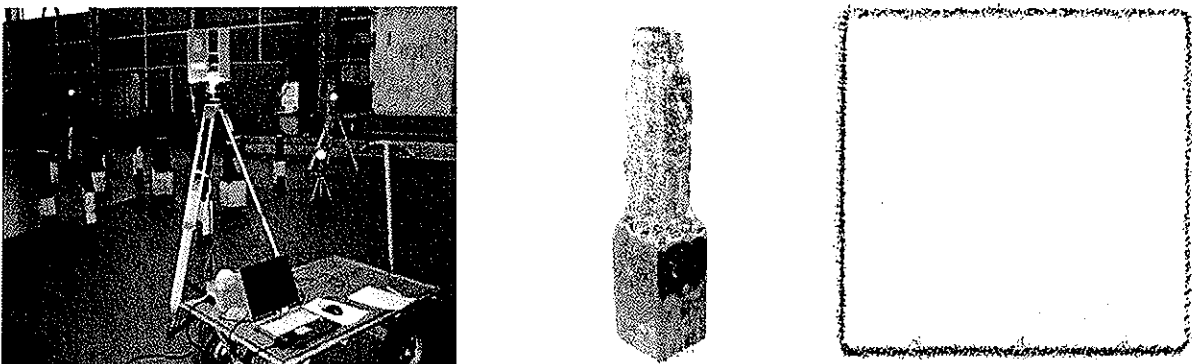
Figure 1   Laser-scanner and burnt-down test specimens (left), three-dimensional model
of connection D 01.1 (middle) and residual cross-section (right)

3

burnt-down timber members as shown in figure 1, middle on the example of connection D 01.1. Furthermore, the residual cross-section can be defined in every section where it is interesting to determine the charring. For the surveying of the residual cross-sections the laser-scanning method was used at the ETH Zurich for the first time and shaped up as a valid alternative to the mainly used manual methods. Figure 1, right shows the data point obtained by the laser-scans as a basis to model the residual cross-section and to determine the charring. The data was processed in two cross-sections of each timber member - the first one in a distance of 60 mm (section B-B), the second one 268 mm (section A-A) from the connection joint. The result can be seen in figure 2 for the timber member I of the connection D 01.1 after removing the char-layer. The charring is given in millimetres.
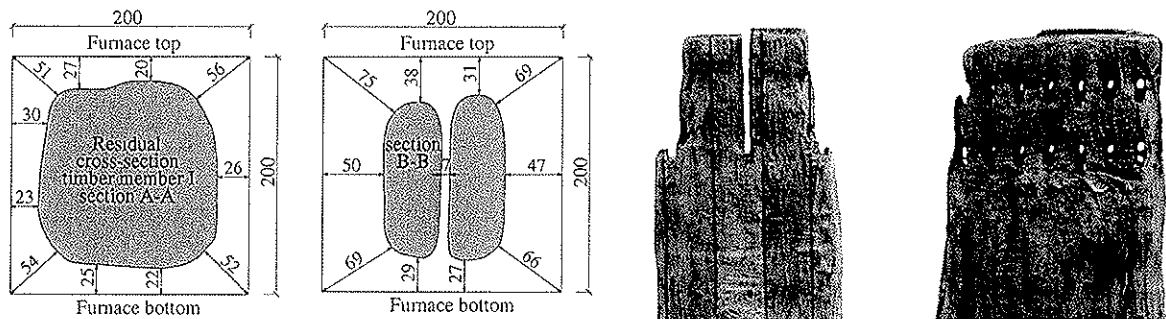
Figure 2   *Residual cross-section A-A and B-B obtained by the laser-scans (left) and test specimen after removing the char-layer of connection D 01.1 (right)*

During the fire exposure the outer timber members of the unprotected connections charred completely and did not contribute to the load-carrying capacity of the connection. On the other hand, for the connection D 01.2 with increased timber covers the outer timber members did not char completely as shown in figure 3. After the fire tests it was observed that the slots for the steel plates were not enlarged. The evaluation of the temperatures near the slots showed that the temperatures were not high enough to increase the charring (see chapter 2.3).
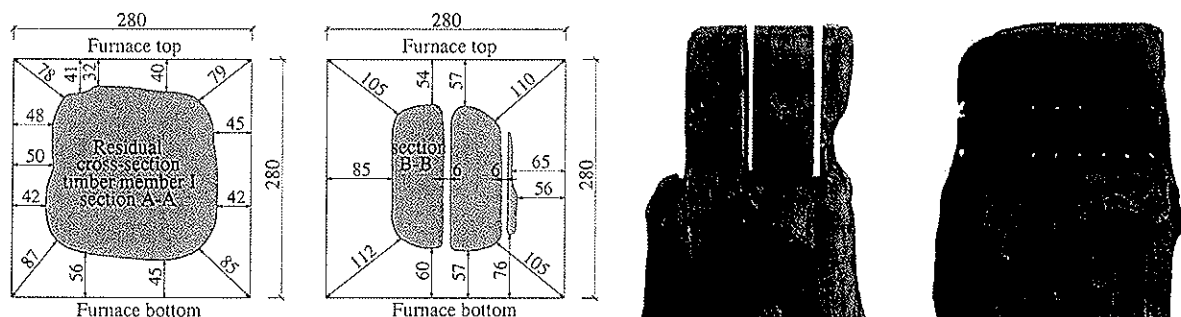
Figure 3   *Residual cross-section A-A and B-B obtained by the laser-scans (left) and test specimen after removing the char-layer of connection D 01.2 (right)*

The laser-scans were carried out with a laser-scanner type Imager 5003 (Zoller + Fröhlich GmbH, D-88239 Wangen i.A.) in the Structural Engineering Laboratory in cooperation with the Institute of Geodesy and Photogrammetry of the ETH Zurich.

2.3   Temperatures

During the fire tests, the temperatures at selected positions on the surface as well as in several depths of the timber members were measured and recorded with thermocouples (TC) of chromel-alumel, type K. The thermocouples were located 3 mm behind the dowels

4

and 12 mm beside the steel plates. The position of the thermocouples is shown in figure 4 and 5 on the hand of the unprotected connection D 01.1 and the connection D 01.2 with increased timber covers.

Figure 4   Position of the thermocouples of the connection D 01.1 (unprotected)
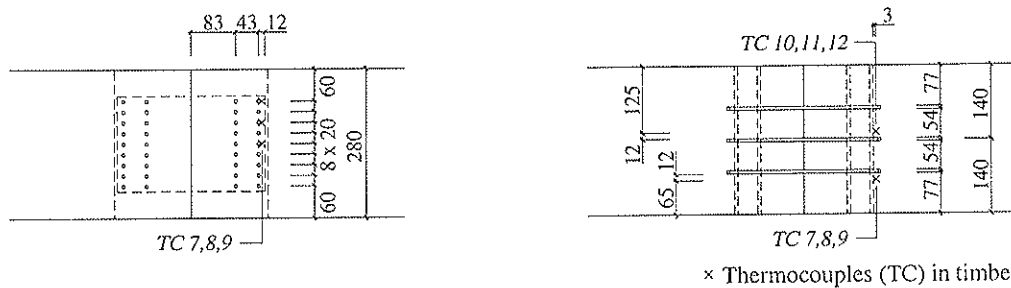
× Thermocouples (TC) in timber

Figure 5   Position of the thermocouples for the connection D 01.2 (increased timber covers)

The measured temperatures are shown in figure 6. It can be seen that the temperatures in the outer timber members (TC 1-3 and TC 7-9) were in most cases higher than next to the slotted-in steel plates in the middle. The temperatures there (TC 5, 6, 11, 12) did not reach more than 150 °C during the fire tests i.e. no charring was observed for the middle slots as aforementioned in chapter 2.2. The typical plateau at a temperature of about 100 °C which lasts several minutes can also be seen in both connection types.
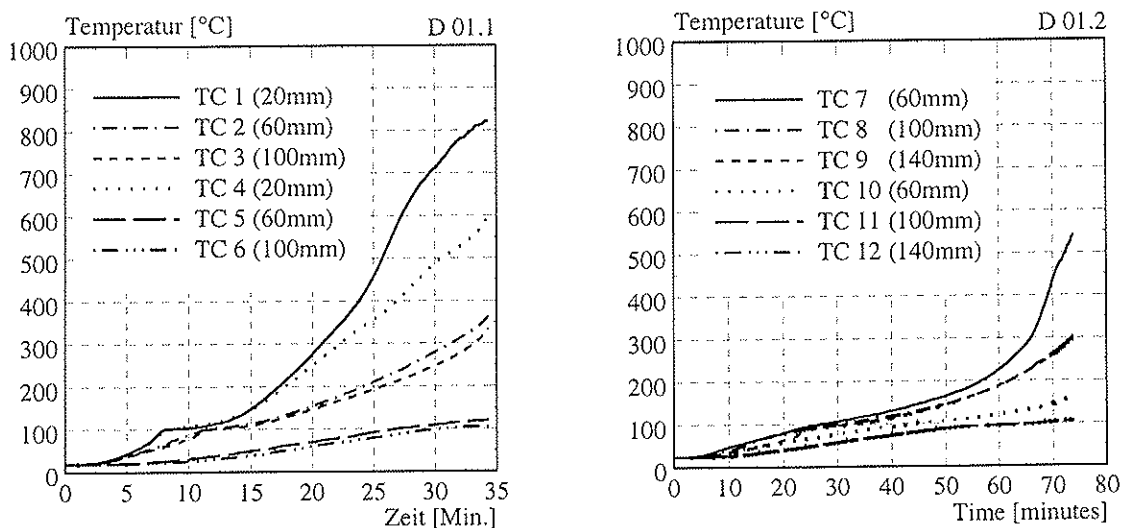
Figure 6   Measured Temperatures in the connection D 01.1 (left) and D 01.2 (right)

In order to observe the effect of the heat flux through the dowels into the timber the measured temperatures were compared to temperatures calculated by equation (1).

$$\Theta_{(x,y)} = 20 + 180 \cdot (\beta_n \cdot t)^\alpha \cdot \left\{ \left(\frac{1}{x}\right)^\alpha + \left(\frac{1}{b-x}\right)^\alpha + \left(\frac{1}{y}\right)^\alpha \right\} \qquad (1)$$

5

where

$\Theta_{(x,y)}$ temperature in °C of any point x,y of the timber cross-section
β_n notional charring rate in mm/min.
t   fire time in minutes
α exponent: $\alpha_{(t)} = 0.025{\cdot}t + 1.75$

This formula was developed originally by Frangi [8] to calculate the temperature in timber members exposed to ISO-fire on three sides. The notional charring rate β_n was determined with the laser-scanning method for connection D 01.1 to 0.7 mm/min. For TC 3 for example the value of x is 25 mm, the y value is 100 mm (figure 4). The calculated temperatures of the thermocouples TC 1-6 according to equation (1) are shown in figure 7.
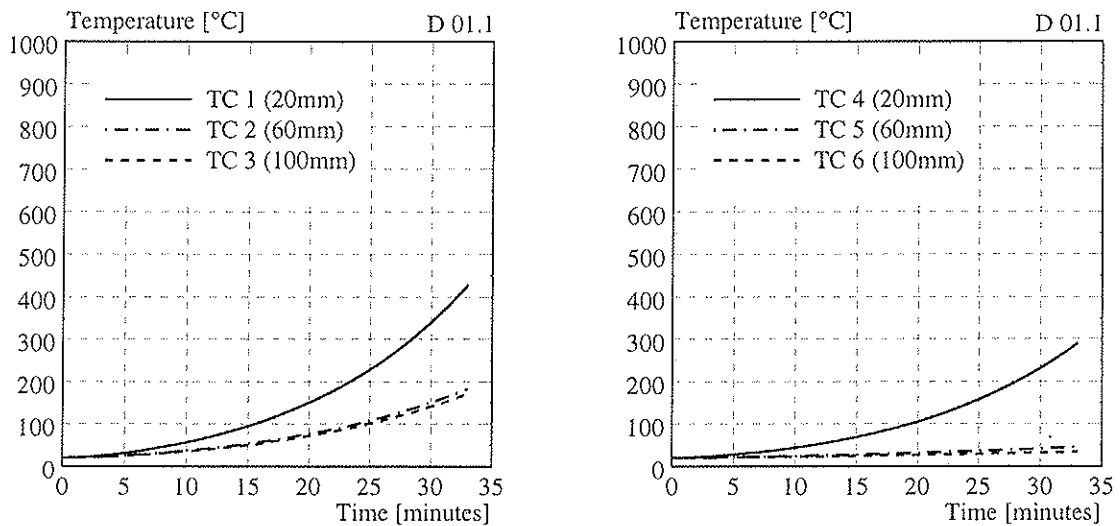
Figure 7   *Calculated temperatures in connection D 01.1 according to equation (1)*

It can be seen that the calculated temperatures are lower than in the experimental tests. Thus, the dowels seem to increase the heat transfer into the timber, however no significant influence of the heat transfer trough the dowels was determined considering the charring. This effect as shown for connection D 01.1 was observed in all other fire tests as well.

2.4   Comparison of the results to Eurocode 5

2.4.1   Simplified rules for unprotected connections

Eurocode 5, part 2 gives also simplified rules for the calculation of the fire resistance of unprotected shear connections with side members of wood designed according to Eurocode 5, part 1 (EN 1995-1-1) [9] at normal temperature. For connections with dowels a fire resistance t_{fi} of 20 minutes is given in EN 1995-1-2. The simplified rules are valid for normal reductions of loads or combinations of loads and partial safety factors used in structural fire design. Further, the connections shall comply with the minimum requirements given in Eurocode 5, part 1 regarding thickness of the timber side members, spacings, edge and end distances of the dowels, diameter of the dowels and width of the steel plates with unprotected edges.

Table 2 gives the minimum spacings, edge and end distances according to the requirements in EN 1995-1-1 as well as the effective spacings and distances used for the test specimens. The provision of the thickness of the side members is given in EN 1995-1-2 to 45 mm to reach a fire resistance of 20 minutes.

Table 2   Comparison of the used distances to the design rules given in EN 1995-1-1 [9]

Spacings and edge/end distances	Minimum spacings or edge/end distances according to EN 1995-1-1	Edge/end distances in the connection type [mm]					
		D 01.1 (d = 6.3 mm)		D 01.2 (d = 6.3 mm)		D 04.1 (d = 12 mm)	
		EN	Test	EN	Test	EN	Test
a_1 (spacing ‖ to grain)	5 x d	31.5	43	31.5	43	60	84
a_2 (spacing ⊥ to grain)	3 x d	18.9	20	18.9	20	36	40
a_3 (end distance loaded end)	max (7 x d; 80 mm)	80	43*	80	83	84	84
a_4 (edge distance loaded edge)	3 x d	18.9	20	18.9	60	36	40

On the other hand, for the unprotected connection D 01.1 the (*)-marked end distance of 43 mm (instead of 80 mm) as well as the thickness of the side members with 37 mm (instead of 45 mm) did not fulfil the requirements of Eurocode 5, part 1. However, also these test specimens showed a fire resistance of more than 30 minutes (table 1). Thus, for multiple shear steel-to-timber connections with slotted-in steel plates and dowels the simplified rules given in EN 1995-1-2 give conservative results.

2.4.2   Evaluation of the parameter k_{flux}

As an alternative method of protecting end and side surfaces of members, the end and edge distances may be increased by a_{fi} in order to increase the fire resistance of the connections. According to EN 1995-1-2 a_{fi} can be calculated as

$$a_{fi} = \beta_n \cdot k_{flux} \cdot (t_{req} - t_{fi}) \quad . \tag{2}$$

where

a_{fi} increase of the side members thickness and the edge and end distances
β_n notional charring rate in mm/min.
t_{req} required standard fire resistance in minutes
t_{fi} fire resistance of the unprotected connection in minutes
k_{flux} coefficient taking into account the increased heat flux through the fasteners.

The coefficient k_{flux} is given to 1.5 and is based on the nail tests by Norén [10], i.e. this value of k_{flux} is only valid for a fire resistance not exceeding 30 minutes and only for nails, screws with non-projecting heads and dowels. For a fire resistance greater than 30 minutes no value of k_{flux} is given in EN 1995-1-2 due to the insufficient experimental background. With the test results of the connection D 01.2 shown in table 1 (40 mm increased side timber members, failure time 73 minutes) in comparison to connection D 01.1 (unprotected, failure time 33 minutes) and a charring rate $\beta_n = 0.7$ mm/min. given in EN 1995-1-2, the coefficient k_{flux} can be determined to 1.4. That means that the given value of k_{flux} of 1.5 in EN 1995-1-2 might to be used in connections with dowels for a fire resistance of more than 30 minutes as well.

2.4.3   Reduced load method

For standard fire exposure, the load-carrying capacity of a connection with fasteners in shear can be calculated according to the "Reduced load method" given in EN 1995-1-2. The relationship between load ratio and time to failure can be described by a one-parameter exponential model

$$\frac{F_{v,R,fi}}{F_{v,R}} = e^{-k \cdot t_{fi}} \tag{3}$$

where

$F_{v,R,fi}$ load-carrying capacity of connections with fasteners in shear at standard fire exposure

$F_{v,R}$ load-carrying capacity of connections with fasteners in shear at normal temperature

k coefficient

t_{fi} fire resistance of the unprotected connection.

The maximum period of validity for the parameter k for unprotected steel-to-wood connections with dowels is 30 minutes. For a greater fire resistance the end and side surfaces of the members have to be protected by wood, wood-based panels, gypsum plasterboards or other materials or the edge and end distances have to be increased.

2.4.4 Calculation of the parameter k

For different wood-to-wood and steel-to-wood connections with nails, screws, bolts and dowels the parameter k given in the calculation model of equation (3) was determined using available test results. For these connection types the parameter k is published in EN 1995-1-2. For lower diameters of the dowels than 12 mm, no value of k is defined for multiple shear steel-to-timber connections with slotted-in steel plates.

In figure 8 the results of the fire tests on multiple shear steel-to-wood connections with dowels are shown in comparison to steel-to-wood connections with bolts (diameter 12 mm) performed similarly according to [11]. In general, it can be seen that the fire resistance of connections with bolts is smaller than of connections with non-projecting dowels, since more heat is transferred into the connection due to the bolt heads. For the connections with dowels a fire resistance of 30 minutes was achieved in every fire test. Furthermore, the fire resistance of the unprotected connections are very close to each other. The effect of the configuration, the diameter and the number of the dowels is not significant.

Figure 8   Load ratio versus time to failure for the carried out connections with dowels in comparison to connections with bolts

The calculation of the parameter k for smaller diameters of the dowels was made on the connections with the same load ratio and the same dowel diameter. Because of the small influence of the number and configuration of the dowels in the fire tests performed, the connections D 02.1 and D 03.1 were also taken into account next to the connection D 01.1 and not considered separately. Figure 9, left shows the calculated exponential curve for the multiple shear steel-to-timber connections with slotted-in steel plates and dowels with a diameter of 6.3 mm and a load ratio of 0.3. The parameter of k for the test series with smaller dowels with a diameter of 6.3 mm was determined to 0.037.

For steel-to-wood connections with dowels with a diameter ≥ 12 mm the parameter k given in EN 1995-1-2 is 0.085. The same value is also given for steel-to-wood connections with bolts with a diameter ≥ 12 mm. Dowels with a diameter of 12 mm were used for the connection D 04.1. On the right side of figure 9, the exponential curve of connection

D 04.1 is shown in comparison to the test results with connections with bolts with a diameter of the bolts of 12 mm given in [11] and to EN 1995-1-2.
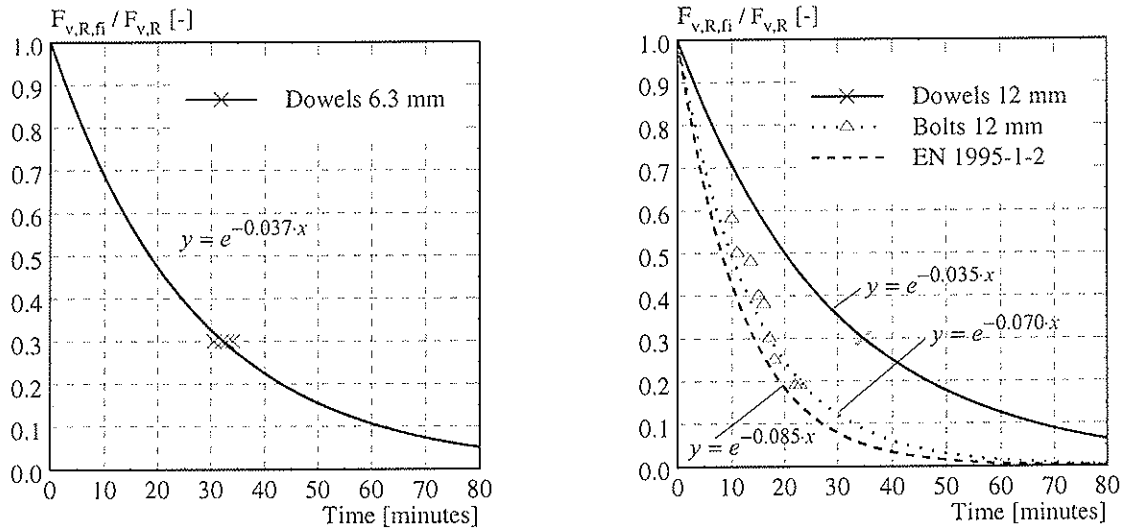
Figure 9   Evaluation of the parameter k for a diameter of the dowels of 6.3 mm (left) and comparison of test results with dowels and bolts to EN 1995-1-2 (right)

The parameter k for the test series D 04.1 for dowels with a diameter of 12 mm was determined to 0.035 and is very similar to the value obtained for dowels with a diameter of 6.3 mm. The value of the parameter k for steel-to-wood connections with bolts and slotted-in steel plates given in [11] is 0.070. While the value of k = 0.085 given in EN 1995-1-2 for steel-to-wood connections with bolts is confirmed by the test results [11], for multiple shear steel-to-timber connections with slotted-in steel plates and dowels a less conservative value may be assumed based on the results of the fire tests performed.

2.4.5   Charring rate

The comparison of the charring with the one-dimensional design charring rates under standard fire exposure given in EN 1995-1-2 is resumed for connection D 01.1 (timber member I) in table 3. The charring rate was determined of the residual cross-section shown on the example of connection D 01.1 in figure 2. After the fire tests the timber members were partially damaged so that it was not possible to evaluate systematically the charring longitudinal to the members occurred at the gap between the members I and II. However, no charring was generally observed at the gap between the members.

Table 3   Comparison of charring rates in connection D 01.1 (timber member I)

D 01.1	Place	Charring depth (mean value) [mm]	Fire resistance [min.]	β_0 [mm/min.]	$\beta_{0,EN\ 1995-1-2}$ [mm/min.]
Timber member I	Left + right side	26.5		0.70	0.65
	Top + bottom side	23.5	38.0	0.62	0.65
	Corners	53.5		1.41	1.30

Regarding the mean values of the charring rates of all experimental tests in section A-A, the charring rate β_0 on the sides, the top and the bottom ranged from 0.54 to 0.88 mm/min. and in the corners (in this case the charring depth was measured diagonally) from 1.19 to 1.48 mm/min. That means a mean value of 0.67 mm/min. and 1.30 mm/min., respectively. It can be seen that - assuming that the charring rate in the corners is twice as big as the one-dimensional charring rate β_0 - the test results are in a good agreement with Eurocode 5.

2.5 Conclusions

The paper analyses the efficiency of different strategies in order to increase the fire resistance of multiple shear steel-to-timber connections with dowels and slotted-in steel plates. Especially connections with a smaller diameter of the dowels were analysed. The laser-scanning method was applied to evaluate the residual cross-section. This method was used at the ETH Zurich for the first time and shaped up as a valid alternative to the mainly used manual methods. Compared to EN 1995-1-2 the charring rates showed a very good agreement. The influence of the heat flux through the fasteners was analysed by comparing the measured temperatures with calculation models developed for timber members without steel elements and fasteners under ISO-fire exposure.

The parameter k used in the "Reduced load method" according to EN 1995-1-2 was determined for a diameter of the dowels of 6.3 mm to 0.037. The results of the fire tests with a diameter of the dowels of 12 mm (connection D 04.1) were compared to EN 1995- 1-2 and to steel-to-wood connections with bolts and slotted-in steel plates with a diameter of the bolts of 12 mm. While the value of k = 0.085 given in EN 1995-1-2 for steel-to-wood connections with bolts and slotted-in steel plates is confirmed by the test results, for multiple shear steel-to-wood connections with dowels and slotted-in steel plates a less conservative value may be assumed based on the results of the fire tests performed.

3 References

[1] Mischler, A., *Bedeutung der Duktilität für das Tragverhalten von Stahl-Holz-Bolzenverbindungen*, PhD Thesis No. 12561, ETH Zurich, 1998.

[2] Gehri, E., Mischler, A., *Multiple shear steel-to-timber joints*, in Madsen, B., *Behaviour of Timber Connections*, Timber Engineering Ltd., North Vancouver, Canada, 2000.

[3] Kolb, J., *Brandschutz in der Schweiz: Das Projekt Brandsicherheit und Holzbau*, 10. DGfH-Brandschutz-Tagung 2004, Berlin, Proceedings published by the German Society of Wood Research (DGfH), Munich.

[4] EN 1995-1-2 (Eurocode 5): *Design of timber structures, Part 1-2: General - Structural fire design*, CEN, Brussel, November 2004.

[5] EN 26891: *Timber structures. Joints made with mechanical fasteners. General principles for the determination of strength and deformation characteristics*, CEN, Brussel 1991.

[6] EN 1363-1: *Fire resistance tests - Part 1: General requirements*, CEN, Brussel, 1999.

[7] Frangi, A., Mischler, A., *Fire tests on timber connections with dowel-type fasteners*, Proceedings of CIB-W18, paper 37-16-2, Edinburgh, Scotland, 2004.

[8] Frangi, A., *Brandverhalten von Holz-Beton-Verbunddecken*, IBK report Nr. 269, Institute of Structural Engineering (IBK), ETH Zurich, September 2001.

[9] EN 1995-1-1 (Eurocode 5): *Design of timber structures, Part 1-1: General - Common rules and rules for buildings*, CEN, Brussel, November 2004.

[10] Norén, J., *Load-bearing capacity of nailed joints exposed to fire*, Fire and Materials 20 (1996), pp. 133-143.

[11] König, J., Fontana, M., *The performance of timber connections in fire - test results and rules of Eurocode 5*, Proceedings of Int. Rilem Symposium, Stuttgart, 2001.

INTERNATIONAL COUNCIL FOR RESEARCH AND INNOVATION
IN BUILDING AND CONSTRUCTION

WORKING COMMISSION W18 - TIMBER STRUCTURES

FIRE TESTS ON LIGHT TIMBER FRAME WALL ASSEMBLIES

V Schleifer

A Frangi

Swiss Federal Institute of Technology, Zurich

SWITZERLAND

Fire tests on light timber frame wall assemblies

Vanessa Schleifer, Andrea Frangi

Swiss Federal Institute of Technology, Zurich, Switzerland

1   Introduction

In the last couple of years, many countries have started to introduce performance-based fire regulations or liberalized the use of timber for buildings. These regulations open the way for new applications, particularly for an extended use of timber structures in multi-storey buildings. In taking advantage of the new possibilities it is essential to verify that the fire safety in timber buildings is not lower than in buildings made of other materials.

Currently, an extensive research project on timber construction in fire is carried out at ETH Zurich. One subproject studies the fire behaviour of light timber frame wall assemblies. The assemblies studied consist of solid timber members (studs) and non-combustible or combustible linings (or combinations) with or without cavity insulation made of rock, glass or wood fibre. Unlike heavy timber structures where the char-layer of fire exposed members performs as an effective protection of the remaining unburned residual cross-section, the fire performance of light timber frame wall assemblies depends on the protection provided by the linings and the cavity insulation.

The objective of the research project is the verification and extension of existing design methods of the separating function of wall and floor assemblies (e.g. as given in the Eurocode 5, part 1-2 [1]). Further new simplified calculation models will be developed based on new experimental and theoretical results.

This paper presents experimental results of an ongoing large testing program planned to enlarge the experimental background of the fire behaviour of light timber frame wall assemblies. Further the test results are compared to design rules given in Eurocode 5, part 1-2. Due to the important influence of the linings on the fire resistance, the type of material, thickness, position within the wall assemblies and number of layers was analysed.

2   Test programme

All fire tests were performed with non-loaded specimens at the Swiss Federal Laboratories for Materials Testing and Research (EMPA) in Dübendorf using ISO-fire exposure. The tests were carried out on the small furnace with the inner dimensions of 1.0 x 0.8 m.

Two different types of linings were tested:

- Non-combustible linings
- Combustible linings

In each test, four different non-combustible linings or two combustible linings were studied. In addition to the different types of linings tested, the thickness and position of the

linings, the number of layers as well as the cavity insulation have been varied. Further also the influence of the type of fasteners used as well as the spacing of the fasteners was analysed. Table 1 gives an overview of the 17 fire tests performed using ISO-fire exposure.

Table 1   Overview of the experimental fire tests

Test No.	Number of boards exposed to fire	Type of lining exposed to fire	Thickness of lining exposed to fire [mm]	Layer behind lining exposed to fire	Remarks
V1	1 (710x910 mm)	gypsum fibreboard (manufacturer 1)	15	no	
V2	4 (355x455 mm)	gypsum fibreboard (manufacturer 1)	15	no	
V3	1 (920x1120 mm)	gypsum fibreboard (manufacturer 1)	15	no	without fastener
V4	4 (355x455 mm)	gypsum fibreboard (manufacturer 1)	15, 2x15	gypsum fibreboard, insulation	
V5	4 (355x455 mm)	gypsum fibreboard (manufacturer 1, 2, 3)	12.5	no	
V6	4 (355x455 mm)	gypsum plasterboard type A and F (manufacturer 2, 3)	15	no	(see figure 1 and 2)
V7	2 (355x910 mm)	gypsum fibreboard (manufacturer 1)	15	no	
V8	4 (355x455 mm)	gypsum fibreboard (manufacturer 1)	18	no	different type and spacing of fasteners
V9	4 (355x455 mm)	gypsum fibreboard (manufacturer 1)	3x10 15	gypsum fibreboard, insulation	
V10	4 (355x455 mm)	gypsum plasterboard type A (manufacturer 3)	12.5, 2x12.5, 25	gypsum plasterboard type A	with gaps
V11	4 (355x455 mm)	gypsum plasterboard type A (manufacturer 3); gypsum plasterboard type F (manufacturer 2)	10+15, 15+10, 2x15, 2x12.5	particle board	
V12	2 (355x910 mm)	wood panelling, multilayer wood panel	54	no	with gaps
V13	2 (355x910 mm)	wood panelling, multilayer wood panel	2x27	no	with gaps
V14	2 (355x910 mm)	OSB (manufacturer 4, 5)	2x25	no	with gaps
V15	2 (355x910 mm)	OSB (manufacturer 4)	12	with and without particle board	with gaps
V16	2 (355x910 mm)	OSB of low flammability; wood fibre	12; 80	Particle board	
V17	4 (355x455 mm)	Gypsum fibreboard (manufacturer 1); Gypsum plasterboard type A (manufacturer 3)	15; 12.5	Particle board, OSB, MDF-board	With gaps

2
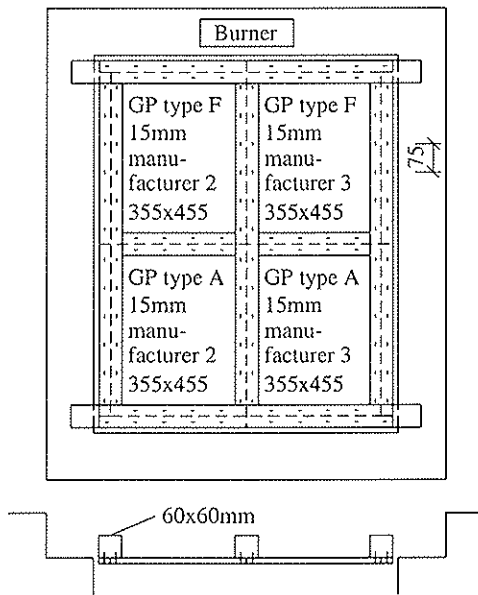
In order to describe the general assembly of the fire test the test specimen of fire test V4 and the position of the thermocouple of fire test V6 are shown in figure 1 and 2 as example. More details about geometry of the test specimens and test arrangements are given in [2].

Figure 1: Test specimen of fire test V6
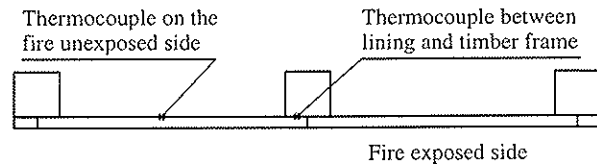
Figure 2: Position of thermocouples in fire test V6

3 Test results

The comparison of temperature measurements for the small-scale fire tests and large-scale fire tests (4.85 x 3.0 m) for the manufacturer 1 showed that the size of the furnace and the size of the specimens did not influence the temperature development of the linings [2]. However, the temperatures within the small furnace varied slightly (ca. $\Delta T = 50°C$). For fire tests with non-combustible linings the temperatures measured close to the burners were a little bit lower than far away of the burners. For fire tests with combustible linings it was observed the opposite case. Therefore the position of the linings in the furnace has a small influence on the temperature development of the linings.

3.1 Non-combustible linings

The non-combustible linings studied were gypsum plasterboard type A and F according to EN 520 [3] as well as gypsum fibreboards.

3.1.1 Gypsum fibreboards

The fire test V5 compared different manufacturers of gypsum fibreboards. The thermocouples were placed on the fire unexposed side as well as between lining and timber frame. The figure 3 shows the temperatures measured of fire test V5 at these locations. It can be seen, that the temperature developments is similar for the three manufacturers, so that the three manufacturers can be considered as equal. Because of the higher temperatures far away from the burner, the temperatures were slightly higher on the fire unexposed side of the gypsum fibreboard of manufacturer 2 (see figure 3a).

According to [4] the fire behaviour of gypsum fibreboards of the manufacturer 1 is better than gypsum plasterboards type F and could be used instead of gypsum plasterboards type F. In the fire tests V2 and V6 gypsum fibreboards (GF) and gypsum plasterboards type F (GPF) were compared (see figure 4). Temperature measurements on the fire unexposed side of the linings showed, that the gypsum fibreboards had the same fire behaviour like the

gypsum plasterboards type F (see figure 4, position T1). Only at high temperatures the gypsum plasterboards type F were slightly better than the fibreboards. However, at the timber frame the gypsum fibreboards behaved more favourable (see figure 4, position T2).
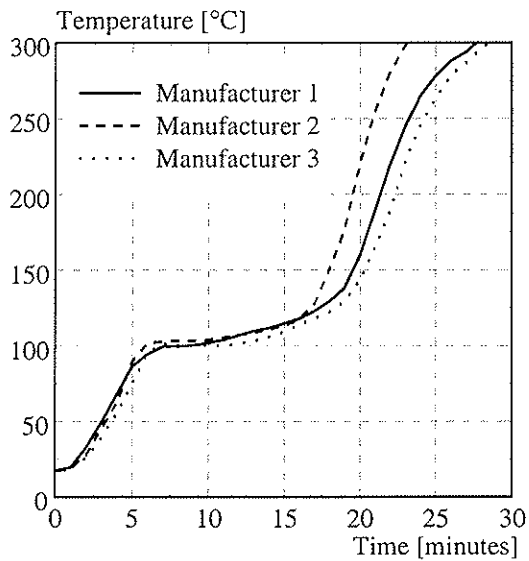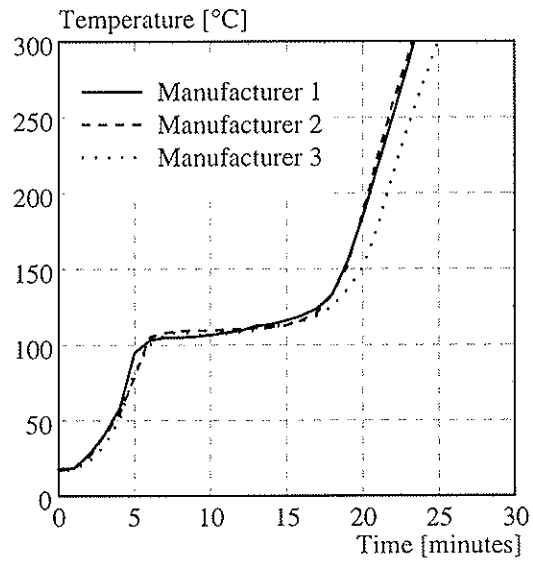
a) Fire unexposed side of the linings   b) Between linings and timber frame

Figure 3   Temperatures developments on the fire unexposed side of gypsum fibreboards (12.5 mm) of the fire test V5
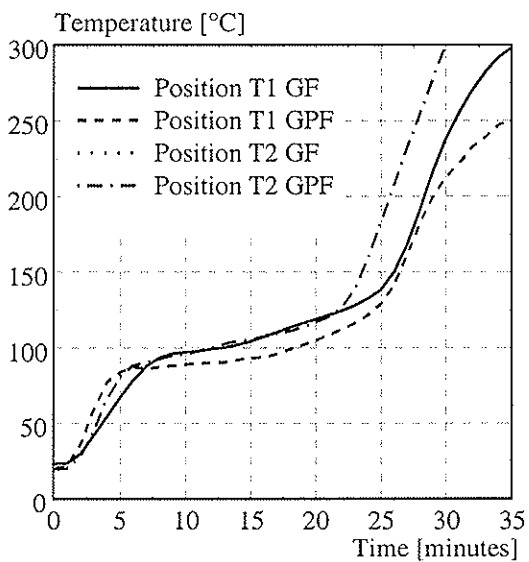
Figure 4 Temperature developments of the fire test V2 (gypsum fibreboards 15 mm) and V6 (gypsum plasterboards 15 mm)
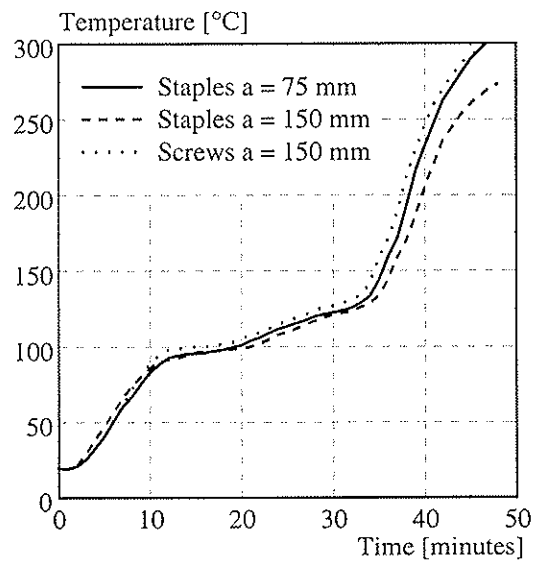
Figure 5 Temperature developments on the fire unexposed side of gypsum fibreboards (18 mm) of the fire test V8

3.1.2 Type and spacing of fastener

In the fire test V8 the type and the spacing of the fasteners was varied. Gypsum fibreboards with a thickness of 18 mm were fixed with staples (50 x 10 x 1.5) and a spacing of a = 75 mm and 150 mm as well as with screws (3.9 x 45) and a spacing of a = 150 mm. The figure 5 showed that the temperatures on the fire unexposed side of the gypsum fibreboard with the different types and spacing of the fasteners were similar. The gypsum fibreboard with staples and a spacing of a = 150 mm was located close to the burners hence the temperatures were slightly lower than those of the other linings.

4

3.1.3 Multilayer linings

Non-combustible linings may show a different fire behaviour when other linings are placed behind them. Figure 6 compares the temperature developments on the fire unexposed side of gypsum fibreboards (15 mm) with no additional linings behind them and with additional non-combustible linings as well as combustible linings (OSB, particle board) behind them. It can be seen, that the combustible linings had an unfavourable influence on the lining exposed to fire. Further, this influence was independent on the material of the combustible linings. On the other hand the gypsum fibreboard with the non-combustible lining showed a better fire behaviour than without a lining behind. A possible reason for the different fire behaviour is that due to the combustible linings the heat was dammed and the non-combustible linings absorbed the heat. The same fire behaviour could be observed in fire tests V10 and V11 with gypsum plasterboards.

3.1.4 Gaps

The gaps of the fire protective cladding have an important influence on the separating function of walls or floors. Therefore the gaps of gypsum plasterboards type A and gypsum fibreboards were studied with the fire tests V10, V11 and V17. For example figure 7 shows the temperature developments of the fire test V10. The gypsum plasterboards type A studied in the fire test V10 had no gaps or gaps with a width of 2 mm. The thermocouples were located directly in the gaps (see figure 7). It can be seen that the temperatures on the fire unexposed side of the gypsum plasterboards and behind the filled or unfilled gaps are similar. However, it has to be considered that due to the shrinkage of the boards the gaps may open more at large scale tests. Therefore also the temperatures may increase at the perimeter adjacent of the gaps.
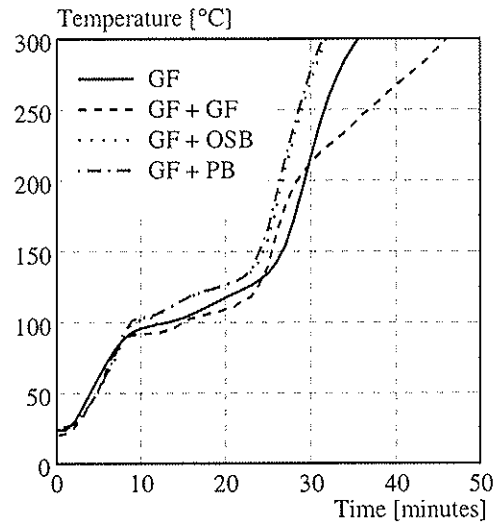
Figure 6   Temperature developments on the fire unexposed side of gypsum fibreboards (GF, 15 mm) with different linings behind
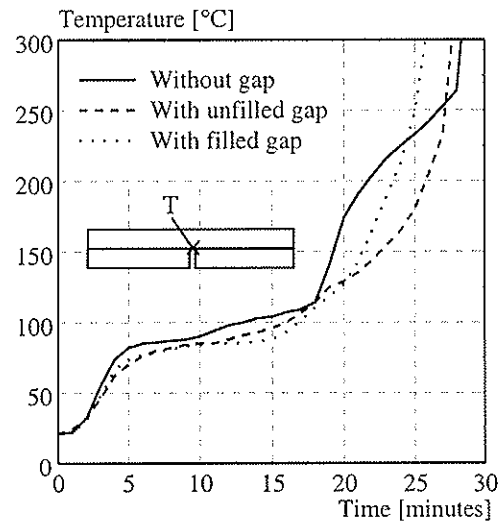
Figure 7   Temperature developments on the fire unexposed side of gypsum plasterboards (12.5 mm) with or without gaps of fire test V10

3.2   Combustible linings

3.2.1   Multilayer panels

The multilayer panels studied consisted of three layer und were compared to wood panelling. The density as well as the moisture content of all linings was similar. Table 2 gives the measured charring depth of the linings after the fire tests.

Table 2   Charring depth of wood panelling and multilayer panels

Fire test	Lining	Thickness [mm]	Fire time [min]	Charring depth $d_{char,0}$ [mm]	Charring depth $d_{char,0}$ at the gap [mm]
V12	Wood panelling	54	38	25	27
V12	Multilayer wood panel	54	38	32.5	50
V13	Wood panelling	2 x 27	28	20	27
V13	Multilayer wood panel	2 x 27	28	35	36

It can be seen that the fire behaviour of the wood panelling is better than in the case of the multilayer panels. For the wood panelling the char-layer performed as an effective protection of the remaining unburned residual cross-section. On the other hand, the multilayer wood panels consist of glued laminated layers. The glue loses its strength at high temperatures. Therefore the char-layer of multilayer wood panels fall off earlier than the char-layer of wood panelling.

4   Comparison to EN 1995-1-2

4.1   Start of charring and failure time

The tests results were compared to design rules given in EN 1995-1-2 [1]. In order to calculate the start of charring and the failure time of linings according to EN 1995-1-2 [1] it shall be differentiated between fire protective claddings, linings used in assemblies whose cavities are completely filled with insulation and linings used in assemblies with void cavities.

In order to determinate the start of charring of the linings tested following temperature criterion was assumed according to the Swiss fire regulations: when the temperature on the unexposed side of the lining reached an average of 250°C or at one location a maximum temperature of 280°C, it is assumed that the wood starts to char. According to EN 13501-2 [5] the maximum temperature is limited to 270°C. The difference between these temperature criterions is negligible and in most of the case the average temperature was reached at first. Therefore the criterion according to the Swiss fire regulations was used. The temperature should be measured on the assemblies behind the lining studied. However, some linings studied had no lining on the fire unexposed side to measure the temperatures at this location. In this case the start of charring measured was corrected by a factor which was determined with fire test V11 ($\Delta t = 1.5$ min) for non-combustible linings.

The failure time of linings of the fire tests were determined by visual observations.

4.1.1 Fire protective cladding

According to EN 1995-1-2 [1] the start of charring t_{ch} and the failure time t_f of protective claddings can be calculated with the following equations:

Wood based panels:
$$t_{ch} = t_f = \frac{h_p}{\beta_{0,\rho,t}} \qquad (3.10, 3.14)$$

Gypsum plasterboards type A and F: $t_{ch} = 2.8 \cdot h_p - 14 \quad \text{gaps} \le 2 \text{ mm} \qquad (3.11)$

Gypsum plasterboards type A: $t_f = t_{ch} \qquad\qquad (3.15)$

The failure time of gypsum plasterboards type F is not specified in the chapter of fire protective claddings. For the comparison with the test results the following equation for pull-out failure of the fastenings was used:

Gypsum plasterboards type F:
$$t_f = t_{ch} + \frac{l_f - l_{a,min} - h_p}{k_s \cdot k_2 \cdot k_n \cdot k_j \cdot \beta_{0,\rho,t}} \qquad (C.9)$$

According to section 3.1.1 the start of charring and the failure time of the gypsum fibreboards were compared to the calculation model for gypsum plasterboards type F.

Table 3   Start of charring and failure time fire protective cladding with gaps (2mm)

Fire protective cladding	Thickness [mm]	Start of charring t_{ch} [min]		Failure time t_f [min]	
		Fire test	Eurocode	Fire test	Eurocode
Gypsum plasterboards type A	12.5	22.5	21	29.5	21
	10 + 15	39.2	35	79	35
	15 + 10	44	42	64.5	42
Gypsum plasterboards type A (without gaps)	2 x 15	71.2	49	> 89	49
Gypsum fibreboard	15	30.5	28	> 39	51.2
	2 x 12.5	59.5	49	80	72.6
Wood panelling	27	> 28	29	> 28	29
Multilayer wood panel	27	22.2	28.5	22.5	28.5
OSB	12	13.9	15.7	17	15.7
	25	30.2	31.6	> 32	31.6
Wood fibre	80	45	56.7	> 64	56.7

From table 3 it can be seen that the calculation model according to EN 1995-1-2 [1] of start of charring for non-combustible fire protective claddings was in a good agreement with the results of the fire tests. Only the calculated failure time of the non-combustible linings was much lower than the test results. However, this difference depends also on the scale effect of the different furnaces.

The calculation model of start of charring and the failure time for combustible fire protective claddings was confirmed by the results of fire tests with wood panelling and OSB. On the other hand, for multilayer wood panels and wood fibres the start of charring was underestimated by the calculation model according EN 1995-1-2. The multilayer wood panels consisted of three glued laminated layers and the wood fibres consisted of four glued laminated layers. Because of the strength loss of the glue by high temperatures the char-layer felt off earlier than the char-layer of solid wood panels. For design purposes an increased charring rate for multilayer wood panels may be used. As shown in table 2 the measured charring rate depends on the thickness of the multilayer wood panel and varied between 0.85 and 1.25 mm/min.

4.1.2 Linings in assemblies with insulation

The determination of the start of charring t_{ch} and the failure time t_f of gypsum plasterboards in assemblies whose cavities are completely filled with insulation according to EN 1995-1-2 [1] are the same as the equations in section 4.1.1.

The gypsum fibreboards were influenced unfavourable by the insulating material behind (see table 4). Mainly this effect influences the separating function of the construction. The calculation model of start of charring according to EN 1995-1-2 [1] makes no difference between gypsum plasterboards with or without insulation behind. Therefore the measured temperatures on the fire unexposed side of the boards without insulation behind were higher than the calculated values. The calculated values based on fire tests, where the thermocouples were located in the middle of the studs behind the boards. However, in the present fire tests the thermocouples were located on the fire unexposed side of the boards in the perimeter adjacent of the insulation. Therefore in the table 4 the calculated results are slightly better than the measured start of charring.

Table 4   Start of charring and failure time of gypsum fibreboards (15 mm) with insulation behind

Insulation	Thickness [mm]	Density [kg/m^3]	Start of charring t_{ch} [min]		Failure time t_f [min]	
			Fire test	Eurocode	Fire test	Eurocode
Rock fibre	40	31	26.1		55	
Rock fibre	80	42	27.4		52	
Rock fibre	40	116	26.5	28	42	51.2
Glass fibre	80	27	27.2		58.5	
Wood fibre	80	178	27.3		44	

4.1.3 Linings in assemblies with void cavities

In order to calculate the start of charring t_{ch} and the failure time t_f of linings in assemblies with void cavities according to EN 1995-1-2 [1] it shall be differentiated between the narrow side and the wide side of members exposed to fire. For the calculation for wood based panels the following equations should be used.

Wood based panels:
$$t_{ch} = t_f = \frac{h_p}{\beta_{0,\rho,t}} - 4 \qquad \text{(C.6, C.7)}$$

Narrow side of the member exposed to fire:
Gypsum plasterboards type A and F: $t_{ch} = 2.8 \cdot h_p - 14$ gaps ≤ 2 mm   (3.11)

Wide side of member facing the cavity:
Gypsum plasterboards type A and F: $t_{ch} = 2.8 \cdot h_p - 11$ spacing ≤ 400 mm (D.4)

Gypsum plasterboards type A: $t_{ch} = t_f$ (D.2)

Gypsum plasterboards type F: (see section 4.1.1)

The calculation of the start of charring on the wide side of the member facing the cavity was compared to the measurement on the fire unexposed side of the linings.
In the fire tests V12, V13 and V14 the wood based panel studied had gaps. As soon as flames have been observed at the gaps on the fire unexposed side, the fire tests were stopped. Therefore the temperature criterion was not reached for these fire tests.
Table 5 shows the significant values of the start of charring of the non-combustible linings.

Table 5   Start of charring and failure time of non-combustible linings in assemblies with void cavities

Lining	Thickness [mm]	Start of charring t_{ch} at wide side of member [min]		Start of charring t_{ch} at narrow side of member [min]		Failure time t_f [min]	
		Fire test	Eurocode	Fire test	Eurocode	Fire test	Eurocode
Gypsum fibreboards	10	18.0	17.0	19.2	14.0	21.5	25.3
	12.5	24.8	24.0	23.5	21.0	> 31	35.3
	15	32.4	31.0	32.5	28.0	> 36	51.2
	18	43.6	39.4	41.7	36.4	> 48	62.3
	2 x 12.5	59.5	52.0	/	49.0	80	66.2
	2 x 15	85.4	64.6	67.3	61.6	82.5	84.8
	3 x 10	60.3	61.8	56.3	58.8	63	70.1
Gypsum plasterboard type F	15	34.5	31	29.5	28	> 32	51.2
Gypsum plasterboard type A	15	29.5	31	29.5	28	> 32	28
	2 x 12.5	41.6	41.5	42.1	38.5	> 46	38.5
	25	> 46	59.0	50.5	56.0	> 46	56

From table 5 it can be seen that the calculation model according to EN 1995-1-2 [1] of start of charring was in a good agreement with the test results. Only for the assembly with three layers and the assembly with a thick lining, the calculation model according to EN 1995-1-2 gives slightly unsafe values than the fire tests.

4.2   Charring depth

The charring depth of timber frames of walls or floors protected by fire protective cladding was studied by König [6]. With the fire test V11 and V13 – V17 the charring depth of wood based panels protected by fire protective claddings was studied.

According to EN 1995-1-2 [1] after the failure time of the fire protective cladding an increased design charring rate for wood based panels should be used. After the time limit t_a the wood based panels is protected by the char-layer and the design charring rate can be used to calculate the charring depth. For fire protective claddings like gypsum plasterboards type F the start of charring is smaller than the failure time. During the time between the start of charring and the failure time a decreased charring rate can be used.

In figure 8 the measured charring depths (solid line) were compared to the calculated charring depths (dashed line) according to the chapter 3.4.3 of EN 1995-1-2 [1].
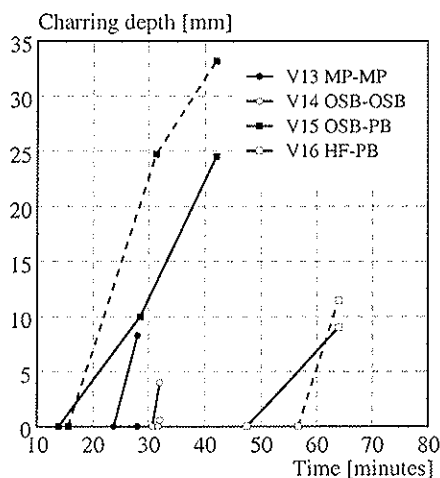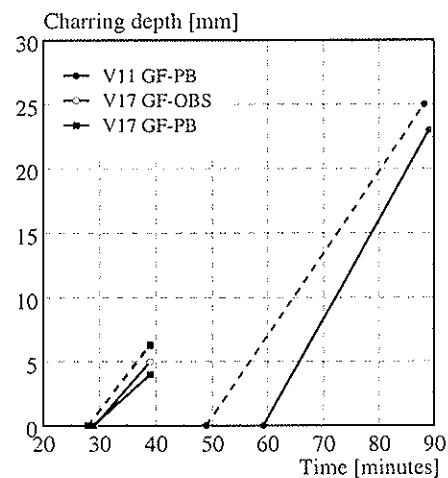
a) Protected by wood based panels   *b) Protected by gypsum fibreboards*
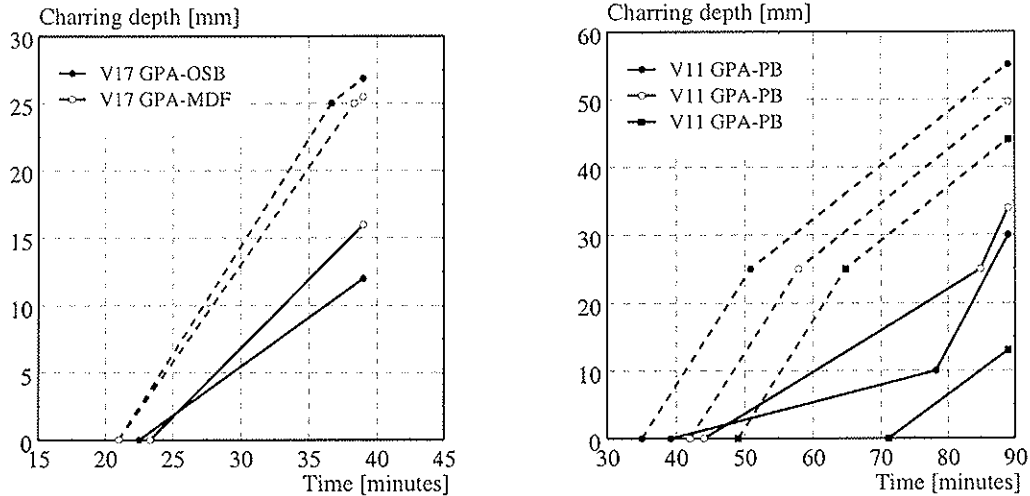
c) *Protected by gypsum plasterboards type A*

Figure 8   Calculated and measured charring depth of wood based panels protected by fire protective cladding (measured – solid line; calculated – dashed line)

The increased charring rate after the failure time of the fire protective cladding according to EN 1995-1-2 [1] could be observed at wood based panels protected by wood based panels. However, in the case of the particle boards protected by wood based panels the increased charring rate was not observed. In addition to the material of the protected lining, the thickness of lining could be a reason of this effect.

The calculated charring depth of wood based panels protected by gypsum fibreboards was in a good agreement with the measured charring depth. The difference of the charring rates was only $\Delta\beta_{0,r,t} = 0.1 - 0.2$ mm/min. Therefore this calculation according EN 1995-1-2 [1] can also be applied on the gypsum plasterboards type F.

For the gypsum plasterboards type A EN 1995-1-2 [1] gives conservative values of the calculated charring depth. The difference between the measured and the calculated charring depths was $\Delta d_{char,0} = 10 - 30$ mm. According to EN 1995-1-2 the failure time of gypsum plasterboards type A is equal to the time of start of charring. Therefore charring depth of the protected panel should be calculated with an increased charring rate after the failure time of the gypsum plasterboards type A. However, this was not observed in the fire tests because the gypsum plasterboards remained in place and still protected the timber panels from fire. The fire behaviour of the gypsum plasterboards type A was similar to the gypsum fibreboards. Therefore it may be possible to differentiate between the failure time and the time of start of charring of gypsum plasterboards type A. However, this assumption has to be confirmed by large scale tests.

5   Conclusions

The fire behaviour of light timber frame wall assemblies is currently analysed by a series of small-scale tests under ISO-fire exposure. The extensive testing program permits to study the influence of different parameters on the fire behaviour of light timber frame wall assemblies. In particular, the influence of the thickness and the position of the linings as well as the number of layers is studied.

All fire tests were conducted on the small furnace at the Swiss Federal Laboratories for Materials Testing and Research (EMPA) in Dübendorf. The linings studied on the fire

exposed side were influenced by the layer behind them. For linings with the same material the fire behaviour of the lining exposed to fire was influenced favourably. An unfavourable influence could be observed for the gypsum plasterboards on the fire exposed side with insulation materials. Further, this influence was independent on the type of the insulation material.

Mainly attention was given to the comparison of the tests results with the calculation model according to EN 1995-1-2 [1]. For the linings studied the time of start of charring, failure time and the charring depth of the layer behind the fire exposed lining were compared. The calculated values were in a good agreement with the test results of the gypsum fibreboards as well as the gypsum plasterboards type F. Only the small gypsum fibreboard with a thickness of 10 mm showed in the tests a slightly unsafe fire behaviour as the calculation. The calculated time of start of charring of gypsum plasterboards type A was also confirmed by the test results. However, the failure time of the fire tests was underestimated and therefore the charring depth of wood based panels protected by gypsum plasterboards type A was smaller than the calculation according EN 1995-1-2. Based on the fire tests the calculated failure time of gypsum plasterboards could be increased. However, this assumption has to be confirmed by large scale tests. Furthermore the calculated time of start of charring of multilayer wood panels should be decreased, because the char-layer of these linings felt off earlier than the char-layer of solid panels.

6 References

[1] EN 1995-1-2, *Eurocode 5 – Design of timber structures, part1-2: General – Structural fire design*, CEN, Brussels, November 2004

[2] V. Schleifer, A. Frangi, M. Fontana, *Fire behaviour of light timber frame wall assemblies*, IASBE Symposium, Lisbon, September 2005

[3] EN 520, *Gypsum plasterboards - Definitions, Requirements, Test Methods*, Draft European Standard , CEN, Brussels, 2003

[4] K. Kordina, C. Meyer-Ottens, *Holz Brandschutz Handbuch*, Deutsche Gesellschaft für Holzforschung e.V., Munich, 1994

[5] EN 13501-2, *Fire classification of construction products and building elements, part 2: Classification using data from the fire resistance tests, excluding ventilation services*, CEN, Brussels, August 2003

[6] J. König, L. Walleij, *One-dimensional charring of timber exposed to standard and parametric fires in initially unprotected and postprotection situations*, Trätek, Rapport I 9908029, Stockholm, August 1999

INTERNATIONAL COUNCIL FOR RESEARCH AND INNOVATION
IN BUILDING AND CONSTRUCTION

WORKING COMMISSION W18 - TIMBER STRUCTURES

ANALYSIS OF CENSORED DATA -
EXAMPLES IN TIMBER ENGINEERING RESEARCH

R Steiger

Swiss Federal Laboratories for Materials Testing and Research EMPA

J Köhler

Swiss Federal Institute of Technology ETH, Zürich

SWITZERLAND

Presented by R Steiger

S Thelandersson commented that one must be careful with consideration of the correlation factor especially in cases when within member correlation of properties may influence and bias the estimation of correlation factor. R Steiger agreed however finding the real correlation factor is difficult.

F Lam commented in the example of proof loading if point estimate is used to estimate a percentile property this technique will not help. If parametric approach is used than this technique is very useful. Work in the US with shear strength data is an example of the use of this technique. R Steiger agreed and stated the excel spreadsheet can be distributed for others to try. BJ Yeh confirmed his work on shear used this technique and the work is reported in previous CIB proceedings. H Larsen also suggested that Denzler's work can be re-analyzed with this technique for improvement.

Analysis of censored data - examples in timber engineering research

R. Steiger [1], J. Köhler [2]

[1] Swiss Federal Laboratories for Materials Testing and Research EMPA, Switzerland

[2] Swiss Federal Institute of Technology ETH, Zurich, Switzerland

1 Introduction

In timber engineering research one is often confronted with situations where test results enclose not only quantitative data e. g. failure loads but also accompanying information. Examples of such situations are:

- modelling mechanical properties with special emphasis to the lower tail of the underlying probability distribution.

- proof loaded specimens with strength higher than the (fixed) threshold,

- "run-outs" in the course of fatigue or duration of load tests, i.e. endurances reached without failure of the specimen, either because the test was terminated at a predetermined limit or because some other part of the specimen failed.

- tensile tests on timber structural joints (glued-in rods as an example) carried out on symmetrical specimens with identical joints at both ends.

- different failure modes within the same test series (e. g. shear and bending failures)

Resulting data in the above mentioned cases is said to be "censored". There are four possible ways to handle censored data:

(i) treating all run-outs as though they were (mode-conform) failure points,

(ii) neglecting the run-outs,

(iii) a graphical analysis (averaging) of all test results within the scatter band,

(iv) the Maximum Likelihood Estimation Technique.

The Maximum Likelihood Method (MLM) was successfully applied to the analysis of fatigue test results by Edwards and Pacheco (1984) [1] as well as by Spindel and Haibach (1979) [2].

Making reference to Lawless (1982) [3] Yeh and Williamson (2001) [4] conducted a censored data analysis to combine shear strength test values of glulam beams with frequently occurring bending failure.

Köhler and Faber (2003) [5] applied MLM for the probabilistic modelling of graded timber material properties. The authors introduced Censored Maximum Likelihood Estimation as a means for estimating the parameters probability density functions (PDF) of timber properties with special emphasis on the lower tail domain and the statistical uncertainty associated with this: only observations in the lower tail domain i.e. below a given predefined threshold value are used explicitly. The other observations are only made use of implicitly to the extent that it is recognized that they exceed the threshold.

Van de Kuilen and Blass (2005) [6] used a similar method reported by Douwen et al (1982) [7] to correct the mean value and the standard deviation when calculating the characteristic values of shear strength derived from tests on beams with two spans, thus accounting for the fact that actually the lower of two possible test values was found.

The paper discusses the influence of regarding/disregarding the additional information provided by the run-outs on the quantification of the parameters of corresponding probability distribution functions by making use of a Censored Maximum Likelihood Estimation Technique. Beside numerical studies of generated samples, as an example calculations are performed on a data set derived from pull-out strength tests of axially loaded steel rods bonded in glulam parallel to the grain and connected to the tension test machine by identical interfaces at both ends of the specimen [8] (Fig. 1, left). In comparison to unsymmetrical configurations (Fig. 2, right) this so-called pull-pull set up has the advantage of being simple when producing the specimens and regarding the transfer of forces from the testing machine into the specimen (Fig. 2).
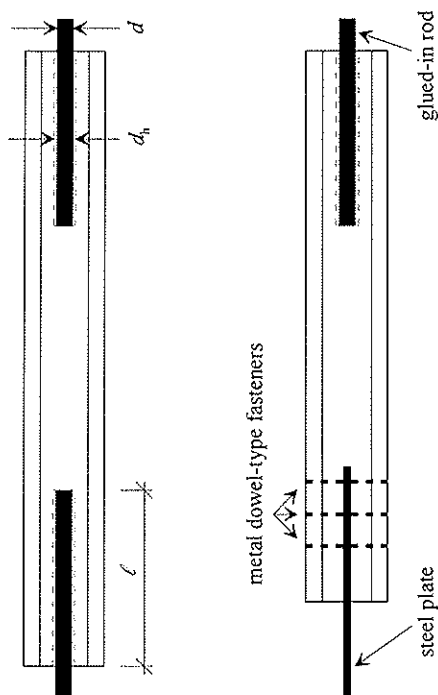
Fig. 1: Symmetrical and unsymmetrical spe-   Fig. 2: Pull-pull configured tensile test on
cimen for pull-out strength tests on   steel rods glued in glulam parallel to
glued-in rods. (The dowel joint has   the grain.
to be stronger then the rod joint!)

The failure loads derived from tests in pull-pull configuration are censored for the following typical reasons:

(i) For symmetrical test set ups (Fig. 1, left) a sample consists of the strength values of the "weaker" side of each of the n specimens but implicitly carries the information that n sides survived the test. I.e. it is also measured that the strength of these survivors is higher than the strength of the opposite joint, which failed.

(ii) For both symmetrical and unsymmetrical test set ups (Fig 1) different failure modes can occur. When optimizing the capacity of a glued-in rod joint, timber shear failure next to the rod (Fig. 3) is aimed. But sometimes steel failures (Fig. 4) or timber tensile failures (Fig. 5) occur. When estimating the probability distribution function of the

2

shear failure data, the measured steel or timber tensile strength has to be considered as exceeding the shear strength.
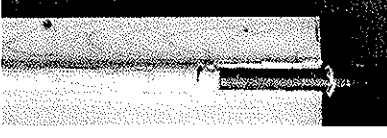
Fig. 3: Glued-in rod pulled out (shear failure in timber.)

Fig. 4: Steel failure of a glued-in rod.
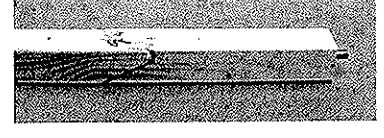
Fig. 5: Timber tensile failure.

2   Theoretical background

2.1   Method of Maximum Likelihood

The Method of Maximum Likelihood (MLM), pioneered by geneticist and statistician Sir Ronald A. Fisher is a method of point estimation, which uses the member of the parameter space that maximizes the likelihood function as an estimate of an unobservable population parameter [9]. The principle of MLM is to find a set of parameters of an assumed probability distribution function (PDF) which most likely reflects the statistical behaviour of the underlying set of data (sample). The format of the method can be derived with the following considerations:

Supposing that the parameters $\theta = (\theta_1,...,\theta_n)^T$ of the distribution of the random variable X are known, the joint probability distribution of a (random) sample X_1, X_2, X_3,..., X_n can be written as

$$f_x(\mathbf{x}|\theta) = f_{X_1,X_2,X_3,...,X_n}(x_1,x_2,x_3,...,x_n|\theta) = f_{X_1}(x_1)f_{X_2}(x_2)\cdots f_{X_n}(x_n) = \prod_{i=1}^{n} f_X(x_i|\theta) \qquad (1)$$

In other words: equation (1) can be regarded as a relative measure for the belief that the sample X_1, X_2, X_3,..., X_n belongs to the distribution function with given parameters $\theta = (\theta_1,...,\theta_n)^T$.

Obviously in general the situation is contrary: A sample $\mathbf{x} = x_1$, x_2, x_3,..., x_n is observed and the set of distribution parameters is not known. Within that context equation (1) can be similarly seen as a relative measure for the likelihood that the distribution determined by θ is reflecting the statistical behaviour of the sample x. Over the entire domain of all possible parameters θ the likelihood L that the parameters belong to the sample is

$$L(\theta|x_1,x_2,x_3,...,x_n) = \prod_{i=1}^{n} f_X(x_i|\theta) \qquad (2)$$

The Maximum Likelihood Estimators can now be defined as the set of parameters $\hat{\theta}$ which are most likely representing the set of sample values, i.e. the set of parameters which maximise the likelihood function $L(\theta|x_1,x_2,x_3,...,x_n)$ over the entire domain of θ.

$$\hat{\theta} = \max_{\theta} L(\theta|x_1,x_2,x_3,...,x_n) \qquad (3)$$

It can be shown that for sufficient large n the estimated parameters are normally distributed with mean values $\mu = \hat{\theta}$.

By taking the log-likelihood function l

$$l = \ln(L) \tag{4}$$

instead of the likelihood function L, the covariance matrix for the parameters θ may be obtained through the inverse of the Fisher information matrix with components given by

$$H_{ij} = -\frac{\partial^2 l}{\partial \theta_i \cdot \partial \theta_j}\bigg|_{\theta=\hat{\theta}} . \tag{5}$$

The Maximum Likelihood Method has the following general properties:

- For large data samples the likelihood function L approaches a Normal distribution.
- Maximum Likelihood Estimates are *consistent*: For large n the estimates converge to the true value of the parameters we wish to determine.
- Maximum Likelihood Estimates are *unbiased*: For all sample sizes the parameter of interest is calculated correctly.
- Maximum Likelihood Estimates are *efficient*: The estimate has the smallest variance.
- Maximum Likelihood Estimates are *sufficient*: They use all the information in the observations.
- The solution of MLM is *unique*.

BUT:

- The *correct probability distribution* for the problem at hand has *to be known*. (Often the PDF to be used when analysing data resulting from tests of timber structural elements or joints is prescribed by corresponding test standards.)

2.2   Predictive distribution

A big advantage of the Maximum Likelihood Estimation Technique is that the parameter estimates are represented as random variables, i.e. the statistical uncertainty and the model uncertainty are taken into account by the randomness of the parameters. The parameters θ are following a Student distribution which for large samples (in the order of magnitude of $n = 10$) converges to a Normal distribution. The information about the uncertain parameters can then be utilized to identify the so-called "predictive distribution".

$$f_{X,pred}(x) = \int_\theta f(x|\theta) f(\theta) \cdot \partial \theta \tag{6}$$

The predictive distribution represents an estimate of the real PDF making use of all information and thus of the whole statistical uncertainty provided by the test results. It is no longer necessary to calculate any confidence intervals.

2.3   Method of Censored Maximum Likelihood

The idea of a Censored Maximum Likelihood Estimation Technique will be explained along the example of strength data derived from glued-in rods test with symmetrical configurations (Fig. 1, left and Fig. 2).

2.3.1 Censoring by symmetry

Consider a test series performed on n symmetrical glued-in rod specimen. The failure mode of all test specimens is timber shear failure and therefore a sample of n observations of shear strengths $(x_1, x_2, ..., x_n)$ is obtained. Assuming that the shear strength can be modelled by a random variable X which follows a PDF with the parameters θ, two likelihood functions can be defined, the first one considering $(x_1, x_2, ..., x_n)$ quantitatively:

$$L_1 = \prod_{i=1}^{n} f(x_i | \theta) \tag{7}$$

The second likelihood function uses the information that n strength values are larger than a realisation of X (The failure loads and the survivors are treated as being independent from each other.):

$$L_2 = \prod_{i=1}^{n} P(X \geq x_i | \theta) \tag{8}$$

with $P(X \geq x_i | \theta) = 1 - F(x_i | \theta)$ (9)

The optimal set of distribution parameters can be found by solving the maximization problem:

$$\hat{\theta} = \max_{\theta}(L_1 \cdot L_2) \tag{10}$$

2.3.2 Censoring by different failure modes

Glued-in rod specimens represent a system of different failure modes. Each failure mode is associated with a different failure mechanism: shear failure in timber or in glue, tension failure in timber net cross-section or in the steel rod. If such a system is tested, the different failure modes and their logical arrangement have to be considered. In the case of a serial arrangement (Fig. 6) only the realisation of the lowest strength can be detected directly. For a sample of n observations of system failure it can by judgement be distinguished between m failure modes. Each failure mode is observed an arbitrary number of times.

$$\text{Failure Mode} = j : (x_1, x_2, ..., x_k)$$

$$\text{Failure Mode} \neq j : (s_1, s_2, ..., s_{n-k})$$
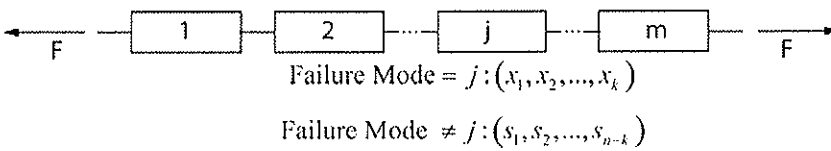
Fig. 6: Serial system of different failure modes.

It is assumed that the strength according to failure mode j, which can be modelled by the random variable X, is observed k times $(x_1, x_2, ..., x_k)$. The parameters of the probability distribution function of X can be found considering $(x_1, x_2, ..., x_k)$ and the observed strength values $(s_1, s_2, ..., s_{n-k})$ where the other failure mechanisms are involved. Two likelihood functions are formulated, the first one considering $(x_1, x_2, ..., x_k)$ quantitatively:

$$L_1 = \prod_{i=1}^{k} f(x_i | \theta) \tag{11}$$

The second likelihood function uses the information that $n - k$ strength values s_i are larger than a realisation of X:

$$L_2 = \prod_{i=1}^{n-k} P\big(X \geq s_i | \theta\big) \tag{12}$$

with $P\big(X \geq s_i | \theta\big) = 1 - F\big(s_i | \theta\big)$ (13)

The optimal set of distribution parameters can be found by solving the maximization problem:

$$\hat{\theta} = \max_{\theta}\big(L_1 \cdot L_2\big) \tag{14}$$

2.4 Special case: Weibull distribution

The Weibull distribution is often used to model phenomena which are results of the weakest link mechanism such as brittle failure and fatigue failure [10] [11]. In timber engineering weakest link considerations were made in the course of quantifying size effects for different strength properties of timber solids [12] [13] [14].

The Weibull distribution can be utilized to relate the strength of n sequentially arranged identical structural solids. In Fig. 7 a serial system of n identical brittle elements is illustrated. The probability distribution of the strength of a serial arrangement of n elements, i.e. the strength of the weakest out of n elements can be modelled with the Weibull distribution with the parameters v and k, where $v = \dfrac{w}{\sqrt[k]{n}}$ and w and k are the Weibull distribution parameters of the strength of one single element.
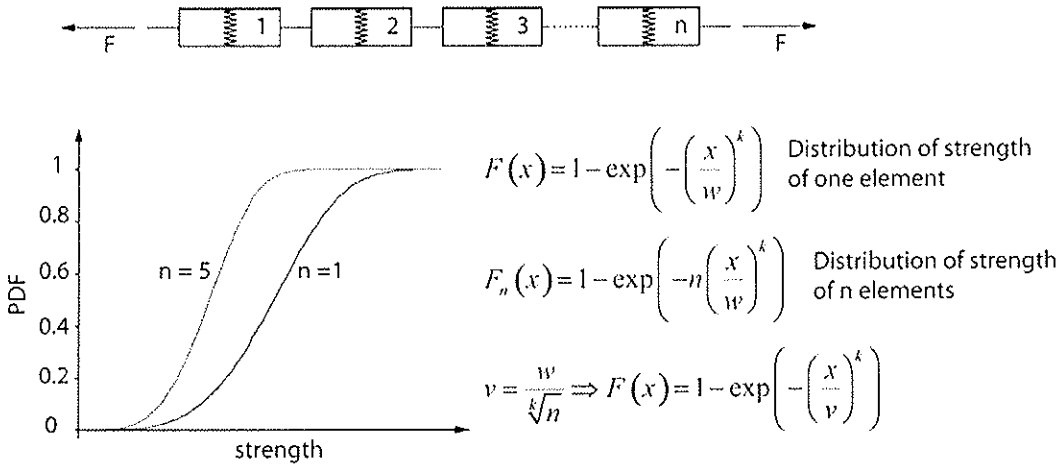
Fig. 7: Weibull's weakest link theory to model the strength probability distribution of a serial system of n identical brittle solids.

In our situation of tensile tests on symmetrically designed specimens with identical joints at both ends, the above principle can be applied with $n = 2$. The analytical solution in the case of a Weibull distribution can be utilized to illustrate the efficiency of the Censored Likelihood Estimation Technique: it can be shown that the parameters estimated by the censored likelihood estimation technique are nearly identical compared to the parameters estimated by using the analytical solution for the Weibull distribution.

3 Example 1: Numerical studies of artificial samples

In order to get an idea on the advantage of using Censored MLM instead of simply taking the sample mean and standard deviation when estimating the parameters or percentiles of the population, the pull-pull situation of glued-in rods (Fig. 1, left) will first be simulated by an artificial data sample: Calculations on Monte Carlo-generated samples with different type of PDF (Normal, Log-normal and Weibull), different sizes and coefficients of variation (COV) are performed. The mean value of the sample was fixed to 100. $2 \cdot n$ paired random failure loads were generated and the minimum of each pair was chosen as actual failure load of the specimen resulting in n values of failure load.

3.1. Influence of probability distribution function

Samples of different types of PDF (Normal, Log-normal and Weibull-2) with COV = 15% and sample sizes $2 \cdot n = 400$ (200 pairs) are compared in Fig. 8. Estimating the parameters by only using the failure load information (MLM) leads to PDF with lower x-values at each quantile of the PDF. Making use of the information that for every failure load a survivor exists (Censored MLM), the resulting PDF shows higher x-values for all quantiles.

Normal distribution

Lognormal distribution

2-parameter Weibull distribution
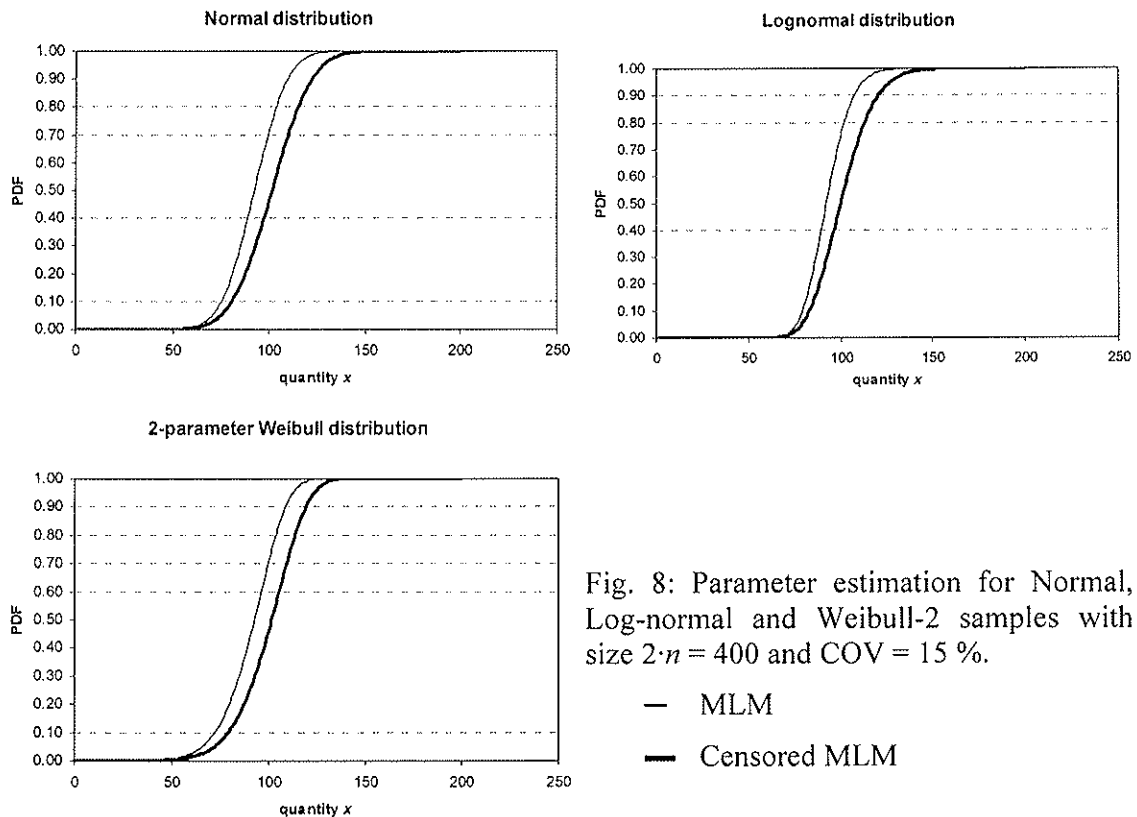
Fig. 8: Parameter estimation for Normal, Log-normal and Weibull-2 samples with size $2 \cdot n = 400$ and COV = 15 %.

— MLM

▬ Censored MLM

Material strength properties are based on low percentiles of the PDF. Timber strength properties are commonly communicated through the 5th percentile values of their PDF. Accordingly the characteristic strength value derived from censored test data is underestimated by 4 to 10% when not including the run-outs (Table 1).

7

Table 1: Difference between 5th percentiles calculated for different PDF the parameters of which were estimated by either MLM or Censored MLM			
PDF	MLM	Censored MLM	Ratio (Censored MLM/MLM)
Normal	70.4	74.9	1.06
Log-normal	75.9	78.9	1.04
Weibull-2	65.6	71.9	1.10

As already mentioned in 2.1 the information about the uncertain parameters can be utilized to identify the predictive distribution. The predictive distribution represents an estimate of the real PDF making use of all information and thus of the whole statistical uncertainty provided by the test results. Fig. 9 shows estimated Log-normal distributions for a small sample ($n = 8$). The sample's mean value again was taken to be 100 and the coefficient of variation (COV) was 15%. The parameters of the PDF were estimated on the basis of Censored Maximum Likelihood and by deriving the predictive distribution which contrary to the Censored MLM not only uses the Maximum Likelihood but rather all Likelihoods within the data range. The difference in 5th percentiles is approximately 1.5%.
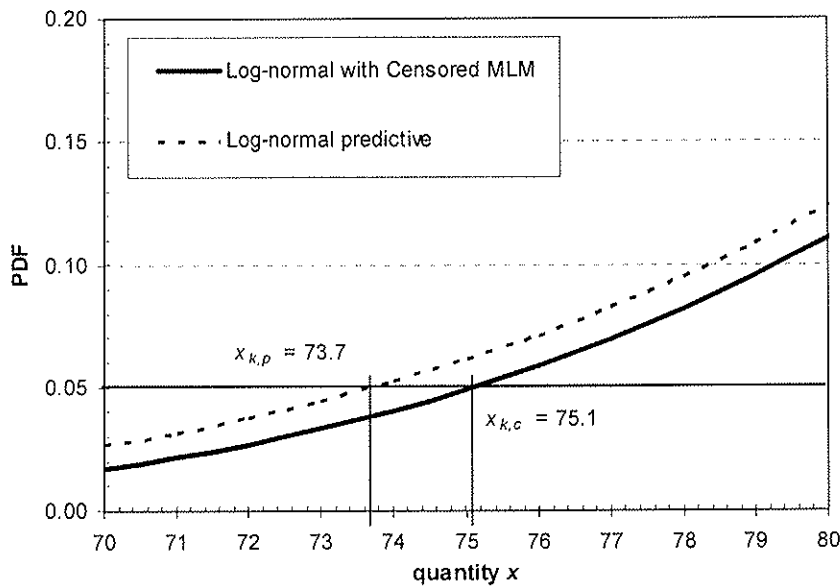
Fig. 9: Predictive distribution compared to PDF estimated by Censored MLM for a log-normally distributed sample with size $n = 8$, COV $= 15\%$ and mean $= 100$.

3.2 Influence of sample variation

The influence of the variation of the test data was studied exclusively on log-normally distributed samples. The sample sizes were $2 \cdot n = 400$ (pairs) resulting in $n = 200$ minima and the sample mean was fixed to 100. The samples were generated with different coefficients of variation (COV = 10, 15, 20 and 30%). The results of this analysis are shown in Fig. 10.
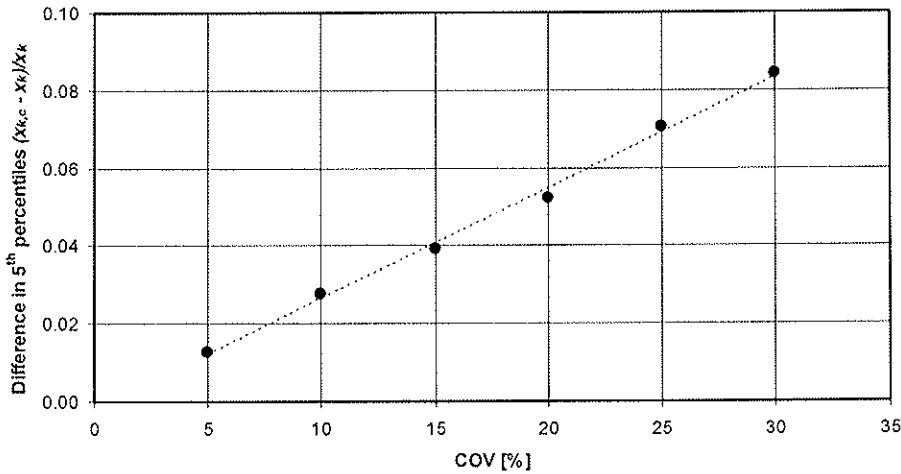
Fig. 10: Difference in 5th percentiles derived from PDF estimated by MLM (x_k) and by Censored MLM $(x_{k,c})$ for log-normally distributed samples (400 pairs, 200 minima) with different COV.

Depending on the COV the difference between the 5th percentiles calculated on the basis of a Log-normal distribution the parameters of which were estimated with MLM (x_k) and Censored MLM respectively $(x_{k,c})$ reaches from approximately 2% for a small COV of 5% to 8% for a high COV of 30%. Thus especially for samples with a bigger variation in the data (COV > 15%) making use of the Censored MLM is of importance.

4 Example 2: Glued-in rods tested in pull-pull configuration

As a second example, the (Censored) Method of Maximum Likelihood will now be applied to a series of tensile tests in pull-pull configuration (Fig. 1, left) performed on axially loaded steel rods with metric thread glued in coniferous glulam parallel to the grain by using an epoxy-type adhesive [8].

The aim of the research project was to identify parameters of significant influence on the pull-out strength of the rod and to suggest an adequate strength model. The tests were performed on rods with diameters M12, M16 and M20. The anchorage lengths varied between 105 and 330 mm. A total of 12 samples with 8 symmetrically designed specimens were tested in tension according to Fig. 2. Each test actually was performed on two joints but only one of them (being the weakest link) failed. The resulting data is censored since for each failure load we know that the rod at the opposite joint did not fail.

According to relevant European pre-standard prEN 14358 [15] the statistical analysis was performed on base of a Log-normal distribution. The characteristic strength values (5th percentiles) were calculated using two different procedures:

(i)   neglecting the information of the stronger joint.

(ii)   by making use of the Censored Maximum Likelihood Method.

In case of larger COV (9.15%) the PDF fitted to the data by either MLM or Censored MLM differ quite much (Fig. 11, right). On the 5th percentile level this difference amounts to 3.3% $(x_k = 94.4$ kN, $x_{k,c} = 97.5$ kN). For a sample with smaller COV (3.15%) the difference between the two PDF is negligible. The characteristic values assigned to the data differs by less than 1% $(x_k = 88.9$ kN, $x_{k,c} = 89.9$ kN).

9
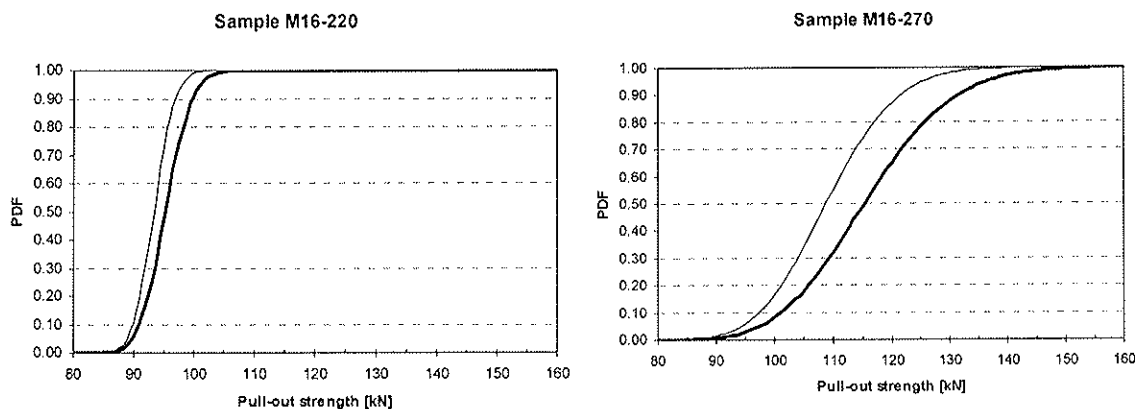
Fig. 11: Log-normal distributions fitted to glued-in rods test data using MLM and Censored MLM parameter estimates. Left: Rods M16, anchorage length 220 mm, n = 8, COV = 3.15%. Right: Rods M16, anchorage length 270 mm, n = 8, COV = 9.15%.

5 Influence of dead weight and of correlation between joint properties

The influence of dead weight of tensile specimens tested in pull-pull configuration (Fig. 2) has to be taken into account for heavy materials like steel or concrete. In such cases a possible increasing frequency of failure of the upper joint might occur. Our tests performed with glulam specimens showed equal frequencies of failures at both joints. The dead weight amounted to less than 1 ‰ of the failure loads.

In the statistical analysis the joints of one single specimen were treated to be independent from each other regarding the mechanical properties. Actually the rods are glued into the same glulam specimen which itself has limited variation in mechanical properties since being a homogenised product. In case of timber shear failure the strengths of the two joints might be correlated. If the correlation would be known, the statistical model to estimate the parameters of the PDF could be improved. The correct correlation however can only be found by testing both joints to failure. After the first joint failed the specimen would have to be cut and a new, stronger joint (for example by using metal dowel type fasteners as shown in Fig.1, right) would have to be added. Since being rather complicated and lavish this procedure will hardly ever be made use of and thus any correlation between the properties of the two joints is suggested to be disregarded.

6 Other similar situations in timber research

The Censored Maximum Likelihood Method (Censored MLM) is a quite interesting tool for several other situations in timber engineering research as well:

6.1 Lower Tail fitting

The tail behaviour of the probability distributions of timber material characteristics plays an important role in the overall probabilistic modelling and reliability analysis. Estimating the parameters of the probability distribution function (PDF) therefore has to be performed with special regard to a good fit of the lower tail. One approach to this is to perform a least

10

squares fit of a suitable PDF such that the value of that PDF in two points is equal to two given lower fractile values (e.g. the 15th and the 5th percentiles) of the sample probability distribution of the material property of interest. This least square fit has the disadvantage of the statistical uncertainty (due to the relative small number of observations on which the fit usually has to be based) not being directly quantified in terms of the uncertainty associated with the distribution parameters of the fitted probability distribution.

Another approach to estimate the probability distribution in the lower tail domain, which was presented by Faber et al. (2004) [16], is by means of the Censored MLM where only observations in the lower tail domain i.e. below a given predefined threshold value are used explicitly. The other observations are only utilized implicitly to the extent that it is recognized that they exceed the threshold. In Fig. 12 the PDF representing all data and the PDF estimated using the Censored Maximum Likelihood Estimation with a threshold corresponding to the lower 30% quantile are compared with the corresponding sample PDF. It can be seen that a significant refinement of the representation of the strength data in the lower tail domain can be achieved by using the distribution model fitted to the lower data set domain.
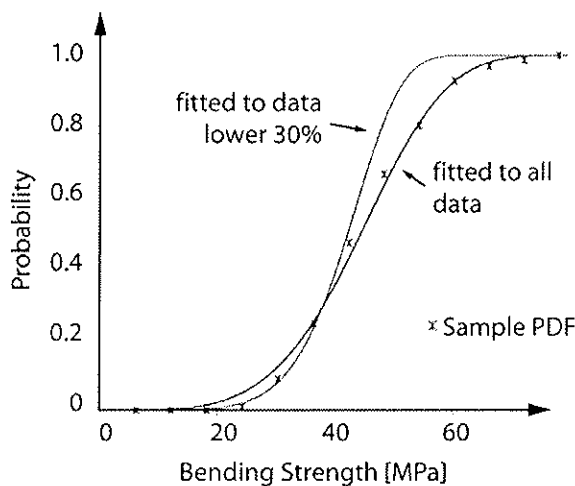
Fig. 12: Weibull-2 PDF with parameters estimated using all data and data below 30%, compared to the sample probability distribution function (Sample PDF).

6.2 Duration of load or fatigue tests

Duration of load or fatigue test results frequently contain "run-outs", that is, values of endurances reached without failure of the specimen at the end of the test, either because the test was terminated at a predetermined limit or because some other part of the specimen failed. In the statistical analysis the survivors can be considered by the Censored Maximum Likelihood Estimation Technique. The procedure has been described by Spindel and Haibach [2] and by Edwards and Pacheco [1].

6.3 Proof loading

In timber engineering proof loading principle is mainly used in the context of „proof loading timber structural components" rather than „proof loading entire structures in situ". When proof loading timber structural elements it can be distinguished between the cases where the entire population or a sample is subjected to a proof load.

An *entire population* may be proven e.g. in form of a permanent means of quality control in the production line. The distribution function of a population entirely subjected to proof

loading thus is truncated and furthermore possible damage of the surviving elements has to be considered, see e.g. Lam et al. (2003) [17].

Proof loading is also applied to *samples*, i.e. only a sample is subjected to the proof load and the indications of the proof loading are used to quantify the characteristics of the population from where the sample is drawn from. The advantage of this technique is that a good indication is obtained from the lower tail domain of the strength distribution while the strong components return to production. Commonly the proof load level is calibrated such that 15% of the components will fail during the proof loading [18]. In general it is assumed that the sample size is small compared to the size of the population, i.e. the effect of returning the strong components does not affect the characteristics of the population. The data obtained from this kind of proof loading is censored in the manner that the strength of say 15% of the sample is observed, but it is also known that the strength of 85% of the sample is larger than the proof load threshold. The presented maximum likelihood estimation technique can be utilized to estimate the distribution parameters of the population by relying not only on the broken pieces but on the whole sample.

6.4   Censoring by judgement

The characteristic value of the bending strength for structural sawn timber according to the European standard EN 384 is derived from 4-point bending tests where pieces are positioned with the critical section between the load points and the tension edge is selected at random in order to simulate the real situation in practice. Performing the tests by systematically orienting the pieces with the weakest zone on the tension edge would be a more economic approach, since fewer tests are to be done (see for example Glos and Denzler (2004) [19]). Strength values derived from such tests are censored by judgement and Censored MLM can be applied to estimate the parameters and percentiles of a predefined PDF to describe the population.

7   Conclusions

When analysing censored data sets the parameters of the underlying probability distribution function (PDF) have to be calculated by means of a Censored Maximum Likelihood Estimation Technique (CMLT) in order not to get wrong results and to take into account all information provided by the tests. The adequate PDF of the problem at hand has either to be known or to be given by standards.

Making use of the censored data information leads to higher characteristic values and thus economizes the design of timber structures. Especially for small samples or samples with a bigger scatter of data (COV > 15%) CMLT is an interesting tool, since it uses all information derived by the tests.

Tensile testing of joints on the basis of symmetric specimens with two identical joints at both ends (pull-pull) can be performed with smaller samples, if all the information provided by the test data is taken into account when calculating parameters or percentiles of PDF.

Censored MLM can be applied to other situations as well occurring in wood research, e.g. duration of load and fatigue tests, proof loading and grading.

8 References

1. Edwards G., Pacheco L.A. 1984: A Bayesian method for establishing fatigue design curves. *Structural Safety* 2(1). p. 27-38.

2. Spindel J.E., Haibach E. 1979: Method of Maximum Likelihood applied to the statistical analysis of fatigue data. *International Journal of Fatigue* 1(2). p. 81-88.

3. Lawless J.F. 1982: Statistical models and methods for lifetime data. John Wiley and Sons, New York, NY.

4. Yeh B., Williamson T.G. 2001: Evaluation of glulam shear strength using a full-size four-point test method. Paper 34-12-2 in Proceedings of CIB-W18 Meeting Thirty-Four. Venice, Italy.

5. Köhler J., Faber M.H. 2003: A probabilistic approach to cost optimal timber grading. Paper 36-5-2 in Proceedings of CIB-W18 Meeting Thirty-Six. Colorado, USA.

6. Van de Kuilen J.W.G., Blass H.J. 2005: Mechanical properties of azobé (Lophira alata). *Holz als Roh- und Werkstoff* 63(1) p. 1-10.

7. Douwen A.A., Kuipers J., Loof H.W. 1982: Corrections to the mean and the standard deviation from test series with symmetrical test specimens. Stevin-Report 4-82-9/oe-5. Technical University Delft, The Netherlands.

8. Steiger R., Gehri E., Widmann R. 2004: Glued-in steel rods: A design approach for axially loaded single rods set parallel to the grain. Paper 37-7-8 in Proceedings of CIB-W18 Meeting Thirty-Seven. Edinburgh, United Kingdom.

9. Benjamin J.R., Cornell C.A. 1970: Probability, statistics, and decision for civil engineers. McGraw-Hill. New York, USA.

10. Weibull W. 1939: A statistical theory of the strength of materials. Royal Swedish Institute for Engineering Research.

11. Bolotin V.V. 1969: Statistical methods in structural mechanics. Holden-Day, San Francisco, USA.

12. Barrett J.D. 1974: Effect of size on tension perpendicular to grain strength of Douglas Fir. *Wood and Fiber* 6(2). p. 126-143.

13. Colling F. 1986: Influence of volume and stress distribution on the shear strength and tensile strength perpendicular to the grain. Paper 19-12-3 in Proceedings of CIB-W18 Meeting Nineteen. Florence, Italy.

14. Madsen B., Buchanan A.H. 1986: Size effects in timber explained by a modified weakest link theory. *Canadian Journal of Civil Engineering* 13(2). p. 218-232.

15. CEN 2004: prEN 14358: Timber structures - Fasteners and wood-based products - Calculation of characteristic 5-percentile value and acceptance criteria for a sample.

16. Faber M.H., Köhler J., Sorensen J.D. 2004: Probabilistic modelling of graded timber material properties. *Structural Safety* 26(3). p. 295-309.

17. Lam F., Abayakoon S., Svensson S., Gyamfi C. 2003: Influence of proof loading on the reliability of members. *Holz als Roh- und Werkstoff* 61(6). p. 432-438.

18. Madsen B. 1992: Structural behaviour of timber. 1st ed. Timber Engineering Ltd. Vancouver, Canada

19. Glos P., Denzler J 2004: Effect of test piece orientation on characteristic bending strength of structural timber. Paper 37-6-2 in Proceedings of CIB-W18 Meeting Thirty-Seven. Edinburgh, United Kingdom.

INTERNATIONAL COUNCIL FOR RESEARCH AND INNOVATION
IN BUILDING AND CONSTRUCTION

WORKING COMMISSION W18 - TIMBER STRUCTURES

ADHESIVE PERFORMANCE AT ELEVATED TEMPERATURES FOR ENGINEERED WOOD PRODUCTS

Borjen Yeh

B Herzog

T G Williamson

APA - The Engineered Wood Association

U.S.A.

Presented by B Yeh

A Buchanan stated that in NZ the fire-fighters will not go up onto the roof of a burning building. Shear failures or other failure modes beside glue failure can occur.

J König made a presentation of his views of this subject. The requirement may be too conservative as the temperature is too high. He presented data of Mischler and Frangi (2001), Fornather et al. (2004). Preheated specimens and short term tests as well as fire test information were presented. Real fire test is lower than preheat specimens and short term test. The reason is that the moisture content below the char level is increased as the moisture front is created during the fire. Influence of the loading rate is also an issue.

The results agree with EN 1995-1-2. The N.A. Curve will punish a lot of adhesive manufacturers. Temperature gradient exists and may be a cause for decrease in strength of the member. Three recommendations were provided by J König: 1) do not ban adhesive that only passed moderate temperature test (200C); 2) specimens with low strength at high temperature should derive an alternative $k_{mod,fi}$ 3) conduct comparative fire tests. BJ Yeh pointed out that some adhesives do have concerns.

A Frangi further explained that the US approach lacks consideration of the critical temperature for the glue. Wood failure between wood and glue is the real reason for failure. Additional failure of the glue from other tests can be considered and combined with EN 1995-1-2. A Frangi results published in Wood Science and Technology is available and will be sent.

BJ Yeh reiterated that the standard does not want to put adhesive manufacturers out of business. They can meet the standard with changes in their formulations. S Thelandersson stated that red curve and the test data may not be entirely comparable. A Frangi stated that some adhesive should not be used. Epoxy for example. All producers have some information.

Adhesive Performance at Elevated Temperatures for Engineered Wood Products

Borjen Yeh, Ph.D., P.E.
Benjamin Herzog
Thomas G. Williamson, P.E.
APA - The Engineered Wood Association, U.S.A.

Abstract

Engineered wood products, such as I-joists and laminated veneer lumber (LVL), have traditionally been manufactured with phenolic-based adhesives in North America. In the last few years, however, an unprecedented number of non-phenolic-based adhesive systems, such as polyurethane-based and isocyanate-based adhesives, have been introduced to the engineered wood products industry. While these relatively new adhesives have demonstrated their compliance with most international adhesive standards, concerns have been raised by the fire services and others on the performance of these adhesives at an elevated temperature, such as just below the ignition temperature of wood.

It is recognized that full-scale fire assembly tests, such as ASTM E119, CAN/ULC S101, or ISO 834, address the fire performance of wood assemblies. However, it is arguable that the adhesive, as a critical component of glued engineered wood products, needs to be evaluated to ensure that the adhesive will not degrade below the wood substrates being adhered when exposed to extreme heat prior to wood ignition. Unfortunately, no international adhesive standards exist in testing the adhesive to such an elevated temperature.

A task committee, as chaired by the first author, was formed in June 2004 by the engineered products industry in North America to address this issue with input from key adhesive suppliers to the industry. Through coordinated efforts, an industry standard was developed and adopted by the engineered wood products industry in March 2005. Test data suggests that this standard can be used to screen out those adhesives that significantly lose adhesive bond strength at the temperature near the wood ignition temperature. This standard has been submitted to the International Code Council (ICC), the U.S. code evaluation agency, and the ASTM Committee on Adhesives (D14.30) for adoption. This paper presents the background information and test data used to develop the industry standard.

1. Introduction

Engineered wood products have traditionally been manufactured with phenolic-based adhesives in North America. Although first commercially developed in the early 1900's, phenolic resins did not attain full-scale commercial significance until being introduced into the plywood industry in the U.S. around 1934. Because of such advantages as good creep resistance, durability, fire performance, and dimensional stability at elevated temperatures, phenolic-based adhesive systems soon became the dominant systems used for such products as softwood and hardwood plywood, oriented strand board, structural glued

1

laminated timber (glulam) laminated veneer lumber (LVL), parallel strand lumber (PSL), and prefabricated wood I-joists.

In the last few years, however, an unprecedented number of non-phenolic-based adhesive systems, such as polyurethane-based and isocyanate-based adhesives, have been introduced to the engineered wood products industry. While these relatively new adhesives have demonstrated their compliance with most international adhesive standards, concerns have been raised regarding the performance of these adhesives at an elevated temperature.

It is recognized that full-scale fire assembly tests address the fire resistance of wood assemblies. These standard test methods for evaluating fire resistance include ASTM E119 [1], CAN/ULC S101 [2], and ISO 834 [3]. Ratings of assemblies are determined by a standard heating curve approximating assumed structural fire conditions. A fire-rated assembly, which is typically composed of fire-protective membranes, such as fire-rated gypsum boards and insulation, and structural elements, is generally required for selected types of buildings, such as multi-family dwellings and commercial buildings, in accordance with the governing fire code. Heavy timber, such as structural glued laminated timber of a significant dimension can also be used for fire-rated assemblies. However, most residential houses in North America are required to be built with neither fire-rated assemblies nor heavy timber. In fact, a vast amount of single-family dwellings in North America are built with an open-frame basement or craw space without any fire-protective membranes.

The fire services in North America have expressed concerns about the light-frame construction built with lightweight materials, such as wood trusses and prefabricated wood I-joists. There have been reported sporadic bans on these engineered wood products in some local jurisdictions around the U.S. and Canada due mainly to the perception that the fire performance of these lightweight engineered wood products is different from that of conventional solid-sawn lumber in unprotected buildings. A frequently asked question by the fire services to the engineered wood products industry has been "does your adhesive melt before wood burns?" By the context of the question, the word "melt" does not mean the glass transition temperature of the adhesive, but the degradation of the adhesive bond strength as a result of heat exposure at a temperature below the wood ignition temperature.

The engineered wood products industry in North America is sensitive to the question raised by the fire services and has a strong desire to ensure the adhesive bonds in engineered wood products will not degrade more than solid wood when exposed to any temperatures up to wood ignition. In April 2004, the industry was made aware of a situation that an adhesive might have been dissociated at a temperature near wood ignition. With the intent to address this issue, an industry task committee, as chaired by the first author, was formed in June 2004. After several intensive meetings and conference calls, and with the input from key adhesive suppliers to the industry, an industry standard, APA/WIJMA AC1000-05, *Standard Test Method for Evaluating the Shear Strength of Adhesive Bonds on Glued Wood Products at Elevated Temperatures*, was approved by the industry in March 2005 (available from APA - The Engineered Wood Association, http://www/apawood.org, and Wood I-Joist Manufacturers Association, http://www.i-joist.org). This paper describes the background information and test data used to develop the standard. Like any new standard, AC1000 is by no means a perfect standard. Since its release, there have been some comments that will be addressed by the task committee in the coming months.

2. Development of the Industry Standard

Based on the Wood Handbook [4], the thermal degradation of wood occurs in three phases: a) dehydration or loss of water vapor (up to 150°C or 302°F), b) non-combustible degradation where gaseous vapors are slowly given off and char begins to form (100 to 250°C or 212° to 482°F) and c) combustible degradation where volatile organic compounds are emitted, which may or may not flame, depending on oven conditions (280° to 500°C or 536° to 932°F). The test method given in APA/WIJMA AC1000-05 is intended to evaluate the condition at the upper end of the second phase of wood degradation, above the hot press temperatures typically used in production of wood composites (149° to 204°C or 300° to 400°F), yet below the ignition temperature of the wood. It is understood that wood ignition is the decomposition (pyrolysis) of material into volatiles and a char residue. The temperature at which the wood ignites is a function of the wood moisture content and species, the temperature and heat flow in the surrounding environment, and the time of exposure at an elevated temperature.

There is no existing standard in the world that addresses the performance of structural adhesives at an elevated temperature near wood ignition. With the understanding that wood will degrade at such a high temperature and the desire of the industry was to ensure the adhesive bond would not degrade more than wood (i.e., the performance of solid wood is the benchmark), the targeted temperatures, test methods, and durations of the heat exposure were identified as critical factors that needed to be considered for the development of the industry standard. A series of coordinated but independent tests were conducted by organizations representing the engineered wood products industry to gather relevant data in October and November 2004.

2.1 Targeted Temperatures

As the objective of the industry standard was to evaluate the adhesive performance at an elevated temperature near wood ignition, a series of tests was conducted at a bond line temperature (not the air temperature) of 177, 204, and 232°C (350, 400, and 450°F). The upper temperature of 232°C (450°F) was selected based on the understanding that the wood ignition temperature is near that temperature and the objective of the industry standard was to evaluate the adhesive performance up to the temperature just before wood ignition. It was understood by the industry that the correlation between these elevated temperatures and the bond line temperatures in end-use applications might be difficult. However, it was believed that if the adhesive bonds meet the performance of solid wood at these temperatures, the performance of the adhesive under actual in-service high temperature conditions could be ensured with a high degree of confidence.

2.2 Test Methods

At the time when the industry effort was initiated in June 2004, a Canadian adhesive standard, CSA O112.9, *Evaluation of Adhesives for Structural Wood Products (Exterior Exposure)* [5], was about to be finalized. Within CSA O112.9, Test Method B2 (Creep Resistance Tests) requires the ASTM D3535 [6] specimens be compression loaded at a constant stress of 2.1 MPa (305 psi) for 2 hours at an air temperature of 180°C (356°F). While the constant-load method at a constant temperature was considered attractive, an

important consideration for the new industry standard was the ability of the engineered wood products plant to conduct in-plant testing. In addition, the ASTM D3535-type specimens are relatively difficult to prepare, as compared to the shear block specimen in accordance with ASTM D905, *Standard test methods for strength properties of adhesive bonds in shear by compression loading* [7], which was also used in CSA O112.9 for shear strength evaluation. Through preliminary tests conducted at a Weyerhaeuser/Trus Joist plant, the industry was in favor of a relatively simple specimen configuration, as shown in Figure 1, and the test method in accordance with ASTM D905. It should be noted that the 3.2-mm (1/8-inch) gap that is typically used in the block shear test jig for evaluation of the block shear strength of wood is not permitted in ASTM D905.
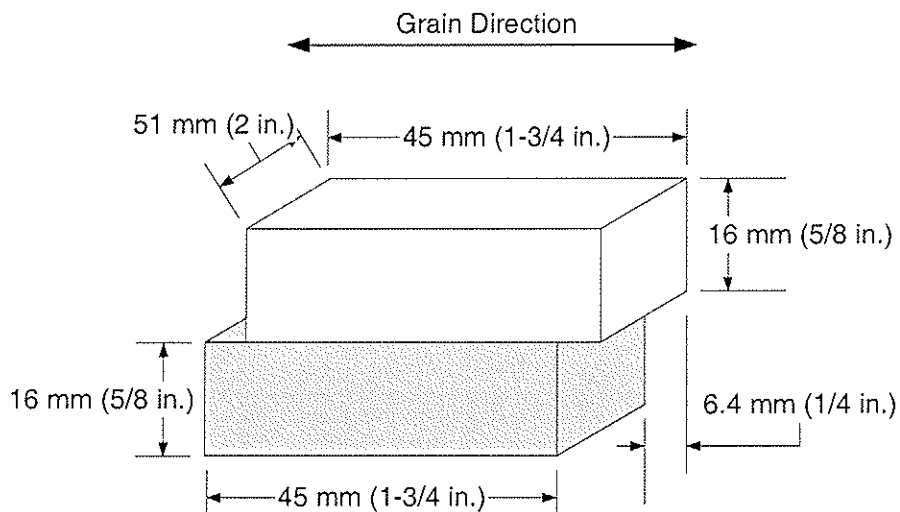
Figure 1. Form and dimensions of a bonded specimen

2.3 Heat Exposure Durations

For the purpose of providing data in determining the shear strength degradation of solid wood when exposed to a constant heat at various temperatures for a 1-hour duration, as measured at the middle of the shear block specimen with a thermocouple, APA - The Engineered Wood Association conducted a study in October 2004 in accordance with ASTM D905 using solid Douglas fir (*Pseudotsuga menziesii*) specimens. Table 1 and Figure 2 show the results.

Table 1. Solid wood (Douglas fir) test results

Adhesive	Temperature, °C (°F)	Mean shear strength, MPa (psi)	COV, %	Residual shear strength	Mean wood failure, %
Control	Ambient [a]	14.6 (2118)	9.8	1.00	100
	177 (350)	6.5 (940)	23.5	0.44	
	204 (400)	4.6 (668)	26.4	0.32	
	232 (450)	3.3 (482)	35.9	0.23	

[a] Approximately 21°C (70°F).

4
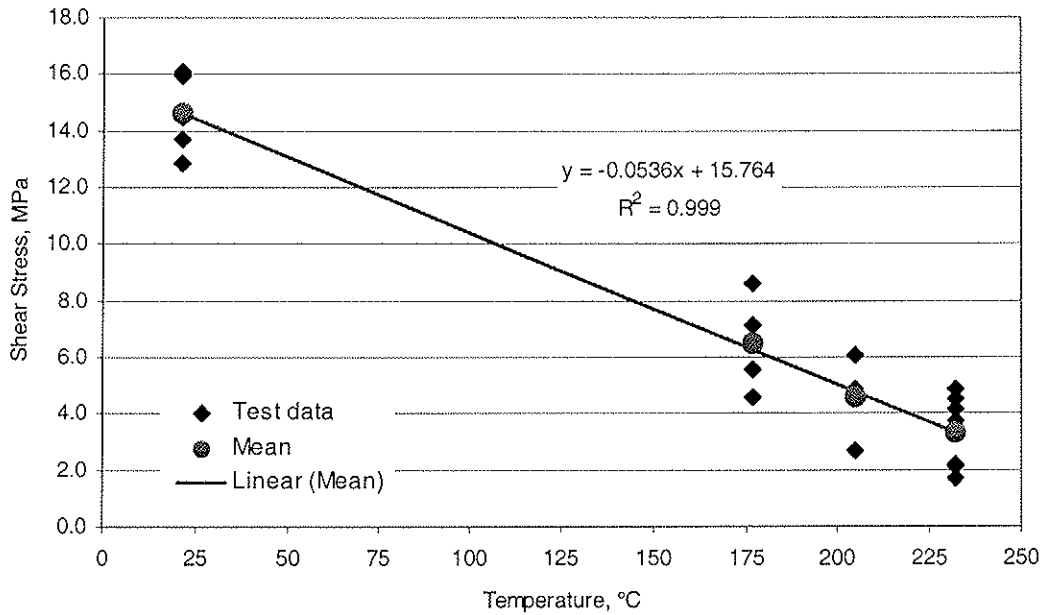
Figure 2. Shear strength of solid wood (Douglas fir) specimens at various temperatures, as measured at the middle of the shear block specimens, for 1-hour duration

As shown in Table 1 and Figure 2, the mean shear strength of the solid wood Douglas fir specimens with a 1-hour constant heat exposure (at the middle of the specimen) at 177°C (350°F), 204°C (400°F), and 232°C (450°F) is 44%, 32%, and 23% of the mean shear strength at the ambient temperature of 21°C (70°F), respectively. From the perspective of engineering design for fire, the mean shear strength at an elevated temperature is expected to remain capable of carrying the design shear. As a result, for LVL products used in the U.S., the allowable shear stress with a typical coefficient of variation of 25% from block shear tests may be expressed as a percentage of the mean shear strength of the same materials tested at the referenced temperature of 21°C (70°F):

$$f_{v,m,te} = F_{v,ts} = \frac{f_{v,k,ts}}{C_a} = \frac{f_{v,m,ts}(1-1.645v)}{C_a} \qquad \text{[Eq. 1]}$$

where $f_{v,m,te}$ = mean shear strength at an elevated temperature

$F_{v,ts}$ = allowable shear stress at the referenced temperature (21°C)

$f_{v,k,ts}$ = characteristic shear strength at the referenced temperature (21°C)

C_a = a factor that accounts for factor of safety and load duration

$f_{v,m,ts}$ = mean shear strength at the referenced temperature (21°C)

v = coefficient of variation

The C_a factor is codified as 3.15 in ASTM D5456, *Standard Specification for Evaluation of Structural Composite Lumber Products* [8]. Therefore,

5

$$f_{v,m,te} = 0.19 \times f_{v,m,ts} \qquad \text{[Eq. 2]}$$

In other words, the mean shear strength at an elevated temperature is expected to be about 20% of the mean shear strength tested at the referenced temperature of 21°C (70°F). Since the objective of the industry standard was to ensure that the strength of engineered wood products, including the adhesive bond strength, is capable of carrying the design loads even at an elevated temperature, it appears that a 1-hour heat exposure is approaching the 20% shear strength at the referenced temperature of 21°C (70°F) if the target exposure temperature is 232°C (450°F). If a lower temperature is selected, the exposure duration may be required to be extended beyond 1 hour to reach the targeted strength ratio of 20%. Therefore, the duration of heat exposure of 1 hour was chosen by the industry with the understanding that it is intended to "protect" the design stress of engineered wood products in an extreme condition of 232°C (450°F), which may or may not exist in end-use applications.

3. Adhesive Tests

Based on the considerations given above, a study was conducted by the industry to evaluate the performance of 6 commercially available adhesives at elevated temperatures, as shown in Table 2.

Table 2. Adhesives tested in this study

Adhesive ID	Adhesive Type
1	2-part Polyurethane Emulsion Polymer (PEP)
2	2-part Emulsion Polymer Isocyanate (EPI)
3	1-part Polyurethane (PUR)
4	1-part Polyurethane (PUR)
5	1-part Polyurethane (PUR)
6	2-part Emulsion Polymer Isocyanate (EPI)

The data reported herein were based on the tests conducted at the APA Research Center in Tacoma, Washington, which is accredited under ISO 17025 by the International Accreditation Service (IAS) in the U.S. and Standards Council of Canada (SCC). All specimens were fabricated by Weyerhaeuser/Trus Joist in accordance with Figure 1 and tested at APA in October and November 2004 in accordance with ASTM D905 after being subjected to three temperatures of 177°C (350°F), 204°C (400°F), and 232°C (450°F) for a 1-hour duration. The bond line temperature was monitored with a thermocouple, as shown in Figure 3. For each adhesive and temperature combination, 5 replicates were tested. Since the industry standard was at the development stage when the tests were conducted, the purpose of the testing was not necessarily to identify any deficient adhesives, but to assess such factors as ease of testing, suitability of prescribed temperatures levels and time durations, and repeatability from one testing facility to another.
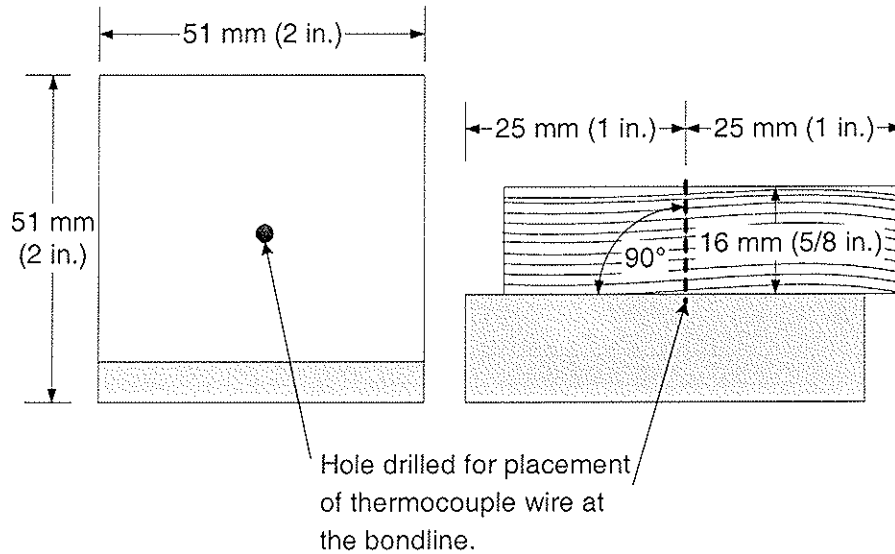
Figure 3. Top view (left) and side view (right) of drilled hole for thermocouple placement

Results from the APA tests are shown in Table 3 and Figure 4. For comparison purposes, the results from control (solid wood) specimens, as previously mentioned in Figure 2, are superimposed in Figure 4. Similar trends were observed from tests conducted by Weyerhaeuser/Trus Joist and other engineered wood product manufacturers.

Table 3. Adhesive test results from APA

Adhesive	Temperature, °C (°F)	Mean shear strength, MPa (psi)	COV, %	Residual shear strength	Mean wood failure, %
1	Ambient [a]	11.1 (1608)	21.5	1.00	99
	177 (350)	7.9 (1147)	11.5	0.71	87
	204 (400)	5.3 (772)	10.4	0.48	71
	232 (450)	3.0 (440)	30.9	0.27	29
2	Ambient [a]	13.4 (1940)	10.2	1.00	89
	177 (350)	6.9 (1006)	16.2	0.52	51
	204 (400)	4.6 (667)	16.7	0.34	30
	232 (450)	2.8 (414)	26.2	0.21	15
3	Ambient [a]	14.3 (2071)	12.7	1.00	100
	177 (350)	8.0 (1167)	9.0	0.56	91
	204 (400)	3.8 (554)	21.0	0.27	38
	232 (450)	0.9 (13)	86.7	0.01	0
4	Ambient [a]	11.0 (1601)	11.3	1.00	97
	177 (350)	4.5 (650)	5.7	0.41	74
	204 (400)	2.3 (328)	17.4	0.20	46
	232 (450)	0.3 (44)	75.8	0.03	0
5	Ambient [a]	12.3 (1793)	10.1	1.00	96
	177 (350)	7.1 (1025)	17.4	0.57	78
	204 (400)	3.5 (503)	36.4	0.28	47
	232 (450)	1.7 (244)	19.4	0.14	22
6	Ambient [a]	11.6 (1678)	9.7	1.00	96
	177 (350)	4.8 (695)	28.9	0.41	27
	204 (400)	3.2 (465)	25.6	0.28	11
	232 (450)	2.0 (285)	33.3	0.17	7

[a] Approximately 21°C (70°F).

7
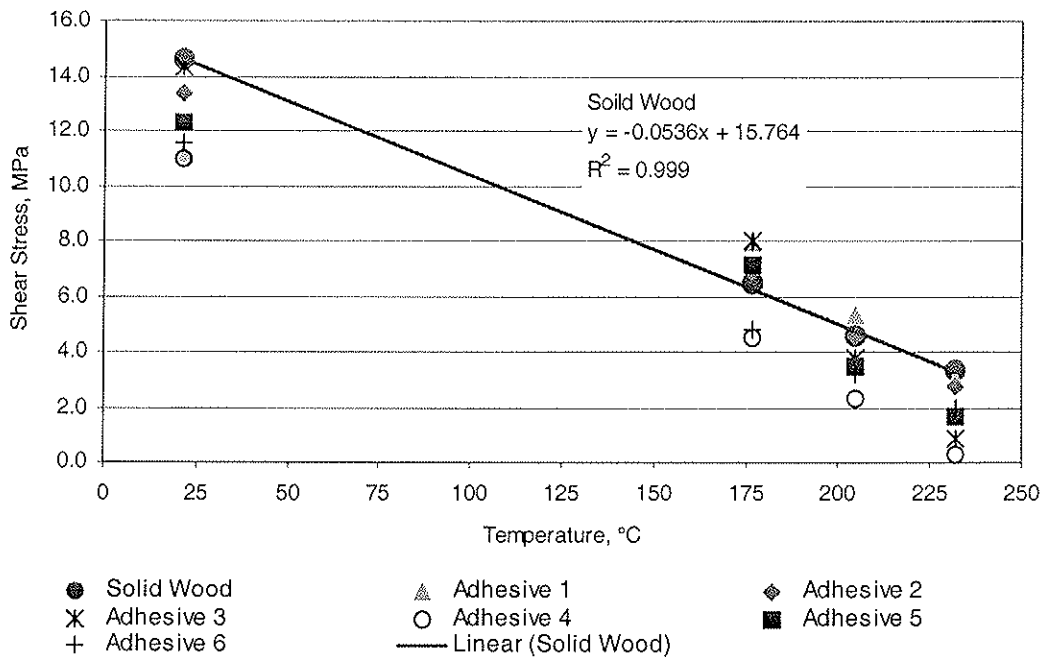
Figure 4. Shear strength of solid wood (Douglas fir) specimens and 6 adhesives at various temperatures, as measured at the middle of the shear block specimens, for 1-hour duration

As noted from Figure 4, the shear strength of some adhesives, such as Adhesives 1 and 2, and to some extent, Adhesives 5 and 6, followed the general trend of the shear strength from solid wood. On the other hand, some adhesives, such as Adhesives 3 and 4, seemed to be completely dissociated at 232°C (450°F) after 1-hour heat exposure (those bonded specimens could be broken in half at the bond line by hand pressure). This drastic loss of bond strength seems to occur for Adhesives 3 and 4 when exposed to an elevated temperature between 204°C (400°F) and 232°C (450°F) after 1-hour heat exposure, as evidenced by the residual shear strength shown in Table 3. The exposure duration could be a significant factor contributing to this behaviour. Unfortunately, no specific data are available to quantify it at this point in time.

These results suggest that some polyurethane-based adhesives may be sensitive to an elevated temperature above 204°C (400°F) for an extended period of time. The test method developed by the industry appears to be capable of segregating adhesive performance at an elevated temperature if the adhesive bond is exposed to a temperature above 204°C (400°F). As previously mentioned, the North American engineered wood products industry has a desire to benchmark solid wood performance. In combination with the relationship between the mean shear strengths at an elevated temperature and the referenced temperature, as given in Equation 2, and the fact that some polyurethane-based adhesives have drastically different response at an elevated temperature above 204°C (400°F), the industry adopted the 1-hour exposure at 232°C (450°F).

It is possible that the ignition temperature of some wood species may fall below the specified temperature of 232°C (450°F). The industry standard permits the tests to be conducted at a lower temperature for such species if it is justified to the satisfaction of the

engineered wood product manufacturer, qualified third-party inspection agency, and code evaluation agency.

4. Acceptance Criteria

Due to test uncertainties, the residual strength at the elevated temperature, as shown in Equation 2, is not meant to be deterministic. As a result, the industry standard specifies the use of matched specimens between solid wood blocks and bonded blocks. Details of the specimen preparation are given in the industry standard. It is generally considered acceptable if the ratio of the mean residual shear strength between 232°C (450°F) and 21°C (70°F) for the bonded specimens is equal to or higher than the lower 95% confidence interval on the ratio of the mean residual shear strength for the solid wood specimens. It should be noted that the wood failure criteria were not specified in the standard because of the difficulty in estimating wood failure after the specimens are exposed to an elevated temperature for 1 hour.

5. Remaining Issues

Since the release of APA/WIJMA AC1000-05 in March 2005, ASTM D14.30 *Subcommittee on Wood Adhesives* has been considering the adoption of the standard. A committee ballot, which contains minor editorial and format changes, is expected to be issued in August 2005. CSA O177, *Qualification Code for Manufacturers of Structural Glued Laminated Timber* [9], is also balloting the adoption of the industry standard by reference. In addition, a proposal to adopt APA/WIJMA AC1000-05 into an acceptance criteria by the International Code Council Evaluation Service (ICC ES) was discussed at the last ICC ES hearing in June 2005.

During the last ICC ES hearing, the adoption of the industry standard was strongly supported by most adhesive suppliers. However, there were concerns raised by two adhesive suppliers on the severity of the standard in terms of the specified temperature and exposure duration. From their viewpoint, it was arguable that the specified temperature and exposure temperature are too severe, as compared to the performance of engineered wood products, such as I-joists, in an unprotected assembly. One adhesive supplier has suggested that the standard be revised to allow either 1) linear temperature rise from ambient to 204°C (400°F) at bond line over a period of 60 minutes or 2) constant air temperature of 180°C (356°F) for 2 hours in accordance with CSA O112.9. These arguments reflect the different viewpoints between some adhesive suppliers and the engineered wood product manufacturers, who tend to take a conservative approach when addressing the concerns raised by the fire services or in response to the issues driven by potential liability. The committee from the engineered wood products industry will be considering the suggestions provided by the adhesive suppliers in September 2005.

6. Conclusions

An industry standard developed by the engineered wood products industry in North America provides an evaluation method on adhesive bond performance at an elevated temperature near wood ignition. The test method appears to be capable of segregating adhesive performance at an elevated temperature if the adhesive bond is exposed to a

temperature above 204°C (400°F) for an extended period of time. However, while this standard is being adopted by a variety of product and test standards, concerns on the severity of the specified temperature and exposure duration remain to be addressed.

7. References

1. ASTM. 2000. *Test Methods for Fire Tests of Building Construction and Materials.* ASTM E 119. ASTM International, West Conshohocken, PA.

2. Underwriters' Laboratories of Canada (UL Canada). 2004. CAN-ULC-S101-04-EN, *Standard Methods of Fire Endurance Tests of Building Construction and Materials.* Toronto, ON.

3. ISO 834-1:1999, *Fire-resistance tests -- Elements of building construction -- Part 1: General requirements.* International Organization for Standardization, Geneva, Switzerland.

4. Forest Products Laboratory. 1999. *Wood handbook—Wood as an engineering material.* General Technical Report FPL–GTR–113. U.S. Department of Agriculture, Forest Service, Forest Products Laboratory, Madison, WI.

5. CSA. 2004. *Evaluation of Adhesives for Structural Wood Products (Exterior Exposure).* CSA O112.9. Canadian Standards Association, Ontario, Canada.

6. ASTM. 2000. *Standard Test Method for Resistance to Deformation Under Static Loading for Structural Wood Laminating Adhesives Used Under Exterior (Wet Use) Exposure Conditions.* ASTM D 3535. ASTM International, West Conshohocken, PA.

7. ASTM. 2003. *Standard test methods for strength properties of adhesive bonds in shear by compression loading.* ASTM D 905. ASTM International, West Conshohocken, PA.

8. ASTM. 2005. *Standard Specification for Evaluation of Structural Composite Lumber Products.* ASTM D5456. ASTM International. West Conshohocken, PA

9. CSA. 1989. *Qualification Code for Manufacturers of Structural Glued Laminated Timber.* CSA O177. Canadian Standards Association, Ontario, Canada.

INTERNATIONAL COUNCIL FOR RESEARCH AND INNOVATION
IN BUILDING AND CONSTRUCTION

WORKING COMMISSION W18 - TIMBER STRUCTURES

NEW GENERATION OF TIMBER DESIGN PRACTICES AND CODE PROVISIONS LINKING SYSTEM AND CONNECTION DESIGN

A Asiz

I Smith

University of New Brunswick

CANADA

New Generation of Timber Design Practices and Code Provisions Linking System and Connection Design

Andi Asiz and Ian Smith
University of New Brunswick, Canada

1. Introduction

During the last several years the Canadian timber design code committee (Canadian Standard Association O86 Technical Committee) has been laying the groundwork for a major overhaul of the national model code CSA Standard O86-O1 'Engineered Design in Wood' (CSA 2001a). Key issues are:

  I. Need for consistency in the objectives, philosophy and technical details that underpin provisions of different sections of the code. For example, if the section dealing with seismic design of braced frames requires use of ductile connections, then the section dealing with detailed design of connections must provide guidance on how to achieve such mechanistic behaviour.

  II. Explicit consideration of the relationships between design provision applicable to individual components (members and connections) and the performance of major structural subsystems and complete structural systems. As in other countries, structural codes in Canada are premised on sequential design of individual components. This premise is coupled with an expectation that if every component is 'strong and stiff' the complete structure will have adequate behaviour. Such an approach leads to great uncertainty about system behaviour at failure. Also, although arguably the current approach is conservative, solutions tend to be uneconomic.

  III. Development of partial coefficients (load and resistance factors) in design equations that reflect 'true' rather than 'nominal' reliability levels.[1] To date partial coefficients in the Canadian timber design code are calibrated to yield essentially the same solutions as were achieved from past Allowable Stress Design (ASD) codes. Structural reliability methods have been used, especially in connection with setting design resistances for small dimension lumber members. However, as the calibration point is always achieving safety indexes under partial coefficient design that maintain parity with ASD within selected calibration problems, it is simply a very fancy way to do so-called 'soft code conversion'. For genuine progress under item II it is essential to deal with real reliability levels, i.e. not bother about parity with ASD solutions.

  IV. Modernise the connection design provisions many of which have their origins in unrecorded committee decisions made in the order of 50 years ago, based on US studies for military purposes at around the time of the Second World War.

  V. Rapid integration of new products, typically proprietary, into the market place. This requires the establishment of a framework and methods that ensures consistency in how design properties are assigned to old and new products.

---

[1] In Canada the terminology limit states design and partial coefficients design (known more frequently as Load and Resistance Factor Design, LRFD) are erroneously taken to be synonymous. Here the authors intend that limit states considerations be considered an integral part of partial coefficients design methods.

There have and will continue to be also be major changes in provisions of the National Building Code of Canada (NRC 2005), i.e. the model document that lays down general -- construction type independent -- design requirement, and specifies the magnitudes of environmental loads and load factors. The 2005 edition (to be published in September) will provides, for the first time, explicit statements of mandatory 'design objectives' and 'functional statements'.[2] The role of the timber code, and other material specific codes, is to provide a basis from which designers can produce solutions that satisfy various objectives listed in the building code. Implicit in items I to V listed above is recognition the potential that changes in the building code releases will only be fully harnessed by the timber construction sector if accompanied by major change in the timber design code.

The last major overhaul of code provisions in Canada that relate to timber connections occurred in the early 1980's. But what was done then was mostly concerned with reformatting information as the code as a whole was transformed from an ASD to a partial coefficients format. Here the need to revise connection design methods is employed as the tool for tying the sections of the national timber design code together, just as actual connections tie timber structures together. This touches on all of the issues I to V.

Extensive use is made below of working documents produced by the University of New Brunswick's Timber Engineering Group under the leadership of Professor Dr. Ian Smith. Specific consideration is given in those documents, and this one, to promoting design practices and provisions that:
- Make it transparent to designers what mode of failure governs the strength of particular connections, and how that relates to system behaviour.
- Embody probabilistic Load and Resistance Factor Design (LRFD) concepts.
- Guide designers toward an appropriate choice of structural systems to resist given sets of loading combinations.
- Guide designers toward appropriate selection of wood and other structural materials.
- Integrate design provisions specific to connections with those pertaining to the overall system design. In the context of CSA Standard O86-O1 this amounts to integration of connection and general design requirements.
- Maximize possibilities for technical harmonization of Canadian and international practice.

What is outlined here is intended to be consistent with activities by other Canadian experts, especially those working on issues related to system behaviour. Although as yet so inconsistencies remain, work reported in the paper "Framework for lateral load design provisions for engineered wood structures in Canada" (Popovski and Karacabeyli 2005) is convergent with what is discussed here. The next three sections discuss the logic for new connection code provisions, general design code provisions that interrelate with design of connections, and current activities.

2. Provisions for Connection Chapter

2.1 Global requirements

Concept here are based on the presumption that the code need specify as the first level decision what are and what are not acceptable modes of connection failure for particular

---

[2] Functional statements help users understand the reasons behind certain requirements.

combinations of Structure Type and Load Combination for Strength and Stability Limit Sates (Table 2.1). The second level of decision is what type of connection to select, knowing what are the acceptable failure modes (Table 2.2). Once appropriate options for connection are identified designers need rules for 'sizing' them (Section 2.2).

The scope of the Connections Chapter should be limited to avoiding attainment of any strength or stability related limit state. When interpreting the permissible failure modes suggested in Table 2.1 it is important to recognize that load paths and/or load resisting mechanisms/components need not be the same for all the load combinations. Table 2.2 is illustrative and deals with only with connections that load fasteners or connectors lateral to the axis of the fastener or connector.

Table 2.1 – Proposed Permissible Failure Modes for Mechanical Connections

Structure Type	Load Combination (Comp. = companion)	Permissible Failure Modes (Allowed nature of connection failures)		
		Brittle	Ductile	Bearing
Light-framing: *not* load-sharing	$\phi R \geq 1.4D$	✗	✔	✔
	$\phi R \geq 1.25D + 1.5L + Comp.$	✗	✔	✔
	$\phi R \geq 1.25D + 1.5S + Comp.$	✗	✔	✔
	$\phi R \geq 1.25D + 1.4W + Comp.$	✗	✔	✔
	$\phi R + effect\ 0.9D \geq 1.4W$ or 1.5L or 1.5S	✗	✔	✗
	$\phi R \geq 1.0D + 1.0E + Comp.$	✗	✔	✗
	$\phi R + effect\ 1.0D \geq 1.0E$	✗	✔	✗
Light-framing: load-sharing *and* statically determinate	$\phi R \geq 1.4D$	✔	✔	✔
	$\phi R \geq 1.25D + 1.5L + Comp.$	✔	✔	✔
	$\phi R \geq 1.25D + 1.5S + Comp.$	✔	✔	✔
	$\phi R \geq 1.25D + 1.4W + Comp.$	✗	✔	✔
	$\phi R + effect\ 0.9D \geq 1.4W$ or 1.5L or 1.5S	✗	✔	✗
	$\phi R \geq 1.0D + 1.0E + Comp.$	✗	✔	✗
	$\phi R + effect\ 1.0D \geq 1.0E$	✗	✔	✗
Light-framing: load sharing *and* statically indeterminate	$\phi R \geq 1.4D$	✔	✔	✔
	$\phi R \geq 1.25D + 1.5L + Comp.$	✔	✔	✔
	$\phi R \geq 1.25D + 1.5S + Comp.$	✔	✔	✔
	$\phi R \geq 1.25D + 1.4W + Comp.$	✔	✔	✔
	$\phi R + effect\ 0.9D \geq 1.4W$ or 1.5L or 1.5S	✔	✔	✔
	$\phi R \geq 1.0D + 1.0E + Comp.$	✗	✔	✗
	$\phi R + effect\ 1.0D \geq 1.0E$	✗	✔	✗
Heavy-framing: *not* self-bracing	$\phi R \geq 1.4D$	✔	✔	✔
	$\phi R \geq 1.25D + 1.5L + Comp.$	✔	✔	✔
	$\phi R \geq 1.25D + 1.5S + Comp.$	✔	✔	✔
	$\phi R \geq 1.25D + 1.4W + Comp.$	✗	✔	✔

	ϕR + effect $0.9D \geq 1.4W$ or $1.5L$ or $1.5S$	✗	✔	✗
	$\phi R \geq 1.0D + 1.0E$ + Comp.	✗	✔	✗
	ϕR + effect $1.0D \geq 1.0E$	✗	✔	✗
Heavy-framing: self-bracing	$\phi R \geq 1.4D$	✗	✔	✔
	$\phi R \geq 1.25D + 1.5L$ + Comp.	✗	✔	✔
	$\phi R \geq 1.25D + 1.5S$ + Comp.	✗	✔	✔
	$\phi R \geq 1.25D + 1.4W$ + Comp.	✗	✔	✔
	ϕR + effect $0.9D \geq 1.4W$ or $1.5L$ or $1.5S$	✗	✔	✗
	$\phi R \geq 1.0D + 1.0E$ + Comp.	✗	✔	✗
	ϕR + effect $1.0D \geq 1.0E$	✗	✔	✗
Arches and shells	$\phi R \geq 1.4D$	✗	✔	✔
	$\phi R \geq 1.25D + 1.5L$ + Comp.	✗	✔	✔
	$\phi R \geq 1.25D + 1.5S$ + Comp.	✗	✔	✔
	$\phi R \geq 1.25D + 1.4W$ + Comp.	✗	✔	✔
	ϕR + effect $0.9D \geq 1.4W$ or $1.5L$ or $1.5S$	✗	✔	✗
	$\phi R \geq 1.0D + 1.0E$ + Comp.	✗	✔	✗
	ϕR + effect $1.0D \geq 1.0E$	✗	✔	✗

✔signifies a failure mode is permissible, while ✗signifies a failure mode is not permissible.

ϕR is factored resistance, D, L, S, W & E are effects dead, live occupancy, snow, wind and earthquake loads respectively.

Load Combinations refers to cases specified in the building code (NRC 2005).

Table 2.2 – Possible Failure Modes According to Connection Type: *Laterally loaded fasteners or connectors* (B = brittle, C = bearing/compressive, D = ductile, EWP = Engineered Wood Products, OSB = Oriented Strand Board)

Connection type	Connected Materials						
	Wood-to-Wood	Ply/OSB-to-wood	Steel-to-wood	Wood-to-concrete/masonry*	Wood-to-EWP+	Ply/OSB-to-EWP	Steel-to-EWP
Dowel fasteners	B, C, D	B, D	B, C, D	B, C	B, D	B, D	B, D
Wood connectors	B	n/a	B, C, D	n/a	B	n/a	n/a
Truss-plates	B, D	n/a	n/a	n/a	B, D	n/a	n/a
Light-gauge framing products	B, C, D	n/a	n/a	n/a	B, C, D	n/a	n/a
Glued-in-rods	B, C, D	n/a	B, C, D	B, C, D	B, C, D	n/a	B, C, D
Carpentry	B, C, D	n/a	n/a	B, C	B, C, D	n/a	n/a
Other	To be determined by testing (Section 2.2.2).						

* If concrete or masonry is reinforced so that local failures cannot propagate, attaining ductile failures is possible.

4

+ For the purposes of connection design EWP's can be thought of as falling into categories of splitting and non-splitting as determined via a standardized test protocol (on going work at University of New Brunswick). Connections with members of splitting EWP materials can exhibit catastrophic failures due to fracturing in EWP members. However, connections with non-splitting EWP materials cannot exhibit catastrophic failures due to fracturing in EWP members.
n/a signifies not appropriate.

2.2 Sizing connections

The reference unit for calculation is the full connection, and not a single fastener or connection as was the case formerly.

2.2.1 By calculation

It is assumed that mechanics based models will be the basis for predicting both the characteristic ultimate load capacity and the associated failure mode. It is presumed that although most models will be based on explicit hand calculations (e.g. existing approach for connections with one bolt – Johansen type yield model), in some instances models will need to be hybrid (e.g. existing design approach for connections with 'timber rivets') or even empirical evidence (e.g. existing approach for connections with multiple bolts). There is no attempt to formulate and provide details of suitable models here but that topic is currently being worked on by researchers at the University of New Brunswick.

Table 2.2.1 specifies the failure mechanisms to be considered for various types of connections. The predicted failure mode for a prospective connection detail is the failure mechanism associated with the minimum estimate of the characteristic ultimate load capacity. The table is very general in its present form and reflects mechanisms possible under arbitrary loading arrangements. In many practical situations a designer would only consider a subset of the listed mechanisms. Where the predicted governing failure mechanism is ductile and the associated characteristic ultimate load capacity is greater than 0.9 times the characteristic ultimate capacity for any alternative mechanism that is brittle, it should be assumed that failure mode would be brittle. However the original estimate for the characteristic ultimate load capacity, for the ductile mode, would still be the value adopted.

Table 2.2.1 – Possible Failure Mechanisms to be considered: ***Laterally loaded fasteners or connectors***

Connection type	Possible Failure Mechanisms						
	Yielding (EYM)	Tear-out	Shear in-the-row	Opening fracture	Shearing fracture	Pull-out	Bearing
Dowel fasteners	✔	✔	✔	✔	✔	*n/a*	*n/a*
Wood connectors	✔	✔	✔	✔	✔	*n/a*	*n/a*
Truss-plates	✔	✔	✔	✔*	✔*	✔	*n/a*
Light-gauge framing products	✔	*n/a*	*n/a*	✔*	✔*	✔	✔
Glued-in-rods	✔	*n/a*	*n/a*	✔	✔	✔	✔
Carpentry	*n/a*	*n/a*	*n/a*	✔	✔	✔	✔
Other	To be determined by testing (Section 2.2.2).						

* the facture could be in either wood or metal.

5

2.2.2 *From test data*

ISO test methods are preferred to promote uniformity in practices and maximize opportunities for exchange of data with foreign colleagues. Tests should be realistic replicating as closely as possible the geometric and loading arrangement, load waveform and frequency, and material conditioning applicable to field situations. The number of test replicates should be enough to reliably characterize average and variability in parameters that characterize any connection's structural response.

The necessary combination of loading regimes will vary depending on the type of connection and the application. Loading regimes that can be applicable are: sustained loads causing static fatigue, fluctuating loads causing low-cycle fatigue, fluctuating loads causing high-cycle fatigue and single or repetitive impact loads. Within cyclic regimes the loading can be applied under either displacement control (*seismic load scenarios*), or load control (*wind loads scenarios*). To date most tests have been carried out using so-called static load where a monotonic load is increased steadily at a rate that causes failure in about 0.1 hours. Static tests mostly employ displacement control. Such load is virtually irrelevant to field applications of connections, but is the simplest and cheapest regime to apply and within the capability of all credible test facilities. The main reason for including static tests within any future research plan is that they provide a basis for comparing results with historical data. Employing realistic loading conditions is prerequisite to proper 'sizing' of connections (and other structural timber components).

The following procedure enables calculation of the *Standardized Specified Resistance* (R_s) from test data, in a manner consistent with established Canadian practice (CSA 2001b).

<u>*STEP 1:*</u> The 5th percentile strengths at 75 % confidence ($R_{0.05,0.75}$) is calculated as:

$$R_{0.05,0.75} = C_f R_{0.05,data}$$

where
$R_{0.05,data}$ = raw data estimate for the 5th percentile strength[3,4]
C_f = data confidence factor
  If sample size (n ≥ 10)
$$C_f = 1 - \frac{2.7V}{\sqrt{n}}$$
  If sample size (n < 10)
$$C_f = R_{min}\left(\frac{n}{27}\right)^V$$
  (based on Leicester, 1986)

---

[3] Strength means the resistance to a defined externally applied force that a connection can develop subject to any deformation constraints appropriate to the connection application being considered. Continuity and displacement compatibility requirements for an overall structural system may prohibit any connection from attaining its ultimate strength. In such a situation the strength would correspond to the resistance at a certain level of deformation and not the ultimate resistance attainable at some unconstrained level of deformation.

[4] When the sample size (n) is ≥ 19 a non-parametric estimate of $R_{0.05,data}$ can be obtained by ranking strength observations in ascending order with the weakest specimen having rank 1 and the strongest specimen having rank n. The 5th percentile value can be estimated by interpolation using the relationship that the cumulative frequency for the ith ranked specimen is $i/_{n+1}$. Otherwise, a parametric estimate of $R_{0.05,data}$ can be obtained by fitting a 2-parameter Weibull, or another appropriate, distribution to the data. ASTM Standard D 5457 provides methods to calculate Weibull distribution parameters.

6

V = coefficient of variation

The coefficient of variation of short-term strength (V) may be estimated by presuming that data is represented by a 2-parameter Weibull, or another appropriate, distribution.

R_{min} = minimum of n test values

<u>STEP 2:</u> The nominal strength, R_n, is calculated as:

$$R_n = B\, R_{0.05,0.75}$$

where

B = reliability normalization factor[5] (accounts for deviations in variance of R from the value used for calibration of resistance factor ϕ within the design equation).

<u>STEP 3:</u> The standardized specified resistance, R_s, is calculated as:

$$R_s = \frac{R_n}{\prod\limits_{i=1,I} k_{test,i}} = \frac{R_{0.05,0.75}B}{\prod\limits_{i=1,I} k_{test,i}}$$

where *for example*: $k_{\text{test, duration of loading}}$ might be given the value $1.25 = 1/0.8$ if resistance for 'standard term' loading is 0.8 time the short-term test strength.

For connections that must resist earthquake combinations, and wind loading combinations causing force reversals, the above can be supplemented by assessment of the ductility class (Popovski and Karacabeyli 2005). Ductility classification of connections by test is simple. Although experiments tend to be expensive, they are probably the most viable approach as few people have the capabilities needed to do ductility classifications via models.

3. Provisions for General Design Chapter

3.1 Control of failure modes

Implicit to the strategy embodied in Section 2 is that designers should not be permitted unfettered choice of combinations of member type and connections for structural arrangements prone to disproportionate or unstable development of local into whole system failures. For some loading combinations it is critical that the connections fail first and not the members, and that even when some connections have failed there is still continuity in the original or an alternative load path(s). Under earthquake and strong wind loading scenarios, this is achieved via connections having adequate ductility. It is presumed here that attaining adequate ductility is a primary requirement under loading combinations that involve earthquake effects and/or wind effects that lead to force reversals.

---

[5] The simple closed form option is to calculate B as (this is consistent with the expression given in Ravinda and Galambos (1978)):

$$B = \exp(\beta_{nom}V_{nom} - \beta_{target}V)$$

where the symbols are: β = reliability index; V = coefficient of variation. The subscript signify: *nom* = nominal values used as the basis of the ϕ specified in the design code; *target* = target value appropriate to the specific type of connection. Actual V is determined from test data or by modeling of the specific type of connection.

General design provisions should require attainment of a certain level of ductility and fatigue life classifications by whole systems and critical connections. What is done needs to be consistent with provisions being developed by the CSA O86 Seismic Design Taskforce (Popovski and Karacabeyli 2005).

The approach underpinning Tables 2.1 and 2.2, and any ductility and fatigue life requirements are part of a strategy for ensuring that designers are guided toward appropriate choices of connections under given loading combinations. However, in themselves these provide no surety that whole systems will be unlikely to be governed by catastrophic member failure. It is necessary to also control likelihood of catastrophic member failures, with the *Capacity Design* approach (Section 3.2) being a suitable vehicle.

3.2 Capacity design

The *Capacity Design concept* has been used for a number of years to design reinforced concrete structures against the effects of seismic loads (Paulay, 1981). The idea is to make it most likely that failure will be in the connections, and not the members, Fig. 1. Chui and Smith (1993) made a preliminary study of how the method might be applied in seismic design of timber structures and concluded that it is viable.
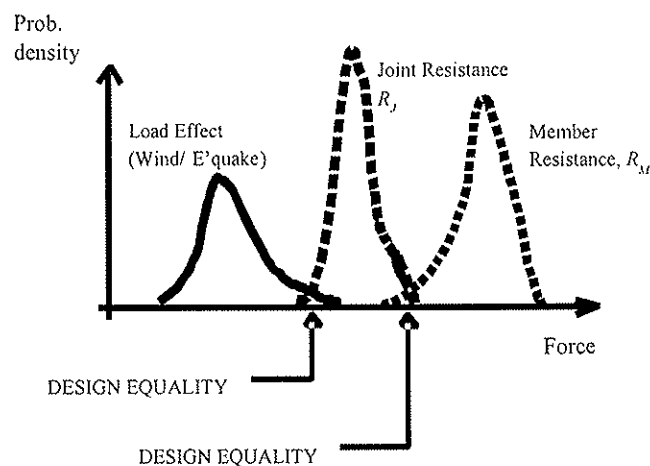
Fig. 1: Logic of the *Capacity Design* concept

It is important to recognize that reasons for enforcing that failures are most likely to occur in the connections would not be the same in the cases of wind and seismic design. Under wind load conditions, design for ductile failure in the connections is desirable because this promotes redistribution of forces between components and subassemblies. This is one of the means of avoiding progressive and disproportionate damage in structural systems. In seismic design, ductile failure in the connections is desired because mechanical connections are the only significant sources of ductility and energy absorption during cyclic loading.

Because of the complexity of many wood-based structural systems, the behaviour of subsystems (diaphragms, shear walls, roof panels and trusses) is hard to predict and thus forces in individual wood elements are not usually predicted with much certainty. However, if load paths are clearly defined within a structural system it is possible to predict the forces

8

in the connections between subsystems with relatively good accuracy, e.g. between the roof and walls, between the walls and foundation. The connections between subsystems often also happen to be locations prone to failure during high wind or seismic events. Capacities of properly designed connections can be controlled to be less variable than the capacities of timber members or subsystems they join (e.g., Larsen and Jensen 2000). Thus, the strength of a whole structural system should be able to be predicted with a high degree of certainty using a capacity design type concept.

The general design equations within CSA Standard O86-O1 for implementation of *Capacity Design* would take the form:

$$\sum LoadEffects \le \phi_{C,L} R_{C,k,L} \quad \text{and}$$

$$\phi_{C,U} R_{C,k,U} \le \phi_M R_{M,k}$$

where

$\phi_{C,L}$ = connection resistance factor associated with the lower characteristic connection strength $R_{C,k,L}$ (typically the 5 percentile value, $R_{C,0.05}$),

$\phi_{C,U}$ = connection resistance factor associated with the upper characteristic connection strength $R_{C,k,U}$ (typically the 95 percentile value, $R_{C,0.95}$),

ϕ_M = member resistance factor associated with the lower characteristic member strength $R_{M,k}$ (typically the 5 percentile value, $R_{M,0.05}$).

Implicitly, the capacity design concept presumes that the design equations are calibrated using structural reliability concepts. As already discussed (Section 1), to be meaningful methods have to be based on true rather than nominal reliability. Neither member nor connection capacities can any longer be based on a soft conversion from ASD to partial coefficients design (LRFD or what is wrongly called Limit States Design in Canada).

4. Current Activities

Reliability analysis of structural timber systems and connections is being conducted at the University of New Brunswick using representative Case Studies. The intent is that within the next year UNB researchers in collaboration with researchers from Forintek Canada Corp. will propose a framework for a Canadian timber design code that is fully consistent with respect to design of structural systems (and large subsystems) and connection design. Ongoing work at UNB is addressing:

- Consistency in reliability approaches: This refers to consistency between the timber design code (CSA Standard O86-01) and the National Building Code of Canada that defines material independent characteristic loads and load factors.
- Definition of failure of a connection: This recognises that failure processes in structural connections must obey overall system requirements for continuity and compatibility (system deformations will not permit various connections to attain excessive deformation). In practical terms this implies that it is inappropriate to simply assume that the reference strength of a connection should equal say the ultimate connection load, or perhaps the "yield load", as observed in tests on isolated connections. The same argument should be applied to members in composite and built-up timber construction, e.g. light-frame construction.
- Definition of the unit of reference: This refers to whether connection reliability is to be controlled at the level of a joint (one end of one member), a member (they usually

have a joint at each end), a connection (several members can be join at a connection), a subsystem (e.g. truss), or a building. Nominally current practices relate to the level of a joint. However, this has had limited reliability implications because traditionally ASD) capacities of connections were assigned based on the concept of controlling the extent of deformation in connections.

- Weak or strong connections: Traditionally under ASD connections were strong elements and tended to be over-designed, but this implies that failures are forced to occur in members and hence that system failures will be brittle. Philosophically at least, designers should be given opportunity to select whether to create connections that are, for example, weak and ductile or strong and stiff.

5. Concluding Comment

Canada is on the cusp of being able to implement a new generation of timber design codes. Although not discussed here, the biggest challenge in achieving major advances is counteracting inertia in a code development system that is not well geared to radical change. The authors invite international colleagues to comment, share ideas and participate in the necessary tasks.

References

CSA. 2001a. Engineering design in wood, *Canadian Standard 086-01*, Canadian Standard Association, Toronto, Canada.

CSA. 2001b. Standard practice relating specified strengths of structural members to characteristic structural properties, *Supplemental document, CSA O86 Technical Committee*, Canadian Standard Association, Toronto, Canada.

Chui, Y.H., Smith, I. 1993. Capacity design of wood structures, *Proc. Annual Conf. Canadian Society for Civil Engineering*, II: 365-374.

Larsen, H.J., Jensen J.L. 2000. Influence of semi-rigidity of joints on the behaviour of timber structures, *Progress in Struct. Eng. and Materials*, 2: 267-277.

Leicester, R.H. 1986. Confidence in estimates of characteristic values, *Proc. 19th Meeting CIB-W18*, International Council for Research and Innovation in Building and Construction, Rotterdam, The Netherlands.

NRC. 2005. *National Building Code*, National Research Council, Ottawa, Canada.

Paulay, T. 1981. Developments in the seismic design of reinforced concrete frames in New Zealand, *Canadian J. Civil Eng*, 8: 91-113.

Popovski, M., and Karacabeyli, E. 2005. Framework for lateral load design provisions for engineered wood structures in Canada, *Proc. 38th Meeting CIB-W18*, International Council for Research and Innovation in Building and Construction, Karlsruhe, Germany.

Ravinda, M.K., and Galambos, T.V. 1978. Load and resistance factor design for steel", *ASCE J. Structural Division*, 104 (ST9): 1337-1353.

INTERNATIONAL COUNCIL FOR RESEARCH AND INNOVATION
IN BUILDING AND CONSTRUCTION

WORKING COMMISSION W18 - TIMBER STRUCTURES

UNCERTAINTIES INVOLVED IN STRUCTURAL TIMBER DESIGN
BY DIFFERENT CODE FORMATS

L Ozola

Department of structural engineering
Latvia University of Agriculture

LATVIA

T Keskküla
Institute of Forestry and Rural Engineering
Estonia University of Agriculture

ESTONIA

Presented by L Ozola

P Kuklic stated it is not proper to compare the Eurocode to the Latvian (Russian) National code as test method is different, safety factors are different, and test methods are different. It is not possible to compare.

Ozola responded that characteristics strengths are different. The work is based on testing of real structural elements not from small clear tests. In terms of connection Ozola agrees that the Eurocode accounts for plastic hinges. Her question is which one is predicted for service life.

J Ehlbeck asked whether the Eurocode is used in Latvia. Ozola said that the code is used by some designers and she taught her students about it. J Ehlbeck stated that one has to wait for national application document.

Uncertainties involved in structural timber design by different code formats

Lilita Ozola

Department of structural engineering
Latvia University of Agriculture, Latvia

Tõnu Keskküla

Institute of Forestry and Rural Engineering
Estonia University of Agriculture, Estonia

1 Abstract

The article presents the comparison of design results of structural timber elements according to different building codes: Eurocode 5 and Russia code SNiP II-25-80. Comparative results of requirements for strength and stability of structural timber elements in axial tension, longitudinal buckling, normal bending and in combined loading are presented and the differences in are discussed.

Key words: *timber structures, codes, design*

2 Motivation for this study

The Eurocodes are expected to enable the functioning of a single European market for products, and to improve the cooperation in construction industry by removing obstacles arising from different nationally codified practices.

Currently design practice of timber structures in East Europa countries maintains the using of two existing codes- Eurocode 5 [1] and Russia SNiP II-25-80 [2], both based on the limit state phylosophy. Yet the methodology, i.e., analytical models and partial factors used in calculations are often taken from well known Russia codes that are not supplemented by improvements made in timber analysis during last decades in West countries.

This study is an extension of topics discussed three years ago in Kyoto meeting [3]. Unfortunately it is still complicated situation with using of different codes in design. It is important to explain and prove the advantages of Eurocode in new EU countries. Traditional design practice based on known Russia SNiP codes is very steady in consciousness of civil engineers. At the same time the permanent treatment and discussion for Eurocode conditions helps to put forward appropriate controversial solutions probably emerging from new interpretation of conditions and design parameters. It is necessary to understand that only a common comprehensive understanding of conditions for structural design may serves for successful development and cooperation in construction industry and the main thing to be taken always into account is ensuring the safety of buildings and sufficient level of reliability.

Some issues for the consideration of engineers and researchers are pointed out by this study.

3 Comparison of design results according to EN 1995-1-1 and SNiP II-25-80

The objective of this chapter is to compare and explore the design conditions of the EN 1995-1-1 and Russia code SNiP II-25-80 with respect to strength and stability of structural timber elements and to determine under what set of conditions and parameters each provides the more economical design.

3.1 Axial tension

Strength verification is the main condition for elements in axial tension. Required section area values per 1 kN of tensile force are calculated as the case of comparative loading and service conditions may be according to both code formats (Table 3.1). It is assumed that characteristic value of wood resistance in tension along the grain is $f_{t,0,k} = 21$ N/mm^2.

Table 3.1   Design results for softwood elements in axial tension

Duration of load	Design resistance $f_{t,0,d}$, N/mm^2		Required section area (mm^2) per 1 kN of force		Economical efficiency
	EN 1995	SNiPR	A_{EN}	A_{SN}	$(1 - A_{EN}/A_{SN})$, %
Environmental conditions (normal): relative humidity of surrounding air up to 65% and temperature of 20°C					
Permanent	9.7	8.0 (6.4)	103.1	125. (156.3)	17.5 (34.0)
Medium-term	12.9	10.0 (8.0)	77.5	100.0 (125)	22.5 (38.0)
Instantaneous	17.8	12.0 (9.6)	56.2	83.3 (104.2)	32.6 (46.0)
Environmental conditions: relative humidity of surrounding air 75-85% and temperature of 20°C					
Permanent	9.7	7.2 (5.8)	103.1	139. (172.4)	25.8 (40.2)
Medium-term	12.9	9.0 (7.2)	77.5	111.0 (139)	30.2 (44.2)
Instantaneous	17.8	10.8 (8.6)	56.2	93.0 (116.0)	39.6 (51.6)
Environmental conditions: relative humidity of surrounding air approximately 95%					
Permanent	8.1	6.8 (5.4)	123.4	147. (185.2)	16.0 (33.4)
Medium-term	10.5	8.5 (6.8)	95.2	117.6 (147)	19.0 (35.2)
Instantaneous	14.5	10.2 (8.2)	69.0	98.0 (122.0)	29.6 (43.4)

In Table 3.1 values presented in brackets refer to tensile elements with symetrically cut edges that are assessed to be as extremely sensitive under limit state according to SNiP approach.

For discussion of this issue it is useful to present there some results of experimental tests from our previous studies [4]. Six softwood (pine) pitched truss models made from boards (width 35 mm) were tested under static load up to failure (see scheme in Fig. 3.1). Rigid joints were made by using of epoxy resin glue in nodes of model. Bottom tensile chord was symmetrically cut for each test specimen, depth of notching vary from 1/9 to 1/7 from full depth of element. Normal stresses determined in netto section under maximal action attached to top node were within the values from 19 to 24 N/mm^2. There were not observed failure of thin section. Thus, results of this case study did not proved the SNiP's assumption on enormously concentration of tensile stresses near notching.
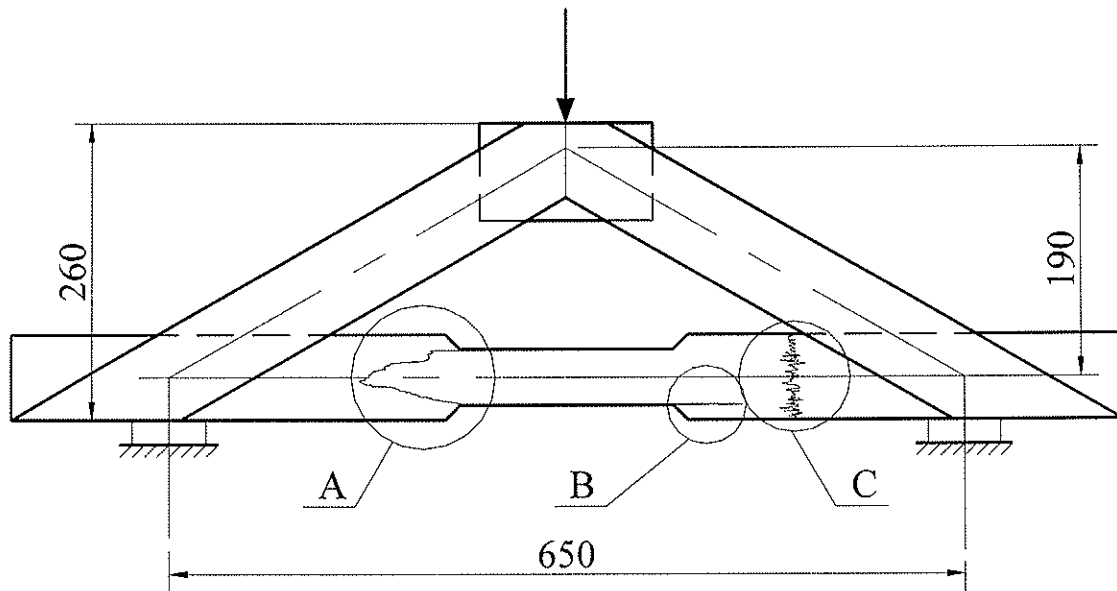
Fig. 3.1   Observed types of fracture modes (A, B, C) for cut tensile element

3.2   Longitudinal buckling

Design results from checking of stability condition in longitudinal buckling $(N_{c,d}/A/k_{c,min}/f_{c,0,d} \leq 1)$ for softwood elements having the slenderness ratio $\lambda_{max} = 80$ are included in Table 3.2. The step forward is made by Eurocode 5 in comparison with SNiP approach as the strength and stiffness properties are included in mathematical model of buckling factor (k_c) as variables. In corresponding model of buckling coefficient φ presented by SNiP mentioned properties are assumed as constants. Comparison of design results of required section area for different slenderness ratio values are showed in Figure 3.2.

Table 3.2   Design results for softwood elements in longitudinal buckling

$f_{c,0,k}$, MPa	$f_{c,0,d}$, MPa (EN)	$E_{0,05}$, MPa	λ_{rel}	$k_{c,min}$	A_{EN}, mm^2/ 1 kN	$f_{c,0,d}$, Mpa (SNiP)	φ_{min}	A_{SN}, mm^2/ 1 kN	c, %
Permanent loading parallel to grain direction in normal conditions									
23	10.6	8000	1.37	0.44	214.4	10.4	0.47	204.6	-4.8
16	7.4	4700	1.49	0.39	346.5	6.8	0.47	312.9	-10.7
Medium term loading parallel to grain direction in normal conditions									
23	14.2	8000	1.37	0.44	160.0	13	0.47	163.7	2.3
16	9.8	4700	1.49	0.39	261.6	8.5	0.47	250.3	-4.6
Instantaneous loading parallel to grain direction in normal conditions									
23	19.5	8000	1.37	0.44	116.6	15.6	0.47	136.4	14.5
16	13.5	4700	1.49	0.39	189.9	10.2	0.47	208.6	8.9
* $c = 100 \times (1 - A_{EN}/A_{SN})$.									

3
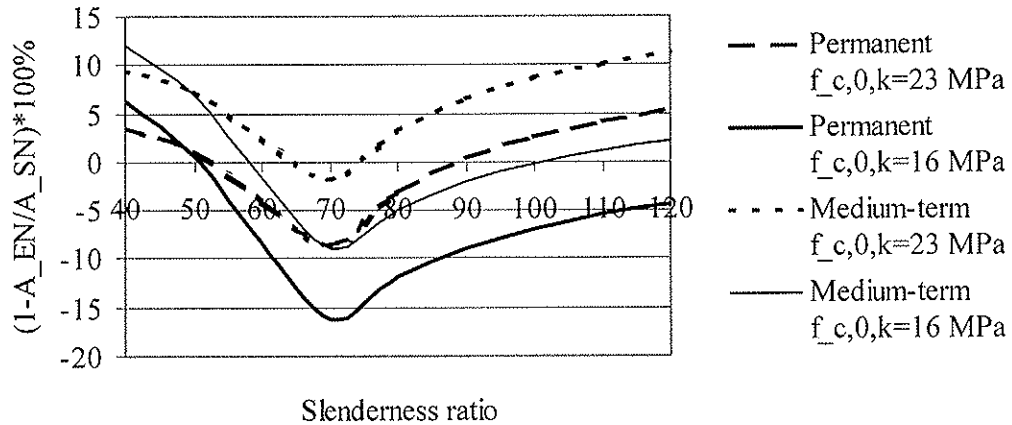
Fig. 3.2   Economical efficiency of buckling elements depending on slenderness ratio

3.3   Bending of solid softwood elements

Solid softwood structural members subjected to flexural loading in normal environmental conditions are calculated according strength condition (Table 3.3). It is assumed that width of beam is one half of depth h (b= h/2). Thus, the section size of beam may be expressed from normal strength condition required for safe behaviour under 1 kNm of bending moment :

$$h = \sqrt[3]{1200000/f_{m,d}} \, . \qquad (1)$$

Table 3.3   Required depths for softwood beams according normal strength condition

Duration of load	$f_{m,k}$, MPa	$f_{m,d}$, MPa (EN 1995)	h_{EN}, mm/ kNm	$f_{m,d}$, MPa (SNiP)	h_{SN}, mm/ kNm	$(1-h_{EN}/h_{SN})$, %
Permanent	24	11.1	47.6	10.4	48.7	2.3
	14	6.5	56.9	6.8	56.1	-1.4
Medium-term	24	14.8	43.3	13	45.2	4.2
	14	8.6	51.9	8.5	52.1	0.4
Instantaneous	24	20.3	39.0	15.6	42.5	8.2
	14	11.8	46.7	10.2	49.0	4.7

Required values of section width b (Table 3.4) necessary for reliable perceiving of shear stresses accompanying with bending, acting along the neutral plane and caused by 1 kN of shear force is expressed from shear strength condition (taking into account that depth $h=2b$):

$$b = \sqrt{750/f_{v,d}} \, . \qquad (2)$$

The environmental conditions are assumed as normal. Differences in design results are more important for low grade elements.

Table 3.4   Design results for softwood beams according shear strength condition

Duration of load	$f_{v,k}$, MPa	$f_{v,d}$, MPa (EN 1995)	b_{EN}, mm/ kN	$f_{v,d}$, MPa (SNiP)	b_{SN}, mm/ kN	$(1-b_{EN}/b_{SN})$, %
Permanent	2.5	1.15	25.5	1.28	24.2	-5.4
	1.7	0.78	31.0	1.28	24.2	-28.1
Medium-term	2.5	1.54	22.1	1.60	21.6	-2.3
	1.7	1.05	26.7	1.60	21.6	-23.6
Instantane ous	2.5	2.12	18.8	1.92	19.8	5.0
	1.7	1.44	22.8	1.92	19.8	-15.2

3.4   Lateral stability in bending

The tendency for failure by buckling in a more flexible plane is always inherent for slender beams subjected to bending moments in its stiff plane. Mathematical models used for verification of lateral stability of timber beams according Eurocode 5 and SNiP II-25-80 differ significantly due to assumed design parameters and restrictions although the theoretical bases are the same.

For illustration of design results using both code formats the design values of the critical moments for softwood beams made from glulam GL24h are calculated for diferent beam section and effective length parametrs (Fig. 3.3) based upon equations:

EN [5]: $M_{crit} = \dfrac{\pi}{\lambda_{ef}} \sqrt{\dfrac{E J_z J_{tor} G}{1 - J_z / J_y}}$ (3)   SNiP [6]: $M_{crit} = \dfrac{\pi}{\lambda_{ef}} \sqrt{E J_z J_{tor} G}$ (4)
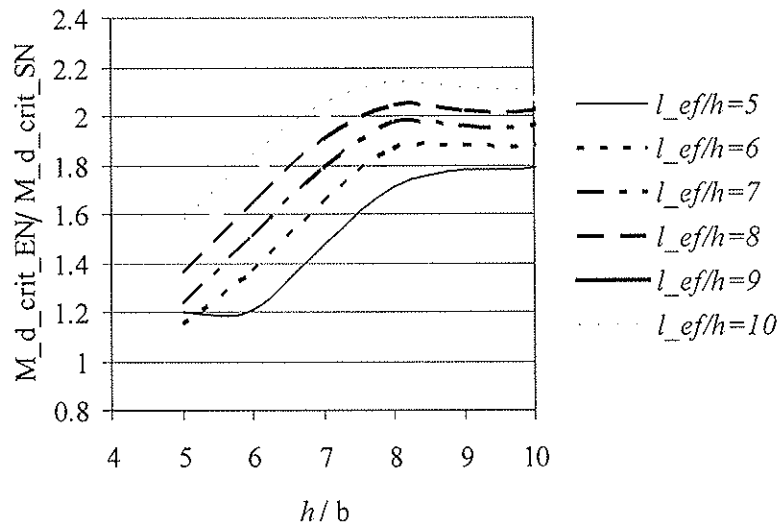
Fig. 3.3   Ratios of critical bending moments calculated according Eurocode 5 and SNiP for different sizes of glulam beams

5

2.5 Combined bending and axial compression

Design conditions for slender elements subjected to combined loading with bending moment and compression force (Fig. 3.4) differ in deterministic approach. The checking of strength and stability conditions (6.23, 6.24, 6.35 [1]) are required by Eurocode 5 and determination of increasing bending moment due to axial force in deformed state falls to part of structural analysis while it is not required to do for each design case. Strength and stability condition for combined loading in compression presented by SNiP code contains parameter ξ involving increase of bending moment in deformed state due to action of axial force.

Design results for glulam (GL24h) element with torsionally restrained supports (Fig. 3.4) are presented in Table 3.5 for illustration of this case study when it is assumed the section sizes of $b=$ 100 mm and $h=$ 528 mm, and slenderness is characterised by ratios $\lambda_z=$ 121 and $\lambda_y=$ 23. Design normal stresses from medium term loading are: $\sigma_{m,d}=$ 7.1 MPa; $\sigma_{c,d}=$ 1.52 MPa.
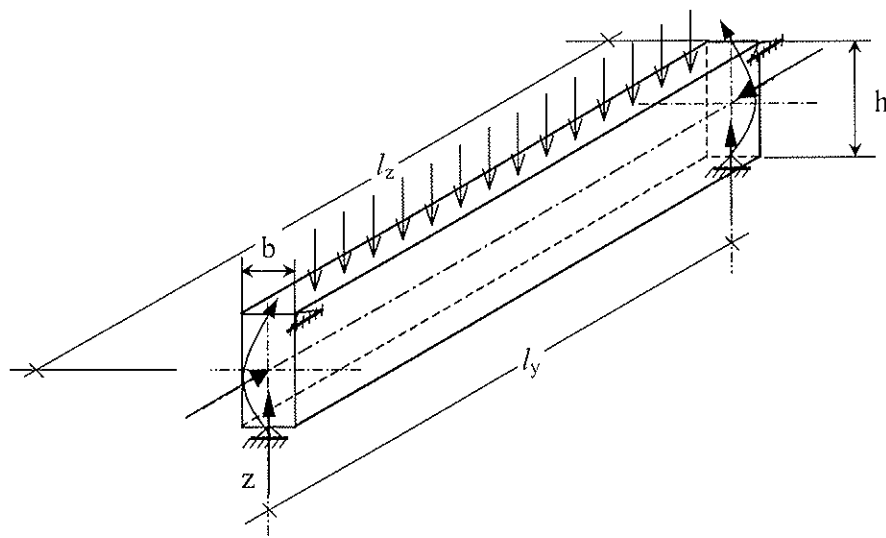
Fig. 3.4   Combined loading with bending moment about the y axis and compression force

Table 3.5   Checking of stability conditions for beam element in combined loading

Code	Design condition	Main parameters	Result
EN 1995	$\left(\dfrac{\sigma_{m,d}}{k_{crit}f_{m,d}}\right)^2 + \dfrac{\sigma_{c,d}}{k_{c,z}f_{c,0,d}} \leq 1$	$\lambda_{rel,m}=$ 0.880; $k_{crit}=$ 0.900; $k_{c,z}=$0.25; $f_{c,0,d}=$ 14.77 MPa; $f_{m,d}=$ 14.96 MPa	0.691
SNiP	$\left(\dfrac{\sigma_{m,d}}{\varphi_M \xi f_{m,d}}\right)^2 + \dfrac{\sigma_{c,d}}{\varphi_z f_{c,0,d}} \leq 1$	$\varphi_M=$ 0.856; $\varphi_z=$ 0.204; $\xi=$ 0.9795; $f_{c,0,d}= f_{m,d}=$ 13 MPa	0.996
Economical efficiency using Eurocode format for this design example: $c=$ 100*(1-0.691/0.996)= 30.6%.			

3.5 Built-up timber columns in longitudinal buckling

Load bearing capacity of built-up timber columns depends from large set of affecting properties and parametrs. Because of it is complicate to characterise the differences in design results using different codes as a whole. In an effort to provide with some useful information on this issue some results through design example is presented below.

Built-up column made by nailing (diameter $d= 6$ mm) of two softwood shafts. Column is assumed as restrained by hinges at the both ends.
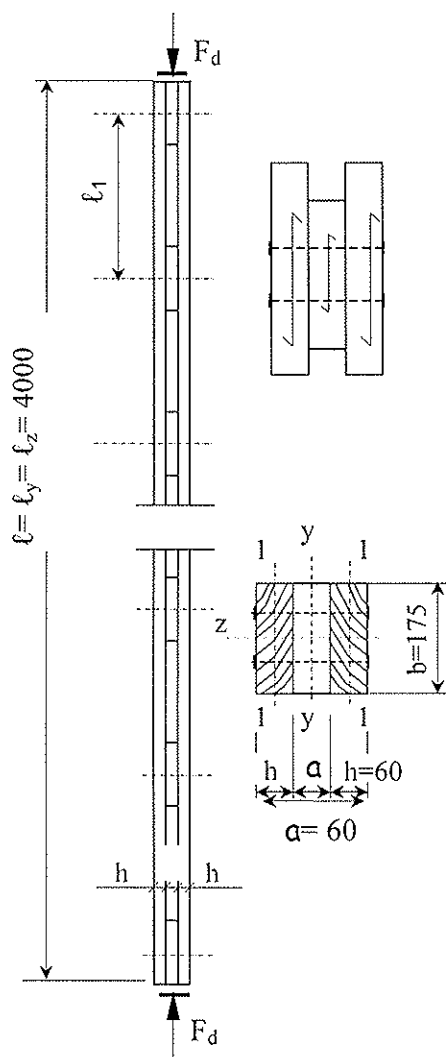
Fig. 3.5   Built-up timber column

Table 3.6   Checking for stability of built-up timber column

EN1995-1-1	SNiP II-25-80
Permanent action $F_d= 40$ kN	
Characteristic resistance of timber $f_{c,0,K}=23$ MPa	
Design resistances for normal environment:	
$f_{c,0,d}= 10.6$ MPa	$f_{c,0,d}= 10.4$ MPa
Slenderness ratio about z axis $\lambda_z= 79.2$	
Slenderness ratio about y axis $\lambda_{ef,y}$:	
$\sqrt{\lambda_y^2 + \eta\, n\lambda_1^2/2} = 89.4$ $= \sqrt{64.1^2 + 4\cdot 31.2^2}$	$\sqrt{(\mu_y\lambda_y)^2 + \lambda_1^2} = 89.8$ $\sqrt{(1.315\cdot 64.1)^2 + 31.2^2}$
Buckling factors:	
$k_{c,y}= 0.37$; $k_{c,z}= 0.45$	$\varphi_y= 0.37$; $\varphi_z= 0.48$
Checking stability condition ($F_d/A/k_c/f_{c,0,d}\leq 1$):	
$\sigma_{ef,z}/f_{c,0,d}= 0.40$; $\sigma_{ef,y}/f_{c,0,d}= 0.49$	$\sigma_{ef,z}/f_{c,0,d}= 0.40$; $\sigma_{ef,y}/f_{c,0,d}= 0.49$
Characteristic resistance of timber $f_{c,0,k}=16$ MPa; Permanent action $F_d= 40$ kN	
$f_{c,0,d}= 7.4$ MPa	$f_{c,0,d}= 6.8$ MPa
$k_{c,z}= 0.39$; $k_{c,y}= 0.32$	$\varphi_y= 0.37$; $\varphi_z= 0.48$;
$\sigma_{ef,z}/f_{c,0,d}= 0.66$; $\sigma_{ef,y}/f_{c,0,d}= 0.81$	$\sigma_{ef,z}/f_{c,0,d}= 0.40$; $\sigma_{ef,y}/f_{c,0,d}= 0.75$

It is useful to point out that load bearing capacity of built-up timber column may be increased by increasing of number or/and diameter of dowels used for fastening together of shafts (upon necessary ones for perceiving of the shear force between the shafts) as it is involved by parameter μ_y in SNiP procedure for calculation of effective slenderness ratio about flexible axis. For example, it is predicted increase of axial load bearing capacity of nailed built-up column for 1.4 times by increasing of fastener's capacity for 2.6 times.

4 Summary

An aspect using of Eurocode design conditions is the increasing the efficiency of the structures that are thought to have "extra capacity"; and thus, indirectly or directly, to reduce the reliability level from the value inherent using SNiP approach. There is a case for reducing of the design safety margins taking into account the need to consider appropriate supervision and quality control measures during erection and maintenance of structures.

SNiPR procedure provides extremely high reliability level for tensile elements which are subjected to brittle failure mode. This may be regarded as "extra capacity" which tends to needless increasing of material consumption.

Eurocode 5 procedure is more flexible in evaluation of the influence of the strength and stiffness properties on the critical axial force in longitudinal buckling, so the characteristics may be used as variables in design procedure. SNiP procedure does not provide sufficient reliability level for buckling elements having lower grade.

The comparison of results from checking of normal strength condition for solid softwood bending elements proves that Eurocode 5 and SNiP assumptions are very nearly equal, yet to satisfy the shear strength condition according Eurocode 5 there is required to increase the width of section up to 30 %.

Significantly differences in design results are revealed by checking of lateral stability of glued timber elements under loading with bending moment and or without axial compressive force. Eurocode 5 procedure allow for much longer free length of members in comparison with the same according SNiP procedure. As this condition always is concerned with safety of large span structures it is recommended to prove and explore further this complicated and serious problem.

In effort to bring the structural timber design methodology up to date Eurocode 5 should be adopted as a basic document by any country. It is the way to achieve the same reliability level of structures in all countries. It is therefore important for the construction engineers of any country to become acquainted with the Eurocodes so that advantage can be taken of the opportunities on implementation. It is necessary to underline that achieving the reliable solutions of structures by using the highly computerised design environment a good erudition in engineering principles is needed first of all.

5 References

[1] ENV 1995-1-1:2004 (E). Eurocode 5: Design of timber structures: Part 1-1: General - Common rules and rules for buildings.

[2] СНиП II-25-80. Деревянные конструкции/ Госстрой СССР.-М.: Стройиздат, 1983

[3] Ozola L., T. Keskküla. Design characteristics and results according to Eurocode 5 and SNiPR procedures. *Proceedings of Meeting Thirty-five, Kyoto, Japan September 2002 of CIB-W18*. Paper 35-102-1. pp. 1-10.

[4] Santa Legzdiņa. Koksnes stiprības un savienojumu nestspējas eksperimentāli pētījumi. Bakalaura darbs. Vadītāja Lilita Ozola. LLU, Jelgava, 2003

[5] Timber Engineering. Step 1. Basis of design, material properties, structural components and joints. Netherlands: Centrum Hout, 1995

[6] Пособие по проектированию деревянных конструкций (к СНиП II-25-80)/ ЦНИИСК им. Кучеренко.- М.: Стройиздат, 1986.- 216 с.

INTERNATIONAL COUNCIL FOR RESEARCH AND INNOVATION
IN BUILDING AND CONSTRUCTION

WORKING COMMISSION W18 - TIMBER STRUCTURES

COMPARISON OF THE EUROCODE 5 AND ACTUAL CROATIAN CODES FOR WOOD CLASSIFICATION AND DESIGN WITH THE PROPOSAL FOR MORE OBJECTIVE WAY OF CLASSIFICATION

V Rajcic

A Bjelanovic

Faculty of Civil Engineering, Zagreb

CROATIA

Presented by V Rajcic

Comparisson of the Eurocode 5 and actual Croatian codes for wood classification and design with the proposal for more objective way of classification

Vlatka Rajcic, Adriana Bjelanovic

Prof.Ph.D., str. eng., Assis. Prof, PH.D., str.eng. Croatia

1   Introduction

The first part of the paper is discussion about wood class system according to EN 338 and the present system of wood classification in Croatia HRN U.D0.001. (for visual classification it is DIN 4074-1 and for the wood classes DIN 4074-2 (12/58). Both standards were taken over in their full content. According to experimental researches from the few collegues and me and datas from the archive of Timber Department at our Faculty, wood species which is the most frequently used for elements in wood constructions in Croatia hardly belong with majority of their characteristics to unique class according EN 338. For the same values of MOE, they have bigger values of the characteristic strengths. [1,2,4,5,6,7,8]. Using values of the classes according to EN 338 wood is wasted because it is overdimensioned.

For countries such as Croatia, which use Eurocode 5 as parallel code to its national but did not make their own tables of characteristic values for mechanical properties for the most used species of wood in wood construction, proposal for classification of wood members using neural network based on the results from non-destructive testings of wood samples is presented.

Second part of the paper gives the differences in dimensions of the wood frame construction designed by Eurocode 5 with characteristic variable action by Croatian NAD for snow and wind load in EC1. For the standard climate conditions there is no big difference in dimensions. But in the case of locations with heavy snow dimensions of timber elements differ more significantly.

2   Wood classification system-how to use wood the most economically?

In Croatia, wood grading is done by traditional visually assesing the elements, taking into account strength reducing factors regarding mainly knots and annual ring width. There are minority of saw mills with possibility of machine strength grading.

The predictive accuracy of visual grading therefore has its limitations since the grading decision depends on the judgement of the grader and it is never objective.

From many experimental investigations [1,2,4,5,6,7,8] and reports regarding testing of mechanical properties of wood which was built in constructions from archive of the Timber Department of our Faculty it was obvious that using strength classes according EN 338 can create economic losses. Especially because Croatia is typically timber exporting country.

There are four the most commonly used species for structural elements in our country: pine (Pinus silvestris), fir (Abies alba), spruce (Picea excelsa) as soft wood and oak (Quercus pedunculata) as hard wood.

Why strength class system according to EN 338 can create economic losses as well as classifying system according present norms has already is created during long period of time?

Starting with the experimental tests and archiv datas for soft wood. From more than hundred specimens for each type of mechanical characteristic following results are obteined from destructive testings, with the moisture content variation from 11,5-14 % (Table 1). All strength and MOE values are deduced to moisture content of 12%. It must be emphasized that the specimen were clear and had a dimension according Croatian standards and their ultimate strengths were tested also according old Croatian norms because all this investigations and reports were made by our standards.

The value of the 5% fractile X_k could be determined according EC5 as:

$$X_k = k_1 \cdot \bar{X} \quad \text{where:} \quad k_1 = e^{\left[-(2.645 + 1/\sqrt{n}) \cdot v(x) + 0.15\right]}$$

Table 1: Values of mechanical properties for soft wood in Croatia [1,2,3,4,5,6,7,8] in comparisson to classes according EN338

Mechanical characteristic	Characteristic value of the mechanical characteristic (Mpa)	Comparative classes according to EN 338	Difference in % *
$E_{0,mean}$	12.0	C27	
$E_{0,05,k}$	7.8	C30	
$f_{m,k}$ bending	55.4	C40*	38%
$f_{c,0,k}$ compression II grain	25.0	C40	
$f_{c,90,k}$ compress ⊥ na grain	7.2	C40*	14%
$f_{t,0,k}$ tension II on grain	35.0	C40*	45%
$f_{v,k}$ shear	6.4	C40*	68%
ρ_{mean} density (kN/m^3)	420	C40	

The same problem of rather big disproportion between MOE and strength values is present for the most commonly used hard wood – oak (Table 2). Hard wood is generally much rarely in use for structural elements then soft woods but people are psyhologicaly connected to this species because it is idea of timber quality, strength and reliability and it was used befor for traditional croatian wood house.

Table 2: Values of mechanical properties for hard wood-oak [1,2,3,7] in Croatia in comparisson to classes according EN338

Mechanical characteristic	Characteristic value of mech. Characteristic (Mpa)	Comparing class according to EN 338	Difference in %
$E_{0,mean}$	13.8	D50	
$E_{0,05,k}$	11.5	D50	
$f_{m,k}$	75.4	D70*	8%
$f_{c,0,k}$	42.0	D70	
$f_{c,90,k}$	12.0	D60-D70	
$f_{t,0,k}$	38.0	D60-D70	
$f_{v,k}$	7.5	D70*	25%
ρ_{mean}	670	D50	

Although the gouvernment trough the Croatian Organisation for standards and norms has taken over EC1, EC2 and EC3 as our national norms with transition period of 5 years for possible use of previous norms. EC5 was not taken over because it was prenorm quite a long time and recently became obligatory to EU countries. Another reason is great innertion of national monopolic firm «Croatian Forests» which is not yet ready for new approach to timber use.

For the countries in transition which currently don't have tables for characteristic values of strengths that are calibrated for most commonly speciesin their countries, this paper brings the information of possibility and procedure which can advance current classification of wood and gives economic savings.

Procedure consists of nondestructive testings of MOE, destructive testings for strength values and use of the "trained" neural network. Input variables of neural network are: dimensions, density, moisture content, boundary conditions, dynamic MOE obteined by nondestructive testings and output variables are strength values obteined for training set by destructive laboratory testings. This procedure make possible advanced classifiation and determination of timber strengths to avoid arbitary visual method for classification which is quite unobjective and adopt it to EC5. On the other hand it is the way to avoid high costs of systems for machine stress grading such as «DIMTER» or «GRECOMATEN». Just with nondestructive testing of element using preliminary trained neural network, values of strengths and static MOE are possible to obteined without any further laboratory destructive testings.

Samples or built up elements in timber construction can be approached by ultrasound sondas. The boundary conditions are not crucial. In the case of MOE obteined by transient excitation by impact that is dynamic MOE, using spectral analyser for determining of first frequency , boundary conditions are very important.

Procedure of classifying with measuring moisture content, dimensions and weight of samples. All these input starts values are put in PC memory. Using one of the nondestructive technique, program calculates dynamic MOE. With RUN-TIME version of neural network, all characteristic strength values could be obteined. Of course it is assumed that neural network is trained on as much as possible testing specimens.
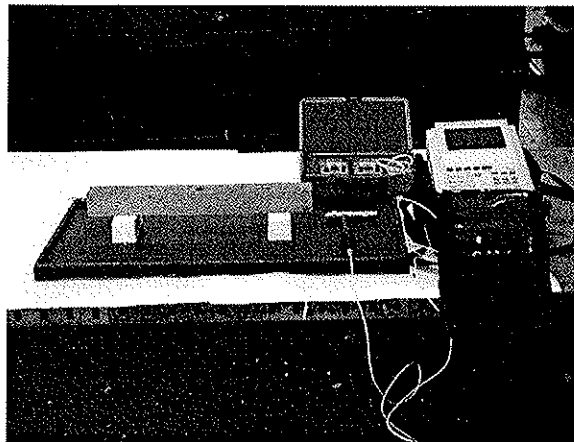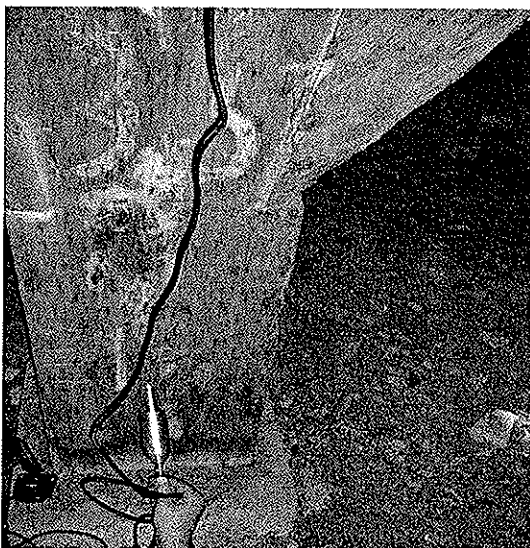

Fig 1: Determination of MOE by spectral analyser.

Fig 2: Ultrasound measuring in built up elements   Fig 3: Ultrasound determination of MOE.
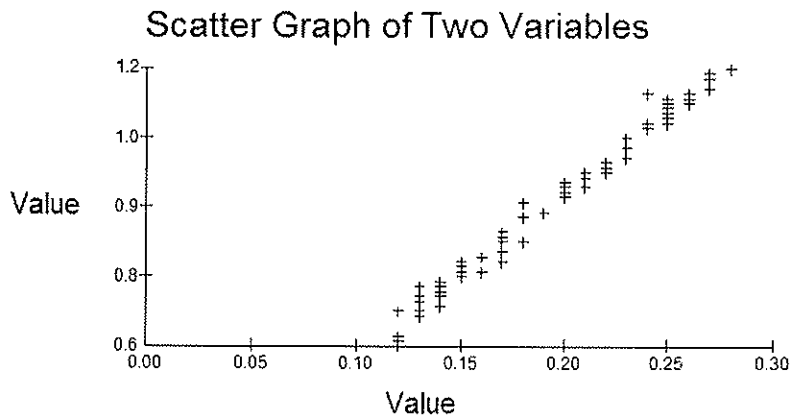
Scatter Graph of Two Variables

Value

Fig. 4. Between each two input or output variables the correlation could be seen ($f_{c,90,k} - f_m$)

Datagrid: E:\klasifneural\M1.pat

File Edit Format Help

Number of row with variable names (blank if none): 1 — ☒ left/right arrow keys end edit
First row containing actual training data: 2 — Size: 179 row 20 columns

Note: This is not a commercial spreadsheet and may not load fast enough for large files. The NeuroShell 2 Options menu allows you to change the datagrid call to your own spreadsheet. Search help file for "datagrid" for detail.

	A	B	C	D	E	F	G	
1	density	moisture	cantilever	beam	frequency	sample	fcii	fcok
2	6.500000000000	0.900000000000	1.000000000000	0.000000000000	2.080000000000	1.000000000000	0.570000000000	
3	6.500000000000	0.900000000000	1.000000000000	0.000000000000	2.040000000000	1.000000000000	0.570000000000	
4	6.100000000000	0.900000000000	1.000000000000	0.000000000000	2.050000000000	1.000000000000	0.560000000000	
5	8.600000000000	0.900000000000	1.000000000000	0.000000000000	1.980000000000	1.000000000000	0.540000000000	
6	8.600000000000	0.900000000000	1.000000000000	0.000000000000	1.950000000000	1.000000000000	0.430000000000	
7	6.640000000000	0.900000000000	1.000000000000	0.000000000000	1.910000000000	1.000000000000	0.560000000000	
8	8.200000000000	0.900000000000	1.000000000000	0.000000000000	1.550000000000	1.000000000000	0.450000000000	
9	9.100000000000	0.900000000000	1.000000000000	0.000000000000	1.700000000000	1.000000000000	0.420000000000	
10	8.400000000000	0.900000000000	1.000000000000	0.000000000000	1.750000000000	1.000000000000	0.440000000000	
11	7.850000000000	0.900000000000	1.000000000000	0.000000000000	1.800000000000	1.000000000000	0.460000000000	
12	6.600000000000	0.900000000000	1.000000000000	0.000000000000	2.130000000000	1.000000000000	0.570000000000	
13	6.200000000000	0.900000000000	1.000000000000	0.000000000000	1.900000000000	1.000000000000	0.450000000000	
14	7.100000000000	0.900000000000	1.000000000000	0.000000000000	2.030000000000	1.000000000000	0.550000000000	
15	6.700000000000	0.900000000000	1.000000000000	0.000000000000	1.950000000000	1.000000000000	0.460000000000	
16	8.430000000000	1.300000000000	1.000000000000	0.000000000000	1.510000000000	1.000000000000	0.450000000000	
17	7.450000000000	1.200000000000	1.000000000000	0.000000000000	1.880000000000	1.000000000000	0.540000000000	
18	8.000000000000	1.300000000000	1.000000000000	0.000000000000	1.630000000000	1.000000000000	0.440000000000	
19	7.980000000000	1.100000000000	1.000000000000	0.000000000000	1.880000000000	1.000000000000	0.540000000000	
20	8.000000000000	1.000000000000	1.000000000000	0.000000000000	1.960000000000	1.000000000000	0.490000000000	
21	7.280000000000	1.400000000000	1.000000000000	0.000000000000	2.010000000000	1.000000000000	0.580000000000	
22	7.880000000000	1.160000000000	1.000000000000	0.000000000000	2.110000000000	1.000000000000	0.580000000000	
23	7.100000000000	1.400000000000	1.000000000000	0.000000000000	1.910000000000	1.000000000000	0.580000000000	
24	6.900000000000	0.900000000000	1.000000000000	0.000000000000	1.670000000000	1.000000000000	0.440000000000	
25	6.960000000000	1.200000000000	1.000000000000	0.000000000000	2.130000000000	1.000000000000	0.570000000000	
26	9.600000000000	1.300000000000	1.000000000000	0.000000000000	1.060000000000	1.000000000000	0.410000000000	
27	7.300000000000	1.100000000000	1.000000000000	0.000000000000	2.130000000000	1.000000000000	0.580000000000	
28	7.500000000000	1.100000000000	1.000000000000	0.000000000000	2.090000000000	1.000000000000	0.580000000000	
29	8.100000000000	1.300000000000	1.000000000000	0.000000000000	1.950000000000	1.000000000000	0.520000000000	
30	8.000000000000	1.400000000000	1.000000000000	0.000000000000	1.880000000000	1.000000000000	0.540000000000	
31	7.840000000000	1.200000000000	1.000000000000	0.000000000000	2.080000000000	1.000000000000	0.580000000000	
32	8.400000000000	1.200000000000	1.000000000000	0.000000000000	1.860000000000	1.000000000000	0.480000000000	
33	8.270000000000	1.200000000000	1.000000000000	0.000000000000	2.100000000000	1.000000000000	0.500000000000	
34	7.300000000000	1.200000000000	1.000000000000	0.000000000000	2.000000000000	1.000000000000	0.570000000000	
35	6.560000000000	1.200000000000	1.000000000000	0.000000000000	2.110000000000	1.000000000000	0.590000000000	
36	7.070000000000	1.200000000000	1.000000000000	0.000000000000	1.960000000000	1.000000000000	0.510000000000	

Start · NEW (D:) · Na zu putu · CiBVRajsc - M... · Windows Med... · NeuroShell 2 -... · Advanced Neu... · Datagrid: E:\... · 13:59

Fig. 5. The data-base: input and output variables in data-grid

3 Proofs of mechanical resistance and stability of timber structures in accordance with HRN codes and Eurocodes - Comparison of results of the structural design

3.1. An example of the timber structure of the three pinned frame with V - columns

The two locations are chosen to be relevant for the comparison. The first one is a coast area of Primorje also known as the zone of very strong winds, and the second one is the neighbouring area of Gorski kotar, the area significant for strong winds as well as for the long-time large snow. The last one is the zone of hills where a height above sea level grows very fast.
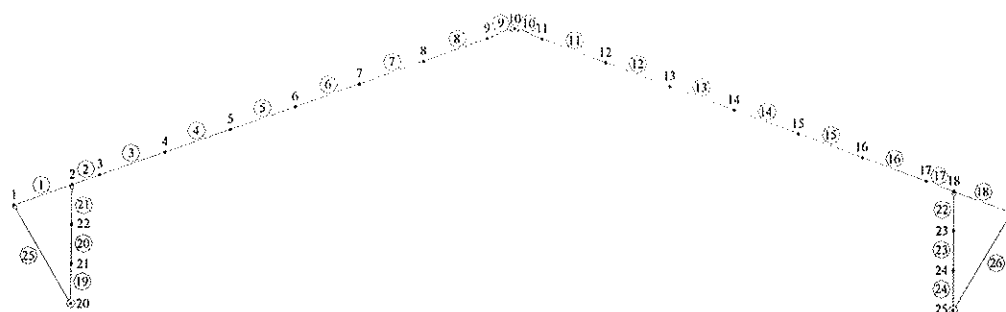

Fig. 6. Model of the main girder of a timber structure used for its computed design

Wooden structure has got the steel-glass facades. Steel panels are provided to cover almost the whole roof, but there is also the cantilever part of frame that is free of covering. That part of beam has got constant depth as well as its adjacent member, but depths on the rests of glulam beams are variable. The vertically part of V-shaped posts are columns of a glued laminated compound cross section. The tensional rod of the each V-shaped column is the glulam as well. The roof slope of the 20° is provided. A total height that measured at the apex of the glulam structure, which is totally exposed to the wind, exceeds the value of 10 meters.

3.2. The coast area location with height above sea level (HASL) of the 100m
A comparison of the estimating results for elements of glulam structure
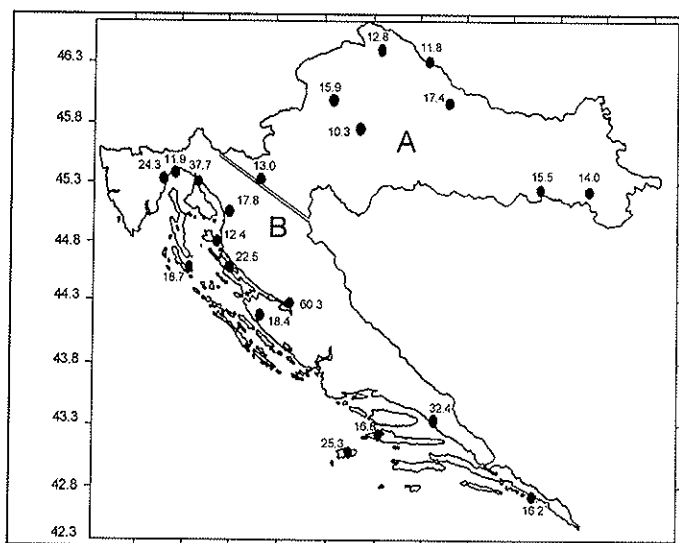
Characteristic values of serviceability loads have been calculated in accordance with the snow and wind features, which are significant for the whole coast area (a low level of snow loading and very strong wind loading, as well).

Fig. 7. A new wind map of Croatia (see zone B) in accordance with EC1

Estimated characteristic values of wind load are as they following:

$w = (c_{e,i} + c_i) \cdot w_0 = (c_{e,i} + c_i)\,1,30\ kN/m^2$ HRN loading codes for zone B (see the map of RC)
$w = 0,40\ kN/m^2$ (for exposed roof area)   Values of coefficients ($c_{e,i}$) are variable (depending of the slope of area that is exposed to the external wind - $c_1 = 0,8$, $c_2 = 1,2 \sin\alpha - 0,4$) and the value of the coefficient $c_i = \pm 0,3$ (internal wind).

$w = 0,83\ kN/m^2$ (for exposed roof area)   EC1 loading codes for zone B (see the map of RC) The estimating of external compression wind load had been based on $v_{ref,0} = 30 m/s$, $\rho = 1,25\ kg/m^3$ and $q_{ref} = 5,63\ kN/m^2$ (ENV 1991 – 2 – 4)

Estimated characteristic values of snow load are as they following:

$s_0 = 0,35\ kN/m^2$ HRN loading codes for zone III.

$s_0 = \mu_i \cdot C_e \cdot C_t \cdot s_k =$
$= 0,8 \cdot 1,0 \cdot 1,0 \cdot 0,45 = 0,36\ kN/m^2$ EC1 loading codes for zone III. (ENV 1991 – 2 – 3) and for the HSAL = 100m circumstances.
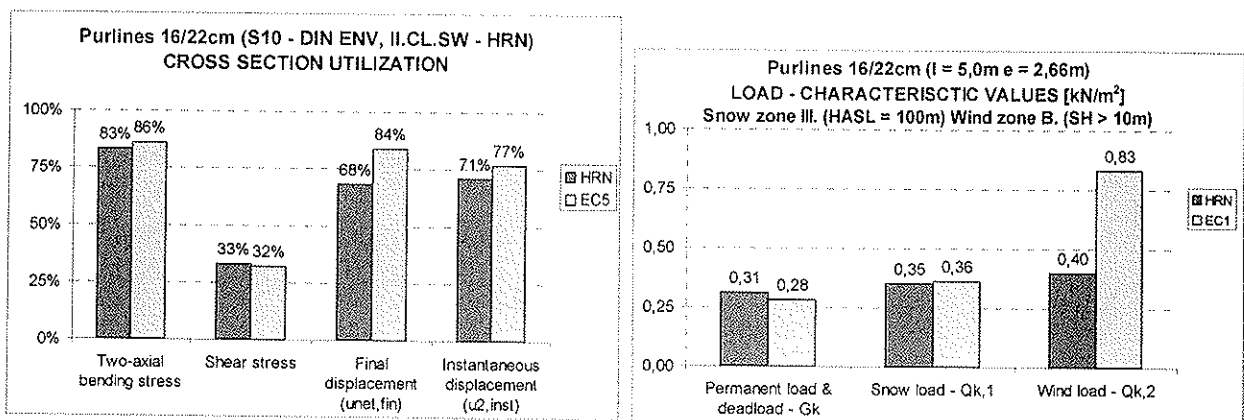

Fig. 8. Purlines of the glulam structure - snow zone III, wind zone B
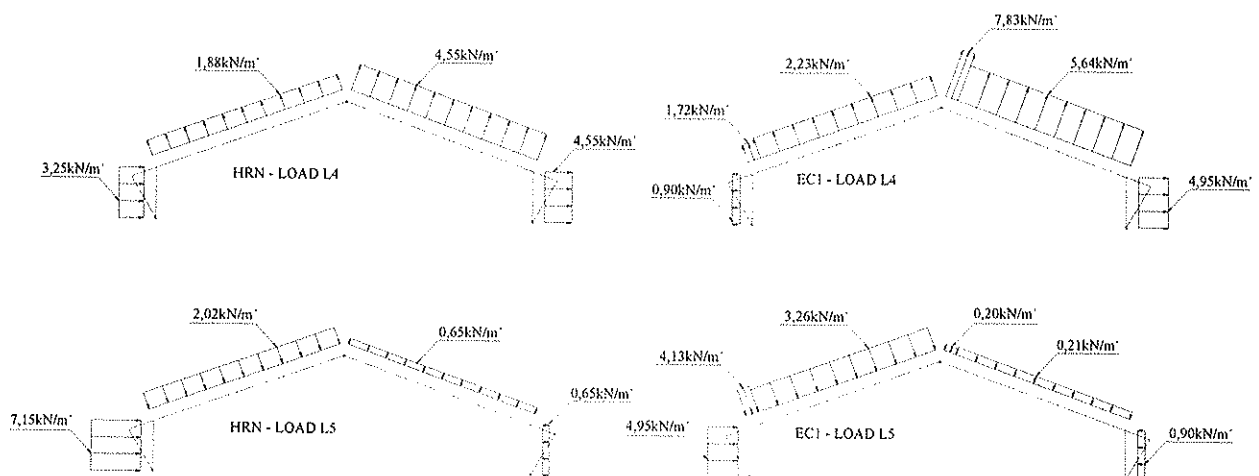A comparison of the results of cross section utilisation and loads

Fig. 9. Model of wind load treatment for the main-girder

Glulam main-girder - 3pinned frame with V-columns (L =30,0m e = 5,0m)
LOAD - CHARACTERISTIC VALUES [kN/m]
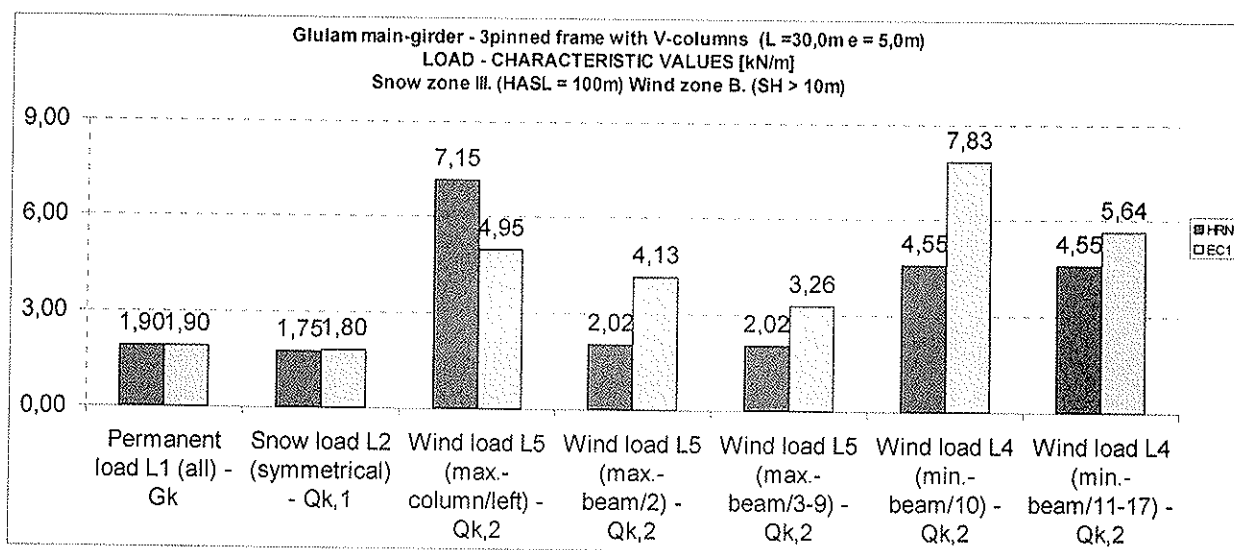Snow zone III. (HASL = 100m) Wind zone B. (SH > 10m)

Fig. 10. A comparison of the results of characteristic load values calculation in accordance with the different standards - estimation for a coast area

Table 3. Serviceability control of main-girder accordingly HRN U.C9.300 and EC5
A comparison of results of joint displacements values and its utilisation

Joint	HRN $u_{net,fin}$ [mm]	EC5 $u_{net,fin}$ [mm]	HRN $u_{2,inst}$ [mm]	EC5 $u_{2,inst}$ [mm]	$u_{net,fin} \leq$ [mm]	$u_{2,inst} \leq$ [mm]	Utilisation			
							$u_{net,fin}$ [%]		$u_{2,inst}$ [%]	
							HRN	EC5	HRN	EC5
18	20,21	16,60	16,24	11,73	27,1	20,3	75%	61%	80%	58%
19	19,34	16,08	14,6	11,41	21,3	14,2	91%	75%	103%	80%
10	24,62	24,78	15,69	14,30	150,0	100,0	16%	17%	16%	14%
7 (14)	41,12	37,5	32,65	31,62	79,8	53,2	52%	47%	61%	59%
23	13,55	11,61	10,92	8,37	20,3	13,5	67%	57%	81%	62%

Table 2. Load bearing capacity control of main-girder accordingly HRN U.C9.300 and EC5
A comparison of results of cross section utilisation that is related on stress values

Part of the main-girder (position and dimensions of an element)	Member (Model)	Stress values (load bearing capacity & stability proofs) [N/mm²]		Cross section utilisation	
		HRN	EC5	HRN	EC5
BEAM (cantilever -20/123)	18	$\sigma_{c,0}$, σ_m		40%	32%
	18 (MJ)	$\sigma_{c,0,neto}$, $\sigma_{m,neto}$		65%	43%
	18 (MJ)	τ_v		75%	64%
BEAM (span -20/123)	2 (MJ)	$\sigma_{c,0,neto}$, $\sigma_{m,neto}$		56%	36%
BEAM (span - 20/83,9)	16	$\sigma_{c,0}$, σ_m		60%	48%
BEAM (apex - 20/60)	10 (MJ)	$\sigma_{c,0}$		18%	36%
	9 (MJ)	τ_v		42%	42%
GLULAM POST (2x20/42)	19 (MS)	$\sigma_{c,0,neto}$, $\sigma_{m,neto}$		14%	32%
	19	$\sigma_{c,0}$, σ_m		20%	13%
	22 (MJ)	$\sigma_{c,0,neto}$, $\sigma_{m,neto}$		30%	21%
GL. TENS. ROD (20/33)	26 (MJ)	$\sigma_{c,0}$, σ_m		26%	26%

3.3. The location in II. snow zone with height above sea level (HASL) of the 800m - a comparison of the estimating results for purlines

Characteristic value of snow load has been calculated in accordance with the snow features in zone II. which is an area of long-time high level snow. Related to the wind, timber structure is located in the B. wind zone, which has been described earlier in the paper.

Estimated characteristic values of snow load (II. zone, HASL = 800m) are as they following:

$s_0 = 1{,}25 + (800 - 500) / 400 = 2{,}0 \ kN/m^2$ HRN loading codes for HASL > 500m

$s_0 = \mu_i \cdot C_e \cdot C_t \cdot s_k =$
$= 0{,}8 \cdot 1{,}0 \cdot 1{,}0 \cdot 4{,}26 = 3{,}41 \ kN/m^2$ EC1 loading codes for II. zone (ENV 1991 – 2 – 3) and for the HSAL = 800m circumstances.
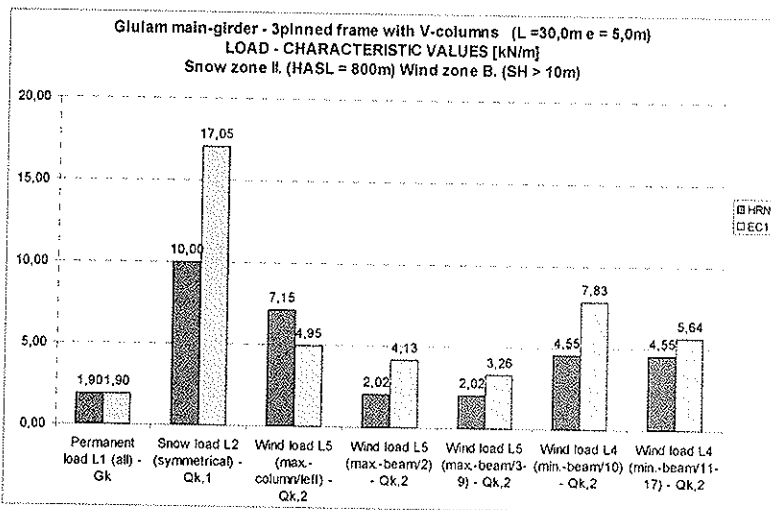

Fig. 11. A comparison of the results of characteristic load values calculation in accordance with the different standards. Estimating for snow zone II and wind zone B
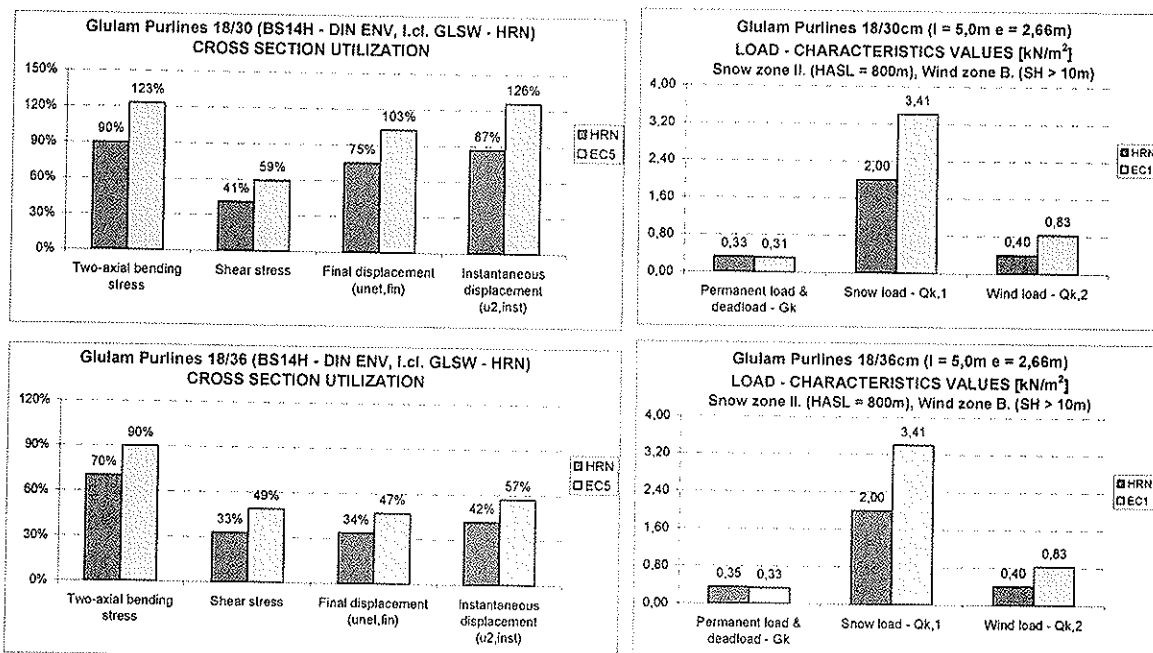

Fig. 12. Purlines of the glulam structure - snow zone II, wind zone B
A comparison of the results of cross section utilisation and loads

Literature:

1. Vlatka Saler (Rajčić): „ NONDESTRUCTIVE METHODS FOR MECHANICAL PROPERTIES DETERMINATION", magistra thesis, University of Zagreb, Faculty of Civil Engineering, Zagreb, January 1996.

2. Vlatka Rajčić: „ CHARACTERISTICS OF COMPOSITE TIMBER-LIGHTWEIGHT (EPS) CONCRETE STRUCTURES", Ph. D. thesis, Faculty of Civil Engineering, Zagreb, July, 2000.

3. Adriana Bjelanović, Vlatka Rajčić: WOODEN STRUCTURES according to european norms, Hrvatska Sveučilišna naklada & Faculty of Civil Engineering, Manualia Universitatis Studiorum Zagrebiensis, book, June , 2006.

4. Miljenko Haiman: ANALYSIS OF THE RELIABILITY OF GLUE-LAMINATED GIRDERS , Ph. D. thesis, Faculty of Civil Engineering, Zagreb, June, 2001.

5. Silva Lozančić: CONTRIBUTION TO KNOWLEDGE ABOUT RHEOLOGY OF COMPOSITE TIMBER-CONCRETE GIRDERS, Ph.D. thesis, Faculty of Civil Engineering , University of J.J. Strossmayer in Osijek, Osijek, December, 2003.

6. Kiril Gramatikov: EXPERIMENTAL AND ANALYTICAL RESEARCH ON TRUSS TIMBER GIRDERS, Ph.D. thesis, Institute for earthquake engineering and seismology, on the University „Kiril i Metodij", Skopje, May, 1990.

7. Željko Đidara: POSSIBILITY OF USING GLUE-LAMINATED GIRDERS FROM HARD WOOD SPECIES OF SMALL DENSITY, Ph.D. thesis, Univesity in Zagreb, Forestry Faculty, Zagreb, May, 1998.

8. Agron E. Gjinolli: ANALYSES OF RELAXATION FLOW OF STRESSES IN CURVED GLUE-LAMINATED ELEMENTS, magistara thesis, University in Zagrebu, Faculty of Civil Engineering, Zagreb, 1997.

9. STEP 1 Blaß, H. J./ Görlacher, R./ Steck, G.: STEP 1, Bemessung und Baustoffe, Fachverlag Holz, Düsseldorf, 1995.